

Mass Spectrometry-based Proteomic Analysis of Forensic Body Fluids, Fingermarks and Fingernail traces

A thesis submitted for fulfilment of the degree of

Doctor of Philosophy

as a combination of research narrative and portfolio of scientific publications by

Sathisha Kamanna, MSc



ADELAIDE • AUSTRALIA

College of Science and Engineering

August 2018

Table of Contents

Declaration.....	VIII
Certificate.....	IX
Abstract.....	X
Acknowledgements.....	XIII
Publications.....	XVI
Conference Proceedings and Presentations.....	XVII
Awards and Achievements.....	XIX
List of abbreviations and symbols.....	XX
Research ethics and safety considerations.....	XXII
Structure of this Thesis.....	XXIII
Chapter 1: INTRODUCTION	1
1.1 Proteomics and mass spectrometry	1
1.2 Matrix Assisted Laser/Desorption Ionization Time of Flight mass spectrometry	2
1.3 The MALDI ion source	4
1.4 The Time of Flight mass analyser	5
1.5 “Top-Down” Mass Spectrometry	6
1.6 Bottom-Up mass spectrometry.....	8
1.7 Post Source Decay.....	10
1.8 MALDI-TOF/TOF (LIFT)	12
1.9 Tandem mass spectrometry	14
1.10 Mass spectrometry imaging (MSI).....	16

1.11	Liquid chromatography mass spectrometry [LC-MS]	17
1.12	Forensic Science.....	18
1.13	Forensic Human Identification.....	19
1.14	Forensic body fluid identification	20
1.14.1	mRNA profiling for body fluid identification.....	21
1.15	Blood.....	23
1.15.1	Presumptive tests.....	23
1.16	Semen.....	25
1.17	Saliva.....	27
1.18	Vaginal Fluid.....	29
1.19	Urine.....	29
1.20	Sweat.....	30
1.21	Fingermarks and other biological-chemical traces.....	31
1.22	Fingernails and biological traces.....	33
1.23	Other Forensic Technologies for the Identification of Body Fluids	34
1.23.1	Fluorescence spectroscopy.....	34
1.23.2	Raman and IR Spectrometry	34
1.23.3	DNA profiling	35
1.24	Mass Spectrometry-based Proteomics for Forensic Body Fluid Identification	36
1.25	Statement of the Problem	38
1.26	Aims of Research	39
Chapter 2: Materials and Methods		42

2.1	Materials and Suppliers.....	42
2.1.1	List of chemicals and materials used in this project.....	42
2.1.2	Instruments and equipment.....	44
2.2	Samples used in this study	45
2.2.1	List of human and non-human body fluid samples used in this project.....	45
2.3	Sample collection.....	46
2.4	Sample Preparation and Experimental Methods for Chapter 3.....	46
2.4.1	Experimental materials and samples	47
2.4.2	Scanning electron microscopy.....	48
2.4.3	MALDI-TOF MS instrumentation	48
2.4.4	MALDI-TOF MS sample preparation.....	49
2.4.4.1	Analysis on MTP 384 polished steel plate.....	48
2.4.4.2	Analysis on ITO-coated slides	49
2.4.4.3	In-solution trypsin digestion	49
2.4.5	Mass spectral and database analysis	50
2.4.6	nLC-ESI-qTOF MS/MS analysis	52
2.5	Chapter four methods.....	53
2.5.1	Materials and chemicals	53
2.5.2	In situ homogenous proteolysis procedure	53
2.5.3	Matrix deposition.....	54
2.5.4	Preparation of finger marks	54
2.5.4.1	Bloodied finger marks.....	54
2.5.4.2	Vaginal fluid-contaminated finger marks	54
2.5.5	Finger mark image capture	55
2.5.6	Preparation of fingernail scrapings.....	55
2.5.7	Finger marks dusted with silver/black powder and lifted.....	55

2.5.8	MALDI-ToF, IMS and data analysis.....	55
2.5.9	nLC-MS/MS and MALDI-ToF analysis of fingernail scrapings	56
2.5.10	DNA profiling of fingernail scrapings.....	56
2.6	Chapter five methods	57
2.6.1	Fingernail preparation and collection of traces using nylon microswabs ...	57
2.6.2	DNA profiling analysis.....	57
2.6.3	Proteomic analysis	57
2.6.3.1	Direct ‘on-fibre’ trypsin digestion	57
2.6.3.2	‘In-solution’ trypsin digestion.....	58
2.6.3.3	nLC-ESI-qTOF MS/MS analysis.....	58
2.6.3.4	MALDI-ToF MS/MS analysis	58
2.6.3.5	Data analysis	58
2.7	Chapter six methods.....	59
2.7.1	Fingermark preparation	59
2.7.1.1	Bloodied fingermarks for MALDI-TOF-IMS.....	59
2.7.2	Homogenous MALDI matrix deposition.....	60
2.7.3	Fingermark image capture	60
2.7.4	Bloodied fingermark enhancement using Amido black stain.....	60
2.7.5	Bloodied fingermarks dusted with silver-black powder and lifted.....	61
2.7.6	Hematrace test	61
2.7.7	In-solution trypsin digestion	61
2.7.8	One-dimensional SDS-PAGE analysis for blood samples	62
2.7.9	In-gel trypsin digestion	63
2.7.10	MALDI-TOF-IMS and data analysis.....	64
2.7.11	nLC-ESI-qTOF MS/MS and protein database analysis	64

Chapter 3: Direct identification of forensic body fluids using matrix-assisted

laser desorption/ionization time-of-flight mass spectrometry	65
3.1 Publication context.....	68
3.2 International Journal of Mass Spectrometry [Kamanna <i>et al.</i> 2016]	70
3.3 Body fluid confirmation by nLC-ESI-qTOF MS/MS analysis.....	71
Chapter:4 A mass spectrometry-based forensic toolbox for imaging and detecting biological fluid evidence in finger marks and fingernail scrapings.....	74
4.1 Manuscript context.....	77
4.2 International Journal of Legal Medicine [Kamanna <i>et al.</i> 2017].....	80
4.3 Comprehensive proteomic analysis of fingernail contaminated vaginal fluid....	81
4.4 DNA profiling of fingernail evidence.....	83
4.5 MALDI-ToF MSI analysis of latent fingermark constituents (endogenous small molecules and large proteins).....	84
Chapter 5: A complementary forensic ‘proteo-genomic’ approach for the direct identification of biological fluid traces under fingernails.....	88
5.1 INTRODUCTION	88
5.2 Fingernail preparation and collection of traces using nylon microswabs.....	91
5.2.1 Data analysis	92
5.3 Results and discussion.....	93
5.3.1 Analysis of fingernail traces using MALDI-ToF-MS/MS	93
5.3.2 Differential proteomic analysis of fingernail traces using nLC-ESI-qToF MS/MS and identification of vaginal fluid and non-human blood protein markers.....	97
5.3.3 Complementary proteomic and genomic analysis of fingernail traces.....	102
5.4 Concluding remarks	104

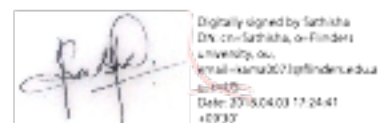
Chapter 6: "Bottom-up" in situ proteomic differentiation of human and non-human haemoglobins for forensic purposes by matrix-assisted laser desorption/ionization time-of-flight tandem mass spectrometry	108
6.1 Manuscript context.....	111
6.2 Rapid Communications in Mass Spectrometry [Kamanna <i>et al.</i> 2017].....	112
6.3 Top-down and bottom-up mass spectrometry analysis for unknown haemoglobins of Australian mammals	116
6.3.1 One-dimensional SDS-PAGE analysis of marsupial blood samples	118
6.4 Bottom-up and tandem mass spectrometry analysis for the differentiation of closely related haemoglobins.....	121
Chapter 7: Conclusions and Future Work	126
7.1 Conclusions	126
7.2 Future Work	129
References	131
Appendices	143

Declaration

I certify that this thesis does not include without acknowledgement any material previously submitted for a degree or diploma in any university; and that to the best of my knowledge and belief it does not contain any material previously published or written by another person except for where due reference is made in the text.

The author acknowledges that copyright of published works contained within this thesis (as listed in publications and the chapters) resides with the copyright holders of those work. I give permission to the University in regards to copy of digital version of my thesis to be made available on the University's digital search repository, the library catalogue, the Australasian Digital Theses Program (ADTP), unless permission has been granted by the University to restrict access for a period of time.

Sathisha Kamanna



CERTIFICATE

This is to certify that thesis entitled “**Mass Spectrometry-based Proteomic analysis of forensic body fluids, fingermarks and fingernail traces**” submitted by Sathisha Kamanna for the degree of Doctor of Philosophy in the College of Science and Engineering is based on the results obtained from the experiments performed by him under my supervision. The thesis or a part there of has not been previously submitted for any other diploma and degree.

Prof. K. Paul Kirkbride

School of Chemical and Physical Sciences

College of Science and Engineering

Abstract

In the past decade, matrix-assisted laser desorption ionization time-of-flight mass spectrometry (MALDI-TOF MS) and mass spectrometry imaging (MSI) have been widely used in clinical and/or biological sciences for the detection, differentiation and mapping of differentially expressed proteins or peptide markers within tissue sections. Recently, MALDI-MS techniques have been applied to forensic science for the analysis of organic small molecules (e.g., illicit drugs and metabolites) and protein biomarkers for identification of body fluids such as blood, saliva, seminal fluid, urine, vaginal fluid and sweat in fingermarks.

The most important forensic test, DNA profiling, can indicate from ‘whom’ biological traces originated. However, it is also very important to determine the ‘type’ of body fluid and differentiate it from non-human fluids, thus providing evidence as to the circumstances surrounding the crime. Furthermore, biological substances such as blood or vaginal fluid and other body fluid mixtures may become smeared on the fingers of the victim or suspect or trapped under their fingernails. If either person touches an object with their “contaminated” finger then a “contaminated” fingermark may be deposited. Such marks could be great value as they can identify not only who deposited the mark, but also who they touched and which part of the body they touched. These trapped biological traces are extremely valuable information to forensic investigation. There is a lack of confirmatory tests for many body fluids and current available presumptive tests often produce false positives, suffer from interferences, lack human-specificity, and cannot distinguish between menstrual blood and venous blood, menstrual fluid and vaginal fluid or mixtures of other bodily fluids.

In this study, mass spectrometry (MS)-based *in-situ* “top-down” and “bottom-up” proteomics analysis was carried out for the direct identification of “protein markers” in body fluids and their mixtures. The work describes a streamlined MALDI-ToF MS-based proteomic methods for the identification of body fluid traces recovered from different, important substrates (e.g., various types of fabric fibres, cotton swabs and nylon microswabs), directly *in situ* on these substrates, and from enhanced latent fingermarks (including “lifted” enhanced marks). Direct identification of intact proteins

(“top-down” analysis) on fabric and microswab fibres using MALDI-MS is often challenging due to low mass axis resolution and accuracy, especially in mixture of body fluids. Thus, the use of “bottom-up” proteomics (peptide mass fingerprint analysis) and *in-situ* MS/MS (tandem mass spectrometry) analysis followed by *de novo* sequencing was investigated in order to enhance the specificity and reliability of protein biomarker identification. The described mass spectrometry methods for the direct identification of differentially expressed protein “markers” in native or dilute solutions of body fluids and in aqueous suspensions of dried body fluid particles on different substrates, offers significant advantages compared to other classical proteomics, including speed of analysis, reduced the cost of complex requirements and elimination of cross-contamination. Even though body fluids of relevance to forensic science are complex mixtures of proteins, they each contain characteristic proteins that are abundantly expressed and they ionize in preference to other proteins that are less abundant. Although MALDI-ToF techniques do not have the performance to discover trace biomarkers in the wide range of tissues and fluids relevant to medical science, the techniques appear to be fit for the purpose of identifying the small range of body fluids that are encountered in forensic biology.

MALDI-MSI techniques were applied for the direct identification and mapping of foreign body fluids (such as blood, vaginal fluid) in fingermarks, including latent fingermarks that were enhanced using silver/black magnetic powder or Amido Black and lifted using double sided Kapton adhesive tape. MALDI-TOF MS provided greater species-specific information as compared to the popular immunochromatographic screening test for human blood (Hematrace[®] ABACard[®]) and fingermark protein staining methods (Amido Black). This thesis also describes for the first time “top-down” and “bottom-up” mass spectrometry-based proteomics approaches for the identification and differentiation of haemoglobins on bloodied fingermarks. It was shown that blood from Australian native animals readily can be differentiated with human blood. Even haemoglobins in mixed blood (human and animal blood) was successfully detected and imaged in bloodied fingermarks. Small endogenous molecules were detected in lifted ridge patterns.

Differential proteome analysis using nLC-ESI-qTOF MS/MS showed a high confidence (>95%) identification and confirmation of body fluid protein markers and detection of

unknown haemoglobins from Australian marsupials blood samples.

A schematic work flow presented in this thesis describes a complementary forensic ‘proteo-genomic’ analysis on a single micro-swab for the direct identification of the “type” of biological fluid present under fingernails and the identity of its “donor”. The analytical strategy (forensic “toolbox”) demonstrated in this work involves two complementary techniques, direct PCR DNA profiling and mass spectrometry-based protein biomarker detection. Post-direct PCR solutions can be used successfully for proteomic identification of haemoglobins, which provides both DNA profiles and proteomic information from the same sample.

The applicability of novel MS-based proteomics (“top-down and “bottom-up”) and tandem mass spectrometry analysis followed by *de novo* sequencing and MALDI-MSI techniques presented in this thesis and the published articles offer significant potential for forensic biology applications.

Acknowledgements

I would like to express my utmost gratitude and appreciation to my supervisors, Prof. Paul Kirkbride, Prof. Nicholas H. Voelcker and Prof. Adrian Linacre for their crucial support and guidance during my doctoral programme.

I would like to start with my primary supervisor Prof. Paul Kirkbride; he was magnificent, cheerful and supportive throughout the research project. All my discussions with him have been thoroughly intellectual and I gained substantial research knowledge in forensic chemistry. I greatly appreciate your support that helped me to go USA conferences, including in San Francisco, the American Society of Mass Spectrometry (ASMS) conference, which was held in Indianapolis, and a workshop trip to Massachusetts (Boston) and New York (awesome!). Thank you for the knowledge shared and gained throughout this study. Your guidance and suggestions and frequent encouragement were also greatly appreciated, and indeed contributed in shaping my PhD research up to a high level.

I wish to express my gratitude to co-supervisor Prof. Adrian Linacre (Chair in Forensic DNA Technology), for his incredible knowledge in the field of biological and genomics analysis – a part of the work in this PhD thesis. Thank you very much for your valuable advice and as well as fruitful collaboration, with respects to knowledge shared and explored in direct PCR DNA profiling and also preliminary work on mRNA/miRNA extraction.

Sincere thanks to my adjunct supervisor Prof. Nicholas H. Voelcker, he currently is the Scientific Director of the Melbourne Centre for Nanofabrication and Professor at the Monash Institute of Pharmaceutical Sciences (Melbourne). I would like to mention special thanks for his assistance and initial discussion in regards to mass spectrometry instrumentation and its applications for forensic science. I greatly appreciated for your valuable suggestions and knowledge shared in this project.

I also greatly acknowledge Dr. Julianne Henry, a chief scientist at Forensic Science SA (FSSA); this work was carried out in collaboration with FSSA and could not have taken place without the assistance of that organization. This project was supported by the Ross

Vining Research Fund, which is administered by FSSA. I therefore express my gratitude to FSSA for providing financial assistance that allowed my project to succeed. I would also like to thank to Dr Jennifer Templeton (Flinders University and FSSA) and Belinda Martin for the helping with initial DNA-profiling experiments.

I would also like to give special thanks to Dr. Daniel Jardine and Mr. Jason Young in the Flinders Analytical and Mass Spectrometry facility. I also thank to Dr. Tim Chataway, proteomics facility head in the Flinders Medical Centre at Flinders University; I gratefully acknowledge both mass spectrometry proteomics facilities allowed me to carry out all the MALDI-TOF MS, imaging experiments and nLC-ESI MS/MS and proteomics analysis.

This project used many types of samples from many volunteers, I wish to thank those who provided fingerprints, fingernails traces, and human body fluid samples and also special thanks to Dr. Ian Hough and Cleland Wildlife Sanctuary for the provision of animal (Australian marsupials) blood samples.

Cheerful gratitude to all the other PhD students from our analytical chemistry and forensic group; thank you for valuable discussions and seminars. I would give respectful thanks to Prof. Claire Lenehan for your valuable suggestions. I also wish to give huge thanks to Nick Lucas for helping to take some good SEM images at Flinders. Also, I wish to acknowledge all the non-academic members (especially Jacqui Hull and Jennie Brand) at the School of Chemical and Physical Sciences, the Faculty of Science and now the College of Science and Engineering.

I greatly acknowledge the Indian Institute of Science (IISc), Professors DC and P Balaram (a former director of IISc) and the mass spectrometry facility, where I worked before starting my PhD.

I wish to thank the *International Journal of Mass Spectrometry-Agilent* and the American Society of Mass Spectrometry (ASMS) for awarding me ‘Best Student Paper Award’ with \$2000 USD for the best applied paper published in 2016. I also like to thank the National Institute of Forensic Science (NIFS) and Australia New Zealand Policing Advisory Agency (ANZPAA) for the ‘Best Paper’ in a Refereed Journal 2016.

Finally, I would especially thank to all my friends and my family members, specifically to Mom, Dad and my brother Dr. Kantharaju (also his wife Abinethri) for their continual encouragement and support right from college days, which enabled me to achieve the knowledge and strength to endeavour for excellence.

Thank you all for helping me complete my PhD journey.

PUBLICATIONS

The publications originating from the research work conducted within this thesis are formed as chapters:

Accepted and published papers:

Sathisha Kamanna, Julianne Henry, Nicholas H. Voelcker, Adrian Linacre, K. Paul Kirkbride, *Direct identification of forensic body fluids using matrix-assisted laserdesorption/ionization time-of-flight mass spectrometry*. **Int. J. Mass Spectrom.** **2016**, 397, 18-26.

Citations: **4** Impact Factor: **1.8**

SCImago Journal Rank (SJR) 27 out of 62 (Spectroscopy category)

Sathisha Kamanna, Julianne Henry, Nicholas H. Voelcker, Adrian Linacre, K. Paul Kirkbride, *A mass spectrometry-based forensic toolbox for imaging and detecting biological fluid evidence in finger marks and fingernail scraping*. **Int J Legal Med** (2017) 131:1413–1422

Citations: **3** Ranking (SCI mago) of the journal: **30/193** (Medicine, Pathology and Forensic Medicine) Impact Factor: **2.4** (2016)

Sathisha Kamanna, Julianne Henry, Nicholas H. Voelcker, Adrian Linacre, K. Paul Kirkbride, *“Bottom-up” in situ proteomic differentiation of human and non-human haemoglobins for forensic purposes by MALDI-ToF-MS/MS*. **Rapid Commun. Mass Spectrom.** **2017**, 31; 22, p1927-1937 (doi: 10.1002/rcm.7986)

Citations: **1** (DOI: 10.1021/acs.analchem.7b04733)

ISI Journal Citation Reports © Ranking (2016): 38/76 (Chemistry Analytical)

Impact Factor: **1.998**

Sathisha Kamanna, Julianne Henry, Nicholas H. Voelcker, Adrian Linacre, K. Paul Kirkbride, *A complementary forensic ‘proteo-genomic’ approach for the direct identification of biological fluid traces under fingernails*. **Analytical and Bioanalytical Chemistry** (2018).

<https://doi.org/10.1007/s00216-018-1223-3>.

Impact Factor: **3.6**

CONFERENCE PROCEEDINGS AND PRESENTATIONS

(Name in bold denotes presenting author)

Sathisha Kamanna, Adrian Linacre, Nico Voelcker, Julianne Henry and Paul Kirkbride, Titled: Mass spectrometry-based forensic “Omics” in direct identification of body fluid protein markers, Received “best poster” presentation award at the 5th International Conference on Forensic Research & Technology (Oct 31-Nov 02, 2016), San Francisco, USA. Sathisha Kamanna et al., J Forensic Res 2016, 7:5 (Suppl)
<http://dx.doi.org/10.4172/2157-7145.C1.021>

Sathisha Kamanna and K. Paul Kirkbride: Integrated Mass Spectrometry-Forensic “Omics” Analysis in Body Fluids/Fingermarks, Poster Presentation at the Analytical and Environmental Chemistry Division (Anachem) Symposium, Adelaide, South Australia, July, 2016

Sathisha Kamanna, school of chemical and physical sciences (CAPS) seminar: Analytical Mass Spectrometry and Forensic Science: Mass Spectrometry-based Proteomic analysis of forensic body fluids, fingermarks and fingernail traces, College of Science and Engineering, Flinders University, May, 2017

Sathisha Kamanna, Adrian Linacre, Julianne Henry, Nico Voelcker, Paul Kirkbride: Integrated “Proteo-Genomics” and MALDI-imaging Analysis in Forensic body fluids and Fingermarks traces, the abstract proceedings has been published in 21st Triennial meeting of the International Association of Forensic Sciences (IAFS), Toronto, CANADA (August, 2017), Forensic Science International 277 (2017) 1–257,
<https://doi.org/10.1016/j.forsciint.2017.07.019>

Sathisha Kamanna, CAPS seminar: Applications of Mass Spectrometry-based Proteomics analysis in Forensic Body Fluids and protein post translational modifications (PTMs), April, 2015

Additional conference/workshop participated

- Attended the 65th American Society of Mass Spectrometry (ASMS) annual conference (Mass Spectrometry and Allied Topics) and workshops, which was held at Indianapolis, USA (June 4-8, **2017**). I have been awarded the ‘best student paper’ award in the conference
- Participated the ASMS Fall Workshop 2017 on “Top-Down” Mass Spectrometry-based proteomics analysis and applications in biomedical sciences, at Hyatt Regency Harborside, Boston, Massachusetts, USA (Nov 1-3, **2017**). I have been awarded the International ASMS travel award (2017)
- 19th Australian Proteomics Symposium, at Lorne, Great Ocean Road, Victoria, Melbourne, Australia (2014)
- Participated advanced mass spectrometry-based proteomics training at Bruker Daltonik GmbH, Bremen, Germany (September 2011)

AWARDS and ACHIEVEMENTS

- American Society of Mass Spectrometry (ASMS)–*International Journal of Mass Spectrometry (IJMS)* and Agilent ‘**Best Student Paper**’ Award for the best applied paper. Received (USD \$2,000) at the 65th ASMS annual conference (Mass Spectrometry and Allied Topics), Indianapolis, USA (**June 2017**).
Elsevier news: <https://www.journals.elsevier.com/international-journal-of-mass-spectrometry/news/ijms-agilent-best-student-paper-awards-2016>
- Australian and New Zealand Forensic Science Society (ANZFSS) and National Institute of Forensic Science (NIFS) ‘**Best Publication Award**’ in Refereed Journal **Web page:** <http://www.anzpaa.org.au/forensic-science/our-work/awards/best-paper/2016> (**2016**)
- **Best Poster Presentation Award** at the 5th International Conference on Forensic Research & Technology (October 31-November 02, **2016**), San Francisco, USA
- **ASMS Fall Workshop** (Top-Down Mass spectrometry) **Student Travel Stipend** (USD \$750) at Hyatt Regency Boston Harbor, Boston, Massachusetts, USA (Nov 1-3, **2017**)
- Elaine Martin International Conference Travel Award (\$ 2,000) **2016**
- Research Higher Degree (RHD) Travel Grant (\$ 1,500) **2017**
- International Postgraduate Research Scholarship (IPRS) award (2013)

List of Abbreviations

Abbreviation	Meaning
ACN	Acetonitrile
ATR	Attenuated total reflectance
AMY1	Salivary Amylase
AMY2	Pancreatic Amylase
AP	Acid Phosphatase
CHCA	. -Cyano-4-hydroxycinnamic acid
CID	Collision Induced Dissociation
CTS	Collaborative Testing Services
CRNN	Cornulin
DTT	Dithiothreitol
Da	Dalton(s)
kDa	Kilo dalton (s)
DNA	Deoxyribonucleic acid
DHB	2, 5-Dihydroxybenzoic acid (Gentisic acid)
ESI-MS	Electrospray Ionization Mass spectrometry
EDS	Energy dispersive X-ray spectrometry
FA	Formic acid
FABP5	Fatty acid-binding protein 5
FT-IR	Fourier Transform Infrared
FSSA	Forensic Science South Australia
HB-A	Hemoglobin Alpha subunit
HB-B	Hemoglobin Beta subunit
HB-D	Hemoglobin Delta subunit
HPLC	High Performance Liquid Chromatography
IAM	Iodoacetamide
IMS/MSI	Imaging mass spectrometry/mass spectrometry imaging
ITO	Indium-tin oxide
KM	Kastle-Meyer
LMG	Leucomalachite green
LIFT	Laser induced fragmentation technology
MALDI	Matrix Assisted Laser Desorption and Ionization
MeOH	Methanol
MS	Mass spectrometry

MS/MS	Tandem mass spectrometry (fragmentation)
mL	Mili litre
μL	Micro litre
mM	Millimolar
m/z	Mass to charge ratio
mRNA	Messenger ribonucleic acid
MTP	Polished steel plate
nLC-MS	Nano-spray Liquid Chromatography-Mass Spectrometry
3-HPA	3-hydroxypicolinic acid
PCR	Polymerase Chain Reaction
PTM	Post translational modifications
PMF	Peptide mass fingerprinting
PPM	Parts per million
PSA	Prostate Specific Antigen
QTOF	Quadrupole Time of Flight
RPM	Revolutions per minute
RP	Reflectron positive
RT-PCR	Reverse Transcription- Polymerase Chain Reaction
RSID	Rapid Stain Identification
SA	Sinapinic acid
SDS	Sodium dodecyl sulfate
SEM	Scanning electron microscopy
SEMG	Semenogelin
SPRR3	Small proline-rich protein 3
TOF	Time-of-flight
TFA	Trifluoroacetic acid
THP	Tamm–Horsfall glycoprotein
UROM	Uromodulin

Research ethics and safety considerations

All human body fluids, fingermarks and fingernail samples in this project were obtained from volunteers Clinical Human Research Ethics Committee Application 440.14 – HREC/14/SAC/455. All experiments conducted on Australian mammals and animal blood samples ethics were obtained under Australian Animal Welfare Committee Application 909/16.

Structure of this Thesis

Chapter 1: An overview of the literature on mass spectrometry instrumentation (principles and applications) and proteomic technologies, forensic science and strengths and weaknesses of current available forensic tests for the detection of body fluids, and MS-based proteomic techniques applicable to the identification of body fluids in trace evidence and fingermarks.

Chapter 2: Materials and experimental methods used in the research described in this thesis.

Chapter 3: Discussion centering on a research article published in *International Journal of Mass Spectrometry* (IJMS). The work presented in this paper describes the direct (or *in situ*) identification of forensic body fluids using matrix-assisted laser desorption/ionization time-of-flight mass spectrometry (MALDI-TOF MS). The work also shows the identification of human body fluid protein markers (“top-down and “bottom-up”) and mixtures of different fluids directly detected on various fabric substrates and ITO-coated slides without classical chromatographic separation.

Chapter 4: Describes an article published in *International Journal of Legal Medicine* (IJLM). The paper demonstrated the usage of a mass spectrometry-based forensic “toolbox” for imaging and detecting biological fluid evidence in fingermarks and fingernail scrapings. This work involved different MS approaches such as MALDI-TOF MS, MALDI-imaging and liquid chromatography-multidimensional nLC-MS/MS analysis for proteomic identification and mapping of biological traces on fingerprint ridges. It also describes fingerprint enhancement using aluminium-containing magnetic powder and then ‘lifting’ of the marks with adhesive tape. The paper describes a novel, matrix-free identification of fingerprint metabolites on lifted fingerprints using MALDI-ToF MS.

Chapter 5: This chapter describes a complementary “proteo-genomics” approach for the identification of biological fluid traces under fingernails. Traces of human and non-human body fluids under fingernails were the detected using MALDI-MS and nLC-ESI-

qTOF MS/MS and the detection limits of the two were presented. The chapter also describes direct ‘on-fiber’ identification of fingernail traces and the single microswab-based ‘proteomic’ (e.g., protein markers I.D) and ‘genomic’ (e.g., direct PCR DNA profiling) analysis. For the first time, we demonstrate that protein (haemoglobins) data can be obtained from post-PCR products. The complementary ‘proteogenomic’ developments has been published in the international peer-reviewed journal *Analytical and Bioanalytical Chemistry*.

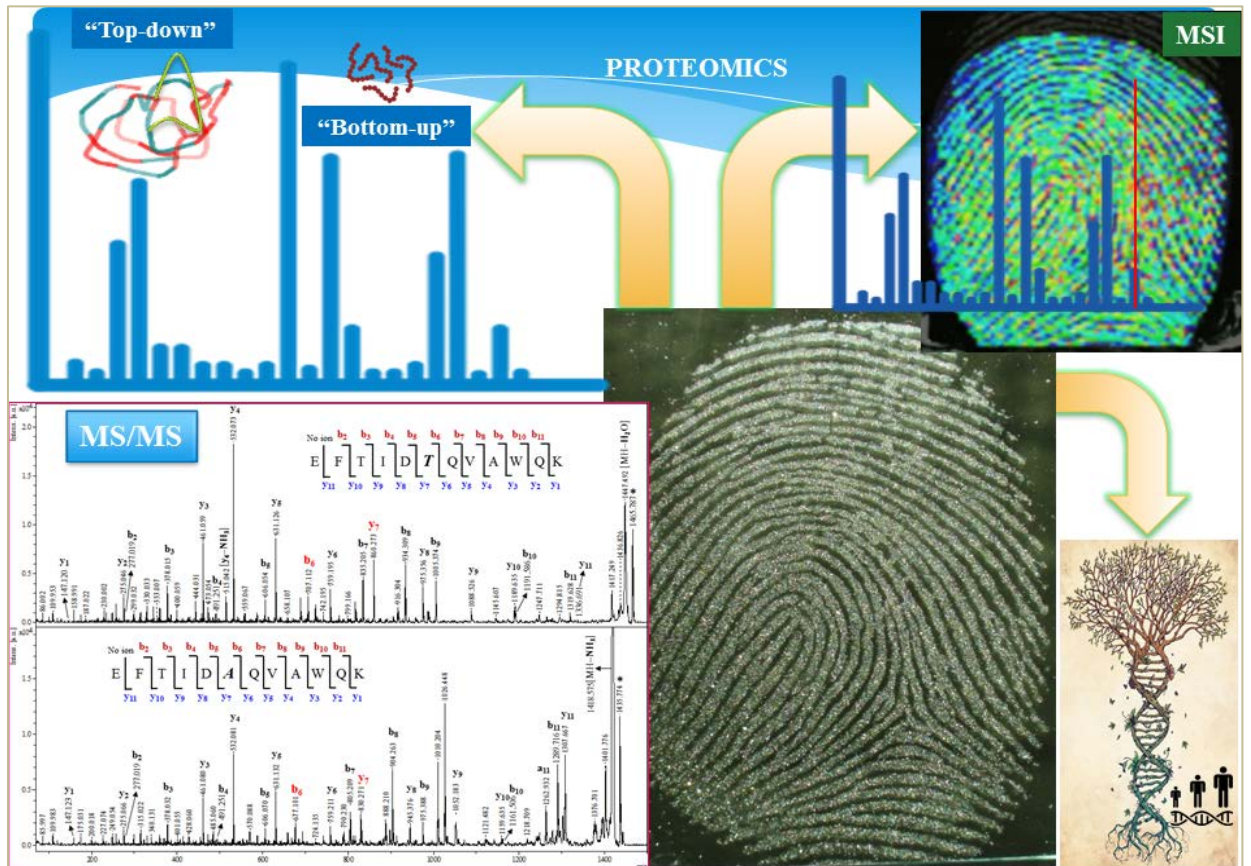
Chapter 6: Centers on a research article published in *Rapid Communications in Mass Spectrometry*. The paper describes novel research work on ‘bottom-up’ in situ proteomic differentiation of human and non-human haemoglobins for forensic purposes by MALDI-ToF-MS/MS. In this chapter, MALDI-imaging mass spectrometry was used on bloodied fingermark for proteomic identification and differentiation of haemoglobin proteins from human and Australian marsupial blood. For Australian native marsupial haemoglobin proteins already on protein databases the haemoglobins were confirmed by ‘bottom-up’ *in silico* methods but *in situ* MS/MS analysis followed by *de-novo* peptide sequencing was used for blood from species not on databases.

Chapter 7: Describes a conclusion and future prospects

References

Appendices

Note: All supplementary data relating to this thesis are presented in the attached DVD.



A picture by Mass Spectrometry Imaging (MSI) is worth a Thousand words!

Chapter 1: INTRODUCTION

1.1 Proteomics and mass spectrometry

The proteome is defined as all proteins expressed by the genome of a given type of cell in biological fluids (e.g., blood serum) or tissue at a specific time and under specific conditions [1-2]. In 1994, the term 'Proteomics' was coined by Wilkins [3] and it refers to the practice of identifying and quantifying those expressed proteins. Proteomics over the past decade has become a widely used technique in the field of clinical biology and even forensic science [2-5]. This is because of not only developments in technology and analytical procedures, but also the innovative and various ways in which the methodologies of protein and peptide analysis have been applied. Proteomics can address challenges that cannot be accomplished by genomic analysis, for instance, in measuring relative abundance of the protein products, protein post-translational modifications (PTMs) as well as protein interactions and functions [6-7]. Studying proteomes is challenging due to the high degree of sample complexity, for example more than 100 PTMs (e.g., phosphorylation, glycosylation, etc.) are possible, human cellular protein levels could change drastically as a result of exposure to altered conditions or mutations and there is a high dynamic range of protein concentration in biological samples [7-8]. Biological samples can be highly complex mixtures (e.g., body fluids and other clinical serum samples), therefore protein separation technique such as two dimensional electrophoresis (2-DE) has been widely used for large proteome analysis. This approach is based on protein separation (first dimension) by isoelectric point followed by separation of molecular weights (second dimension) using poly-acrylamide gel electrophoresis (PAGE) [9]. The 2-DE method is capable of the identification of hundreds of differentially expressed proteins [10]. Another simple proteomic separation technique such as sodium dodecyl sulfate (SDS) - PAGE electrophoresis [11] has been widely used for macromolecular and/or protein characterization in biomedical, forensic science and other life science laboratories. When the proteins are mixed with SDS (anionic detergents), they acquire a net negative charge and then the proteins separated in a PAGE based on their molecular weights [12].

Mass Spectrometry (MS) is a powerful high-throughput analytical tool in various

disciplines and specifically in a wide range of applications in biological and/or clinical research. It can allow label-free and multiplexed detection of a wide variety of biochemical analytes. Mass spectrometry has found wide application in proteomics, especially when liquid chromatography (LC) fractionation of proteins is followed by electrospray ionization mass spectrometry-mass spectrometry (ESI-MS/MS), which is a “soft” ionization process (Yamashita and Fenn 1984) [13]. Later developments in mass spectrometry were extended to include peptides obtained from protein digestion in complex biological mixtures followed by matrix assisted laser desorption ionization - time of flight mass spectrometry-mass spectrometry (MALDI-TOF MS/MS) analysis [14-15].

1.2 Matrix Assisted Laser/Desorption Ionization Time of Flight mass spectrometry

As indicated above, MALDI-ToF MS is one of the powerful techniques widely used in proteome analysis to identify and/or confirm the unknown proteins. This “soft” ionization technique was developed in 1988 by Karas and Hellenkamp [16] and it is capable of the identification of protein molecular masses exceeding 10,000 Daltons. The typical MALDI-ToF mass spectrometer consists of MALDI ion source, mass analyser (ToF instrument) and a detector, as shown in Figure 1.1. Importantly, MALDI allows generation of molecular ions without significant ion fragmentations (i.e., is a soft ionization technique). The instrument has a wide range of advantages: it can detect down to the femtomolar concentration range, no chemical labelling is required, it is not limited only to known proteins, and it can also use to identify lipids, metabolites and other chemical small molecules. Additionally, mixtures of proteins can be analyzed simultaneously (i.e., without chromatographic separation).

In brief, when the sample, mixed with a crystalline matrix, is bombarded by a laser pulse, a bundle of ions is produced. An electric potential applied to the sample plate causes the ions to move away from the plate into an electrostatic field that accelerates the ions and brings those that have equivalent charge into a tight bundle with regards to kinetic energy and spatial spread (i.e., into focus) at the beginning of a field free region (which is the ToF tube in the diagram), through which the ions drift at their own particular velocity. The heavier ions will travel slower than lighter ions. In high resolution instruments the ions are reflected in order to increase the distance travelled

and to focus ions with the same mass to charge ratio (m/z) before hitting the detector, thus maximizing the difference in flight time between light and heavy ions. In linear detection, large proteins (e.g., 0-500 kDa) can be measured in the linear detector after a relatively short flight path. Higher mass accuracy is achieved for peptide and/or polypeptide (0-7 kDa) measurement using the reflector detector, which is located approximately twice as far from the ion source as the linear detector. When high voltage (20-30 kV) is applied to the region immediately before the ToF tube, all the produced ions or charged particles are given the same kinetic energy (i.e., $\frac{1}{2}mv^2 = zV$ (V is 21-30 kV and z is the charge on the ion)). Consequently, ionised molecules with the same charge but different masses will have different velocities, thus, different times of flight. However, due to non-homogeneous and inconsistency in ionization, molecules with same m/z value could have broad velocity distribution and hence, different times of flight. This would cause peak broadening and poor mass resolution. The precursor ion selector (PCIS) functions as a mass filter for chosen ion and fragments, which is extremely useful in the identification of target species (peptide and/or proteins) using MS/MS. These basic principles are discussed in more detail below.

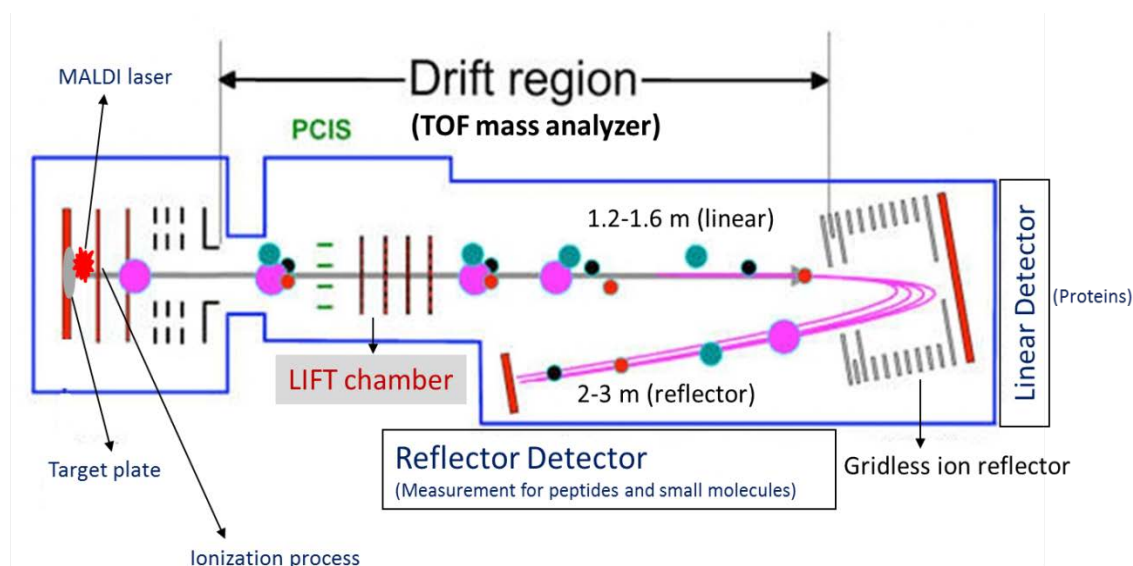


Figure 1.1 A basic principles of matrix-assisted laser desorption/ionization (MALDI) time of flight (ToF) mass spectrometry. Figure is adapted from Bruker Daltonics tutorial, Bremen, Germany, MALDI theory mass spectrometry, 2004 [17].

1.3 The MALDI ion source

The ionization mechanism of MALDI was described by Karas and Hillenkamp in 1988 [16, 18]. The Bruker MALDI ToF-MS (Autoflex/Ultraflex) ion source used in the research described in this thesis employs a neodymium- doped yttrium aluminium garnet [Nd: YAG $\lambda=355$ nm] solid state laser to produce gaseous phase ions under vacuum conditions [19]. Two models for ion formation have been developed, the older model was described by Karas *et al.* 1987. This group proposed that photoionization of the matrix molecules in the matrix crystals was the initial step followed by charge transfer to the neutral analyte molecules in the MALDI plume [16]. A more recent model [20-21] proposes that singly charged molecular ions detected in the spectrometer are “lucky survivors” and assumes that proteins present in the matrix as charged species are predominantly re-neutralized within desorbed clusters of matrix and analyte. The sample, generally peptide proteolytic digests or intact proteins, is crystallized in the presence of low molecular weight organic matrices [22] on the MALDI target plate (e.g., Bruker MTP ground steel, hydrophilic Anchor Chip spots). The matrix is chosen based on their mass extinction coefficient (i.e., how strongly a particles absorbs light) at wave length matched to the MALDI laser. The MALDI matrices have a strong optical absorption in either IR (e.g., succinic acid) or UV range (e.g., 3-hydroxy picolinic acid), hence they rapidly and efficiently absorb the radiation. Typical UV absorption coefficient ranges from about 5×10^4 to 5×10^5 cm^{-1} at a laser wavelength of 337 (nitrogen lasers) or 355 nm (usually solid state or SmartbeamTM laser). MALDI matrices are generally crystalline solids with low vapour pressure that can become volatilised to form ions in a vacuum. The organic matrix plays a key role by absorbing laser energy and results in causing the crystallized target substrate (solid) to vaporize (see Figure 1.1). The advantage of the matrix is its mediator role between the laser and the analyte, assisting in the desorption (absorb laser energy), vaporization and enhancing ionization of analyte molecules, thus, the name matrix assisted laser desorption and ionization (MALDI). When the laser is applied onto the crystallized sample, the charged (protonated) molecules transfer from matrix to drift region (e.g., $\text{MH}^+ + \text{A} = \text{M} + \text{AH}^+$). In peptide mass fingerprint (PMF, i.e., analysis of proteolytic digests of proteins, explained in more detail below) analysis the most commonly used matrices are α -cyano-4 hydroxy cinnamic acid (α -CHCA) [23] and 2, 5 dihydroxy benzoic acid (DHB) [24]. Sinapinic acid (SA) matrix can be used for identification of whole proteins

[25]. For these matrices, 337 or 355 nm lasers are utilized. Unfortunately, there is no single MALDI matrix or a sample preparation procedure suited to all analytical problems and analytes in MALDI MS analysis. So-called “smart beam” sources using a range of wavelengths (ultra-violet) have been developed to optimize ionization. Ideally, the MALDI ion sources should generate singly charged molecular ions to optimize limits of detection and minimize signal overlaps [16].

1.4 The Time of Flight mass analyser

Time of flight [ToF] mass analyzers are generally coupled with MALDI ion sources as they can cope with ions that are generated discontinuously and can provide accurate measurements of mass-to-charge (m/z) ratio with good resolution and signal-to-noise (S/N) [20, 26]. The ion signal detected at a microchannel plate (MCP) is plotted versus arrival time at the detector using a digital storage oscilloscope. On applying a high voltage between 20-30kV in the region just before the ToF tube, all generated ions arrive at the ToF tube with the same kinetic energy (i.e., $\frac{1}{2} mv^2 = zV$, where V is 20-30 kV and z is the charge on the ion) and at the same time. In the ToF tube ions of different masses have different velocities and hence, different time of flights over the given length of the ToF tube, from which " v " and m/z can be determined.

A mass spectrum exhibits a number of key characteristics including, mass accuracy, mass resolution, sensitivity and/or limit of detection, and signal/noise (S/N) ratio. Mass accuracy (the difference between the theoretical mass of an ion and its measured mass) is commonly presented in parts per million (PPM). Mass accuracy is restricted by the quality of the internal [ToF instrument (determination of peak center and theoretical peak shape)] and external calibration [e.g., peptide standard mix]. Mass resolution can be calculated from the peak height (ion mass) and width of the mass peak by following equation $R = (m/z)/W_{1/2}$, where $W_{1/2}$ =peak width at half height (e.g., 0.5 Da). A poor resolution would degrade the mass accuracy because the centroid of broad peaks can not be found with high accuracy. Resolution can be improved in the ToF instrument by delayed extraction (DE) of ions produced at high vacuum conditions. DE usually refers to the operation mode of vacuum ion sources when the onset of the electric field responsible for acceleration and/or extraction of the ions into the flight tube is delayed by a short time (e.g., 100–500 ns) after the ionization (or desorption/ionization) event. The flight times of ions is

measured from the application of the DE field (i.e., time-zero). In the small mass range upto several thousand Da (useful for peptide measurements), mass resolutions of 20,000 to 80,000 (modern instruments) can be achieved with TOF mass spectrometers (e.g., Bruker ultrafleXtreme and rapifleX). However, at higher molecular weights (>30 kDa) DE gradually decreases its power for enhancing mass resolution. The limit of detection (LOD) of the ToF mass analyser determined as the smallest quantity of an analyte that can be confidently detected (i.e., at a signal strength of three times root-mean-squared background noise). When using complex biological sample (e.g., mixture body fluids), the chemical background can be significant, making the signal-to-noise ratio for analytes present at very low concentration low.

MALDI-TOF can be operated in two modes: linear and reflectron. In linear mode, the accelerated ions travel in one direction in the field free region and are detected in the linear detector, which is about 1.2-1.6 meter from the ion source. Usually, linear positive (LP) mode is used whenever analytes or large molecules are not stable enough to survive the high electric fields kV in reflector TOF. In the reflectron mode, ions are diverted into the secondary detector, which extends the flight distance (2-3 meter) and therefore high resolution and mass accuracy (peptides upto 6000 Da) are possible. In addition, the reflectron TOF unit is also suitable for MS/MS structural analysis in the post source decay [PSD] or LIFT mode, where the precursor ion selection and subsequent fragmentations of it take place (Figure1.1) [26].

1.5 Top-down Mass Spectrometry

Top-down mass spectrometry-based proteomics approach is an emerging technique that involves analysis of proteins in their intact form (i.e., distinct from bottom-up approaches, which involve analysis of peptides derived from proteins using digestions). Top-down approaches are used for whole-proteome analysis while preserving the innate utility of an intact protein characterization including post-translational modifications (PTMs, e.g. phosphorylation, glycosylation, etc.). Top-down proteomics analysis is a potentially disruptive technology in biological sciences. Figure 1.2 shows the mass spectrum acquired for intact haemoglobin proteins and Figure 1.3 shows multiply charged ions acquired from an intact kinase enzyme. Different top-down mass spectrometry “technologies” including MALDI-ToF MS/MS, LC-ESI-MS/MS,

Fourier Transform Ion Cyclotron Resonance Mass Spectrometry (FT-ICR MS), Orbitrap and ESI-qTOF mass spectrometer have been used for the analysis [27-29]. TOF mass analyzer (e.g. MALDI, ESI-qTOF) can be used for top-down analysis of smaller proteins (between 5-40 kDa), whereas hybrid mass analyzers (FT-ICR and Orbitrap) can extend to large (up to 200 kDa) proteins [30].

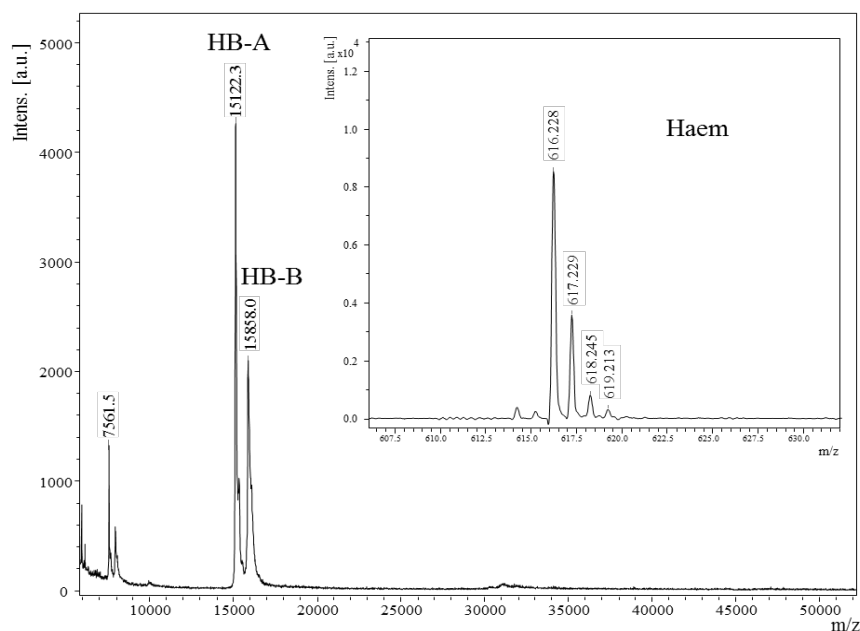


Figure 1.2. Typical ‘Top-Down’ MALDI-TOF mass spectrum of human α - and β -hemoglobin proteins. The spectrum is adapted from Kamanna *et al.* [31].

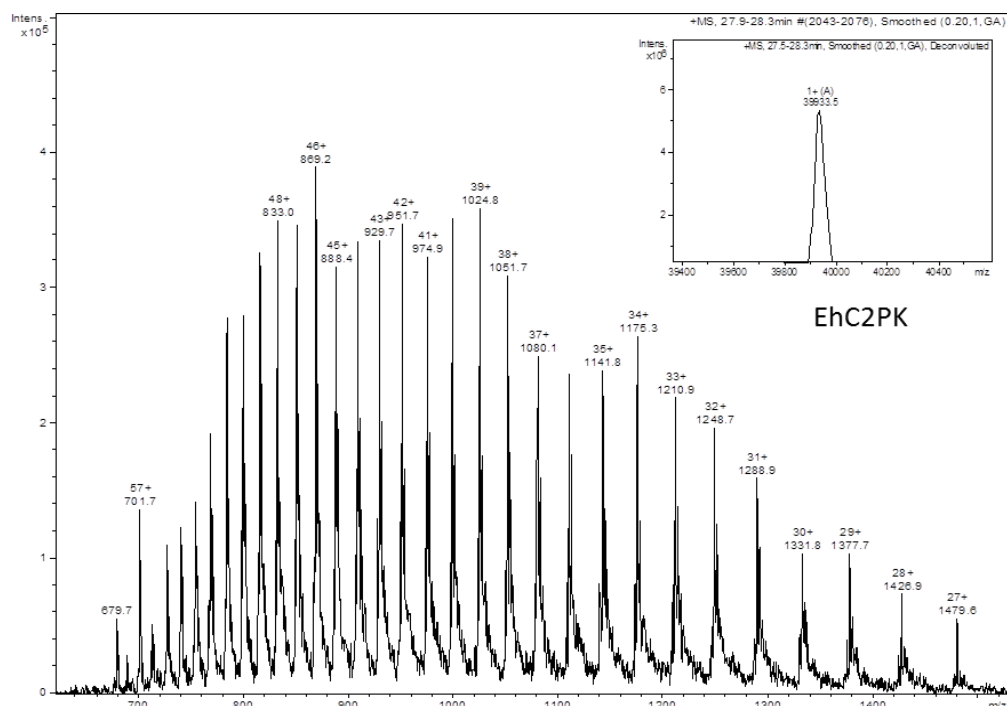


Figure 1.3. Example of ‘Top-Down’ LC-ESI deconvoluted mass spectra of *Entamoeba histolytica* C2 domain-containing protein kinase (EhC2PK). The intact protein mass was determined to be 39.93 kDa. The Figure is adapted from Somlata and Kamanna *et al.* [7].

In regards to top-down PTMs and protein sequencing analysis, high resolution and high mass accuracy instruments are required (e.g., FT-ICR, Orbitrap MS); these techniques offer great potential for protein characterization. Various top-down fragmentation methods such as in-source decay (ISD), collision induced dissociation (CID), recent growing MS/MS tandem platforms including electron transfer dissociation (ETD) [7], electron capture dissociation (ECD), proton transfer reaction (PTR) approaches are available for the top-down proteomic characterization and PTMs structural elucidation [32-33]. The advantages of top-down techniques are that there is less additional complexity as enzymatic digestion is not required and there is capability to measure all proteoforms. Top-down mass spectrometry “technologies” have played a significant role in biomedical applications by providing the information with genetic variations of cellular signalling of healthy and diseased states [34]. MALDI-ToF based top-down mass spectrometry has been widely used for the identification of intact microorganisms and microbial protein biomarkers [35]. Recently, the MALDI Biotyper (Bruker Daltonics) has been utilized for the top-down identification of bacterial and microbial pathogens from whole cells or crude extracts matching by the database containing biomarkers [36]. The current challenges of high-throughput top-down mass spectrometry includes the need to separate intact proteins (e.g. membrane proteins and biological body fluids), samples must be free of salts or buffers, sensitivity for sequence coverage from MS/MS data, database tools for identification of complex proteins, and techniques for discovery of novel biomarkers and PTMs localization. To address complex biological mixtures and achieve highly robust analysis, bottom-up MS methods can be used as a complementary approach to top-down proteomic analysis.

1.6 Bottom-Up mass spectrometry

In the bottom-up proteomic approach (state-of-the-art proteomics analysis), enzymatic digestion is performed to cleave intact proteins into peptides. What is obtained from MS is a digested peptide mass fingerprint (PMF). **Fig 1.4** displays an example of bottom-up mass spectrometry-based proteomic identification of auto phosphorylated peptides from EhC2PK protein [7]. In some cases bottom-up analysis involves protein separation and enrichment prior to enzymatic digestion, for instance by protein chromatographic

techniques (e.g., HPLC, FPLC) or separation of proteins through SDS-PAGE electrophoresis followed by in-gel digestion of proteins and MALDI-TOF MS/MS or LC-ESI-MS/MS analysis.

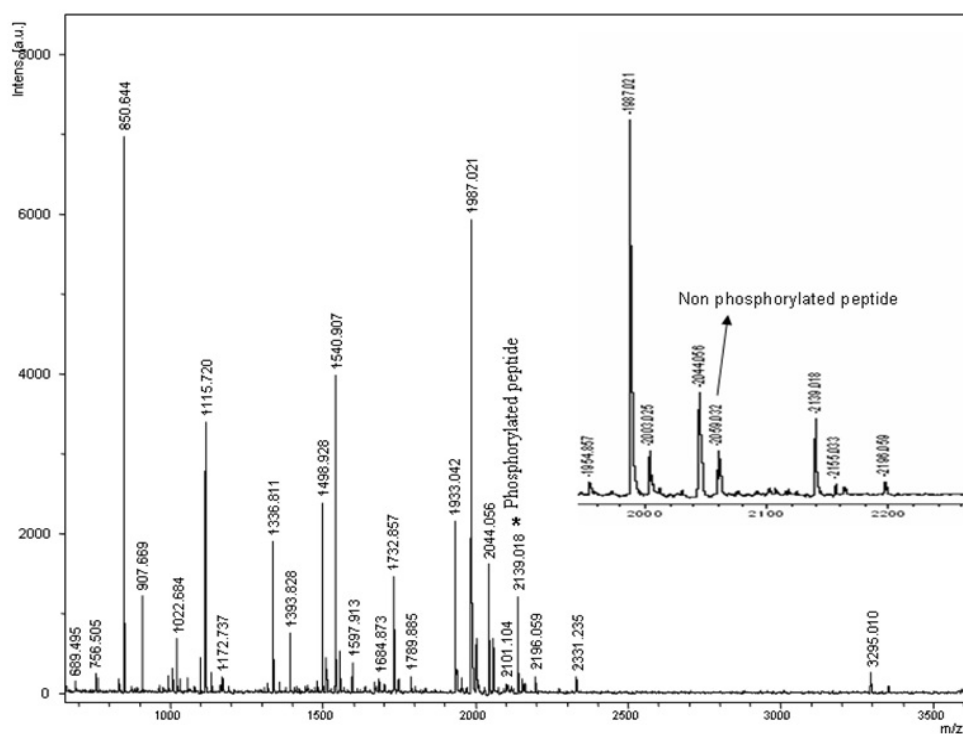


Figure 1.4. Typical MALDI-TOF MS spectra of bottom-up proteomic approach (Fig.1.3 protein). The PMF spectrum (EhC2PK) were adapted from [7].

Protein identification is usually accomplished by identifying matched tryptic peptides through *in silico* (or computer-based) protein database analysis. As described later, if peptides cannot be identified *in-silico*, it is possible to subject protein digests to tandem mass spectrometry (MS/MS) in order to determine the amino acid sequence of peptides, which is a process referred to as *de-novo* sequencing. The advantages of the bottom-up approach includes robustness, sensitivity, high mass accuracy and the analysis is able to provide a high confidence identification of protein sequences since the analysis is carried out in the low *m/z* detection region. However, the approach often provides an incomplete proteoform mapping and loss of labile PTMs, and may result in limited protein sequences from identified peptides. Several emerging computational-based proteomics software applications are available for both bottom-up and top-down tandem mass spectrometry analysis. Mascot search engine (Matrix Science) has been widely used for bottom-up analysis [37-39]. For the top-down proteomic database analysis, a few *in silico* tools such as MascotTD, PIITA (precursor ion independent top-down algorithm),

and ProSight are available for the protein identification [40-42]. However, analysis of large (over 110 kDa) and complex proteins (e.g., membrane proteins and PTMs) often is difficult due to large data sets as well as lack of top-down bioinformatics tools. Sample preparation is a key factor for successful top-down and bottom-up mass spectrometry analysis, for example salts and detergents in the sample often cause ionization issues in the ESI-MS, but it may be good for MALDI-TOF MS analysis. In some cases top-down analysis does not always provide good MS/MS results from the core of the protein, this is due to presence of high thiol (-SH) groups or some other complex subunits (e.g., post translational modifications). Traditional bottom-up proteomic analysis may overcome the above issues by removing the salts and separating the proteins through SDS-PAGE electrophoresis. Commercially available detergent such as RapiGest™ Surfactant (Waters Ltd) can be used for solubilizing the membrane proteins to enhance the protein sequences. In summary top-down and bottom-up proteomic strategies are complementary.

1.7 Post Source Decay

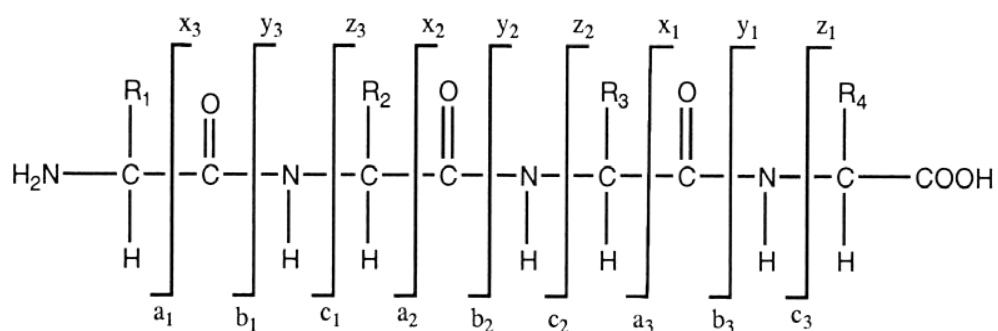
As a result of the MALDI ionization process some molecular ions undergo spontaneous fragmentation in flight between the ion source and the analyser, which is referred to as post source decay (PSD) [43]. This process can be enhanced and controlled by a Laser Induced Fragmentation Technology (LIFT) device, a function of laser power and pulse characteristics (pulse width and output energy per pulse), or by collision induced dissociation (CID). PSD is valuable because it can provide structural information (e.g., amino acid sequence in regards to proteins and peptides) on a mass-selected precursor ion.

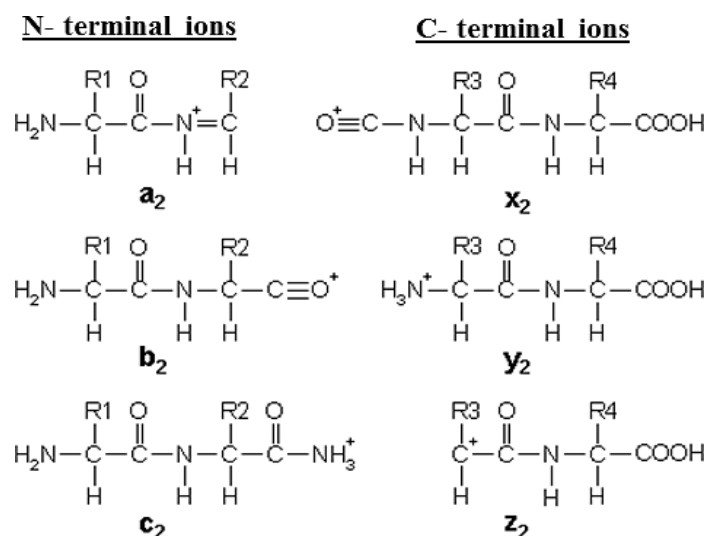
After leaving the ion source the precursor ions all have equivalent kinetic energy. However, when these ions fragment they produce fragments with similar velocity but quite different and lower kinetic energy due to their reduced mass compared to the parent ion. The fragmented ions are then differentiated as a function of their kinetic energy (hence their mass). Larger fragment ions (with higher kinetic energy) will penetrate deeper into the reflectron than the smaller ion fragment ions and hence they appear at a later time on the resulting reflectron time of flight spectrum.

The MALDI-PSD technique is becoming a major field of application in structural analysis and sequencing of peptides. Types of fragment ions obtained from MS/MS are based on various factors such as primary sequence, the amount of internal energy, charge state of molecules and type of energy applied for the fragmentation.

Peptide *de novo* sequencing is usually obtained with protonated adducts $[M+H]^+$ in MALDI or electro spray (ESI) ionization conditions. The protonated species (precursor ions) are then subjected to *in-situ* fragmentation resulting in product ions. The fragmentation of a peptide or protein molecule is largely determined by its chemical properties and the nature of ionization and/or activation modes used for the fragmentation events. The fragmentation pattern produced by a particular peptide is referred to as a peptide mass fingerprint (PMF). The obtained product ions allow determination of the composition of amino acids, their sequence, and type of peptide backbone [e.g., amide group, PTMs (Phosphorylated/N-glycosylated modifications)] and size of the molecules. In a typical proteomics analysis, it is possible to determine the amino acid sequence of a peptide by searching its PMF data against a database (referred to as *in-silico* sequencing) but for peptides from unlisted proteins *de-novo* sequencing is required, where the following rules (see Scheme 1.0) are applied in order to deduce a sequence.

Scheme 1.0 Nomenclature for product ions and their chemical structures produced from backbone fragmentation of protonated adduct. This was first proposed by Roepstorff and Fohlman, 1984 [44], subsequently updated by Johnson, 1987 [45] and Biemann Klaus, 1990 [46].





As shown in Scheme 1 and Figure 1.5, generally the PSD or LIFT spectrum is recorded from singly charged peptide molecules and mass signals come from predictable fragmentation locations within the peptide chain to give products such as immonium ions [47], N- terminal fragment ions (a, b, c, and d-type ions) [48-49], and C- terminal fragment ions (x, y, and z type ions) [50-51]. In MALDI-PSD analysis the most abundant fragment types such as ‘a, b and y’ ions can be observed during peptide fragmentation.

1.8 MALDI-TOF/TOF (LIFT)

The Bruker Daltonics MALDI TOF/TOF mass spectrometer (Autoflex-III, as used in the research described in this thesis) uses a MALDI ion source, delayed ion extraction (DE) electronics, timed ion selectors (TIS), LIFT device, reflector unit and fast ion detectors [26]. The instrument ion source was equipped with a neodymium-doped yttrium aluminum garnet Smart Beam 200 Hz solid-state laser operating at 355 nm. Suckau *et al.*, 2003 was the first to report MALDI-TOF MS (Ultraflex TOF/TOF) equipped with the “LIFT” technique, which provides high sensitivity (attomole range) and better sequence information for PMF. They have also shown that it is possible to analyze fragment ions generated by any one of three different modes of dissociation such as LIFT and/or laser induced dissociation (LID), high energy collision induced dissociation (CID) and in source decay (ISD) in the reflectron mode of the mass analyser. The range of dissociation depends on the quantity of energy deposited to the ions through the ion formation. For the data acquisition of PMF, reflectron positive

(RP) ion mode can be used with 20 kV accelerating voltage. Precursor ions of a particular m/z value can be manually selected prior to laser-induced fragmentation using the Bruker proprietary LIFT technique.

In the standard LIFT mode (ion source 2), the Autoflex TOF/TOF employs “laser induced dissociation” (LID) or LIFT reacceleration cell (attached between the two TOF tubes) for the generation of product ions. Re-acceleration of product ions and re-focusing (resolution) of the ions is applied in the secondary ion source. MALDI-LIFT MS/MS is a straightforward way to accomplish peptide backbone fragmentation (b, y-type ions) [26]. The fragmentation spectra can be used to derive partial sequence information (sequence tags) or even the full peptide sequence [see Figure 1.5]. The resulting sequence information is highly useful for the confirmation of peptides and proteins (even unknown peptides).

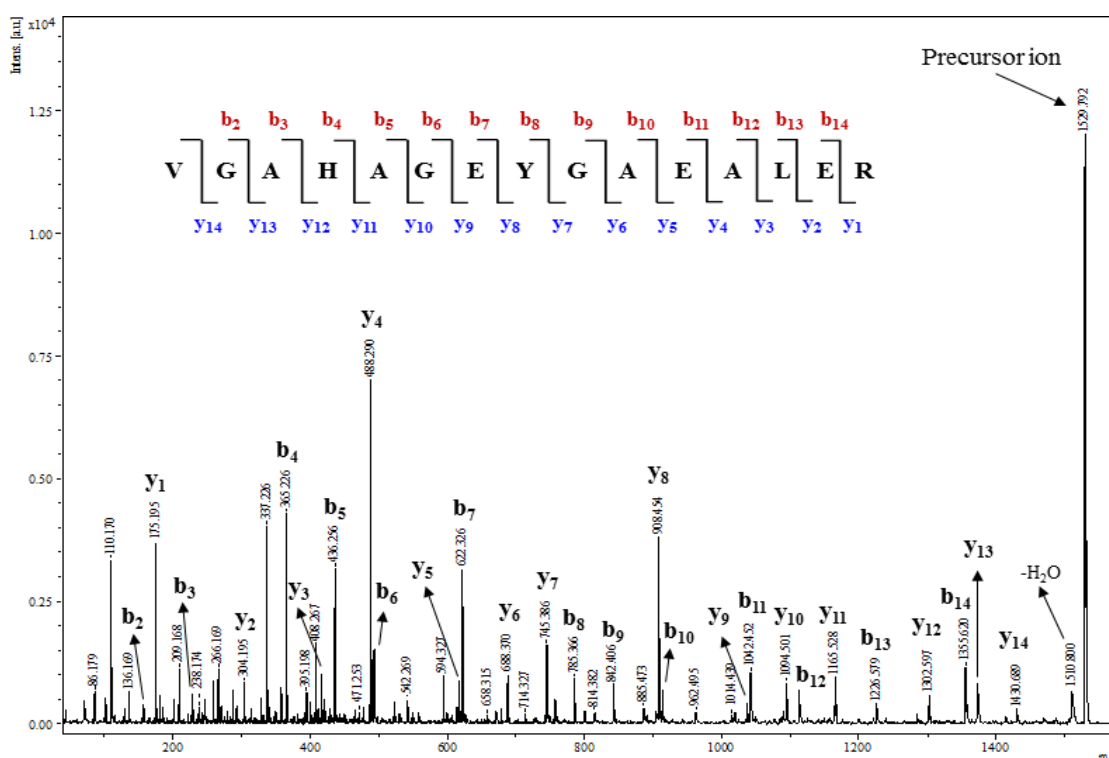


Figure 1.5. Typical MALDI-LIFT mass spectrum of $[M + H]^+$ precursor ion at m/z 1529.79 of a protein hemoglobin sub unit alpha. Fragmentation pattern showing the product ions and matched “b” and “y” ions are indicated in the spectra. The spectrum was adapted from **Kamanna et al.** [31].

Distinct compositions of MALDI matrix and collision gas determine the amount of internal energy deposited by the MALDI process and the CID process [52]. The CHCA matrix is most frequently used matrix for peptide analysis, because it is relatively “hot”

and induces unimolecular decomposition [53]. DHB is a “cooler” matrix [53-54] and it is also suitable for the analysis of peptides and/or glycopeptides, carbohydrates/sugars, and higher molecular weight species as they normally yield more abundant signals by this matrix compared to CHCA.

Collision induced dissociation and/or decomposition (CID) is the most commonly used ion activation method. In this fragmentation process, the precursor ions suffer inelastic collisions with neutral target gas yielding product ions. Some factors influencing the CID process are the amount of energy deposited during the activation, the probable number of collisions, and the nature of target gas. Low energy CID fragmentation can be carried out in triple quadrupole, ion trap and FT-ICR instruments. High energy CID fragmentation provides additional side chain cleavage and higher relative intensity of internal fragments. This technique can be used as optional applications for *de-novo* sequencing (enhanced immonium ions), differentiation of isobaric amino acids (e.g. by detecting L and I variation) [45], and detailed glycosylation analysis. CID yields additional types of fragments, which carry specific structural information of peptides (d-, w-, and z-ions) [18, 53]. In a typical CID-LIFT MS/MS experiment, the TOF/TOF allows the use of collision gas (i.e. Argon) for fragmentation to produce structural information. The modern fragmentation techniques such as high energy CID, ETD and other top-down fragmentation methods provide a high sequence coverage with regards to side chain post-translational modifications and confident identification of targeted proteins [7, 51].

In-source decay (ISD) is a rapid fragmentation process in the MALDI source prior to ion extraction. ISD fragments undergo further metastable decay in the TOF1 region. The ions generated by the desorption/ionization event yield product ions via two main pathways, radical induced pathway that generates c-, z-, w-, and d-ions, and a thermally activated pathway that produces y-, b-, and a-ions [18].

Instrument available at Flinders were capable of MALDI-LIFT and CID (in ESI-qTOF MS) fragmentation techniques and both were used for MS/MS analysis and the *de novo* sequencing of peptides and protein identification presented here.

1.9 Tandem mass spectrometry

Tandem Mass Spectrometry (MS/MS) is the process of selecting an ion, and generating a mass spectrum of the resulting product ions. The tool can be used for many analytical tasks regarding various structural aspects of biomolecular complexes such as protein

sequence analysis and database searching, determination of reaction pathways, conformational studies and characterization of protein PTMs [7, 55]. In tandem mass spectrometry, a particular ‘precursor ion’ or ‘parent ion’ can be selected and subjected to fragmentation resulting in the generation of ‘product ions’ or ‘fragment ions’. This fragmentation process is referred as MS/MS or MS² analysis. But, often secondary stages of fragmentation could be carried out in which a product ion further fragmented, and so forth. These experiments are called “MSⁿ” experiments. The obtained product ions can be analyzed either through database search engine or manual ‘*de novo*’ peptide sequencing. High mass accuracy and high resolution tandem fragmentation strategies are required in regards to confident assignment of fragmented ions. LC-ESI combined with fragmentation methods such as CID, ECD and ETD MS/MS can be used for maximizing the protein sequence coverage (i.e. maximizing the match between the measured *m/z* ions and theoretical sequences in the protein database, the protease cleavage specificity and the product ion pattern in the MS/MS spectrum) as well as the cleavage of modified peptide backbone (e.g. phosphorylation or glycosylation sites).

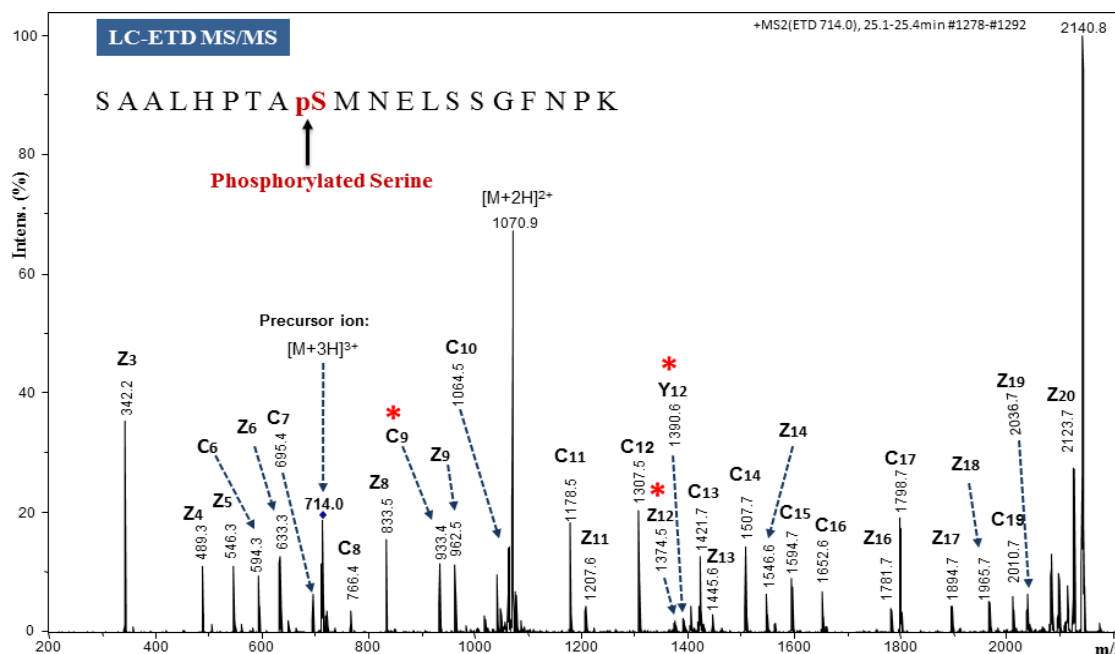


Figure 1.6. Typical tandem mass spectrometry (LC-ESI-ETD MS/MS) results of [M+3H]³⁺ precursor ion *m/z* 714.0 matched “z” and “c” fragment ions are indicated in the spectra and in the peptide sequence, the 9th serine is found to be phosphorylated. *indicates phosphorylated ions. The tandem mass spectrum was adapted from Somlata and Kamanna et al. [7].

Fig. 1.6 displays the typical example of tandem LC-ESI-ETD MS/MS spectrum of phosphorylated peptide $[M+3H]^{3+}$ precursor ion m/z 714.0 (singly charged at m/z 2140.8). The identified autophosphorylation at Ser428 of EhC2PK protein is a key role in regulating erythrophagocytosis in the parasite *Entamoeba histolytica* [7]. In this work, the power of top-down and bottom-up mass spectrometry-based proteomics analysis to understanding the molecular mechanisms and identification of protein post-translational modification at the sequence-specific level was demonstrated.

1.10 Mass spectrometry imaging (MSI)

Over the past decade, matrix-assisted laser desorption ionization-time of flight-mass spectrometry (MALDI-ToF-MS) has become a powerful technique that has been widely used in clinical and/or biological sciences for the direct detection and molecular imaging of peptides, proteins and/or small molecules within tissues [56-59]. The mass spectrometry imaging (MSI) experiment is typically performed either on multiple distinct regions of interest within a specimen to generate tissue specific molecular profiles (i.e. MALDI-profiling), or at high resolution (i.e. MALDI-imaging) to obtain a spatial abundance of hundreds of analytes (e.g., peptides, metabolites, proteins) across entire areas of tissue sections or other heterogeneous specimens. A typical MALDI-MSI process and a molecular ion (spatially distributed m/z) images obtained from a tissue section is shown in Fig. 1.7. MSI can be used for simultaneous detection and visualization of the two dimensional concentration profiles of “molecules” in or on the surface of specimens (e.g. clinical tissues, fingerprints and etc.). The application of MALDI-MSI and other modern high resolution imaging mass spectrometry is expected to have a significant role in biomedical sciences and proteomics research with respect to “biomarker” discovery. Currently, proteomics research is focusing on finding novel biomarkers (e.g., proteins, glycoproteins or lipids) that indicate a certain disease state (e.g., normal v/s tumor tissue) or the exposure of an organism to environmental substances, and identification of differentially expressed protein markers in biological systems.

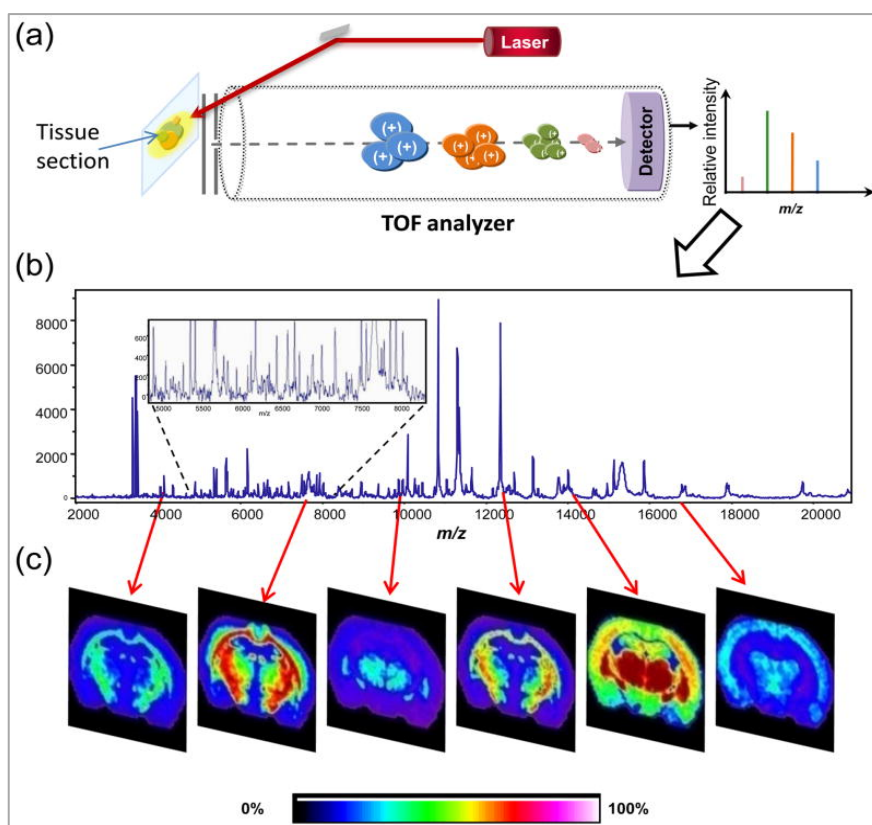


Figure 1.7. Typical schematic of MALDI-MSI process. It shows a) tissue (e.g., mouse brain) section on a conductive slide (ITO-coated) placed in the MALDI source. Laser power applied onto the surface and the sample is rastered with respect to the laser. Molecules are desorbed and ionized at each pixel, and they are separated in the time of flight (TOF) analyzer and detected using reflector or linear mode. b) A mass spectrum collected from one pixel in the tissue section. c) Molecular ion images produced by plotting abundance of particular m/z values at each pixels collected for the specimen. These maps demonstrate the spatial distribution of particular proteins. Total abundance of ions at each pixel can be plotted to demonstrate the spatial distribution of total protein. The figure was adapted from Seeley and Caprioli 2011 [60].

1.11 Liquid chromatography mass spectrometry [LC-MS]

Recent advances in hyphenated mass spectrometry, techniques such as nano liquid chromatography (nLC) coupled to MALDI-TOF/TOF MS (nLC-MALDI) and electrospray ionization (ESI) MS (nLC-ESI MS), can provide identification of proteins from complex mixtures with high confidence.

The basic principle behind liquid chromatography-mass spectrometry LC-MS as applied

to separation of complex mixtures of peptides is that a reverse phase (RP) HPLC column packed with C18 hydrocarbon modified silica particles (generally for peptides) is used to reversibly bind peptide samples through their hydrophobic interactions with the stationary phase. By increasing the organic solvent concentration in the elution buffer, different peptides elute at different times based on their hydrophobicity and as they elute they are passed on to the mass spectrometer for analysis. LC-MALDI-MS or MS/MS methods integrated with LC-ESI MS/MS (or even higher levels of multidimensional MS) have substantial application in crude separation and simultaneous detection and/or analysis of complex peptide samples [61, 62]. Classical proteome analysis using LC-MS/MS technologies has been widely used in biomedical sciences for the separation of complex biological matrices and the identification of candidate biomarkers and/or protein markers [63, 64].

1.12 Forensic Science

The role of the forensic scientist is to provide the justice system with unbiased, scientifically meticulous, robust and reliable information. Such information is crucial in establishing whether any links exist between the suspect, victim and/or crime scene. Forensic science historically has integrated fields such as biology, chemistry, biochemistry and molecular biology together in criminal investigations. A new frontier is proteomic analysis.

The examination of body fluids is a key aspect of forensic science in regards to crimes against the person such as murder, assault and rape. An examination can be considered in regards to two tasks. One task is to find or locate deposits of body fluids (such as stains or fingerprints) at the crime scene or on crime-related items (such as garments). Location of material can be difficult as crime scenes can be large in area, many objects might be present and deposits might be small and/or invisible. The second task is forensic analysis of traces of body fluid evidence in order to establish the identity of the victim or the individual committing the crime. Leading the way in the latter endeavour is DNA profiling. DNA evidence can be present in body fluid and/or tissue samples, from suspect and victim, and can be received for analysis either on swabs or as a physical material such as a stained garment or a lifted fingerprint. DNA profiling followed by DNA data base comparison or comparison against samples from a

suspect are crucial steps in investigations in forensic science [65]. DNA-based identification of individuals involved in crime has now been established for over three decades. However, determining the type of fluid present in biological evidence can also be important in reconstructing the circumstances of the crime that has taken place and in corroborating/refuting the statements of victim/suspect. Current standard DNA profiling alone does not specify if the DNA arrived from semen, saliva, vaginal fluids, urine or any other sources, nor can it indicate cross contamination of material during sample collection or at other times [66] – it “simply” indicates the person from whom the biological material originated.

1.13 Forensic Human Identification

Over the last 3 decades, DNA fingerprinting then DNA profiling [67-68] has become a very widely used technique for the accurate identification of suspects and victims from their biological materials or body fluid traces. Currently the DNA profiling method of choice involves measurement of the length of short-tandem repeats (STRs) using capillary gel electrophoresis and fluorescence detection. An individual acquires two sets of many different STRs, one from each parent, and the length of each STR present will also be determined by parentage. As there are many billions of permutations of STR length variations possible very good differentiation between individuals can be achieved even when a set of only 24 STRs is measured. A major enabler of forensic DNA profiling is the polymerase chain reaction (PCR). This chemistry allows copies of STRs to be generated selectively, thus allowing just a small number of copies of DNA in trace evidence to be multiplied into an amount that can be analyzed comfortably.

Recent forensic genomic research, carried out mainly by one of the supervisors of the research described in this thesis, has been directed towards the development of increasingly-sensitive tests and the streamlining of sample treatment processes through innovations such as direct-PCR DNA profiling [69-70]. In this direct PCR technique, a small portion of a biological sample or a swab used to collect biological material is placed directly into the PCR reaction mixture, which not only accomplishes the exponential multiplication of target DNA sequences but also obviates the need for cell lysis and DNA extraction steps. This approach minimizes the loss of DNA and maximizes the potential to obtain a DNA profile as compared to the conventional DNA isolation-profiling methods.

1.14 Forensic body fluid identification

Many body fluid stains are difficult to locate by the naked eye as many are colourless and therefore are not easily discriminated from the background material. It is also the case that mixtures of body fluids are encountered in forensic cases and thus one body fluid may be masked by another.

Currently, physical (e.g. microscopy) and/or biochemical tests can be performed on questioned stains to identify a body fluid or to confirm the absence of one. In forensic investigations the most common body fluids encountered are blood, semen, saliva, urine and vaginal fluid [71, 72]. Of interest, but less commonly encountered are foetal blood, perspiration, and menstrual blood. The body fluids each have a unique composition related to their functions and site of secretion within the body. The main functions of body fluids include transport (blood), digestion (saliva), reproduction and excretion (semen and urine), and lubrication and defence (vaginal fluid).

Table 2-1. The main components of human body fluids. Adapted from [72-75]

Blood	Saliva	Semen	Urine	Vaginal fluid	Sweat
Hemoglobin	Amylase	Acid phosphatase	Urea	Acid phosphatase	Urea
Fibrinogen	Proteins/glycoproteins	Prostate specific-antigen (PSA)	Sodium	Mucin	Lactic acid
Erythrocytes	Mucin	Semenogelin	Creatinine	Lactic acid	Chloride
Albumins	Lysozyme	Spermatozoa	Uric acid	Citric acid	Sodium
Glucose	Urea	Choline	Glucose	Albumin	Calcium
Immunoglobulins (Ig)	Glucose	Spermine	Chlorine	Urea	Potassium
Electrolytes	Amino acids	Lactic acid	Phosphate	Vaginal peptidase	Immunoglobulins
RBCs	Thiocyanate	Citric acid	Bicarbonate	Glycogen	Other metabolites
	Lipids	Zinc	Tamm Horsfall-glycoprotein (THP)	Acetic acid	
	Uric acid	Fructose		Squalene	
	Ig	Urea		Pyridine	
	Bicarbonate	Ascorbic acid		Amino acids	
	Chloride	Ig		Phospholipids	
	Potassium			Sodium	
	Sodium			Lactoferrin	
	Phosphate			Ig	

The different compositions in one body fluid versus another fluid provide the basis of its current and future identification methods. The commonly encountered forensic body fluids and their main constituents are shown in Table 2-1. It can be seen that some of the components are present in many body fluids and in many household or environmental substances (such as sodium or potassium). It is risky to base a forensic identification of

body fluids on markers such as those. In some of the body fluids there are many components that are common to more than one fluid, but there are differences in their relative abundances. For instance, a large quantity of amylase is present in saliva compared to less amounts in semen and vaginal fluids. Another example is urea, a component of urine, semen and perspiration.

1.14.1 mRNA profiling for body fluid identification

One approach being actively investigated involves messenger-ribose nucleic acid (mRNA) analysis to identify species-specific and tissue/fluid-specific nucleic acids. The mRNA is an intermediate template directly involved in the biosynthesis of proteins. Figure 1.8 represents schematic of the central dogma of molecular biology, which involve two-steps process, DNA replication to transcription (RNA synthesis) and translation (protein synthesis). During protein synthesis the mRNA plays a crucial role in the translation of the genetic code of DNA in the cell into what type of protein is made at the ribosome. The genes expressed within the diverse range of tissues and fluids in the human body are tissue specific, for instance the cells present in brain and blood or saliva have different functions and thus require different proteins. Therefore different cell types within body fluids have different mRNA markers present.

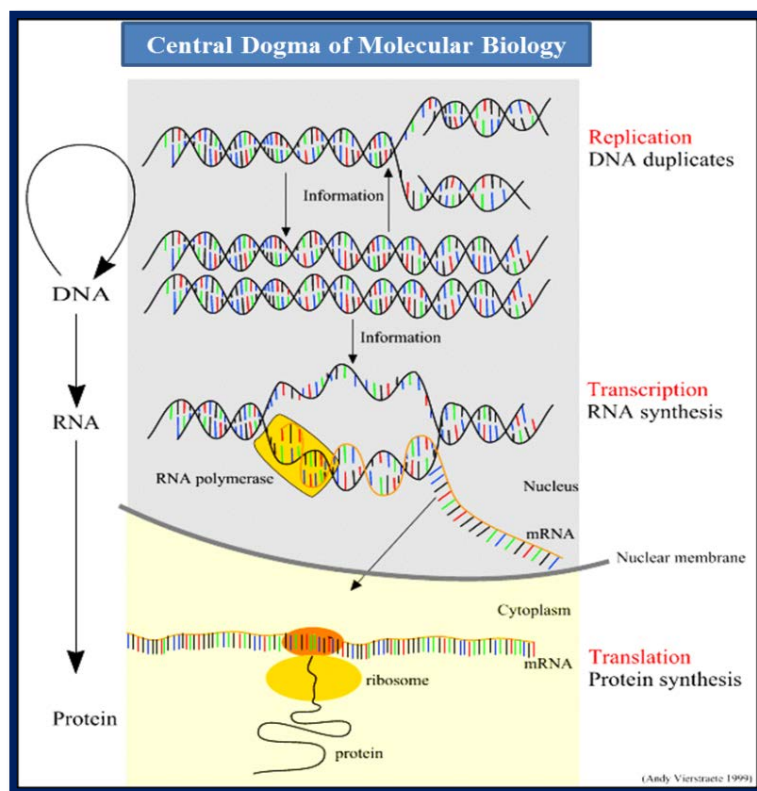


Figure 1.8. A schematic diagram of the “Central Dogma of Molecular Biology” showing the molecular information from DNA via transcription (RNA synthesis) to protein synthesis. The term “central dogma” was originally proposed by Francis Crick (Nature, 1970) [76]. Figure is adapted from: <https://users.ugent.be/~avierstr/index.html>

Recently a number of articles have been published that focus on the practical considerations of mRNA profiling for determination of the type of body fluid and/or tissue based on gene expression patterns [77-80]. This test could have advantages compared to traditional methods because both DNA and RNA can be extracted in a single sample and the RNA tests have good sensitivity and specificity. Reverse transcription-polymerase chain reaction (RT-PCR) followed by electrophoresis are used to identify mRNA species that are cell type specific for instance by multiplex mRNA profiling by RT-PCR [81] for forensic purposes were used to identify vaginal fluid based on the presence of human beta-defensin 1 (HBD-1) and mucin 4 (MUC4) markers; these genes have also amplified in menstrual blood. The same authors also identified semen stains using mRNA markers of semen-specific genes such as protamine 1 (PRM1) and PRM2, and semenogelin genes are SEMG1 and SEMG2 [82].

A recent study by Donfack *et al.* has reported that mass spectrometry based cDNA (complementary DNA) and/or mRNA profiling is a potential tool for forensic human body fluid identification (venous blood, saliva and semen) [83]. These authors concluded that MALDI-TOF-MS is a potential fluorescent dye free alternative method for body fluid identification in forensic case work. They have also indicated the problems associated with the use of mRNA/cDNA profiling such as intrinsic issues of low amounts of mRNA, a complicated extraction and reverse transcription process, and mRNA is readily degraded by environmental exposures or long-term storage [83, 84]. This degradation will negatively impact the detection of mRNA. Using PCR-based analysis in some cases may introduce false positive results from nonspecific amplification or allelic drop-in (due to mis-copying or strand slippage) because of the thermal cycling steps. Another additional problem of identifying body fluids/tissues by mRNA/cDNA methods is PCR inhibition due to blood and soil (arising from hemoglobin and humic acid, respectively) [84] and blood samples submitted to forensic laboratories are regularly washed with ultrapure water to remove hemoglobin before carrying out DNA analysis. To remove hemoglobin completely and extract and/or purify the DNA/mRNA prior to PCR analysis involves various procedures. These additional steps are time consuming, require more reagents/chemicals, may not completely remove inhibitors and could lead to losses of required DNA/mRNA. On the other hand, compared to nucleic acids, proteins are abundant in body fluids, they are very stable over time, and their isolation and analysis are more straightforward. Considering all the above limitations, proteomics-based analysis has the potential to be more reliable, faster and economical for identification of biomarkers in body fluids/tissue at a molecular level.

The following sections deal with the composition of each of these fluids, current available forensic techniques for their location and identification, and the significance of characteristic nucleic acids and proteins that may have potential as markers.

1.15 Blood

1.15.1 Presumptive tests

Blood is one of the most common biological fluids observed at crime scenes,

particularly at violent crimes. There are some presumptive tests and confirmatory tests available. Presumptive blood tests are generally based on the colour change or chemiluminescence of a particular reagent when it comes into contact with the haemoglobin present in blood. Ultraviolet (UV) light is the simplest test that can be used as a presumptive test to detect blood stains present on dark background materials. However, certain UV wavelengths can damage and/or degrade the DNA evidence [85, 86] which is crucial material present in a blood, hence caution must be taken. Another sensitive presumptive test presently in use is the luminol test [87], which has been used for over 40 years. The presence of blood causes chemiluminescence, emission of blue-green light, to take place in the presence of hydrogen peroxide. The reaction is catalysed by heme group (iron) present in haemoglobin within the blood sample. However, luminol is known to cross react with other materials such as bleach, saliva, and other animal and fruit/vegetable proteins (e.g., peroxidases). The luminol test remains despite a relatively high false positive rate because it has a low false negative rate in comparison to other screening methods and the fact that it is not as hazardous as other reagents [88].

Another popular presumptive catalytic technique is the Kastle-Meyer (KM) test, also known as the phenolphthalein test. This test has limits of detection in the 1:10000 blood dilution range. Phenolphthalein is added to the questioned blood samples and upon addition of hydrogen peroxide will turn pink colour if blood is present as a result of the solution turning alkaline. KM test produces false positives similar to other tests, but tests on other body fluids do not yield a positive result. One of the other common presumptive catalytic tests for blood used in forensic laboratory is Leucomalachite green (LMG) [72]. This test is performed under acidic conditions and uses catalytic properties of haemoglobin to produce a green colour. Other catalysts occur widely in nature in cytochromes, plant peroxidases and other catalase enzymes and these give false positive results as do copper salts [89].

Hemastix™, a test strip used to test for occult blood in faeces, have also been used as a presumptive test for blood. Although the test is simple and convenient, limits of detection are relatively high. Another routinely used forensic test is the Hematrace® ABACard® kit, which has very low limits of detection and very high specificity for human blood (only higher primate blood and ferret blood are known to result in false positives) [90-92]. The test has high specificity because a positive result is only achieved if the unknown material has a chromatographic movement the same as human

haemoglobin and if the unknown material binds with a polyclonal anti-human hemoglobin (hHb)-antibody.

As haemoglobin is common to many animals it can be important in forensic science to confirm that a blood stain is of human origin rather than animal. For example, if an item has traces of human saliva and animal blood present (perhaps as a result of meat preparation), DNA analysis will yield a profile of the saliva and presumptive tests (with the exception of Hematrace) will indicate the presence of blood, but there will be no indication that the blood is not human. In this case the blood will just not take part in the human-specific polymerase chain reaction (PCR) and effectively be invisible. In this case the incorrect assumption might be made that the blood is human and originated from the person who left the saliva.

As human blood is often an extremely important form of evidence, a significant amount of research has been carried out to validate the performance of the Hematrace test and it is now widely used in forensic laboratories. Nevertheless, a significant research effort is being undertaken to find other means by which human blood can be positively identified. The goals of this research are to provide a method that can corroborate results provided by Hematrace, an alternative method for those cases where Hematrace does not work or to provide a “universal” method that can be used to identify blood and other fluids that are present. An example of new capability being sought relates to differentiating between menstrual blood and venous blood. This information can be crucial in a sexual assault case where it might be important to establish whether the female has been injured or whether she is undergoing menses.

1.16 Semen

The other most common body fluid encountered at crime scenes, specifically in sexual assaults, is semen. Deposits not only play a critical role in identifying the perpetrator and linking him to the crime scene, but its positive identification as semen can be vital in corroborating or refuting victim’s or suspect’s statements because it is not a body fluid usually left by accident. There are some presumptive tests available to identify seminal fluid in forensic practice. The following sections describe the major forensic techniques that are used for detection of seminal fluid. The same as with blood, semen can also be identified using an alternative light source (ALS) for example Wood’s Lamp and/or UV source. The Wood’s Lamp emits UV wavelength (365 nm) and it is

inexpensive, safe and easy to use. When exposed to UV light at this wavelength semen can be seen to fluoresce on the surface of the skin, but this test is subject to false positive results from some ointments and creams; a study reported that it is not possible to distinguish between semen and other common products [93].

The most commonly used biochemical test for the indication of seminal fluid is the acid phosphatase (AP) test [94], which was developed in the late 1950s. This test involves two steps; in step one the AP enzyme present within semen catalyses the hydrolysis reaction of substrate α -naphthyl phosphate to sodium phosphate and α -naphthol. In the second step, α -naphthol then reacts with the chromagen, Brentamine fast blue, to produce a purple colour. The AP test has been reported to give some false positive colour changes with plant material (e.g., tea plants) [89], substances found within vaginal fluids and female urine as well as semen [95]. This could lead to confusion when identifying the body fluids of rape case, where identifying fluid samples must indicate whether sexual intercourse had occurred or not. Furthermore, the disadvantage of AP test is that the enzyme can degrade when exposed to environmental factors such as heat, mold, putrefaction, or chemicals. Another way to confirm the presence of semen is to establish the presence of spermatozoa microscopically or by conducting enzymatic determination using the choline test [96]. The Christmas tree stain, hematoxylin and eosin stains are commonly used for staining the DNA within the sperm head to aid detection and identification of spermatozoa by light microscopy. In some case circumstances small sperm counts can be encountered or might be absent completely if the donor is suffering from azoospermia or if they have had a vasectomy. Useful identification methods therefore should be based upon identifying the components of seminal fluid.

The prostate-specific antigen (PSA) marker or p30, a glycoprotein produced in the prostate gland, can be detected by enzyme-linked immunosorbent assay (ELISA) [97] and overcomes the issues listed above. This method has advantages compared to other presumptive tests, because semen of azoospermic persons will still contain PSA protein because it is present in seminal plasma. Although PSA can be detected in semen at very low concentration (106 dilutions) in other body fluids (e.g.. breast milk and vaginal fluid) the low levels do not cause false positive reactions. However, the PSA test can also give false positive results in male and/or female urine [98]. An advantage of

detecting PSA is the ability to detect it on contaminated or deficient samples including laundered fabrics and decomposed cadavers [99]. Hochmeister *et al.*, 1999, demonstrated the presence of seminal fluids using a PSA membrane assay method using supernatant solution from the DNA extraction procedure and shown that low sensitivity PSA (4 ng PSA/mL) can be detected within 10 minutes from vasectomized individuals [98]. Authors, Pang and Cheung (2007) [100] compared commercially available rapid stain identification (RSID) test (based upon the detection of semenogelin [Sg] protein within semen) with PSA strips for analyzing semen. No cross reactivity was seen with other body fluids. In future developments in forensic science a non-destructive semen screening method would be very useful in sexual assault cases that depend on DNA evidence not being destroyed by screening techniques.

Recently, emerging mRNA-based techniques is available for the confirmatory identification of semen sample. In the past decade, many researchers described the various mRNA markers, for example Protamine 1 (PRM1) and Protamine 2 (PRM2) is a semen-specific marker [101]. Juusola and Ballantyne [2005] proposed the reverse transcriptase-polymerase chain reaction (RT-PCR) for detection of the semen-specific genes PRM1 and PRM2 [81]. This group also described mRNA and DNA co-isolation method for forensic casework analysis. Fang *et al.* in 2006 applied a real-time PCR assays for the detection of semen-specific mRNA marker genes such as, semenogelin-1 (SEMG1), semenogelin-2 (SEMG2) and human prostate transglutaminase-type 4 (TGM4) [82], these genes are highly expressed in semen and considered as a forensic markers. Additional information about mRNA markers related to seminal fluid can be referred in section 2.2.1.

1.17 Saliva

In addition to blood and semen, saliva is another body fluid commonly found at forensic scenes. Saliva is clear liquid produced in the mouth to act as lubrication for food and to facilitate enzymatic breakdown of carbohydrates by amylase protein. Saliva has a significance role in identifying criminals in sexual assault cases, on cigarette butts, or around the rim of the glass bottles and other surfaces at crime scenes. There are some presumptive tests available for saliva, but until recently there is no readily-used specific confirmatory test for saliva. Similar to blood and semen, a UV light and/or ALS can be used to locate saliva stains, which show as a visible bluish-

white colour. Due to its high water content (~98%), saliva is harder to detect than other fluid (e.g. semen). The most popular detection techniques depend on the detection of α -amylase activity. Two isoforms of α -amylase are present in the human body. These isoforms are coded by chromosome 1, specifically by salivary amylase (AMY1A and AMY1B) and pancreatic amylase (AMY2A) genes. The AMY1 locus is expressed in saliva and at much lower levels in breast milk and sweat, while the AMY2A locus is expressed in the pancreas, semen and vaginal fluids. Thus detection of the activity of amylase can give only presumptive information since it is not exclusive to saliva [72]. The other popular test widely used in forensic laboratories for the detection of α -amylase is Phadebas test, which includes amylopectin-procion red. This test consists of a blue dye immobilized in a starch matrix on paper. Water is sprayed onto the paper, which is placed onto the item on which saliva is suspected to be present. The presence of α -amylase enzyme within saliva hydrolyses α 1-4 glycosidic bonds in the starch and releases the blue dye, which is free to diffuse in the paper and form a visible blue stain. The Phadebas test is relatively cheap and quick, but one study has shown that false positive results are produced by hand cream, face lotion, semen, urine and feces [102]. Another recently used presumptive colorimetric test is SALIgAE[®] also available for the detection of saliva [74], when reaction buffer mixed with saliva sample it turn to yellow colour. Similar to blood and semen, immune-chromatographic test strips (RSID[™]) are available for saliva testing using anti human salivary (amyA) antibodies. This test is more sensitive in the detection of saliva than the Phadebas test and no cross reactivity was observed with other human body fluids [103]. A recent investigation by Ricci *et al.* that involved the RSID analysis of a suspected robber's saliva [104] showed that false positive salivary amylase results were produced by citrus fruits (calamondin trees). Results were established to be false positives by human DNA testing, which did not indicate the presence of any human DNA. Similar to blood and semen, there are some emerging mRNA techniques available for the detection of saliva. Alvarez et al. described the co-isolation of RNA and DNA method that can be applied to saliva samples for detection of histatin 3 (HTN3) [101]. Another study by Juusola and Ballantyne proposed the RT-PCR analysis for the detection of saliva-specific genes statherin (STATH) [81]. These mRNA markers can be potentially considered as a forensic confirmatory assay.

1.18 Vaginal Fluid

Vaginal fluid is not as common at crime scenes as compared to other body fluids but this evidence can play an important part in sexual assault cases where vaginal contact takes place. There are not many methods available to test for the indication of this fluid, possibly because not been as extensively investigated as other fluids. The traditional method involves an enzymatic detection of a biochemical marker such as vaginal peptidase that is found in vaginal fluids. An electrophoresis method has been used in a starch gel at a pH of 7.4 in which the enzyme hydrolyses the dipeptide substrate L-valyl-L-leucine [105]. Positive results have been observed in mixtures of vaginal fluid, semen and blood. A chemical method involving periodic acid-Schiff (PAS) reagent can be used for the detection of cytoplasm of glycogenated epithelial cells present in the vaginal fluid; a positive result is the production of a crimson colour. However, glycogenation changes depending on the pre or post-menopausal cycle, therefore this method could easily give false negative results [106]. Another significant limitation of this test is that it requires a high amount of sample and that may destroy critical DNA evidence in the sample. A presumptive method involving the measurement of the lactic acid: citric acid ratio using capillary electrophoresis and comparing it to the ratio present in semen is reported to identify vaginal fluid alone or its presence in a mixture with semen [107]. Recently, a simple method for the identification of vaginal secretions based on the quantification of *Lactobacillus* species (an abundant microorganism in the vagina) by real time PCR has been described [108].

Juusola and Ballantyne's method of multiplex messenger RNA (mRNA) profiling by RT-PCR [81] for forensic purposes were used to identify vaginal fluid based on the presence of human beta-defensin 1 (HBD-1) and mucin 4 (MUC4) markers, although these genes have also amplified in menstrual blood [109]. The same method has been patented to the invention of ribonucleic acid (RNA) based assay kit for body fluid marker identification [110].

1.19 Urine

Urine is another body fluid encountered less frequently than blood, semen and saliva in forensic practice but can be encountered in sexual assault, rape or murder, harassment

and/or mischief cases.

The traditional method for identifying urine is based on the detection of urea or urea nitrogen [111]. Urine is difficult to detect due to the low sensitivity of urea tests and many false positive results could be anticipated from this method due to the ubiquity of urea. Similar to above mentioned body fluids, it will also give fluorescence when exposed to UV light. Another method for urine stain visualization is radial diffusion using urease enzyme and bromothymol blue as an indicator for released ammonia [112]. However, semen and sweat stains also display weak false positive results because of their urea content. Another chemical analysis widely used in forensic examination involves detection of creatinine (Jaffe test), which is present in high amounts in urine. This test uses a picric acid in benzene solution; creatinine reacts with picric acid to produce a creatinine picrate (a red precipitate) [74, 106]. Scanning electron microscopy (SEM) integrated with energy-dispersive X-ray (EDX) spectroscopy can be used for the relative concentration of sodium, sulfur, phosphorous, chlorine, potassium, calcium, and traces of other elements in urine [106]. Tamm-Horsfall glycoprotein (THP), also known as uromodulin, has been used as a target in immunochromatographic tests (RSID™) for the detection of urine, but it is not a human-specific test [113].

The study by Nakazono *et al.* 2002 [114] presented a method for indication of human urine by detecting five major 17-ketosteroid conjugates using- liquid chromatography coupled to electrospray ionization-mass spectrometry (LC-ESI-MS). Simultaneously they carried out DNA extraction and purification on the same sample. This prevents destruction of DNA evidence, which is a positive aspect for forensic analysis. However, DNA profiling for human urine stains is limited by the quantity of DNA (cells) available in the samples. It is remarkable that male urine stain contains less DNA than the female urine stains [115].

1.20 Sweat

Sweat is also a less commonly encountered fluid in forensic investigations. The fluid has a similar composition to urine, but low amounts of urea and creatinine [74]. The main current presumptive test available for sweat is SEM-EDX, which is used for measure the relative concentrations of elements such as, sodium, phosphorous, chlorine, sulfur,

calcium, potassium, and traces of other elements. However, this test has low sensitivity and would give false positive results due to similar compositions present in other body fluid (e.g. semen and urine) [74, 75].

Sweat is less refined than other body fluids and not many forensic tests are available for the detection of fluid-specific components. An emerging technique using enzyme-linked immunosorbent assay (ELISA) has been reported for the identification of sweat-specific protein (G-81) using monoclonal antibody and a Western blot technique [116].

Sweat is an excretion or perspiration process that may contain many endogenous and exogenous molecules present on the skin surface or arising as a result of ingestion. A very important attribute of sweat is that it is component of fingerprints, which are very important evidence at crime scenes and on crime-related items.

1.21 Fingerprints and other biological-chemical traces

Fingerprints contain many eccrine or apocrine gland bio-chemical substances ranging from salts (e.g. sulphates, phosphates and ammonia), amino acids, and enzymes (such as the anti-microbial peptide, dermcidin) to metabolites of ingested drugs and other foreign materials that a person might have touched [117, 118]. In addition to the biometric information present in a fingerprint (which is a very important way of identifying criminals) the chemical information present in fingerprints can provide information regarding the circumstances surrounding a crime [119]. Fingerprints made in human blood are especially important evidence because they indicate violence and the ridge pattern may identify the perpetrator. It is the case that fingerprints at the crime scene are often invisible to the naked eye (referred to as latent fingerprints) and require some form of enhancement in order to make them visible and allow the ridge pattern to be imaged. This process, including recording the image, can be carried out at the crime scene or back at a laboratory if the enhanced mark is “lifted” off the surface it is on using an adhesive sheet.

During violent criminal acts biological material such as blood or other body fluids may become smeared on the fingers of victim or suspect and then transferred to objects at the crime scene. As well as the biometric pattern in the mark it can be extremely important in a criminal case to establish exactly what the mark consists of. For instance, a domestic violence casualty is investigated and a fingerprint testing positive to blood is

found on a kitchen surface; DNA analysis of the mark indicates the typing of the victim. In this case it is important to ascertain whether the mark contains human or animal haemoglobin [119], such as from chicken or cow blood. If animal blood is present then the mark is not likely to be relevant to the crime and the victim's DNA could be on the surface due to "innocent" activity. Sexual assault cases can also involve the deposition of fingermarks containing traces of semen or vaginal fluid. Marks such as these can have great value as they have the potential to identify not only the individual who deposited the mark but also provides information regarding who they touched and which part of the body they touched.

As discussed in previous body fluid (blood) section, there are some presumptive tests such as Kastle-Meyer test and recently medical test kits such as Hemastix and Hematrace® are used for the detection of blood traces on the contaminated fingermark. However, these tests require a sampling of the suspected blood traces, which in the case of a fingermark means destroying some of the ridge pattern (that is critical for the identification of the person who deposited the mark). These tests also cannot indicate whether the body fluid is only present in the ridges of the mark (and therefore the person who deposited the mark has the fluid on their finger) or more generally on the surface (and therefore was most likely present before the surface was touched).

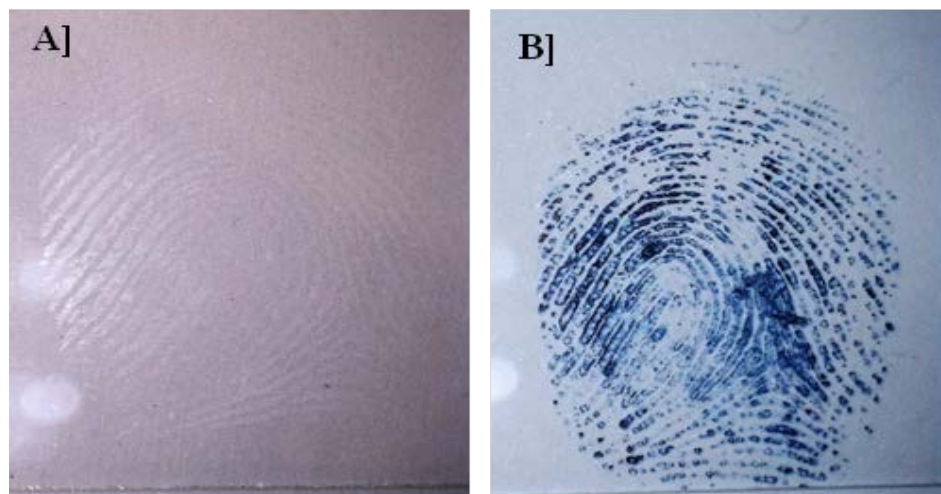


Figure 1.9. A] Microscopic image of bloodied fingermark on a glass slide. B] Same mark stained with Amido black solution (Image from Kamanna *et. al.* 2017 [119]).

Instead of these tests, fingermark examiners apply one of a number of protein dyes, such as Amido black (Acid black1), Acid violet 17 and Acid yellow [120] in order to enhance the mark if they suspect that it contains blood. Figure 1.9 shows images of a latent

“bloodied” fingermark and its appearance after enhancement using Amido black. The successful enhancement of a mark with these reagents does not prove that blood is present in the mark, simply that a protein is present, and furthermore it is not specific for human proteins. Clearly in the case depicted in Figure 1.9, the protein is present in the ridges of the mark and not generally distributed over the surface.

If blood is not suspected then any of a range of fingermark enhancement dusts will be applied at the scene (such as aluminium powder) and they do not give any information as to what the mark is made from.

1.22 Fingernails and biological traces

A nail is a hard protective envelope of thick keratinized proteins. During violent crimes such as sexual assault, rape or homicides, touching or violent contact may take place between suspect and the victim. This could result in traces of bodily fluids becoming trapped under the fingernails. Some recently published articles described the current DNA typing and direct-PCR DNA profiling techniques for the identification of individuals from biological material present in fingernail scrapings and fingernail clippings [66, 69-70]. DNA profiling of fingernail scrapings can be very valuable in the investigation of violent crimes against the person because it can show contact between victim and suspect [121]. However, it can be important to determine the type of body fluid present in order to provide add evidence as to the circumstances surrounding the contact. The presence of blood under fingernails, for instance, indicates that contact with the person from whom the blood originated was sufficiently forceful to cause violence. In a sexual assault case, the victim’s fingernails may collect traces of body fluid from the assailant (such as semen) or the assailant’s fingernails might collect traces of vaginal fluid originating from the victim. In a sexual assault investigation the detection of a trace of the victim’s DNA under the alleged assailant’s fingernails would indicate contact between the two individuals but the identification of the trace as vaginal fluid would provide additional circumstantial evidence (intimate contact). On the other hand, the identification of the trace as saliva would indicate an entirely different set of circumstances.

1.23 Other Forensic Technologies for the Identification of Body Fluids

1.23.1 Fluorescence spectroscopy

Over the past decades this technique has been applied to forensic investigation of trace materials. In fluorescence spectroscopy, excitation radiation (e.g. ultraviolet light) is absorbed by a fluorophore (fluorescent compound), which is a chemical group in an analyte (e.g. proteins, nucleic acids and lipids). The fluorophore then emits radiation at a longer wavelength than the excitation radiation. The intensity of the emitted radiation is proportional to the concentration of the fluorophore. Fluorescence is also widely used for the direct detection of dried saliva stains and other body fluids on surfaces such as clothing, carpets etc. [122]. However, this technique could be destructive due to photo degradation of the DNA and RNA in a sample due to prolonged exposure to ultraviolet light. Another disadvantage is the poor performance when analyzing mixtures and other components. This technique is not a confirmatory method because it is neither specific to particular body-fluid stains nor species-specific.

1.23.2 Raman and IR Spectrometry

Raman spectrometry is like infrared (IR) spectrometry in that it accesses fundamental modes of vibration and/or rotation in molecules. It is usually suitable for small molecule identification rather than protein identification. Unlike infrared spectrometry however, Raman spectrometry is not sensitive to water, which is a benefit in analysis of body fluids. Raman spectrometry uses the scattering of low intensity laser light on a sample. In the past decades this technique has played some role in forensic science for the identification and differentiation of body fluids. Using Raman spectrometry different body fluids have been tested including semen, vaginal fluid, saliva, sweat and blood. The resulting spectra from each body fluid were shown to be significantly different [72]. Studies in 2014 have shown that discrimination of human and animal blood traces is possible using Raman spectrometry and partial least squares-discriminant analysis (PLS-DA) [123]. Recently, another study reported a comparison of Raman and Infrared (IR) spectrometry for discrimination between blood from human, feline (cat) and canine (dog) species; Raman was found to be more suitable (Figure 1.10) [73].

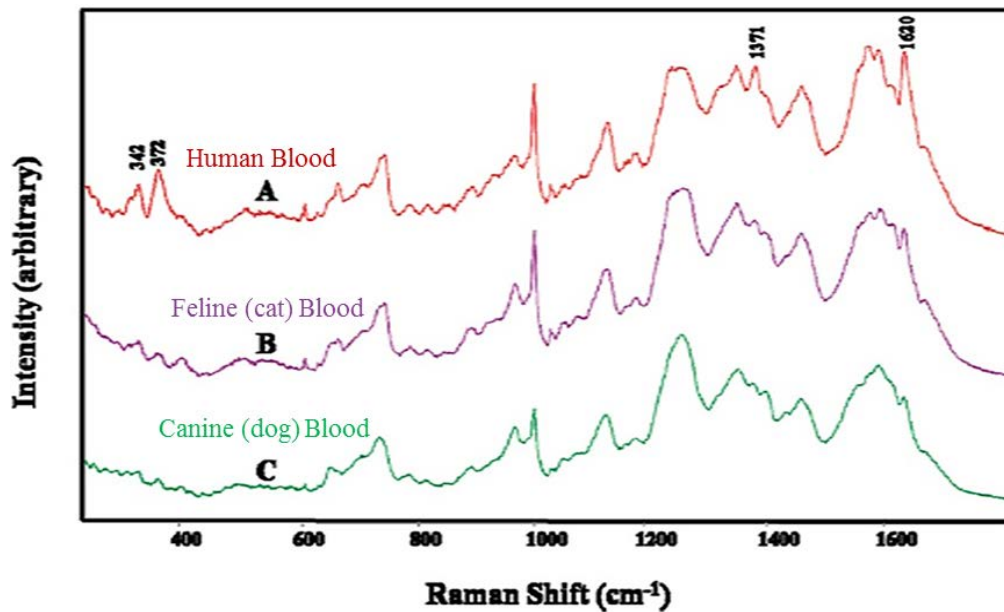


Figure 1.10. Typical Raman spectra of human blood (A), cat blood (B) and canine blood (C). The Figure is adapted from Zapata *et al.* 2015 [73].

However, the obtained spectra of all three species of blood samples all contain very similar components and broad bands, and there does not appear to be much scope for this technique to resolve mixed stains [72] or to be applied to very small quantities of fluid.

Recently, a vibrational based technique, attenuated total reflectance Fourier transform infrared (ATR FT-IR) spectrometry, has been used for rapid presumptive detection and discrimination of human body fluids [124, 125]. FT-IR spectrometry has also used for biomedical examination and identification of biomolecule components and their structures in human tissues, cells and body fluids [124]. Elkins *et al.* evaluated the FT-IR detection of various human fluids and other materials. IR spectra were collected in their raw solution or on substrate materials (e.g., fabric or white paper) [125].

Similar to Raman spectrometry, IR spectrometry exhibits broad bands and very subtle features that indicate that the technique could not be applied to mixtures of fluids or to trace samples. This was confirmed in a brief evaluation of the applicability of ATR FT-IR carried out as part of the research described in this thesis; the results are presented in **Appendix 5** and are not discussed further in the main body of this thesis.

1.23.3 DNA profiling

DNA profiling is the main forensic test currently used for determining the individual's DNA profile. DNA evidence can be present in body fluid and/or tissue samples, from suspect and victim, and can be received for analysis either on swabs or as a physical material (piece of stained garment or a lifted fingerprint). Recently forensic genomic research has been focused towards the development of progressively-sensitive tests and the simplified sample treatment processes through innovations such as direct-PCR DNA profiling [70, 121]. In this technique, a small quantity of a biological sample or a swab used to collect biological material is placed directly into the PCR, which not only achieve the exponential multiplication of target DNA sequences but also avoid the need for cell lysis and DNA extraction steps. DNA profiling followed by DNA data base comparison or comparison against samples from a suspect are crucial steps in investigations in forensic science [65]. However, determining the type of fluid present in biological evidence could also be important in reconstructing the crime that has taken place and in confirming/refuting the statements of victim/suspect. DNA profile analysis alone does not specify if the DNA arrived from semen, saliva, vaginal fluids, urine or any other sources, nor can it indicate cross contamination of material during sample collection or at other times [66] – it “simply” indicates the person from whom the biological material originated.

1.24 Mass Spectrometry-based Proteomics for Forensic Body Fluid Identification

All body fluids, even watery ones such as sweat and urine, contain proteins and sometimes proteins are the most abundant component and present as a complex mixture. Mass spectrometric methods are increasingly being applied to proteomics and that also includes the analysis of body fluids for forensic purposes.

At the time that the research described in this thesis commenced, several articles relating to the forensic use of mass spectrometry for the detection of small molecules in body fluids [126, 127, 128, 129, 130], the examination of fingerprints [131-137] and the detection of proteins in body fluids [138, 139, 140] had been published. It was shown that finger sweat contains small molecule exogenous compounds, such as traces of ingested drugs that can be detected using mass spectrometry [126-129], as well as many small-molecule endogenous compounds [129-133]. For the research that deals with exogenous

compounds, most makes use of fingerprints that have been artificially enriched with the compounds, but detection of ingested drugs and their metabolites in fingerprints has been reported [128]. It was shown that it is possible to map fingerprint ridge pattern simultaneously to traces of condom lubricants present in the fingerprint region [141, 142].

MS methods have been reported over a number of years for the identification of haemoglobin variants in blood [for example 143] and many other tissues and fluids. More recently, a few research groups have shown the applicability of LC-MS based proteomic analysis for the identification and evaluation of potential forensic marker proteins in biological fluids [138, 139, 140, 144, 145 & 146]. In the most recent of these articles Yang *et al.* [138, 139] used LC-MALDI based proteomic analysis for the identification and differentiation of venous blood, menstrual blood and vaginal fluid. Van Steendam *et al.* [146] performed an MS-based classical proteomics approach to identify biological matrices in forensic science. This group identified different markers in mixtures of several biological fluids using nLC-ESI MS/MS. Their results have shown that an MS approach can identify different proteins at the same time and identify several biological fluids in one sample. Multiple markers for each type of body fluid increases the confidence of correct identification.

While work relating to this thesis was being carried out, several articles were published by Francese's research group that extended the application of MSI to examination of fingerprints, especially those containing blood [147, 148, 149, 150]. Recently Igoh *et al.* described the emerging mass spectrometry-based proteomics analysis using LC-MS/MS approach for the identification of potential forensic protein markers in vaginal fluid [151]. This group identified two human small proline-rich protein 3 (SPRR3) isoforms and fatty acid-binding protein 5 (FABP5), potential protein markers that may be used for the identification of vaginal fluid in forensic science. Another recently published article [140] reports a specific protein marker method using comparative proteome fractionation followed by liquid chromatography–mass spectrometry/mass spectrometry (LC-MS/MS) analysis. The authors identified a panel of 29 candidate protein markers and recommended specific indicators of human urine, vaginal fluid, peripheral blood and menstrual blood.

The above studies show that MALDI-based techniques can detect body fluid biomarker proteins accurately, reproducibly, and with high sensitivity even in mixtures. The technique has been shown to be effective for imaging proteins. A major advantage of MS techniques, including MALDI-based techniques, is the fact that analysis can make use of the typical DNA extraction processes, since the protein-rich component of the extract can be used, which is otherwise discarded [see Fig. 1.11]. Similar to other MS-based techniques, no prior knowledge of an unknown stain nor how many body fluids it contains is required to perform the test using MALDI-ToF MS. It can be used to detect at pico- to femto-mole concentrations of protein in body fluid. Simultaneously multiple peptides from numerous protein markers can be detected and effectively confirmed by sequencing.

When the speed of MALDI-ToF-MS analysis is considered and the fact that it can be used for imaging (“mapping”) of proteins, the technique appears to be well-suited to dealing with the analysis of forensic items. The existing challenges to the implementation of MALDI-imaging mass spectrometry to analysis of forensic items include the wide concentration range of substances in forensic items, which necessitates a wide dynamic range in analysis, difficulties regarding sample preparation and optimization, sample topography, data analysis and data interpretation is highly complex.

1.25 Statement of the Problem

As demonstrated above, there is a lack of confirmatory tests for many body fluids and current available presumptive tests for determining the origin of fluids produce false positives, suffer from interferences, lack human-specificity, cannot distinguish between menstrual blood and venous blood, are difficult to carry out when mixtures of fluids are present, and are destructive to the sample, so subsequent DNA analysis to identify the donor or confirm human origin cannot be carried out on the same sample. For some fluids, such as sweat and urine, reliable presumptive tests are not available. Furthermore, most tests cannot be used to “map” body fluid deposits with high enough spatial resolution to detect and identify fluids in fingerprint ridge patterns.

Analysis of nucleic acid and protein biomarkers offer solutions to these problems, however, the former cannot be used to “map” body fluid deposits in fingerprints and, at

the time when the research described in this thesis commenced, detection and analysis of protein biomarkers was not well-developed and usually involved the use of liquid chromatography.

Research to extend the scope and coverage of protein biomarker analysis using mass spectrometry, particularly MALDI-ToF-MS, and to streamline approaches was warranted.

1.26 Aims of Research

The current issues of human body fluid identification and opportunities for innovation and improvement were considered when designing the aims of this study. New developments in forensic science, analytical biochemistry and mass spectrometry-based proteomics were evaluated to develop a new technique with the potential for identifying a range of protein markers in body fluids without some of the present disadvantages.

The aim was to develop novel, direct and simplified MALDI-ToF MS-based proteomic methods for the identification of body fluid traces recovered from different, important substrates (e.g. various types of fabric fibres, cotton swabs and nylon micro-swabs), directly *in situ* on these substrates, and from enhanced latent fingermarks (including “lifted” enhanced marks).

As blood protein sequences are not available in the literature for many Australian native marsupials (a number of which are used as food or are involved in “road-kill”, and therefore traces of blood from these animals might be found on members of the public, their homes and cars) research was carried out to demonstrate the specificity of an MS-based approach in Australia.

Some research concentrated on the examination of traces of fluids under fingernails (i.e. fingernail scrapings) as published methodology for such examinations is scarce.

Finally, in recognition of the fact that the amount of body fluid present in fingernail scrapings, fingermarks and swabs is limited and the fact that it is vital to carry out DNA profiling of fluid in these items, research was carried out with the view to fully integrating MS-based proteomic analysis with forensic DNA STR profiling technology.

This project was sub-divided into six distinct tasks designed to accomplish the aims. These were:

1. To optimize MALDI-TOF MS/MS techniques for direct (or *in-situ*) trypsin digestion and analysis of body fluids ‘on-fibres’ plucked from fabrics and swabs (including fingernail trace swabs), for analysis of raw body fluids, and in fingermarks (including enhanced and lifted marks).
2. To use nLC-ESI-qTOF MS/MS to confirm the identity of major protein markers (both human and animal) in blood, semen, urine, vaginal fluid and saliva as determined by *in situ* MALDI-TOF MS/MS.
3. To establish a mass spectrometry-based forensic “toolbox” containing MALDI-TOF MS/MS, MALDI TOF MS-imaging and nLC-ESI-qTOF MS/MS methods for detecting biological fluid traces in latent fingermarks and fingernail scrapings.
4. To demonstrate a complementary forensic ‘proteo-genomic’ approach on a single micro-swab for the direct identification of the type of biological fluid present and the identity of its “donor”.
5. To explore both “top-down” and “bottom-up” approaches and to carry out *de-novo* sequencing of Australian marsupial blood peptides that are not currently listed in databases.

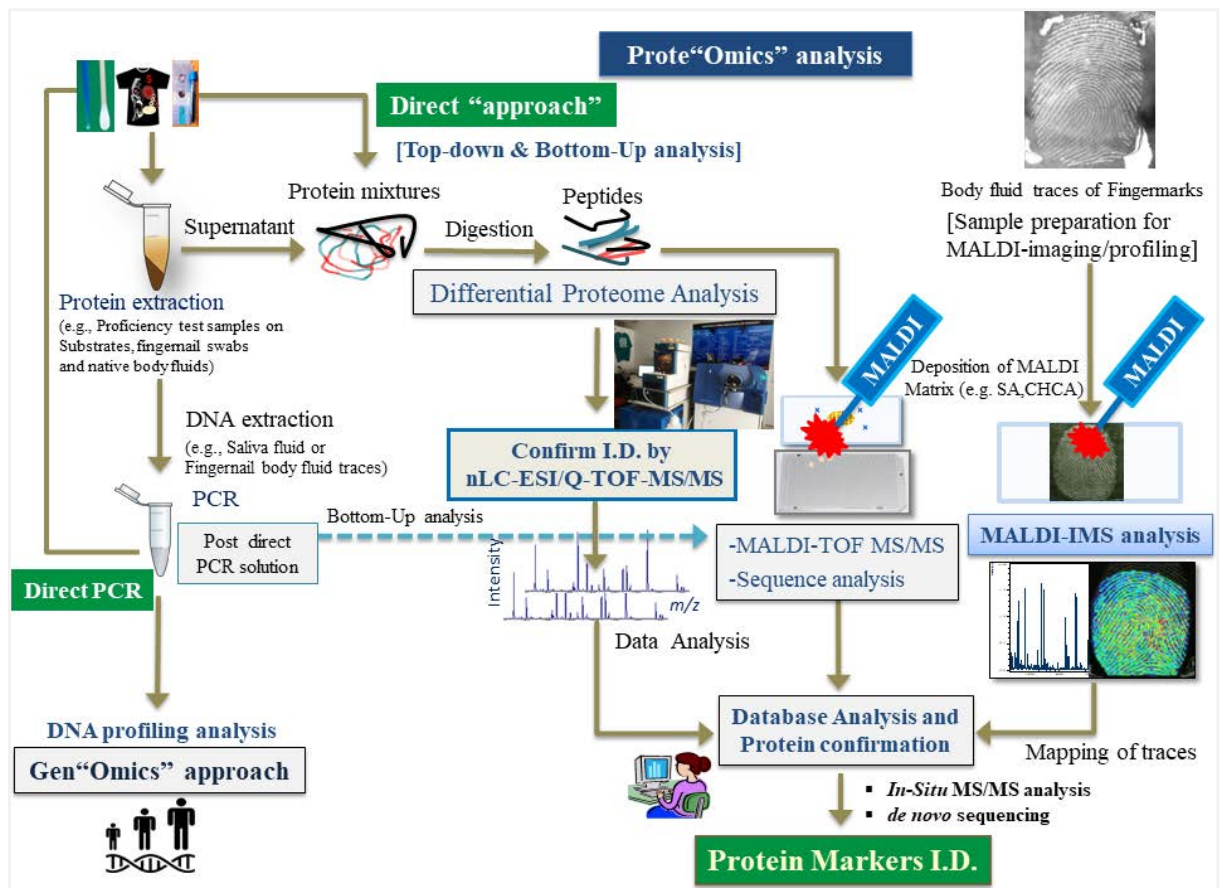


Figure 1.11. A schematic diagram representing different stages of a comprehensive MS-based experimental workflow for the identification of body fluids and fingerprint traces. Initially, the samples (e.g., human volunteer’s body fluids, animal fluid specimens, crime stains, and proficiency test samples) are extracted from substrates (e.g., fabric materials or cotton and nylon micro-swabs and native solution) and with the resulting supernatant solution, direct fibres (containing debris of body fluid traces) or raw liquid fluid can be carried out for “Top-Down” and “Bottom-Up” proteomics analysis. The main advantage of this technique is that it does not interfere with mRNA and/or DNA analysis, because genomic material is precipitated as a pellet. Direct PCR DNA-profiling is performed for fingernail micro-swabs and post-PCR (direct) solutions still can be analyzed for proteomic identification. The identified body fluid protein markers can be sequenced and confirmed by MALDI-TOF MS/MS and tandem mass spectrometry techniques (nLC-ESI-Q-TOF MS/MS). Fingerprint enhancement and MALDI-imaging (MSI) techniques are used for the identification and mapping of exogenous/endogenous small metabolites and body fluid traces (e.g., blood, vaginal fluid) from the contaminated mark. The Schematic Figure is adapted from my publications.

Chapter 2: Materials and Methods

Chapter 2: Materials and Methods

2.1 Materials and Suppliers

2.1.1 List of chemicals and materials used in this project.

Chemicals and Materials	Manufacturer/Suppliers
Acetonitrile (ACN) HPLC grade	Sigma-Aldrich (NSW, Australia)
Ammonium bicarbonate (NH ₄ HCO ₃)	Sigma
Acetic acid glacial	Sigma
Amido Black (No. LV501)	SIRCHIE [®] Inc. USA
ABAcad [®] Hematrace [®] kit (#808426)	Abacus Diagnostics Inc. (California, USA)
Dithiothreitol (DTT)	Sigma
Iodoacetamide (IAM)	Sigma
LC-MS grade water	Sigma
Trifluoroacetic acid (TFA)	Sigma
α -Cyano-4-hydroxycinnamic acid (CHCA)	Sigma
Sinapinic acid (SA)	Sigma
Picolinic acid (PA)	Sigma
2, 5-Dihydroxybenzoic acid (DHB)	Sigma
Trypsin Gold, MS grade (V5280)	Promega (Madison, USA)
Modified porcine Trypsin (V5111)	Promega (Madison, USA)
Formic acid	Sigma
Methanol	Sigma
Microscopic slides	Paul Marienfeld GmbH & Co. KG
Sodium dodecyl sulfate (SDS)	Bio-Rad [®] , USA
SDS-PAGE Molecular Weight Standards	Bio-Rad [®]
Mini-PROTEAN [®] TGX Stain-Free gels (Cat# 456-8123)	Bio-Rad [®]
Indium-tin oxide (ITO) coated slides (25 x 75 x 1.1 mm)	HTX Technologies, USA
ImagePrep solution vails	Bruker Daltonics (Bremen, GmbH, Germany)
ImagePrep slide cover slips (267942)	
MTP 384 polished steel plate	Bruker Daltonics
MTP slide adaptor	Bruker Daltonics

Pepmix calibrants (P.N: 206195)	Bruker Daltonics
Protmix standard-I (P.N: 206355)	Bruker Daltonics
Ethanol (Absolute)	Sigma
Aluminium foil	Supermarket
Bromophenol blue	Sigma
Surfactant RapiGest™-SF (Part #186001860)	Waters Ltd, NSW, Australia
Silver-black magnetic powder	Sirchie Inc.(North Carolina)
Black magnetic powder	Sirchie Inc. USA
Magnetic powder applicator	Sirchie Inc.
Double-sided Kapton tape (1 inch, 0.1 mm total thickness)	Ted Pella Inc. California, USA)
Cover-Up (teaching mark)	Marbig, Australia
Sterile micro syringe	Livingstone International Ltd, NSW, Sydney, Australia.
Kimwipes	KIMTECH SCIENCE, USA
Eppendorf tubes	Hamburg, Germany
50 mL sterile plastic sample containers	SARSTEDT (Australia)
VACUETTE® blood collection tubes (3 mL), with sodium citrate anticoagulant 3.2 %	Greiner Bio-One (Austria)
Sterile cotton swabs (8150CIS)	COPAN (Australia)
Microswabs (nylon # 18-903)	Premium Plus™, Australia
2 mL chromatography sample vials	Agilent Ltd, Sydney, Australia
0.2 mL thin-walled PCR tube	Eppendorf, Vic, Australia
GlobalFiler PCR kit	Thermo Fisher, Australia
SuperScript® IV Reverse Transcriptase	Invitrogen, California, USA
Oligo d(T) ₂₀ primers	Thermo Fisher, Australia
QIAamp Mini spin columns	QIAGEN
Hi Di formamide	Thermo Fisher, Australia
3500 Genetic Analyser	Thermo Fisher, Australia
Aluminum SEM stubs (12.5 mm) with carbon tape	
Pieces of 100% nylon, polyester, cotton and cellulose acetate fabric (white)	ProSciTech, Australia Spotlight (South Australia)

2.1.2 Instruments and equipment

Instrument	Company/source
Autoflex-III MALDI-ToF mass spectrometry	Bruker Daltonics, Bremen, Germany
AB Sciex TripleTOF® 5600+ mass spectrometer	AB Sciex, Framingham, MA, USA
Attenuated total reflectance Fourier transform infrared (ATR FT-IR) spectrometer	Thermo Nicolet Corporation Framingham, USA
Centrifuge 5816 R	Eppendorf, Hamburg, Germany
C18 column (75 mm x 150 mm)	Nikkyo Technos, Tokyo, Japan
DP21 digital camera	Olympus Ltd, Tokyo Japan
Digitech USB microscope (5 megapixel camera with integrated white LED light source)	Jaycar Electronics Pty Ltd (Adelaide, Australia)
Eksigent Ekspert 415 nano LC	AB Sciex, Framingham, MA, USA
EZ Omnic (v8.3) software	Thermo Nicolet Corporation, USA
FEI Inspect F50 instrument (scanning electron microscope)	FEI Corporation, USA
FlexImaging 3.3 software	Bruker Daltonics, Bremen, Germany
Flex Analysis 3.3 software	Bruker Daltonics, Bremen, Germany
GeneMapper IDX™	Thermo Fisher, Australia
ImagePrep station	Bruker Daltonics, Bremen, Germany
MTP slide adaptor-II	Bruker Daltonics, Bremen, Germany
Mini-PROTEAN® Gel chamber	Bio-Rad®, USA
Olympus XZS2 stereo microscope	Olympus Ltd, Tokyo Japan
Proflex PCR Machine	Thermo Fisher, Australia
Protein pilot version 4.5.	AB SCIEX™, Australia

2.2 Samples used in this study

2.2.1 List of human and non-human body fluid samples used in this project.

Origin of sample	Type of sample	No. of volunteers /samples
Human body fluids	Blood	10
	Seminal fluid	12
	Saliva	10
	Vaginal fluid	15
	Urine	8
	Fingermarks (dusting and lifting)	20
	Bloodied (human) fingermarks	20
	Bloodied (human and animal blood mixture) fingermarks	10
	Vaginal contaminated fingermarks	15
	Fingernail scrapings (Microswabs) control	5
	Fingernail scrapings of vaginal fluid traces	22
	Fingernails of non-human blood traces	20
	Dried body fluid particles on different fabric types (nylon, cotton, polyester and cellulose acetate)	20
	Proficiency tests from CTS (Virginia, USA)	Batch number 04-571(January 2004), mixture of blood and semen
11-573 (May2011)		4
12-584 (July 2012)		4
14-582 (March 2014)		4
Non-human blood/fluids	Dama wallaby	1
	Koala	1
	Swamp wallaby	1
	Western grey kangaroo	1
	Brushtail possum	1
	Kangaroo island (K.I) kangaroo	1
	Tasmanian devil	1
	Red kangaroo	2
	Kangaroo meat fluid	3
	Chicken liver fluid (meat)	2
FSSA test samples of dog breeds	10	

2.3 Sample collection

All the human body fluid samples were sourced and collected from volunteers from Forensic Science, SA (FSSA) and Flinders University. Semen samples were sourced from patient volunteers from Flinders Fertility (Flinders Medical Centre), Adelaide, South Australia. All samples were collected pursuant to Southern Adelaide Clinical Human Research Ethics Committee Application 440.14 – HREC/14/SAC/455. Prior to sample collection all the donors read consent participation form (provided in Appendix) and signed to carry out this research study. Saliva and urine samples were collected in 50 mL sterile containers (SARSTEDT, Australia) from healthy volunteers. Semen samples (12) were collected in 30 mL Eppendorf centrifuge tubes and stored at -20°C prior to the experiments. Fingernail scrapings containing vaginal fluid were collected by inserting a clean finger into a vagina for about 10 s. Vaginal fluid samples were not sampled during their menses to avoid a cross contamination of menstrual blood. The fingernail deposited biological fluid (e.g. blood and vaginal fluid) evidence was collected using nylon dental microswabs [Premium Plus™, Australia]. The tip of the microswab was moistened with deionized water and then rolled around under the nail and in the gap at the side of the nail in order to collect any persisting biological fluid. The microswab was then allowed to air dry before being inserted through the septum of a chromatography sample vial (2 mL, Agilent Pty Ltd., Sydney, Australia) and sealed, ensuring that the microswab tip did not touch the wall of the vial.

For the collection of bloodied fingermarks, small droplets of human blood were produced by pricking a clean finger using a sterile syringe (Livingstone International Pty Ltd). A small volume of blood (Approx. 1 to 2 µL) was rubbed on another clean index fingertip and then dried at room temperature prior to office work. The bloodied mark was then deposited and/or collected onto indium tin oxide (ITO) coated glass slides.

For the collection of vaginal fluid-contaminated fingermarks, a clean finger was placed into a vagina for approximately 5 s, air dried for ~10 min and then finger marks were deposited onto ITO slides. Two donors provided samples for ten experiments. The proficiency test samples provided by Collaborative Testing Services (CTS) Incorporated (Stirling, Virginia, USA) such as test 04-571 (provided by CTS in January 2004), 11-573 (May 2011), 12-584 (July 2012) and 14-582 (March 2014) were provided to

Forensic Science SA (FSSA, Adelaide, South Australia) as part of their quality assurance program. Each test involved four pieces of fabric stained with various body fluids; they were manufactured to resemble typical stained items that might be encountered in investigation of crimes. Samples were stored after their initial receipt from CTS at room temperature in sealed paper and plastic bags in the dark.

Australian Mammal blood samples from brushtail possum [*Trichosurus vulpecula*], koala [*Phascolarctos cinereus*], red kangaroo [*Macropus rufus*], Western grey kangaroo and its Kangaroo Island sub-species [*Macropus fuliginosis* and *Macropus fuliginosus fuliginosus*, respectively], dama wallaby [*Macropus eugenii*], Eastern grey kangaroo [*Macropus giganteus*], swamp wallaby [*Wallabia bicolor*], Tasmanian devil [*Sarcophilus harrisi*] were obtained from the Cleland Wildlife Sanctuary (Adelaide, South Australia) pursuant to Australian Animal Welfare Committee Application 909/16. The native animal blood samples were collected “opportunistically” by Dr Ian Hough, consulting veterinarian for Cleland Wildlife Reserve (Adelaide), using the DEWNR Wildlife Ethics Committee “Collection of Blood from Wildlife Policy” guidelines. All the liquid blood samples were collected (about 1 mL) into VACUETTE[®] blood collection tubes containing a coagulation sodium citrate (3.2 %) solution. No animals were handled or anaesthetized for the sole purpose of blood collection. The species listed above are important to forensic science because are used as meat (and therefore might be found on blood stained household items and garments), are animals that might become roadkill (and therefore might be on bloodstained cars and garments). Some Australian native animals are not already on protein databases.

2.4 Sample Preparation and Experimental Methods for Chapter 3

Some of methods described here are presented as they given in the manuscript.

2.4.1 Experimental materials and samples

Pieces of 100 % fabric materials (cotton, cellulose acetate, nylon and polyester, all

white) were laundered in lukewarm water for 30 min using non-enzymatic laundry powder (“Fab” brand, Colgate-Palmolive, Pty Ltd.) at the level recommended by the manufacturer. The fabric pieces were then rinsed several times in fresh cold water and left to dry naturally. Comprehensive list of all other chemicals and reagents are shown in the section 2.1.

Deposition of body fluid on fabric materials:

The crude individual body fluids and their mixtures were deposited on pieces of nylon, cotton and cellulose acetate fabric. Individual fabric body fluid specimens were prepared by spotting 10 μ L of each type of body fluids (blood, semen and saliva) on the fabric. For body fluid mixtures, samples containing blood (5 μ L of 1:50 dilution in water) mixed with semen (10 μ L), or blood (5 μ L of 1:50 dilution in water) mixed with saliva (15 μ L) were deposited on each of the fabric materials. The concentration of blood used and its ratio to the other body fluids in these mixtures was calculated to balance the amounts of protein from each body fluid. All fabric specimens were dried at stored room temperature for 3 days before prior to analysis.

2.4.2 Scanning electron microscopy

Scanning electron microscopy (SEM) images were collected using an FEI Inspect F50 instrument. Fibers plucked from clean fabric pieces and from pieces that had been exposed to liquid semen were attached to aluminum SEM stubs (12.5 mm) using double sided adhesive carbon tape discs and then coated with platinum metal (13 nm thick). Images were collected using 5 keV beam energy, spot size of 6.3 μ and magnification between 100 \times and 3000 \times .

2.4.3 MALDI-TOF MS instrumentation

All mass spectrometric analysis was performed using an Autoflex-III MALDI-TOF-MS [Bruker Daltonics, Bremen, Germany] mass spectrometer (see **Figure 2.1**). The instrument ion source was equipped with a neodymium-doped yttrium aluminum garnet [Nd: YAG λ = 355 nm] Smart Beam 200 Hz solid state laser. Reflectron positive (RP) ion mode was used with 20 kV accelerating voltage and delayed extraction ions of 200 ns for detection of peptides in the m/z detection range of 600–4000. Large protein data (m/z detection range 5000–110,000) were acquired using linear positive (LP) ion mode.

All the MALDI instrumental parameters including laser power, mass detection range, voltage, delayed extraction and laser offset were set using Flexcontrol 3.3. Each mass spectrum collected represented the sum of the data from 2000 laser shots. In order to account for inhomogeneous distribution of matrix, summed spectra were collected at several locations in the body fluid deposit and an average spectrum was produced. A standard peptide mixture (P.N: 206195, Bruker pepmix calibrants) and protein standard-I (P.N: 206355) were used for external calibration.



Figure 2.1 A photograph to show the Autoflex-III MALDI-TOF-MS [Bruker Daltonics, GmbH, Germany] mass spectrometer. Photograph taken in house [Flinders Analytical].

2.4.4 MALDI-TOF MS sample preparation

2.4.4.1 Analysis on MTP 384 polished steel plate

The volunteer neat body fluid mixtures were prepared for “top-down” intact protein analysis as follows: 2 μL of 1:50 dilution of blood in water, 3 μL of raw semen and 5 μL of raw saliva were mixed and from this 1 μL was treated with an equal volume of a saturated matrix solution of sinapinic acid (SA) in 50% LC-MS grade acetonitrile/ H_2O

with 0.1% trifluoroacetic acid. These mixtures (2 μL) were deposited on MTP 384 polished steel plate. Urine samples of 1 μL were spotted with an equal volume of saturated α -cyano-4-hydroxycinnamic acid (CHCA) matrix in 50% LC–MS grade acetonitrile/ H_2O with 0.2% trifluoroacetic acid.

2.4.4.2 Analysis on ITO-coated slides

In the direct MALDI-TOF MS analysis of body fluid on dried fabric fibers, a small tuft of fibres from each of the semen-treated fabrics (<0.5 cm) were directly deposited onto an ITO-coated conductive glass slide and then 3 μL of SA matrix in 50% LC–MS grade acetonitrile/ H_2O with 0.1% TFA was deposited on the fibers. The slide was dried at room temperature and then inserted into an Autoflex-III MALDI-TOF MS using a MALDI-imaging slide adaptor-II.

2.4.4.3 In-solution trypsin digestion

The individual body fluids and mixtures were subjected to enzymatic in-solution trypsin digestion for “bottom-up” protein analysis. Briefly, 10 μL samples of blood diluted in water (1:500), semen diluted in water (1:200), saliva diluted in water (1:5) or urine diluted in water (1:10) were vortexed and centrifuged at 14,000 rpm for 5 min. The samples were reduced with 1.5 μL of 100 mM dithiothreitol (DTT) stock solution and incubated at 55°C temperature on a hot water bath for 30 min. After this step, the samples were alkylated using iodoacetamide (IAM, 3 μL of 100 mM solution in LC–MS grade water) and incubation at room temperature, in the dark, for 50 min. Enzymatic digestion was carried out by incubating the reaction mixture with trypsin gold (3 μL of a 0.1 $\mu\text{g}/\mu\text{L}$ solution in 25 mM NH_4HCO_3) overnight at 37°C. The trypsin digested samples (1 μL) were mixed with an equal volume of saturated matrix solution of CHCA matrix (10 mg/mL in 50% acetonitrile/ H_2O with 0.2% TFA) and spotted onto a MTP 384 polished steel plate.

2.4.5 Mass spectral and database analysis

After acquisition of MS data from the body fluid samples, the data were processed by Bruker Daltonics FLEX analysis software version 3.3. The resulting MALDI-TOF MS peptide mass fingerprints (PMF) for the “bottom-up” approach and intact protein data for the “top-down” approach were compared with Swiss-Prot and/or mascot databases

using matrix science software [http://www.matrixscience.com/search_form_select.html]. Theoretical peptide masses were calculated for proteins contained in these databases and compared against experimentally obtained tryptic peptide masses. A peptide mass tolerance of 100 ppm and one maximum missed cleavage were included as the database search parameters. Alkylation of cysteine residues (carbamidomethylation) as fixed modification and oxidation of methionine was set as variable modifications [see **Figure 2.2**] since they are common modifications on proteins and/or peptides. MS/MS analysis allowed *de novo* sequencing; matched amino acid sequences in the mass spectra were manually annotated.

MASCOT Peptide Mass Fingerprint

Your name: Sathisha Email: _____

Search title: _____

Database(s): Vertebrates_EST, contaminants, cRAP, NCBIprot, SwissProt Enzyme: Trypsin

Allow up to: 1 missed cleavages

Taxonomy: Homo sapiens (human)

Fixed modifications: Carbamidomethyl (N-term) mTRAQ (N-term), mTRAQ (Y), mTRAQ:13C(3)15N(1) (K), mTRAQ:13C(3)15N(1) (N-term), mTRAQ:13C(3)15N(1) (Y), mTRAQ:13C(6)15N(2) (K), mTRAQ:13C(6)15N(2) (N-term), mTRAQ:13C(6)15N(2) (Y), NIPCAM (C), Oxidation (HW), Phospho (ST)

Variable modifications: Oxidation (M)

Protein mass: _____ kDa Peptide tol. ±: 100 ppm

Mass values: MH⁺ M_r M-H⁻ Monoisotopic: Average

Data input: Data file: Choose File SK17_E01_...FN-VF.mgf Query

Decoy: Report top: AUTO hits

Start Search ... Reset Form

Figure 2.2 An example of the MASCOT peptide mass fingerprint (PMF) search engine screen with desired search parameters.

2.4.6 nLC-ESI-qTOF MS/MS analysis

Where possible MALDI-ToF identifications of proteins were confirmed using nLC-ESI-qTOF MS/MS. The in-solution trypsin digested body fluid mixtures [pooled samples of 1:500 blood, 1:200 semen and 1:5 dilutions of saliva, 5 μ L] was analysed and the protein markers confirmed using an AB Sciex TripleTOF 5600⁺ mass spectrometer (see **Figure 2.3**) equipped with a Nano spray source (AB Sciex). Tryptic digested peptides were applied to a Polar 3 μ m precolumn (0.3 x 10 mm, SGE Analytical Science) and eluted onto a spray tip 5 μ m C18 column (75mm x 150 mm with a bead pore size of 100Å) (Nikkyo Technos), using an Eksigent Ekspert 415 nano LC (AB Sciex). The peptides were eluted using a 35-minute gradient from 5% to 25% acetonitrile containing 0.1% formic acid at a flow rate of 300 nL/minute over 35 minutes, followed by a second gradient to 40% Acetonitrile over 7 minutes and a further step to 95% acetonitrile for 11 minutes. The mass spectrometer was operated in positive-ion mode with one MS scan of mass/charge (m/z) 350–1,500, followed by collision-induced dissociation fragmentation of +2 to +5 charge state ions that were greater than 250 counts per second for a maximum of 100 candidate ions. The nLC-MS/MS data was analyzed using Protein pilot software (version 4.5) followed by Swiss-Prot protein database analysis.



Figure 2.3 A photograph to show the Nano-spray LC [Eksigent Ekspert 415] system coupled to AB Sciex TripleTOF 5600+ mass spectrometer [photograph taken in house (Flinders Proteomics facility)].

2.5 Chapter four methods

Note: Some of methods described here are presented as they appeared in the manuscript.

2.5.1 Materials and chemicals

A comprehensive list of materials, chemical and the instruments are shown in the section 2.1.

2.5.2 In situ homogenous proteolysis procedure

A 1:1 mixture of Trypsin Gold (66 ng/ μ L) and 0.1% RapiGestTMSF (200 μ L) in 25 mM NH_4HCO_3 was sprayed onto ITO slides containing finger marks using an ImagePrep station (Bruker Daltonics GmbH, Germany) [see **Figure 2.4**]. The solutions were deposited with five layers and 10 min of incubation between each layer. After the deposition was completed, the ITO slide was incubated in a humid chamber at 37 °C for 2 h.

2.5.3 Matrix deposition

Matrix deposition (CHCA, 7 mg/mL in 50% ACN and 0.2% TFA) was deposited onto digested finger marks using an automated ImagePrep station and an operator-modified Bruker Daltonics default method optimized for sensor-controlled nebulization of the matrix.



Figure 2.4 A Photograph to show the ImagePrep station (Bruker Daltonics, Bremen, Germany) used for the automated homogenous sample preparation [Photo taken in the Flinders Mass Spectrometry Facility].

2.5.4 Preparation of finger marks

2.5.4.1 *Bloodied finger marks*

Small droplets of human blood were produced by pricking a clean finger using a sterile syringe (Livingstone International Pty Ltd., Sydney, Australia). A small volume of blood ($\sim 2 \mu\text{L}$) was rubbed on another clean index fingertip, which was then dried at room temperature. After 3 h of normal routine computer work, bloodied finger marks were deposited onto ITO-coated glass slides. For finger marks bloodied with animal blood, a small volume ($\sim 2 \mu\text{L}$) was applied to a finger (single volunteer), rubbed with another finger and a mark made on an ITO slide once the deposit had dried. A single volunteer donated bloodied finger marks for four separate experiments.

2.5.4.2 *Vaginal fluid-contaminated finger marks*

A clean finger was placed into a vagina for approximately 5 s, air dried for ~ 10 min and

then finger marks were deposited onto ITO slides. One donor provided samples for eight experiments.

2.5.5 Finger mark image capture

Optical images of all finger marks were taken before carrying out MALDI TOF-imaging experiments using either an Olympus XZS2 stereomicroscope equipped with a white light fibre optic source and a DP21 digital camera (Olympus Pty Ltd., Tokyo, Japan) or a Digitech USB microscope/5 megapixel camera with integrated white LED light source (Jaycar Electronics Pty Ltd., Adelaide, Australia).

2.5.6 Preparation of fingernail scrapings

Detail is presented in Chapter four and the related manuscript.

2.5.7 Finger marks dusted with silver/black powder and lifted

Finger marks (uncharged or charged with koala blood, $\sim 2 \mu\text{L}$), were deposited onto new glass microscope slides and dusted using silver/black magnetic powder. The dusted marks were lifted using double-sided adhesive Kapton tape, which was then stuck down, mark uppermost, onto an ITO-coated glass slide. All finger mark optical images were collected using the stereomicroscope. Finger marks were donated by a single male individual for five separate experiments.

2.5.8 MALDI-ToF, IMS and data analysis

All mass spectrometry imaging analysis was performed using an Autoflex-III MALDI-ToF-MS (Bruker Daltonics GmbH, Bremen, Germany) mass spectrometer [see Figure 2.1]. Finger marks of tryptic peptides imaging was performed in the m/z detection range of 800–3500 with a spatial resolution of 200 μm . MALDI-MS/MS data were acquired manually using the Bruker LIFT technique and a summed response from 4000 laser shots. For detection of intact proteins in finger marks (in situ, or dusted and lifted), data were acquired over a detection range of 3500–30,000 m/z . A standard peptide mixture (P.N 206195, Bruker pepmix calibrants) and protein standard-I (P.N 206355) was used for external calibration and CHCA was used as matrix. A similar procedure was followed for the detection of small molecules in dusted and lifted latent finger marks,

but data were acquired over a detection range 20–1000 m/z and CHCA was not required as the enhancement powder itself assisted ionization.

All the parameters in MALDI-TOF including laser power, mass detection range, voltage, delayed extraction and laser offset were set using Flexcontrol 3.3. FlexImaging 3.3 software was used to collect ion intensity maps of tryptic peptides and small molecules and to control Autoexecute MALDI-imaging method.

2.5.9 nLC-MS/MS and MALDI-ToF analysis of fingernail scrapings

Fingernail scrapings (traces of body fluid deposited) were collected from nylon microswabs by extraction with 50% ACN. The extracted 15 μ L solutions were treated with 5 μ L of 0.1% RapiGest™ and 5 μ L of Trypsin Gold (100 ng/ μ L). The solutions were incubated at 37 °C overnight; 3 μ L of the digested sample was analysed using an AB Sciex TripleTOF 5600+ mass spectrometer equipped with a nano-spray source (AB Sciex) and MALDI-TOF MS/MS. Detailed mass spectrometry data analysis of this section is described in chapter four.

2.5.10 DNA profiling of fingernail scrapings

Several fibres were plucked from a microswab that was used to collect vaginal fluid traces from under a fingernail (see Chapter 4). These fibres were placed directly into a 0.2-mL thin-walled PCR tube (Eppendorf, Vic, Australia). Direct PCR was carried out using the Global Filer kit (Thermo Fisher, Sydney, Australia) by adding into each PCR tube 8 μ L of PCR mix and 2 μ L of primers plus 15 μ L of sterile H₂O. Amplification was conducted on a Proflex PCR Machine (Thermo Fisher) following the manufacturer's recommendations. From each PCR, 0.5 μ L was added to 10 μ L HiDi formamide and separated on a 3500 Genetic Analyser (Thermo Fisher). The data were analysed using Genemapper IDX™ (version 3.2).

2.6 Chapter five methods

The aim of chapter five experimental methods was to demonstrate a complementary forensic 'proteo-genomic' approach on a single micro-swab for the direct identification of the "type" of biological fluid present and the identity of its "donor".

2.6.1 Fingernail preparation and collection of traces using nylon microswabs

Detailed fingernail preparation of this section is described in chapter five and section 2.3.

2.6.2 DNA profiling analysis

Microswabs were irradiated with ultraviolet light (254nm) for 6 minutes using a Stratalinker (Stratagene, Sydney, Australia). The microswabs containing traces of vaginal fluid or non-human blood traces (*Macropus rufus*) were prepared as described above.

For combined MALDI and direct PCR, approximately 50-60% of the fibres were directly plucked from the head of the device and placed into a 0.2-mL thin-walled PCR tube (Eppendorf, Vic, Australia). For standard direct PCR experiments the whole swab-head was used. Direct PCR was performed using the GlobalFiler™ kit (Thermo Fisher,) by adding into each PCR tube 8 µL of PCR mix and 2 µL of primers plus 15 µL of sterile water. Amplification was conducted on a Proflex PCR Machine (Thermo Fisher, Sydney, Australia) following the manufacturer's recommendations. From each PCR, 0.5 µL was added to 10 µL HiDi formamide and separated on a 3500xL Genetic Analyzer (Thermo Fisher). The data were analysed using GeneMapper ID-X™ (version 3.2).

For conventional forensic PCR analysis, DNA was extracted from microswabs using the Promega DNA-IQ System (Promega Corporation, WI, USA) as per the manufacturer's protocol with a final elution volume of 60 µL. The total amount of DNA recovered was determined by real-time PCR using the Quantifiler™ Trio DNA Quantification kit (Thermo Fisher). Either 0.4 ng of DNA or 15 µL of DNA extract (when 0.4 ng was not available) was amplified using the GlobalFiler™ PCR amplification kit (Thermo Fisher) and products separated on a 3500xL Genetic Analyzer as described above. Profile data were analysed using GeneMapper ID-X™ (version 1.4)

2.6.3 Proteomic analysis

2.6.3.1 Direct 'on-fibre' trypsin digestion

Several fibres were plucked from microswabs that were used for the collection of

vaginal fluid and blood traces from underneath fingernail and deposited onto an indium-oxide (ITO)-coated slide. The fibres were then treated with 5 μL of 0.2% RapiGest™ reagent and 5 μL of Trypsin Gold (125 ng/ μL) in 25 mM NH_4HCO_3 . ‘On-fibre’ enzymatic digestion was carried out on the ITO slide in a humid chamber at 37°C for 3 h. The ‘on-fibre’ digests were treated with 5 μL of MALDI matrix (CHCA in 60% ACN and 0.2% TFA) and subjected to MALDI-ToF MS/MS analysis.

2.6.3.2 ‘In-solution’ trypsin digestion

Microswabs were placed in LC-MS grade water (50 μL for swabs exposed to vaginal fluid, 200-300 μL for swabs exposed to blood) .. an Eppendorf tube (1 mL), left at room temperature for about 5 min and then the swab was removed and the tube was vortexed for around 60 s. For the 2 μL of post PCR (direct) product was diluted with 8 μL of water and then all the tube contents were centrifuged at 14,000 rpm for 5 min. Aliquots of the supernatant (10 μL) were mixed with aqueous NH_4HCO_3 solution (2 μL , 100 mM) and treated with aqueous RapiGest™ solution (5 μL , 0.2%) and aqueous Trypsin Gold solution (5 μL , 125 ng/ μL). The reaction mixtures were incubated at 37 °C overnight.

2.6.3.3 nLC-ESI-qTOF MS/MS analysis

Detailed mass spectrometry analysis for this section is presented in Chapter 3 and 5.

2.6.3.4 MALDI-ToF MS/MS analysis

All the ‘in-solution’ and ‘on-fibres’ digested fingernail residue samples were analyzed using an Autoflex-III MALDI-ToF-MS (Bruker Daltonics GmbH, Bremen, Germany) mass spectrometer (refer section 2.4.3).

Detailed MALDI-TOF MS analysis relating to this section can be found in chapter 5.

2.6.3.5 Data analysis

MALDI-ToF MS/MS peptide mass fingerprinting (PMF) data were processed with FlexAnalysis (version 3.3) software and the PMF list of m/z values was used to search the Swiss-Prot or NCBI nr protein databases with the search tool Matrix Science (<http://www.matrixscience.com>) (version 2.5). Mass tolerance up to 0.5 Da with no fixed modifications and one maximum missed cleavage were selected as the search parameters. Protein identifications were based on the presence of at least two unique

peptides and significant sequence coverage. The protein match and sequence coverage were also cross validated with theoretical and observed protein masses.

For the identification and evaluation of protein markers by nLC-ESI-qTOF MS/MS, the raw data were processed with MS converter software by generating the mascot generic file (.mgf). The file was then uploaded into Protein pilot software version 4.5 (AB Sciex, Massachusetts, USA) and searched the data against the ‘Swiss-Prot’ database by selecting a “Homo sapiens” as a taxonomy. For the identification of non-human (*Macropus rufus*) blood traces, the MS data were searched by selecting the taxonomy “All-organisms”. After database searches were completed, the protein data were exported as a text file and imported into Microsoft Excel. The Excel data were manually analysed for the presence of protein markers that arose from the material deposited underneath fingernails; only peptides of greater than 95 % confidence were considered for this data analysis step. Statistical analysis of these data was carried out in the Microsoft Excel sheet.

For the identification of DNA profiles from the direct PCR analysis, DNA loci were analysed and interpreted using Genemapper IDX™ (version 3.2, Thermo Fisher Scientific).

2.7 Chapter six methods

The aim of the work described in chapter six was to explore both “top-down” and “bottom-up” proteomic approaches and to carry out *de-novo* sequencing of Australian marsupial blood peptides that are not currently listed in databases.

2.7.1 Fingerprint preparation

2.7.1.1 Bloodied fingerprints for MALDI-TOF-IMS

A small droplet of human blood was produced by pricking a clean finger using a sterile syringe (Livingstone International Pty Ltd). A small volume of pricked blood (~2 µL) and an equal volume of dama wallaby (*Macropus eugenii*) or koala (*Phascolarctos cinereus*) blood were deposited onto a glass microscope slide and then rubbed on another clean index fingertip. The deposit was air-dried at room temperature. After 2 h of normal routine computer work, bloodied fingerprints were deposited onto an ITO-

coated glass slide. The ITO slides were marked with teaching points using Cover-Up (Marbig, Blacktown, New South Wales, Australia) white liquid. Bloodied marks on ITO slides were subjected to homogenous proteolysis by spraying them with a 1:1 mixture of Trypsin Gold (125 ng/ μ L) and 0.2% RapiGestTM-SF (200 μ L) in 25 mM NH_4HCO_3 using an ImagePrep station (Bruker Daltonics GmbH, Bremen, Germany). The solutions were deposited with 5 layers and 10 min incubation between each layer. After the deposition was completed, the ITO-coated slide was incubated in a humid chamber at 37°C for 3 h.

2.7.2 Homogenous MALDI matrix deposition

CHCA (7 mg/mL) in 60% ACN and 0.2% TFA was deposited onto digested bloodied fingerprints using an ImagePrep station and an operator-modified Bruker Daltonics default method optimised for sensor controlled nebulisation of the matrix spray conditions such as layer dryness and thin-layer deposition of the matrix.

2.7.3 Fingerprint image capture

Fingerprint image capture procedures can be referred in methods section 2.5.5

2.7.4 Bloodied fingerprint enhancement using Amido black stain

Bloodied fingerprints were prepared by rubbing 1:1 blood mixtures (human and dama wallaby or Tasmanian devil blood) on the index fingertip, allowing the deposit to dry for around 40 min at room temperature while carrying out normal computer work, and then depositing marks onto ITO-coated slides. The Amido Black stain solution was prepared by dissolving 1 g of Amido Black powder in a solution of methanol (450 mL) and glacial acetic acid (50 mL). The prepared mark was enhanced by immersing the ITO-coated slide in the Amido Black solution for 1 min, rinsing for 1 min with a wash solution containing acetic acid in methanol (10%), rinsing with a wash solution containing acetic acid in water (5%) and finally rinsing using distilled water to remove excess dark blue dye from the mark and the glass slide background. After the enhanced mark had dried in air at room temperature its optical images were collected using the stereomicroscope and USB microscope then subjected to both "top-down" and "bottom-up" proteomics analysis using MALDI TOF-MS. Sinapinic acid (SA) and CHCA

matrices were used to acquire intact proteins and tryptic peptides data, respectively.

2.7.5 Bloodied fingermarks dusted with silver-black powder and lifted

Bloodied fingermarks prepared using mixed red kangaroo or dama wallaby blood and human blood (1:1) were deposited onto new microscope glass slides and dusted using silver-black magnetic powder. The dusted marks were lifted using double-sided adhesive Kapton tape, which was then fixed onto an ITO-coated glass slide (s) with the dusted mark uppermost. The lifted marks were then rinsed (1 min) with absolute ethanol solution (to remove particles or other debris) and the marks were trypsin digested at 37°C for 3 h in a humid chamber. CHCA (7 mg/mL in 60% ACN and 0.2% TFA) matrix was spotted on distinct regions and the marks were then used for MS analysis. Optical images of fingermarks were collected using the stereomicroscope and USB microscope.

2.7.6 Hematrace test

The Amido Black stained bloodied fingermarks were swabbed (approx. 0.5 mm on dark blue region of ridge patterns) using microswabs or cotton swabs moistened with Hematrace extraction buffer. The swabs were then extracted with a further 500 µL of the buffer. Approximately 200 µL of extraction solution was added into the sample (S) region of the immunochromatographic device and allowed to migrate. The results were read within 10 min. The Hematrace test was also carried out using the CTS proficiency test bloodstains.

2.7.7 In-solution trypsin digestion

Human and all animal blood samples were diluted (1:500) in LC/MS grade water then centrifuged at 14,000 rpm for 3 min. Supernatant (8 µL) was mixed with 2 µL of 100 mM NH₄HCO₃, and then solutions were treated with 5 µL of 0.1% RapiGest™ and 5 µL of Trypsin Gold (125 ng/µL). The samples were digested by incubating at 37°C overnight. Intact and digested samples (1 µL) were spotted onto a 384-well polished steel Bruker target plate and treated with CHCA matrix solution (1 µL, 10 mg/mL) in 60% ACN and 0.2% TFA, and allowed to dry.

2.7.8 One-dimensional SDS-PAGE analysis for blood samples

The extracted blood samples (human and animal) were subjected to one-dimensional (1D) sodium dodecyl sulphate polyacrylamide gel electrophoresis (SDS-PAGE) using the mini-PROTEAN[®] TGX Stain-Free Precast gels (BIO-RAD) [see **Figure 2.5**]. Briefly, the mini gels were attached to the Bio-Rad holder, the sides were closed gently, and then placed in the tank. Prepared 1x running buffer [containing 0.025 M Tris, 0.192 M Glycine and 0.06 % SDS] was placed into the gel holder first to ensure there is no leakage. Then the tank was filled up to the marked line with 1X running buffer. The desired amount of each sample was mixed with 4X loading/sample buffer (containing 4 mg of DTT, Coomassie blue, mixture of SDS and Tris buffer) to make final volume of 20 μ L mixture [10 μ L sample + 5 μ L H₂O + 5 μ L 4X loading buffer]. The samples were denatured at 95°C on a heating block for about 2 min. The samples were centrifuged and then 15 μ L of sample mixture was loaded per well. Appropriate 5 μ L of protein standard (BIO-RAD) was loaded as protein markers. The gel was run at 200 volts for about 30 min. After electrophoresis, gels were stained with Colloidal Coomassie Blue G-250 (mixed with 40 mL of stock in 10 mL of Methanol) and left for overnight shaking. The gel slab was rinsed with HPLC grade water to remove the excess coomassie stain until minimizing the background staining. The SDS gel bands were scanned using Gel Doc[™] EZ Imager [BIO-RAD].

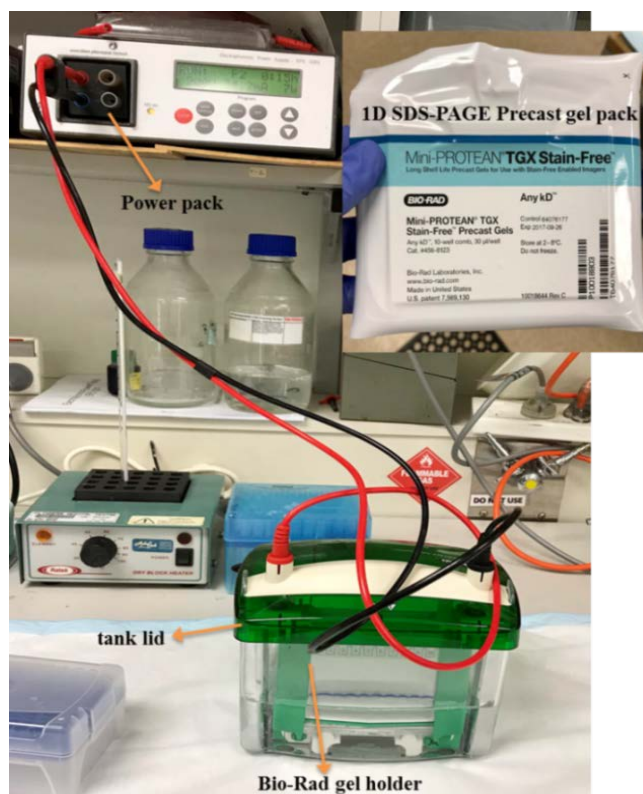


Figure 2.5 A Photograph to show the SDS-PAGE set up unit (BIO-RAD) and Precast Gels pack (Any kD mini PROTEAN[®]-stain free) used for the analysis of blood proteins. The picture was taken in house.

2.7.9 In-gel trypsin digestion

The purified SDS-PAGE protein bands were excised and subjected to in-gel trypsin digestion. Briefly, the excised band was sliced into small pieces, transferred to sterile Eppendorf tubes and destained by multiple washing with 50 mM NH_4HCO_3 and 50% acetonitrile followed by 100% ACN wash. The proteins in the gel pieces were reduced with 100 μL of freshly prepared 50 mM DTT in 50 mM NH_4HCO_3 for 30 min at 56°C on hot water bath. The supernatant was discarded and 100 μL of freshly prepared 100 mM iodoacetamide in 50 mM NH_4HCO_3 was added, and then the mixture was incubated in the dark for 30 min at room temperature.

The supernatant was removed from the gel pieces which were then dehydrated for 5 min in 100 μL of ACN and 50 mM NH_4HCO_3 . The gel pieces were dried at room temperature and enzymatic digestion was carried out by treating the pieces with Trypsin Gold (66 ng/ μL in 25 mM NH_4HCO_3) at 37 °C overnight (~ 14 h). The tryptic peptide mixture was extracted (using 50% ACN and 1% TFA) and extracts were analysed using

MALDI-TOF MS/MS and nLC-ESI-qTOF MS/MS.

2.7.10 MALDI-TOF-IMS and data analysis

All mass spectrometry analysis and fingerprint imaging analysis were performed using an Autoflex-III MALDI-TOF-MS (Bruker Daltonics) mass spectrometer. Detailed mass spectrometry analysis relating to this section is given in chapter six and the related manuscript.

2.7.11 nLC-ESI-qTOF MS/MS and protein database analysis

All in-gel digested samples were analyzed for the protein identification using the AB Sciex TripleTOF 5600+ mass spectrometer equipped with an Eksigent Ekspert 415 nano LC (AB Sciex) separation technique. Detailed mass spectrometry information and protein database analysis for human and Australian marsupial blood peptides can be found in methods section 2.4.6 and in chapter six.

Chapter 3

Chapter 3: Direct identification of forensic body fluids using matrix-assisted laser desorption/ionization time-of-flight mass spectrometry

Int. J. Mass Spectrom. 2016, 397, 18-26. <https://doi.org/10.1016/j.ijms.2016.01.002>

Sathisha Kamanna¹, Julianne Henry², Nicholas H. Voelcker³, Adrian Linacre⁴, K. Paul Kirkbride^{1*}

¹School of Chemical and Physical Sciences, Flinders University, Sturt Road, Bedford Park, 5042 Adelaide, South Australia, Australia

²Forensic Science SA, 21 Divett Place, 5000 Adelaide, South Australia, Australia

³Future Industries Institute, University of South Australia, Mawson Lakes, 5095 South Australia, Australia

⁴School of Biological Sciences, Flinders University, Sturt Road, Bedford Park, 5042 Adelaide, South Australia, Australia

Selected supplementary information relating to this research article will appear in this chapter and remaining data are provided in the appendix of this thesis.

Journal Impact Factor: 1..

SCImago Journal Rank (SJR) 27 out of 62 (Spectroscopy category)

Number of citations: 4

This article has 4 social media (Twitter) interactions (relating to an International Journal of Mass Spectrometry “best paper” award presented at the ASMS conference)

Statement of Authorship for Chapter 3 manuscript

Title of Paper	Direct identification of forensic body fluids using matrix-assisted laserdesorption/ionization time-of-flight mass spectrometry
Publication Status	Published
Publication details	Published in International Journal of Mass Spectrometry 2016 , 397, 18-26

AUTHOR CONTRIBUTIONS

By signing the Statement of Authorship, below mentioned each author certified that their stated contribution to the publication is accurate and that permission is granted for the research article to be included in the candidate's thesis.

Name of Principal Author (Candidate)	Sathisha Kamanna		
Contribution to the paper	Designed the research and experimental method. Performed all laboratory work and analysis, interpreted data and drafted/edited the manuscript.		
Signature		Date	March, 2018

Name of Co-author	Julianne Henry		
Contribution to the paper	Provided manuscript draft assistance/evaluation, industry/forensic biology advice, provided access to proficiency test/volunteer samples for analysis and acted as industry research co-supervisor.		
Signature		Date	March, 2018

Name of Co-author	Nicholas H. Voelcker		
-------------------	----------------------	--	--

Contribution to the paper	Provided manuscript draft assistance/evaluation, specialist mass spectrometry advice and acted as an external academic research co-supervisor.		
Signature		Date: 15/03/2018	March, 2018

Name of Co-author	Adrian Linacre		
Contribution to the paper	Provided manuscript draft assistance/evaluation, forensic biology advice and research co-supervision.		
Signature		Date	March, 2018

Name of Co-author	K. Paul Kirkbride		
Contribution to the paper	Supervised research, provided manuscript draft assistance/evaluation and acted as corresponding author.		
Signature		Date	March, 2018

3.1 Publication context

At the time when the research described in this chapter commenced, only a few research articles were published that described the identification of candidate protein markers in biological fluids for forensic purposes using mass spectrometry [142, 143, 145]. These involved comparative proteomic fractionation-mass spectrometric techniques such as liquid chromatography–mass spectrometry/mass spectrometry (LC-MS/MS) and LC–matrix-assisted laser desorption/ionization time of flight mass spectrometry (LC–MALDI-ToF-MS). These differential proteomics techniques are important in biological mass spectrometry for **discovery** of “biomarkers” in body fluids and tissues. However, once relevant biomarkers have been discovered it may not necessarily be the case that the same techniques have to be used in more routine biomarker **detection** tasks involving those fluids and tissues, such as in forensic casework. Fractionation of complex mixtures of proteins, is time consuming, complex and carries with it the risk of column carry over between samples; therefore research aimed at detecting biomarkers using a less complex, more streamlined approach suitable for high-throughput and cost-sensitive for forensic casework was warranted.

The current issues and practices of human body fluid identification (such as forensic presumptive tests, DNA profiling analysis and classical proteomic technologies) and opportunities for innovation and improvement were considered when designing the research aims of this chapter and the manuscript. In particular, the work of Bradshaw et al. [147], which showed that MALDI-ToF (in imaging mode) was capable of detecting blood proteins in fingerprints, was considered and extended.

Here is presented a manuscript that titled “Direct Identification of Forensic Body Fluids using Matrix-Assisted Laser Desorption/Ionization Time-of-Flight Mass Spectrometry” [MALDI-TOF MS]. It describes work that was directed towards developing a simple and streamlined proteomics assay based upon mass spectrometry that would be suitable for examining the types of body fluid specimens received by forensic biologists in relation to the investigation of serious crimes against the person, such as murder and sexual assault. This research article describes a single-step confirmatory methodology for the positive identification of blood, semen, saliva and urine, especially mixtures of them, using MALDI-TOF MS. In this study we have used two different MALDI sample preparation strategies [see Figure 3.1]: the analysis of untreated aliquots of liquid fluids

(or extracts or suspensions of dried flakes of them); or analysis of body fluid deposits in situ on tufts of fibres plucked from stained fabrics (e.g., various types of fabric fibres) and swabs (cotton and nylon microswabs). Two different ionization substrates, Bruker MTP polished steel plate and indium tin oxide (ITO) coated glass slides, were used depending upon which sample preparation strategy was chosen. Aged stains were successfully analysed; blood proteins were easily detected in an eleven years old proficiency test stain. Hemoglobin was used as a marker for blood, α -amylase for saliva, semenogelins, prostate-specific antigen and acid phosphatase for seminal fluid and uromodulin for urine. In this article were reported initial findings in regards to the development of the simplified methodology. Additionally, the body fluid protein markers were confirmed using nLC-ESI-qTOF MS/MS analysis. The key to the methodology is that although body fluids are complex mixtures of proteins, MALDI-ToF is capable of detecting only the most abundant proteins, which in the case of forensically-relevant fluids are biomarker proteins. Although a particular biomarker may be found in other tissues, it will be present at such a low level in those tissues that it cannot be detected using MALDI-ToF and/or those tissues are not likely to be encountered in evidence. This finding was published in the International Journal of Mass Spectrometry and the full article is presented here.

3.2 International Journal of Mass Spectrometry [Kamanna *et al.* 2016]

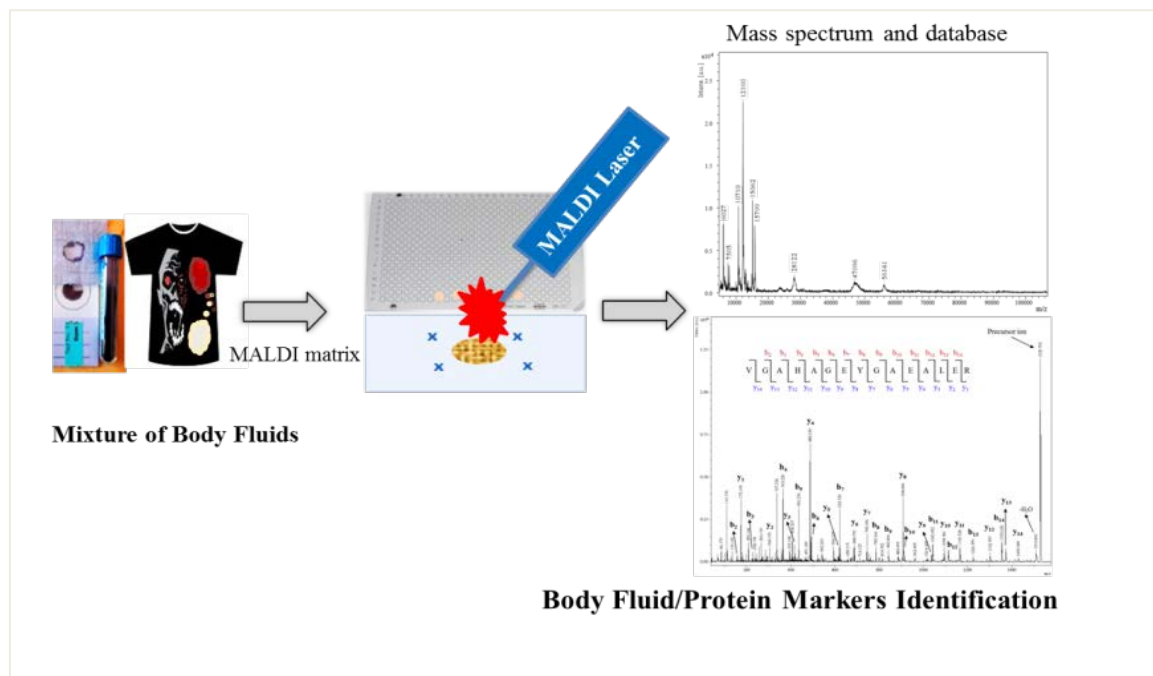


Figure 3.1 A graphical abstract for the article showing the two different MS ionization substrates for direct detection of body fluid protein markers from various types of fabric substrates and liquid fluids.



Direct identification of forensic body fluids using matrix-assisted laser desorption/ionization time-of-flight mass spectrometry



Sathisha Kamanna^a, Julianne Henry^b, Nicholas H. Voelcker^c, Adrian Linacre^d,
K. Paul Kirkbride^{a,*}

^a School of Chemical and Physical Sciences, Flinders University, Sturt Road, Bedford Park, 5042 Adelaide, South Australia, Australia

^b Forensic Science SA, 21 Divett Place, 5000 Adelaide, South Australia, Australia

^c Future Industries Institute, University of South Australia, Mawson Lakes, 5095 South Australia, Australia

^d School of Biological Sciences, Flinders University, Sturt Road, Bedford Park, 5042 Adelaide, South Australia, Australia

ARTICLE INFO

Article history:

Received 6 October 2015

Received in revised form

16 December 2015

Accepted 14 January 2016

Available online 8 February 2016

Keywords:

Matrix-assisted laser desorption/ionization
time-of-flight mass spectrometry
(MALDI-ToF MS)

Body fluids

Fabric substrates

Forensic science

Protein biomarkers

ABSTRACT

The examination of body fluids such as blood, seminal fluid, urine or saliva is a key aspect of forensic science in regards to investigation of crimes against the person such as murder and rape. This article describes a streamlined and simplified approach for the identification of body fluids using matrix-assisted laser desorption/ionization time-of-flight mass spectrometry (MALDI-ToF-MS) that avoids fractionation or isolation of proteins. It is applicable to the examination of microliter quantities (or less) of neat fluids, extracts or suspensions of dried fluids or deposits of fluids in situ on tufts of fibers plucked from fabrics, which has practical application in the examination of crime-related items such as underwear or face masks. Hemoglobin was used as a marker for blood, α -amylase for saliva, semenogelins, prostate-specific antigen and acid phosphatase for seminal fluid and uromodulin for urine. Aged stains were successfully analyzed; blood proteins were easily detected in an 11-year-old blood stain.

© 2016 Elsevier B.V. All rights reserved.

1. Introduction

The examination of body fluids such as blood, seminal fluid, urine or saliva is a key aspect of forensic science in regards to crimes against the person such as murder and rape. The main test carried out on fluid deposits is DNA profiling in order to establish from whom the body fluid originated. However, it can be extremely important in a case, sometimes even crucially important, to establish the identity of the fluid(s) in the crime deposit in order to establish a link between a body fluid and the resulting DNA profile. Body fluids can be encountered in crime investigation as mixtures, for example blood and semen, semen and saliva, or mixtures containing urine. Several presumptive tests for body fluids are available but they can be ambiguous or provide false negative or false positive results, especially in the case of mixed deposits.

Chemical tests (such as the luminol, Kastle–Meyer, leucomalachite green, and benzidine tests [1,2]) have been used for over 40 years as presumptive tests for blood and more recently medical test kits such as Hemastix and Hematrace [3] have been brought into use. In regards to chemical tests and Hemastix, the detection is based upon chemical reactions catalyzed by the heme group (iron) present in hemoglobin within the blood, but cross reactivity with other materials such as bleach, saliva, and other animal and fruit/vegetable proteins (e.g., peroxidases) is known [4,5]. Hematrace kits, being based upon immunochromatography, are much more specific but can lead to false negatives when high concentrations of hemoglobin are present, give rise to false positives in the presence of blood from ferrets and higher primates other than humans, and rely upon the epitope (the target for the antibody) being intact. Furthermore, these presumptive tests cannot distinguish between related body fluids such as venous blood and menstrual blood. Ultraviolet (UV) light can be used to stimulate fluorescent emission from semen stains, which is not only useful in presumptively indicating the presence of semen but it can be used by investigators to search a crime scene for invisible semen stains. However, emission can be quenched by various domestic substances or swamped by emission from other fluorophores present in items such as clothing [6]. The

* Corresponding author. Tel.: +61 882013011.

E-mail addresses: kama0073@flinders.edu.au (S. Kamanna),

Julianne.Henry@sa.gov.au (J. Henry), Nico.Voelcker@unisa.edu.au (N.H. Voelcker), adrian.linacre@flinders.edu.au (A. Linacre), paul.kirkbride@flinders.edu.au (K.P. Kirkbride).

prostatic acid phosphatase (AP) test [7], which was developed in the late 1950s, has been reported to give some false positive color changes with plant material (e.g., tea plants [8]), and substances found within vaginal fluids and female urine as well as semen [9]. This could lead to confusion when identifying the body fluids of rape cases, where identifying fluid samples must indicate whether sexual intercourse had occurred or not. In addition, enzymes can degrade when exposed to environmental factors such as heat, mold, putrefaction, or denaturing chemicals. Immunochromatographic tests for the detection of semenogelin, prostate specific antigen (PSA), and prostatic acid phosphatase are now available [10–14]. For saliva, the most popular and simple test that is widely used in forensic laboratories for the detection of salivary α -amylase is the Phadebas assay [15]. The presence of α -amylase enzyme in a saliva sample or stain hydrolyses α -1-4 glycosidic bonds of a dye-labeled starch impregnated in a test paper, releasing the dye that forms a visible blue stain in the paper. However, it has been shown that false positive results are produced by hand cream, face lotion, urine and feces [16]. Immunochromatographic tests also are available for saliva, but false positive salivary amylase results have been reported for certain citrus fruits (the calamondin, or cumquat, [17]). Urine is another body fluid encountered in sexual assault, rape or murder, harassment and/or mischief cases. The traditional method for identifying urine is based on the detection of urea or urea nitrogen [18]. Urine is difficult to detect due to the low sensitivity of urea tests and many false positive results can be expected from this assay due to the ubiquity of urea. Previous studies [19] presented a method for indication of human urine by detection of five major 17-ketosteroid conjugates using HPLC–MS analysis. Another method relies upon the reaction between urine and a urease enzyme to form ammonia that in turn causes a color change in bromothymol blue indicator [20]. However, semen and sweat stains also display weak false positive results because of their urea content. The Tamm–Horsfall glycoprotein (THP), also known as uromodulin, has been used as a target in immunochromatographic tests (RSID™) for urine, but it is not a human-specific test [21].

While current forensic practices in regards to the identification of some body fluids using immunochromatographic tests are quite reliable, there are some significant shortcomings including: a shortage of immunochromatographic tests for a number of body fluids of forensic interest; the need to verify presumptive tests with confirmatory tests; and, as the presumptive tests respond to a single fluid, the requirement for a combination of tests in order to fully characterize a fluid or mixture. For these reasons, alternative ways to identify body fluids for forensic purposes are being sought.

Recently, research articles have been published that describe the use of mass spectrometry-based techniques for the identification of protein biomarkers for forensic purposes in biological fluids including hemoglobin in blood, α -amylase in saliva, and PSA and semenogelin protein markers in semen [22–25]. It has been shown that mass spectrometry-based techniques can detect body fluid biomarker proteins accurately, reproducibly and with high sensitivity. Identification is at the molecular level (i.e., protein sequence level), is species-specific and multiple markers for each type of body fluid can be used to increase the confidence of identification.

In 2013, Yang et al. used liquid chromatography–matrix-assisted laser desorption/ionization time of flight mass spectrometry (LC–MALDI–ToF–MS) for the identification of protein markers in different body fluids [22]. Another recently published article [24] describes a specific protein marker approach using comparative proteome fractionation followed by liquid chromatography–mass spectrometry/mass spectrometry (LC–MS/MS) analysis. The authors identified a panel of 29 candidate protein markers and suggested specific indicators of human urine, vaginal fluid, peripheral blood and menstrual blood [24]. These “classical” proteomics methods can play a significant role in

the biological mass spectrometry for biomarker discovery in body fluids for forensic purposes. However, these technologies rely on some level of fractionation of the complex mixture of proteins, are time consuming, complex and bear the risk of column carry over between samples [26]. In other recent work, which extended an on-going theme of employing MALDI for the direct detection of endogenous and exogenous small molecules in fingerprints, it was indicated that MALDI can be used for the direct detection of blood proteins in fingerprints [25].

The aim of the research described in this paper was to extend and simplify MS-based identification of protein biomarkers and develop a methodology that is appropriate and practical for use in forensic casework. Here, we present a direct methodology for the positive identification of a broad range of body fluids of interest to forensic science (e.g., blood, semen, saliva and urine), including mixtures, using MALDI–TOF MS. In this study, we have used two different MALDI sample preparation strategies; the particular method chosen depended upon the nature of the evidence under examination. In the first strategy, untreated aliquots of liquid fluids or extracts or suspensions of dried flakes of them (such as would be found on non-porous surfaces) can be analyzed. In the second strategy, which can be applied to deposits on porous evidence such as garments or swabs, we present a novel and elegant approach that simply involves plucking single fibers (or a small tuft of them) from the fabric and directly analysing the body fluid deposits in situ. Two different ionization substrates, Bruker MTP polished steel plate and indium tin oxide (ITO) coated glass slides, were used depending upon which sample preparation strategy was chosen. We then combine these two sampling strategies with both “top-down” proteomic analysis (which is a rapid process ideal for screening of samples) and bottom-up analysis (which is used as a confirmation step).

2. Experimental

2.1. Materials

α -Cyano-4-hydroxycinnamic acid (CHCA), sinapinic acid (SA), dithiothreitol (DTT), iodoacetamide (IAM), LC–MS grade water, acetonitrile (ACN) and trifluoroacetic acid (TFA) were purchased from Sigma–Aldrich (NSW, Australia). Trypsin gold (MS grade) was obtained from Promega (Madison, WI, USA). Indium–tin oxide (ITO) coated slides were purchased from Shimadzu (NSW, Australia). Polished steel plate (MTP) and protein/peptide mixture of external calibrants was obtained from Bruker Daltonics (Bremen, Germany).

Pieces of 100% nylon, cotton and cellulose acetate fabric (all white) were purchased from Spotlight (Adelaide, South Australia) and were laundered in lukewarm water for 30 min using non-enzymatic laundry powder (“Fab” brand, Colgate–Palmolive, Pty Ltd.) at the level recommended by the manufacturer. The fabric pieces were then rinsed several times in cold water and left to dry naturally.

Body fluid samples were sourced from eight volunteers from FSSA and Flinders University and semen samples were sourced from six patient volunteers from Flinders Fertility, Adelaide, South Australia pursuant to Southern Adelaide Clinical Human Research Ethics Committee Application 440.14 – HREC/14/SAC/455. Four proficiency test kits provided by Collaborative Testing Services (CTS) Incorporated (Stirling, Virginia, USA) were used. The tests used were 04-571 (provided by CTS in January 2004), 11-573 (May 2011), 12-584 (July 2012) and 14-582 (March 2014), which were provided to Forensic Science SA (FSSA, Adelaide, South Australia) as part of their quality assurance program. Each test involved four pieces of fabric stained with various body fluids; they were manufactured to resemble typical stained items that might be

encountered in investigation of crimes. Samples were stored after their initial receipt from CTS at room temperature in sealed paper and plastic bags in the dark.

2.2. Scanning electron microscopy

Scanning electron microscopy (SEM) images were collected using an FEI Inspect F50 instrument. Fibers plucked from clean fabric pieces and from pieces that had been exposed to liquid semen were attached to aluminum SEM stubs (12.5 mm) using double sided adhesive carbon tape discs and then coated with platinum metal (13 nm thick). Images were collected using 5 keV beam energy, spot size of 6.3 and magnification between 100× and 3000×.

2.3. MALDI-TOF MS instrumentation

All mass spectrometric analysis was performed using an Autoflex-III MALDI-TOF-MS (Bruker Daltonics, Bremen, Germany) mass spectrometer. The instrument ion source was equipped with a neodymium-doped yttrium aluminum garnet [Nd:YAG $\lambda = 355$ nm] Smart Beam 200 Hz solid state laser. Reflectron positive (RP) ion mode was used with 20 kV accelerating voltage and delayed extraction ions of 200 ns for detection of peptides in the m/z detection range of 600–4000. Large protein data (m/z detection range 5000–110,000) were acquired using linear positive (LP) ion mode. All the MALDI instrumental parameters including laser power, mass detection range, voltage, delayed extraction and laser offset were set using Flexcontrol 3.3. Each mass spectrum collected represented the sum of the data from 2000 laser shots. In order to account for inhomogeneous distribution of matrix summed spectra were collected at several locations in the body fluid deposit and

an average spectrum was produced. A standard peptide mixture (P.N: 206195, Bruker pepmix calibrants) and protein standard-I (P.N: 206355) were used for external calibration.

2.4. MALDI-TOF MS sample preparation

2.4.1. Deposition of body fluid on fabric materials

The crude individual body fluids and their mixtures were deposited on pieces of nylon, cotton and cellulose acetate fabric. Individual fabric body fluid specimens were prepared by spotting 10 μL of each type of body fluids (blood, semen and saliva) on the fabric. For body fluid mixtures, samples containing blood (5 μL of 1:50 dilution in water) mixed with semen (10 μL), or blood (5 μL of 1:50 dilution in water) mixed with saliva (15 μL) were deposited on each of the fabric materials. The concentration of blood used and its ratio to the other body fluids in these mixtures was calculated to balance the amounts of protein from each body fluid. All fabric specimens were dried at stored room temperature for 3 days before prior to analysis.

2.4.2. Analysis on MTP 384 polished steel plate

The volunteer neat body fluid mixtures were prepared for “top-down” intact protein analysis as follows: 2 μL of 1:50 dilution of blood in water, 3 μL of raw semen and 5 μL of raw saliva were mixed and from this 1 μL was treated with an equal volume of a saturated matrix solution of sinapinic acid (SA) in 50% LC-MS grade acetonitrile/ H_2O with 0.1% trifluoroacetic acid. These mixtures (2 μL) were deposited on MTP 384 polished steel plate. Urine samples of 1 μL were spotted with an equal volume of saturated α -cyano-4-hydroxycinnamic acid (CHCA) matrix in 50% LC-MS grade acetonitrile/ H_2O with 0.2% trifluoroacetic acid.

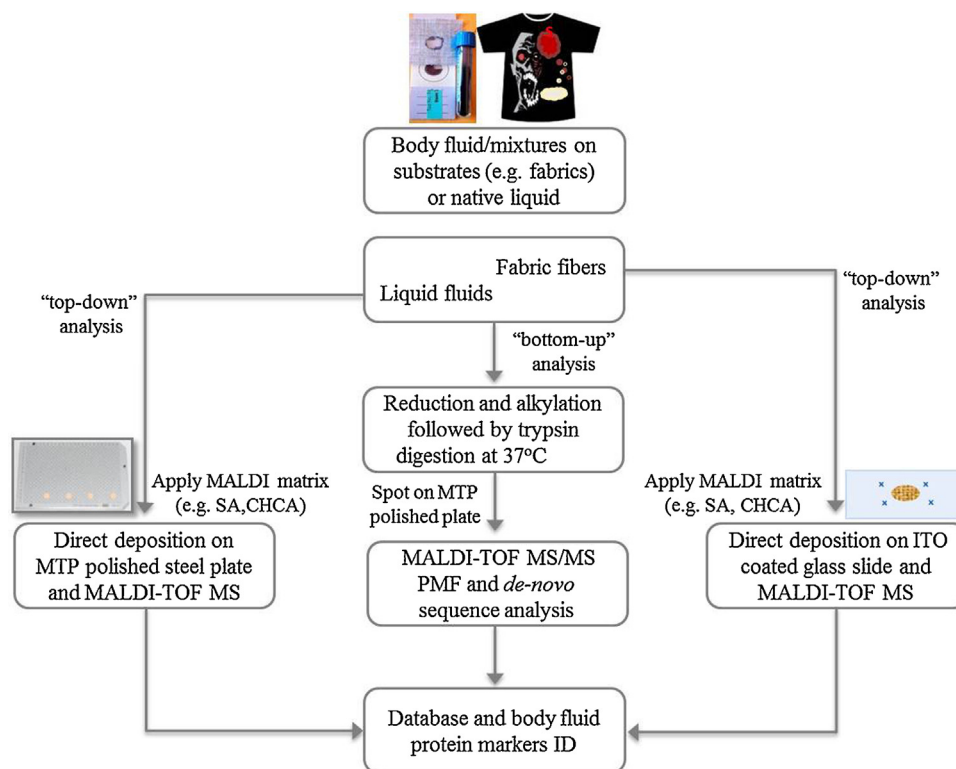


Fig. 1. A schematic of the overall experimental design developed for direct identification of protein markers from body fluid mixtures (e.g., blood and semen, semen and saliva, urine and/or other stains) using MALDI-TOF MS. The workflow consists of two different MALDI sample preparation strategies (the analysis of body fluid deposits in situ on fabric or the analysis of untreated aliquots of liquid fluids and extracts) using two different ionization substrates (Bruker MTP polished steel plate for neat samples or extracts and ITO-coated glass slides for fiber samples).

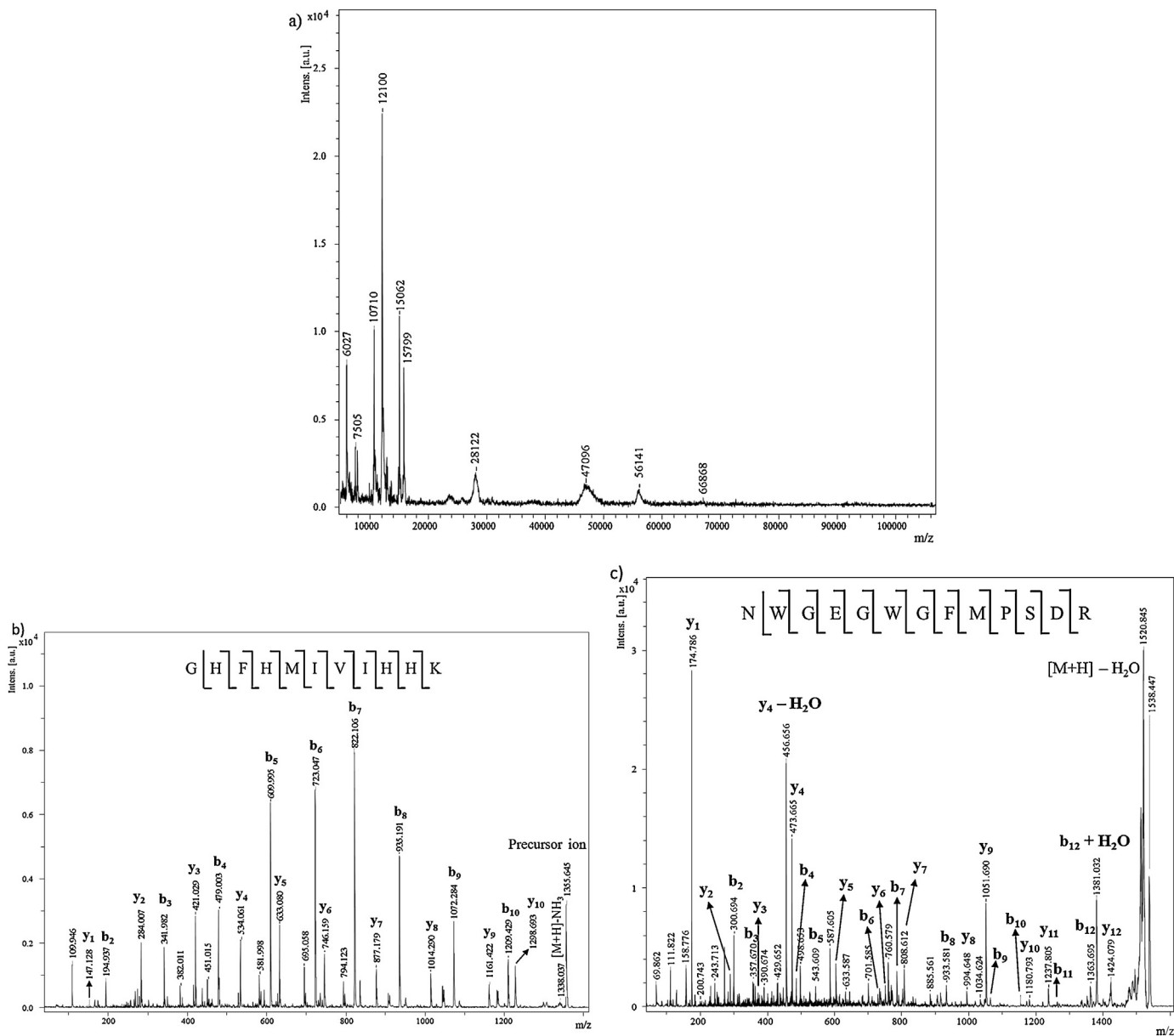


Fig. 2. (a) Typical MALDI-TOF MS protein profiles of volunteer body fluids mixture (1:50 blood + raw semen + raw saliva). The mixtures were spotted with equal volume of SA matrix and the data acquired in linear positive mode. (b) MALDI-MS/MS spectrum of precursor ion m/z 1355.64 of a protein fragment of semenogelin 2 (semen). (c) MS/MS spectrum of precursor ion m/z 1538.44 of a protein fragment of alpha amylase 1 (saliva) and matched “b” and “y” ions are indicated in the spectra. The 1 μ L of body fluid samples were directly mixed with an equal volume of MALDI matrix (α -CHCA 10 mg/mL in 50% LC-MS grade ACN/H₂O) and mixture was spotted on MTP polished steel plate.

Table 1

List of most abundant proteins identified from direct analysis of volunteers body fluid samples and the approximate amounts of proteins present in them.

Body fluid	Protein detected	Accession number	Swiss-Prot entry name	Sequence coverage (%)	Number of matched peptides	% of total protein (Ref.)
Blood	Hemoglobin subunit beta	P68871	HBB_HUMAN	94	15	~55 [29]
	Hemoglobin subunit alpha	P69905	HBA_HUMAN	71	10	
	Hemoglobin subunit delta	P02042	HBD_HUMAN	48	7	
Saliva	Alpha-amylase 1	P04745	AMY1_HUMAN	51	22	~30–50 [30–32]
	Alpha-amylase 2B	P19961	AMY2B_HUMAN	47	21	
	Pancreatic α -amylase	P04746	AMYP_HUMAN	38	18	
Semen	Semenogelin 2	Q02383	SEM2_HUMAN	31	17	~40 [33]
	Semenogelin 1	P04279	SEM1_HUMAN	25	12	
	Prostate specific antigen (PSA)	P07288	KLK3_HUMAN	32	8	
Urine	Uromodulin	P07911	UROM_HUMAN	19	14	~30 [34]

Bold font indicates the major protein markers with a high sequence coverage.

2.4.3. Analysis on ITO-coated slides

In the direct MALDI-TOF MS analysis of body fluid on dried fabric fibers, a small tuft of fibers from each of the semen-treated fabrics (<0.5 cm) were directly deposited onto an ITO-coated conductive glass slide and then 3 μ L of SA matrix in 50% LC-MS grade acetonitrile/H₂O with 0.1% TFA was deposited on the fibers. The slide was dried at room temperature and then inserted into an Autoflex-III MALDI-TOF MS using a MALDI-imaging slide adaptor-II.

2.4.4. In-solution trypsin digestion

The individual body fluids and mixtures were subjected to enzymatic in-solution trypsin digestion for “bottom-up” protein analysis. Briefly, 10 μ L samples of blood diluted in water (1:500), semen diluted in water (1:200), saliva diluted in water (1:5) or urine diluted in water (1:10) were reduced with 1.5 μ L of 100 mM dithiothreitol (DTT) stock solution and incubated at 55 °C temperature on a hot water bath for 30 min. After this step, the samples were alkylated using iodoacetamide (IAM, 3 μ L of 100 mM solution in LC-MS grade water) and incubation at room temperature, in the dark, for 50 min. Enzymatic digestion was carried out by incubating the reaction mixture with trypsin gold (3 μ L of a 0.1 μ g/ μ L solution in 25 mM NH₄HCO₃) overnight at 37 °C. The trypsin digested samples (1 μ L) were mixed with an equal volume of saturated matrix solution of CHCA matrix (10 mg/mL in 50% acetonitrile/H₂O with 0.2% TFA) and spotted onto a MTP 384 polished steel plate.

2.5. Mass spectral and database analysis

After acquisition of MS data from the body fluid samples, the data were processed by Bruker Daltonics FLEX analysis software version 3.3. The resulting MALDI-TOF MS peptide mass fingerprints (PMF) for the “bottom-up” approach and intact protein data for the “top-down” approach were compared with Swiss-Prot and/or mascot databases using matrix science software [http://www.matrixscience.com/search_form_select.html]. Theoretical peptide masses were calculated for proteins contained in these databases and compared against experimentally obtained tryptic peptide masses. A peptide mass tolerance of 100 ppm and one maximum missed cleavage were included as the database search parameters [27]. Alkylation of cysteine residues (carbamidomethylation) as

fixed modification and oxidation of methionine was set as variable modifications since they are common modifications on proteins and/or peptides [28]. MS/MS analysis allowed de novo sequencing; matched amino acid sequences in the mass spectra were manually annotated. The scheme of overall experimental workflow of the mass spectrometry based approach for direct identification of body fluid mixtures on substrates or native liquid (e.g., blood, semen, saliva and urine and/or other statins) is represented in Fig. 1.

3. Results and discussion

3.1. Top-down MALDI-TOF measurement of intact body fluid mixtures

To identify intact protein markers, mixtures were prepared using diluted blood (2 μ L of 1:50 dilution in water), raw semen (2 μ L) and raw saliva (5 μ L) and from this 1 μ L was mixed with an equal volume of saturated SA matrix solution. The mixtures were then deposited on the MTP polished steel plate, dried at room temperature, and the sample target plate was loaded into the MALDI-TOF mass spectrometer. Fig. 2a displays typical protein profiles over the m/z range 5–120 kDa. All proteins were detected using linear, positive mode: blood (m/z ~ 15.0 and 15.7 kDa), semen (~28.1 kDa, 47.0 kDa and its fragment proteins at 6.0 and 10.7 kDa) and saliva (~56.1 and 12.1 kDa).

3.2. Body fluids protein digestion and “bottom-up” identification

To positively identify the marker proteins using sequence confirmation, body fluids were mixed with 100 mM NH₄HCO₃, reduced with DTT, alkylated with 100 mM IAM and digested overnight at 37 °C with trypsin. Each digested sample (1 μ L) was mixed with an equal volume of saturated matrix solution (α -CHCA in 50% LC-MS grade acetonitrile/H₂O with 0.2% TFA) and deposited on an MTP 384 ground steel target plate prior to MALDI-TOF-MS/MS in positive reflectron mode.

The obtained PMF results and molecular mass values were assessed using either Swiss-Prot or NCBI nr protein database and matrix science search engine [http://www.matrixscience.com/search_form_select.html].

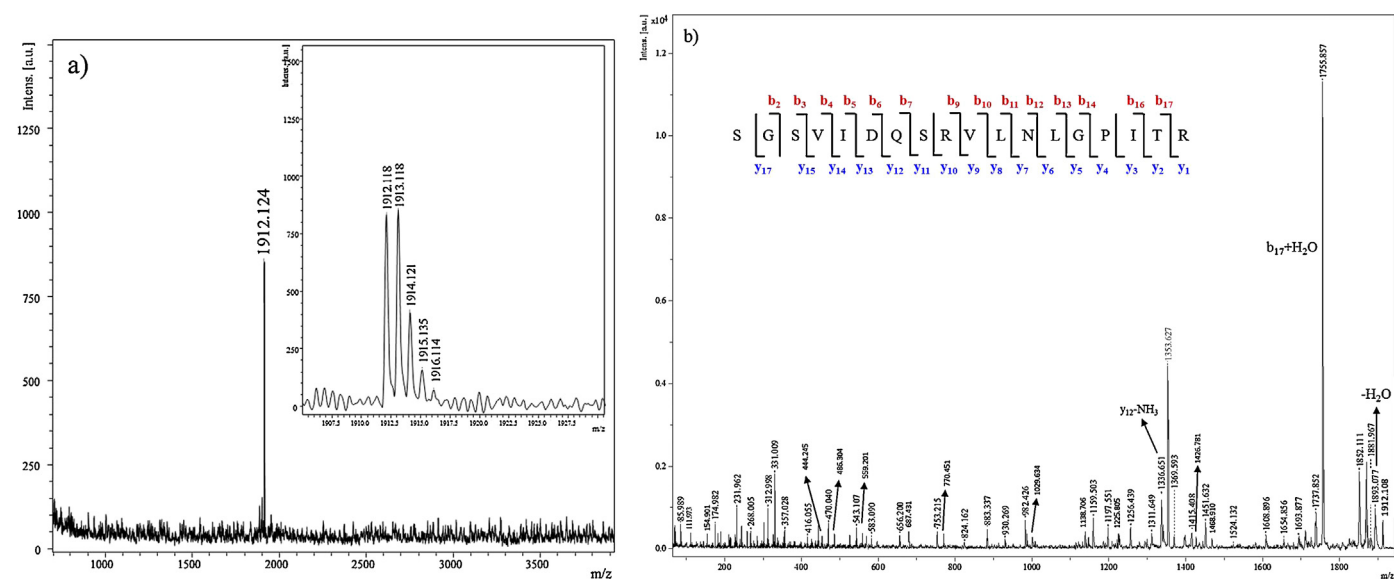


Fig. 3. (a) MALDI-TOF mass spectrum of human urine. 1 μ L of urine samples were directly spotted with α -CHCA matrix on MTP target and the endogenous peptide (m/z 1912.12) of uromodulin was identified using database analysis (Swiss-Prot). Inset: a mass spectrum showing isotopic pattern of the peptide. (b) MALDI-MS/MS data of urine peptide m/z 1912.12 and matched ion fragment masses are identified on X-axis, intensities on Y-axis.

A typical proteomic analysis of body fluids results in the detection of tens to hundreds of proteins, some of which can be detected at high levels in a wide range of tissues and fluids and some that are differentially expressed, that is, present in abundance in one particular fluid and in low amounts in other fluids. For example, PSA is present in abundance in seminal fluid but it is also found in lower levels in vaginal fluid. In the direct approach described here, only the most abundant proteins in a fluid (or mixture of fluids) are detected and those that are present in low abundance are not. Using the example of PSA again, direct analysis of seminal fluid results in the detection of PSA but the direct analysis of vaginal fluid does not (results not shown). This situation is repeated for other body fluids of forensic interest and as a consequence, despite the simplicity of the direct approach, it is fit for the purpose of distinguishing between body fluids for forensic purposes. It is therefore neither necessary nor desirable to isolate (fractionate) the differentiated proteins from body fluids prior to mass spectrometry or to perform an assay to determine the relative abundance of these proteins. Of course, in mixtures of fluids where one

component greatly exceeds the amount of the other then only the most abundant proteins in the most abundant component will be detected and the minor contributor to the mixture will most likely not be detected. However, the operational range observed for the direct method is nevertheless still practical for many forensic investigations.

Table 1 indicates the most abundant proteins detected in samples of each body fluid, together with the reported amounts of total protein present in them. A complete list of proteins matched within each body fluid and peptide ranking based on the confidence level for each protein is given in Supplementary Data 1.

The following were selected as practical “biomarkers” for forensic purposes: semenogelin I and II and PSA for semen; α - and β -subunits of uromodulin for blood; α -amylase 1 and 2 for saliva; and uromodulin for urine. Although MALDI-MS data for hemoglobin, semenogelins and amylases have been described previously [22], such data do not appear to be available in the literature for uromodulin. Fig. 3 shows MALDI MS and MS/MS data obtained for uromodulin.

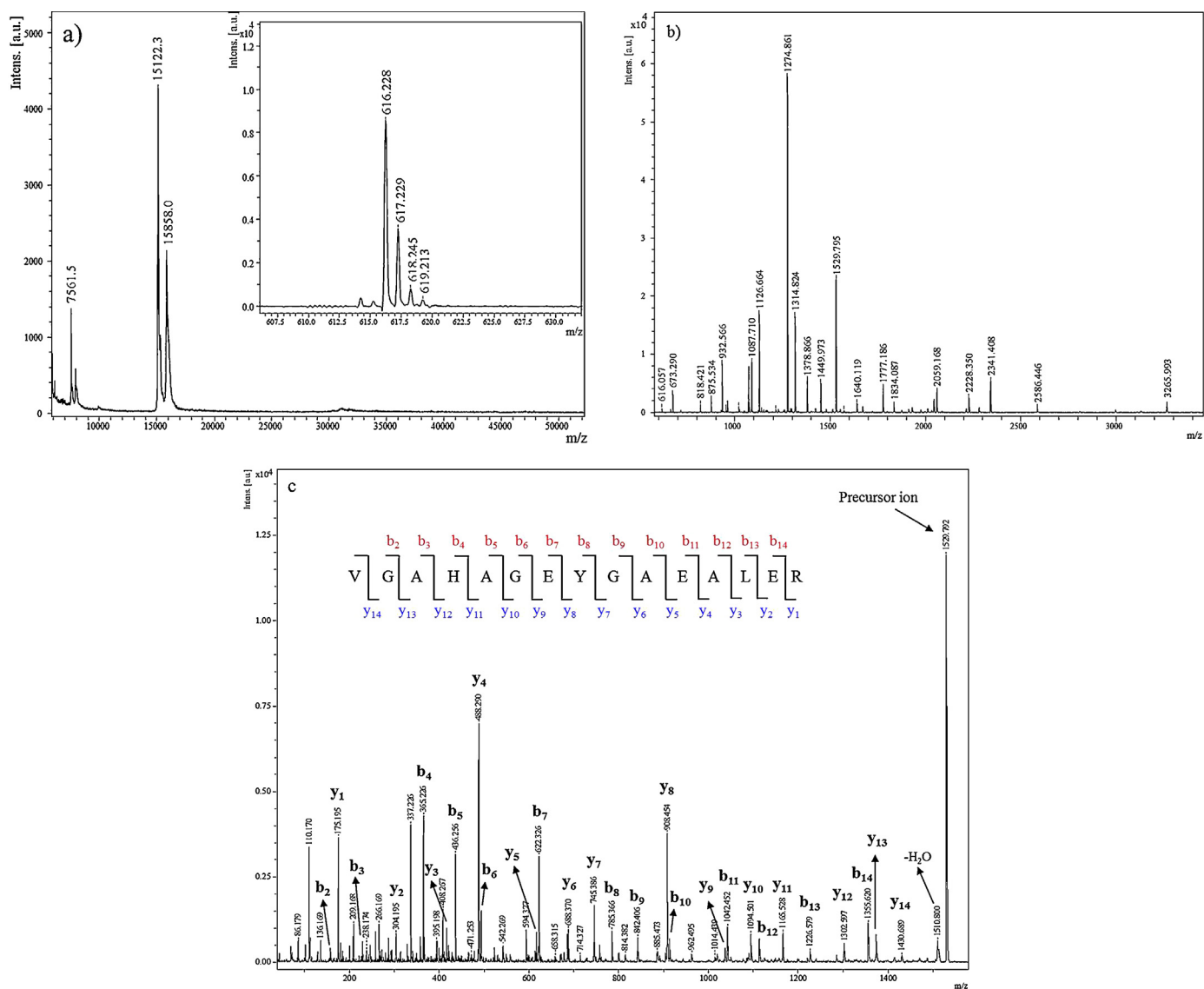


Fig. 4. MALDI-TOF mass spectra of an 11-year-old proficiency test sample from the “victim’s” shirt. (a) Intact protein mass matched to human α - and β -hemoglobin proteins, inset spectrum indicates the presence of heme group (m/z 616.2). (b) Tryptic peptides (PMF), (c) MS/MS spectrum of precursor ion m/z 1529.79 of α -subunit of hemoglobin. Inset: sequence of the corresponding peptide based on MALDI-LIFT fragmentation pattern; matched “b” and “y” ions are indicated in the spectra.

3.3. MALDI-TOF analysis of aged samples

In order to evaluate the stability of marker proteins and the performance limits of the direct approach for forensic body fluid identification, historical proficiency test samples from CTS Inc. were examined. These samples are provided on a regular basis

to hundreds of forensic laboratories around the world for quality assurance of their DNA profiling operations. Each test involved four pieces of fabric stained with various body fluids, which were manufactured to resemble typical stained items as might be recovered from victims and suspects of crime. The items examined ranged in age from about 12 months to 11 years and they were stored

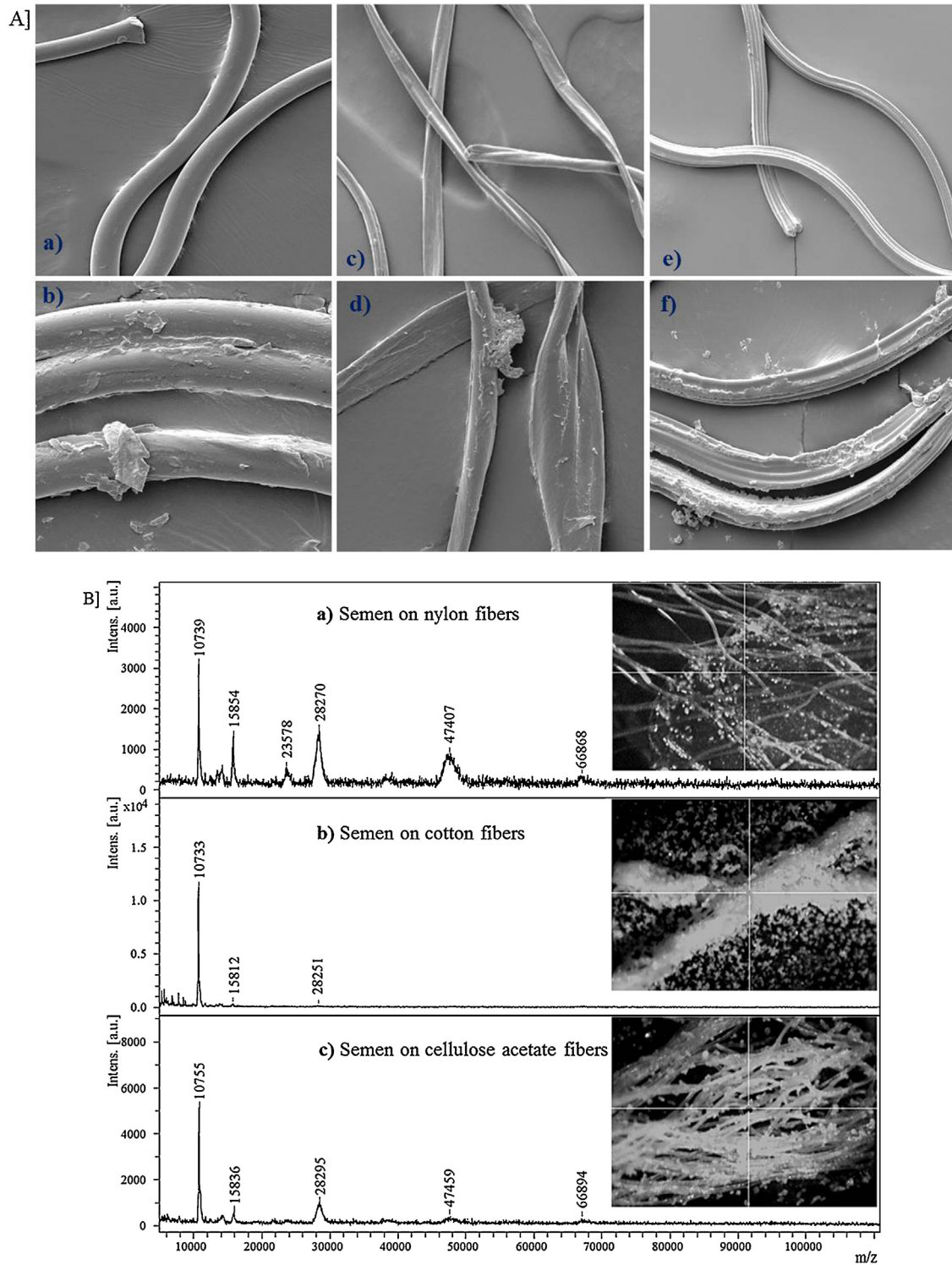


Fig. 5. (A) SEM images of fabric fibers, top row (a, c and e) are untreated nylon, cotton and cellulose acetate respectively, bottom row (b, d and f) depicts fibers from the same fabrics that have been treated with semen. (B) Protein profiles obtained by MALDI-TOF MS from semen-treated fabric fibers. The intact protein profiles were acquired using linear positive mode, all fabric fibers were directly deposited onto ITO-coated glass slides with SA matrix (10 mg/mL in 50% ACN/H₂O with 0.1% TFA). Inset images show the matrix applied to the fibers and the regions analyzed.

after their initial receipt from CTS at room temperature in sealed paper and plastic bags in the dark. Test items were extracted and supernatant (1 μ L) was treated with an equal amount of saturated SA matrix solution and MS data acquired in linear positive mode using MALDI-TOF. Fig. 4a shows typical signals for intact proteins extracted from the 11-year-old item mass matched to hemoglobin α - (15,122 Da) and β -subunits (15,858 Da); also an indication of the heme group (m/z 616.2) can be seen in the inset spectrum. For further confirmation, samples were reduced, alkylated and then trypsin digested at 37 °C overnight. The obtained tryptic peptides (Fig. 4b) were analyzed using MALDI-TOF and their identity confirmed using the Swiss-Prot database. Fig. 4c shows the MS/MS spectrum of precursor ion m/z 1529.79 of the α -subunit of hemoglobin, with the corresponding sequence of the peptide fragmentation pattern and matched “b” and “y” ions in the spectrum. These MS results show the surprising stability of hemoglobin proteins on fabric substrates, even when the stains are stored under less than optimal conditions. This is of practical value in the investigation of unsolved (“cold”) cases and even routine case in laboratories that are operating under a backlog.

3.4. Direct analysis of raw semen on different fabrics

Direct proteomic analysis of body fluids in situ on different substrates (e.g., fabrics, swabs) as received in forensic case investigations would be an elegant solution to operational demands for high analytical throughput. The practicality of this approach was investigated using replicated casework samples prepared by applying body fluid sample stains (semen, blood and saliva) to pieces of clean fabric and then applying MALDI-MS directly to small tufts of a few fibers plucked from the stained area. Fabrics (white cotton, cellulose acetate and nylon) were chosen to represent the range found in garments typically encountered in casework (e.g., underpants, petticoats and other foundation garments, face masks, shirts and trousers) and to include both man-made and natural fibers and hydrophilic and hydrophobic fibers. Only results relating to tests involving semen are discussed here as some differences in protein detection were noted in regards to this fluid; blood and saliva produced the expected positive results on all fibers tested. The small tufts of semen-treated fabric fibers were deposited with the MALDI matrix (SA) onto ITO-coated slides and directly analyzed using MALDI-TOF MS. Fig. 5 (panel A) shows typical SEM images for fibers from each type of fabric, both untreated (top row, a, c, and e) and treated with semen (bottom row, b, d and f). Fig. 5 (panel B) shows the intact protein profiles obtained by MALDI-TOF MS from semen-treated fabric fibers (linear positive (LP) ion mode, m/z detection range 5000–120,000 Da) together with an image of the specimen region from which mass spectral data were acquired.

PSA (m/z ~28 kDa), semenogelin-I (~47 kDa) and semenogelin-II (~66 kDa) ionized well on nylon but less well on cellulose acetate. Only traces of semenogelin-I, semenogelin-II and PSA were detected on the cotton substrate. These results show that the type of substrate strongly affects the ion yields for intact proteins in this direct approach to analysis. The fibers themselves do not contribute to spectral chemical noise (see supplementary data, Fig. 2), but it does appear (Fig. 5, panel A, image d) that the hydrophilic fiber (cotton) substantially absorbs seminal fluid and possibly strongly hydrogen-bonds the gel-forming semenogelin proteins too, thus reducing their availability for ionization. The cotton fibers under the SEM were mostly smooth with very few of the characteristic irregular-shaped semen deposits (of the type seen toward the top of the center fiber in micrograph d in Fig. 5) present on their surface. On the other hand, seminal fluid appears to form a distinct and heavy crust on the surface of

the other two fiber types, thus presenting abundant material for ionization.

4. Conclusion

Here, we report initial findings in regards to the development of a simple and direct method for the direct MS identification of differentially expressed protein “markers” in dilute solutions of body fluids and in aqueous suspensions of dried body fluid particles. Although body fluids are complex mixtures of proteins, and even though the “marker” proteins detected in this reported method are not unique to any one fluid, the simple and direct approach for body fluid identification is nevertheless effective. This is because “marker” proteins detected by this approach are the most abundant proteins in those fluids that are important in forensic casework. This of course means that the direct approach might not be effective for the detection of trace levels of one fluid mixed with another; however, mixtures (even ternary mixtures) of body fluids of the type likely to be involved in casework have been resolved using this approach. Protein biomarkers from blood, semen and saliva were all readily detected and positively identified in addition to human uromodulin from urine, which is a “biomarker” that has not been described in literature dealing with the detection of proteins of forensic relevance. Less than one hour is all that is required to obtain an initial “top-down” indication or screen as to the protein markers in an unknown fluid using MALDI-ToF-MS/MS with confirmation using a “bottom-up” tryptic digest accomplished after a 12 h incubation period. Less than 1 μ L of saliva and semen were required for successful production of abundant, high m/z ions. The reported method is extremely sensitive to the presence of blood proteins; 1 μ L of highly diluted stain is all that is required for successful detection and identification of blood. Furthermore, blood markers appear to be quite stable over time – an 11-year-old sample of blood was successfully analyzed. This is of relevance to case investigations where deposits are not fresh, such as in laboratories that are operating under high backlogs or in regards to unsolved crime investigations (“cold cases”).

Simple deposition of fluid and matrix on a polished stainless steel target plate (Bruker MTP) is all that is required for analysis, which indicates that high-throughput, automated screening is possible. For each body fluid more than one marker was detected, thus conferring a high degree of reliability to the assay. The direct technique offers significant advantages compared to classical proteomics, including speed of analysis, reduced equipment requirements and elimination of cross-contamination or carry over during isolation/fractionation. Species-specific information is generated; compared to genomic and immunochromatographic assays a combination of assays is not required in order to fully evaluate an unknown fluid or mixture.

The direct approach can be elegantly extended to the direct, in situ identification of body fluids on textile fibers, including mixed deposits, both of which are capabilities of particular relevance to forensic examination of garments and other fabric-based items seized in relation to crime. Small tufts containing a few individual fibers plucked from stains on nylon, cotton and cellulose acetate fabrics were successfully analyzed by mixing them with matrix on ITO-coated glass slides. However, sensitivity toward semenogelin and PSA proteins is poor on cotton substrates. It may be that semenogelin (which is a gel-forming protein) strongly binds to the hydrophilic cellulose of cotton, thus reducing the availability of the former for ionization. None of the textiles tested interfered with the body fluid assay.

The simple and direct approach described here shows significant potential for application in forensic casework.

Acknowledgements

The authors would like to acknowledge Flinders Analytical and Flinders Proteomics at Flinders University. We also wish to thank Forensic Science SA for in-kind support and financial assistance from the Ross Vining Research Fund, which is administered by Forensic Science SA. Finally we wish to thank the volunteers who provided body fluid samples.

Appendix A. Supplementary data

Supplementary data associated with this article can be found, in the online version, at <http://dx.doi.org/10.1016/j.ijms.2016.01.002>.

References

- [1] J.L. Webb, J.I. Creamer, T.I. Quickenden, A comparison of the presumptive luminol test for blood with four non-chemiluminescent forensic techniques, *Luminescence* 21 (4) (2006) 214–220.
- [2] S.S. Tobe, N. Watson, N.N. Daeid, Evaluation of six presumptive tests for blood, their specificity, sensitivity, and effect on high molecular-weight DNA, *J. Forensic Sci.* 52 (1) (2007) 102–109.
- [3] J. Connie, A.J.G.S. Swander, Evaluation of the ABACard HemaTrace for the Forensic Identification of Human Blood, *Association of Forensic Scientist*, 1998, pp. 1–5.
- [4] S. Baj, T. Krawczyk, An investigation into the reaction of hemin-catalysed luminol oxidation by peroxy compounds, *J. Photochem. Photobiol. A: Chem.* 183 (1–2) (2006) 111–120.
- [5] J.H. An, K.J. Shin, W.I. Yang, H.Y. Lee, Body fluid identification in forensics, *BMB Rep.* 45 (10) (2012) 545–553.
- [6] K. Virkler, I.K. Lednev, Analysis of body fluids for forensic purposes: from laboratory testing to non-destructive rapid confirmatory identification at a crime scene, *Forensic Sci. Int.* 188 (1–3) (2009) 1–17.
- [7] F. Lundquist, Medicolegal identification of seminal stains using the acid phosphatase test, *AMA Arch. Pathol.* 50 (4) (1950) 395–399.
- [8] M. Vennemann, G. Scott, L. Curran, F. Bittner, S.S. Tobe, Sensitivity and specificity of presumptive tests for blood, saliva and semen, *Forensic Sci. Med. Pathol.* 10 (1) (2014) 69–75.
- [9] H.C. Graves, G.F. Sensabaugh, E.T. Blake, Postcoital detection of a male-specific semen protein. Application to the investigation of rape, *N. Engl. J. Med.* 312 (6) (1985) 338–343.
- [10] B.C. Pang, B.K. Cheung, Identification of human semenogelin in membrane strip test as an alternative method for the detection of semen, *Forensic Sci. Int.* 169 (1) (2007) 27–31.
- [11] N. Khaldi, A. Miras, K. Botti, L. Benali, S. Gromb, Evaluation of three rapid detection methods for the forensic identification of seminal fluid in rape cases, *J. Forensic Sci.* 49 (4) (2004) 749–753.
- [12] A. Bjartell, J. Malm, C. Moller, M. Gunnarsson, A. Lundwall, H. Lilja, Distribution and tissue expression of semenogelin I and II in man as demonstrated by in situ hybridization and immunocytochemistry, *J. Androl.* 17 (1) (1996) 17–26.
- [13] M. Robert, C. Gagnon, Semenogelin I: a coagulum forming, multifunctional seminal vesicle protein, *Cell. Mol. Life Sci.* 55 (6–7) (1999) 944–960.
- [14] M.N. Hochmeister, B. Budowle, O. Rudin, C. Gehrig, U. Borer, M. Thali, R. Dirnhöfer, Evaluation of prostate-specific antigen (PSA) membrane test assays for the forensic identification of seminal fluid, *J. Forensic Sci.* 44 (5) (1999) 1057–1060.
- [15] D.G. Casey, J. Price, The sensitivity and specificity of the RSID-saliva kit for the detection of human salivary amylase in the Forensic Science Laboratory, Dublin, Ireland, *Forensic Sci. Int.* 194 (1–3) (2010) 67–71.
- [16] J.R. Myers, W.K. Adkins, Comparison of modern techniques for saliva screening, *J. Forensic Sci.* 53 (4) (2008) 862–867.
- [17] U. Ricci, I. Carboni, F. Torricelli, False-positive results with amylase testing of citrus fruits, *J. Forensic Sci.* 59 (5) (2014) 1410–1412.
- [18] K. Sato, H. Tsutsumi, H.H. Htay, K. Tamaki, H. Okajima, Y. Katsumata, Identification of human urinary stains by the quotient uric acid/urea nitrogen, *Forensic Sci. Int.* 45 (1–2) (1990) 27–38.
- [19] T. Nakazono, S. Kashimura, Y. Hayashiba, T. Hisatomi, K. Hara, Identification of human urine stains by HPLC analysis of 17-ketosteroid conjugates, *J. Forensic Sci.* 47 (3) (2002) 568–572.
- [20] J.L. Bedrosian, M.D. Stolorow, M.A. Tahir, Development of a radial gel diffusion technique for the identification of urea in urine stains, *J. Forensic Sci.* 29 (2) (1984) 601–606.
- [21] T. Akutsu, H. Ikegaya, K. Watanabe, H. Fukushima, H. Motani, H. Iwase, K. Sakurada, Evaluation of Tamm–Horsfall protein and uroplakin III for forensic identification of urine, *J. Forensic Sci.* 55 (3) (2010) 742–746.
- [22] H. Yang, B. Zhou, H. Deng, M. Prinz, D. Siegel, Body fluid identification by mass spectrometry, *Int. J. Legal Med.* 127 (6) (2013) 1065–1077.
- [23] K. Van Steendam, M. De Ceuleneer, M. Dhaenens, D. Van Hoofstat, D. Deforce, Mass spectrometry-based proteomics as a tool to identify biological matrices in forensic science, *Int. J. Legal Med.* 127 (2) (2013) 287–298.
- [24] K.M. Legg, R. Powell, N. Reisdorph, R. Reisdorph, P.B. Danielson, Discovery of highly specific protein markers for the identification of biological stains, *Electrophoresis* 35 (21–22) (2014) 3069–3078.
- [25] R. Bradshaw, S. Bleay, M.R. Clench, S. Francese, Direct detection of blood in fingerprints by MALDI MS profiling and imaging, *Sci. Just.* 54 (2) (2014) 110–117.
- [26] J. Chen, L. Canales, R.E. Neal, Multi-segment direct inject nano-ESI-LTQ-FT-ICR-MS/MS for protein identification, *Proteome Sci.* 9 (2011) 38.
- [27] D.B. Kristensen, J.C. Brønd, P.A. Nielsen, J.R. Andersen, O.T. Sørensen, V. Jørgensen, K. Budin, J. Matthiesen, P. Venø, H.M. Jespersen, C.H. Ahrens, S. Schandorff, P.T. Ruhoff, J.R. Wisniewski, K.L. Bennett, A.V. Podtelejnikov, Experimental peptide identification repository (EPIR): an integrated peptide-centric platform for validation and mining of tandem mass spectrometry data, *Mol. Cell. Proteomics* 3 (10) (2004) 1023–1038.
- [28] D.N. Perkins, D.J. Pappin, D.M. Creasy, J.S. Cottrell, Probability-based protein identification by searching sequence databases using mass spectrometry data, *Electrophoresis* 20 (18) (1999) 3551–3567.
- [29] E. Beutler, J. Waalen, The definition of anemia: what is the lower limit of normal of the blood hemoglobin concentration? *Blood* 107 (5) (2006) 1747–1750.
- [30] L.H. Schneyer, Amylase content of separate salivary gland secretions of man, *J. Appl. Physiol.* 9 (3) (1956) 453–455.
- [31] R.E. Noble, Salivary alpha-amylase and lysozyme levels: a non-invasive technique for measuring parotid vs submandibular/sublingual gland activity, *J. Oral Sci.* 42 (2) (2000) 83–86.
- [32] E. Benedek-Spat, The composition of unstimulated human parotid saliva, *Arch. Oral Biol.* 18 (1) (1973) 39–47.
- [33] E. de Lamirande, K. Yoshida, T.M. Yoshiike, T. Iwamoto, C. Gagnon, Semenogelin, the main protein of semen coagulum, inhibits human sperm capacitation by interfering with the superoxide anion generated during this process, *J. Androl.* 22 (4) (2001) 672–679.
- [34] O. Devuyst, K. Dahan, Y. Pirson, Tamm–Horsfall protein or uromodulin: new ideas about an old molecule, *Nephrol. Dial. Transplant.* 20 (7) (2005) 1290–1294.

3.3 Body fluid confirmation by nLC-ESI-qTOF MS/MS analysis

Above manuscript described the usage of MALDI-ToF MS for the direct identifications of body fluids proteins on different fabric substrates and aged proficiency analysis. Furthermore, the research work has been extended for the confirmation of body fluid protein markers using nLC-ESI-qTOF MS/MS. The in-solution trypsin digested body fluid mixtures (pooled samples of 1:500 blood, 1:200 semen and 1:5 dilutions of saliva, 5 μ L) was analyzed using an AB Sciex TripleTOF 5600+ mass spectrometer equipped with a Nano spray source (AB Sciex). The nLC-MS/MS data for body fluid mixtures were searched with taxonomy set to 'Homo sapiens' using Protein pilot software (version 4.5) followed by Swiss-Prot protein database analysis. **Table 3.1** displays the list of identified and confirmed abundant and/or major protein markers from the diluted solutions of body fluid mixtures (blood, semen and saliva) by differential proteome analysis.

Table 3.1 List of identified abundant protein markers in mixture of volunteer's body fluid samples [Blood 1:500, semen 1:200, saliva 1:5] using nLC-ESI-qTOF MS/MS analysis.

No.	Identified protein markers	UniProt accession number	Swiss-Prot entry name	Protein Sequence coverage (%)	Peptides (>95% CL)
1	Semenogelin-2	Q02383	SEMG2_HUMAN	55.12	90
2	Semenogelin-1	P04279	SEMG1_HUMAN	63.9	75
3	Alpha-amylase 1	P04745	AMY1_HUMAN	55.42	44
4	Alpha-amylase	B7ZMD7	B7ZMD7_HUMAN	53.45	43
5	Hemoglobin subunit beta	P68871	HBB_HUMAN	97.6	43
6	Hemoglobin subunit alpha	P69905	HBA_HUMAN	93.96	43
7	Alpha-2 globin chain	D1MGQ2	D1MGQ2_HUMA	93.96	43
8	Hemoglobin subunit delta	P02042	N	85.71	39
9	Serum albumin	P02768	HBD_HUMAN	46.48	30
10	cDNA FLJ54371, highly similar to Serum albumin	B4DPP6	ALBU_HUMAN B4DPP6_HUMAN	44.82	29
11	Ig alpha-1 chain C region	P01876		40.81	16
12	Prostate-specific antigen	P07288	IGHA1_HUMAN	30.46	9
13	Kallikrein 3 , (Prostate specific antigen), isoform CRA	Q546G3	KLK3_HUMAN Q546G3_HUMAN	30.46	9

14	Prostate-specific antigen (Fragment)	M0R1F0	M0R1F0_HUMAN	27.36	9
15	Zinc-alpha-2-glycoprotein	P25311	ZA2G_HUMAN	26.83	9
16	Mucin-5B OS=Homo sapiens	Q9HC84	MUC5B_HUMAN	4.91	12
17	Mucin-6	Q6W4X9	MUC6_HUMAN	4.1	7
18	Mucin 5AC, oligomeric mucus/gel-forming	A7Y9J9	A7Y9J9_HUMAN	3.43	9
19	Clusterin	P10909	CLUS_HUMAN	19.38	10
20	Cystatin-SN	P01037	CYTN_HUMAN	16.48	4
21	Clusterin-S	P01036	CYTS_HUMAN	24.11	4
22	Prolactin-inducible protein	P12273	PIP_HUMAN	24.6	9
23	Hemoglobin subunit gamma-2	P69892	HBG2_HUMAN	28.17	5
24	Hemoglobin subunit gamma-1	P69891	HBG1_HUMAN	28.17	5
25	Fibronectin	P02751	FINC_HUMAN	4.4	7
26	Isoform 3 of Fibronectin	P02751-3	FINC_HUMAN	21.06	7
27	Isoform 17 of Fibronectin	P02751-17	FINC_HUMAN	20.10	7
28	Lactotransferrin	P02788	TRFL_HUMAN	17.97	9
29	Lactoferrin	W8QEY1	W8QEY1_HUMAN	11.95	9
30	Ig kappa chain C region	P01834	IGKC_HUMAN	33.51	8
31	Ig alpha-2 chain C region	P01877	IGHA2_HUMAN	20.77	8
32	Carbonic anhydrase 1	P00915	CAH1_HUMAN	20.39	7
33	Carbonic anhydrase 1 (Fragment)	E5RH81	E5RH81_HUMAN	19.12	6
34	Carbonic anhydrase 1 Isoform	V9HWE3	V9HWE3_HUMAN	20.39	7
35	Apolipoprotein A-I	P02647	APOA1_HUMAN	50.56	9
36	Serotransferrin	P02787	TRFE_HUMAN	29.10	9
37	Prostatic acid phosphatase	P15309	PPAP_HUMAN	25.91	9
38	Isoform 3 of Prostatic acid phosphatase	P15309-3	PPAP_HUMAN	24.38	8
39	Isoform 2 of Prostatic acid phosphatase	P15309-2	PPAP_HUMAN	18.70	6
40	Peroxiredoxin-2	P32119	PRDX2_HUMAN	27.80	6
41	Extracellular matrix protein 1	Q16610	ECM1_HUMAN	21.85	8
42	Isoform 4 of Extracellular matrix protein 1	Q16610-4	ECM1_HUMAN	24.70	8
43	Immunoglobulin J chain	P01591	IGJ_HUMAN	44.03	6
44	Epididymal secretory protein E1	B4DQV7	B4DQV7_HUMAN	44.80	6
45	Hemopexin	P02790	HEMO_HUMAN	30.10	3
46	Haptoglobin	H3BMJ7	H3BMJ7_HUMAN	27.83	3
47	Cysteine-rich secretory protein	P54107	CRIS1_HUMAN	12.03	3
48	Actin cytoplasmic 1	P60709	ACTB_HUMAN	29.60	4
49	Ig gamma-2 chain C region	P01859	IGHG2_HUMAN	32.85	5
50	Ig lambda-2 chain C regions	P0CG05	LAC2_HUMAN	62.26	3
51	Ig gamma-1 chain C region	P01857	IGHG1_HUMAN	26.70	4

52	Lipocalin-1	P31025	LCN1_HUMAN	40.35	2
53	Serotransferrin	P02787	TRFE_HUMAN	4.14	4
54	Transferrin	Q06AH7	Q06AH7_HUMAN	3.1	2
55	IGH@ protein	Q6P089	Q6P089_HUMAN	26.67	12

Bold font indicates the abundant or rich protein markers with high sequence coverage and considered as marker proteins in semen, saliva and blood.

The following differentially expressed proteins were selected as practical “biomarkers” for forensic purposes: semenogelin I and II and PSA for semen; α -and- β subunits of hemoglobin for blood; α -amylase 1 and 2 for saliva; and uromodulin [also called as Tamm–Horsfall glycoprotein (THP)] for urine (see manuscript Table 1). These protein markers are over-expressed in the specified body fluid and they have also critical role for clinical applications in regards to detection of certain types of early stage cancers (e.g. prostate-specific antigen (PSA) and the level or quality of semen for fertility examination (semenogelin and spermatozoa). It can be seen that the classical proteomic analysis using nLC-ESI-qToF MS/MS has a much lower limit of detection for the fluid biomarkers and would be the “gold standard method” of choice for the identification of bodily fluids and unknown biological mixtures beyond the scope applicable to forensic science. In that context the technique has high throughput, uses low volumes of extract and dilute protein solutions and it has ability to separate hundreds to thousands of tryptic peptides from body fluid mixtures through nano-capillary column chromatographic separation and detection of the protein markers using high resolution mass spectrometry (triple quadrupole ESI-TOF MS (Sciex 5600+).

Furthermore to the manuscript context and related to this chapter, a complete list of proteins matched (database identification) within the individual body fluids and peptide ranking based on the confidence level for each protein is given in **Appendix-1A** attached to this thesis. All fabric backgrounds were acquired in linear positive mode (m/z detection range 5000–120,000 Da) by MALDI-TOF MS; the fabric fibres themselves do not contribute to spectral chemical noise. The spectra data for each control fabric (100% of nylon, cotton and cellulose acetate) fibres were provided in this Thesis **Appendix-1B**.

Chapter 4

Chapter:4 A mass spectrometry-based forensic toolbox for imaging and detecting biological fluid evidence in finger marks and fingernail scrapings

Int J Leg Med. 2017; 131 (5): pp 1413-1422. [DOI: 10.1007/s00414-017-1587-5](https://doi.org/10.1007/s00414-017-1587-5)

Sathisha Kamanna¹, Julianne Henry², Nicholas H. Voelcker³, Adrian Linacre⁴, K. Paul Kirkbride^{1*}

¹School of Chemical and Physical Sciences, Flinders University, Sturt Road, Bedford Park, 5042 Adelaide, South Australia, Australia

²Forensic Science SA, 21 Divett Place, 5000 Adelaide, South Australia, Australia

³Monash Institute of Pharmaceutical Sciences, 381 Royal Parade, Parkville, VIC 3052, Australia

⁴School of Biological Sciences, Flinders University, Sturt Road, Bedford Park, 5042 Adelaide, South Australia, Australia

Selected supplementary information relating to this research article will appear in this chapter and remaining data were provided in the appendix of this thesis.

Journal Impact Factor: **2.4**

SCImago Journal Rank (SJR): 30 out of 193 [Medicine, Pathology and Forensic Medicine]

Number of citations: **2**

Statement of Authorship for Chapter 3 manuscript

Title of Paper	A mass spectrometry-based forensic toolbox for imaging and detecting biological fluid evidence in finger marks and fingernail scrapings
Publication Status	Published
Publication details	Published in International Journal of Legal Medicine. 2017 ; 131 (5): pp 1413-1422.

AUTHOR CONTRIBUTIONS

By signing the Statement of Authorship, below mentioned each author certified that their stated contribution to the publication is accurate and that permission is granted for the research article to be included in the candidate's thesis.

Name of Principal Author (Candidate)	Sathisha Kamanna		
Contribution to the paper	Designed the research and experimental method. Performed all laboratory work and analysis, interpreted data and drafted/edited the manuscript.		
Signature		Date	March, 2018

Name of Co-author	Julianne Henry		
Contribution to the paper	Provided manuscript draft assistance/evaluation, industry/forensic biology advice, provided access to proficiency test/volunteer samples for analysis and acted as industry research co-supervisor.		
Signature		Date	March, 2018

Name of Co-author	Nicholas H. Voelcker		
Contribution to the paper	Provided manuscript draft assistance/evaluation, specialist mass spectrometry advice and acted as an external academic research co-supervisor.		
Signature		Date: 15/03/2018	March, 2018

Name of Co-author	Adrian Linacre		
Contribution to the paper	Provided manuscript draft assistance/evaluation, forensic biology advice and research co-supervision.		
Signature		Date	March, 2018

Name of Co-author	K. Paul Kirkbride		
Contribution to the paper	Supervised research, provided manuscript draft assistance/evaluation and acted as corresponding author.		
Signature		Date	March, 2018

4.1 Manuscript context

During violent crimes such as homicide or sexual assault the hands and fingers of the assailant or victim can become smeared with body fluids such as blood or vaginal fluid. If either of these individuals touches something at the crime scene they could leave fingerprints containing fluid that could persist and provide evidence. Furthermore, if the assailant is apprehended within a certain time frame, evidence of contact could be present in traces under their fingernails.

Our published article [118] describes research in an important area of mass spectrometry-based proteomics applications for forensic science in regards to body fluids, fingerprints and fingernail traces. DNA profiling has revolutionized forensic science as it is able to identify the source of even minute traces of cellular material. However, a major limitation of this test has been that DNA profiling cannot indicate what type of cellular material is present in evidence, "just" the identity of person from whom the material originated. Specific identification of what a biological and/or chemical deposit consists of can be crucial to a case investigation. For example, in a sexual assault where there is an allegation of finger penetration there is a reasonable expectation that the fingernails of the suspect would trap traces of vaginal fluid and if the suspect had touched something at the crime scene then their fingerprints would also contain vaginal fluid. Very few articles in the literature deal with the examination of fingernail deposits. Until the article described in this chapter was published, all that could be achieved is a determination that the victim's DNA was present in the mark or under their nails - it is very important to determine whether the cellular material is vaginal fluid (which would support the allegation) or whether it is some other material such as saliva or skin cells (which could support another scenario).

In forensic investigations, detection of fingerprints with a clear ridge pattern is crucial information and/or evidence in regards to the identification of the perpetrator. However, it is also important to identify circumstances surrounding the event that could be found in chemical and biological fluid traces from different sources (e.g., from human and animal biological fluids) present in the ridge pattern of fingerprints.

The current limitations and practices of human body fluid identification (such as

forensic presumptive tests, DNA profiling analysis and classical proteomic technologies) and opportunities for innovation and improvement were considered when designing the research aims of this chapter and the manuscript. Published work by Bradshaw *et al.* [137] demonstrated the practical issues of integrating mass spectrometry imaging (MSI) with traditional finger mark enhancement and biometric identification methods. At the time when research described in this thesis was being undertaken, there had been little forensic research work carried out that integrated mass spectrometry (MS) techniques with a DNA profiling or genomic technique. Additionally, there was a lack of specific forensic test available for the examination of sweat (including metabolites, exogenous chemical and biological molecules) in fingermarks and under fingernails. The current statement of issues and implementation of human body fluid identification and opportunities for innovation and improvement were considered when designing the research aims of this chapter and the manuscript. The main aim of this chapter was to establish a MS-based proteomic and forensic “toolbox” containing MALDI-TOF MS/MS, MALDI TOF MS-imaging and nLC-ESI-qTOF MS/MS methods for detecting and mapping the biological fluid traces in latent fingermarks and fingernail scrapings.

In this article, preliminary work demonstrated the identification of biological fluid traces under fingernails or creating images of their distribution in fingermarks. Therefore the article [118] presents a valuable contribution to the techniques available for the forensic investigation of serious crime. The work describes MS-based analysis carried out on fingermarks that have been treated using standard fingermark visualization techniques. Here we demonstrated the application of matrix-assisted laser desorption ionization-time of flight-MS (MALDI-TOF MS) for the detection and mapping (MSI) of proteins and peptides from body fluids in finger marks, including marks that have been dusted with aluminum-containing magnetic powder and “lifting” using adhesive tape. Nano-spray liquid chromatography combined with multidimensional tandem MS (nLC-MS/MS) was successful for the detection of protein biomarkers characteristic of vaginal fluid and blood trapped under fingernails, even after hands had been washed. The research described in this article is therefore very practical and can be implemented in forensic casework. An extension of this work, presented in a later chapter, deals with exactly how long traces of biomarkers under fingernails persist.

The technique offers potential for indicating whether a person (through their fingerprints and touch chemistry analysis) has handled chemicals such as drugs or explosives. In addition, for the first time, the article has demonstrated an MS technique combined with a DNA profiling technique (direct PCR analysis). The integrated "MS-based forensic toolbox" offers potential for forensic investigations that can provide simultaneous identification of the 'type' of biological traces present in contaminated fingerprints and under fingernails, and identification of the person from whom the trace originated. In this research article an extremely complex mass spectrometry technique has been elegantly simplified and a method is described that is very conducive to implementation in criminal investigations.

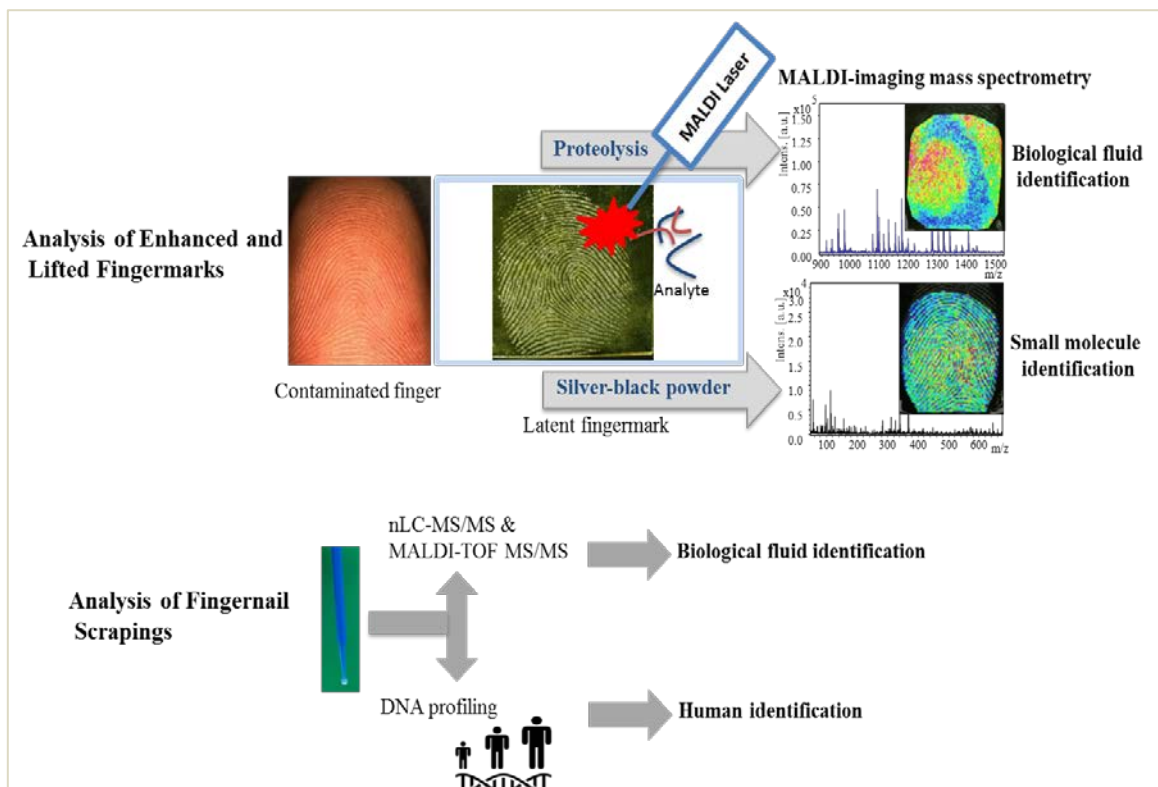


Figure 4.1 A graphical representation of the different mass spectrometry techniques and DNA profiling (direct-PCR) analysis used for the identification of body fluid traces and individual DNA profile from fingermarks and fingernail scrapings. The figure was designed based on experimental work carried out by Kamanna *et al.* 2017.

What follows is a peer-review version of the article published in the International Journal of Legal Medicine. The final authenticated version is available online at: <http://dx.doi.org/10.1007/s00414-017-1587-5>.

4.2 A mass spectrometry-based forensic toolbox for imaging and detecting biological fluid evidence in finger marks and fingernail scrapings

Sathisha Kamanna, ¹

Julianne Henry, ²

Nicolas H. Voelcker, ³

Adrian Linacre, ⁴

K. Paul Kirkbride, ^{1,*}

Phone 61 8 82013011

Email paul.kirkbride@flinders.edu.au

¹ Flinders University, School of Chemical and Physical Sciences, GPO Box 2100, Adelaide, South Australia, 5001 Australia

² Forensic Science SA, Forensic Science Centre, Adelaide, South Australia, 5000 Australia

³ Monash Institute of Pharmaceutical Sciences, 381 Royal Parade, Parkville, VIC, 3052 Australia

⁴ Flinders University, School of Biological Sciences, GPO Box 2100, Adelaide, South Australia, 5001 Australia

Abstract

During a crime, biological material such as blood or vaginal fluid may become smeared on the fingers of the victim or suspect or trapped under their fingernails. The type of trapped fluid is extremely valuable forensic information. Furthermore, if either person touches an object at the crime scene with their 'contaminated' finger then a

'contaminated' finger mark may be deposited. Such marks have great value as they could identify not only who deposited the mark but also who they touched and which part of the body they touched. Here, we describe preliminary work towards a 'toolbox' of techniques based on mass spectrometry (MS) for the identification of biological fluid traces under fingernails or the imaging of them in finger marks. Liquid chromatography-multidimensional MS was effective for the detection of protein biomarkers characteristic of vaginal fluid and blood trapped under fingernails, even after hands had been washed. In regard to examination of finger marks for the presence of biological fluids, the most practical implementation of any technique is to integrate it with, but after, routine crime scene finger mark enhancement has been applied. Here, we demonstrate the usage of matrix-assisted laser desorption ionization-time of flight-MS for the detection and mapping of proteins and peptides from body fluids in finger marks, including marks enhanced using aluminium-containing magnetic powder and then 'lifted' with adhesive tape. Hitherto, only small molecules have been detected in enhanced, lifted marks. In a novel development, aluminium in the enhancement powder assisted ionization of small molecules in finger marks to the extent that conventional matrix was not required for MS.

Keywords

Haemoglobin
Cornulin
MALDI-MS/IMS
Proteins
Fingerprint

Electronic supplementary material

The online version of this article (doi: 10.1007/s00414-017-1587-5) contains supplementary material, which is available to authorized users.

Introduction

During homicide, assault, sexual assault and other crimes against a person, touching or violent contact may take place. This can result in the deposition of two types of evidence: traces of body fluids may become trapped under the fingernails of the victim or suspect; and smears of foreign body fluids may be transferred to fingers that can then deposit finger marks at the crime scene. While current DNA profiling methods provide routine and accurate identification of individuals from biological material, the circumstances and events surrounding the crime can be difficult to determine. However, identification of the body fluids that are present in biological traces can be a crucial indicator of events. For example, in a case where there is an accusation of a sexual assault involving digital penetration, examination of fingernail scrapings taken from the suspect could indicate that DNA from both the victim and suspect are present. While this finding adds weight to the accusation, the crux of the matter is to establish whether the material from the victim is vaginal fluid (which would strongly support the allegation) or some other cellular material (which would be more suggestive of casual contact).

Mass spectrometric techniques are becoming widely used in clinical and/or biological sciences for the detection of peptides, proteins and/or small molecules within tissues. One particular technique, matrix-assisted laser desorption ionization-time of flight-mass spectrometry (MALDI-ToF-MS), has the particular advantage of allowing the distribution of analytes within biological specimens to be mapped using imaging mass spectrometry (IMS) [1, 2, 3, 4]. Applications of MALDI-ToF-MS to forensic science have involved biomarker discovery in traces of body fluids such as blood, seminal fluid, vaginal fluid, saliva and sweat [5, 6, 7]. While several articles have described the use of mass spectrometric methods for the identification of body fluids and mixtures of them on some simulated crime items (e.g. the presence of semen on textile fibres [6] and aged bloodstains [6, 7]), experiments involving fingernail scrapings have hitherto not been reported. The preliminary investigation reported here describes the first means to detect the presence of body fluids in fingernail scrapings, even after hand washing.

Finger marks with sufficiently clear ridge patterns are valuable evidence at a crime scene because they may allow identification of the perpetrator of the crime. However, additional valuable chemical and biological evidence as to the circumstances surrounding the crime could be present in the ridge pattern of the mark. Using an alleged case of a digital penetration as an example once again, evidence supporting the accusation would be obtained if a surface at the crime scene was found to have a clear finger mark originating from the suspect that contained traces of vaginal fluid only in the ridge marks of the pattern. It is reasonable to assume that as a result of vaginal penetration, a finger would have foreign fluid both on the ridges and in the valleys. If that finger then lightly touches a surface, then a ridge pattern in fluid would be left behind because only the ridges would touch and contaminate the surface. However, if the contact pressure was high enough for the both ridges and valleys to make contact, then the presence of fluid would be consistent across the mark with a ridge pattern 'embossed' into it, assuming the pressure is not so high as to obliterate any pattern. The pattern resulting when high pressure is involved might be difficult to differentiate from an alternative situation where the suspect touched a stain of fluid already on the surface at the crime scene, but only if the stain is smaller than the finger making the mark, otherwise, there would be fluid obvious on the surface outside the finger mark. Clearly, a pattern where fluid is absent between the ridges pattern would be very unlikely to be formed when a finger touches fluid already present on the object. In the latter this situation, any absence of fluid would likely be where the finger ridges touched the deposit; therefore, a pattern with fluid in the valleys rather than the ridges would result. A more likely scenario involving a pre-existing stain at a crime scene and the presence of a clear mark containing foreign fluid in the ridges of the pattern is when indirect transfer is involved, for example, where the suspect touches a surface that has fluid present and then touches another surface.

Finger marks deposited contemporaneously to the crime are likely to be rich in body fluid, and, because proteins in body fluid deposits have been reported to be stable [6, 7], the evidence can be expected to persist

for days or weeks until such time as it is gathered by the crime scene investigator. This is in contrast to foreign body fluid deposits on the body of the victim or assailant, which can be expected to persist only for a short time as a result of unintentional activity such as sweating and contact with clothing, or deliberate activity such as washing.

Techniques for detection of body fluids in finger marks are therefore valuable for law enforcement purposes, and significant progress recently has been made in regard to the detection and mapping of foreign body fluids in finger marks using imaging mass spectrometry (IMS) [8, 9, 10, 11]. In addition, it is well established that finger sweat contains small-molecule exogenous compounds, such as traces of ingested drugs [12], as well as many small-molecule endogenous compounds. Many methods for the detection of one, the other or both of these classes of substances in finger marks using a range of techniques, including IMS, have been reviewed [13]. For the research that deals with exogenous compounds, most make use of finger marks that have been artificially enriched with the compounds, but detection of ingested drugs and their metabolites in finger marks has been reported [14, 15].

Standard procedure for the treatment of finger marks at a crime scene, which are marks that are practically invisible to the unaided eye and are called latent marks, is to apply a dust that enhances the ridge patterns and makes them visible [16]. The pattern is then photographed in order to allow its comparison to a fingerprint database or reference prints from a suspect in order to identify who made the mark. As a consequence, any practical application of IMS in regard to examination of real, crime-related finger marks must be compatible with, and follow, the ridge pattern enhancement techniques employed by the police. Furthermore, it is likely that crime-related finger marks will be deposited on rough, uneven surfaces or on objects such as door frames, windows, etc., none of which are suitable for *in situ* examination using IMS. The most practical way to involve IMS in the examination of a real crime-related mark is to apply an adhesive sheet to the mark after it has been enhanced and 'lift' it off for analysis. The work of Bradshaw et al. [17] deals with the practical issues of integrating IMS with traditional finger mark enhancement and biometric identification methods. Their work involves the mixing of traditional

finger mark enhancement powders with traditional MALDI matrices for the detection of many endogenous small molecules and some exogenous compounds (e.g. alkylammonium antimicrobials). Guinan et al. [18] describe the usage of treated porous silicon microparticulate dust for both the enhancement of latent finger marks and, after lifting, the ionization and mapping of chemicals in the ridges by use of nanostructure-initiator mass spectrometry (NIMS). The identification of small molecules in the ridges of a finger mark can provide valuable contextual information surrounding a crime. For example, the detection of improvised lubricants allegedly used in an assault could confirm the victim's account of events. Results described in the present article are initial findings in regard to streamlining and extending the integration of traditional finger mark enhancement techniques with MALDI IMS. Detection of high-molecular-weight body fluids in finger marks has been achieved using traditional matrix. In addition, small molecules could be detected in the absence of a traditional MALDI matrix, with the dusting powder itself stimulating ionization.

Experimental section

Materials and chemicals

HPLC–MS-grade acetonitrile (ACN), methanol, water and trifluoroacetic acid (TFA) was purchased from Sigma–Aldrich (NSW, Australia).

Surfactant RapiGest™-SF was purchased from Waters Ltd. (Sydney, Australia) and Trypsin Gold (MS grade) was obtained from Promega (Melbourne, Australia). Indium-tin oxide (ITO)-coated slides were

purchased from Shimadzu (Sydney, Australia). α -Cyano-4-

hydroxycinnamic acid (CHCA) and protein/peptide mixture of external calibrants was obtained from Bruker Daltonics (Melbourne, Australia).

Double-sided Kapton tape (1 in, 0.1 mm total thickness) was purchased from Ted Pella Incorporated (Redding, California, USA). Silver-black magnetic powder and magnetic powder applicator were purchased from Sirchie Incorporated (Youngsville, North Carolina, USA). Finger marks and body fluid samples were obtained from volunteers pursuant to

Clinical Human Research Ethics Committee Application

440.14—HREC/14/SAC/455. Animal blood samples were obtained under Australian Animal Welfare Committee Application 909/16.

In situ homogenous proteolysis procedure

A 1:1 mixture of Trypsin Gold (66 ng/ μ L) and 0.1% RapiGestTMSF (200 μ L) in 25 mM NH_4HCO_3 was sprayed onto ITO slides containing finger marks using an ImagePrep station (Bruker Daltonics GmbH, Germany). The solutions were deposited with five layers and 10 min of incubation between each layer. After the deposition was completed, the ITO slide was incubated in a humid chamber at 37 °C for 2 h.

Matrix deposition

CHCA (7 mg/mL) in 50% ACN and 0.2% TFA was deposited onto digested finger marks using an automated ImagePrep station and an operator-modified Bruker Daltonics default method optimized for sensor-controlled nebulization of the matrix.

Preparation of finger marks

Bloodied finger marks

Small droplets of human blood were produced by pricking a clean finger using a sterile syringe (Livingstone International Pty Ltd., Sydney, Australia). A small volume of blood (\sim 2 μ L) was rubbed on another clean index fingertip, which was then dried at room temperature. After 3 h of normal routine computer work, bloodied finger marks were deposited onto an ITO-coated glass slides. For finger marks bloodied with animal blood, a small volume (\sim 2 μ L) was applied to a finger (single volunteer), rubbed with another finger and a mark made on an ITO slide once the deposit had dried. A single volunteer donated bloodied finger marks for four separate experiments.

Vaginal fluid-contaminated finger marks

A clean finger was placed into a vagina for approximately 5 s, air dried for \sim 10 min and then finger marks were deposited onto ITO slides. One donor provided samples for eight experiments.

Finger mark image capture

Optical images of all finger marks were taken before carrying out MALDI-imaging experiments using either an Olympus XZS2 stereomicroscope equipped with a white light fibre optic source and a

DP21 digital camera (Olympus Pty Ltd., Tokyo, Japan) or a Digitech USB microscope/5 megapixel camera with integrated white LED light source (Jaycar Electronics Pty Ltd., Adelaide, Australia).

Preparation of fingernail scrapings

Fingernail scrapings containing vaginal fluid were prepared by inserting a clean finger into a vagina for about 10 s. The finger was then washed under cold running water for about 1 min and then typical office work was carried out for a range of time periods up to 5 h prior to collection of the scraping. A single donor provided samples for 12 experiments. Collection was carried out with the aid of a microswab (illustrated later) designed by one of us (AL) and manufactured by Flinders Technology (Adelaide, Australia). The tip of the microswab was moistened with deionized water, flicked to remove excess liquid and then rolled around under the nail and in the gap at the side of the nail in order to collect any persisting vaginal fluid. The microswab was then allowed to air dry before being inserted through the septum of a chromatography sample vial (2 mL, Agilent Pty Ltd., Sydney, Australia) and sealed, ensuring that the microswab tip did not touch the wall of the vial. A control specimen was prepared by using a moistened microswab to collect matter from under a fingernail that had not been exposed to vaginal fluid.

Fingernail scrapings containing blood were prepared by placing approximately 3 μ L of animal blood (koala, *Phascolarctos cinereus*) under a fingernail. Human blood was not used for these experiments for two reasons. First, it was to ensure that any haemoglobin detected was from the deposited blood rather than as a result of a small injury to the nail bed during collection of the scrapings. Second, it was part of a continuing validation exercise to ensure that human haemoglobin can be differentiated using MALDI techniques from haemoglobin from common food meat and road-kill blood that a person suspected of a crime might innocently encounter. After deposition of the blood, the hand was rinsed under cold running water for about 30 s and normal office duties were carried out for a measured time prior to collection of the deposited fluid; collection was carried out using exactly the same process as described for collection of residual

vaginal fluid. A single individual made a finger available for three experiments.

Finger marks dusted with silver/black powder and lifted

Finger marks, uncharged or charged with koala blood (~2 μL), were deposited onto new glass microscope slides and dusted using silver/black magnetic powder. The dusted marks were lifted using double-sided adhesive Kapton tape, which was then stuck down onto an ITO-coated glass slide. Finger mark optical images were collected using the stereomicroscope. Finger marks were donated by a single male individual for five separate experiments.

Scanning electron microscopy

Scanning electron microscopy (SEM) images were collected using an FEI Inspect F50 instrument (FEI Corporation, Hillsboro, Oregon, USA) using 10 keV beam energy, a spot size of 6.3 and magnifications between 100 \times and 2000 \times .

MALDI-ToF, IMS and data analysis

All mass spectrometry imaging analysis was performed using an Autoflex-III MALDI-ToF-MS (Bruker Daltonics GmbH, Bremen, Germany) mass spectrometer. The instrument ion source was equipped with a neodymium-doped yttrium aluminium garnet Smart Beam 200 Hz solid-state laser operating at 355 nm. Reflectron positive (RP) ion mode was used with 20 kV accelerating voltage and delayed extraction ions of 200 ns for finger marks of tryptic peptides imaging in the m/z detection range of 800–3500 with a spatial resolution of 200 μm . MS/MS data were acquired manually using the Bruker LIFT technique and a summed response from 4000 laser shots.

For detection of intact proteins in finger marks (in situ, or dusted and lifted), data were acquired over a detection range of 3500–30,000 m/z . A standard peptide mixture (P.N 206,195, Bruker pepmix calibrants) and protein standard-I (P.N 206,355) was used for external calibration and CHCA was used as matrix. A similar process was followed for the detection of small molecules in dusted and lifted latent finger marks, but data were acquired over a detection range 20–1000 m/z and CHCA

was not required as the enhancement powder itself assisted ionization. For detection of tryptic peptides in finger marks, digestion was carried out as described above followed by automated deposition of CHCA.

All the MALDI instrumental parameters including laser power, mass detection range, voltage, delayed extraction and laser offset were set using Flexcontrol 3.3. FlexImaging 3.3 software was used to collect ion intensity maps of tryptic peptides and small molecules and to control Autoexecute MALDI-imaging.

nLC-MS/MS and MALDI-ToF analysis of fingernail scrapings

Microswabs were extracted with 50% ACN, and then 15 μL of extract was treated with 5 μL of 0.1% RapiGestTM and 5 μL of Trypsin Gold (100 ng/ μL). The solutions were incubated at 37 °C overnight; 3 μL of the digested sample was analysed using an AB Sciex TripleTOF 5600+ mass spectrometer fitted with a nanospray source (AB Sciex). Tryptic digested peptides were applied to a Polar 3 μm precolumn (0.3 \times 10 mm, SGE Analytical Science) and eluted onto a spray tip 5 μm C18 column (75 mm \times 150 mm with a bead pore size of 100 Å) (Nikkyo Technos), using an Eksigent Ekspert 415 nano LC. Peptides were eluted using a 35-min gradient from 5 to 25% acetonitrile containing 0.1% formic acid at a flow rate of 300 nL/min over 35 min, followed by a second gradient to 40% acetonitrile over 7 min and a further step to 95% acetonitrile for 11 min. The mass spectrometer was operated in positive-ion mode with one MS scan of mass/charge (m/z) 350–1500, followed by collision-induced dissociation fragmentation of +2 to +5 charge state ions that were greater than 250 counts per second for a maximum of 100 candidate ions. The MS data were analysed with protein pilot version 4.5. This experiment was carried out in duplicate.

DNA profiling of fingernail scrapings

Several fibres were plucked from a microswab that was used to collect vaginal fluid traces from under a fingernail as described previously (single donor). These fibres were placed directly into a 0.2-mL thin-walled PCR tube (Eppendorf, Vic, Australia). Direct PCR was performed using the GlobalFiler kit (Thermo Fisher, Sydney, Australia) by adding into each PCR tube 8 μL of PCR mix and 2 μL of primers

plus 15 μL of sterile H_2O . Amplification was conducted on a Proflex PCR Machine (Thermo Fisher, Sydney, Australia) following the manufacturer's recommendations. From each PCR, 0.5 μL was added to 10 μL HiDi formamide and separated on a 3500 Genetic Analyser (Thermo Fisher). The data were analysed using Genemapper IDX™ (version 3.2).

Results and discussion

Analysis of fingernail scrapings

As discussed above, fingernails can retain valuable evidence of contact between the assailant and victim in offences such as assaults and sexual assaults. Hard plastic or wooden sticks with fine tips can be used to collect the scrapings; however, these were not used in this research because it was felt that the hardness and the sharpness of the collection device might remove keratinized cellular material originating from the person being sampled or could result in micro-injury of the person being sampled, thus resulting in the presence of haemoglobin in the scrapings. While neither of these events are an issue if genetic testing is to be carried out on the scrapings (the purpose for which these collection devices are designed), keratin and haemoglobin both ionize very readily and might ionize in preference to other proteins, especially any traces originating from the other party. In order to avoid any issues, scrapings were recovered using a custom-made microswab device that is depicted in Fig. 1. The device has a very slender and flexible plastic tip that tapers to a fine point (~1 mm). This point is encased in a minute ball-shaped flock brush that does not injure skin.

Fig. 1

Fingernail residues typical of those present after a sexual assault were collected using the microswab at up to 6 h after an 'assault' and after a single, simple hand wash using cold running water. Extraction of the microswabs followed by in-solution tryptic digestion and nLC-MS/MS was successful in the detection of proteins characteristic of vaginal

fluid at up to 3 h after the assault. Proteins characteristic of vaginal fluid that were detected are cornulin (CRNN, the most abundant protein in vaginal fluid), small proline-rich protein 3 (SPRR3), cystatin (CST) A & B, peroxiredoxin-1 and glutathione S-transferase P (GSTP). Dermcidin and lactotransferrin were also detected; these are skin antimicrobial proteins and they are most likely to arise from the finger itself rather than the deposited vaginal fluid. A complete list of proteins detected is presented in Supplementary Information, Fig. S1.

Genomic analysis of a small fraction of a microswab that had been used to collect vaginal fluid from under fingernails was carried out using a standard forensic DNA profiling system combined with direct PCR [19, 20]. As expected, a mixed male/female typing was obtained (Fig. S2). In the research described here, proteomic and genomic analysis were carried out using separate swabs. However, the limits of detection of the techniques are such that debris collected on a single microswab could be used for both tests. Work is currently being finalized in our laboratory in regard to a combined workflow that elegantly incorporates both forensic genomic and proteomic examination of a single swab, which allows streamlined and efficient identification of the individuals involved in a crime and the type of body fluid exchanged between the two.

A trace of koala blood (~2 µL) was placed under a fingernail. The hands were then washed and the fingernail sampled using a moistened microswab after 3 h of office work. Extraction of the swab and in-solution digestion followed by MALDI-ToF MS allowed the detection of weak but characteristic signals arising from haem and HB-B (see Fig. S3 for blood MS data and also data acquired from a control fingernail scraping). Human blood and koala blood (and other animals tested so far by us and others [7]) are quite easily differentiated (data not shown).

MALDI-ToF IMS analysis of finger marks containing vaginal fluid and blood

It was found that proteolysis of finger marks containing body fluids can be carried out very rapidly (2 h) using RapiGest-SF surfactant. This is a considerable improvement in the time required for conventional proteolysis (approximately 12 h) and can allow preservation of the

spatial distribution of substances in the mark, including some ridge detail, which is not the case with conventional proteolysis. These findings confirm those of Deininger et al. [11].

A mark made by a finger exposed to vaginal fluid was subjected to homogenous proteolysis prior to MALDI-ToF IMS analysis. Figure 2a shows the resultant spectra and maps related to the peptides of CRNN (m/z 1501, 994) and human cytoskeletal keratin protein (m/z 1179). In this case, it can be observed that the CRNN forms some ridges in the mark; therefore, if it were a case sample then there would be support for the hypothesis that vaginal fluid was present on the finger rather than already present on the substrate that it touched.

Fig. 2

The CRNN protein sequence was confirmed by the MS/MS spectrum of the precursor ion $[M + H]$ 1501.91 (EQGQTQTQPGSGQR); matched ion fragments of 'b' and 'y' and loss of NH_3 are identified in Fig. 2.

Database (SwissProt and UniProt) analysis was performed on MALDI profiling data of tryptic peptides to confirm the protein matches and sequence analysis; the tryptic peptides identified from the database are provided in the supplementary data (Fig. S4).

Figure 3a shows maps of tryptic peptides including m/z 1529 matched to the α -subunit of haemoglobin (HB-A), and m/z 1274 and 1314 matched peptides of β -haemoglobin (HB-B) from finger marks charged with human blood (CHCA was used as matrix). Several human keratin peptides were detected in the finger marks in addition to those from haemoglobin. For instance, m/z 1707 matched to cytoskeletal-10 of

keratin type-I proteins and matched correlation can be seen in the ion maps. In a subsequent 'top-down' MALDI-profiling experiment, the presence of intact HB-A and HB-B haemoglobin proteins were identified by spotting a drop of CHCA onto an undigested mark. Additional MALDI data relating to the bloodied finger mark, a control finger mark (i.e. one made by a finger that had not been exposed to blood) and showing the benefits of using RapiGest can be found in the supplementary results (Fig. S5). Figure 3b displays the MS/MS spectrum of precursor ion m/z 1314.87 of HB-B, with the corresponding confirmatory sequence of the peptide fragmentation pattern. Matched b and y ions are indicated in the inset. Although the results meet the criteria for the identification of blood proposed by Patel et al. [20], and the maps clearly show ridges in the top right of the mark, ridges are not visible in the region where blood was detected (centre-left of the mark). Therefore, if this were evidence from a crime scene, then it would not be possible to deduce whether the blood was on the finger that caused the mark or already on the surface before the finger touched it.

Fig. 3

MALDI-ToF IMS analysis of low molecular weight and high molecular weight components of lifted finger marks

As indicated in the introduction, crime-related finger marks are usually latent (i.e. practically invisible) and require enhancement in order to locate them within the crime scene and to produce enough contrast between the mark and the surface on which it is deposited before their

biometric information can be exploited. Any practical application of IMS must therefore follow common crime scene latent mark enhancement techniques and be compatible with them. Given that IMS requires a smooth, thin and flat specimen, the most practical way to deal with an enhanced mark is to apply an adhesive sheet to it after it has been enhanced and 'lift' the mark off for analysis. Here, for the first time, the integration of a standard finger mark enhancement technique with lifting and matrix-free MALDI-ToF IMS is reported.

As a first step, the composition of silver/black magnetic powder and its compatibility with MALDI-ToF IMS was evaluated. A finger was charged with sebaceous deposit by rubbing it on the back of the neck and then a mark was deposited on a clean glass microscope slide. The mark was dusted using silver/black magnetic powder and a magnetic wand and then lifted using carbon adhesive tape attached to a SEM stub. SEM-energy dispersive X-ray spectrometry (EDS) showed that the ridge pattern in the lifted mark was rich in aluminium and contained some iron; this composition contrasted starkly to that of the valley regions, which showed the response expected only for carbon tape (Fig. 4a–c). Another groomed finger mark was prepared and dusted in the same way as above, but this time, it was lifted using a square of Kapton double-sided adhesive tape (about 25 mm × 25 mm) that was then fixed to an ITO-coated glass slide and subjected to MALDI-ToF IMS. Figure 4d–h shows the ridge detail achieved by plotting the Al (m/z 26.79) and Fe (m/z 55.68) ion abundances. Relatively low spatial resolution settings were chosen for data acquisition in order to reduce the time required for mapping.

Fig. 4

a, f SEM images of portion of a finger mark dusted with silver/black magnetic powder and collected on double-sided carbon adhesive tape showing ridge and valley detail. **b, c** EDS spectra of ridge and valley regions for the finger mark, respectively. **d, e** mass spectra acquired in the ridge and valley region of the finger mark. **g, h** MALDI-ToF IMS homogenous ion distribution maps of Al and Fe in the finger mark

The data in Fig. 4 also show that the signal obtained from the ridges contains ions from more than just the metals present in the powder; these ions are not detected in just the powder alone (see Fig. S6a) nor in the regions between the ridges (i.e. in the valleys). These data and tentative assignments for the ions detected in the ridges are listed in Fig. S6b. Despite the absence of a conventional matrix (although CHCA clusters were used as an external mass calibrant), good detection of ions was achieved as their protonated, sodiated, potassiated and aluminated adducts. As can be seen in Fig. 5, finger mark ridge patterns can be observed using intensity maps of several of the ions derived from small molecules present in the mark.

Fig. 5

Microscopic images of **a** a latent finger mark, **b** the same finger mark dusted with silver/black magnetic powder, **c** the dusted mark lifted on Kapton double-sided adhesive tape (note that the lifted pattern is shown in its natural inverted form rather than corrected) and right MALDI-ToF IMS maps of ions of small molecules arising from the latent, lifted mark. CHCA was not necessary for the acquisition of these data; the silver/black magnetic powder was all that was required

Several molecules that were detected (triacylglycerols, cholesterol, diacylglycerols and oleic acid) have been previously reported by Yagnik et al. [10] and Bradshaw et al. [17]. Quaternary alkylammonium species, presumably arising from liquid soaps, appear to be a consistent xenobiotic in finger marks as they were detected in the present work (behentrimonium) and have been reported previously [10, 17, 18, 21, 22].

In order to examine the scope for imaging molecules in a dusted and lifted finger mark without the aid of conventional matrices, an experiment aimed at the detection of intact haemoglobin and smaller proteins was carried out. For this experiment, ~2 μ L of koala blood was smeared over a fingertip and a finger mark applied to a clean glass slide, dusted with silver/black powder and lifted with Kapton tape. It was observed that proteins ionized poorly. However, when CHCA

(~0.4 μL) was added, haemoglobin and dermcidin were readily detected (see Fig. 6). This result provides an interesting counterpoint to the work of Bradshaw et al. [17], where it was reported that the presence of aluminium suppressed ion formation when CHCA was used as a traditional matrix for MALDI-ToF IMS.

Fig. 6

a MALDI-ToF mass spectrum of intact protein (low mass range) profiles of a control finger mark. **b** MALDI-ToF mass spectrum of a dusted and lifted bloodied finger mark (using koala (*Phascolarctos cinereus*) blood) showing HB-A (m/z 15329), and HB-B (m/z 16118). CHCA was used as matrix in both experiments

Figure S7 shows MALDI-profiling data derived from a small portion of the dusted and lifted bloodied finger mark that was subjected to a trypsin digest and treatment with CHCA matrix. The presence of signals from HB-B and heme were confirmed. Amongst a number of peaks in the control finger mark prior to digestion is a signal arising from dermcidin (see Fig. 6, 4819 m/z); peptide fragments of dermcidin were not detected after trypsin digestion.

Conclusion

This article describes an initial investigation of the application of mass spectral techniques for the examination of fingernail scrapings and latent finger marks that have been treated with aluminium-containing magnetic powder and lifted using adhesive tape.

Fingernail scrapings from a victim or suspect can contain valuable evidence as to violent close contact between the two. Due to the tight confines between the finger and nail, it is likely that fluid residues under the nail will persist longer than fluid on exposed skin surfaces from which deposits can be expected to be shed readily as a result of sweating, contact with clothing or deliberate removal. We report here for the first time the successful identification of blood and vaginal fluids in fingernail scrapings even after the ‘assailant’ had washed their hands. Although MALDI-ToF MS can be used for

examination of scrapings, the time between 'the crime' and collection of scrapings must be of the order of about 1 h if successful detection of vaginal fluid is to be accomplished; the use of nLC-MS/MS extends that window to about 2 h and the data obtained are much richer. MALDI-ToF MS can be used to detect blood in fingernail scrapings taken up to 3 h after a crime. We have not yet evaluated the impact that delays between collection of scrapings and their analysis might have upon the analytical results, and the experiments reported here were carried out using single volunteers; therefore, inter-donor variability has not been assessed.

The limits of detection of mass spectrometry and forensic genetic profiling are such that there is the possibility that proteomic and genomic analysis may be carried out on a single sample, thus maximizing the forensic evidence or intelligence that might be generated in regard to an investigation. Methodology for a streamlined, integrated genomic and proteomic assay is currently being finalized in our laboratory.

Finger marks at a crime scene are an extremely valuable biometric, but in addition, they might also carry a record as to intimate or violent contact between the victim and suspect. If finger marks are deposited contemporaneously to the alleged crime, then it follows that they are likely to be rich in body fluid and can be expected to persist for days or weeks as proteins in body fluid deposits seem to be quite stable [6, 7]. This is in contrast to foreign body fluid deposits on the body of the victim or assailant, which can be expected to only persist for a few hours at most. We have extended 'bottom-up' enzymatic proteomic analysis to the detection of foreign proteins in finger marks contaminated with vaginal fluid (and saliva, data not shown), which contains much lower levels of protein than blood. It is possible to identify ridge patterns in finger marks formed when a finger contaminated with foreign body fluids touches a surface. When the signal from the foreign protein is not present in the 'valleys' of the mark, this is good evidence that the protein cannot have been on the surface prior to it being touched. However, the presence of a ridge and valley pattern is of course highly dependent upon whether the foreign protein smear on the finger is sparse or abundant and upon the pressure

with which the finger touches the surface. A finger with an abundance of smeared foreign protein on it will most likely produce a mark where the ridge pattern is obliterated and thus, it will be difficult to determine whether the protein was actually on the finger or not when it touched the surface. In summary, given a sufficient quantity of foreign protein in a finger mark, the limitations in regard to inferences that can be drawn from protein maps will be more dependent upon the circumstances surrounding the deposition of the mark rather than the imaging technology. We concur with findings elsewhere [8] as to the value of including RapiGest in the proteolysis step because it greatly enhances the rate of digestion and preserves the finger mark ridge chemical pattern.

Direct mapping of foreign body fluids in finger marks, as described in the previous section, represents a valuable capability for forensic science when a mark fortuitously is found on a surface that can be placed directly into a MALDI-ToF mass spectrometer (e.g. if a mark is on a plastic bag). However, the implementation of imaging mass spectrometry (IMS) that is most practical for law enforcement involves the examination of finger marks that have been treated with industry-standard mark enhancement techniques for biometric capture and then lifted from the object upon which they were deposited in order to carry out MS. We report here that IMS can be carried out on finger marks that have been enhanced using silver/black magnetic powder and lifted using double-sided Kapton adhesive tape; small endogenous molecules could be detected in lifted ridge patterns. In a novel and significant development, matrix was not required for ionization of small molecules. The scope for application of the matrix-free approach for analytical chemistry more generally and for the detection of forensically relevant small molecules such as drug metabolites and explosives in lifted finger marks is currently being investigated by us. Proteins and tryptic peptides could be detected in lifted finger marks, but CHCA matrix was required for strong ionization.

Acknowledgements

This project was supported by the Ross Vining Research Fund, which is administered by Forensic Science SA. The authors would like to

acknowledge Flinders Analytical and the Proteomics Centre at Flinders University. Finally, we wish to thank the volunteers who provided fingerprints and body fluid samples and Dr. Ian Hough and Cleland Wildlife Sanctuary for the provision of animal blood samples.

Electronic supplementary material

ESM 1

(PDF 290 kb)

ESM 2

(PDF 573 kb)

ESM 3

(PDF 561 kb)

ESM 4

(PDF 540 kb)

ESM 5

(PDF 769 kb)

ESM 6

(PDF 101 kb)

ESM 7

(PDF 107 kb)

References

1. Caprioli RM, Farmer TB, Gile J (1997) Molecular imaging of biological samples: localization of peptides and proteins using MALDI-TOF MS. *Anal Chem* 69:4751–4760
2. Meriaux C, Franck J, Wisztorski M, Salzet M, Fournier I (2010) Liquid ionic matrixes for MALDI mass spectrometry imaging of lipids. *J Proteome* 73:1204–1218
3. Groseclose MR, Massion PP, Chaurand P, Caprioli RM (2008) High-throughput proteomic analysis of formalin-fixed paraffin-embedded tissue microarrays using MALDI imaging mass spectrometry. *Proteomics* 8:3715–3724
4. Seeley EH, Oppenheimer SR, Mi D, Chaurand P, Caprioli RM (2008) Enhancement of protein sensitivity for MALDI imaging mass spectrometry after chemical treatment of tissue sections. *J Am Soc Mass Spectrom* 19:1069–1077
5. Yang H, Zhou B, Deng H, Prinz M, Siegel D (2013) Body fluid identification by mass spectrometry. *Int J Legal Med* 127:1065–1077
6. Kamanna S, Henry J, Voelcker NH, Linacre A, Kirkbride KP (2016) Direct identification of forensic body fluids using matrix-assisted laser desorption/ionization time-of-flight mass spectrometry. *Int J Mass Spectrom* 397–398:18–26
7. Patel E, Cicatiello P, Deininger L, Clench MR, Giardina MP, Langenburg G, West A, Marshall P, Sears V, Francese S (2016) A proteomic approach for the rapid, multi-informative and reliable identification of blood. *Analyst* 141:191–198
8. Patel E, Clench MR, West A, Marshall PS, Marshall N, Francese S (2015) Alternative surfactants for improved efficiency of *in situ* tryptic proteolysis of fingerprints. *J Am Soc Mass Spectrom* 26:862–872

9. Ferguson LS, Wulfert F, Wolstenholme R, Fonville JM, Clench MR, Carolan VA, Francese S (2012) Direct detection of peptides and small proteins in fingermarks and determination of sex by MALDI mass spectrometry profiling. *Analyst* 137:4686–4692
10. Yagnik GB, Korte AR, Lee YJ (2013) Multiplex mass spectrometry imaging for latent fingerprints. *J Mass Spectrom* 48:100–104
11. Deininger L, Patel E, Clench MR, Sears V, Sammon C, Francese S (2016) Proteomics goes forensic: detection and mapping of blood signatures in fingermarks. *Proteomics* 16:1707–1717
12. De Giovanni N (2016) Sweat as an alternative biological matrix. In: Davies S, Johnston A, Holt D (eds) *Forensic toxicology: drug use and misuse*. Royal Society of Chemistry, Cambridge, pp 438–478
13. Su B (2016) Recent progress on fingerprint visualization and analysis by imaging ridge residue components. *Anal Bioanal Chem* 408:2781–2791
14. Bailey MJ, Bradshaw R, Francese S, Salter TL, Costa C, Ismail M, Webb P, Bosman R, Wolff I, de Puit M (2015) Rapid detection of cocaine, benzoylecgonine and methylecgonine in fingerprints using surface mass spectrometry. *Analyst* 140:6254–6259
15. Guinan T, Dela Vedova C, Kobus H, Voelcker NH (2015) Mass spectrometry imaging of fingerprint sweat on nanostructured silicon. *Chem Commun* 51:6088–6091
16. Ramotowski RS (2012) Powder methods. In: Ramotowski RS (ed) *Advances in fingerprint technology*, 3rd edn. CRC, Boca Raton, pp 1–17
17. Bradshaw R, Bleay S, Wolstenholme R, Clench MR, Francese S (2013) Towards the integration of matrix assisted laser desorption ionisation mass spectrometry imaging into the current finger mark examination workflow. *Forensic Sci Int* 232:111–124

18. Guinan T, Kobus H, Voelcker NH (2016) Nanostructured silicon based fingerprint dusting powders for enhanced visualization and mass spectrometry detection. *ChemPlusChem* 81:258–261
19. Templeton J, Ottens R, Paradiso V, Handt O, Taylor D, Linacre A (2013) Genetic profiling from challenging samples: direct PCR of touch DNA. *Forensic Sci Int* 4:e224–e225
20. Ottens R, Taylor D, Linacre A (2015) DNA profiles from fingernails using direct PCR. *Forensic Sci Med Pathol* 11:99–103
21. Guinan T, Gustafsson O, McPhee G, Kobus H, Voelcker NH (2015) Silver-coating for high mass accuracy imaging mass spectrometry of fingerprints on nanostructured silicon. *Anal Chem* 87:11195–11202
22. Bailey MJ, Bright NJ, Croxton RS, Francese S et al (2012) Chemical characterization of latent fingerprints by matrix-assisted laser desorption ionization, time-of-flight secondary ion mass spectrometry, mega electron volt secondary mass spectrometry, gas chromatography/mass spectrometry, X-ray photoelectron spectroscopy, and attenuated total reflection Fourier transform infrared spectroscopic imaging: an intercomparison. *Anal Chem* 84:8514–8523

4.3 Comprehensive proteomic analysis of fingernail contaminated vaginal fluid

The article describes the applicability of MALDI-ToF MS and MALDI-mass spectrometry imaging (MSI) to the detection and mapping of biological fluid or chemical trace evidence from fingermarks and fingernail scrapings. Additionally, the research work has been extended to the identification of fingernail contaminated fluid protein markers using nLC-ESI-qTOF MS/MS. **Table 4.1** Shows the list of identified major protein markers from the fingernail scrapings of vaginal fluid (after 2 h deposition) searched with taxonomy set to ‘Homosapiens’ using Protein pilot software (version 4.5) followed by Swiss-Prot protein database analysis.

Table 4.1: List of proteins (selected) identified from fingernail scrapings of vaginal fluid (after the 2 h deposition). The extracted samples were in-solution trypsin digested and analyzed using nLC-ESI qTOF MS/MS.

No.	Accession Number	Identified protein name	Function	% Seq Cov (95)	No. of Peptides (>95% CL)
1	P13646	Keratin, type I cytoskeletal 13	Structural molecule activity; cellular response to retinoic acid	67	105
2	P19013	Keratin, type II cytoskeletal 4	Structural molecule activity; epithelial cell differentiation	66	99
3	P04264	Keratin, type II cytoskeletal 1	Regulate the activity of kinases; carbohydrate binding; fibrinolysis	62	91
4	P35527	Keratin, type I cytoskeletal 9	Plays a role in keratin filament assembly ; spermatogenesis	63	72
5	Q09666	Neuroblast differentiation-associated protein	Required for neuronal cell differentiation.	22	66
6	Q9UBG3	Cornulin	Calcium binding; response to heat	80	64
7	P04083	Annexin A1	Plays important roles in the innate immune response	60	37
8	K7EK18	Periplakin	Cornified envelope of keratinocytes; keratinization	19	35
9	P15924	Desmoplakin	Cell adhesive protein binding; cell communication	12	34
10	P06702	Protein S100-A9	Key role in the regulation of inflammatory processes and immune response	81	33
11	P07476	Involucrin	Protein binding; peptide cross linking; keratinization	58	30
12	Q9UBC9	Small proline-rich protein 3	Cross-linked envelope protein of keratinocytes	54	25
13	P63261	Actin, cytoplasmic 2	Involved in cell motility and are ubiquitously expressed in all eukaryotic cells	45	21
14	P60709	Actin, cytoplasmic 1	-	45	21
15	B1AN48	Small proline-rich protein 3 (Fragment)	Cornified envelope precursor proteins	44	20
16	P07355	Annexin A2	Calcium-regulated membrane-binding protein; body fluid secretions	47	19
17	P07355-2	Isoform 2 of Annexin A2	-	45	19
18	P04792	Heat shock protein beta-1	Involved in stress resistance; intracellular signal transduction	60	17
19	P29508	Serpin B3	Papain-like cysteine protease inhibitor to modulate the host immune response against tumor cells	41	16

20	Q92817	Envoplakin	Cornified envelope of keratinocytes	9	16
21	P04080	Cystatin-B	Intracellular thiol proteinase inhibitor	74	12
22	P04406	Glyceraldehyde-3-phosphate dehydrogenase	Role in glycolysis and nuclear functions	34	12
23	O95171	Sciellin	Regulation of proteins in the cornified envelope	19	12
24	P02768	Serum albumin	Regulation of the colloidal osmotic pressure of blood; transporting	16	12
25	P05109	Protein S100-A8	Regulation of inflammatory processes and immune response	69	11
26	O95171-3	Isoform 3 of Sciellin	-	19	11
27	Q6UWP8	Suprabasin	Epidermal differentiation.	26	10
28	P08107-2	Isoform 2 of Heat shock 70 kDa protein 1A/1B	-	18	10
29	Q06830	Peroxiredoxin-1	Peroxidase activity; cell proliferation	34	7
30	H3BQN4	Fructose-bisphosphate aldolase A	Glycolysis and carbohydrate degradation	22	7
31	P06733	Alpha-enolase	Glycolysis and carbohydrate degradation	20	7
32	P04279	Semenogelin-1	Participates in the formation of a gel matrix	12	7
33	Q01469	Fatty acid-binding protein, epidermal	Fatty acids metabolism and keratinocyte differentiation	46	6
34	Q16610	Extracellular matrix protein 1	Involved in endochondral bone formation	12	6
35	Q02383	Semenogelin-2	Participates in the formation of a gel matrix	11	6
36	P27482	Calmodulin-like protein 3	Calcium ion binding	44	6
37	P01040	Cystatin-A	Intracellular thiol proteinase inhibitor	42	5
38	P09211	Glutathione S-transferase P	Role in detoxification by catalyzing the conjugation of many hydrophobic and electrophilic compounds with reduced glutathione	30	5
39	P62937	Peptidyl-prolyl cis-trans isomerase A (Cyclophilin A)	Accelerate the folding of proteins and most abundantly expressed isozyme	30	5
40	P00338	L-lactate dehydrogenase A chain	Pyruvate fermentation to lactate	15	5
41	P04279-2	Isoform 2 of Semenogelin-1	-	10	5
42	P14618	Pyruvate kinase PKM	Glycolysis and carbohydrate degradation	10	4
43	P07900	Heat shock protein HSP 90-alpha	Chaperone and Stress response	6	4
44	P10599	Thioredoxin	Oxidoreductase activity ; cell-cell signalling	23	3
45	P81605	Dermcidin	Antimicrobial activity/defence response	27	3
46	P06396	Gelsolin	Calcium-regulated ; ciliogenesis	4	3
47	F5H397	Epithelial membrane protein 1	Cell growth	61	3
48	P02787	Serotransferrin	Cellular iron ion homeostasis	3	2
49	O15231	Zinc finger protein 185	Regulation of cellular proliferation	3	2
50	P02788	Lactotransferrin	Iron ion binding; antimicrobial activity	1	1

Those associated with vaginal fluid are in **RED** font. CL; confidence level

As expected, many keratinized and epithelium proteins (e.g., keratin 1 and 13) were detected even after diluted samples of fingernail scrapings were analyzed. The following vaginal fluid associated and differentially expressed protein markers were considered for forensic purposes: cornulin (CRNN), small proline-rich protein 3 (SPRR3), involucrin, Fatty acid-binding protein (FABP5), peroxiredoxin-1, serum

albumin, glutathione S-transferase P (GSTP) and desmoplakin (cell adhesive protein binding) [126, 152]. These proteins (see marked RED font in the Table 4.1) are over-expressed in the specified body fluid and they have also critical role for biomedical and/or clinical applications (detection of early stage cancers (e.g., cervical, squamous epithelial) [152]. Recently, using cDNA microarray analysis, researchers have demonstrated (both *in vitro* and *in vivo* characterization) the function of cornulin (CRNN) is a tumor suppressive gene that plays a crucial tumor suppressive role in esophageal squamous cell carcinoma (ESCC) and the CRNN protein help to maintain the barrier function in squamous epithelium in response to injury [153, 154].

Further information to this section, a complete list of detected proteins (database identification) within the fingernail fluid evidence and peptide ranking based on the confidence level for each protein, is given in Appendix-2A (nLC-MS/MS data) attached to this thesis.

Additionally, fingernail evidence analysis was extended for the detection of blood traces from washed hands. In order to ensure that the blood detected was not from the donor of the fingernail scrapings, koala blood was used for experiments. The fingernail traces were digested as similar to vaginal fluid and analyzed by MALDI-TOF MS. Identified mass spectra of peptides from β -haemoglobin proteins (HB-B) and the haem group with the database results for fingernail koala blood traces and control fingernails are provided in this thesis Appendix-2B.

4.4 DNA profiling of fingernail evidence

Direct-PCR DNA profiling (using Proflex PCR Machine) was carried on small portion of microswab fibres that had been used to collect vaginal fluid evidence from under fingernails [70, 124]. The profiles were analyzed using Genemapper IDXTM (version 3.2). As expected, a mixed profile of male and female short tandem repeats (STR) was obtained (see Figure 4.2). The figure indicates the STR loci plus three gender markers. Alleles from one or both contributors of DNA were recorded at 12 loci. Direct-PCR DNA profiling has made a significant application to forensic genomic research and this streamlined approach is a special area of investigation for one of the supervisors of the research described in this thesis.

This direct approach reduces the loss of DNA and increases the potential to obtain a DNA profile as compared to the conventional DNA isolation-profiling methods.

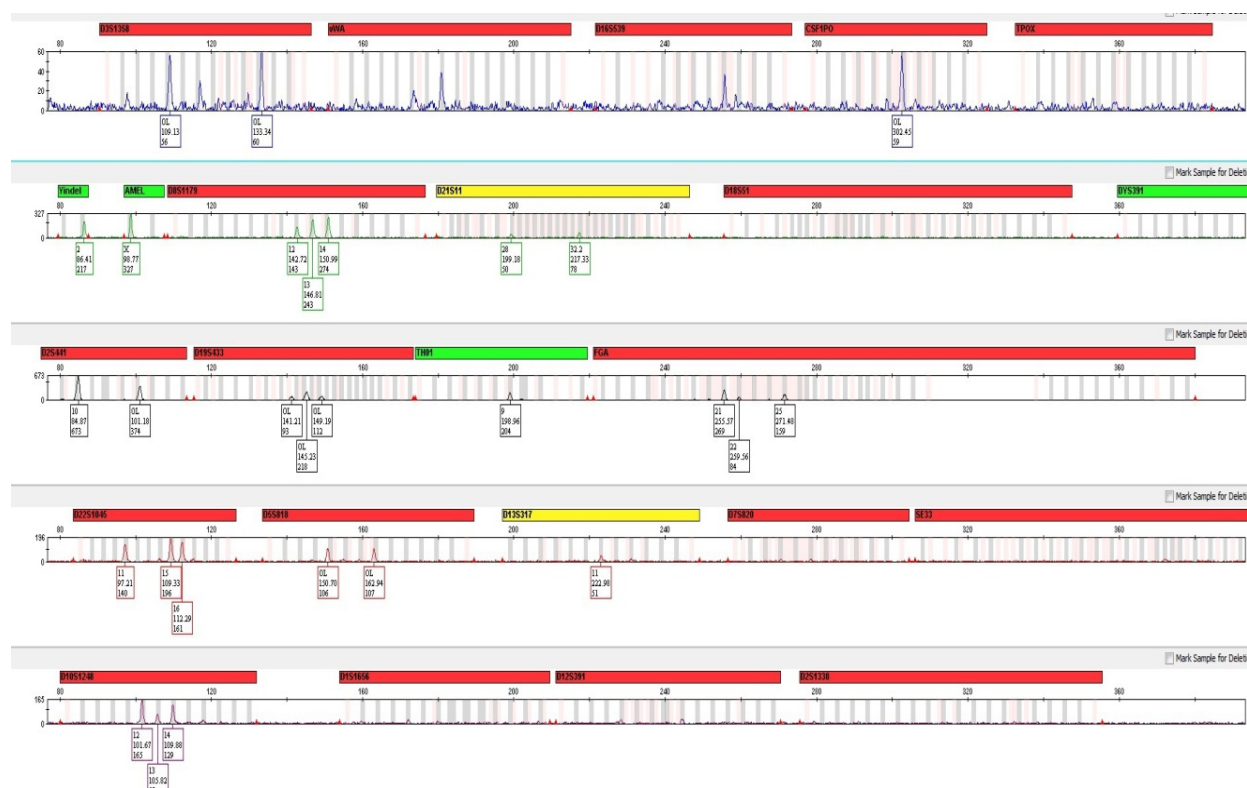


Figure 4.2. Direct-PCR DNA profile data of fingernail scrapings of vaginal fluid present in a few fibres plucked from a microswab. The process amplifies short tandem repeats (STR) plus three gender markers. Alleles from one or both contributors of DNA were recorded at 24 loci.

4.5 MALDI-ToF MSI analysis of latent fingerprint constituents (endogenous small molecules and large proteins)

For the detection of fingerprint small molecules (endogenous and xenobiotics or exogenous small chemicals), a finger was charged with sebaceous deposit by rubbing it on the back of the neck and then a mark was deposited on a clean glass microscope slide. The mark was dusted using silver/black magnetic powder (which contains iron and aluminium dust) and then lifted using a square of Kapton double-sided adhesive tape (about 25 mm × 25 mm) that was then fixed to an ITO-coated glass slide; the slide

was then subjected to MALDI-ToF and MSI analysis. Table 4.1 displays the list of small molecules and/or ions detected (e.g., fatty acids, behentrimonium, etc.) in the fingerprint ridges and ion maps are shown in Fig. 5 in the article. In these experiments conventional matrix (CHCA) was not used for the detection of low molecules ions (although CHCA clusters were used as an external mass calibrant), all the observed ions were achieved as their protonated, sodiated, potassiated, and aluminated adducts. This “matrix-less” approach could be important for forensic analysis of drugs and their metabolites, xenobiotics and endogenous molecules detections to provide additional information (i.e. what they have ingested) about the suspects or victims. Our results provide an interesting counterpoint to the work of Bradshaw *et al.* [137] where it was described that the presence of aluminium suppressed ion formation when CHCA was used as a traditional matrix for MALDI-ToF IMS.

Table 4.1. List of low molecular weight ions detected in a latent fingerprint dusted with silver-black magnetic powder lifted with Kapton double sided tape. Abbreviations: PC phosphatidylcholine; MG monoacylglyceride.

analyte	analyte theor <i>m/z</i>	ion formula	<i>m/z</i> ob [M + analyte adducts] ⁺
NaCl	-	[Na ₂ Cl] ⁺	81.445
KCl/NaCl	-	[KNaCl] ⁺	96.892
KCl	-	[K ₂ Cl] ⁺	112.877
Asparagusic acid	150.219	[C ₄ H ₆ O ₂ S ₂ + H] ⁺	150.286
N-lactoyl ethanolamine	133.145	[C ₅ H ₁₁ NO ₃ + Na] ⁺	156.213
2-Hydroxycinnamic acid	164.158	[C ₉ H ₈ O ₃ + H] ⁺	165.488
1-isothiocyanato-3-methylbutane	129.223	[C ₆ H ₁₁ NS + K] ⁺	168.015
4-Hydroxyphenylacetaldehyde	136.148	[C ₈ H ₈ O ₂ + K] ⁺	174.270
Ethyl 4-(acetylthio) butyrate	190.066	[C ₈ H ₁₄ O ₃ S + H] ⁺	190.981
Tetrahydrofurfuryl butyrate	172.221	[C ₉ H ₁₆ O ₃ K]	211.329
Palmitoleic acid	254.410	[C ₁₆ H ₃₀ O ₂ + H] ⁺	255.349
Oleic acid [-H ₂ O]	282.461	[C ₁₈ H ₃₂ O ₁ + H] ⁺	265.290
Pentadecanoic acid	242.397	[C ₁₅ H ₃₀ O ₂ + K] ⁺	281.742
Cyclohexaneundecanoic acid	268.434	[C ₁₇ H ₃₂ O ₂ + Na] ⁺	291.890
Glutamylarginine	303.314	[C ₁₁ H ₂₁ N ₅ O ₅ + H] ⁺	304.010
Heptanoylcarnitine	273.368	[C ₁₄ H ₂₇ NO ₄ + K] ⁺	312.180
MG (0:0/15:0/0:0), MG(15:0/0:0/0:0)	316.476	[C ₁₈ H ₃₆ O ₄ + Na] ⁺	339.972
Behentrimonium [-Cl]	404.160	[C ₂₅ H ₅₄ N] ⁺	368.394
Cholesterol	386.653	[C ₂₇ H ₄₆ O+Al] ⁺	413.458
Niveusin C	378.416	[C ₂₀ H ₂₆ O ₇ + K] ⁺	417.096
Squalene	410.718	[C ₃₀ H ₅₀ + K] ⁺	449.307
Fatty acids, propylene glycol mono- and diesters	510.832	[C ₃₂ H ₆₂ O ₄ + K] ⁺	549.349
Triacylglycerol (45:1)	763.224	[C ₄₈ H ₉₀ O ₆ + Na] ⁺	785.648
PC (o-18:0/18:0)	775.645	[C ₄₄ H ₉₀ NO ₇ P + Na] ⁺	798.661
Triacylglycerol (48:1)	805.304	[C ₅₁ H ₉₆ O ₆ + Na] ⁺	827.698

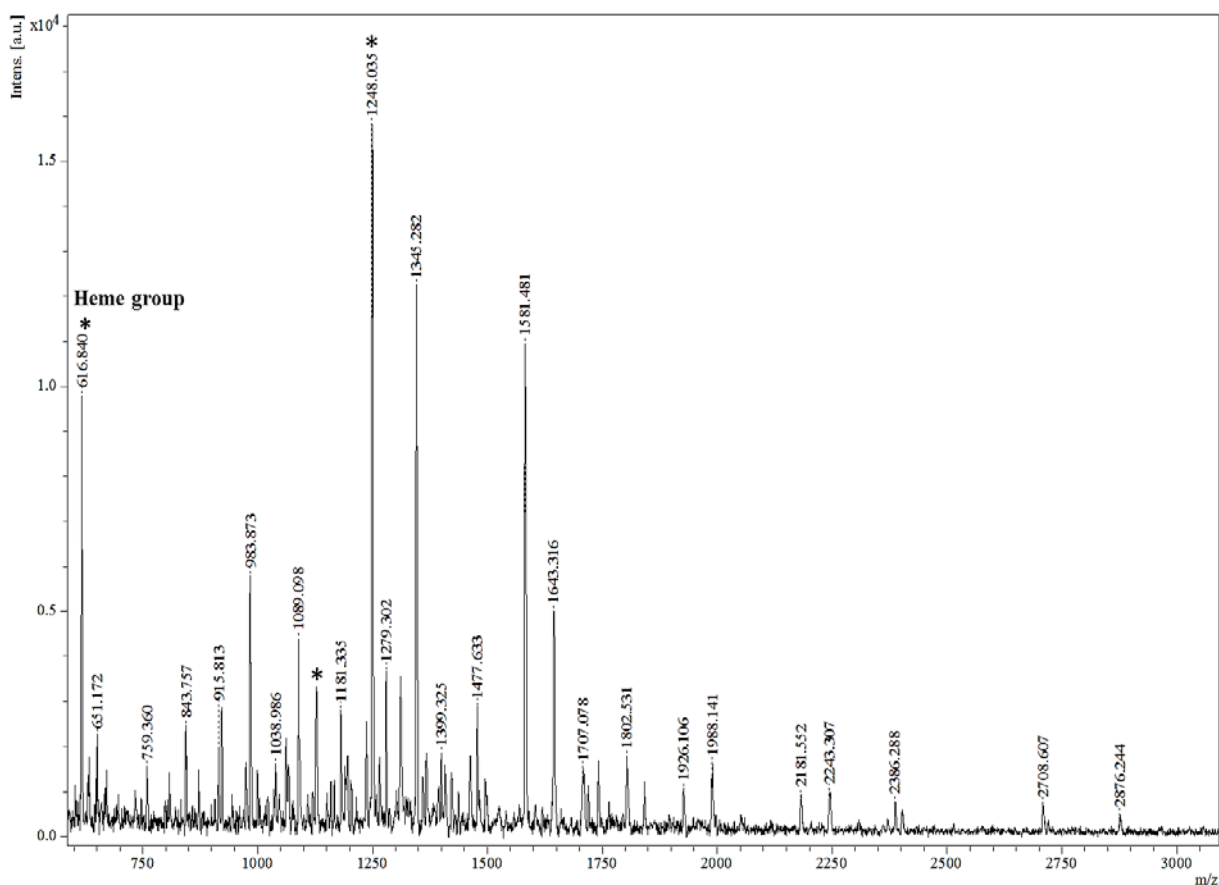


Figure 4.3. MALDI-spectra of a dusted and lifted fingermark made by a finger smeared with koala blood. A small section of the lifted mark was subjected to on-tape digestion with trypsin for 2hrs, at 37°C. CHCA matrix (1 μ L of) was placed on top of the digested fingermark region. On-tape calibration was carried out using Pepmix calibrants. Mass error upto 1.5 Da.

The applicability of MALDI-TOF MS was extended for the detection of higher protein molecules in latent fingermarks, in this experiment a finger was smeared with koala blood (around 2 μ L) and the mark was made onto a clean glass slide, dusted with silver/black magnetic powder and lifted with Kapton double sided tape. Top-down protein analysis was performed on the lifted material (Fig. 6b in the article). In order to confirm the top-down analysis, on-tape bottom-up proteomic digestion (MALDI-profiling at selected region) was carried out at 37°C, for 2hrs. Figure 4.3 displays the MALDI-TOF spectrum of bloodied fingermark indicating the presence of heme group (m/z 616), and successfully detected HB-B peptides (m/z 1248). Many additional keratin tryptic peptides were also detected in the mark. A mass error was observed upto 1.5 Da due to height of sample substrate causing a mass shift during MALDI-ionization.

Our article demonstrated for the first time, the combination of magnetic powder

fingermark enhancement with and matrix-free MALDI-ToF MSI for the detection and mapping both of small molecules and larger proteins (haemoglobins). This makes a valuable contribution to extending the information that can be gathered from a very important type of evidence.

The following additional data relating to this chapter and the article are attached to this thesis:

Appendix-2A. List of vaginal fluid associated proteins detected by Nano spray LC-MS/MS.

Appendix-2B. MALDI spectrum of koala blood recovered from under a fingernail 3hrs after deposition and after brief washing.

Appendix-2C. MALDI-TOF MS and database report for control fingermarks.

Appendix-2D. Article supplementary information for Figure 2 & 3 (MALDI-MSI results for fingermark of vaginal fluid and human blood).

Appendix-2E. MALDI spectrum of silver-black magnetic dusting powder prior to exposure to fingermarks.

Chapter 5

Chapter 5: A complementary forensic ‘proteo-genomic’ approach for the direct identification of biological fluid traces under fingernails

The main aim of the work in this chapter was to develop a complementary ‘proteomic-genomic’ approach on a single micro-swab for the direct identification of the type of biological fluid present and the identity of its “donor”. The traces under fingernails represent valuable forensic evidence because DNA profiling can indicate from whom the trace originated and proteomic methods can be used to determine the type of fluid in the trace, thus providing evidence as to the circumstances surrounding the crime. In this chapter, an analytical strategy is presented that involves two complementary techniques, direct PCR DNA profiling and mass spectrometry (MS)-based protein biomarker detection, for the comprehensive examination of traces of biological fluids gathered from underneath fingernails.

These developments are presented in this thesis as chapter 5 and the complementary ‘proteo-genomic’ approach of manuscript has been accepted for publication in international peer-reviewed journal (**Analytical and Bioanalytical Chemistry**). <https://doi.org/10.1007/s00216-018-1223-3>.

5.1 INTRODUCTION

One type of valuable evidence arising during a violent offence is foreign biological material trapped under the fingernails of the victim or offender. The type of fluid present can provide extremely valuable evidence as to the circumstances surrounding an allegation – the detection of blood under fingernails, for example, confirms that contact with the person from whom it originated was sufficiently vigorous to result in bloodshed. During a sexual assault, the victim’s fingernails may collect traces of body fluid from the assailant (such as semen) or the assailant’s fingernails might collect traces originating from the victim (such as vaginal fluid). DNA profiling of the foreign trace material under fingernails in these cases is extremely valuable as it will indicate from whom the traces originated [70]. Recently, mass spectrometry (MS) has been shown to

be valuable in determining the type of biological material present [118, 138, 139, 146, 155].

A characteristic of fingernail deposits that limits the application both of DNA profiling and mass spectrometry to their examination is the very small amounts of material available for analysis. Over the years, forensic genomic research has been directed towards the development of increasingly-sensitive tests and the streamlining of sample treatment processes through innovations such as direct polymerase chain reaction (PCR) DNA profiling [70, 121]. In that technique, a small portion of a biological sample or a swab used to collect biological material is placed directly into the PCR, which not only accomplishes the exponential multiplication of target DNA sequences but also obviates the need for cell lysis and DNA extraction steps. This approach minimises the loss of DNA and maximises the potential to obtain a DNA profile.

Recently (2017) Legg *et al.* [156] detected high-specificity protein markers of vaginal fluid. In particular, cornulin, neutrophil gelatinase-associated lipocalin, suprabasin and Ly6/PLAUR containing protein 3 were consistently detected in their set of vaginal fluid samples and it was proposed that these markers may be used for analysis of questioned stains [140]. The authors also concluded these vaginal fluid markers were not detected in saliva, seminal fluid or peripheral blood samples. Legg *et al.* also concluded that using current analytical methods for differentiation of menstrual fluid from mixtures of peripheral blood and vaginal fluid is often difficult and there is no specific marker for the detection of menstrual fluid. Another recently published article [151] had shown an emerging mass spectrometry-based proteomics analysis approach using LC-MS/MS for the identification of potential forensic protein markers in vaginal fluid [151]. This work identified two human small proline-rich protein 3 (SPRR3) isoforms (m/z 17,237 and 18,063) and fatty acid-binding protein 5 (FABP5, m/z 15,075) as potential protein markers that may be used for the identification of vaginal fluid.

The research described in the present study relates to an extension of previous work described in this thesis related to the detection of protein biomarkers in forensically-relevant body fluids such as blood, semen, saliva and vaginal fluid. Earlier it was shown that traces of vaginal fluid or blood underneath fingernails could be collected using a flock microswab and protein biomarkers characteristic of the fluids could be detected in microswab extracts using MALDI-ToF MS/MS [118].

Even though body fluids are complex mixtures of proteins, and MALDI-ToF MS/MS was used without chromatographic fractionation of the mixture, the approach is nevertheless effective as a forensic technique because characteristic biomarkers are highly-expressed in forensically-relevant body fluids (such as haemoglobin in blood). Under MALDI ionization conditions the most abundant proteins or peptides ionize in preference to those present at lower levels. Using the example of prostate-specific antigen (PSA), a body fluid other than semen in which PSA is present in trace amounts, such as blood, would not yield a detectable PSA signal using MALDI-ToF-MS as the more abundant protein, in this case haemoglobin, would ionize preferentially. Furthermore, it has been demonstrated earlier in this thesis and published that small tufts of fibres plucked from pieces of fabric (i.e. nylon, cotton, cellulose acetate) that had been stained with biological fluids (blood, semen) can be subjected to direct MALDI-ToF MS and intact protein biomarkers could readily be detected [31]. Given that only a small portion of a microswab containing biological material is required for generation of a direct PCR DNA profile [70, 121], the elegant extension that small tufts of fibres plucked from a single microswab could be used for both direct PCR DNA profiling and direct MALDI-ToF-MS analysis of fluid protein biomarkers was investigated.

Direct detection and identification of intact proteins (“top-down” analysis) on fibres using MALDI-MS is challenging due to limitations in mass axis resolution and accuracy, especially if a mixture of body fluids is present. Hence, the use of “bottom-up” proteomic analysis was also investigated in order to enhance the specificity and reliability of protein biomarker identification.

Compared to evidence such as a visible bloodstain, debris that may collect under fingernails as a result of person-to-person contact during a crime such as homicide or sexual assault is present at the trace level. Classical techniques for the extraction of proteins from fingernail traces present the risk that valuable analyte may be lost, thus affecting the identification of the biological material present. It has been shown previously in this thesis and the associated publication [31] that it is possible to carry out in situ or direct MALDI-ToF MS analysis of intact proteins and their tryptic digests on minute tufts of textile fibres (e.g. nylon, cotton) that had been plucked from garments that had been exposed to human body fluids such as blood and semen.

That research involved the use of cotton, polyester, rayon and nylon textile fibres. As part of on-going research into the applications of direct PCR genomic analysis to forensic science [157], nylon microswabs were identified as an effective tool for recovery of trace biological material from a variety of surfaces. It was therefore a logical extension of both these research streams to examine the scope and limitations of *in situ* MALDI-ToF MS analytical techniques for the identification of minute traces of human body fluid ‘evidence’ collected from under fingernails using nylon microswabs. For this work, dental microswabs were employed.

Whilst the transfer of biological traces during an assault obviously determines what might be detected after the event, the persistence of traces is an important consideration. Regardless of the amount or type of foreign material transferred, everyday activities, such as handwashing or showering, or the passage of time might cause the deposit to be lost. Therefore, although it is important to determine which techniques can be applied to the identification of foreign biological deposits under fingernails, an evaluation of the impact that the time delay has between deposition and recovery is also very important.

This chapter explores the relative abilities of MALDI-ToF-MS and n-LC-MS/MS to identify biological fluids under fingernails when there is a delay between deposition of the fluid and analysis. The aim of this study was to carry out a comprehensive forensic examination of traces of vaginal fluid or foreign blood trapped under fingernails using a complementary proteomic and genomic approach.

5.2 Fingernail preparation and collection of traces using nylon microswabs

Before deposition of biological fluids under fingernails, the hands were washed with normal tap water. Fingernail deposits containing vaginal fluid were prepared by inserting a clean finger into a vagina for about 5-10 s and then typical office work was carried out for a range of time intervals (between 1-8 h) prior to the collection of any deposit remaining under the nail. The samples were provided from four donors over 16 experiments. Collection of fingernail traces was carried out using microswabs, which feature a very small tip approximately 1 mm wide x 2 mm long made from flocked short, thin nylon fibres [118]. These swabs are many times smaller than the swabs currently used in forensic laboratories and do not absorb significant quantities of fluid.

The tip of the microswab was moistened with deionized water, flicked to remove liquid droplets and then it was rolled underneath the fingernail to collect any persisting vaginal fluid. After it was dried in air for about 10 min, the microswab tip was sealed in an HPLC sample (2 mL) until used in analysis, which was usually within 12 hrs. The small size of the microswabs, together with their flocked hydrophobic construction, resulted in very little moisture being retained and thus a relatively short drying time. A control sample of fingernail scrapings (finger not exposed to fluid) was examined for all donors. Fingernail traces containing blood were mocked-up by placing 1 μ L of animal blood (Red kangaroo, *Macropus rufus*) under a clean fingernail. Human blood was not used for these experiments in order to remove uncertainty that any blood detected might have arisen by injury of the finger during sampling of the nail. After deposition of the blood, the hands were rinsed under cold running water about 1 min and normal office duties or other daily routine work (e.g., computer work, coffee preparation, with washing) were carried out prior to collection of the deposited blood, which took place 6-24 h after it was deposited. Sampling was carried out using exactly the same process as described above for the collection of vaginal fluid traces. Three individuals contributed samples for more than 20 experiments.

The detailed sample preparation and mass spectrometry analysis of this chapter can be referred in Materials and Methods section (chapter 2).

5.2.1 Data analysis

MALDI-ToF MS/MS peptide mass fingerprinting (PMF) data were processed with FlexAnalysis (version 3.3) software and the PMF list of m/z values was used to search the Swiss-Prot or NCBIInr protein databases with the search tool Matrix Science (<http://www.matrixscience.com>) (version 2.5). Mass tolerance up to 0.5 Da with no fixed modifications and one maximum missed cleavage were selected as the search parameters. Protein identifications were based on the presence of at least two unique peptides and significant sequence coverage. The protein match and sequence coverage were also cross validated with theoretical and observed protein masses. For the identification and evaluation of protein markers by nLC-ESI-qTOF MS/MS, the raw data were processed with MS converter software by generating the mascot generic file (.mgf).

The file was then uploaded into Protein pilot software version 4.5 (AB Sciex, Massachusetts, USA) and searched the data against the ‘Swiss-Prot’ database by selecting a “Homo sapiens” as a taxonomy. For the identification of non-human (*Macropus rufus*) blood traces, the MS data were searched by selecting the taxonomy “All-organisms”. After database searches were completed, the protein data were exported as a text file and imported into Microsoft Excel. The Excel data were manually analysed for the presence of protein markers that arose from the material deposited underneath fingernails; only peptides of greater than 95 % confidence were considered for this data analysis step. Statistical analysis of these data was carried out in the Microsoft Excel sheet. For the identification of DNA profiles from the direct PCR analysis, DNA loci were analysed and interpreted using Genemapper IDX™ (version 3.2, Thermo Fisher Scientific).

5.3 Results and discussion

5.3.1 Analysis of fingernail traces using MALDI-ToF-MS/MS

First, a sample of vaginal fluid from a volunteer was analysed using MALDI-TOF MS/MS to determine the intact protein profiles from a control. Fig. 5.1A shows average molecular values attributed to small proline-rich protein 3 (SPRR3) isoforms (17.2 and 18.03 kDa) and fatty acid-binding protein 5 (FABP5) at approximate mass of 15.02 kDa. These proteins were considered as biomarkers for the detection of vaginal fluid for this research and a recent study using classical proteomic methods confirmed the validity of this approach [151]. Intact cornulin (CRNN) was not detected, possibly due to the complexity of the mixture or the lower sensitivity of MALDI-ToF-MS towards the higher molecular weight (~58 kDa) of CRNN. Fig. 5.1B represents the MALDI-MS/MS spectrum of peptide m/z 967.56 matched to small proline-rich 2B (SPRR2B) protein and its sequence (matched ‘b’ and ‘y’ product ions are indicated in the spectra). Classical proteomics analysis by nLC-ESI-qTOF MS/MS confirmed the CRNN and SPRR3 marker proteins (see Appendix-3A).

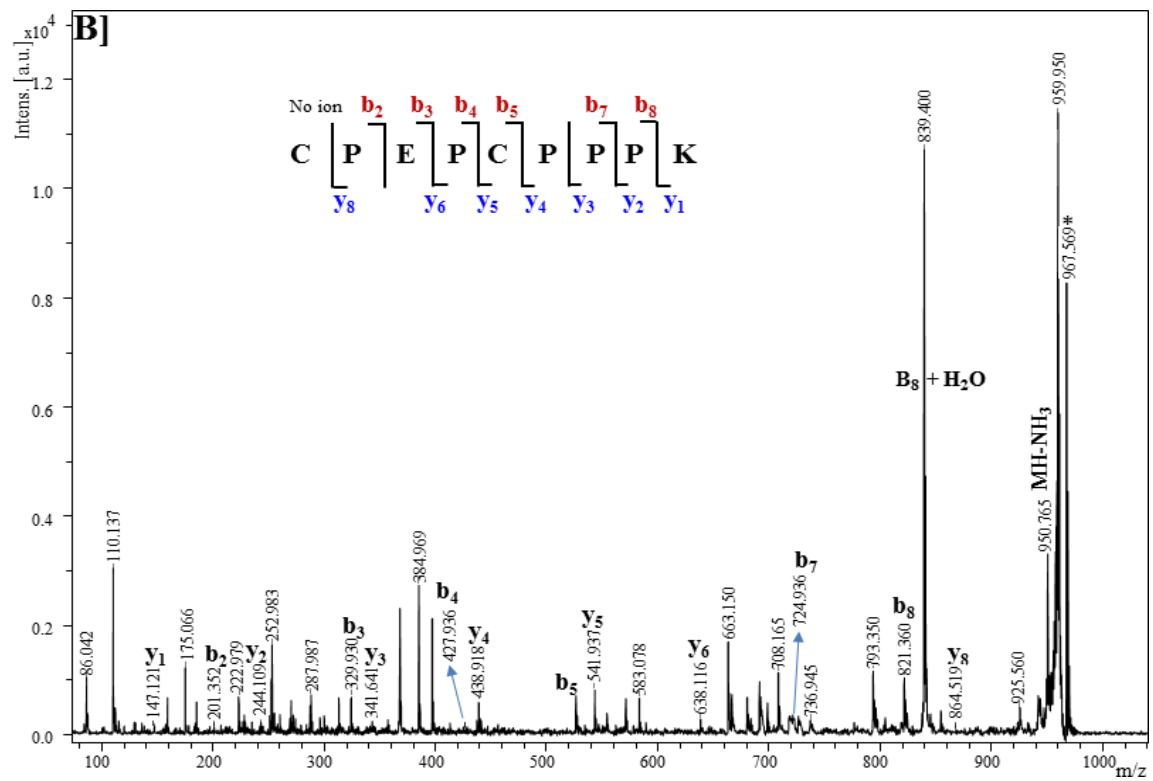
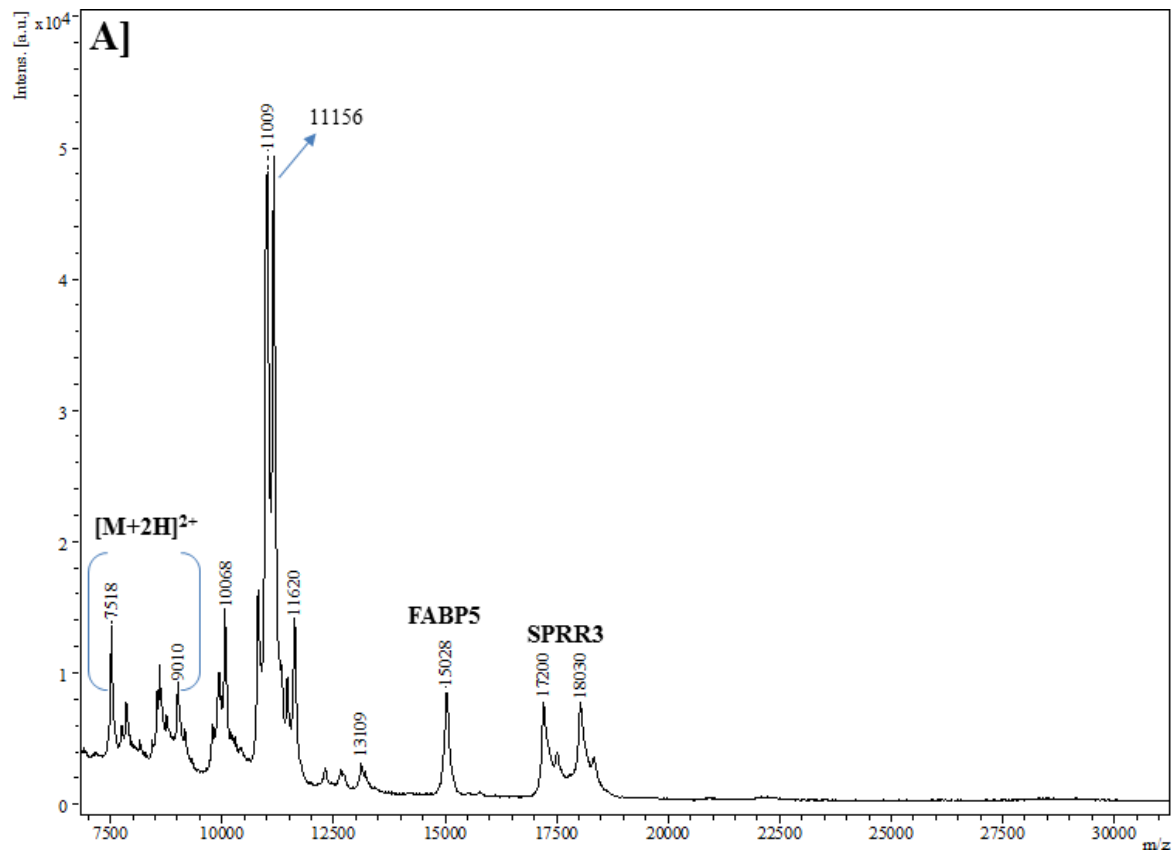


Figure 5.1. A) MALDI-TOF MS protein profiles of vaginal fluid. A microswab containing vaginal fluid was extracted and acquired MS spectrum using linear positive

mode. B] MALDI-LIFT MS/MS spectrum of peptide m/z 967.56 of matched small proline-rich 2B (SPRR2B) protein. Inset: sequence of the corresponding peptide; matched 'b' and 'y' fragmented ions are indicated in the spectra. CHCA (60% ACN/H₂O and 0.2%TFA) matrix was used.

In regards to detection of intact proteins in traces collected from underneath fingernails, neither haemoglobin nor vaginal fluid biomarkers ionised well using MALDI. In addition, significant mass errors were observed that would make defendable identification of proteins difficult. However, **Fig. 5.2A** displays a typical MALDI-ToF trypsin digest PMF successfully acquired directly from several fibres plucked from a nylon microswab that had been used to collect traces from under a fingernail exposed to vaginal fluid 3 h previously. The manual interpretation of the MALDI-PMF spectra and a Mascot database search resulted in the positive identification of 14 peptides originating from cornulin (CRNN), which is the most abundant protein in vaginal fluid [156, 158] and is not present in other fluids can be expected to be found under fingernails such as blood, saliva and semen [31, 156].

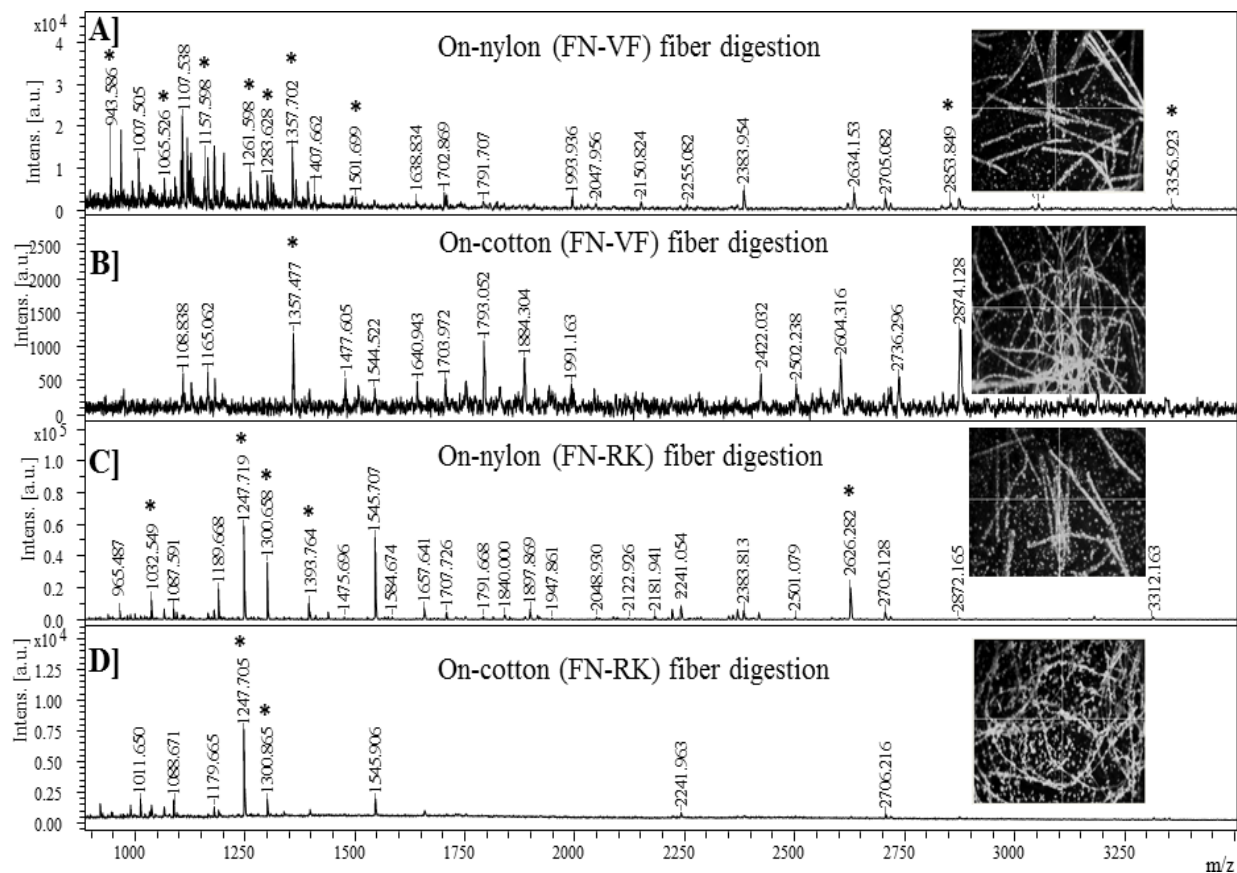


Figure 5.2. ‘On-fibre’ MALDI-ToF MS analysis of trypsin digests for vaginal fluid (A] and B]) and blood traces (C] and D]) collected from under fingernail 3 h and 6 h after deposition, respectively, using cotton and nylon swabs. Peaks marked with asterisks (*) in A] and B] indicate the matched peptides originating from human cornulin while in C] and D] the asterisks signify β -haemoglobin peptides (*Macropus rufus*). Insets are images of the collection of fibres on the ITO slide with matrix.

Fig. 5.2B shows an *in situ* PMF collected from vaginal fluid traces present under a fingernail that were collected using a cotton swab. Signals due to CRNN are not evident. Earlier work described in this thesis and published [31] has shown that cotton is also a poor substrate for detection of human semen, but saliva and blood biomarkers can readily be detected using ‘on-fibre’ digestion and MALDI-ToF MS with cotton fibres. At present, the erratic performance achieved using cotton swabs cannot be explained. However, as described earlier and published, it is clear that the nylon microswab offers consistent performance with all the fluids examined so far and it is a very convenient device for the collection of minute traces from the small gap under fingernails [118]. Signals obtained (MALDI-TOF) from control cotton and nylon fibres report can be seen in this thesis Appendix-3B. A replicate analysis using ‘in-solution’ digestion was also successful for the detection of CRNN, but only 9 peptides could be identified (report provided in the Appendix-3B). This suggests that the direct, *in situ* approach is preferable to the classical, in-solution digestion approach for evidence examination.

Fig. 5.2C shows a typical *in situ* PMF derived from non-human blood (1 μ L, *Macropus rufus*) that been deposited under a fingernail and collected using a nylon microswab (in this case after the blood had been in place for 3 h before it was recovered). As can be seen from **Fig. 5.2D**, blood traces can be detected directly on cotton fibres.

A critical aspect of the *in situ* analytical approach with regards to its application to casework is whether it can be applied to traces of body fluids that have been trapped under fingernails for a length of time. Over several experiments it was determined that the time limit for detection of blood traces under fingernails using the *in situ* approach is up to 14 h with up to 5 h being the limit for vaginal fluid traces. This will be discussed later in comparison to techniques involving nLC-MS/MS.

5.3.2 Differential proteomic analysis of fingernail traces using nLC-ESI-qToF MS/MS and identification of vaginal fluid and non-human blood protein markers

A potential issue with regards to the analysis of fingernail traces using MALDI methods is that, in addition to foreign biological material, the traces will contain keratinized cellular material from the finger itself and possibly traces of nail keratin if evidence recovery is not gentle. As a consequence, fingernail traces are likely to contain keratin that might swamp traces of other proteins during digestion and ionization. This may compromise the ability to detect foreign body fluids in fingernail traces if their concentration is low, either as a result of brief or gentle contact between victim and assailant or as a result of a long time delay between trace deposition and its recovery. The performance limitations of MALDI-ToF-MS/MS were compared to those applicable to nLC-ESI-qToF MS/MS, where keratin is chromatographically separated from target biomarkers. Differential proteomic analysis of a small group of fingernail trace samples collected after a range of collection time periods was carried out. Fingernail traces of vaginal fluid and non-human blood (1 μ L, *Macropus rufus*) were collected using nylon microswabs. The swabs were extracted in LC-MS grade water, followed by in-solution enzymatic protein digestion and then analysed using nLC-ESI-qToF MS/MS and MALDI-ToF MS/MS. Resulting data were searched against Swiss-Prot database by selecting 'Homo sapiens' for the identification of vaginal fluid markers using search engine Matrix Science (v2.5; London, UK). nLC-ESI-qToF MS/MS data for *Macropus rufus* blood traces were searched with taxonomy set to 'All organisms' and for the MALDI-ToF-MS/MS PMF data 'Other Mammalia' was selected to identify specific haemoglobin protein markers.

Figure 5.3A summarises the nLC-ESI-qToF MS/MS results with regards to the detection of vaginal fluid associated peptides and other proteins in fingernail traces versus the time delay between deposition of vaginal fluid traces and their recovery onto a microswab (3-8 h range). The results displayed were obtained from a single volunteer, but the experiment was repeated twice more with similar results, (data not shown). First, it can be seen that the control fingernail swab does not show the presence of any CRNN and other vaginal-related characteristic proteins but there was a "background" of 65 different, non vaginal proteins. Second, after deposition of vaginal fluid, fingernail

traces show a marked increase in the number of specific peptides originating from CRNN, small proline-rich protein 3 (SPRR3), fatty acid binding protein 5 (FABP5) and serum albumin that drops-off over the experimental time-frame. By 8 h, these peptides were no longer detected. **Fig. 5.3A** also shows that the fingernail traces are enriched in proteins generally as a result of exposure of fingers to vaginal fluid and there is also a drop-off in their numbers as well almost to approximately background level after 8 h. Many non-vaginal associated proteins (cervico-vaginal) identified are found in the vaginal cavity but cannot be considered as a specific biomarker for that environment, such as Annexin and protein S 100 (calcium binding and immune response), Desmoplakin (involved in cornification and structural integrity), Involucrin (cornified cell envelope of stratified squamous epithelia), Cystatin-A and -B (intracellular proteinase inhibitor), Heat shock proteins (HSP) and enzymes involved in oxidative stress defence (such as glutathione S-transferase P (GSTP), thioredoxin and peroxiredoxin proteins), lactotransferrin (iron ion binding and antimicrobial activity), neuroblast differentiation-associated protein AHNAK and various epithelial membrane associated proteins [151, 156 & 158]. A complete Microsoft Excel list of all identified proteins detected in vaginal fluid fingernail traces (3-8 h delay between deposition and collection), control vaginal fluid and the fingernail data can be found in this thesis Appendix-3A. **Fig. 5.3B** shows the MS/MS data for the CRRN peptide ion m/z 1503.71 detected at 7 h and its associated sequence.

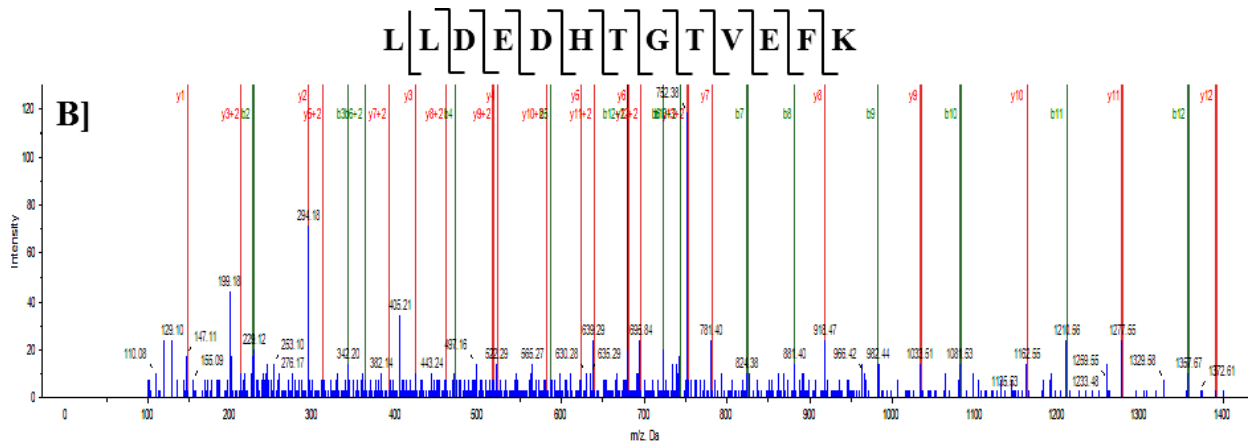
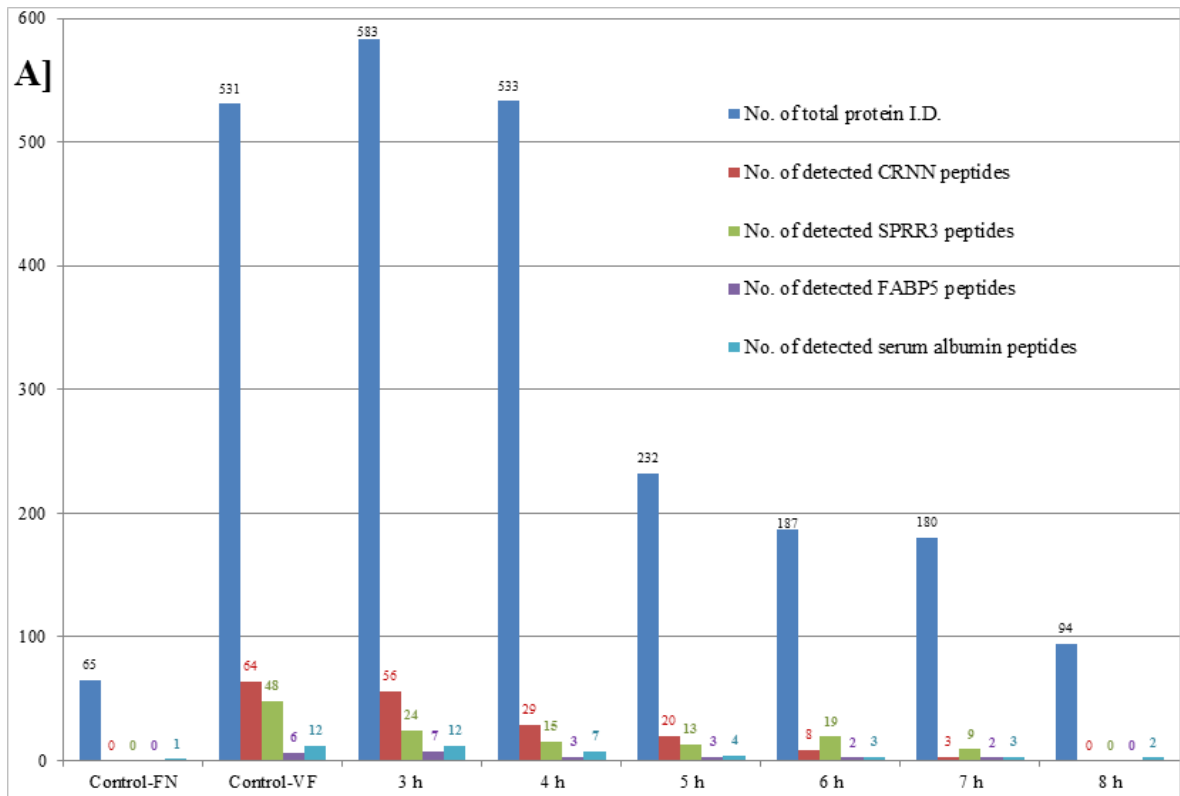


Figure 5.3. nLC-MS/MS analysis of fingernail traces containing vaginal fluid evidence. A] The graph represents the identified total proteins from a control fingernail (FN), control vaginal fluid (VF) and deposited vaginal fluid traces collected after different time periods (3-8h). B] nLC-MS/MS spectrum of CRNN tryptic peptide at m/z 1503.71(LLDEDHTGTVEFK) arising from the 7 h fingernail trace.

A similar time-series experiment (6-24 h) was carried out using deposition and recovery of non-human blood (1 μ L, *Macropus rufus*) under fingernails. Non-human blood was used to guard against the (slight) possibility that the trace recovery process injured the nail bed and caused bleeding of the volunteers. The traces collected on microswabs were

treated in the same way as vaginal fluid traces. **Fig. 5.4** displays the graph of haemoglobin peptide markers and different proteins (including keratinized and matched haemoglobins proteins to various other species) in general identified in fingernail traces using nLC-ESI-qToF MS/MS. The results displayed were collected from a single volunteer but are typical of the replicate experiments (data not shown).

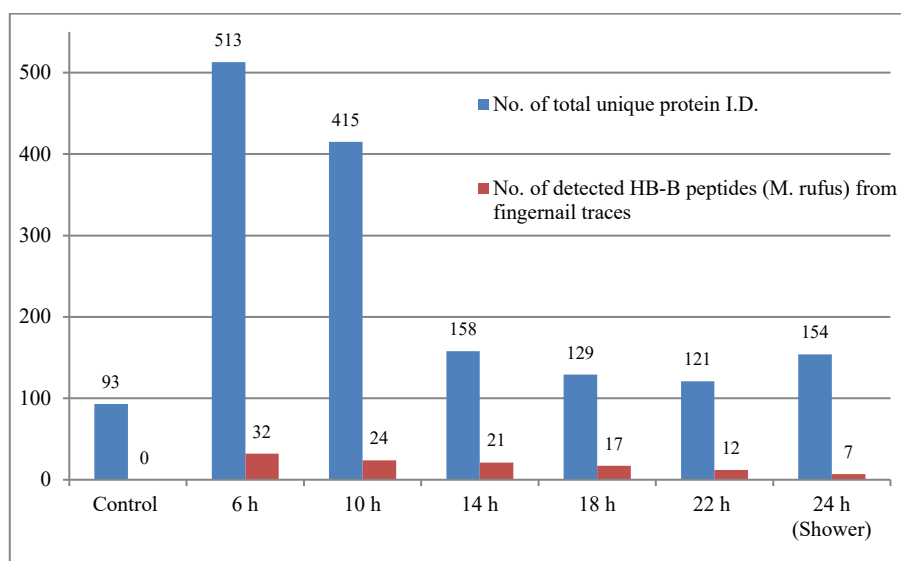


Figure 5.4. Number of identified proteins and haemoglobin-specific peptides ..-haemoglobin, (HB-B)) from fingernail traces containing *Macropus rufus* blood (1 μ L) using nLC-ESI-qToF MS/MS.

As for the results relating to vaginal fluid deposition and collection, target peptides were not detected in the control. When nails were exposed to blood, the numbers of proteins in general and β -haemoglobin (HB-B) peptides rose and then decreased as the time between deposition and collection lengthened from 6 to 24 h. The result at 24 h is remarkable in that the volunteer showered between deposition of blood and collection of traces (for all other time points volunteers carried out normal office duties and had washed their hands). A list of total identified unique proteins from control and all fingernail traces (6-24 h delay between deposition and collection) are provided in this thesis **Appendix-3C**. Compared to vaginal fluid traces under fingernails, blood traces show a much wider time window for recovery and successful identification.

The same samples of tryptic peptide solution that were used for nLC-ESI-qToF MS/MS were analysed using MALDI-ToF MS/MS (aliquots of 0.8 μ L were pipetted directly

onto a steel plate and treated with CHCA matrix, referred to here as the “in-solution” process). **Table 5.1** shows a comparison of the results achieved using nLC-ESI-qToF MS/MS and in-solution MALDI-ToF MS/MS. It can be seen that the classical proteomic analysis using nLC-ESI-qToF MS/MS has a much lower limit of detection for the fluid biomarkers and would be the method of choice for examination of swabs collected many hours after an alleged offence or when the offence is likely to involve the transfer of low levels of biological material. It can also be seen that the *in situ* approach of analyzing fluid digests directly on fibres from a microswab using MALDI performs as well as the in-solution MALDI method when vaginal fluid or blood are involved. Thesis supporting information Appendix-3D, 3E, 3F and 3G contain all the PMF data and database search results that were used to produce **Table 1**.

Table 5.1. The number of tryptic peptides from CRNN (human vaginal fluid) and haemoglobin (*Macropus rufus*) recovered from under fingernails as detected using MALDI-ToF MS/MS and nLC-ESI-qToF MS/MS.

Analysed fingernail scraping samples	No. of identified peptides from deposited fluid	
	nLC-MS/MS Analysis	MALDI-MS Analysis
<u>Fingernail with vaginal fluid traces</u>	CRNN	CRNN
3 h	56	14
4 h	29	12
5 h	20	7
6 h	8	ND
7 h	3	ND
8 h	ND	ND
<u>Fingernail with <i>Macropus rufus</i> blood traces</u>	HB-B	HB-B
6 h	32	8
10 h	24	7
14 h	21	5
18 h	17	ND
22 h	12	ND
24 h (after shower)	7	ND

CRNN: Cornulin (human), ND: not detected, HB-B: β -subunit of haemoglobin (*Macropus rufus*).

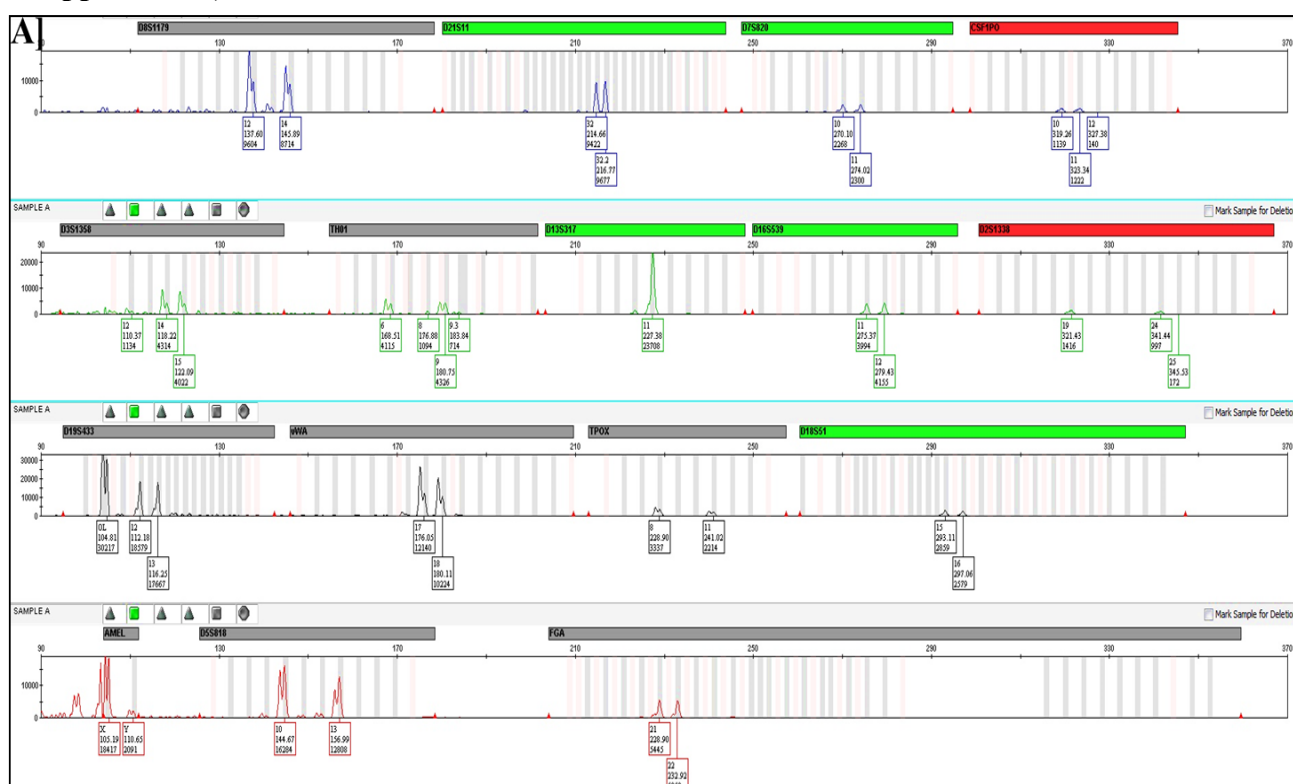
5.3.3 Complementary proteomic and genomic analysis of fingernail traces

In a forensic examination of fingernail traces collected in regards to a serious offence such as homicide or sexual assault, the ideal goal is to obtain information as to both the type of body fluid present as well as the identity of the person from whom it originated, rather than just information relating to one or the other. The most elegant and practical approach is a complementary one, where the examination can accommodate a single collection of evidence rather than one where a sample is collected for proteomic analysis and an additional one is collected for genomic analysis. Dual sampling presents the risk that the first sampling collects all the evidence that is present, leaving nothing for the second swab to collect, or that both samples do not contain sufficient material for successful analysis. There are two potential complementary analytical approaches: one is to use a single swab to collect the evidence and use some of the swab for proteomic analysis and some of it for genomic analysis; the other is carry out genomic analysis as a priority (as it yields the most valuable evidence) and then use either surplus DNA extract or PCR product as the sample for proteomic analysis. Both of these approaches were investigated.

In regards to the first approach, it has been shown above in this thesis (Figure 5.2) and the associated publication [118] that it is feasible to carry out *in situ*, bottom up identification of body fluids present on only a few fibres plucked from a microswab that was used to collect traces from under fingernails. Therefore, experiments were carried out where direct MALDI-ToF MS/MS was performed on a few fibres plucked from a microswab used to collect vaginal fluid traces from under fingernails 1 hr after deposition and then direct PCR combined with capillary electrophoresis [121, 157] was performed on some fibres plucked from the same microswab.

A strong female DNA profile (see **Fig. 5.5A**) and a PMF indicating the presence of CRNN were obtained (see **Appendix-3H**); the electropherogram shows signs that too much DNA was present in the PCR but no attempts were made to optimize the process in this proof of concept. A similar experiment was carried out where fingernail traces containing *Macropus rufus* blood were collected 6 hr after deposition. Direct PCR of a few fibres from the swab yielded the profile of only the human volunteer, which is to be expected as the profiling process uses human-specific PCR primers, and direct MALDI-ToF MS yielded a PMF consistent with *Macropusrufus HB-B* (see **Appendix-3I**).

For a trace of blood that was recovered 6 h post-deposition, post-PCR residue (2 μ L) from the direct PCR genomic analysis of the same sample was also subjected to MALDI-ToF MS and MS/MS. Top down identification of *Macropus rufus* haemoglobin was achieved and confirmed using bottom up techniques. **Fig. 5.5B** shows the MALDI-ToF-MS/MS spectrum of precursor ion $[M+H]^+$ m/z 1247.74 (sequence LLIVYPWTSR), which was confirmed using the Swiss-Prot database as a peptide associated with the HB-B subunit unit of *Macropus rufus* haemoglobin (see **Appendix-3I**). For comparison, conventional forensic DNA profiling (i.e. a process involving cell lysis and magnetic bead clean-up of nucleic acids prior to PCR) was carried out using fingernail traces gathered 3 hrs after blood (*Macropus rufus*) had been deposited underneath fingernails. Both purified DNA extract and post-PCR solution were spotted onto stainless steel plates and subjected to MALDI-ToF MS. As expected, HB was not detected in either the DNA extract nor the downstream PCR product; the extraction solution includes a protease enzyme and purification of DNA using a magnetic bead-based protocol is very effective at removing traces of proteins and peptides. Strong signals due to bovine serum albumin and possibly a non-ionic surfactant were detected (see **Appendix-3J**).



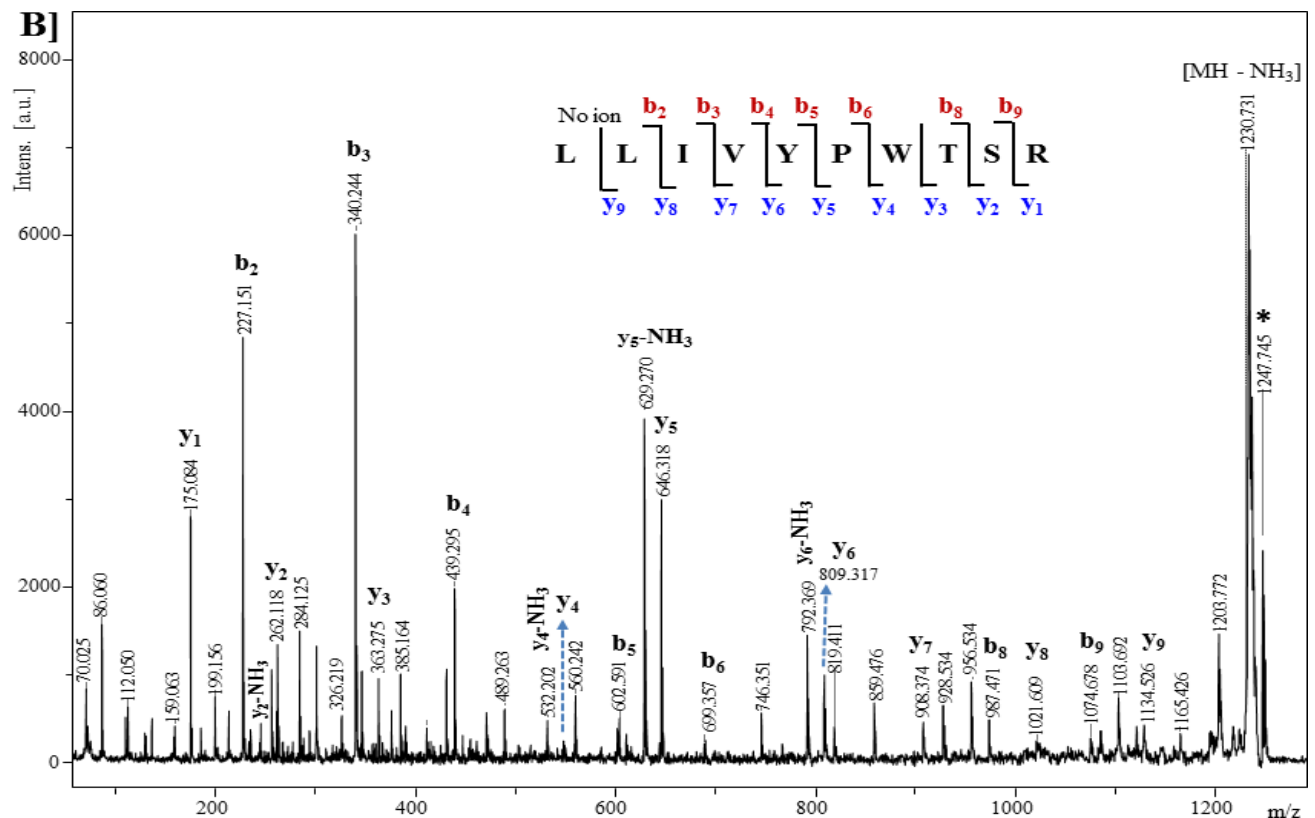


Figure 5.5. A) Direct-PCR DNA profile data (selected loci) from fingernail traces containing vaginal fluid (fibres plucked from a deposit collected on a microswab 1 h after deposition). B) MALDI-ToF MS/MS spectrum acquired from a tryptic peptide product obtained from post-PCR solution of fingernail trace of *Macropus rufus* blood (collected 6 h after deposition). MS/MS data were acquired from precursor ion at m/z 1247.74, which arose from the HB-B subunit of *Macropus rufus* blood. Matched “b” and “y” product ions are indicated in the sequence.

5.4 Concluding remarks

This study has shown that it is possible to carry out a comprehensive forensic examination of traces of vaginal fluid or foreign blood trapped under fingernails using a complementary proteomic and genomic approach.

A summary of the analytical strategy and individual steps that comprise the complementary approach is given in **Fig 5.6**.

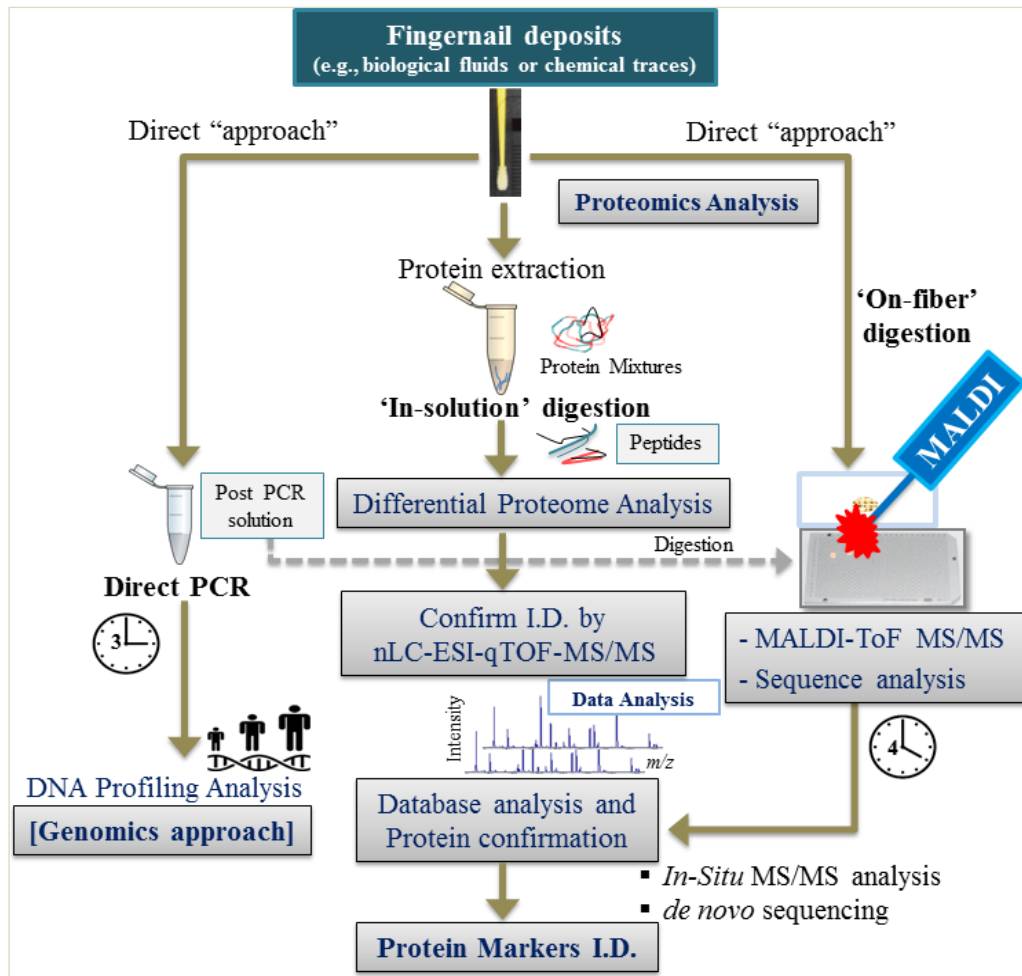


Figure 5.6. A schematic workflow for a complementary proteomic and genomic analysis of fingernail debris present in a single microswab. The right-hand workflow illustrates ‘on-fibre’ tryptic digestion of fingernail traces present on a few fibres taken from a microswab followed by direct (or *in situ*) MALDI-TOF MS/MS analysis. The elapsed time for this workflow is approximately 4 h. The left-hand workflow depicts direct PCR analysis carried out using a few fibres taken from the same microswab. The elapsed time for this workflow is about 3 h. The workflow in the centre shows ‘in-solution’ tryptic digestion of residues present on the microswab. This workflow requires about 18 h to accomplish but compared to MALDI-TOF MS/MS analysis much lower limits of detection are achievable. Dotted lines indicate that post-PCR solutions from the genomic analysis and ‘in-solution’ tryptic digest solutions can be analysed using MALDI-TOF MS/MS.

In an investigation where there is an allegation of sexual assault committed by a particular individual, it has been shown in this thesis that a direct or *in situ* MALDI-ToF-MS approach may detect human CRNN and other abundant protein markers for vaginal fluid including CRNN, SPRR3, FABP5 on a few fibres plucked from a single

microswab used to collect evidence from under the assailant's fingernails. Not surprisingly, proteins that cannot be uniquely attributed to vaginal fluid, such as serum albumin, were also detected. The on-fibre, *in situ* approach is quick and convenient and may be less risky when only small traces of evidence are present on the swab. Furthermore, a few more fibres from that swab may be used to identify of the human source of that fluid *via* direct PCR. On the other hand, solutions must be prepared anyway if MALDI results are to be confirmed by nLC-MS/MS and the topography of the sample in the on-fibre approach causes some mass error.

The presence of CRNN *and* DNA attributable to the victim in traces under an individual's fingernails would provide valuable evidence in establishing that genital contact has occurred. The limitation in a scenario such as this is that sampling of the suspect would need to occur within about 5 h of the alleged offence and in our experiments the volunteer did not wash their hands. The impact of hand washing on the persistence of CRNN under the fingernails is an important subject for further research.

In regards to an allegation of an assault that could have resulted in a victim or offender collecting foreign blood under their fingernails, it has been shown that MALDI-ToF MS/MS proteomic examination could indicate the presence of haemoglobin up to 14-18 h after the alleged offence. The *in situ* approach avoids the prefractionation steps and contamination issues associated with techniques involving liquid chromatography MS. By using Rapigest for bottom-up analysis only 4 h is required to get a proteomic result, which is only slightly longer than the time required for direct PCR DNA profiling (3 h). In the event that a microswab has been completely consumed for direct PCR, post-direct PCR solutions can be used successfully for proteomic examination. In the experiments described here, β -subunits of haemoglobin (*Macropus rufus*) could be detected in post-PCR solutions of blood traces collected 3 h after deposition; no attempt was made to examine detection of blood longer times after deposition. However, β -subunits of haemoglobin could not be detected in conventional DNA extracts (or their downstream PCR products) as the DNA extraction process was very effective at removing the target proteins and significant chemical noise was evident in the resultant mass spectra. Compared to analysis using MALDI-MS, the use of nLC-ESI-qToF MS/MS extends the window for vaginal protein markers (i.e. CRNN, SPRR3 & FABP5) detection to about 7 h and the data obtained are richer.

This classical proteomics analysis has shown the high sensitivity detection for vaginal fluid evidence from fingernails. Detection of haemoglobin was extended to at least 24 h and this was possible even if the volunteer had washed their hands several times and even showered. Although nLC-ESI-qToF MS/MS extends the detection window for biomarkers and the dataset is rich, the entire content of a microswab is consumed in this approach and the analytical procedure takes longer to accomplish (approximately 18 h).

Nylon microswabs make an important contribution to this complementary analytical approach. They are quite small and convenient for the collection of trace material from tight confines. In addition, they are not likely to injure the nail bed (which could result in a false positive result for haemoglobin) and do not abrade the nail, which would introduce more keratin into the recovered trace and the risk of suppression of the desired biomarker signal. Nylon fibres do not seem to interfere with the ionisation process in MALDI-ToF MS, nor do they contribute chemical noise to the mass spectrum. Finally, they are integral to the complementary approach of dual genomic and proteomic analysis because small tufts of fibres can be plucked from a single swab for each analysis.

The following additional data relating to this chapter are attached to this thesis:

Appendix-3A. nLC-MS/MS protein data for control vaginal fluid, control fingernails and the fingernail traces containing vaginal fluid evidence.

Appendix-3B. MALDI-ToF MS spectra and database report for control nylon microswab and cotton swabs.

Appendix-3C. nLC-MS/MS protein data for fingernail traces of *Macropus rufus* blood traces.

Appendix-3D. MALDI-PMF data for FN-VF (Supporting Information for Table 5.1)

Appendix-3E. MALDI-PMF data for FN-RK (red kangaroo blood traces)

Appendix-3F. FN-VF mascot database report (Table 5.1)

Appendix-3G. FN-RK mascot database report (Table 5.1)

Appendix-3H. MALDI-TOF spectrum and database report for FN-VF (Fig.5.5A)

Appendix-3I. Direct-PCR DNA profile data, MALDI-PMF spectra and database report for post PCR products (Fig. 5.5B).

Appendix-3J. MALDI-PMF spectra of post-PCR products (conventional PCR solutions)

Chapter 6

Chapter 6: "Bottom-up" in situ proteomic differentiation of human and non-human haemoglobins for forensic purposes by matrix-assisted laser desorption/ionization time-of-flight tandem mass spectrometry

Rapid Commun Mass Spectrom. 2017; 31:1927–1937. [DOI: 10.1002/rcm.7986](https://doi.org/10.1002/rcm.7986)

Sathisha Kamanna¹, Julianne Henry², Nicholas H. Voelcker³, Adrian Linacre¹, K. Paul Kirkbride^{1*}

¹College of Science and Engineering, Flinders University, Bedford Park, Adelaide, South Australia 5001, Australia

²Forensic Science SA, 21 Divett Place, 5000 Adelaide, South Australia, Australia

³Monash Institute of Pharmaceutical Sciences, 381 Royal Parade, Parkville, Melbourne, VIC 3052, Australia

*Correspondence

K. P. Kirkbride, College of Science and Engineering,

Flinders University, Bedford Park,

Adelaide, South Australia 5001, Australia.

Email: paul.kirkbride@flinders.edu.au

Selected supplementary information relating to this research article will appear in this chapter and remaining data were provided in the appendix of this thesis.

Journal Impact Factor: **2.2**

ISI Journal Citation Reports © Ranking: 2016: 18/42 (Spectroscopy); 38/76 (Chemistry Analytical); 51/78 (Biochemical Research Methods)

Number of citations: **1** ([DOI: 10.1021/acs.analchem.7b04733](https://doi.org/10.1021/acs.analchem.7b04733))

Statement of Authorship for Chapter 3 manuscript

Title of Paper	"Bottom-up" in situ proteomic differentiation of human and non-human haemoglobins for forensic purposes by matrix-assisted laser desorption/ionization time-of-flight tandem mass spectrometry
Publication Status	Published
Publication details	Published in Rapid Communications in Mass Spectrometry . 2017; 31:1927–1937.

AUTHOR CONTRIBUTIONS

By signing the Statement of Authorship, below mentioned each author certified that their stated contribution to the publication is accurate and that permission is granted for the research article to be included in the candidate's thesis.

Name of Principal Author (Candidate)	Sathisha Kamanna		
Contribution to the paper	Designed the research and experimental method. Performed all laboratory work and analysis, interpreted data and drafted/edited the manuscript.		
Signature		Date	March, 2018

Name of Co-author	Julianne Henry		
Contribution to the paper	Provided manuscript draft assistance, industry/forensic biology advice, provided access to proficiency test/volunteer samples for analysis and acted as industry research co-supervisor.		
Signature		Date	March, 2018

Name of Co-author	Nicholas H. Voelcker		
Contribution to the paper	Provided manuscript draft assistance and acted as an external academic research co-supervisor.		
Signature		Date: 15/03/2018	March, 2018

Name of Co-author	Adrian Linacre		
Contribution to the paper	Provided manuscript draft assistance and research co-supervision.		
Signature		Date	March, 2018

Name of Co-author	K. Paul Kirkbride		
Contribution to the paper	Supervised research, provided manuscript draft assistance/evaluation and acted as corresponding author.		
Signature		Date	March, 2018

6.1 Manuscript context

The manuscript is titled "Bottom-up" in situ proteomic differentiation of human and non-human haemoglobins for forensic purposes by matrix-assisted laser desorption/ionization time-of-flight tandem mass spectrometry. The application of MALDI-TOF and MSI techniques to forensic examination of body fluids is best described as emerging and extremely promising. However, in order for the technique to be adopted by forensic laboratories a certain amount of validation must be carried out.

This paper [119] describes some noteworthy improvements and extensions in regards to the usage of mass spectrometry (including MALDI-imaging techniques) for forensic investigation of serious crimes that result in blood deposits or bloodied fingermarks. Blood is, arguably, the most important body fluid in forensic science as its presence at a scene is often as a result of violence. In this context it is vitally important to demonstrate that MALDI is capable of differentiating between human blood at a crime scene or on a person and that from animals, which is usually not associated with a crime but as a result of handling meat or handling an animal after a vehicle accident. While *in silico* sequencing of haemoglobin proteins in blood stains has shown in a number of cases that MALDI is valid, protein databases only contain a small number of entries for haemoglobin from Australian native animals. In the investigation of crime in Australia this is a validation gap as some native animals are used for food and others are often involved in road kill.

Here, we demonstrated for the first time “top-down” and “bottom-up” mass spectrometry-based proteomics approaches for the identification and differentiation of haemoglobins on bloodied fingermarks. It was shown that blood from Australian native animals cannot be confused with human blood, and therefore extends the scope of validity of MALDI for forensic casework.

We also present data for forensic scientists who wish to evaluate MALDI against traditional immunochromatographic screening tests for blood. This work shows that MALDI is at least as sensitive as traditional techniques and slightly more specific.

Finally, in this article we also described a capability to carry out mass spectrometry on latent fingerprints that have been processed by forensic investigator using their standard techniques and lifted off surfaces. Haemoglobins even from mixed blood (human and animal blood readily can be detected and imaged in bloodied fingerprints that have been enhanced using Amido Black or silver-black magnetic powder. This shows that MALDI can be integrated with current technology and can complement it by helping to prove who had blood on their hands. Integration is extremely important because forensic agencies have substantial “sunken costs” in current fingerprinting technology and there would be strong resistance to changing this technology.

This article also presents fully our *de novo* sequencing data gathered during research in the hope that it might be of benefit to biologists outside forensic science who study Australian native animals, archaeologists and wildlife crime investigators. The majority of blood protein (haemoglobin sequences are similar between all the native species, but there are regions where there are some differences. At present there is only a small amount of published, MS-based proteomics analysis that describes the identification of blood proteins of native Australian mammal (marsupial) species. Sequences have not yet been uploaded to any reference database.

What follows is a peer-review version of the article published in Rapid Communications in Mass Spectrometry. The final authenticated version is available online at: <http://dx.doi.org/10.1002/rcm.7986>.

6.2 “Bottom-up” *in situ* proteomic differentiation of human and non-human haemoglobins for forensic purposes by MALDI-ToF-MS/MS

KEYWORDS

Body fluids

Protein biomarkers

Fingerprints

Forensic science

RATIONALE:

The detection and identification of human blood on crime-related items is of particular relevance to many investigations because shed blood can provide evidence of violent contact between individuals. However, for any detection and identification technique, specificity is a critical performance characteristic to assess, that is, whether the technique has capability to differentiate between human blood (which usually is of relevance to a criminal investigation) and non-human blood (which usually would not be associated with a crime but may be detected incidentally).

METHODS:

MALDI-ToF-MS approaches using “top-down” (detection of intact proteins) and “bottom-up” (detection of tryptic peptide markers) were used to detect and identify haemoglobin in blood from humans and that from a range of Australian native mammals; the technique could be carried out directly on blood stains without the need to extract proteins (i.e., *in situ* measurement). Imaging of haemoglobin was achieved in bloodied fingermarks, including those that had been enhanced using two “industry standard” fingerprint enhancement processes.

RESULTS:

Differentiation of intact haemoglobin proteins in human and non-human blood using “top-down” MALDI-ToF-MS, was difficult. However, *in situ* “bottom-up” approaches using

MS/MS and *de novo* sequencing of tryptic digest peptides allowed unambiguous differentiation. Imaging mass spectrometry of human haemoglobin, even when it was mixed with animal blood, was achieved in bloodied fingermarks that had been enhanced using two common processes (staining with Amido Black or dusted with magnetic powder) and “lifted” using adhesive tape.

CONCLUSIONS:

The MALDI-ToF MS-based *in situ* “bottom-up” proteomic methodology described here shows great promise for the detection of human blood and even imaging of blood in bloodied fingermarks. The approach is sensitive, can differentiate between human blood and that from many animals (including several Australian native animals) and can be implemented after traditional crime scene fingermark enhancement techniques have been carried out.

INTRODUCTION

Over the past decade, applications of matrix-assisted laser desorption ionization (MALDI) mass spectrometry (MS) and imaging mass spectrometry (IMS) have been widely used in clinical and/or biological sciences for the detection, differentiation and mapping of proteins or peptide markers within tissue sections.^[1-5] The advantages of these approaches include the capability to provide reproducible high-resolution mass measurement of intact proteins or, following their tryptic digestion, the collection of characteristic peptide profiles known as peptide mass fingerprints (PMF) and peptide sequences if tandem mass spectrometry (MS/MS) is used. These techniques are applicable to solutions of proteins and peptides after they have been deposited on a surface and dried, but it is also possible to analyse proteins and peptides directly in samples without resorting to their dissolution (i.e., *in situ* measurement).

To date, most applications of MALDI MS techniques to forensic science have focussed on the analysis of miscellaneous small organic molecules (e.g. illicit drugs) and biomarker discovery for identification of body fluids such as blood, saliva, seminal fluid, vaginal fluid and sweat in fingermarks.^[6-11] Blood in particular is a complex body fluid containing hundreds of proteins and peptides. However, we have indicated previously^[6] that haemoglobin or peptides derived from it are the most abundant high molecular weight substances detected in blood (or its digest) and MALDI-MS using a time of flight mass spectrometer (MALDI-ToF-MS) is capable of revealing their presence practically to the exclusion of all other substances. In forensic investigations, the detection of human blood is of high significance because bloodshed is often a consequence of violent contact between individuals; therefore MALDI MS has the potential to be an extremely valuable forensic technique. Earlier work^[6,12,13] has shown that MALDI MS has very low limits of detection for haemoglobin, even in aged bloodstains. It is therefore extremely important to determine whether MALDI MS is sufficiently specific to indicate when a blood deposit does not relate to a crime but to previous contact with non-human blood, for example as a result of meat preparation or dealing with the aftermath of roadkill. Earlier work by Kamanna et al.^[9], Yang et al.^[14] and Espinoza et al.^[15] illustrate that mass spectrometry and peptide sequencing are capable of differentiating human haemoglobin from that originating from “old world” mammal species. However, in the context of Australian crime investigation, haemoglobin peptide sequences are known only for a handful of indigenous Australian mammals and therefore the specificity of MS techniques within the Australian context is not known. The primary motivation of the research described in the present article was to assess

whether it is possible to differentiate between human blood and that from certain Australian native animals using MALDI MS techniques.

During violent crimes against a person, human blood may become smeared on the fingers of victims or assailants and then deposited as fingermarks at the crime scene. Marks of this type can be valuable evidence because they may carry finger-ridge pattern information and/or DNA attributable to a victim or a suspect. Although obvious bloodied fingermarks are found at crime scenes, many more marks are practically invisible and cannot be photographed; these are referred to as latent fingermarks. It is therefore an inconvenient reality that many marks must be enhanced in order to make the ridge pattern visible. Furthermore, the object upon which the mark is deposited may be immovable. Depending upon circumstances, enhanced marks may be photographed in place or perhaps “lifted” (using adhesive sheet) in order to preserve and relocate the evidence prior to biometric exploitation. Depending upon the offence under investigation and the particular investigative procedures where the crime is being investigated, the lifted mark might not be available for subsequent testing that would destroy the ridge pattern.

In the event that an investigator suspects that a bloodied latent mark might have been deposited during a crime, one of a number of dyes that react with proteins, such as Amido Black (Acid Black1), Acid Violet 17 and Acid Yellow,^[16] may be applied in order to enhance the mark. The successful enhancement of a mark with reagents such as Amido Black does not prove that blood is present in the mark, simply that a protein is present in the mark. If there is no indication that a fingermark contains blood then examiners would choose one of a number of other options available for mark enhancement, the choice being driven mainly by whether the surface upon which the mark is present is porous or not. One choice for enhancement of marks on non-porous surfaces is silver magnetic powder, which contains aluminium dust. IMS techniques are becoming popular for the examination of fingermarks, including for the identification of body fluids that might be present in the ridge patterns.^[9, 16] The second goal of the research described in the present article was to examine whether MALDI IMS can be used for the identification and mapping of blood in “lifted” latent prints that have been enhanced using Amido Black or magnetic powder.

Currently, if it is important in a criminal investigation to verify whether a mark actually does contain blood, a few options are available. One is to use the Hematrace[®] ABACard[®] kit (herein after referred to as Hematrace), which has very low limits of detection and very high specificity

for human blood (only higher primate blood and ferret blood are known to result in false positives).^[17-19] However, the Hematrace test requires sampling of the suspected blood, which in the case of a fingerprint means destroying some of the ridge pattern. The final goal of the research described here was to compare MALDI-based methods for blood identification with Hematrace.

In achieving these goals, *de novo* sequencing of haemoglobin peptides from a number of Australian native mammal species was carried out. Sequence data are presented here for the benefit of those investigating wildlife crimes, archaeologists or biologists studying native mammals.

EXPERIMENTAL

Materials and biological samples

All solvents including HPLC–MS grade acetonitrile (ACN), methanol, ethanol, glacial acetic acid, water and trifluoroacetic acid (TFA) were purchased from Sigma–Aldrich (Sydney, New South Wales, Australia). Surfactant RapiGest™-SF was purchased from Waters Ltd (Sydney, Australia) and Trypsin Gold (MS grade) was obtained from Promega (Melbourne, Victoria, Australia). Sterile syringes were obtained from Livingstone International Pty Ltd, Sydney, Australia. Indium-tin oxide (ITO) coated slides were purchased from Shimadzu (Sydney, New South Wales, Australia). α -Cyano-4-hydroxycinnamic acid (CHCA), sinapinic acid (SA) and protein/peptide mixture of external calibrants was obtained from Bruker Daltonics (Melbourne, Victoria, Australia). Double-sided Kapton tape (1 inch, 0.1 mm total thickness) was purchased from Ted Pella Incorporated (Redding, California, USA). Amido Black (#LV501) powder, silver-black magnetic powder, black magnetic powder, and magnetic powder applicator were purchased from Sirchie Incorporated (Youngsville, North Carolina, USA). Microswabs (ultrafine, Premium Plus™ disposable applicators, # 18-903) were purchased from City Dental Supplies (Adelaide, South Australia, Australia). Copan sterile cotton swabs (8150CIS) were obtained from Interpath Services (Melbourne, Australia). ABACard® Hematrace® kit (#808426) was obtained from Abacus Diagnostics Inc. (Los Angeles, California, USA). Proficiency test samples (e.g. 04-571 (January 2004) and 11-573) are received from Collaborative Testing Services (CTS) Incorporated (Sterling, Virginia, USA). All fingerprints and human body fluid samples were obtained from volunteers pursuant to Clinical Human Research Ethics Committee Application 440.14 –HREC/14/SAC/455. Mammal blood samples (brushtail possum [*Trichosurus vulpecula*], koala [*Phascolarctos cinereus*], red kangaroo

[*Macropus rufus*], western grey kangaroo and its Kangaroo Island sub-species [*Macropus fuliginosus* and *Macropus fuliginosus fuliginosus*, respectively], dama wallaby [*Macropus eugenii*], eastern grey kangaroo [*Macropus giganteus*], swamp wallaby [*Wallabia bicolor*], Tasmanian devil [*Sarcophilus harrisii*]) were obtained from Cleland Wildlife Sanctuary, Adelaide, South Australia pursuant to Australian Animal Welfare Committee Application 909/16.

Fingermark preparation

Bloodied fingermarks for MALDI-ToF-IMS

A small droplet of human blood was produced by pricking a clean finger using a sterile syringe (Livingstone International Pty Ltd, Sydney, Australia). A small volume of pricked blood (~2 μL) and an equal volume of dama wallaby (*Macropus eugenii*) or koala (*Phascolarctos cinereus*) blood was deposited onto a glass microscope slide and then rubbed on another clean index fingertip. The deposit was air-dried at room temperature. After 2 h of normal routine computer work, bloodied fingermarks were deposited onto an ITO coated glass slide. The ITO slides were marked with teaching points using Cover-Up (Marbig, Australia) white liquid. Bloodied marks on ITO slides were subjected to homogenous proteolysis by spraying them with a 1:1 mixture of Trypsin Gold (125 ng/ μL) and 0.2% RapiGestTMSF (200 μL) in 25 mM NH_4HCO_3 using an ImagePrep station (Bruker Daltonics GmbH, Germany). The solutions were deposited with 5 layers and 10 min incubation between each layer. After the deposition was completed, the ITO slide was incubated in a humid chamber at the 37°C, for 3 h.

Homogenous MALDI matrix deposition

CHCA (7 mg/mL) in 60% ACN and 0.2% TFA was deposited onto digested bloodied fingermarks using an ImagePrep station and an operator-modified Bruker Daltonics default method optimised for sensor controlled nebulisation of the matrix spray conditions such as layer dryness and thin layer deposition of the matrix.

Fingermark image capture

Optical images of all fingermarks were taken before carrying out MALDI-imaging experiments using either an Olympus XZS2 stereo microscope equipped with a white light fibre optic source and a DP21 digital camera (Olympus Pty Ltd, Tokyo, Japan) or a Digitech USB microscope/5

megapixel camera with integrated white LED light source (Jaycar Electronics Pty Ltd, Adelaide, Australia).

Bloodied fingermark enhancement using Amido Black stain

Bloodied fingermarks were prepared by rubbing 1:1 blood mixtures (human and dama wallaby or Tasmanian devil blood) on the index fingertip, allowing the deposit to dry for around 40 min at room temperature while carrying out normal computer work, and then depositing marks onto ITO-coated slides. Amido Black stain solution was prepared by dissolving 1 g of Amido Black powder in a solution of methanol (450 mL) and glacial acetic acid (50 mL). The prepared mark was enhanced by immersing the ITO slide in the Amido Black solution for 1 min, rinsing for 1 min with a wash solution containing acetic acid in methanol (10%), rinsing with a wash solution containing acetic acid in water (5%) and finally was rinsed using distilled water to remove excess dark blue dye from the mark and the glass slide background. After the enhanced mark had dried in air at room temperature its optical images were collected using the stereo microscope and USB microscope then subjected to both “top-down” and “bottom-up” proteomic analysis using MALDI-ToF-MS. SA and CHCA matrices were used for acquiring intact proteins and tryptic peptides data, respectively.

Bloodied fingermarks dusted with silver-black powder and lifted

Bloodied fingermarks prepared using red kangaroo or dama wallaby blood and human blood (1:1) were deposited onto new microscope glass slides and dusted using silver-black magnetic powder. The dusted marks were lifted using double-sided adhesive Kapton tape, which was then fixed onto an ITO-coated glass slide (s). Lifted marks were then rinsed (1 min) with absolute ethanol solution (to remove particles or other debris) and the marks were trypsin digested at the 37°C, for 3 h in a humid chamber. CHCA (7 mg/mL in 60 % ACN and 0.2 % TFA) matrix was spotted on distinct regions and then the marks were used for MS analysis. Optical images of fingermarks were collected using the stereomicroscope and USB microscope.

Hematrace test

The Amido Black stained bloodied fingermarks were swabbed (approx. 0.5mm on dark blue region of ridge patterns) using microswabs or cotton swabs moistened with Hematrace extraction buffer. Then the swabs were extracted with a further 500 µL of the buffer.

Approximately 200 μL of extraction solution was added into the sample (S) region of the immunochromatographic device and allowed to migrate. Results were read within 10 minutes. The Hematrace test was also carried out using the CTS proficiency test blood stains.

In-solution trypsin digestion

Human and all animal blood samples were diluted (1:500) in LC-MS grade water then centrifuged at 14,000 rpm for 3 min. Supernatant (8 μL) was mixed with 2 μL of 100 mM NH_4HCO_3 , and then solutions were treated with 5 μL of 0.1% RapiGestTM and 5 μL of Trypsin Gold (125 ng/ μL). The samples were digested by incubating at 37°C overnight. Intact and digested samples (1 μL) were spotted onto 384-well polished steel Bruker target plate and treated with CHCA matrix solution (1 μL , 10 mg/mL) in 60 % ACN and 0.2 % TFA, and allowed to dry.

MALDI-ToF-IMS and data analysis

All mass spectrometry analysis was performed using an Autoflex-III MALDI-ToF-MS (Bruker Daltonics GmbH, Bremen, Germany) mass spectrometer. The instrument ion source was equipped with a neodymium-doped yttrium aluminum garnet Smart Beam 200 Hz solid state laser operating at 355 nm. Reflectron positive (RP) ion mode was used with 20 kV accelerating voltage and delayed extraction of ions (200 ns). Peptide mass fingerprints (PMF) for in-solution digests and *in situ* digested fingermarks were collected in the m/z detection range of 800–3700. MSI analyses were performed at a raster width of 200 μm . Parent ions of a particular m/z value were manually selected prior to laser-induced fragmentation using the Bruker proprietary LIFT technique. Summed responses were gathered from 4500 laser shots and the spectra were processed using flexAnalysis 3.3 software (Bruker Daltonics). A standard peptide mixture (P.N: 206195, Bruker pepmix calibrants) and protein standard-I (P.N: 206355) were used for external calibration and CHCA was used as matrix. For detection of tryptic peptides (PMF) from human and native mammal blood (including in fingermarks, and enhanced and lifted fingermarks), digestion was carried out as described above followed by treatment with CHCA matrix (1 μL). On-tape pepmix calibration was performed for lifted latent fingermark (PMF) data acquisition. The MALDI-PMF data were searched using publicly available Matrix Science software (Mascot version 2.5) (<http://www.matrixscience.com>) against the SwissProt database, with mass tolerance up to 0.5-0.8 m/z and no fixed modifications. All MALDI instrumental parameters including laser power, mass detection range, voltage, delayed extraction and laser

offset were set using Flexcontrol 3.3. FlexImaging 3.3 software (Bruker Daltonics) was used to collect ion intensity maps of tryptic peptides and to control Autoexecute MALDI-imaging.

RESULTS AND DISCUSSION

The surface of hands, clothing and objects can be exposed to blood from non-human sources from a range of activities not related to crime, such as meat preparation or vehicle accidents involving animals. Intact protein (i.e., “top down”) analysis using MS and tryptic peptide sequencing (i.e., “bottom up” analysis) using tandem MS are extremely powerful techniques for the identification blood from many domestic and “old world” mammals (including humans). However, protein and sequence data for a number of native Australian mammals (actually marsupials) that are available as food, or are commonly involved in road accidents, are not known. As a consequence, a number of blood samples originating from humans and marsupials indigenous to Australia were prepared for MALDI MS or MS/MS analysis using “top-down” and “bottom-up” approaches. Those for which specific database sequences were not available are: koala (*Phascolarctos cinereus*), western grey kangaroo (*Macropus fuliginosus*), swamp wallaby (*Wallabia bicolor*), brushtail possum (*Trichosurus vulpecula*) and Tasmanian devil (*Sarcophilus harrisi*).

In a typical “top-down” experiment, 0.5 μL of SA matrix and 0.5 μL of the extracted blood samples were placed onto a stainless steel MALDI plate. Intact haemoglobin protein profiles display a few variations between the examined species. **Table 1** shows the list of abundant proteins identified from each sample. All the measured intact haemoglobin protein m/z values and peptide mass fingerprints (PMF) of blood proteins and theoretical masses from the SwissProt protein database search reports using Mascot for mammalian species and homo sapiens can be found in the Supporting information (**S1a** and **S1b**). What is striking in the protein profiles is the clarity of the signal arising from haemoglobin and haem as a result of the absence of spectral contributions from other proteins

TABLE 1

The MS signals arising from intact haemoglobin (HB) are broad and there can be significant variance between observed and theoretical m/z values (see Table 1), which makes it difficult to

differentiate between human blood and that originating from other animals. “Bottom-up” approaches must therefore be used to identify and resolve species reliably.

“Bottom-up” analysis involved extraction and in-solution enzymatic (trypsin) digestion of the sample at 37°C overnight with the detergent RapiGestTM-SF (0.1%). RapiGestTM was used as this increases the solubility of proteins without the need to reduce and alkylate amino acids. As can be seen from **Table 1** (which shows sequence coverage of matched peptides and theoretical m/z values from the SwissProt peptide database) and supporting information (**S2**), peptide mass fingerprints (PMF) and MS/MS of particular peptides obtained from trypsin digests allow simple differentiation of blood from the different species (including humans) that were examined. The tryptic peptide derived from the β - subunit of HB (HB-B) gave an $[M+H]^+$ ion at m/z 1247 to which a peptide sequence (LLIVYPWTSR) was assigned. Similar sequences were found for the other Australian species studied. In addition, all but two of the native marsupial blood samples analysed showed a $[M+H]^+$ signal for the α - subunit of HB (HB-A) at m/z 1515 (VGGHAGEYAAEGLER); the blood data for the brushtail possum and Tasmanian devil were different to the blood data from the other Australian species examined and the closest match on the SwissProt database was the *Virginia opossum* (native to North America).

The dama wallaby and red kangaroo blood samples exhibited a close similarity to each other with regards to their PMF data. However, $[M+H]^+$ ions at m/z 1465.78 and 1435.77, respectively, were observed that differentiated the two species. *De novo* sequencing was carried out, which provided the following sequences EFTIDTQVAWQK and EFTIDAQVAWQK (see Supporting information, **S3**).

All the “top-down and “bottom-up” results were reproducible and replicated multiple times (data not shown) using the same digestion conditions.

IMS and proteomic analysis of human and non-human haemoglobins in fingerprints

In order to determine if this technique is human species-specific even in complex mixtures and in imaging experiments, bloodied fingerprints were prepared using mixtures of human and non-human blood.

Bottom-up MS analysis of bloodied fingerprints, including IMS, can be carried out using rapid (3 h), *in situ* homogenous proteolysis (i.e., without extraction) using RapiGest-SF surfactant. Due to the high abundance of haemoglobin proteins within the blood mixtures, a trypsin

concentration of 125 ng/ μ L and surfactant (0.2%) were deposited (approx. 200 μ L) onto bloodied fingermarks. This is a considerable improvement in the time required for conventional *in situ* proteolysis for “bottom-up” analysis (approximately 12 h) and is sufficiently rapid to preserve some spatial distribution of substances in the mark, including some ridge detail, which is not the case with conventional proteolysis.

FIGURE 1

IMS data acquisition was carried out using a spatial resolution of 200 μ m and only a selected region of the fingermark was analysed in order to minimise the time taken to acquire images (**Fig. 1A, light grey region**). The resulting normalised spectra (**Fig. 1B**) are used to construct a heat map of the abundance of tryptic peptides in the fingermark. It can be seen from the maps that the blood proteins are more abundant on the fingermark ridges. The presence and distribution of human blood proteins was simply and effectively determined by mapping $[M+H]^+$ ions m/z 1274 and 1314 and m/z 1529, corresponding to HB-B and HB-A, respectively. This was achieved despite the co-localisation of haemoglobin proteins arising from admixed dama wallaby blood, which produces $[M+H]^+$ signals at m/z 1247 and 1300 for HB-B and m/z 1515 for HB-A, respectively. The supporting information (**Fig. S4a**) provides PMF results for the mixed blood stain. Additionally, a negative control fingermark (i.e. one made by a finger that had not been exposed to blood) was examined; haemoglobin signals were not detected in the control (see Supporting Information **Fig. S4b**).

To confirm the tryptic peptides in bloodied fingermarks containing a mixture of human and dama wallaby blood, *in situ* MS/MS analysis was performed. **Fig. 2A** represents the MALDI-ToF-MS/MS spectrum of precursor ion $[M+H]^+$ m/z 1529.91 (sequence VGAHAGEYGAEALER), which was confirmed as a peptide associated with the HB-A subunit of human haemoglobin. The product ion spectrum of $[M+H]^+$ m/z 1515.79 corresponds to the sequence VGGHAGEYAAEGLER, which a SwissProt database search indicated was a tryptic peptide of the HB-A subunit of haemoglobin from the dama wallaby. The differences in amino acid residues glycine and alanine between species were readily detected by the bottom-up approach, even when the blood was presented as a mixture from two species. **Fig. 2B** displays results obtained from a mixture of blood from a human and a Tasmanian devil, which also was readily resolved. The product ion spectrum of $[M+H]^+$ at m/z 1247.76 corresponds to a sequence LLIVYPWTSR, which was attributed to a peptide originating from Tasmanian devil HB-B whereas $[M+H]^+$ ion at m/z 1274.78 was confirmed as a peptide from

originating from human HB-B (sequence LLVVYPWTQR). **Fig. S5** contains data for the tryptic peptide sequence for $[M+H]^+$ m/z 1314 originating from human HB-B.

FIGURE 2

Fingerprint enhancement and proteomic identification of blood

The fingerprints discussed in the previous section were deposited on “convenient” substrates and analysed *in situ*. While it is possible to find fingerprints on “convenient” substrates at a crime scene (such as plastic bags or polymer banknotes), many are deposited on “inconvenient” surfaces such as windows, door frames etc. In addition, fingerprints are often practically invisible and must be enhanced in order to render them visible and facilitate exploitation of their biometric content. A typical process after enhancement is to lift the mark with an adhesive sheet in order to form a permanent record of the ridge pattern. When a crime scene examiner suspects that a mark contains blood, enhancement is carried out using a reagent such as Amido Black dye solution ^[16], otherwise a range of other techniques will be applied, such as dusting with powders that target other substances such as lipids. Amido Black forms a stain with many proteinaceous materials, therefore it cannot be used as proof that a fingerprint is formed from blood, let alone human blood. If MS-based proteomic techniques are to contribute to the examination of real crime scene fingerprints and prove the presence of human blood then they must be capable of being applied after enhancement has been carried out.

Although it has been demonstrated that Amido Black does not interfere with the detection of haemoglobin,^[13] the detection of haemoglobin in lifted marks enhanced with Amido Black has not been reported. Therefore bloodied fingerprints were deposited onto glass slides, treated with Amido Black stain solution using standard techniques, lifted off using adhesive tape and examined using MALDI-ToF-MS. **Fig. 3A** shows MALDI-PMF spectra of Amido Black stained bloodied fingerprint containing 1:1 human and dama wallaby blood and **Fig. S6** provides intact protein data. The PMF data were searched against the SwissProt database (taxonomic class Mammalia) and both human and dama wallaby haemoglobin proteins were successfully identified. However, the PMF of Amido Black stained bloodied fingerprint indicated that predominantly HB-A subunits of haemoglobin were detected; signals for HB-B subunits were very weak.

FIGURE 3

Currently, a popular conventional way in which to confirm the presence of human blood in the mark is to subject it to the Hematrace immunochromatographic test. This test is very sensitive to haemoglobin (about 0.0125 $\mu\text{g}/\text{mL}$)^[20] and whilst it is very selective towards human haemoglobin it is reported to give positive results with haemoglobin from higher primates and ferrets. A region of the protein-stained mark discussed above (approximately 5 mm x 5 mm) was swabbed using a microswab and the extracted solution was subjected to the Hematrace test. A pink coloured band at the test region (T) confirmed the presence of human blood (**Fig. 3C**), but the response was weak. A further comparison of MALDI-ToF-MS and the Hematrace test was carried out using an aged proficiency test sample (CTS test 04-571, January 2004). A sample of the test stain was extracted into the Hematrace buffer and the majority of the stain (~200 μL) was subjected to the Hematrace test. A small fraction of the extract (0.5 - 0.8 μL) was deposited onto a MALDI plate and treated with matrix. Hematrace produced a positive result that appeared to be close to the limit of detection whereas MALDI-ToF-MS yielded data that allowed identification of haemoglobin well above limits of detection (**Fig. S7**). As can be seen in **Fig. S6**, MALDI-ToF-MS can differentiate between human blood and that from higher primates, although this is not a point of differentiation between the techniques that is of high significance.

In the event that a latent mark at a crime scene is not suspected to contain blood it is likely to be enhanced using one of variety techniques other than Amido Black. We have shown previously⁹ that certain body fluid markers (such as cornulin in vaginal fluid) can be detected in fingermarks that had been enhanced with silver-black magnetic powder and lifted with tape. As the abundance of haemoglobin in blood is much higher than protein markers in other body fluids, it was expected that it would be a simple matter to detect blood in marks that had been dusted with magnetic powder. This expectation was tested to see if MALDI-ToF-MS can be used to examine enhanced marks for the presence of blood in those cases where its presence was not initially suspected but later becomes relevant.

Fingermarks containing blood were prepared by smearing mixtures of human and non-human blood on a fingertip and then placing it on a clean glass microscope slide (see **Fig. 4A**, which depicts a mixture of human and dama wallaby blood). Again, mixtures were used to illustrate the high species specificity that the technique is capable of even in mixtures. The bloodied mark was then enhanced using silver-black magnetic powder and lifted off using a square of Kapton double-sided adhesive tape and fixed onto ITO-coated glass slide (**Fig. 4B & C**). **Fig. 4D** displays the “top-down” protein profiles from the bloodied mark. Although it is possible to

identify that the mark contains haemoglobin, due to the relatively low mass accuracy in linear mode and chemical noise the closely related intact m/z values of human and dama wallaby haemoglobin subunits could not be distinguished. However, despite the minor differences between the haemoglobins from the two species, differentiation was readily achieved by “bottom-up”, *in situ* MS/MS analysis. **Fig. 4E** shows tryptic peptides of $[M+H]^+$ ion at m/z 1248 and 1516 (confirmed HB peptides sequence of dama wallaby) and $[M+H]^+$ ion at m/z 1275 and 1530 (human HB) with a mass error observed up to 1.5 Da after on-tape calibration with pepmix standard solutions. Haemoglobin was not detected in controls although the antimicrobial peptide dermicidin ($[M+H]^+$ at m/z 4819) was readily observed (**Fig. S8**).

FIGURE 4

CONCLUSIONS

It is becoming evident that MS, particularly *in situ* MALDI methods, can be used to detect small and large molecules present in items of forensic interest, such as biological stains and fingerprints, which can assist in elucidating the circumstances surrounding a crime. Furthermore, in imaging mode, MALDI is capable of mapping molecules contained within a fingerprint, including those contained only within the ridges.

MALDI-ToF-MS displays high sensitivity towards haemoglobin and high ionisation selectivity towards it, despite the presence of a multitude of other proteins in blood. This is of high value in forensic examinations. However, as non-human blood can be present at the crime scene or on individuals as a result of activities not related to crime, it is important to demonstrate that MALDI-ToF-MS has high specificity towards human blood. Fortunately, blood protein data from many “old world” mammals are present on databases and our work and that of others indicates that MALDI-ToF-MS is capable of high species specificity. Here, we show that human haemoglobin can readily be distinguished from that originating from several Australian native marsupial species as well. Although it is unlikely that a mixed blood stain might be relevant to a forensic investigation, blood mixtures were investigated in order to demonstrate specificity in a “worst-case” scenario. In the Supplementary Information we have provided sequence data applicable to haemoglobin from several native species in the hope that the data might also be of use to biologists studying Australian native mammals, archaeologists and wildlife crime investigators.

In linear mode MALDI-ToF-MS cannot differentiate between intact human haemoglobin and closely related animal haemoglobins. However, “bottom-up” analysis allows discrimination even when mixtures of haemoglobin from human and blood from other species are examined.

Even when it is mixed with animal blood, human blood readily can be detected and imaged in bloodied fingermarks that have been enhanced using Amido Black or silver-black magnetic powder. While the enhancement of latent marks using Amido Black did not result in chemical noise that precluded identification of blood, for some reason it did result in the loss of signals due to HB-B peptides.

MALDI-ToF-MS shows comparable or possibly better sensitivity towards human blood than the Hematrace test and, based on the limited work done so far, at least equivalent specificity. One major difference between Hematrace and MALDI-ToF-MS is that the former required the mark to be swabbed, which in the case of fingermarks means that some of the biometric information is destroyed.

Acknowledgements

This project was supported by the Ross Vining Research Fund, which is administered by Forensic Science SA (South Australia). The authors would like to acknowledge Flinders Analytical and the Proteomics Centre at Flinders University. Finally, we wish to thank the volunteers who provided fingerprints and body fluid samples and Dr Ian Hough, veterinary surgeon, and the Cleland Wildlife Sanctuary, Adelaide South Australia for the provision of non-human blood samples.

REFERENCES

- 1] Caprioli, R. M.; Farmer, T. B.; Gile, J. Molecular imaging of biological samples: localization of peptides and proteins using MALDI-TOF MS. *Anal. Chem.* **1997**, *69*, 4751-4760.
- 2] Groseclose, M. R.; Massion, P. P.; Chaurand, P.; Caprioli, R. M. High-throughput proteomic analysis of formalin-fixed paraffin-embedded tissue microarrays using MALDI imaging mass spectrometry. *Proteomics* **2008**, *8*, 3715-3724.
- 3] Khatib-Shahidi, S.; Andersson, M.; Herman, J. L.; Gillespie, T. A.; Caprioli, R. M. Direct Molecular Analysis of Whole-Body Animal Tissue Sections by Imaging MALDI Mass Spectrometry. *Anal. Chem.* **2006**, *78*, 6448-6456.
- 4] Panderi, I.; Yakirevich, E.; Papagerakis, S.; Noble, L.; Lombardo, K.; Pantazatos, D. Differentiating tumor heterogeneity in formalin-fixed paraffin-embedded (FFPE) prostate adenocarcinoma tissues using principal component analysis of matrix-assisted laser desorption/ionization imaging mass spectral data. *Rapid Commun. Mass Spectrom.* **2017**, *31*, 160-170.

- 5] F. Hillenkamp, T. W. Jaskolla and M. Karas, MALDI MS, Wiley-VCH Verlag GmbH & Co. KGaA, 2013, pp. 1–40, DOI: 10.1002/9783527335961.ch1.
- 6] Kamanna, S.; Henry, J.; Voelcker, N. H.; Linacre, A.; Kirkbride, K. P. Direct identification of forensic body fluids using matrix-assisted laser desorption/ionization time-of-flight mass spectrometry. *Int. J. Mass Spectrom.* **2016**, *397*, 18-26.
- 7] Ferguson, L. S.; Wulfert, F.; Wolstenholme, R.; Fonville, J. M.; Clench, M. R.; Carolan, V. A.; Francese, S. Direct detection of peptides and small proteins in fingerprints and determination of sex by MALDI mass spectrometry profiling. *Analyst* **2012**, *137*, 4686-4692.
- 8] Wolstenholme, R.; Bradshaw, R.; Clench, M. R.; Francese, S. Study of latent fingerprints by matrix-assisted laser desorption/ionisation mass spectrometry imaging of endogenous lipids. *Rapid Commun. Mass Spectrom.* **2009**, *23*, 3031-3039.
- 9] Kamanna, S.; Henry, J.; Voelcker, N. H.; Linacre, A.; Kirkbride, K. P., A mass spectrometry-based forensic toolbox for imaging and detecting biological fluid evidence in fingerprints and fingernail scrapings. *Int J Legal Med*, **2017**. *131* (5), 1413-1422.
- 10] Guinan, T.; Della Vedova, C.; Kobus, H.; Voelcker, N. H. Mass spectrometry imaging of fingerprint sweat on nanostructured silicon. *Chem. Commun.* **2015**, *51*, 6088-6091
- 11] Guinan, T. M.; Kirkbride, P.; Della Vedova, C. B.; Kershaw, S. G.; Kobus, H.; Voelcker, N. H. Direct detection of illicit drugs from biological fluids by desorption/ionization mass spectrometry with nanoporous silicon microparticles. *Analyst* **2015**, *140*, 7926-7933.
- 12] Patel, E.; Cicatiello, P.; Deininger, L.; Clench, M. R.; Marino, G.; Giardina, P.; Langenburg, G.; West, A.; Marshall, P.; Sears, V.; Francese, S. A proteomic approach for the rapid, multi-informative and reliable identification of blood. *Analyst* **2016**, *141*, 191-198.
- 13] Bradshaw, R.; Bleay, S.; Clench, M. R.; Francese, S. Direct detection of blood in fingerprints by MALDI MS profiling and imaging. *Sci. Justice* **2014**, *54*, 110-117.
- 14] Yang, H.; Zhou, B.; Prinz, M.; Siegel, D. Proteomic analysis of menstrual blood. *Mol. Cell. Proteomics: MCP* **2012**, *11*, 1024-1035.
- 15] Espinoza, E. O.; Lindley, N. C.; Gordon, K. M.; Ekhoﬀ, J. A.; Kirms, M. A. Electrospray Ionization Mass Spectrometric Analysis of Blood for Differentiation of Species. *Anal. Biochem* **1999**, *268*, 252-261.
- 16] Bossers, L. C.; Roux, C.; Bell, M.; McDonagh, A. M. Methods for the enhancement of fingerprints in blood. *Forensic Sci. Int.* **2011**, *210*, 1-11.
- 17] Johnston, S.; Newman, J.; Frappier, R. Validation Study of the Abacus Diagnostics ABACard® HemaTrace® Membrane Test for the Forensic Identification of Human Blood. *Can. Soc. Forensic Sci. J.* **2003**, *36*, 173-183.
- 18] Johnston, E.; Ames, C. E.; Dagnall, K. E.; Foster, J.; Daniel, B. E. Comparison of Presumptive Blood Test Kits Including Hexagon OBTI. *J. Forensic Sci.* **2008**, *53*, 687-689.
- 19] Cox, M. A study of the sensitivity and specificity of four presumptive tests for blood. *J. Forensic Sci.* **1991**, *36*, 1503-1511.
- 20] Kristaly, A., & Smith, D.A.S., . Validation of the OneStep ABACard HemaTrace™ for the rapid forensic identification of human blood. *Unpublished paper* **1999**.

6.3 Top-down and bottom-up mass spectrometry analysis for unknown haemoglobins of Australian mammals

As described in the manuscript, only a few marsupials (e.g., dama wallaby, grey kangaroo) haemoglobin sequences are available in the SWISSPROT database, but no other native Australian animal. The main important hypothesis of this research was to identify and distinguishing human haemoglobin proteins from a range of common, relevant animal haemoglobins. The established methodology that would be useful for forensic purposes in regards to identification of suspected stains or body fluid mixtures from contaminated sources. In this research context, blood samples from human and animal fluids were extracted and analyzed by mass spectrometry.

Figure 6.1 displays the “top-down” mass spectra of native Australian mammals; the intact protein profiles of native species were obtained from MALDI-TOF MS analysis. The acquired haemoglobin protein profiles display a few m/z variations between the examined species (see Table 1 in the article and Fig. 6.1). This could be due to presence of closely related haemoglobin sequences and similar masses between the other Australian marsupials. However, top-down protein analyses often gave broad or low resolution mass spectra (poor mass accuracy in linear mode) which makes it difficult to distinguish between blood from different species (human or marsupial). Therefore, mass spectrometry based “bottom-up” proteomic approaches were used for the identification of species-specific protein information at molecular level. A complete list of MALDI-PMF data (mass spectrum) and the theoretical masses from the SwissProt protein database search reports using Mascot for mammalian species and *Homo sapiens* can be found in this thesis **Appendix-4A and 4B**. Unknown haemoglobin protein sequences from Australian marsupials gave spurious matches to other organisms in the SwissProt database, and for some tryptic peptides the database report indicated that many amino acids were identical to those from other mammalian species.

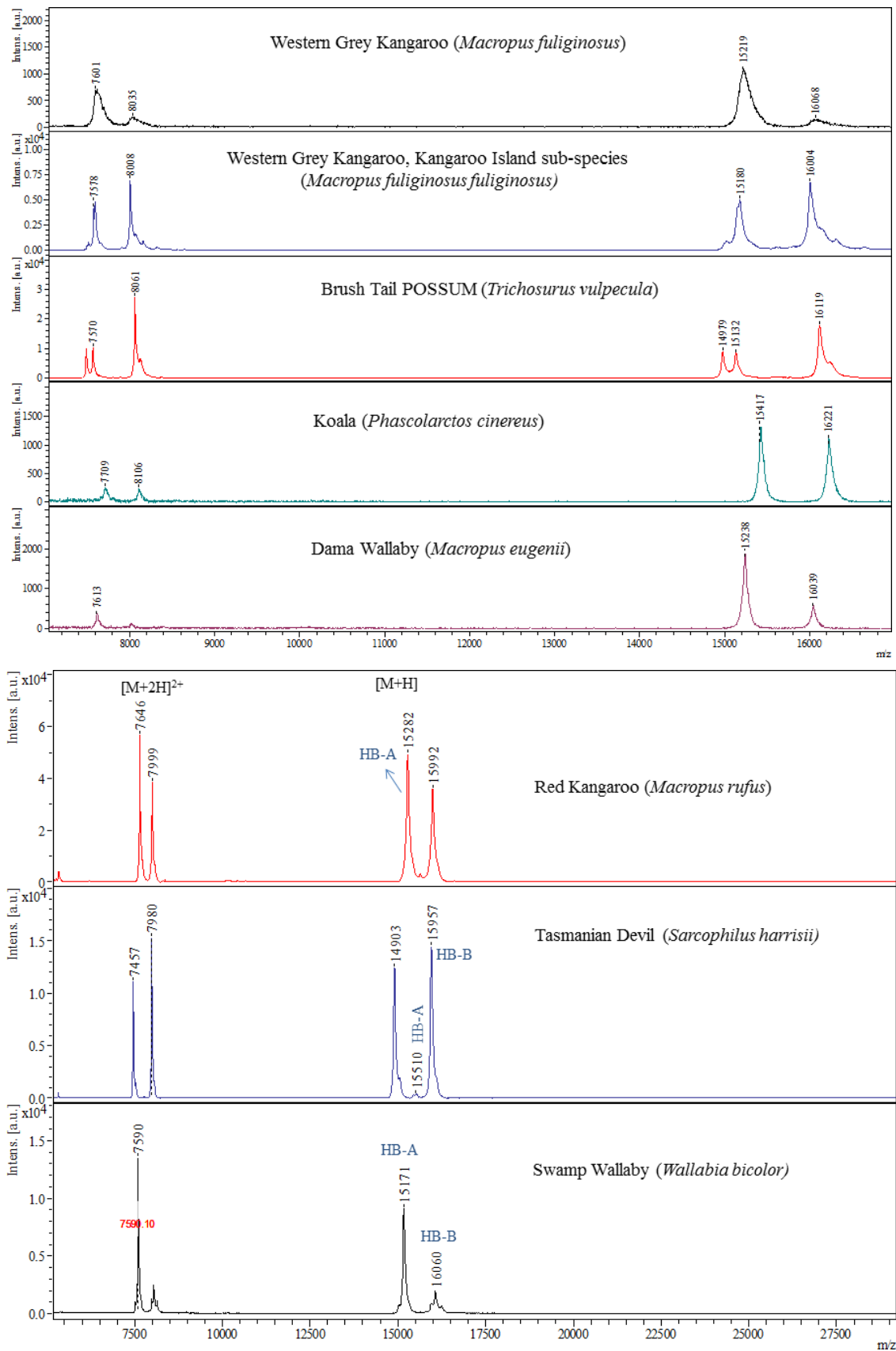


Figure 6.1. MALDI-ToF MS data for intact proteins from Australian marsupials blood samples. Sinapinic acid in 60 % ACN and 0.2 % TFA was used as matrix. Spectra were acquired in linear positive mode with detection range of m/z 5000 – 30000.

6.3.1 One-dimensional SDS-PAGE analysis of marsupial blood samples

The analysis of Australian marsupial blood samples was further extended to confirm the haemoglobin sequences by classical proteomics approaches. The extracted blood samples (both human and mammalian) were subjected to one-dimensional (1D) sodium dodecyl sulphate polyacrylamide gel electrophoresis (SDS-PAGE) using the mini-PROTEAN® TGX Stain-Free Precast gels (BIO-RAD). A detailed SDS-PAGE electrophoresis methodology can be referred in the material and methods section [Chapter-2].

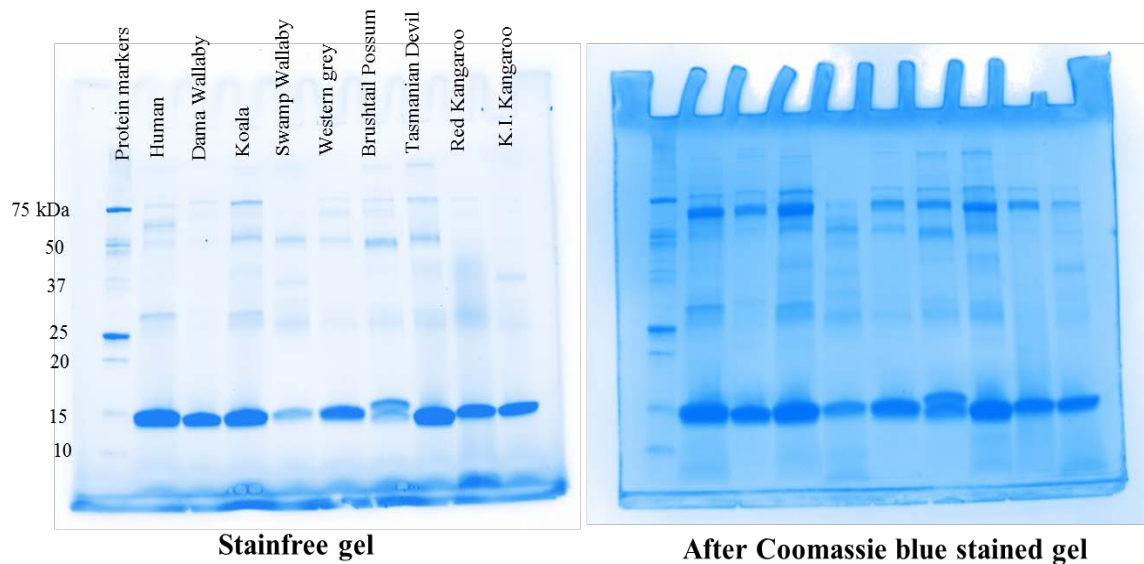


Figure 6.2. 1D-SDS PAGE images of Australian mammalian blood samples. Lane-1 displays the protein standard (BIO-RAD) as protein markers and the gels slab were stained with Colloidal Coomassie Blue G-250.

Fig. 6.2 shows the SDS-PAGE results of mammalian blood samples, the image indicated separated haemoglobin masses at around 15 kDa region. Due to the low resolution of the SDS gel most of the haemoglobin bands appear in the same lane and were difficult to differentiate from each other. *Trichosurus vulpecula* (Brushtail Possum) shows the 2 distinct bands that could be lysozyme at m/z 14.9 kDa (see Figure 6.1 and Fig. 6.2) and haemoglobins. Similarly, top-down protein profiles of *Sarcophilus harrisii* (Tasmanian devil) displays a 14.9 kDa peak and one for haemoglobin but only a

single band was observed in the SDS-PAGE electrophoresis. It is known that lysozyme proteins have antimicrobial properties and they play a crucial role in the immune protection of marsupial newborns during their pouch life [159]. These proteins are secreted through skin of the post-reproductive pouch that may critical for the decreased population of certain bacteria in the pouch. However, except for our published article [119], there is no mass spectrometry-based proteomic study for the characterization of unknown proteins of Australian marsupials.

SDS bands were subjected to in-gel trypsin digestion followed by bottom-up mass spectrometry analysis for the confirmation of haemoglobins. All in-gel digested samples were analyzed for protein identification using MALDI-TOF MS/MS (Bruker Daltonics, Germany) and confirmed by AB Sciex TripleTOF 5600+ mass spectrometer equipped with an Eksigent Ekspert 415 nano LC (AB Sciex) separation technique. **Table 6.1** displays the list of haemoglobin protein markers identified from human and marsupials blood samples. Classical proteomic analysis using nLC-MS/MS provided a high confidence (>95%) identification of protein markers from the Australian mammalian samples. All the blood samples were replicated multiple times utilizing both MALDI-TOF MS/MS and nLC-ESI-MS/MS.

Table 6.1. List of abundant haemoglobin protein markers identified in human and animal blood samples by nLC-ESI-qTOF MS/MS analysis.

Analyzed blood samples	Proteins detected	Matched organism	UniProt Accession number	Sequence coverage (95%)	No. of matched peptides (95%CL)
Human	HB-A	<i>Homo sapiens</i>	P69905	78.87	49
	HB-B	<i>Homo sapiens</i>	P68871	85.71	60
	HB-D	<i>Homo sapiens</i>	P02042	91.16	35
	HB-G1	<i>Homo sapiens</i>	P69891	43.54	5
Dama Wallaby (<i>Macropus eugenii</i>)	HB-A	<i>Macropus eugenii</i>	P81043	88.02	60
		<i>Macropus giganteus</i>	P01975	100	63
		<i>Pan troglodytes</i>	P69907	77.46	15
	HB-B	<i>Macropus eugenii</i>	Q6H1U7	98.64	67
		<i>Macropus giganteus</i>	P02106	98.62	70
		<i>Macropus rufus</i>	P02107	98.62	67
<i>Sminthopsis crassicaudata</i>		Q28932	73.47	46	
Koala (<i>Phascolarctos cinereus</i>)	HB-A	<i>Macropus eugenii</i>	P81043	57.04	8
		<i>Macropus giganteus</i>	P01975	57.45	8
	HB-B	<i>Macropus eugenii</i>	Q6H1U7	60.54	20
		<i>Macropus giganteus</i>	P02106	56.16	19
		<i>Macropus rufus</i>	P02107	56.16	19

Swamp Wallaby (<i>Wallabia bicolor</i>)	HB-A	<i>Macropus eugenii</i>	P81043	60.56	12
		<i>Macropus giganteus</i>	P01975	61.00	12
	HB-B	<i>Macropus rufus</i>	P02107	63.70	17
		<i>Macropus giganteus</i>	P02106	63.70	17
<i>Macropus eugenii</i>		Q6H1U7	55.10	16	
Western grey Kangaroo (<i>Macropus fuliginosus</i>)	HB-A	<i>Macropus giganteus</i>	P01975	60.28	30
		<i>Homo sapiens</i>	P69905	28.17	3
	HB-B	<i>Macropus giganteus</i>	P02106	89.73	39
		<i>Chrysocyon brachyurus</i>	P60526	28.08	6
<i>Canis latrans</i>		P60525	28.08	6	
Brushtail Possum (<i>Trichosurus vulpecula</i>)	HB-A	<i>Macropus eugenii</i>	P81043	33.8	3
		<i>Macropus giganteus</i>	P01975	34.04	3
	HB-B	<i>Macropus rufus</i>	P02107	56.16	7
		<i>Macropus giganteus</i>	P02106	56.16	7
<i>Macropus eugenii</i>		Q6H1U7	55.78	7	
K.I. Kangaroo (<i>Macropus fuliginosus fuliginosus</i>)	HB-A	<i>Macropus eugenii</i>	P81043	79.6	25
		<i>Macropus giganteus</i>	P01975	80.14	25
	HB-B	<i>Macropus giganteus</i>	P02106	94.52	43
		<i>Macropus rufus</i>	P02107	89.73	41
		<i>Macropus eugenii</i>	Q6H1U7	86.40	41
<i>Sminthopsis crassicaudata</i>		Q28932	49.67	7	
Tasmanian Devil (<i>Sarcophilus harrisii</i>)	HB-A	<i>Dasyurus viverrinus</i>	P07419	30.46	9
	HB-B	<i>Sminthopsis crassicaudata</i>	Q28932	73.48	43
		<i>Macropus eugenii</i>	Q6H1U7	64.64	15
		<i>Macropus rufus</i>	P02107	65.07	15
		<i>Macropus giganteus</i>	P02106	65.07	15
HB-T	<i>Sus scrofa</i>	P04246	37.68	17	
Red Kangaroo (<i>Macropus rufus</i>)	HB-B	<i>Macropus rufus</i>	P02107	87.68	36
		<i>Sminthopsis crassicaudata</i>	Q28932	49.67	11
	HB-A	<i>Macropus eugenii</i>	P81043	73.95	22
		<i>Macropus giganteus</i>	P01975	74.48	22
		<i>Varecia variegata</i> (HB-A1)	P20018	24.12	3
<i>Dasyurus viverrinus</i>		P07419	14.03	2	
<i>Eulemur fulvus fulvus</i>		P01936	14.18	2	

α -haemoglobin (HB-A), β -haemoglobin (HB-B), δ -haemoglobin (HB-D), Hemoglobin subunit gamma-1 (HBG1), Hemoglobin subunit theta (HB-T), CL; confidence level

Note that entries for koala, swamp wallaby, western grey kangaroo, brushtail possum, Kangaroo Island (K.I.) kangaroo, Tasmanian devil and Red kangaroo (HB-A) are not present on the database. These haemoglobin proteins were spuriously matched to closest organisms in the database. The nLC-MS/MS analysis shows that most of the haemoglobin peptide sequences are found to be similar between other marsupial species (e.g., HB-B peptides from *Macropus eugenii* was also matched to *Macropus giganteus*, and *Macropus rufus*).

6.4 Bottom-up and tandem mass spectrometry analysis for the differentiation of closely related haemoglobins

As described in this thesis introduction, there are lack of presumptive tests for the accurate detection and differentiation of body fluid in biological mixtures (for instance, blood mixed with semen, human fluid contaminated and/or mixed with other non-human body fluids). In typical forensic investigation, it is very important to differentiate the type of biological fluid present in the contaminated fluid traces from other biological sources. Therefore, “bottom-up” proteomic approach using *in situ* MS/MS (tandem mass spectrometry) and followed by the *de novo* sequencing was carried out for the unambiguous differentiation of closely related unknown haemoglobin tryptic peptides from the mammalian blood. **Figure 6.3** displays the MALDI-MS PMF spectra for blood samples of *Macropus rufus* and *Macropus eugenii*. The obtained PMF spectra containing tryptic peptides exhibited a close similarity between these species. But, *in situ* MS/MS followed by *de novo* sequencing allowed a differentiation of molecular ion at m/z 1465.78 and 1435.77, which provided the following sequence with single amino acid variants (bold italic) of the peptide, EFTID***T***QVAWQK and EFTID***A***QVAWQK (see **Figure 6.4**). The tandem mass spectrum clearly differentiated by the product ions at ‘b₆’ and ‘y₇’ masses (with a difference of 30 Daltons). The results clearly demonstrated that MALDI-TOF MS/MS and sequencing has potential for the identification and differentiation of closely related proteins and provide species-specific information. Furthermore, the in-gel tryptic peptides and the sequences of haemoglobins matched to the Australian mammals were confirmed by nLC-ESI-MS/MS (**Table 6.1**).

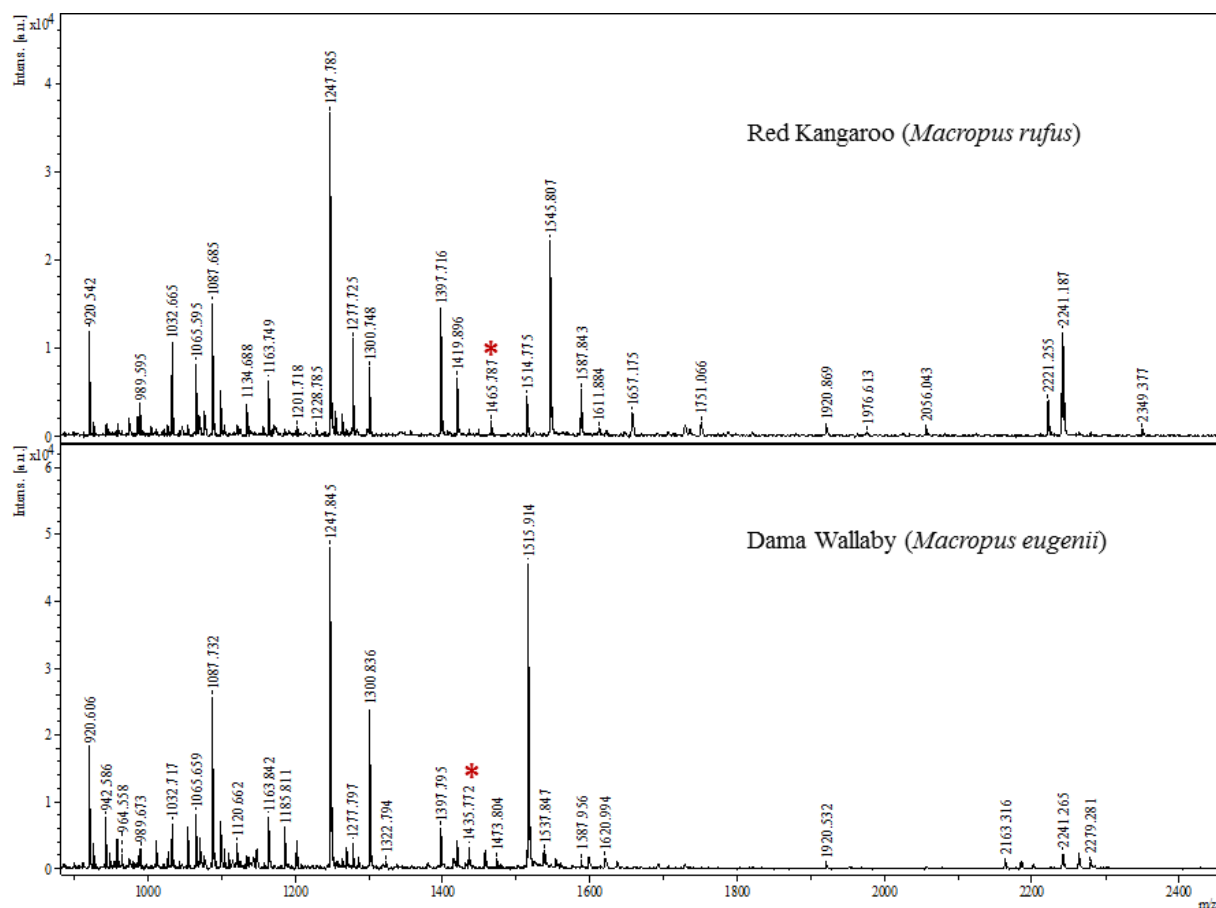


Figure 6.3. MALDI-ToF PMF spectra for blood samples of *Macropus rufus* and *Macropus eugenii*. The samples were extracted and digested at the 37°C , for 4 h. CHCA (in 60 %ACN and 0.2% TFA) was used as MALDI matrix. *Tryptic peptides (β -Hbs) used for *in-situ* MS/MS analysis (see below). Most of the tryptic peptides identified are identical between the species.

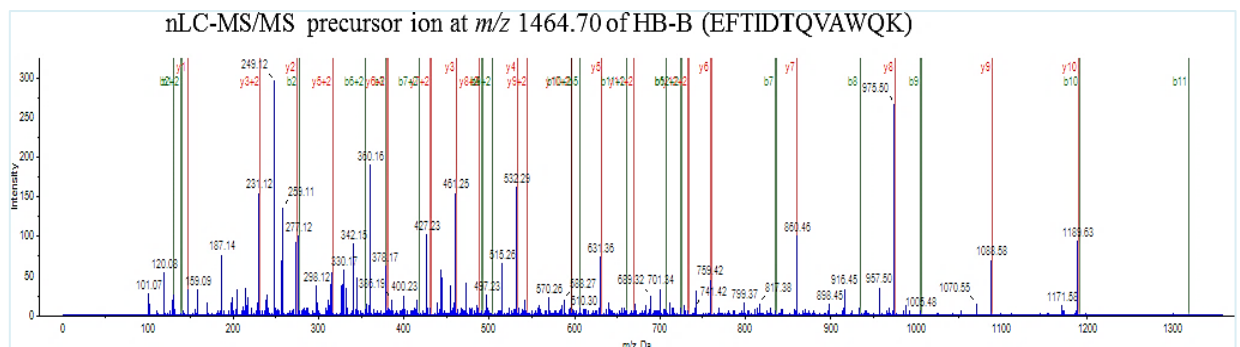
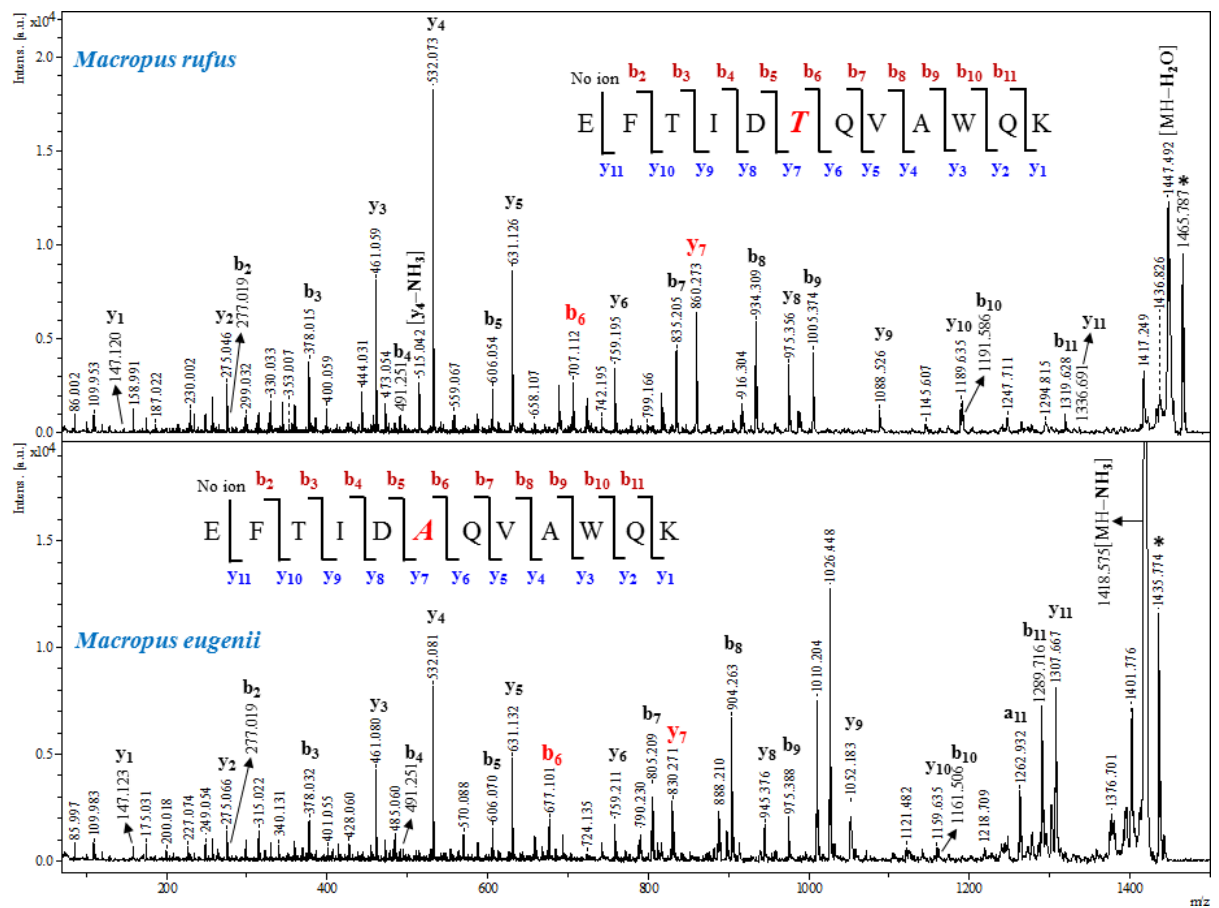


Figure 6.4. MALDI-ToF MS/MS spectrum acquired from precursor ions (*) at $[M+H]$ m/z 1465.78 and m/z 1435.77 for tryptic peptides of HB-B subunits of *Macropus rufus* and *Macropus eugenni* blood. Matched “b” and “y” product ions were interpreted manually and indicated in the sequences. **Bottom:** displays the nLC-ESI MS/MS spectrum (automated sequencing comparison) of same peptide (m/z 1464.70) matched to HB-B of *Macropus rufus* and product ions sequences were assigned automatically using Protein pilot software (v4.5).

The Australian mammal's haemoglobin sequences not available in the SwissProt database are: koala (*Phascolarctos cinereus*), swamp wallaby (*Wallabia bicolor*), brushtail possum (*Trichosurus vulpecula*), western grey kangaroo (*Macropus fuliginosus*), and Tasmanian devil (*Sarcophilus harrisi*); sequences for the α -subunit of haemoglobin (HB-A) were not available for red kangaroo (*Macropus rufus*). Most of these species were spuriously matched to closet protein sequences available in the SwissProt database. For example, in-gel digested tryptic peptides of Tasmanian devil blood were matched to HB-B of *Sminthopsis crassicaudata* (fat-tailed dunnart). Additional information in regards to the number of matched peptides and the *in-situ* nLC-MS/MS spectrum of assigned 'b' and 'y' product ions can be seen in Table 6.1 and **Figure 6.5**, respectively.

Furthermore, research work is required for the detection and validation of unknown haemoglobins. This work has been extended in regards to proteomic identification and differentiation of unknown haemoglobins using classical proteomics approach.

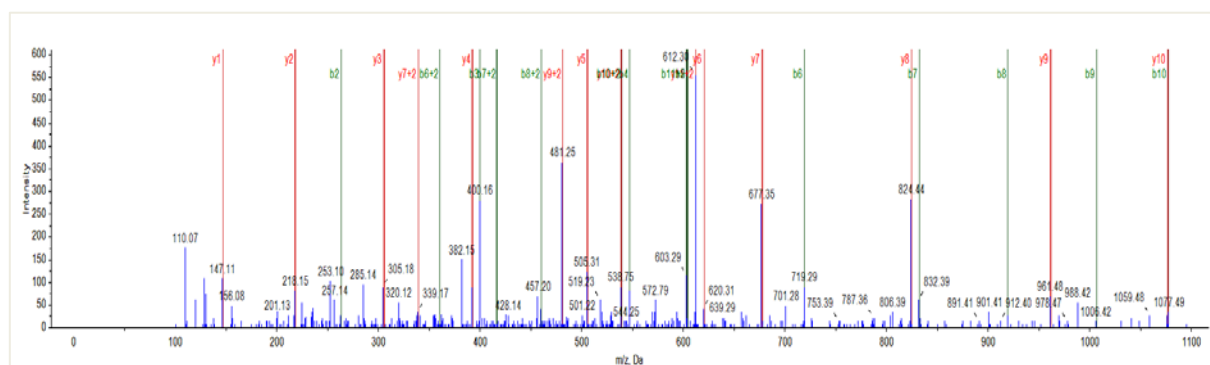


Figure 6.5. nLC-ESI-MS/MS spectrum of HB-B tryptic peptide at m/z 1222.56 (FDHFGDLSSAK) matched to *Sminthopsis crassicaudata* (fat-tailed dunnart). The SDS-PAGE band (see Fig 6.2) of Tasmania devil blood (Lane 8) was in-gel digested and analyzed using AB Sciex TripleTOF 5600+ mass spectrometer.

The following additional data relating to this chapter and the article are attached to this thesis:

Appendix-4A. MALDI-ToF MS tryptic peptide mass fingerprints (PMF) for human and non-human blood samples (Supporting information for Table 1 in the article).

Appendix-4B. SwissProt database search results of the MALDI-PMF data obtained from human and animal blood (Table 1 in the article).

Appendix-4C. MALDI- PMF spectrum of Human and Dama Wallaby blood mixture (1:1), the spectrum was acquired on a bloodied fingermark (Supporting information for Figure 1 in the article).

Appendix-4D. MALDI-MS/MS spectrum acquired from precursor ion m/z 1314.87 with its matched peptide sequence of human HB-B. Spectrum was acquired on bloodied fingermark (Figure 1).

Appendix-4E. MALDI-MS top-down protein profiles and mascot database report for amido black stained bloodied fingermark (Supporting information for Figure 3A and B).

Appendix-4F. ABACard Hematrace® test results and MALDI-MS intact proteins of aged (10 years) proficiency test blood sample (Supporting information for Figure 3C).

Appendix-4G. MALDI-TOF-MS intact protein profiles of a control fingermark (Supporting information for Figure 4).

Appendix-4H. nLC-ESI qTOF MS/MS data for Australian marsupial blood samples (Supporting information for Table 6.1).

Chapter 7

Chapter 7: Conclusions and Future Work

7.1 Conclusions

The original aims of research, as described in **Chapter 1**, were:

1. To optimize MALDI-TOF MS/MS techniques for direct (or *in-situ*) trypsin digestion and analysis of body fluids ‘on-fibres’ plucked from fabrics and swabs (including fingernail trace swabs), for analysis of raw body fluids, and in fingerprints (including enhanced and lifted marks).
2. To use nLC-ESI-qTOF MS/MS to confirm the identity of major protein markers (both human and animal) in blood, semen, urine, vaginal fluid and saliva as determined by *in situ* MALDI-TOF MS/MS.
3. To establish a mass spectrometry-based forensic “toolbox” containing MALDI-TOF MS/MS, MALDI TOF MS-imaging and nLC-ESI-qTOF MS/MS methods for detecting biological fluid traces in latent fingerprints and fingernail scrapings.
4. To demonstrate a complementary forensic ‘proteo-genomic’ approach on a single micro-swab for the direct identification of the type of biological fluid present and the identity of its “donor”.
5. To explore both “top-down” and “bottom-up” approaches and to carry out *de-novo* sequencing of Australian marsupial blood peptides that are not currently listed in databases.

In **Chapter 3**, achievement of project aims 1-3 are presented as an article published in *International Journal of Mass Spectrometry* [31]. The work presented in this paper reported the direct (or *in situ*) identification of forensic body fluids using *matrix-assisted laser desorption/ionization time-of-flight mass spectrometry* (MALDI-TOF MS). This work also shows the identification of human body fluid protein markers (“top-down and “bottom-up” analysis) and mixtures of different fluids were directly detected on various fabric substrates and ITO-coated slides without classical chromatographic separation.

The direct “approach” can be elegantly extended to the direct, time-saving *in situ* identification of body fluids on textile fibers, including mixed deposits, both of which are capabilities of particular relevance to forensic identification of traces on garments and other fabric-based items seized in relation to crime. Blood ‘markers’ appear to be quite stable over time – haemoglobin in an 11-year-old proficiency sample of blood was successfully detected.

Despite the fact that body fluids are complex mixtures of proteins and the MALDI-based method used did not involve chromatographic fractionation of fluids, the method is nevertheless practical and fit for purpose for forensic examinations. This is because characteristic protein markers are over-expressed and highly abundant in the body fluids relevant to forensic science and they are ionized in preference to the trace proteins present. Haemoglobin, for example, is probably present at trace levels in many body fluids, but those fluids are not encountered in crime stains and the more abundant proteins present in the fluids are the ones that would be detected using the direct MALDI method. This does indicate one limitation of the direct MALDI method. The presence of trace levels of saliva, for example, in another relevant body fluid (such as blood) might not be detected. Techniques using nLC-ESI-qTOF MS/MS are more effective for resolving mixtures where one fluid is present at the trace level.

In **Chapter 4**, the usage of MALDI-TOF MS and mass spectrometry imaging (MSI) techniques was applied to the identification and mapping of body fluid traces in fingermarks, including matrix free detection and visualization of endogenous or xenobiotic small molecules in enhanced (silver/black magnetic powders) and lifted fingermarks. This chapter addresses aims 2 and 4, and was extended to include the analysis of biological traces under fingernails. Described for the first time the successful identification of blood and vaginal fluids in fingernail scrapings even after the ‘assailant’ had washed their hands. Chapter 4 was written around an article published in *The International Journal of Legal Medicine* [118]. This chapter confirms that direct MALDI-TOF MS techniques can be integrated with standard forensic techniques and does not require crime scene examiners or forensic scientists to adapt their procedures to suit the new technique developed.

Chapter 5 demonstrated a further integration of new methodology with existing methodology, which achieves aim 5. A complementary forensic ‘proteo-genomic’ approach using a single micro-swab is described for the direct identification of the type of biological fluid present on the swab and the identity of its “donor”. This chapter explores the persistence of traces of vaginal fluid or foreign blood trapped under fingernails and the relative performance of MALDI-TOF MS techniques and “gold standard” analysis using nLC-ESI-MS/MS. Blood was surprisingly persistent under fingernails, it could be detected about a day after deposition, but vaginal fluid deposits could not be detected about 5-8hrs after deposition. This indicates that fingernail traces must be collected from a suspect of a sexual assault quite promptly for them to yield good evidence. Alternatively, as was demonstrated in Chapter 4, crime scene examiners could be encouraged to seek objects that the assailant might have touched after the sexual assault as vaginal fluid traces would persist much longer in fingermarks and they can be detected in fingermarks. The complementary ‘proteo-genomic’ developments has been published in the international peer-reviewed journal *Analytical and Bioanalytical Chemistry* [163].

Aim 6 is discussed briefly in **chapter 6**. It describes both “top-down” and “bottom-up” approaches followed by *de-novo* sequencing of Australian marsupial blood peptides. For the first time, unknown haemoglobins of Australian mammals were identified and described for the forensic and biological research applications. Top-down and bottom-up tandem mass spectrometry approaches were used for the characterization of haemoglobins from *Phascolarctos cinereus*, *Macropus fuliginosus*, *Wallabia bicolor*, *Trichosurus vulpecula*, and *Sarcophilus harrisii* and etc.). As expected, in linear mode MALDI-TOF-MS cannot differentiate between intact human haemoglobin and closely related animal haemoglobins, however, "bottom-up" proteomics followed by the *de novo* sequencing analysis allowed a differentiation even when mixtures of haemoglobin from human and blood from other mammalian species are examined. These findings of unknown haemoglobins were subsequently published in *Rapid Communications in Mass Spectrometry* [119]. The achievement of Aim 6 was important because it demonstrates that identification of human blood using proteomics is valid in the Australian context. That is, blood from native species, which may be present at the crime scene, on a suspect or on a motor vehicle due to “innocent” means, is easily differentiated from human blood. In addition, it has been demonstrated that if an investigation involves trafficking of a protected native species or perhaps an animal cruelty offence then proteomics could be used to provide evidence.

MALDI-MS had shown that better sensitivity towards human blood than the Hematrace and other presumptive tests, and compared to any technique that involves swabbing to recover evidence (including DNA profiling), MALDI imaging allows the spatial distribution of the fluids in a stain to be mapped. This includes mapping of proteins in fingerprints, even after enhancement techniques have been carried out.

7.2 Future Work

The research described in this thesis explored many analytical and/or proteomic strategies to establish streamlined methodology for the detection of protein markers from body fluids and their traces on various substrates. This section describes some of the future directions in which research may carry out based on this thesis content and the published data.

The research was carried out using volunteer samples and as some sample collections were quite invasive this initial research involved only a few different volunteers. A large cohort study would now be valuable to highlight any differences between individuals in regards to vaginal fluid biomarkers and more analysis of menstrual fluid would be valuable. Also the persistence study also involved only a small number of individuals, time points and activities after deposition of fluids. A more extensive study with more individuals would be valuable. Additional work is required to explore the effect of very abundant proteins such as albumin or haemoglobin on MALDI detection in different ratios of undiluted body fluids.

Work towards the detection of multiple biomarkers for particular body fluids would be valuable because this could increase the sensitivity and specificity of body fluid identification.

The majority of current available genomics assays (including conventional DNA analysis) typically involve capillary electrophoresis (CE) or quantitative RT-PCR platforms. However, these methods require the use of high-cost fluorescently labelled primers or probes. Therefore, streamlined methodology and cost effective complementary novel “techniques” are advantageous for implementation in forensic casework.

The proteomic application and mechanism of MALDI-MS was introduced by Karas and Hillenkamp [16, 18]. This group has also shown the usage of MALDI mass spectrometry for the DNA sequencing analysis and suggested that MALDI-MS could be a high throughput method for future alternative conventional sequencing procedures and screening of genetic mutations [160]. Recently, for forensic applications a number of articles have been published that focus on the practical considerations of mRNA profiling for determination of the type of body fluid and/or tissue based on gene expression patterns [77-80]. A recent study by Donfack et al. has reported that mass spectrometry based cDNA and/or mRNA profiling is a potential tool for forensic human body fluid identification (venous blood, saliva and semen) [83]. These authors have shown that MALDI-TOF MS is a potential fluorescent dye-free or labelled PCR primers-free alternative method for body fluid identification in forensic casework. The use of mass spectrometry for both detection of protein biomarkers and mRNA markers in forensic samples would be very powerful. The two techniques combined would provide mutual confirmation of a body fluid identification.

In future work use of MS tools for both protein analysis and genomic analysis of top-down DNA patterns, DNA methylation, DNA base pair content or DNA sequencing fragments micro RNA (miRNA), mRNA and single nucleotide polymorphisms (SNPs) could be investigated. Using PCR and direct electrospray ionization mass spectrometry can be advantageous for automated analysis of sequence polymorphism in STR alleles [161]. Such analysis could be valuable to forensic science by gathering an abundance of proteomic and genomic information from the same sample.

Recently, researchers have focused on the applications of SNP genotyping (multiple SNPs can be genotyped in a single MALDI experiment), DNA methylation analysis, expression profiling, and mutation detection using MALDI-TOF MS. A MALDI matrix such as 3-hydroxypicolinic acid (3-HPA) has been widely used for the DNA and oligonucleotides analysis [162] in positive ion mode; however, this matrix may cause depurination and/or loss of bases and adduct formation (i.e. sodium and potassium) with DNA oligonucleotides. Hence, the search for novel sample preparation conditions and suitable matrices for better MALDI ionization and the detection of DNA molecules is warranted. Since the DNA molecule contains negatively charged phosphate groups, electrospray ionization mass spectrometry (ESI-MS) could be another choice for better ionization (i.e. using negative ESI mode).

References

1. Hu, S., J.A. Loo, and D.T. Wong. *Human body fluid proteome analysis*. *Proteomics*, 2006. 6(23): p. 6326-6353.
2. Paulo JA, Kadiyala V, Banks PA, Steen H, Conwell DL. *Mass spectrometry based proteomics for translational research: a technical overview*. *Yale J Biol Med*. 2012; 85 (1):59-73.
3. Wilkins MR. *From proteins to proteomes: large scale protein identification by two dimensional electrophoresis and amino acid analysis*. *Bio/technology* (Nature Publishing Company). 1996; 14(1):61-5.
4. Wunschel Dea. *Forensic proteomics of poxvirus production*. *The Analyst*. 2013; 138 (21):6385- 97.
5. Dammeier S, Nahnsen S, Veit J, Wehner F, Ueffing M, Kohlbacher O. *Mass-Spectrometry-Based Proteomics Reveals Organ-Specific Expression Patterns To Be Used as Forensic Evidence*. *J. Proteome Res.*, 2016;15(1):182-92.
6. Olsen JV, Mann M. *Status of large scale analysis of post translational modifications by mass spectrometry*. *Mol Cell Proteomics*. 2013; 12 (12):3444-52.
7. Somlata, **Kamanna S**, Agrahari M, Bhattacharya S, and Bhattacharya A. *Autophosphorylation of Ser (428) of EhC2PK Plays a Critical Role in Regulating Erythrophagocytosis in the Parasite Entamoeba histolytica*. *J Biol Chem*. 2012, 287:10844-10852.
8. Licker V, Burkhard PR. *Proteomics as a new paradigm to tackle Parkinson's disease research challenges*. *Advances in Integrative Medicine*. 2014;4–5(0):1-17.
9. O'Farrell, P.H. High resolution two-dimensional electrophoresis of proteins. *J Biol Chem*, 1975. 250(10): p. 4007-21.
10. Vanrobaeys, F., et al., *Profiling of myelin proteins by 2D-gel electrophoresis and multidimensional liquid chromatography coupled to MALDI TOF-TOF mass spectrometry*. *J Proteome Res*, 2005. 4(6): p. 2283-93.
11. Banga, J.P., *SDS-Polyacrylamide Gel Electrophoresis (SDS-Page) A2 - Delves, Peter J, in Encyclopedia of Immunology* (Second Edition). 1998, Elsevier: Oxford. p. 2143-2144.
12. Saraswathy, N. and P. Ramalingam. *Introduction to proteomics, in Concepts and Techniques in Genomics and Proteomics*. 2011, Woodhead Publishing. p. 147-158.
13. Yamashita, M. and J.B. Fenn. *Electrospray ion source: Another variation on the free-jet theme*. *J Phys Chem*, 1984. 88 (20): p. 4451-4459.

14. Chaurand, P., F. Luetzenkirchen, and B. Spengler. *Peptide and protein identification by matrix-assisted laser desorption ionization (MALDI) and MALDI-post-source decay time-of-flight mass spectrometry*. J. Am. Soc. Mass Spectrom. 1999. 10(2): p. 91-103.
15. Landry, F., C.R. Lombardo, and J.W. Smith. *A method for application of samples to matrix-assisted laser desorption ionization time-of-flight targets that enhances peptide detection*. Anal. Biochem. 2000. 279 (1): p. 1-8.
16. Karas, M. and F. Hillenkamp. *Laser desorption ionization of proteins with molecular masses exceeding 10,000 daltons*. Anal Chem, 1988. 60(20): p. 2299-2301
17. *MALDI Theory Mass Spectrometry* (2004 application report). Bruker Daltonics, Bremen GmbH, Germany.
18. F. Hillenkamp, T. W. Jaskolla and M. Karas, MALDI MS, Wiley-VCH Verlag GmbH & Co. KGaA, 2013, pp. 1–40, DOI: 10.1002/9783527335961.ch1.
19. Morrical BD, Ferguson DP, Prather KA. *Coupling two-step laser desorption/ionization with aerosol time of flight mass spectrometry for the analysis of individual organic particles*. Journal of American Society for Mass Spectrometry. 1998; 9 (10):1068-73.
20. Ehring, H., M. Karas, and F. Hillenkamp, *Role of photoionization and photochemistry in ionization processes of organic molecules and relevance for matrix-assisted laser desorption ionization mass spectrometry*. Organic Mass Spectrometry, 1992. 27(4): p. 472-480.
21. Karas M, Gluckmann M, Schafer J. *Ionization in matrix-assisted laser desorption/ionization: singly charged molecular ions are the lucky survivors*. J. Mass Spectrom. 2000; 35 (1):1-12.
22. Padliya ND, Wood TD. *Improved peptide mass fingerprinting matches via optimized sample preparation in MALDI mass spectrometry*. Analytica chimica acta. 2008;627 (1):162-8.
23. Gobom J, Schuerenberg M, Mueller M, Theiss D, Lehrach H, Nordhoff E. *Alphacyano α hydroxycinnamic acid affinity sample preparation. A protocol for MALDI MS peptide analysis in proteomics*. Anal chem. 2001; 73(3):434-8.
24. Bourcier S, Bouchonnet S, Hoppilliard Y. *Ionization of 2,5-dihydroxybenzoic acid (DHB) matrix-assisted laser desorption ionization experiments and theoretical study*. Int. J Mass Spectrom. 2001; 210–211(0):59-69.
25. Schreiner M, Strupat K, Lottspeich F, Eckerskorn C. *Ultraviolet matrix assisted laser desorption ionization mass spectrometry of electroblotted proteins*. Electrophoresis. 1996; 17(5):954-61.
26. Suckau D, Resemann A, Schuerenberg M, Hufnagel P, Franzen J, Holle A. *A novel MALDI LIFT- TOF/TOF mass spectrometer for proteomics*. Anal. Bioanal. Chem. 2003; 376(7):952-65.

27. Liu, Z. and K.L. Schey. *Optimization of a MALDI TOF-TOF mass spectrometer for intact protein analysis*. J. Am. Soc. Mass Spectrom. 2005, 16 (4): p. 482-490.
28. Sampson, J.S., K.K. Murray, and D.C. Muddiman. *Intact and Top-Down Characterization of Biomolecules and Direct Analysis Using Infrared Matrix-Assisted Laser Desorption Electrospray Ionization Coupled to FT-ICR Mass Spectrometry*. J. Am. Soc. Mass Spectrom. 2009, 20(4): p. 667-673.
29. Catherman, A.D., O.S. Skinner, and N.L. Kelleher. *Top Down Proteomics: Facts and Perspectives*. Biochem Biophys Res Commun, 2014. 445 (4): p. 683-93
30. Han, X., et al., *Extending top-down mass spectrometry to proteins with masses greater than 200 kilodaltons*. Science, 2006. 314(5796): p. 109-12.
31. **Kamanna, S.**; Henry, J.; Voelcker, N. H.; Linacre, A.; Kirkbride, K. P. *Direct identification of forensic body fluids using matrix-assisted laser desorption/ionization time-of-flight mass spectrometry*. Int. J. Mass Spectrom. 2016, 397, 18-26.
32. Laskin, J. and J.H. Futrell. *Collisional activation of peptide ions in FT-ICR mass spectrometry*. Mass Spectrom Rev, 2003. 22(3): p. 158-81.
33. Syka, J.E., et al., *Peptide and protein sequence analysis by electron transfer dissociation mass spectrometry*. Proc Natl Acad Sci USA, 2004. 101(26): p. 9528-33.
34. Cui, W., H.W. Rohrs, and M.L. Gross. *Top-Down Mass Spectrometry: Recent Developments, Applications and Perspectives*. The Analyst, 2011. 136 (19): p. 3854-3864.
35. Wynne, C., et al., *Top-down identification of protein biomarkers in bacteria with unsequenced genomes*. Anal Chem, 2009. 81(23): p. 9633-42.
36. Sauget, M., et al., *Can MALDI-TOF Mass Spectrometry Reasonably Type Bacteria?*Trends Microbiol, 2017. 25(6): p. 447-455.
37. Perkins DN, Pappin DJC, Creasy DM, Cottrell JS. Electrophoresis. 1999; 20:3551–3567.
38. Kapp EA, Schutz F, Connolly LM, Chakel JA, Meza JE, Miller CA, Fenyo D, Eng JK, Adkins JN, Omenn GS, Simpson RJ. Proteomics. 2005; 5:3475–3490.
39. Ramachandran S, Venugopal A, **Sathisha K**, Reshmi G, Charles S, Divya G, Pillai MR, Kartha CC. 2012. *Proteomic profiling of high glucose primed monocytes identifies cyclophilin A as a potential secretory marker of inflammation in type 2 diabetes*. Proteomics 12:2808-2821.
40. Kellie, J.F., et al., *The emerging process of Top Down mass spectrometry for protein analysis: biomarkers, protein-therapeutics, and achieving high throughput*. Mol Biosyst, 2010. 6(9): p. 1532-9.
41. Tsai, Y.S., et al., *Precursor ion independent algorithm for top-down shotgun proteomics*. J Am Soc Mass Spectrom, 2009. 20(11): p. 2154-66.
42. Zamdborg, L., et al., *ProSight PTM 2.0: improved protein identification and characterization for top down mass spectrometry*. Nucleic Acids Res, 2007. 35(Web Server issue): p. W701-6.

43. Kaufmann R, Wingerath T, Kirsch D, Stahl W, Sies H. *Analysis of carotenoids and carotenol fatty acid esters by matrix-assisted laser desorption ionization (MALDI) and MALDI-post source-decay mass spectrometry.* Anal. Biochem. 1996;238 (2):117-28.
44. Roepstorff P, Fohlman J. *Proposal for a common nomenclature for sequence ions in mass spectra of peptides.* Biomedical mass spectrometry. 1984;11(11):601.
45. Johnson, R.S., et al., *Novel fragmentation process of peptides by collision-induced decomposition in a tandem mass spectrometer: differentiation of leucine and isoleucine.* Anal. Chem. 1987; 59(21): p. 2621-2625.
46. Biemann, K., Appendix 5. *Nomenclature for peptide fragment ions (positive ions).* Methods Enzymol, 1990. 193: p. 886-7.
47. Parthasarathi R, He Y, Reilly JP, Raghavachari K. *New insights into the vacuum UV photodissociation of peptides.* J. Am. Chem. Soc. 2010;132 (5):1606-10.
48. Yalcin T, Csizmadia IG, Peterson MR, Harrison AG. *The structure and fragmentation of B_n (n>=3) ions in peptide spectra.* J Am Soc Mass Spectrom. 1996;7(3):233-42.
49. Yalcin T, Khouw C, Csizmadia IG, Peterson MR, Harrison AG. *Why Are B ions stable species in peptide spectra?* J Am Soc Mass Spectrom. 1995;6(12):1165-74.
50. Fang S, Takao T, Satomi Y, Mo W, Shimonishi Y. *Novel rearranged ions observed for protonated peptides via metastable decomposition in matrix assisted laser desorption/ionization time of flight mass spectrometry.* J Am Soc Mass Spectrom. 2000;11(4):345-51.
51. Han, H., Y. Xia, and S.A. McLuckey, *Ion Trap Collisional Activation of c and z(•) Ions Formed via Gas-Phase Ion/Ion Electron Transfer Dissociation.* J. Proteome Res. 2007. 6(8): p. 3062-3069.
52. Medzihradszky KF, Campbell JM, Baldwin MA, Falick AM, Juhasz P, Vestal ML, et al. *The characteristics of peptide collision-induced dissociation using a high-performance MALDI TOF/TOF tandem mass spectrometer.* Anal. Chem. 2000;72(3):552-8.
53. Stimson E, Truong O, Richter WJ, Waterfield MD, Burlingame AL. *Enhancement of charge remote fragmentation in protonated peptides by high-energy CID MALDI-TOF-MS using "cold" matrices.* Int J Mass Spectrom Ion Process. 1997;169-170(0):231-40.
54. Karas, M., et al., *Matrix Dependence of Metastable Fragmentation of Glycoproteins in MALDI TOF Mass Spectrometry.* Anal. Chem. 1995; 67(3): p. 675-679.
55. Vestal ML, Campbell JM. *Tandem time-of-flight mass spectrometry.* Methods Enzymol, 2005;402:79-108.
56. Caprioli, R. M.; Farmer, T. B.; Gile, J. *Molecular imaging of biological samples: localization of peptides and proteins using MALDI-TOF MS.* Anal. Chem. 1997, 69, 4751-4760.

57. Meriaux, C.; Franck, J.; Wisztorski, M.; Salzet, M.; Fournier, I. *Liquid ionic matrixes for MALDI mass spectrometry imaging of lipids*. J. Proteom. 2010, 73, 1204-1218.
58. Groseclose, M. R.; Massion, P. P.; Chaurand, P.; Caprioli, R. M. *High-throughput proteomic analysis of formalin-fixed paraffin-embedded tissue microarrays using MALDI imaging mass spectrometry*. Proteomics 2008, 8, 3715-3724.
59. Seeley, E. H.; Oppenheimer, S. R.; Mi, D.; Chaurand, P.; Caprioli, R. M. *Enhancement of protein sensitivity for MALDI imaging mass spectrometry after chemical treatment of tissue sections*. J. Am. Soc. Mass Spectrom 2008, 19, 1069-1077.
60. Seeley, E.H. and R.M. Caprioli, *MALDI imaging mass spectrometry of human tissue: method challenges and clinical perspectives*. Trends Biotechnol, 2011. 29(3): p. 136-43.
61. Mirgorodskaya E, Braeuer C, Fucini P, Lehrach H, Gobom J. *Nanoflow liquid chromatography coupled to matrix assisted laser desorption/ionization mass spectrometry: sample preparation, data analysis, and application to the analysis of complex peptide mixtures*. Proteomics. 2005; 5(2):399- 408.
62. Sorensen LK, Hasselstrom JB. *A hydrophilic interaction liquid chromatography electrospray tandem mass spectrometry method for the simultaneous determination of gamma hydroxybutyrate and its precursors in forensic whole blood*. Forensic Sci. Int. 2012; 222(1-3):352-9.
63. Tsai, T.H., et al., *LC-MS/MS-based serum proteomics for identification of candidate biomarkers for hepatocellular carcinoma*. Proteomics, 2015. 15(13): p. 2369-81.
64. Mbeunkui, F., et al., *Identification of Differentially Secreted Biomarkers Using LC-MS/MS in Isogenic Cell Lines Representing a Progression of Breast Cancer*. J. Proteome Res., 2007, 6(8): p. 2993-3002.
65. Panneerchelvam, S. and M.N. Norazmi, *Forensic DNA Profiling and Database*. Malays J Med Sci., MJMS, 2003. 10(2): p. 20-26.
66. Hebda LM, Doran AE, Foran DR. *Collecting and analyzing DNA evidence from fingernails: a comparative study*. J Forensic Sci. 2014; 59(5):1343-50.
67. Gill P, Jeffreys AJ, Werrett DJ. *Forensic application of DNA 'fingerprints'*. Nature. 1985; 318(6046):577-9.
68. Roewer, L., *DNA fingerprinting in forensics: past, present, future*. Investigative Genetics, 2013. 4(1): p. 22.
69. Oz, C. and A. Zamir, *An evaluation of the relevance of routine DNA typing of fingernail clippings for forensic casework*. J Forensic Sci, 2000. 45(1): p. 158-60.
70. Ottens, R., D. Taylor, and A. Linacre, *DNA profiles from fingernails using direct PCR*

- Forensic Sci Med Pathol, 2015. 11(1): p. 99-103.
71. An JH, Shin KJ, Yang WI, Lee HY. *Body fluid identification in forensics*. BMB reports. 2012; 45(10):545-53.
 72. Virkler K, Lednev IK. *Analysis of body fluids for forensic purposes: from laboratory testing to non-destructive rapid confirmatory identification at a crime scene*. Forensic Sci. Int. 2009; 188(1-3):1-17.
 73. Zapata, F., M.Á. Fernández de la Ossa, and C. García-Ruiz. *Emerging spectrometric techniques for the forensic analysis of body fluids*. Trends Analyt Chem. 2015, 64: p. 53-63.
 74. R. Li, *Forensic Biology*. CRC Press, Boca Raton. 2008.
 75. Robinson, S. and A.H. Robinson. *Chemical composition of sweat*. Physiol Rev, 1954. 34(2): p. 202-20.
 76. Crick, F., *Central dogma of molecular biology*. Nature, 1970. 227(5258): p. 561-563.
 77. Wang Z, Zhang SH, Di Z, Zhao SM, Li CT. *Messenger RNA profiling for forensic body fluid identification: research and applications*. Fa yi xue za zhi. 2013; 29(5):368-74.
 78. Hanson, E.K. and J. Ballantyne. *Rapid and inexpensive body fluid identification by RNA profiling-based multiplex High Resolution Melt (HRM) analysis*. F1000Research, 2013. 2: p. 281.
 79. An, J.H., et al., *Body fluid identification in forensics*. BMB Rep, 2012. 45(10): p. 545-553.
 80. Vennemann, M. and A. Koppelkamm. *mRNA profiling in forensic genetics I: Possibilities and limitations*. Forensic Sci Int, 2010. 203(1-3): p. 71-5.
 81. Juusola, J. and J. Ballantyne. *Multiplex mRNA profiling for the identification of body fluids*. Forensic Sci Int, 2005. 152(1): p. 1-12.
 82. Fang, R., et al., *Real-time PCR assays for the detection of tissue and body fluid specific mRNAs*. International Congress Series, 2006. 1288: p.685-687.
 83. Donfack J, Wiley A. *Mass spectrometry-based cDNA profiling as a potential tool for human body fluid identification*. Forensic Sci. Int. Genet. 2015; 16:112-20.
 84. Al-Soud WA, Radstrom P. *Purification and characterization of PCR-inhibitory components in blood cells*. J. Clin. Microbiol. 2001; 39(2):485-93.
 85. Pang BC, Cheung BK. *One-step generation of degraded DNA by UV irradiation*. Anal. Biochem. 2007; 360(1):163-5.
 86. Andersen J, Bramble S. *The effects of fingermark enhancement light sources on subsequent PCR-STR DNA analysis of fresh bloodstains*. J Forensic Sci. 1997; 42(2):303-6.
 87. Webb JL, Creamer JJ, Quickenden TI. *A comparison of the presumptive luminol test*

- for blood with four non-chemiluminescent forensic techniques. Luminescence: the journal of biological and chemical luminescence. 2006; 21(4):214-20.*
88. Castelló A, Alvarez M, Verdú F. *Accuracy, Reliability, and Safety of Luminol in Bloodstain Investigation. Can. Soc. Forensic Sci. J. 2002; 35(3):113-21.*
 89. Vennemann M, Scott G, Curran L, Bittner F, Tobe SS. *Sensitivity and specificity of presumptive tests for blood, saliva and semen. Forensic science, medicine, and pathology. 2014; 10(1):69-75.*
 90. Johnston, S.; Newman, J.; Frappier, R. *Validation Study of the Abacus Diagnostics ABACard® HemaTrace® Membrane Test for the Forensic Identification of Human Blood. Can. Soc. Forensic Sci. J. 2003, 36, 173-183.*
 91. Johnston, E.; Ames, C. E.; Dagnall, K. E.; Foster, J.; Daniel, B. E. *Comparison of Presumptive Blood Test Kits Including Hexagon OBTL. J Forensic Sci. 2008, 53, 687-689.*
 92. Cox, M. *A study of the sensitivity and specificity of four presumptive tests for blood. J Forensic Sci. 1991, 36, 1503-1511.*
 93. Santucci KA, Nelson DG, McQuillen KK, Duffy SJ, Linakis JG. *Wood's lamp utility in the identification of semen. Pediatrics. 1999; 104(6):1342-4.*
 94. Lundquist F. *Medicolegal identification of seminal stains using the acid phosphatase test. AMA archives of pathology. 1950; 50(4):395-9.*
 95. Lewis, J., et al., *Improved detection of semen by use of direct acid phosphatase testing. Science & Justice, 2013. 53(4): p. 385-394.*
 96. Noppinger K, Morrison R, Jones NH, Hopkins H, 2nd. *An evaluation of an enzymatic choline determination for the identification of semen in casework samples. J Forensic Sci. 1987; 32(4):1069-74.*
 97. Tsuda R, Hara M, Sagawa K. [*Demonstration of seminal stains by sandwich ELISA using monoclonal gamma seminoprotein antibody bound to acrylbutadienestyrene beads. Forensic immunological studies of body fluids and secretion. Report XXIII]. Jpn J Legal Med 1984; 38 (1):83-7.*
 98. Hochmeister MN, Budowle B, Rudin O, Gehrig C, Borer U, Thali M, et al. *Evaluation of prostate specific antigen (PSA) membrane test assays for the forensic identification of seminal fluid. J Forensic Sci. 1999;44(5):1057-60.*
 99. Healy DA, Hayes CJ, Leonard P, McKenna L, O'Kennedy R. *Biosensor developments: application to prostate specific antigen detection. Trends Biotechnol. 2007; 25(3):125-31.*
 100. Pang BC, Cheung BK. *Identification of human semenogelin in membrane strip test as an alternative method for the detection of semen. Forensic Sci. Int. 2007; 169(1):27-31.*

101. Alvarez, M., J. Juusola, and J. Ballantyne. *An mRNA and DNA co-isolation method for forensic casework samples*. *Anal Biochem*, 2004. 335(2): p. 289-98.
102. Myers JR, Adkins WK. *Comparison of modern techniques for saliva screening*. *J Forensic Sci*. 2008; 53(4).
103. Casey DG, Price J. *The sensitivity and specificity of the RSID- saliva kit for the detection of human salivary amylase in the Forensic Science Laboratory, Dublin, Ireland*. *Forensic Sci. Int.* 2010; 194(1-3):67-71.
104. Ricci U, Carboni I, Torricelli F. *False-positive results with amylase testing of citrus fruits*. *J Forensic Sci*. 2014; 59(5):1410-2.
105. Divall GB. *A new peptidase isozyme which may assist in the identification of vaginal debris*. *Forensic Sci. Int.* 1984; 24(4):239-46.
106. Stuart H. James, J.J.N., Ph.D., Suzanne Bell, *Forensic Science: An Introduction to Scientific and Investigative Techniques*. CRC Press, Boca Raton, Fourth ed. 2014:
107. Martin, P.D. and S.K. Cheshire, *A Comparative Study of the Citrate and Lactate Concentrations in Stains from Semen, Vaginal Secretion and Mixtures of the Two Using Isotachophoresis*, *Adv. Forensic Haemogen.* 1 (1986) p299-303.
108. Doi, M., et al., *A simple identification method for vaginal secretions using relative quantification of Lactobacillus DNA*. *Forensic Sci. Int. Genet.* 2014, 12: p. 93-99.
109. Haas, C., et al., *mRNA profiling for body fluid identification by reverse transcription endpoint PCR and realtime PCR*. *Forensic Sci Int Genet*, 2009. 3(2): p. 80-8.
110. Ballantyne, J. and J. Juusola. *Messenger RNA profiling: body fluid identification using multiplex reverse transcription-polymerase chain reaction (RT-PCR)*. Foundation of The University of Central Florida Inc., USA, 2007, Patents.
111. Sato, K., et al., *Identification of human urinary stains by the quotient uric acid/urea nitrogen*. *Forensic Sci Int*, 1990. 45(1-2): p. 27-38.
112. Bedrosian, J.L., M.D. Stolorow, and M.A. Tahir, *Development of a radial gel diffusion technique for the identification of urea in urine stains*. *J Forensic Sci*, 1984. 29(2): p. 601-6.
113. Akutsu, T., et al., *Evaluation of Tamm-Horsfall protein and uroplakin III for forensic identification of urine*. *J Forensic Sci*, 2010. 55(3): p. 742-6.
114. Nakazono T, Kashimura S, Hayashiba Y, Hisatomi T, Hara K. *Identification of human urine stains by HPLC analysis of 17 ketosteroid conjugates*. *J Forensic Sci*. 2002; 47(3):568-72.
115. Nakazono T, Kashimura S, Hayashiba Y, Hara K, Matsusue A, Augustin C. *Dual examinations for identification of urine as being of human origin and for DNA-typing*

- from small stains of human urine.* J Forensic Sci. 2008; 53(2):359-63.
116. Sagawa, K., et al., *Production and characterization of a monoclonal antibody for sweat-specific protein and its application for sweat identification.* Int J Legal Med, 2003. 117(2): p. 90-5.
117. Girod, A., R. Ramotowski, and C. Weyermann. *Composition of fingerprint residue: A qualitative and quantitative review.* Forensic Sci Int, 2012. 223(1): p. 10-24.
118. **Kamanna S.**, Henry J., Voelcker N.H., Linacre A, Kirkbride K.P. *A mass spectrometry based forensic toolbox for imaging and detecting biological fluid evidence in finger marks and fingernail scrapings.* Int J Legal Med, 2017. 131 (5), 1413-1422.
119. **Kamanna S.**, Henry J., Voelcker N.H., Linacre A, Kirkbride K.P. *"Bottom-up" in situ proteomic differentiation of human and non-human haemoglobins for forensic purposes by matrix-assisted laser desorption/ionization time-of-flight tandem mass spectrometry.* Rapid Commun. Mass Spectrom. 2017, 31(22): p. 1927-1937.
120. Bossers, L.C., et al., *Methods for the enhancement of fingerprints in blood.* Forensic Sci Int, 2011. 210(1-3): p. 1-11.
121. Templeton J.E.L., Taylor D., Handt O., Skuza P. et al., *Direct PCR Improves the Recovery of DNA from Various Substrates.* J. Forensic Sci. 2015;60(6):1558-6.
122. Soukos, N.S., et al., *A rapid method to detect dried saliva stains swabbed from human skin using fluorescence spectroscopy.* Forensic Sci Int, 2000. 114(3): p. 133-138.
123. McLaughlin G, Doty KC, Lednev IK. *Discrimination of human and animal blood traces via Raman spectroscopy.* Forensic Sci. Int. 2014; 238:91-5.
124. Orphanou, C. M.; Walton-Williams, L.; Mountain, H.; Cassella, J. *The detection and discrimination of human body fluids using ATR FT-IR spectroscopy.* Forensic Sci. Int. 2015, 252, e10-16.
125. Elkins, K. M. *Rapid presumptive "fingerprinting" of body fluids and materials by ATR FT-IR spectroscopy.* J. Forensic Sci. 2011, 56, 1580-1587.
126. De Giovanni, N. *Sweat as an Alternative Biological matrix.* In *Forensic Toxicology : Drug Use and Misuse*; Calavia, P. G. R., D.A.; Davies, S.; Johnston, A.; Holt, D., Eds.; Royal Society of Chemistry: Cambridge, UK, 2016; Chapter 22, pp438-478.
127. Guinan, T.M., et al., *Direct detection of illicit drugs from biological fluids by desorption/ionization mass spectrometry with nanoporous silicon microparticles.* Analyst, 2015. 140(23): p. 7926-33.
128. Bailey, M. J.; Bradshaw, R.; Francese, S.; Salter, T. L.; Costa, C.; Ismail, M.; Webb, P.; Bosman, R.; Wolff, I.; de Puit, M. *Rapid detection of cocaine, benzoylecgonine and methylecgonine in fingerprints using surface mass spectrometry.* Analyst 2015, 140, 6254-6259.

129. Guinan, T.; Dela Vedova, C.; Kobus, H.; Voelcker, N.H. *Mass Spectrometry Imaging of Fingerprint Sweat on Nanostructured Silicon*. Chem. Commun. 2015, 51, 6088 - 6091.
130. Bradshaw, R., et al., *Separation of overlapping fingermarks by matrix assisted laser desorption ionisation mass spectrometry imaging*. Forensic Sci Int, 2012. 222(1-3): p. 318-26.
131. Yagnik, G. B.; Korte, A. R.; Lee, Y. J. *Multiplex mass spectrometry imaging for latent fingerprints*. J. Mass Spectrom. 2013, 48, 100-104.
132. Wolstenholme, R.; Bradshaw, R.; Clench, M. R.; Francese, S. *Study of latent fingermarks by matrix-assisted laser desorption/ionisation mass spectrometry imaging of endogenous lipids*. Rapid Commun Mass Spectrom 2009, 23, 3031-3039.
133. Su, B. *Recent progress on fingerprint visualization and analysis by imaging ridge residue components*. Anal. Bioanal. Chem. 2016, 408, 2781-279.
134. Bradshaw, R., et al., *A novel matrix-assisted laser desorption/ionisation mass spectrometry imaging based methodology for the identification of sexual assault suspects* Rapid Commun. Mass Spectrom. 2011. 25(3): p. 415-422.
135. Ferguson, L., et al., *Two-Step Matrix Application for the Enhancement and Imaging of Latent Fingermarks*. Anal. Chem. 2011, 83(14): p. 5585-5591.
136. Ferguson, L.S., et al., *Efficiency of the dry-wet method for the MALDI-MSI analysis of latent fingermarks*. J. Mass Spectrom. 2013, 48(6): p. 677-684.
137. Bradshaw, R., et al., *Towards the integration of matrix assisted laser desorption ionisation mass spectrometry imaging into the current fingerprint examination workflow*. Forensic Sci Int, 2013. 232(1-3): p. 111-24.
138. Yang H., Zhou B., Prinz M., Siegel D. *Proteomic analysis of menstrual blood*. Mol. Cell. Proteomics: 2012, 11, 1024-1035.
139. Yang, H., Zhou, B., Deng, H., Prinz, M., Siegel, D. *Body fluid identification by mass spectrometry*. Int J Legal Med, 2013; 127(6):1065-77.
140. Legg, K.M., et al., *Discovery of highly specific protein markers for the identification of biological stains*. Electrophoresis, 2014. 35(21-22): p. 3069-78.
141. Spencer, S.E., et al., *Matrix-assisted laser desorption/ionization-time of flight-mass spectrometry profiling of trace constituents of condom lubricants in the presence of biological fluids*. Forensic Sci Int, 2011. 207(1-3): p. 19-26.
142. Bradshaw, R., N. Denison, and S. Francese. *Implementation of MALDI MS profiling and imaging methods for the analysis of real crime scene fingermarks*. Analyst, 2017. 142(9): p. 1581-1590.

143. Basilico F, Di Silvestre D, Sedini S, Petretto A, Levreri I, Melioli G, et al. *New approach for rapid detection of known hemoglobin variants using LC MS/MS combined with a peptide database.* J. Mass Spectrom. 2007; 42(3):288-92.
144. Van Bocxlaer, J.F., et al., *Liquid chromatography-mass spectrometry in forensic toxicology.* Mass Spectrom Rev, 2000. 19(4): p. 165-214.
145. Wood, M., et al., *Recent applications of liquid chromatography-mass spectrometry in forensic science.* J Chromatogr A, 2006. 1130(1): p. 3-15.
146. Van Steendam, K., et al., *Mass spectrometry-based proteomics as a tool to identify biological matrices in forensic science.* Int J Legal Med. 2013. 127(2): p. 287-298.
147. Bradshaw, R.; Bleay, S.; Clench, M. R.; Francese, S. *Direct detection of blood in fingerprints by MALDI MS profiling and imaging.* Sci. Justice. 2014, 54, 110-117.
148. Deininger, L.; Patel, E.; Clench, M. R.; Sears, V.; Sammon, C.; Francese, S. *Proteomics goes forensic: Detection and mapping of blood signatures in fingerprints.* Proteomics 2016, 16, 1707-1717.
149. Francese, S., R. Bradshaw, and N. Denison. *An update on MALDI mass spectrometry based technology for the analysis of fingerprints - stepping into operational deployment.* Analyst, 2017,142, 2518-2546.
150. Francese, S. *Techniques for Fingerprint Analysis Using MALDI MS: A Practical Overview, in Advances in MALDI and Laser-Induced Soft Ionization Mass Spectrometry,* R. Cramer, Editor. 2016, Springer International Publishing: Cham. p. 93-128.
151. Igoh, A., Y. Doi, and K. Sakurada. *Identification and evaluation of potential forensic marker proteins in vaginal fluid by liquid chromatography/mass spectrometry.* Anal Bioanal Chem, 2015. 407(23): p. 7135-44.
152. Zegels, G., et al., *Comprehensive proteomic analysis of human cervical-vaginal fluid using colposcopy samples.* Proteome Science, 2009. 7: p. 17-17.
153. Chen, K., et al., *Characterization of Tumor Suppressive Function of cornulin in Esophageal Squamous Cell Carcinoma.* PLoS ONE, 2013. 8(7): p. e68838.
154. Zhang, W., et al., *Genetic variants of C1orf10 and risk of esophageal squamous cell carcinoma in a Chinese population.* Cancer Sci, 2009. 100(9): p. 1695-700.
155. Patel, E., Cicatiello, P., Deininger, L., Clench, M. R. et al., *A proteomic approach for the rapid, multi informative and reliable identification of blood.* Analyst. 2016; 141:191-198.
156. Legg, K.M., et al., *Verification of protein biomarker specificity for the identification of biological stains by quadrupole time-of-flight mass spectrometry.* ELECTROPHORESIS, 2017. 38(6): p. 833-845.

157. Ottens R., Templeton J., Paradiso V., Taylor D. et al., *Application of direct PCR in forensic casework*. *Forensic Sci. Int. Genet.* 2013; 4(1):e47-e8.
158. Dasari S., Pereira L., Reddy A.P., Michaels J.E. et al., *Comprehensive proteomic analysis of human cervical-vaginal fluid*. *J. Proteome Res.* 2007; 6(4):1258-68.
159. Cheng, Y. and K. Belov. *Antimicrobial Protection of Marsupial Pouch Young*. *Frontiers in Microbiology*, 2017. 8: p. 354.
160. Kirpekar F., Nordhoff E., Roepstorff P., Hillenkamp F.. *DNA sequence analysis by MALDI mass spectrometry*. *Nucleic Acids Research*, 1998. 26(11): p. 2554-2559.
161. Planz, J. V., et al. (2012). *Automated analysis of sequence polymorphism in STR alleles by PCR and direct electrospray ionization mass spectrometry*. *Forensic Sci. Int. Genet.* 6, 594-606.
162. Wu, K.J., T.A. Shaler, and C.H. Becker. *Time-of-flight mass spectrometry of underivatized single-stranded DNA oligomers by matrix-assisted laser desorption*. *Anal Chem*, 1994. 66(10): p. 1637-45.
163. **Kamanna, S.**, et al., *A complementary forensic 'proteo-genomic' approach for the direct identification of biological fluid traces under fingernails*. *Anal Bioanal Chem* (2018). <https://doi.org/10.1007/s00216-018-1223-3>.

APPENDICES

Appendix-1A (Selected data)

nLC-ESI MS/MS data relating to blood in water (1:500) and semen in water (1:200) and saliva in water (1:5) are provided in the attached DVD)

Body fluid: Blood

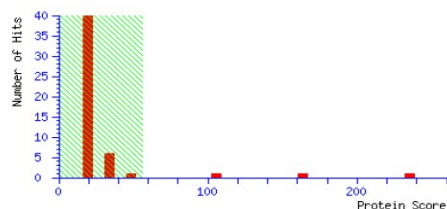
Protein ID: 1) Hemoglobin subunit beta OS=Homo sapiens

MASCOT SCIENCE Mascot Search Results

User : Satish
Email : satish@gmail.com
Search title :
Database : SwissProt 2015_08 (549008 sequences; 195692017 residues)
Taxonomy : Homo sapiens (human) (20204 sequences)
Timestamp : 27 Jul 2015 at 05:36:11 GMT
Top Score : 235 for **Mixture 1**, HBB_HUMAN + HBA_HUMAN

Mascot Score Histogram

Protein score is $-10 \cdot \log(P)$, where P is the probability that the observed match is a random event.
Protein scores greater than 56 are significant ($p < 0.05$).



Protein sequence coverage: 94%

Matched peptides shown in **bold red**.

1 **MVHLTPEEK**S AVTALWGKVN VDEVGGEALG RLLVVYPWTQ RFFESFGDLS
51 **TPDAVMGNPK** VKAHGKKVLG AFSDGLAHLN NLKGTFFATLS ELHCDKLHVD
101 **PENFRLLGNV** LVCVLAHHFG KEFTPPVQAA YQKVVAGVAN ALAHKYH

Start	End	Observed masses	Theoretical masses	Missed cleavage	Peptide Sequence
2	-9	952.552	951.5447	0	M.VHLTPEEK .S
10	-18	932.56	931.5527	0	K.SAVTALWGK .V
10	-31	2228.35	2227.3427	1	K.SAVTALWGKVN VDEVGGEALGR.L
19	-31	1314.824	1313.8167	0	K.VNVDEVGGEALGR .L
32	-41	1274.861	1273.8537	0	R.LLVVYPWTQR .F
42	-60	2059.168	2058.1607	0	R.FFESFGDLSTPDAVMGNPK .V
68	-83	1670.078	1669.0707	0	K.VLGA FS DGLAHLN LK.G
68	-96	3129.903	3128.8957	1	K.VLGA FS DGLAHLN LKGTFFATLS ELHCDKL
84	-96	1478.878	1477.8707	0	K.GTFFATLS ELHCDK.L
84	-105	2586.446	2585.4387	1	K.GTFFATLS ELHCDKLHVDPENFR.L
97	-105	1126.664	1125.6567	0	K.LHVD PENFR.L
106	-121	1777.186	1776.1787	0	R.LLGNV LVCVLAHHFGK.E
122	-133	1378.866	1377.8587	0	K.EFTPPVQAAYQK .V
134	-145	1149.7	1148.6927	0	K.VVAGVAN ALAHK.Y
134	-147	1449.973	1448.9657	1	K.VVAGVAN ALAHKYH

2) Hemoglobin subunit alpha OS=Homo sapiens

Protein sequence coverage: 71%

Matched peptides shown in **bold red**.

1 MVLSPADKTN VK**AAWGK**VGA HAGEYGAEAL ERMFLSFPTT KTYFP**PHDLS**
 51 **HGSAQVK**GHG **KKVADAL**TNA VAHVDDMPNA LSALS**DLHAH** KLRVDPV**NFK**
 101 LLSHCLLVTL AAHLPAEFTP AVHASL**DKFL** ASVSTVL**TSK** YR

Start	End	Observed masses	Theoretical masses	Missed cleavage	Peptide Sequence
13	32	2043.194	2042.1867	1	K.AAWGKVG AHAGEYGAEAL ER.M
18	32	1529.928	1528.9207	0	K.VGAHAGEYGAEALER.M
33	41	1071.642	1070.6347	0	R.MFLSFPTTK.T
42	57	1834.087	1833.0797	0	K.TYFP PHDLSHGSAQVK .G
42	61	2213.282	2212.2747	1	K.TYFP PHDLSHGSAQVKGHGK .K
63	91	2996.757	2995.7497	0	K.VADALTN AVAHVDDMPNALSALS DLHAHK.L
63	93	3265.993	3264.9857	1	K.VADALTN AVAHVDDMPNALSALS DLHAHKLR.V
92	100	1087.71	1086.7027	1	K.LRVDPV NFK .L
94	100	818.421	817.4137	0	R.VDPV NFK .L
129	142	1572.052	1571.0447	1	K.FLASVSTVL TSKYR

3) Hemoglobin subunit delta OS=Homo sapiens

Protein sequence coverage: 47%

Matched peptides shown in **bold red**.

1 **MVHLTPEEK**T AVNALWGK**VN** **VDAVGGEALG** **RLLVVYPWTQ** RFFESFGDLS
 51 SPDAVMGNPK VKAHG**KKVLG** **AFSDGLAHL**D NLKGTFSQLS ELHCDKL**HVD**
 101 **PENFRLLGNV** LVCV**LARNFG** KEFT**PQM**QAA YQ**KVVAGVAN** **ALAHKYH**

Start	End	Observed masses	Theoretical masses	Missed cleavage	Peptide Sequence
2	9	952.552	951.5447	0	M.VHL TPEEK .T
19	31	1256.77	1255.7627	0	K.VN VDAVGGEALGR .L
32	41	1274.861	1273.8537	0	R.LLV VYPWTQR .F
68	83	1670.078	1669.0707	0	K.VL GAFSDGLAHL DNLK.G
97	105	1126.664	1125.6567	0	K.LH VDPENFR .L
134	145	1149.7	1148.6927	0	K.V VAGVANALAHK .Y
134	147	1449.973	1448.9657	1	K.V VAGVANALAHKYH

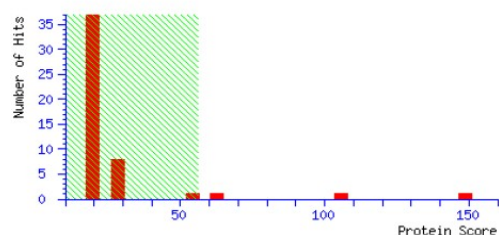
Body fluid: Semen

MASCOT SCIENCE Mascot Search Results

User : Satish
 Email : satish@gmail.com
 Search title :
 Database : SwissProt 2015_08 (549008 sequences; 195692017 residues)
 Taxonomy : Homo sapiens (human) (20204 sequences)
 Timestamp : 9 Aug 2015 at 06:26:44 GMT
 Top Score : 149 for Mixture 1, SEMG2_HUMAN + SEMG1_HUMAN + KLK3_HUMAN

Mascot Score Histogram

Protein score is $-10 \cdot \log(P)$, where P is the probability that the observed match is a random event. Protein scores greater than 56 are significant ($p < 0.05$).



Protein: Semenogelin-2

Start	End	Observed masses	Theoretical masses	Missed cleavage	Peptide Sequence
45	52	964.456	963.4487	0	K.GQHYFGQK.D
61	80	2428.101	2427.0937	0	K.GSFSIQHTYHVDINDHDWTR.K
121	131	1355.723	1354.7157	0	K.GHFHMIVIIHKK.G
121	153	3525.613	3524.6057	1	K.GHFHMIVIIHKKGGQAHHGTQNPSQDQGNPSGK.G
132	153	2189.209	2188.2017	0	K.GGQAHHGTQNPSQDQGNPSGK.G
228	233	716.162	715.1547	0	R.EEHSSK.L
234	251	2063.58	2062.5727	1	K.LQTSLHPAHQDRLQHGPK.D
326	342	1972.928	1971.9207	0	K.SQNQVTIHSQDQEHGK.E
326	345	2344.024	2343.0167	1	K.SQNQVTIHSQDQEHGKKNK.I
357	363	857.289	856.2817	0	R.HLNCGEK.G
364	371	816.368	815.3607	1	K.GIQKGVSK.G
392	402	1257.64	1256.6327	0	R.IPSQAQEYGHK.E
466	477	1460.705	1459.6977	1	K.MSYQSSSTEERR.L
477	483	807.499	806.4917	1	R.RLNYGGK.S
484	500	1911.96	1910.9527	1	K.STQKDVSSISFQIEK.L
527	543	1857.946	1856.9387	1	K.SGQSADSKQDLLSHEQK.G
535	543	1097.52	1096.5127	0	K.QDLLSHEQK.G

Protein: Semenogelin-1

Start	End	Observed masses	Theoretical masses	Missed cleavage	Peptide Sequence
32	52	2387.103	2386.0957	1	R.LPSEFSQFPHGQKQHYSGQK.G
99	114	1801.905	1800.8977	1	R.HLGGSQLLNKQEGR.D

119	125	868.473	867.4657	1	K.SKGFHHR.V
126	131	732.673	731.6657	0	R.VVIHHK.G
126	134	974.509	973.5017	1	R.VVIHHKGGK.A
154	165	1370.682	1369.6747	0	K.GISSQYSNTEER.L
154	173	2291.093	2290.0857	1	K.GISSQYSNTEERLWVHGLSK.E
228	233	716.162	715.1547	0	R.EEHSSK.V
326	342	1996.369	1995.3617	1	K.SQKQITIPSQEQEHSQK.A
329	342	1652.82	1651.8127	0	K.QITIPSQEQEHSQK.A
386	394	982.63	981.6227	0	K.SQIQAPNPK.Q
448	462	1789.91	1788.9027	1	R.HLAQHLNNDRNPLFT

Protein: Prostate-specific antigen (KLK3_Human)

Start	End	Observed masses	Theoretical masses	Missed cleavage	Peptide Sequence
34	45	1407.801	1406.7937	0	K.HSQPWQVLVASR.G
46	68	2557.119	2556.1117	1	R.GRAVCGGVLVHPQWVLTAHCIR.N
48	68	2344.024	2343.0167	0	R.AVCGGVLVHPQWVLTAHCIR.N
126	137	1272.59	1271.5827	0	R.LSEPAELTDAVK.V
170	191	2587.981	2586.9737	1	K.KLQCVDLHVISNDVCAQVHPQK.V
246	250	673.116	672.1087	0	K.VVHYR.K
246	251	801.46	800.4527	1	K.VVHYRK.W
252	261	1156.584	1155.5767	1	K.WIKDTIVANP

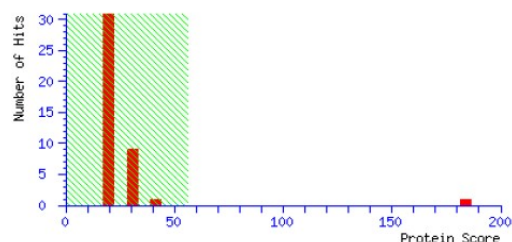
Body fluid: Saliva

MATRIX SCIENCE Mascot Search Results

User : Satish
 Email : satish@gmail.com
 Search title :
 Database : SwissProt 2015_08 (549008 sequences; 195692017 residues)
 Taxonomy : Homo sapiens (human) (20204 sequences)
 Timestamp : 31 Jul 2015 at 09:23:14 GMT
 Top Score : 184 for **AMY1_HUMAN**, Alpha-amylase 1 OS=Homo sapiens GN=AMY1A PE=1 SV=2

Mascot Score Histogram

Protein score is $-10 \cdot \log(P)$, where P is the probability that the observed match is a random event.
 Protein scores greater than 56 are significant ($p < 0.05$).



Protein: Alpha-amylase 1 OS=Homo sapiens

Start	End	Observed masses	Theoretical masses	Missed cleavages	Peptide Sequence
26	35	1287.712	1286.7047	0	R.TSIVHLFEWR.W
36	45	1290.663	1289.6557	0	R.WVDIALECER.Y
51	76	2990.27	2989.2627	0	K.GFGGVQVSPNENVAIHNPFRPWWER.Y
88	95	953.362	952.3547	0	R.SGNEDEFN.N
88	100	1554.696	1553.6887	1	R.SGNEDEFNRMVTR.C
140	155	1814.877	1813.8697	0	R.DFPAVPYSGWDFNDGK.C
158	173	1739.873	1738.8657	0	K.TGSGDIENYNDATQVR.D
259	267	1002.466	1001.4587	0	K.SSDYFGNGR.V
294	306	1538.717	1537.7097	0	K.NWGEGWGFMPSTR.A
307	318	1427.766	1426.7587	0	R.ALVFVDNHDNR.G
307	334	3024.48	3023.4727	1	R.ALVFVDNHDNRGHGAGGASILTFWDAR.L
319	334	1615.869	1614.8617	0	R.GHGAGGASILTFWDAR.L
338	352	1697.88	1696.8727	0	K.MAVGFMLAHPYGFTR.V
353	358	758.256	757.2487	0	R.VMSSYR.W + Oxidation (M)
353	361	1181.606	1180.5987	1	R.VMSSYRWPR.Y
353	361	1197.672	1196.6647	1	R.VMSSYRWPR.Y + Oxidation (M)
362	383	2465.025	2464.0177	1	R.YFENGKDVNDWVGPPNDNGVTK.E
384	402	2303.019	2302.0117	0	K.EVTINPDTCGNDWVCEHR.W
408	413	780.22	779.2127	0	R.NMVNFR.N
414	436	2585.062	2584.0547	0	R.NVVDGQPFTNWDNNGSNQVAFGR.G
482	489	896.367	895.3597	0	K.IYVSDDGK.A
490	510	2271.104	2270.0967	0	K.AHFSISNSAEDPFIAIHAESK.L

Protein: Alpha-amylase 2B OS=Homo sapiens

Start	End	Observed masses	Theoretical masses	Missed cleavages	Peptide Sequence
26	35	1287.712	1286.7047	0	R.TSIVHLFEWR.W
36	45	1290.663	1289.6557	0	R.WVDIALECER.Y
51	76	2990.27	2989.2627	0	K.GFGGVQVSPNENVAIHNPFRPWWER.Y
88	95	953.362	952.3547	0	R.SGNEDEFN.N
88	100	1554.696	1553.6887	1	R.SGNEDEFNRMVTR.C
140	155	1814.877	1813.8697	0	R.DFPAVPYSGWDFNDGK.C
158	173	1739.873	1738.8657	0	K.TGSGDIENYNDATQVR.D
259	267	1002.466	1001.4587	0	K.SSDYFGNGR.V
294	306	1538.717	1537.7097	0	K.NWGEGWGFMPSTR.A
307	318	1427.766	1426.7587	0	R.ALVFVDNHDNR.G
307	334	3024.48	3023.4727	1	R.ALVFVDNHDNRGHGAGGASILTFWDAR.L
319	334	1615.869	1614.8617	0	R.GHGAGGASILTFWDAR.L
338	352	1697.88	1696.8727	0	K.MAVGFMLAHPYGFTR.V
353	358	758.256	757.2487	0	R.VMSSYR.W + Oxidation (M)

353	361	1181.606	1180.5987	1	R.VMSSYRWPR.Q
353	361	1197.672	1196.6647	1	R.VMSSYRWPR.Q + Oxidation (M)
384	402	2303.019	2302.0117	0	K.EVTINPDTTTCGNDWVCEHR.W
408	413	780.22	779.2127	0	R.NMVNFR.N
414	436	2585.062	2584.0547	0	R.NVVDGQPFTNWDNGSNQVAFGR.G
482	489	896.367	895.3597	0	K.IYVSDDGK.A
490	510	2271.104	2270.0967	0	K.AHFSISNSAEDPFIAIHAESK.L

Protein: Pancreatic alpha-amylase OS=Homo sapiens

Start	End	Observed masses	Theoretical masses	Missed cleavages	Peptide Sequence
26	35	1287.712	1286.7047	0	R.TSIVHLFEWR.W
36	45	1290.663	1289.6557	0	R.WVDIALECER.Y
88	95	953.362	952.3547	0	R.SGNEDEFR.N
88	100	1554.696	1553.6887	1	R.SGNEDEFRNMVTR.C
140	155	1814.877	1813.8697	0	R.DFPAVPYSGWDFNDGK.C
158	173	1739.873	1738.8657	0	K.TGSGDIENYNDATQVR.D
259	267	1002.466	1001.4587	0	K.SSDYFGNGR.V
307	318	1427.766	1426.7587	0	R.ALVFVDNHDNQR.G
307	334	3024.48	3023.4727	1	R.ALVFVDNHDNQRGHGAGGASILTFWDAR.L
319	334	1615.869	1614.8617	0	R.GHGAGGASILTFWDAR.L
338	352	1697.88	1696.8727	0	K.MAVGFMLAHPYGFTR.V
353	358	758.256	757.2487	0	R.VMSSYR.W + Oxidation (M)
353	361	1181.606	1180.5987	1	R.VMSSYRWPR.Q
353	361	1197.672	1196.6647	1	R.VMSSYRWPR.Q + Oxidation (M)
384	402	2303.019	2302.0117	0	K.EVTINPDTTTCGNDWVCEHR.W
414	436	2585.062	2584.0547	0	R.NVVDGQPFTNWDNGSNQVAFGR.G
482	489	896.367	895.3597	0	K.IYVSDDGK.A
490	510	2271.104	2270.0967	0	K.AHFSISNSAEDPFIAIHAESK.L

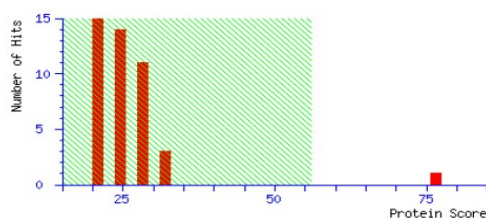
Body fluid: Urine

MATRIX SCIENCE Mascot Search Results

User : Satish
Email : satish@gmail.com
Search title :
Database : SwissProt 2015_08 (549008 sequences; 195692017 residues)
Taxonomy : Homo sapiens (human) (20204 sequences)
Timestamp : 3 Aug 2015 at 04:55:15 GMT
Top Score : 76 for UROM_HUMAN, Uromodulin OS=Homo sapiens GN=UMOD PE=1 SV=1

Mascot Score Histogram

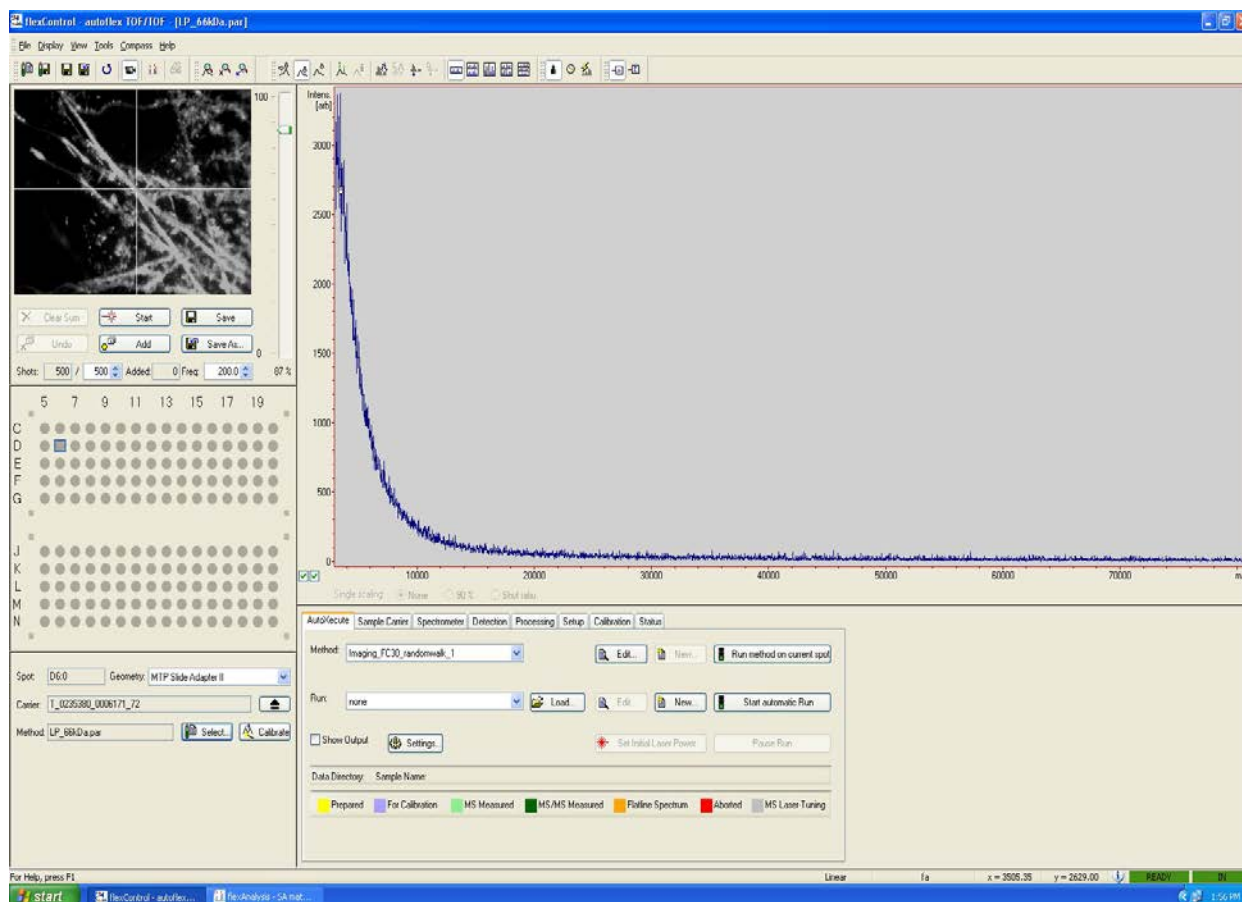
Protein score is $-10 \cdot \log(P)$, where P is the probability that the observed match is a random event.
Protein scores greater than 56 are significant ($p < 0.05$).



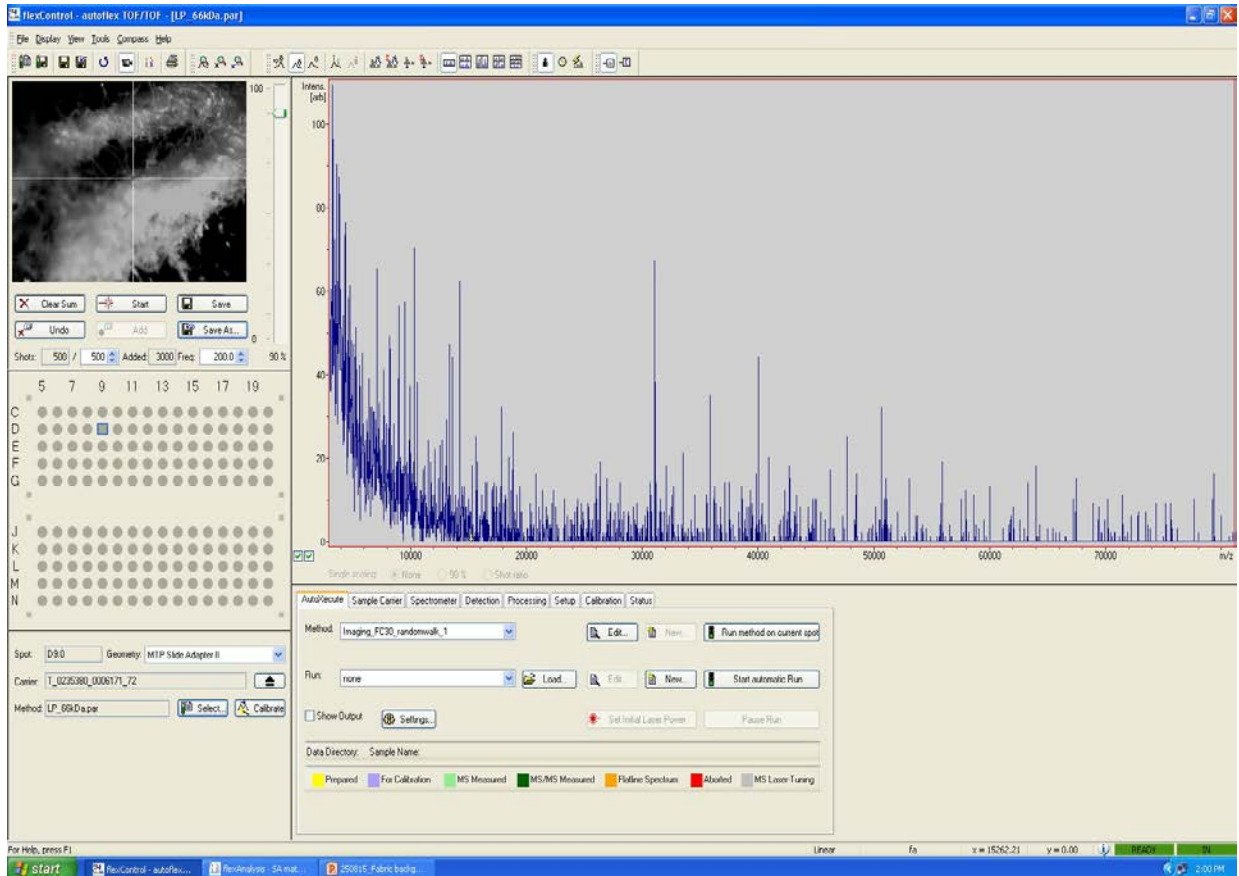
Start	End	Observed masses	Theoretical masses	Missed cleavages	Peptide Sequence
179	185	982.364	981.3567	0	R.TLDEYWR.S
186	200	1736.303	1735.2957	0	R.STEYGEGYACDLDL.R
205	212	791.243	790.2357	0	R.FVGQGGAR.M
213	222	1175.346	1174.3387	0	R.MAETCVPVLR.C
319	332	1683.85	1682.8427	0	K.QDFNITDISLLEHR.L + Gln->pyro-Glu (N-term Q)
319	332	1700.9	1699.8927	0	K.QDFNITDISLLEHR.L
357	365	1117.298	1116.2907	0	K.VFMYLSDSR.C
376	385	1129.374	1128.3667	0	R.DWVSVVTPAR.D
386	395	1075.301	1074.2937	0	R.DGPCGTVLTR.N
437	449	1413.429	1412.4217	0	K.TALQPMVSALNIR.V
450	459	1024.32	1023.3127	0	R.VGGTGMFTVR.M
548	554	914.278	913.2707	0	R.FSVQMFR.F
587	597	1251.409	1250.4017	1	R.FRSGSVIDQSR.V
589	597	948.475	947.4677	0	R.SGSVIDQSR.V

Appendix 1B

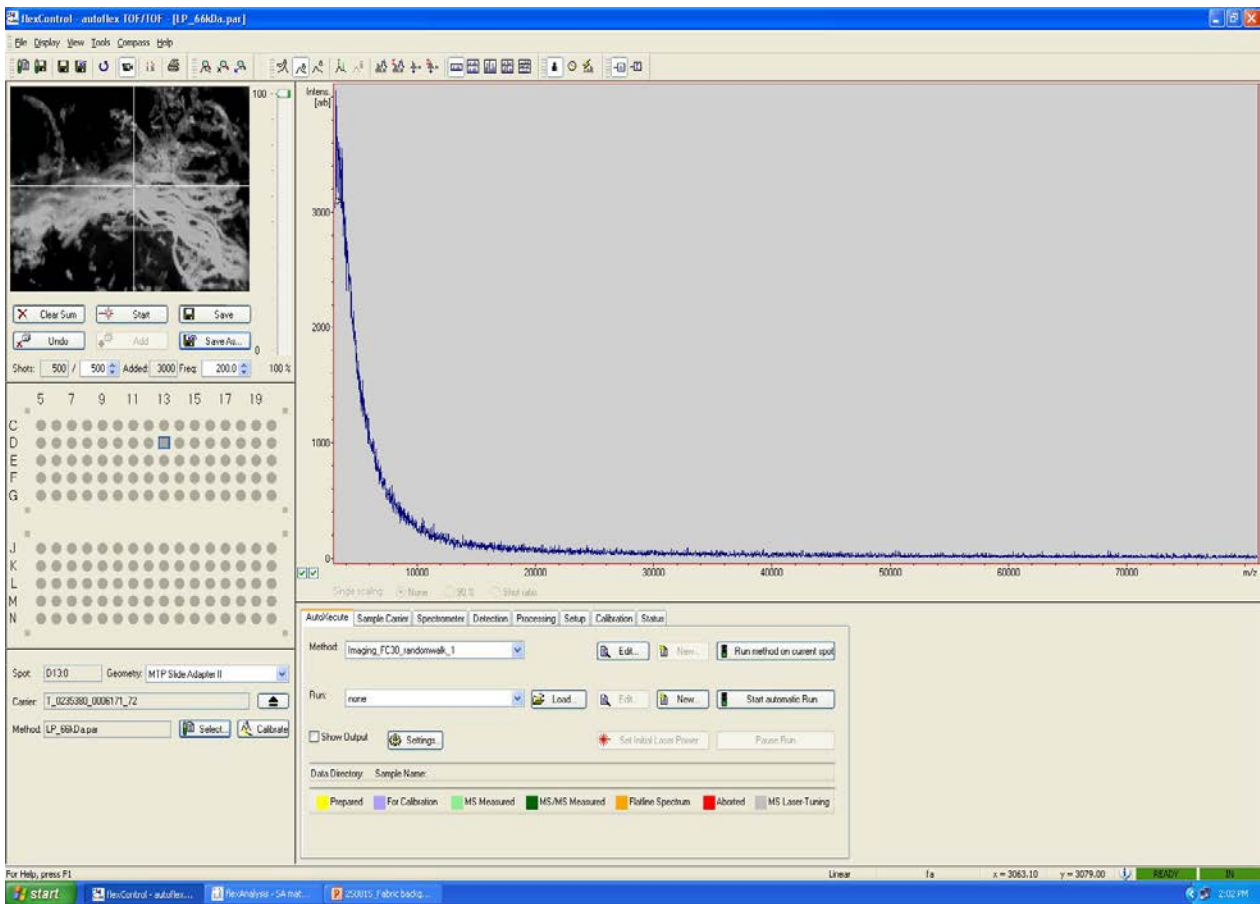
100 % Nylon fabric fibers



100 % Cotton fabric fibers



100 % Cellulose acetate fibers



Appendix-2A

List of proteins detected by nanospray LC-MS/MS. Those associated with vaginal fluid are in **RED** font

N	Unused	Total	%Cov	%Cov(5)	%Cov(95)	Accession	Protein Name	Species	No. of Peptides(>95%)
1	119.18	119.18	35.18	27.72	22.4600002	sp Q09666 AHNK_HUMAN	Neuroblast differentiation-associated protein AHNK OS=Homo sapiens GN=AHNK PE=1 SV=1	HUMAN	66
2	108.28	108.28	69.85	69.1	65.7299995	sp P19013 K2C4_HUMAN	Keratin, type II cytoskeletal 4 OS=Homo sapiens GN=KRT4 PE=1 SV=4	HUMAN	99
3	105.85	105.85	74.45	73.8	67.0300007	sp P13646 K1C13_HUMAN	Keratin, type II cytoskeletal 13 OS=Homo sapiens GN=KRT13 PE=1 SV=4	HUMAN	105
4	92.75	103.36	69.25	64.6	61.3399982	sp P04264 K2C1_HUMAN	Keratin, type II cytoskeletal 1 OS=Homo sapiens GN=KRT1 PE=1 SV=6	HUMAN	91
4	0	103.36	69.25	64.6	61.3399982	cont 000135	cra hCP1609934.2 keratin 1 (epidermolytic hyperkeratosis) [Homo sapiens (contaminant)]	Homo sapien	91
4	0	103.36	69.25	64.6	61.3399982	cont 000134	rf NP_006112.2 keratin 1 [Homo sapiens (contaminant)]	Homo sapien	91
5	72.68	72.68	70.95	62.76	62.7600014	sp P35527 K1C9_HUMAN	Keratin, type I cytoskeletal 9 OS=Homo sapiens GN=KRT9 PE=1 SV=3	HUMAN	72
6	67.79	81.04	64.65	61.28	57.3700011	cont 000126	spt P48666 Keratin, type II cytoskeletal 6C (Cytokeratin 6C) (CK 6C) (K6c keratin) [Homo sa	Homo sapien	72
7	64.07	64.13	29.42	21.04	18.9300001	tr K7EKI8 K7EKI8_HUMAN	Periplakin OS=Homo sapiens GN=PPL PE=1 SV=1	HUMAN	35
7	0	64.13	28.7	21.01	18.9099997	sp O60437 PEPL_HUMAN	Periplakin OS=Homo sapiens GN=PPL PE=1 SV=4	HUMAN	35
8	60.98	60.98	21.04	13.58	11.3499999	sp P15924 DESP_HUMAN	Desmoplakin OS=Homo sapiens GN=DSP PE=1 SV=3	HUMAN	34
9	59.82	74.4	73.24	60.42	58.3299994	cont 000136	cra hCP1812051 keratin 10 (epidermolytic hyperkeratosis; keratosis palmaris et plantaris) [Homo sapien	Homo sapien	64
9	0	74.4	76.54	64.55	62.3300016	cont 000129	trm Q8N175 Keratin 10 [Homo sapiens (contaminant)]	Homo sapien	64
9	0	74.4	71.58	64.55	62.3300016	sp P13645 K1C10_HUMAN	Keratin, type I cytoskeletal 10 OS=Homo sapiens GN=KRT10 PE=1 SV=6	HUMAN	64
9	0	74.34	73.86	62.06	61.3799989	cont 000133	pir KRHU0 keratin 10, type I, cytoskeletal - human [Homo sapiens (contaminant)]	Homo sapien	64
9	0	74.34	73.86	62.06	61.3799989	cont 000122	spt P13645 Keratin, type I cytoskeletal 10 (Cytokeratin 10) (K10) (CK 10) [Homo sapiens (c	Homo sapien	64
10	53.54	53.54	84.85	79.6	79.6000004	sp Q9UBG3 CRNN_HUMAN	Corneulin OS=Homo sapiens GN=CRNN PE=1 SV=1	HUMAN	64
11	50.1	66.78	68.64	65.47	62.5	sp P02533 K1C14_HUMAN	Keratin, type I cytoskeletal 14 OS=Homo sapiens GN=KRT14 PE=1 SV=4	HUMAN	59
12	44.56	44.56	67.34	61.56	59.5399976	sp P04083 ANXA1_HUMAN	Annexin A1 OS=Homo sapiens GN=ANXA1 PE=1 SV=2	HUMAN	37
13	43.81	43.81	61.71	59.49	58.1200004	sp P07476 INVO_HUMAN	Involucrin OS=Homo sapiens GN=IVL PE=1 SV=2	HUMAN	30
14	32.84	32.84	85.96	80.7	80.6999981	sp P06702 S10A9_HUMAN	Protein S100-A9 OS=Homo sapiens GN=S100A9 PE=1 SV=1	HUMAN	33
15	28.58	28.58	55.75	51.92	46.6100007	sp P07355 ANXA2_HUMAN	Annexin A2 OS=Homo sapiens GN=ANXA2 PE=1 SV=2	HUMAN	19
15	0	28.58	52.94	49.3	44.2600012	sp P07355-2 ANXA2_HUMAN	Isoform 2 of Annexin A2 OS=Homo sapiens GN=ANXA2	HUMAN	19
16	28.53	29.16	22.19	11.24	9.0999982	tr K7EKI0 K7EKI0_HUMAN	Envoplakin OS=Homo sapiens GN=EVPL PE=1 SV=1	HUMAN	16
16	0	29.16	22.43	11.36	9.19800028	sp Q29817 EVPL_HUMAN	Envoplakin OS=Homo sapiens GN=EVPL PE=1 SV=3	HUMAN	16
17	27.9	62.3	65.96	64.69	61.7299974	sp P08779 K1C16_HUMAN	Keratin, type I cytoskeletal 16 OS=Homo sapiens GN=KRT16 PE=1 SV=4	HUMAN	56
18	26.33	26.33	50.4	48.53	45.3299999	sp P63261 ACTG_HUMAN	Actin, cytoplasmic 2 OS=Homo sapiens GN=ACTG1 PE=1 SV=1	HUMAN	21
18	0	26.33	50.4	48.53	45.3299999	sp P60709 ACTB_HUMAN	Actin, cytoplasmic 1 OS=Homo sapiens GN=ACTB PE=1 SV=1	HUMAN	21
19	24.6	47.79	46.17	42.57	35.9899998	sp P35908 K2E2_HUMAN	Keratin, type II cytoskeletal 2 epidermal OS=Homo sapiens GN=KRT2 PE=1 SV=2	HUMAN	30
20	23.4	66.47	62.33	52.39	47.9699999	sp P13647 K2C5_HUMAN	Keratin, type II cytoskeletal 5 OS=Homo sapiens GN=KRT5 PE=1 SV=3	HUMAN	59
21	22.13	48.76	50.76	45.18	39.5900011	tr F5GWP8 F5GWP8_HUMAN	Junction plakoglobin OS=Homo sapiens GN=JUP PE=1 SV=1	HUMAN	34
22	21.76	21.76	22.82	19.62	18.6000004	sp O95171 SCEL_HUMAN	Scellin OS=Homo sapiens GN=SCEL PE=1 SV=2	HUMAN	12
22	0	19.94	22.16	18.86	17.8100005	sp O95171-2 SCEL_HUMAN	Isoform 2 of Scellin OS=Homo sapiens GN=SCEL	HUMAN	11
22	0	19.71	23.22	19.81	18.7299997	sp O95171-3 SCEL_HUMAN	Isoform 3 of Scellin OS=Homo sapiens GN=SCEL	HUMAN	11
23	21.33	21.33	45.13	41.54	41.0299987	sp P29508 SPB3_HUMAN	Serpin B3 OS=Homo sapiens GN=SERPINB3 PE=1 SV=2	HUMAN	16
24	19.52	19.52	66.34	60	60.0000024	sp P04792 HSPB1_HUMAN	Heat shock protein beta-1 OS=Homo sapiens GN=HSPB1 PE=1 SV=2	HUMAN	17
25	18.58	18.58	42.69	36.72	33.7300003	sp P04406 G3P_HUMAN	Glyceraldehyde-3-phosphate dehydrogenase OS=Homo sapiens GN=GAPDH PE=1 SV=3	HUMAN	12
26	18.25	18.25	29.56	25.45	16.0899997	sp P02768 ALBU_HUMAN	Serum albumin OS=Homo sapiens GN=ALB PE=1 SV=2	HUMAN	12
27	18.08	29.28	33.85	29.81	26.3500005	sp Q8N1N4 K2C78_HUMAN	Keratin, type II cytoskeletal 78 OS=Homo sapiens GN=KRT78 PE=2 SV=2	HUMAN	19
27	0	25.18	34.88	30.4899991	sp Q8N1N4-2 K2C78_HUMAN	Isoform 2 of Keratin, type II cytoskeletal 78 OS=Homo sapiens GN=KRT78	HUMAN	19	
28	18.07	18.07	20.75	16.38	16.3800001	sp P08107 HSP71_HUMAN	Heat shock 70 kDa protein 1A/1B OS=Homo sapiens GN=HSPA1A PE=1 SV=5	HUMAN	10
28	0	18.07	22.7	17.92	17.9199994	sp P08107-2 HSP71_HUMAN	Isoform 2 of Heat shock 70 kDa protein 1A/1B OS=Homo sapiens GN=HSPA1A	HUMAN	10
29	17.62	17.62	73.29	53.42	53.4200013	tr F5GZ12 F5GZ12_HUMAN	Small proline-rich protein 3 OS=Homo sapiens GN=SPRR3 PE=4 SV=1	HUMAN	24
29	0	17.62	74.56	50.89	50.8899987	sp Q9UBC9 SPRR3_HUMAN	Small proline-rich protein 3 OS=Homo sapiens GN=SPRR3 PE=1 SV=2	HUMAN	24
29	0	17.62	68.99	43.67	43.6699986	tr B1AN48 B1AN48_HUMAN	Small proline-rich protein 3 (Fragment) OS=Homo sapiens GN=SPRR3 PE=4 SV=2	HUMAN	20
30	15.79	15.79	28.92	12.05	12.0499998	sp P02545 LMNA_HUMAN	Prelamin-A/C OS=Homo sapiens GN=LMNA PE=1 SV=1	HUMAN	8
30	0	15.79	31.27	13.03	sp P02545-6 LMNA_HUMAN	Isoform 6 of Prelamin-A/C OS=Homo sapiens GN=LMNA	HUMAN	8	
30	0	15.79	33.57	13.99	13.9899999	sp P02545-2 LMNA_HUMAN	Isoform C of Prelamin-A/C OS=Homo sapiens GN=LMNA	HUMAN	8
30	0	15.79	34.83	16.29	16.2900001	tr Q5TCI8 Q5TCI8_HUMAN	Prelamin-A/C OS=Homo sapiens GN=LMNA PE=1 SV=1	HUMAN	8
30	0	15.79	30.27	14.16	14.1599998	sp P02545-5 LMNA_HUMAN	Isoform 5 of Prelamin-A/C OS=Homo sapiens GN=LMNA	HUMAN	8
30	0	15.79	29.79	13.94	13.9400005	sp P02545-4 LMNA_HUMAN	Isoform 4 of Prelamin-A/C OS=Homo sapiens GN=LMNA	HUMAN	8
30	0	13.77	28.08	10.41	10.4099996	sp P02545-3 LMNA_HUMAN	Isoform A/Delta10 of Prelamin-A/C OS=Homo sapiens GN=LMNA	HUMAN	7
31	14.05	14.05	42.71	42.17	34.1699988	sp Q06830 PRDX1_HUMAN	Peroxiredoxin-1 OS=Homo sapiens GN=PRDX1 PE=1 SV=1	HUMAN	7
32	13.43	13.43	81.63	81.63	73.4700024	sp P04080 CYTB_HUMAN	Cystatin-B OS=Homo sapiens GN=CSTB PE=1 SV=2	HUMAN	12
33	12.84	12.84	30.51	26.27	26.2699991	sp Q6UWP8 SBSN_HUMAN	Suprabasin OS=Homo sapiens GN=SBSN PE=2 SV=2	HUMAN	10
34	12.83	12.84	29.44	25.39	25.8100003	sp P31947 14335_HUMAN	14-3-3 protein sigma OS=Homo sapiens GN=SFN PE=1 SV=1	HUMAN	7
34	0	12.84	33.8	29.63	29.6299994	sp P31947-2 14335_HUMAN	Isoform 2 of 14-3-3 protein sigma OS=Homo sapiens GN=SFN	HUMAN	7
35	12.63	12.63	14.6	10.43	8.67199972	sp O43707 ACTN4_HUMAN	Alpha-actinin-4 OS=Homo sapiens GN=ACTN4 PE=1 SV=2	HUMAN	7
35	0	12.12	17.2	12.86	11.4200003	sp O43707-2 ACTN4_HUMAN	Isoform ACTN4ISO of Alpha-actinin-4 OS=Homo sapiens GN=ACTN4	HUMAN	7
36	12.18	12.18	76.34	76.34	68.8199997	sp P05109 S10A8_HUMAN	Protein S100-A8 OS=Homo sapiens GN=S100A8 PE=1 SV=1	HUMAN	11
37	12.13	12.13	22.64	14.96	13.1899998	sp P07237 PDIA1_HUMAN	Protein disulfide-isomerase OS=Homo sapiens GN=P4HB PE=1 SV=3	HUMAN	7
37	0	12.1	22.63	16.38	14.4400001	tr H7B294 H7B294_HUMAN	Protein disulfide-isomerase OS=Homo sapiens GN=P4HB PE=1 SV=2	HUMAN	7
37	0	12.1	23.28	16.85	14.8599997	tr F5H8J2 F5H8J2_HUMAN	Uncharacterized protein OS=Homo sapiens GN=P4HB PE=1 SV=1	HUMAN	7
38	11.89	11.89	32.72	24.42	19.8200002	sp P06733 ENOA_HUMAN	Alpha-enolase OS=Homo sapiens GN=ENO1 PE=1 SV=2	HUMAN	7
39	11.66	11.66	49.59	41.87	36.9899988	tr E7EX29 E7EX29_HUMAN	14-3-3 protein zeta/delta (Fragment) OS=Homo sapiens GN=YWHAZ PE=1 SV=1	HUMAN	8
39	0	11.66	49.8	42.04	37.1399999	sp P63104 14332_HUMAN	14-3-3 protein zeta/delta OS=Homo sapiens GN=YWHAZ PE=1 SV=1	HUMAN	8
40	11.17	11.17	19.79	13.19	13.1899998	sp P30740 ILEU_HUMAN	Leukocyte elastase inhibitor OS=Homo sapiens GN=SERPINB1 PE=1 SV=1	HUMAN	6
40	0	9.1	21.93	17.54	15.4000004	tr B4DNT0 B4DNT0_HUMAN	Leukocyte elastase inhibitor OS=Homo sapiens GN=SERPINB1 PE=1 SV=1	HUMAN	5
41	10.3	10.3	59.06	48.99	48.9999993	sp P27482 CALL3_HUMAN	Calmodulin-like protein 3 OS=Homo sapiens GN=CALML3 PE=1 SV=2	HUMAN	5
42	10.02	10.02	13.42	11.26	11.2599999	sp P04279 SEMG1_HUMAN	Semenogelin-1 OS=Homo sapiens GN=SEMG1 PE=1 SV=2	HUMAN	7
42	0	8.01	11.94	9.453	9.45300013	sp P04279-2 SEMG1_HUMAN	Isoform 2 of Semenogelin-1 OS=Homo sapiens GN=SEMG1	HUMAN	5
43	9.86	9.86	24.18	20.92	20.9199995	tr J3KPS3 J3KPS3_HUMAN	Aldolase A, fructose-bisphosphate, isoform CRA_b OS=Homo sapiens GN=ALDOA PE=1 SV=1	HUMAN	7
43	0	9.86	24.65	21.33	21.3300005	tr H3BQN4 H3BQN4_HUMAN	Fructose-bisphosphate aldolase A OS=Homo sapiens GN=ALDOA PE=1 SV=1	HUMAN	7
43	0	9.86	24.45	21.15	21.1500004	sp P04075 ALDOA_HUMAN	Fructose-bisphosphate aldolase A OS=Homo sapiens GN=ALDOA PE=1 SV=2	HUMAN	7
43	0	9.86	21.29	18.42	18.4200004	sp P04075-2 ALDOA_HUMAN	Isoform 2 of Fructose-bisphosphate aldolase A OS=Homo sapiens GN=ALDOA	HUMAN	7
43	0	9.83	27.7	23.38	23.3799994	tr H3BPS8 H3BPS8_HUMAN	Fructose-bisphosphate aldolase A (Fragment) OS=Homo sapiens GN=ALDOA PE=1 SV=1	HUMAN	6
44	9.78	9.78	35.43	35.43	33.1800014	cont 000143	pdb 1FNI_A A Chain A, Crystal Structure Of Porcine Beta Trypsin With 0.01% Polydocanol [Sus scrofa (cc	11
44	0	9.78	34.2	34.2	32.0300013	cont 000141	spt P00761 Trypsin precursor [E.C.3.4.21.4] [Sus scrofa (contaminant)]	Sus scrofa (cc	11
44	0	9.78	35.43	35.43	33.1800014	cont 000040	gi 2914482 pdb 1TFX A Chain A, Complex Of The Second Kunitz Domain Of Tissue Factor P	Sus scrofa (cc	11
44	0	9.78	63.2	63.2	59.2000008	cont 000032	gi 1942351 pdb 1AKS A Chain A, Crystal Structure Of The First Active Autolysate Form Of T	Sus scrofa (cc	11
44	0	9.78	35.43	35.43	33.1800014	cont 000023	gi 494360 pdb 1MCT A Chain A, Trypsin [E.C.3.4.21.4] Complexed With Inhibitor From Bitt	Sus scrofa (Cr	11
44	0	9.78	30.24	30.24	30.2400017	cont 000142	pdb 1EPT_B B Chain B, Porcine E-Trypsin [E.C.3.4.21.4] [Sus scrofa (contaminant)]	Sus scrofa (cc	11
44	0	8.27	30.94	30.94	28.7	cont 000144	pdb 1AN1_E E Chain E, Leech-Derived Trypsin Inhibitor TRYPSIN COMPLEX [Sus scrofa (co	Sus scrofa (cc	9
45	9.57	9.57	33.33	33.33	33.3299994	sp Q9BTM1 H2A1_HUMAN	Histone H2A.J OS=Homo sapiens GN=H2AFJ PE=1 SV=1	HUMAN	5
45	0	9.57	28.48	28.48	28.4799993	sp Q9BTM1-2 H2A1_HUMAN	Isoform 2 of Histone H2A.J OS=Homo sapiens GN=H2AFJ	HUMAN	5
45	0	9.57	33.59	33.59	33.5900009	sp Q99878 H2A11_HUMAN	Histone H2A type 1-J OS=Homo sapiens GN=HIST1H2AJ PE=1 SV=3	HUMAN	5
45	0	9.57	33.59	33.59	33.5900009	sp Q96K65 H2A1H_HUMAN	Histone H2A type 1-H OS=Homo sapiens GN=HIST1H2AH PE=1 SV=3	HUMAN	5
45	0	9.57	33.08	33.08</					

45	0	9.57	33.08	33.08	33.0799997	sp P04908 H2A18_HUMAN	Histone H2A type 1-B/E OS=Homo sapiens GN=HIST1H2AB PE=1 SV=2	HUMAN	5
45	0	7.53	36.96	36.96	36.9599998	tr HOYFX9 HOYFX9_HUMAN	Histone H2A (Fragment) OS=Homo sapiens GN=H2AFJ PE=3 SV=1	HUMAN	4
46	8.91	8.91	48.54	48.54	38.8300002	sp P62805 H4_HUMAN	Histone H4 OS=Homo sapiens GN=HIST1H4A PE=1 SV=2	HUMAN	6
47	8.8	8.8	8.803	4.333	4.33299989	sp A8K2U0 A2ML1_HUMAN	Alpha-2-macroglobulin-like protein 1 OS=Homo sapiens GN=A2ML1 PE=1 SV=3	HUMAN	6
47	0	8.03	8.367	4.084	4.08399999	tr HOYGG5 HOYGG5_HUMAN	Alpha-2-macroglobulin-like protein 1 (Fragment) OS=Homo sapiens GN=A2ML1 PE=4 SV=1	HUMAN	4
47	0	8.03	8.723	4.258	4.25800011	tr F5H222 F5H222_HUMAN	Alpha-2-macroglobulin-like protein 1 OS=Homo sapiens GN=A2ML1 PE=4 SV=1	HUMAN	4
48	8.78	8.78	19.59	13.75	10.17	sp P14618 KPYM_HUMAN	Pyruvate kinase PKM OS=Homo sapiens GN=PKM PE=1 SV=4	HUMAN	4
48	0	8.78	19.59	13.75	10.17	sp P14618-2 KPYM_HUMAN	Isoform M1 of Pyruvate kinase PKM OS=Homo sapiens GN=PKM	HUMAN	4
48	0	6.72	18.02	12.02	8.3329998	sp P14618-3 KPYM_HUMAN	Isoform 3 of Pyruvate kinase PKM OS=Homo sapiens GN=PKM	HUMAN	3
48	0	6.71	16.7	12.16	8.24699998	tr H3BTNS H3BTNS_HUMAN	Pyruvate kinase (Fragment) OS=Homo sapiens GN=PKM PE=1 SV=1	HUMAN	3
49	8.18	8.18	47.62	34.29	30.0000012	sp P09211 GSTP1_HUMAN	Glutathione S-transferase P OS=Homo sapiens GN=GSTP1 PE=1 SV=2	HUMAN	5
49	0	8	45.98	29.89	29.8900008	tr A8MX94 A8MX94_HUMAN	Glutathione S-transferase P OS=Homo sapiens GN=GSTP1 PE=1 SV=1	HUMAN	4
50	8.14	8.14	14.07	8.47	6.0109999	sp P07900 HS90A_HUMAN	Heat shock protein HSP 90-alpha OS=Homo sapiens GN=HSP90AA1 PE=1 SV=5	HUMAN	4
50	0	8.14	12.06	7.26	5.15200011	sp P07900-2 HS90A_HUMAN	Isoform 2 of Heat shock protein HSP 90-alpha OS=Homo sapiens GN=HSP90AA1	HUMAN	4
51	8.09	8.09	15.06	14.46	14.4600004	sp P00338 LDHA_HUMAN	L-lactate dehydrogenase A chain OS=Homo sapiens GN=LDHA PE=1 SV=2	HUMAN	5
51	0	8.09	13.85	13.3	13.3000001	sp P00338-3 LDHA_HUMAN	Isoform 3 of L-lactate dehydrogenase A chain OS=Homo sapiens GN=LDHA	HUMAN	5
51	0	6.07	16.06	15.33	15.3300002	sp P00338-4 LDHA_HUMAN	Isoform 4 of L-lactate dehydrogenase A chain OS=Homo sapiens GN=LDHA	HUMAN	4
52	8.06	8.06	24.82	15.18	15.1800007	sp Q16610-2 ECM1_HUMAN	Isoform 2 of Extracellular matrix protein 1 OS=Homo sapiens GN=ECM1	HUMAN	6
52	0	8.03	17.41	11.67	11.6700001	sp Q16610 ECM1_HUMAN	Extracellular matrix protein 1 OS=Homo sapiens GN=ECM1 PE=1 SV=2	HUMAN	6
52	0	8.03	16.58	11.11	11.1100003	sp Q16610-4 ECM1_HUMAN	Isoform 4 of Extracellular matrix protein 1 OS=Homo sapiens GN=ECM1	HUMAN	6
53	7.37	7.37	33.33	29.7	29.6999991	tr P62937 PPIA_HUMAN	Peptidyl-prolyl cis-trans isomerase A OS=Homo sapiens GN=PPIA PE=1 SV=2	HUMAN	5
53	0	6.33	35.24	35.24	35.2400005	tr Q567Q0 Q567Q0_HUMAN	Peptidyl-prolyl cis-trans isomerase A OS=Homo sapiens GN=PPIA PE=1 SV=1	HUMAN	4
54	7.3	7.3	24.89	16.45	13.8500005	sp Q5V7E0 EF1A3_HUMAN	Putative elongation factor 1-alpha-like 3 OS=Homo sapiens GN=EEF1A1P5 PE=5 SV=1	HUMAN	9
54	0	7.3	24.89	16.45	13.8500005	sp P68104 EF1A1_HUMAN	Elongation factor 1-alpha 1 OS=Homo sapiens GN=EEF1A1 PE=1 SV=1	HUMAN	9
55	7.21	7.21	47.62	47.62	46.6699988	sp P31949 S10A8_HUMAN	Protein S100-A11 OS=Homo sapiens GN=S100A11 PE=1 SV=2	HUMAN	5
56	7.14	7.14	24.22	24.22	21.2899998	sp Q9UBD6 RHCG_HUMAN	Ammonium transporter Rh type C OS=Homo sapiens GN=RHCG PE=1 SV=1	HUMAN	7
56	0	4.89	23.37	23.37	20.2199996	tr F5HOA6 F5HOA6_HUMAN	Ammonium transporter Rh type C OS=Homo sapiens GN=RHCG PE=4 SV=1	HUMAN	6
57	6.79	6.79	60.2	41.84	41.8399999	sp P01040 CYTA_HUMAN	Cystatin-A OS=Homo sapiens GN=CSTA PE=1 SV=1	HUMAN	5
58	6.71	13.06	33.17	15.95	14.0400007	tr E9PKE3 E9PKE3_HUMAN	Heat shock cognate 71 kDa protein OS=Homo sapiens GN=HSPA8 PE=1 SV=1	HUMAN	9
58	0	13.06	32.2	15.48	13.11442	HSP7C_HUMAN	Heat shock cognate 71 kDa protein OS=Homo sapiens GN=HSPA8 PE=1 SV=1	HUMAN	9
58	0	13.05	29.61	18.05	15.6200007	sp P11142-2 HSP7C_HUMAN	Isoform 2 of Heat shock cognate 71 kDa protein OS=Homo sapiens GN=HSPA8	HUMAN	8
58	0	8.87	33.33	20.83	16.99	tr E9PN89 E9PN89_HUMAN	Heat shock cognate 71 kDa protein (Fragment) OS=Homo sapiens GN=HSPA8 PE=1 SV=1	HUMAN	6
59	6.37	6.37	53.33	45.93	45.9300011	sp Q01469 FABP5_HUMAN	Fatty acid-binding protein, epidermal OS=Homo sapiens GN=FABP5 PE=1 SV=3	HUMAN	6
60	6.3	6.3	15.73	15.73	13.29	sp P60174 TPIS_HUMAN	Triosephosphate isomerase OS=Homo sapiens GN=TP11 PE=1 SV=3	HUMAN	3
60	0	6.3	26.95	26.95	22.7500007	sp P60174-4 TPIS_HUMAN	Isoform 4 of Triosephosphate isomerase OS=Homo sapiens GN=TP11	HUMAN	3
60	0	6.3	18.07	18.07	15.2600005	sp P60174-1 TPIS_HUMAN	Isoform 2 of Triosephosphate isomerase OS=Homo sapiens GN=TP11	HUMAN	3
60	0	4.23	29.2	29.2	23.0100006	tr U3KP20 U3KP20_HUMAN	Triosephosphate isomerase (Fragment) OS=Homo sapiens GN=TP11 PE=1 SV=1	HUMAN	2
61	6.28	6.28	36.51	30.16	30.1600009	sp Q98799 H2B1M_HUMAN	Histone H2B type 1-M OS=Homo sapiens GN=HIST1H2BM PE=1 SV=3	HUMAN	7
61	0	6.28	22.89	22.89	22.89	tr U3KXK0 U3KXK0_HUMAN	Histone H2B OS=Homo sapiens GN=HIST1H2BN PE=1 SV=1	HUMAN	7
61	0	6.28	22.89	22.89	22.89	tr B4DR52 B4DR52_HUMAN	Histone H2B OS=Homo sapiens GN=HIST1H2BF PE=1 SV=1	HUMAN	7
61	0	6.28	30.16	30.16	30.1600009	sp Q98880 H2B1L_HUMAN	Histone H2B type 1-L OS=Homo sapiens GN=HIST1H2BL PE=1 SV=3	HUMAN	7
61	0	6.28	30.16	30.16	30.1600009	sp Q98877 H2B1N_HUMAN	Histone H2B type 1-N OS=Homo sapiens GN=HIST1H2BN PE=1 SV=3	HUMAN	7
61	0	6.28	30.16	30.16	30.1600009	sp Q93079 H2B1H_HUMAN	Histone H2B type 1-H OS=Homo sapiens GN=HIST1H2BH PE=1 SV=3	HUMAN	7
61	0	6.28	30.16	30.16	30.1600009	sp Q8N257 H2B3B_HUMAN	Histone H2B type 3-B OS=Homo sapiens GN=HIST3H2BB PE=1 SV=3	HUMAN	7
61	0	6.28	30.16	30.16	30.1600009	sp Q5QNW6 H2B2F_HUMAN	Histone H2B type 2-F OS=Homo sapiens GN=HIST2H2BF PE=1 SV=3	HUMAN	7
61	0	6.28	28.36	28.36	28.3600003	sp Q5QNW6-2 H2B2F_HUMAN	Isoform 2 of Histone H2B type 2-F OS=Homo sapiens GN=HIST2H2BF	HUMAN	7
61	0	6.28	30.16	30.16	30.1600009	sp Q16778 H2B2E_HUMAN	Histone H2B type 2-E OS=Homo sapiens GN=HIST2H2BE PE=1 SV=3	HUMAN	7
61	0	6.28	30.16	30.16	30.1600009	sp P62807 H2B1C_HUMAN	Histone H2B type 1-C/E/F/G/I OS=Homo sapiens GN=HIST1H2BC PE=1 SV=4	HUMAN	7
61	0	6.28	30.16	30.16	30.1600009	sp P58876 H2B1D_HUMAN	Histone H2B type 1-D OS=Homo sapiens GN=HIST1H2BD PE=1 SV=2	HUMAN	7
61	0	6.28	30.16	30.16	30.1600009	sp P57053 H2BFS_HUMAN	Histone H2B type F-S OS=Homo sapiens GN=H2BFS PE=1 SV=2	HUMAN	7
61	0	6.28	30.16	30.16	30.1600009	sp P33778 H2B1B_HUMAN	Histone H2B type 1-B OS=Homo sapiens GN=HIST1H2BB PE=1 SV=2	HUMAN	7
61	0	6.28	30.16	30.16	30.1600009	sp P23527 H2B1O_HUMAN	Histone H2B type 1-O OS=Homo sapiens GN=HIST1H2BO PE=1 SV=3	HUMAN	7
61	0	6.28	30.16	30.16	30.1600009	sp P06899 H2B1J_HUMAN	Histone H2B type 1-J OS=Homo sapiens GN=HIST1H2BJ PE=1 SV=3	HUMAN	7
61	0	6.28	30.16	30.16	30.1600009	sp O60814 H2B1K_HUMAN	Histone H2B type 1-K OS=Homo sapiens GN=HIST1H2BK PE=1 SV=3	HUMAN	7
61	0	6.05	22.05	22.05	22.0500007	sp Q96A08 H2B1A_HUMAN	Histone H2B type 1-A OS=Homo sapiens GN=HIST1H2BA PE=1 SV=3	HUMAN	5
62	6.14	78.19	61.7	61.7	57.2700024	sp P04259 K2C6B_HUMAN	Keratin, type II cytoskeletal 6B OS=Homo sapiens GN=KRT6B PE=1 SV=5	HUMAN	67
62	0	79.49	61.99	59.15	55.2399993	cont 000127	sp P48668 Keratin, type II cytoskeletal 6E (Cyto keratin 6E) (CK 6E) (K6e keratin) [Homo sa	Homo sapien	69
63	6.07	6.07	31.43	22.86	22.8599995	sp P10599 THIO_HUMAN	Thioredoxin OS=Homo sapiens GN=TXN PE=1 SV=3	HUMAN	3
63	0	6.07	38.82	28.24	28.2400012	sp P10599-2 THIO_HUMAN	Isoform 2 of Thioredoxin OS=Homo sapiens GN=TXN	HUMAN	3
64	6.04	8.06	15.46	10.65	10.65	sp Q02383 SEM62_HUMAN	Semenogelin-2 OS=Homo sapiens GN=SEM62 PE=1 SV=1	HUMAN	6
65	6.04	6.04	16.89	12.89	12.8900006	tr HOYD33 HOYD33_HUMAN	Calpastatin (Fragment) OS=Homo sapiens GN=CAST PE=1 SV=1	HUMAN	4
65	0	6.04	16.34	12.47	12.4700002	tr HOY9H6 HOY9H6_HUMAN	Calpastatin (Fragment) OS=Homo sapiens GN=CAST PE=1 SV=1	HUMAN	4
65	0	6.04	17.43	13.3	13.3000001	tr HOY7F0 HOY7F0_HUMAN	Calpastatin (Fragment) OS=Homo sapiens GN=CAST PE=1 SV=1	HUMAN	4
65	0	6.04	11.95	9.19	9.19190029	tr E9PDE4 E9PDE4_HUMAN	Calpastatin OS=Homo sapiens GN=CAST PE=1 SV=1	HUMAN	4
65	0	6.04	11.29	8.618	8.61800015	tr E9PCH5 E9PCH5_HUMAN	Calpastatin OS=Homo sapiens GN=CAST PE=1 SV=1	HUMAN	4
65	0	6.04	10.97	8.369	8.36900026	tr E7EYV3 E7EYV3_HUMAN	Calpastatin OS=Homo sapiens GN=CAST PE=1 SV=1	HUMAN	4
65	0	6.04	9.883	7.542	7.54199997	tr E7ESM9 E7ESM9_HUMAN	Calpastatin OS=Homo sapiens GN=CAST PE=1 SV=1	HUMAN	4
65	0	6.04	11.84	9.034	9.03400034	tr E7ES10 E7ES10_HUMAN	Calpastatin (Fragment) OS=Homo sapiens GN=CAST PE=1 SV=1	HUMAN	4
65	0	6.04	17.63	13.46	13.4599999	tr E7EQAO E7EQAO_HUMAN	Calpastatin OS=Homo sapiens GN=CAST PE=1 SV=1	HUMAN	4
65	0	6.04	17.97	13.71	13.7099996	tr E7EQ12 E7EQ12_HUMAN	Calpastatin OS=Homo sapiens GN=CAST PE=1 SV=1	HUMAN	4
65	0	6.04	10.95	8.357	8.35700035	tr B7Z574 B7Z574_HUMAN	Calpastatin OS=Homo sapiens GN=CAST PE=1 SV=1	HUMAN	4
65	0	6.04	10.08	7.692	7.69200027	tr B7Z468 B7Z468_HUMAN	Calpastatin OS=Homo sapiens GN=CAST PE=1 SV=1	HUMAN	4
65	0	6.04	10.73	8.192	8.19199979	sp P20810 ICAL_HUMAN	Calpastatin OS=Homo sapiens GN=CAST PE=1 SV=4	HUMAN	4
65	0	6.04	10.13	7.733	7.73300007	sp P20810-9 ICAL_HUMAN	Isoform 9 of Calpastatin OS=Homo sapiens GN=CAST	HUMAN	4
65	0	6.04	11.08	8.455	8.45500007	sp P20810-8 ICAL_HUMAN	Isoform 8 of Calpastatin OS=Homo sapiens GN=CAST	HUMAN	4
65	0	6.04	9.845	7.513	7.51300007	sp P20810-7 ICAL_HUMAN	Isoform 7 of Calpastatin OS=Homo sapiens GN=CAST	HUMAN	4
65	0	6.04	9.608	7.332	7.33200014	sp P20810-6 ICAL_HUMAN	Isoform 6 of Calpastatin OS=Homo sapiens GN=CAST	HUMAN	4
65	0	6.04	10.05	7.672	7.67199993	sp P20810-5 ICAL_HUMAN	Isoform 5 of Calpastatin OS=Homo sapiens GN=CAST	HUMAN	4
65	0	6.04	11.39	8.696	8.69600028	sp P20810-4 ICAL_HUMAN	Isoform 4 of Calpastatin OS=Homo sapiens GN=CAST	HUMAN	4
65	0	6.04	12.88	9.831	9.83100012	sp P20810-3 ICAL_HUMAN	Isoform 3 of Calpastatin OS=Homo sapiens GN=CAST	HUMAN	4
65	0	6.04	10.94	8.345	8.3449997	sp P20810-2 ICAL_HUMAN	Isoform 2 of Calpastatin OS=Homo sapiens GN=CAST	HUMAN	4
66	6.03	6.03	10.16	4.774	3.67200002	sp P22735 TGM1_HUMAN	Protein-glutamine gamma-glutamyltransferase K OS=Homo sapiens GN=TGM1 PE=1 SV=4	HUMAN	3
67	6.02	6.02	11.54	10.26	10.2600001	sp Q96H7 ERO1A_HUMAN	ERO1-like protein alpha OS=Homo sapiens GN=ERO1L PE=1 SV=2	HUMAN	5
68	6.02	6.02	34.78	22.46	22.4600002	sp P29373 RABP2_HUMAN	Cellular retinoic acid-binding protein 2 OS=Homo sapiens GN=CRABP2 PE=1 SV=2	HUMAN	3
68	0	6.02	46.34	37.8	37.7999991	tr Q5SY24 Q5SY24_HUMAN	Cellular retinoic acid-binding protein 2 (Fragment) OS=Homo sapiens GN=CRABP2 PE=1 SV=1	HUMAN	3
69	6.01	6.01	41.91	30.15	24.2599994	sp P47929 LEG7_HUMAN	Galectin-7 OS=Homo sapiens GN=LGALS7 PE=1 SV=2	HUMAN	4
70	6	49.06	66.2	57.18	52.0799994	sp Q04695 K1C17_HUMAN	Keratin, type I cytoskeletal 17 OS=Homo sapiens GN=KRT17 PE=1 SV=2	HUMAN	35
70	0	21.84	64.5	52.07	42.8600013	tr K7EPJ9 K7EPJ9_HUMAN	Keratin, type I cytoskeletal 17 (Fragment) OS=Homo sapiens GN=KRT17 PE=1 SV=1	HUMAN	17
71	6	6	29.58	10.21	10.21	sp P67936-2 TPM4_HUMAN	Isoform 2 of Tropomyosin alpha-4 chain OS=Homo sapiens GN=TPM4	HUMAN	3
71	0	6	33.06	11.69	11.6899997	sp P67936 TPM4_HUMAN	Tropomyosin alpha-4 chain OS=Homo sapiens GN=TPM4 PE=1 SV=3	HUMAN	3
71	0	6	34.64	16.2	16.2	tr K7ENT6 K7ENT6_HUMAN	Tropomyosin alpha-4 chain (Fragment) OS=Homo sapiens GN=TPM4 PE=1 SV=1	HUMAN	3
71	0	6	32.35	17.06	17.0599997	tr K7ERG3 K7ERG3_HUMAN	Tropomyosin alpha-4 chain (Fragment) OS=Homo sapiens GN=TPM4 PE=1 SV=1	HUMAN	3
71	0	6	22.58	11.69	11.6899997	sp P07951-3 TPM2_HUMAN	Isoform 3 of Tropomyosin beta chain OS=Homo sapiens GN=TPM2	HUMAN	3
71	0	6	15.84	9.006	9.00600031	tr Q5TCU8 Q5TCU8_HUMAN	Tropomyosin beta chain OS=Homo sapiens GN=TPM2 PE=1 SV=1	HUMAN	3
71	0	6	17.96	10.21	10.21	tr Q5TCU3 Q5TCU3_HUMAN	Tropomyosin beta chain OS=Homo sapiens GN=TPM2 PE=1 SV=1	HUMAN	3
71	0	6	17.96	10.21	10.21	sp P07951 TPM2_HUMAN	Tropomyosin beta chain OS=Homo sapiens GN=TPM2 PE=1 SV=1	HUMAN	3
71	0	6	16.9	10.21	10.21	sp P07951-2 TPM2_HUMAN	Isoform 2 of Tropomyosin beta chain OS=Homo sapiens GN=TPM2	HUMAN	3
71	0	4	39.58	19.79	19.7899997	tr K7EPV9 K7EPV9_HUMAN	Tropomyosin alpha-4 chain (Fragment) OS=Homo sapiens GN=TPM4 PE=1 SV=1	HUMAN	2

71	0	4	37.25	18.63	18.6299995	tr K7EMUS K7EMUS_HUMAN	Tropomyosin alpha-4 chain (Fragment) OS=Homo sapiens GN=TPM4 PE=1 SV=1	HUMAN	2
71	0	4	21.01	13.77	13.7700006	tr K7EP68 K7EP68_HUMAN	Tropomyosin alpha-4 chain (Fragment) OS=Homo sapiens GN=TPM4 PE=1 SV=1	HUMAN	2
72	6	6	8.824	3.708	3.70800011	sp P06396 GELS_HUMAN	Gelsolin OS=Homo sapiens GN=GSN PE=1 SV=1	HUMAN	3
72	0	6	6.631	3.924	3.92399989	sp P06396-4 GELS_HUMAN	Isoform 4 of Gelsolin OS=Homo sapiens GN=GSN	HUMAN	3
72	0	6	6.604	3.908	3.90800014	sp P06396-3 GELS_HUMAN	Isoform 3 of Gelsolin OS=Homo sapiens GN=GSN	HUMAN	3
72	0	6	6.703	3.967	3.96700017	sp P06396-2 GELS_HUMAN	Isoform 2 of Gelsolin OS=Homo sapiens GN=GSN	HUMAN	3
72	0	4	8.247	4.124	4.12399992	tr Q5TOH9 Q5TOH9_HUMAN	Gelsolin OS=Homo sapiens GN=GSN PE=1 SV=1	HUMAN	2
73	6	6	10.85	6.074	6.07400015	tr F5H7U0 F5H7U0_HUMAN	Uncharacterized protein OS=Homo sapiens GN=PGD PE=1 SV=1	HUMAN	3
73	0	6	10.35	5.797	5.79699986	sp P52209 6PGD_HUMAN	6-phosphogluconate dehydrogenase, decarboxylating OS=Homo sapiens GN=PGD PE=1 SV=1	HUMAN	3
73	0	6	10.64	5.957	5.95699996	sp P52209-2 6PGD_HUMAN	Isoform 2 of 6-phosphogluconate dehydrogenase, decarboxylating OS=Homo sapiens GN=PGD PE=1 SV=1	HUMAN	3
73	0	4	13.67	8.203	8.20299983	tr K7EPF6 K7EPF6_HUMAN	6-phosphogluconate dehydrogenase, decarboxylating (Fragment) OS=Homo sapiens GN=PGD PE=1 SV=1	HUMAN	2
73	0	4	21.88	13.12	13.1200001	tr K7EMN2 K7EMN2_HUMAN	6-phosphogluconate dehydrogenase, decarboxylating (Fragment) OS=Homo sapiens GN=PGD PE=1 SV=1	HUMAN	2
73	0	4	17.07	10.24	10.2399997	tr K7EM49 K7EM49_HUMAN	6-phosphogluconate dehydrogenase, decarboxylating (Fragment) OS=Homo sapiens GN=PGD PE=1 SV=1	HUMAN	2
74	6	6	7.595	6.329	6.329	sp P25705 ATPA_HUMAN	ATP synthase subunit alpha, mitochondrial OS=Homo sapiens GN=ATP5A1 PE=1 SV=1	HUMAN	3
74	0	6	17.07	17.07	17.0699999	tr K7ERX7 K7ERX7_HUMAN	ATP synthase subunit alpha, mitochondrial (Fragment) OS=Homo sapiens GN=ATP5A1 PE=1 SV=1	HUMAN	3
74	0	4	14.57	11.06	11.0600002	tr K7ENJ4 K7ENJ4_HUMAN	ATP synthase subunit alpha, mitochondrial (Fragment) OS=Homo sapiens GN=ATP5A1 PE=1 SV=1	HUMAN	2
74	0	4	14.01	10.63	10.6299996	tr K7EK77 K7EK77_HUMAN	ATP synthase subunit alpha, mitochondrial (Fragment) OS=Homo sapiens GN=ATP5A1 PE=1 SV=1	HUMAN	2
74	0	4	5.65	4.331	4.33100015	sp P25705-3 ATPA_HUMAN	Isoform 3 of ATP synthase subunit alpha, mitochondrial OS=Homo sapiens GN=ATP5A1	HUMAN	2
74	0	4	5.765	4.374	4.37400006	sp P25705-2 ATPA_HUMAN	Isoform 2 of ATP synthase subunit alpha, mitochondrial OS=Homo sapiens GN=ATP5A1	HUMAN	2
75	6	6	38.26	28.7	28.7	sp P05387 RLA2_HUMAN	60S acidic ribosomal protein P2 OS=Homo sapiens GN=RPLP2 PE=1 SV=1	HUMAN	3
75	0	4	33.7	21.74	21.7399999	tr HOYD08 HOYD08_HUMAN	60S acidic ribosomal protein P2 (Fragment) OS=Homo sapiens GN=RPLP2 PE=1 SV=1	HUMAN	2
76	5.82	5.82	17.27	9.697	9.69699994	sp P01857 IGHG1_HUMAN	Ig gamma-1 chain C region OS=Homo sapiens GN=IGHG1 PE=1 SV=1	HUMAN	3
77	5.23	5.23	10.28	7.712	7.71199986	tr B7Z7A9 B7Z7A9_HUMAN	Phosphoglycerate kinase OS=Homo sapiens GN=PGK1 PE=1 SV=1	HUMAN	4
77	0	5.23	9.592	7.194	7.19399974	sp P00558 PGK1_HUMAN	Phosphoglycerate kinase 1 OS=Homo sapiens GN=PGK1 PE=1 SV=3	HUMAN	4
78	5.1	5.1	26.36	26.36	26.3599992	sp P81605 DCD_HUMAN	Dermcidin OS=Homo sapiens GN=DCD PE=1 SV=2	HUMAN	3
78	0	5.1	26.36	26.36	26.3599992	cont 000124	spt P81605 Dermcidin precursor (Preproteolysin) [Contains: Survival-promoting peptide; D Homo sapien	HUMAN	3
78	0	4	24.79	18.18	18.1799993	sp P81605-2 DCD_HUMAN	Isoform 2 of Dermcidin OS=Homo sapiens GN=DCD	HUMAN	2
79	4.86	4.86	4.643	3.214	3.21400017	sp Q08554-2 DSC1_HUMAN	Isoform 1B of Desmocollin-1 OS=Homo sapiens GN=DSC1	HUMAN	3
79	0	4	3.579	2.237	2.23699994	sp Q08554 DSC1_HUMAN	Desmocollin-1 OS=Homo sapiens GN=DSC1 PE=1 SV=2	HUMAN	2
80	4.83	4.83	44.34	29.25	29.2499989	tr J3QTR3 J3QTR3_HUMAN	Ubiquitin (Fragment) OS=Homo sapiens GN=RPS27A PE=1 SV=1	HUMAN	3
80	0	4.83	30.13	19.87	19.8699996	sp P62979 RS27A_HUMAN	Ubiquitin-40S ribosomal protein S27a OS=Homo sapiens GN=RPS27A PE=1 SV=2	HUMAN	3
80	0	4.83	52.46	40.66	40.6599998	tr Q96C32 Q96C32_HUMAN	Polyubiquitin-C OS=Homo sapiens GN=UBC PE=2 SV=1	HUMAN	3
80	0	4.83	63.49	49.21	49.21	tr MOR1V7 MOR1V7_HUMAN	Ubiquitin-60S ribosomal protein L40 (Fragment) OS=Homo sapiens GN=UBA52 PE=4 SV=1	HUMAN	3
80	0	4.83	49.46	39.78	39.7799999	tr J3Q539 J3Q539_HUMAN	Ubiquitin (Fragment) OS=Homo sapiens GN=UBB PE=4 SV=1	HUMAN	3
80	0	4.83	53.88	40.78	40.7799989	tr J3QKNO J3QKNO_HUMAN	Ubiquitin (Fragment) OS=Homo sapiens GN=UBB PE=4 SV=1	HUMAN	3
80	0	4.83	53.75	42.5	42.5000012	tr F5H747 F5H747_HUMAN	Polyubiquitin-C (Fragment) OS=Homo sapiens GN=UBC PE=1 SV=2	HUMAN	3
80	0	4.83	58.2	43.44	43.4399992	tr F5H6Q2 F5H6Q2_HUMAN	Polyubiquitin-C (Fragment) OS=Homo sapiens GN=UBC PE=4 SV=2	HUMAN	3
80	0	4.83	51.61	40	40.0000006	tr F5H388 F5H388_HUMAN	Polyubiquitin-C (Fragment) OS=Homo sapiens GN=UBC PE=4 SV=1	HUMAN	3
80	0	4.83	52.21	38.97	38.9699996	tr F5H223 F5H223_HUMAN	Polyubiquitin-C (Fragment) OS=Homo sapiens GN=UBC PE=4 SV=1	HUMAN	3
80	0	4.83	53.69	41.61	41.6099995	tr F5H265 F5H265_HUMAN	Polyubiquitin-C (Fragment) OS=Homo sapiens GN=UBC PE=4 SV=1	HUMAN	3
80	0	4.83	51.07	40.72	40.7200009	tr F5H041 F5H041_HUMAN	Polyubiquitin-C OS=Homo sapiens GN=UBC PE=4 SV=1	HUMAN	3
80	0	4.83	52.99	39.55	39.5500004	tr F5GYU3 F5GYU3_HUMAN	Polyubiquitin-C (Fragment) OS=Homo sapiens GN=UBC PE=4 SV=1	HUMAN	3
80	0	4.83	45.56	40.23	40.2399987	tr F5GKX7 F5GKX7_HUMAN	Polyubiquitin-C (Fragment) OS=Homo sapiens GN=UBC PE=4 SV=1	HUMAN	3
80	0	4.83	52.29	40.52	40.5200005	tr B4DV12 B4DV12_HUMAN	Ubiquitin OS=Homo sapiens GN=UBB PE=2 SV=1	HUMAN	3
80	0	4.83	31.25	24.22	24.2200002	sp P62987 RL40_HUMAN	Ubiquitin-60S ribosomal protein L40 OS=Homo sapiens GN=UBA52 PE=1 SV=2	HUMAN	3
80	0	4.83	52.55	40.73	40.7299995	sp P0CG48 UBC_HUMAN	Polyubiquitin-C OS=Homo sapiens GN=UBC PE=1 SV=3	HUMAN	3
80	0	4.83	52.4	40.61	40.6100005	sp P0CG47 UBB_HUMAN	Polyubiquitin-B OS=Homo sapiens GN=UBB PE=1 SV=1	HUMAN	3
80	0	2.74	72.09	51.16	51.1600018	tr J3QSA3 J3QSA3_HUMAN	Ubiquitin (Fragment) OS=Homo sapiens GN=UBB PE=4 SV=1	HUMAN	2
80	0	2.74	77.07	19.21	19.2100003	tr J3QRK5 J3QRK5_HUMAN	Protein UBBP4 OS=Homo sapiens GN=UBBP4 PE=1 SV=1	HUMAN	2
80	0	2.74	23.66	19.64	19.6400002	tr J3QLP7 J3QLP7_HUMAN	Protein UBBP4 OS=Homo sapiens GN=UBBP4 PE=4 SV=1	HUMAN	2
80	0	2.74	50.82	36.07	36.0700011	tr F5GZ39 F5GZ39_HUMAN	Polyubiquitin-C (Fragment) OS=Homo sapiens GN=UBC PE=4 SV=1	HUMAN	2
81	4.72	31.45	53.25	36.5	30.5000007	sp P08727 K1C19_HUMAN	Keratin, type I cytoskeletal 19 OS=Homo sapiens GN=KRT19 PE=1 SV=4	HUMAN	32
82	4.44	4.65	16.37	13.04	9.97399986	sp Q9UIV8 SPB13_HUMAN	Serpin B13 OS=Homo sapiens GN=SERPINB13 PE=1 SV=2	HUMAN	4
82	0	4.22	15.34	11.5	7.96499997	sp Q9UIV8-2 SPB13_HUMAN	Isoform 2 of Serpin B13 OS=Homo sapiens GN=SERPINB13	HUMAN	3
83	4.39	8.54	15.75	10.7	9.32699963	sp P11021 GRP78_HUMAN	78 kDa glucose-regulated protein OS=Homo sapiens GN=HSPA5 PE=1 SV=2	HUMAN	6
84	4.31	4.31	6.768	2.574	2.57399995	sp Q02413 DSG1_HUMAN	Desmoglein-1 OS=Homo sapiens GN=DSG1 PE=1 SV=2	HUMAN	3
85	4.17	4.17	43.69	32.04	32.04	sp Q96FQ6 S10AG_HUMAN	Protein S100-A16 OS=Homo sapiens GN=S100A16 PE=1 SV=1	HUMAN	3
86	4.12	4.12	23.14	12.94	9.80399996	sp P62258 1433E_HUMAN	14-3-3 protein epsilon OS=Homo sapiens GN=YWHAE PE=1 SV=1	HUMAN	2
86	0	4.11	21.89	14.16	10.7299998	sp P62258-2 1433E_HUMAN	Isoform SV of 14-3-3 protein epsilon OS=Homo sapiens GN=YWHAE	HUMAN	2
87	4.08	4.08	38.89	25.56	24.4399995	sp P06703 S10AG_HUMAN	Protein S100-A6 OS=Homo sapiens GN=S100A6 PE=1 SV=1	HUMAN	3
87	0	4	31.76	17.65	17.6499993	tr R4GN98 R4GN98_HUMAN	Protein S100-A6 (Fragment) OS=Homo sapiens GN=S100A6 PE=1 SV=1	HUMAN	2
88	4.08	4.08	14.96	11.02	11.0200003	sp P18669 PGAM1_HUMAN	Phosphoglycerate mutase 1 OS=Homo sapiens GN=PGAM1 PE=1 SV=2	HUMAN	3
89	4.01	4.01	8.3	2.544	2.544	sp Q13835 PKP1_HUMAN	Plakophilin-1 OS=Homo sapiens GN=PKP1 PE=1 SV=2	HUMAN	2
89	0	4.01	8.54	2.617	2.61700004	sp Q13835-2 PKP1_HUMAN	Isoform 1 of Plakophilin-1 OS=Homo sapiens GN=PKP1	HUMAN	2
90	4	4	10.49	3.933	3.93299982	tr F5H3X9 F5H3X9_HUMAN	Serine/threonine-protein phosphatase 2A 65 kDa regulatory subunit A alpha isoform OS=Ho	HUMAN	2
90	0	4	9.508	3.565	3.565	sp P30153 2A_A_HUMAN	Serine/threonine-protein phosphatase 2A 65 kDa regulatory subunit A alpha isoform OS=Ho	HUMAN	2
90	0	4	11.71	5.122	5.12199998	tr B3KQV6 B3KQV6_HUMAN	Serine/threonine-protein phosphatase 2A 65 kDa regulatory subunit A alpha isoform OS=Ho	HUMAN	2
90	0	2	8.861	2.785	2.78500002	tr C9J9C1 C9J9C1_HUMAN	Serine/threonine-protein phosphatase 2A 65 kDa regulatory subunit A alpha isoform (Fragm	HUMAN	1
90	0	2	7.576	2.757	2.75799995	tr E9PH38 E9PH38_HUMAN	Serine/threonine-protein phosphatase 2A 65 kDa regulatory subunit A alpha isoform (Fragm	HUMAN	1
91	4	4	8	4.471	4.47099991	tr Q3SYB4 Q3SYB4_HUMAN	SERPINB12 protein OS=Homo sapiens GN=SERPINB12 PE=2 SV=1	HUMAN	2
91	0	2	5.679	1.975	1.97500009	sp Q96P63 SPB12_HUMAN	Serpin B12 OS=Homo sapiens GN=SERPINB12 PE=1 SV=1	HUMAN	1
92	4	4	9.333	3.474	3.4740001	sp Q86VZ3 HORN_HUMAN	Hornerin OS=Homo sapiens GN=HRNR PE=1 SV=2	HUMAN	3
93	4	4	12.4	7.851	7.85100013	sp P31944 CASPE_HUMAN	Caspase-14 OS=Homo sapiens GN=CASP14 PE=1 SV=2	HUMAN	2
94	4	4	13.72	10.18	10.1800002	sp P16401 H15_HUMAN	Histone H1.5 OS=Homo sapiens GN=HIST1H15 PE=1 SV=3	HUMAN	2
95	4	4	7.492	7.492	7.49199986	tr F8W6I7 F8W6I7_HUMAN	Heterogeneous nuclear ribonucleoprotein A1 OS=Homo sapiens GN=HNRNPA1 PE=1 SV=2	HUMAN	2
95	0	4	9.957	9.957	9.95699987	tr F8VZ49 F8VZ49_HUMAN	Heterogeneous nuclear ribonucleoprotein A1 (Fragment) OS=Homo sapiens GN=HNRNPA1 F	HUMAN	2
95	0	4	20.35	20.35	20.3500003	tr F8VYN5 F8VYN5_HUMAN	Heterogeneous nuclear ribonucleoprotein A1 (Fragment) OS=Homo sapiens GN=HNRNPA1 F	HUMAN	2
95	0	4	7.187	7.187	7.18699992	sp Q32P51 RA1L2_HUMAN	Heterogeneous nuclear ribonucleoprotein A1-like 2 OS=Homo sapiens GN=HNRNPA1L2 PE=	HUMAN	2
95	0	4	6.183	6.183	6.18299991	sp P09651 ROA1_HUMAN	Heterogeneous nuclear ribonucleoprotein A1 OS=Homo sapiens GN=HNRNPA1 PE=1 SV=5	HUMAN	2
95	0	4	8.614	8.614	8.61399993	sp P09651-3 ROA1_HUMAN	Isoform 2 of Heterogeneous nuclear ribonucleoprotein A1 OS=Homo sapiens GN=HNRNPA1	HUMAN	2
95	0	4	7.187	7.187	7.18699992	sp P09651-2 ROA1_HUMAN	Isoform A1-A of Heterogeneous nuclear ribonucleoprotein A1 OS=Homo sapiens GN=HNRN	HUMAN	2
95	0	2	5.236	5.236	5.23599982	tr HOYH80 HOYH80_HUMAN	Heterogeneous nuclear ribonucleoprotein A1 (Fragment) OS=Homo sapiens GN=HNRNPA1 F	HUMAN	1
95	0	2	8.333	8.333	8.3329998	tr F8W646 F8W646_HUMAN	Heterogeneous nuclear ribonucleoprotein A1 (Fragment) OS=Homo sapiens GN=HNRNPA1 F	HUMAN	1
95	0	2	8.897	8.897	8.89700022	tr F8VTQ5 F8VTQ5_HUMAN	Heterogeneous nuclear ribonucleoprotein A1 (Fragment) OS=Homo sapiens GN=HNRNPA1 F	HUMAN	1
96	4	4	60.87	60.87	60.8699977	tr F5H397 F5H397_HUMAN	Epithelial membrane protein 1 OS=Homo sapiens GN=EMPI1 PE=4 SV=1	HUMAN	3
96	0	4	28.77	28.77	28.7699997	tr F5GYV0 F5GYV0_HUMAN	Epithelial membrane protein 1 (Fragment) OS=Homo sapiens GN=EMPI1 PE=4 SV=1	HUMAN	3
96	0	4	29.79	29.79	29.7899991	tr B4DRR1 B4DRR1_HUMAN	Epithelial membrane protein 1 OS=Homo sapiens GN=EMPI1 PE=2 SV=1	HUMAN	3
96	0	4	26.75	26.75	26.7500013	sp P54849 EMPI1_HUMAN	Epithelial membrane protein 1 OS=Homo sapiens GN=EMPI1 PE=2 SV=3	HUMAN	3
97	3.77	3.77	4.203	2.977	2.97699999	tr J3KN47 J3KN47_HUMAN	Serotransferrin OS=Homo sapiens GN=TF PE=1 SV=1	HUMAN	2
97	0	3.77	4.238	2.435	2.43599992	sp P02787 TRFE_HUMAN	Serotransferrin OS=Homo sapiens GN=TF PE=1 SV=3	HUMAN	2
97	0	3.77	7.463	7.463	7.46299997	tr C9JVG0 C9JVG0_HUMAN	Serotransferrin (Fragment) OS=Homo sapiens GN=TF PE=1 SV=1	HUMAN	2
97	0	1.57	3.39	0.9887	0.98869996	tr E7ER44 E7ER44_HUMAN	Kalocin-1 OS=Homo sapiens GN=LTF PE=1 SV=1	HUMAN	1
97	0	1.57	3.448	1.006	1.00600002	tr E7EQB2 E7EQB2_HUMAN	Kalocin-1 (Fragment) OS=Homo sapiens GN=LTF PE=1 SV=1	HUMAN	1
97	0	1.57	3.38	0.9859	0.98590003	sp P02788 TRFL_HUMAN	Lactotransferrin OS=Homo sapiens GN=LTF PE=1 SV=6	HUMAN	1
97	0	1.57	3.604	1.051	1.05100004	sp P02788-2 TRFL_HUMAN	Isoform DeltaL of Lactotransferrin OS=Homo sapiens GN=LTF	HUMAN	1
97	0	1.57	4.895	4.895	4.89500016	tr H7C5E8 H7C5E8_HUMAN	Serotransferrin (Fragment) OS=Homo sapiens GN=TF PE=1 SV=1	HUMAN	1
97	0	1.57	0.9485	0.9485	0.94849998	sp P08582 TRFM_HUMAN	Melanotransferrin OS=Homo sapiens GN=MF12 PE=1 SV=2	HUMAN	1
97	0	1.57	2.318	2.318	2.31800005	sp P08582-2 TRFM_HUMAN	Isoform 2 of Melanotransferrin OS=Homo sapiens GN=MF12	HUMAN	1

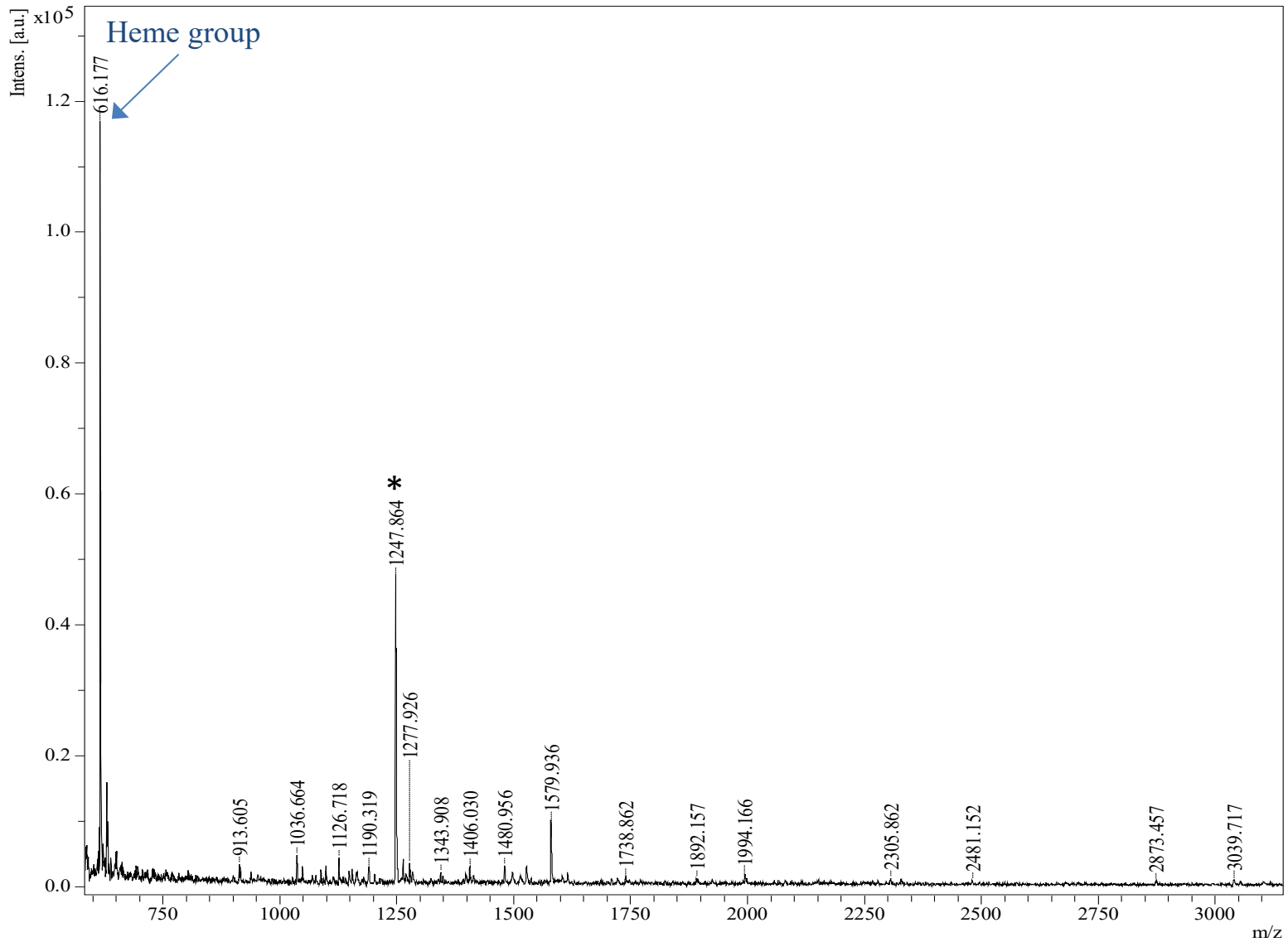
98	3.75	3.75	14.44	7.04	5.59599996	tr E7EQR4 E7EQR4_HUMAN	Ezrin OS=Homo sapiens GN=EZR PE=1 SV=2	HUMAN	4
98	0	3.75	13.65	6.655	5.29000014	sp P15311 EZRI_HUMAN	Ezrin OS=Homo sapiens GN=EZR PE=1 SV=4	HUMAN	4
98	0	2	4.859	0.3966	0.39659999	sp Q5T2A2 CROCC_HUMAN	Rootletin OS=Homo sapiens GN=CROCC PE=1 SV=1	HUMAN	1
98	0	2	5.111	0.6102	0.61019999	tr B1AKD8 B1AKD8_HUMAN	Rootletin (Fragment) OS=Homo sapiens GN=CROCC PE=4 SV=2	HUMAN	1
98	0	2	5.331	0.6093	0.60930001	sp Q5T2A2-2 CROCC_HUMAN	Isoform 2 of Rootletin OS=Homo sapiens GN=CROCC	HUMAN	1
99	3.56	3.56	24.04	24.04	24.04000001	sp Q9HCY8 S10AE_HUMAN	Protein S100-A14 OS=Homo sapiens GN=S100A14 PE=1 SV=1	HUMAN	3
100	3.53	5.66	27.42	14.52	11.68999997	sp P06753-6 TPM3_HUMAN	Isoform 6 of Tropomyosin alpha-3 chain OS=Homo sapiens GN=TPM3	HUMAN	3
100	0	5.66	27.53	14.52	11.73999998	sp P06753-3 TPM3_HUMAN	Isoform 3 of Tropomyosin alpha-3 chain OS=Homo sapiens GN=TPM3	HUMAN	3
100	0	5.66	27.42	14.52	11.68999997	sp P06753-2 TPM3_HUMAN	Isoform 2 of Tropomyosin alpha-3 chain OS=Homo sapiens GN=TPM3	HUMAN	3
100	0	5.66	25	15.52	12.5	tr Q5VU59 Q5VU59_HUMAN	Uncharacterized protein OS=Homo sapiens GN=TPM3 PE=1 SV=1	HUMAN	3
100	0	5.66	19.65	12.63	10.18000002	tr J3KN67 J3KN67_HUMAN	Tropomyosin alpha-3 chain OS=Homo sapiens GN=TPM3 PE=1 SV=1	HUMAN	3
100	0	5.53	21.77	11.69	11.68999997	sp P06753-5 TPM3_HUMAN	Isoform 5 of Tropomyosin alpha-3 chain OS=Homo sapiens GN=TPM3	HUMAN	3
100	0	5.53	21.86	11.74	11.73999998	sp P06753-4 TPM3_HUMAN	Isoform 4 of Tropomyosin alpha-3 chain OS=Homo sapiens GN=TPM3	HUMAN	3
100	0	5.53	14.74	10.18	10.18000002	sp P06753 TPM3_HUMAN	Tropomyosin alpha-3 chain OS=Homo sapiens GN=TPM3 PE=1 SV=2	HUMAN	3
100	0	3.53	20.63	11.66	8.51999968	tr Q5VU61 Q5VU61_HUMAN	Tropomyosin alpha-3 chain OS=Homo sapiens GN=TPM3 PE=1 SV=2	HUMAN	2
100	0	3.42	13.92	12.03	12.03000002	sp P06753-7 TPM3_HUMAN	Isoform 7 of Tropomyosin alpha-3 chain OS=Homo sapiens GN=TPM3	HUMAN	2
101	3.48	5.59	19.7	15.15	15.15000002	sp P32119 PRDX2_HUMAN	Peroxiredoxin-2 OS=Homo sapiens GN=PRDX2 PE=1 SV=5	HUMAN	3
101	0	3.48	20.59	13.97	13.96999996	tr A6NIW5 A6NIW5_HUMAN	Peroxiredoxin 2, isoform CRA_a OS=Homo sapiens GN=PRDX2 PE=1 SV=2	HUMAN	2
101	0	2	13.38	7.042	7.04199997	sp P32119-2 PRDX2_HUMAN	Isoform 2 of Peroxiredoxin-2 OS=Homo sapiens GN=PRDX2	HUMAN	1
102	3.43	3.43	22.6	18.49	13.00999997	sp Q9NZT1 CALL5_HUMAN	Calmodulin-like protein 5 OS=Homo sapiens GN=CALL5 PE=1 SV=2	HUMAN	3
103	3.11	3.11	4.809	2.186	2.18599998	tr E9PLK3 E9PLK3_HUMAN	Puromycin-sensitive aminopeptidase OS=Homo sapiens GN=NPEPPS PE=1 SV=1	HUMAN	2
103	0	3.11	5.244	2.384	2.38400009	tr B72463 B72463_HUMAN	Uncharacterized protein OS=Homo sapiens GN=NPEPPS PE=1 SV=1	HUMAN	2
103	0	3.11	4.788	2.176	2.17599999	sp P55786 PSA_HUMAN	Puromycin-sensitive aminopeptidase OS=Homo sapiens GN=NPEPPS PE=1 SV=2	HUMAN	2
103	0	3.09	7.95	4.184	4.18399982	tr I3L083 I3L083_HUMAN	Protein LOC101929950 OS=Homo sapiens GN=LOC101929950 PE=4 SV=1	HUMAN	2
103	0	3.09	8.817	4.64	4.63999994	tr HOYAQ6 HOYAQ6_HUMAN	Protein LOC101929950 (Fragment) OS=Homo sapiens GN=LOC101929950 PE=4 SV=1	HUMAN	2
103	0	3.09	7.966	4.193	4.19300012	tr E7EWZ2 E7EWZ2_HUMAN	Protein LOC101929950 OS=Homo sapiens GN=LOC101929950 PE=4 SV=2	HUMAN	2
103	0	3.09	8.068	4.246	4.24599983	tr ESR124 ESR124_HUMAN	Protein LOC101929950 (Fragment) OS=Homo sapiens GN=LOC101929950 PE=4 SV=1	HUMAN	2
103	0	3.09	7.95	4.184	4.18399982	tr A6NEC2 A6NEC2_HUMAN	Puromycin-sensitive aminopeptidase-like protein OS=Homo sapiens GN=NPEPPL1 PE=2 SV=1	HUMAN	2
103	0	3.08	6.173	6.173	6.17300011	tr F5GZV4 F5GZV4_HUMAN	Protein LOC101929950 OS=Homo sapiens GN=LOC101929950 PE=4 SV=1	HUMAN	2
103	0	2	4.183	4.183	4.18299995	sp A6NCE2-2 PSAL_HUMAN	Isoform 2 of Puromycin-sensitive aminopeptidase-like protein OS=Homo sapiens GN=NPEPP_HUMAN	HUMAN	1
104	2.62	2.62	9.77	9.77	9.76999998	tr E9PR44 E9PR44_HUMAN	Alpha-crystallin B chain (Fragment) OS=Homo sapiens GN=CRYAB PE=3 SV=1	HUMAN	2
104	0	2.62	16.04	16.04	16.04000003	tr E9PNH7 E9PNH7_HUMAN	Alpha-crystallin B chain (Fragment) OS=Homo sapiens GN=CRYAB PE=3 SV=1	HUMAN	2
104	0	2.62	13.18	13.18	13.17999996	tr E9PIL7 E9PIL7_HUMAN	Alpha-crystallin B chain (Fragment) OS=Homo sapiens GN=CRYAB PE=3 SV=2	HUMAN	2
104	0	2.62	15.74	15.74	15.73999997	tr A0A024R3B9 A0A024R3B9_HUMAN	Alpha-crystallin B chain OS=Homo sapiens GN=CRYAB PE=3 SV=1	HUMAN	2
104	0	2.62	9.714	9.714	9.71399993	sp P02511 CRYAB_HUMAN	Alpha-crystallin B chain OS=Homo sapiens GN=CRYAB PE=1 SV=2	HUMAN	2
104	0	2	5.161	5.161	5.16100004	tr E9PRA8 E9PRA8_HUMAN	Alpha-crystallin B chain OS=Homo sapiens GN=CRYAB PE=4 SV=1	HUMAN	1
105	2.46	2.46	9.959	7.64	4.63799983	sp Q9GTA1-2 NIBL1_HUMAN	Isoform 2 of Niban-like protein 1 OS=Homo sapiens GN=FAM129B	HUMAN	3
105	0	2.46	8.445	7.507	7.50799997	sp Q9GTA1 NIBL1_HUMAN	Niban-like protein 1 OS=Homo sapiens GN=FAM129B PE=1 SV=3	HUMAN	3
106	2.33	2.33	8.35	0.7691	0.2197	sp Q15149-6 PLEC_HUMAN	Isoform 6 of Plectin OS=Homo sapiens GN=PLEC	HUMAN	1
106	0	2.33	8.247	0.7697	0.2199	sp Q15149-4 PLEC_HUMAN	Isoform 4 of Plectin OS=Homo sapiens GN=PLEC	HUMAN	1
106	0	2.33	7.857	0.7472	0.2135	sp Q15149 PLEC_HUMAN	Plectin OS=Homo sapiens GN=PLEC PE=1 SV=3	HUMAN	1
106	0	2.33	8.118	0.7721	0.2206	sp Q15149-9 PLEC_HUMAN	Isoform 9 of Plectin OS=Homo sapiens GN=PLEC	HUMAN	1
106	0	2.33	8.133	0.7735	0.22100001	sp Q15149-8 PLEC_HUMAN	Isoform 8 of Plectin OS=Homo sapiens GN=PLEC	HUMAN	1
106	0	2.33	8.151	0.7752	0.22150001	sp Q15149-7 PLEC_HUMAN	Isoform 7 of Plectin OS=Homo sapiens GN=PLEC	HUMAN	1
106	0	2.33	8.093	0.7697	0.2199	sp Q15149-5 PLEC_HUMAN	Isoform 5 of Plectin OS=Homo sapiens GN=PLEC	HUMAN	1
106	0	2.33	8.045	0.7652	0.21860001	sp Q15149-2 PLEC_HUMAN	Isoform 2 of Plectin OS=Homo sapiens GN=PLEC	HUMAN	1
106	0	2.33	7.899	0.7659	0.21879999	sp Q15149-3 PLEC_HUMAN	Isoform 3 of Plectin OS=Homo sapiens GN=PLEC	HUMAN	1
107	2.24	2.24	14.29	6.95	3.86100002	tr F8VPV9 F8VPV9_HUMAN	ATP synthase subunit beta OS=Homo sapiens GN=ATP5B PE=1 SV=1	HUMAN	2
107	0	2.24	13.99	6.805	3.78100015	sp P06576 ATP5B_HUMAN	ATP synthase subunit beta, mitochondrial OS=Homo sapiens GN=ATP5B PE=1 SV=3	HUMAN	2
107	0	2.24	17.4	9.945	5.52500002	tr HOYH81 HOYH81_HUMAN	ATP synthase subunit beta (Fragment) OS=Homo sapiens GN=ATP5B PE=1 SV=1	HUMAN	2
107	0	2.24	14.44	10.21	7.04199997	tr F8W079 F8W079_HUMAN	ATP synthase subunit beta, mitochondrial (Fragment) OS=Homo sapiens GN=ATP5B PE=1 SV=1	HUMAN	2
108	2.19	2.19	10.91	6.181	6.18100017	sp P20930 FILA_HUMAN	Filaggrin OS=Homo sapiens GN=FLG PE=1 SV=3	HUMAN	8
109	2.18	2.19	17.45	5.296	3.11500002	tr D6REE5 D6REE5_HUMAN	Guanine nucleotide-binding protein subunit beta-2-like 1 (Fragment) OS=Homo sapiens GN=HUMAN	HUMAN	1
109	0	2.19	20.82	6.32	3.71700004	tr D6RAC2 D6RAC2_HUMAN	Guanine nucleotide-binding protein subunit beta-2-like 1 OS=Homo sapiens GN=GNB2L1 PE_HUMAN	HUMAN	1
109	0	2.19	17.67	5.363	3.15500014	sp P63244 GBLP_HUMAN	Guanine nucleotide-binding protein subunit beta-2-like 1 OS=Homo sapiens GN=GNB2L1 PE_HUMAN	HUMAN	1
109	0	2	6.536	6.536	6.53600022	tr E9PD14 E9PD14_HUMAN	Guanine nucleotide-binding protein subunit beta-2-like 1 OS=Homo sapiens GN=GNB2L1 PE_HUMAN	HUMAN	1
109	0	2	4.292	4.292	4.29200009	tr D6RHH4 D6RHH4_HUMAN	Guanine nucleotide-binding protein subunit beta-2-like 1 OS=Homo sapiens GN=GNB2L1 PE_HUMAN	HUMAN	1
109	0	2	14.08	14.08	14.07999999	tr D6RKG8 D6RKG8_HUMAN	Guanine nucleotide-binding protein subunit beta-2-like 1 OS=Homo sapiens GN=GNB2L1 PE_HUMAN	HUMAN	1
109	0	2	5.076	5.076	5.07600009	tr D6RFZ9 D6RFZ9_HUMAN	Guanine nucleotide-binding protein subunit beta-2-like 1 (Fragment) OS=Homo sapiens GN=HUMAN	HUMAN	1
109	0	2	5.155	5.155	5.15500009	tr D6RFK4 D6RFK4_HUMAN	Guanine nucleotide-binding protein subunit beta-2-like 1 (Fragment) OS=Homo sapiens GN=HUMAN	HUMAN	1
109	0	2	6.25	6.25	6.25	tr D6RBD0 D6RBD0_HUMAN	Guanine nucleotide-binding protein subunit beta-2-like 1 (Fragment) OS=Homo sapiens GN=HUMAN	HUMAN	1
109	0	2	6.803	6.803	6.80299997	tr D6RAU2 D6RAU2_HUMAN	Guanine nucleotide-binding protein subunit beta-2-like 1 OS=Homo sapiens GN=GNB2L1 PE_HUMAN	HUMAN	1
109	0	2	4.237	4.237	4.23699999	tr D6R921 D6R921_HUMAN	Guanine nucleotide-binding protein subunit beta-2-like 1 (Fragment) OS=Homo sapiens GN=HUMAN	HUMAN	1
109	0	2	3.333	3.333	3.33300009	tr D6R9L0 D6R9L0_HUMAN	Guanine nucleotide-binding protein subunit beta-2-like 1 (Fragment) OS=Homo sapiens GN=HUMAN	HUMAN	1
109	0	2	8.621	8.621	8.62099975	tr D6R909 D6R909_HUMAN	Guanine nucleotide-binding protein subunit beta-2-like 1 OS=Homo sapiens GN=GNB2L1 PE_HUMAN	HUMAN	1
110	2.17	80.44	61.7	61.17	57.2700024	sp P02538 K2C6A_HUMAN	Keratin, type II cytoskeletal 6A OS=Homo sapiens GN=KRT6A PE=1 SV=3	HUMAN	72
110	0	80.44	61.81	61.28	57.3700011	cont 000125	sp P02538 Keratin, type II cytoskeletal 6A (Cytokeratin 6A) (CK 6A) (K6a keratin) [Homo sa Homo sapien	HUMAN	72
111	2.16	2.17	14.97	14.97	14.9700001	sp P30086 PEBP1_HUMAN	Phosphatidylethanolamine-binding protein 1 OS=Homo sapiens GN=PEBP1 PE=1 SV=3	HUMAN	3
112	2.15	2.15	10.36	5.18	5.18000014	sp Q3ZCM7 TBB8_HUMAN	Tubulin beta-8 chain OS=Homo sapiens GN=TUBB8 PE=1 SV=2	HUMAN	2
112	0	2.15	10.34	5.169	5.1690001	sp P68371 TBB4B_HUMAN	Tubulin beta-4B chain OS=Homo sapiens GN=TUBB4B PE=1 SV=1	HUMAN	2
112	0	2.15	10.36	5.18	5.18000014	sp P04350 TBB4A_HUMAN	Tubulin beta-4A chain OS=Homo sapiens GN=TUBB4A PE=1 SV=2	HUMAN	2
112	0	2	8.982	8.982	8.98199975	tr MOR278 MOR278_HUMAN	Tubulin beta-4A chain (Fragment) OS=Homo sapiens GN=TUBB4A PE=4 SV=1	HUMAN	1
112	0	2	14.56	14.56	14.56000006	tr MORX0 MORX0_HUMAN	Tubulin beta-4A chain OS=Homo sapiens GN=TUBB4A PE=4 SV=1	HUMAN	1
112	0	2	9.554	9.554	9.55400002	tr MOQZL7 MOQZL7_HUMAN	Tubulin beta-4A chain (Fragment) OS=Homo sapiens GN=TUBB4A PE=4 SV=2	HUMAN	1
112	0	2	14.02	14.02	14.02000004	tr MOQY85 MOQY85_HUMAN	Tubulin beta-4A chain (Fragment) OS=Homo sapiens GN=TUBB4A PE=4 SV=1	HUMAN	1
112	0	2	13.76	13.76	13.76000005	tr MOQY37 MOQY37_HUMAN	Tubulin beta-4A chain OS=Homo sapiens GN=TUBB4A PE=4 SV=1	HUMAN	1
112	0	2	13.64	13.64	13.63999999	tr MOQX14 MOQX14_HUMAN	Tubulin beta-4A chain OS=Homo sapiens GN=TUBB4A PE=4 SV=1	HUMAN	1
113	2.11	10.42	18.26	11.68	8.99299979	tr P14923 PLAK_HUMAN	Junction plakoglobin OS=Homo sapiens GN=JUP PE=1 SV=3	HUMAN	7
114	2.11	2.11	16.45	16.45	16.44999998	tr J3KND3 J3KND3_HUMAN	Myosin light polypeptide 6 OS=Homo sapiens GN=MYL6 PE=1 SV=1	HUMAN	2
114	0	2.11	30.12	30.12	30.12000002	tr HOYI43 HOYI43_HUMAN	Myosin light polypeptide 6 (Fragment) OS=Homo sapiens GN=MYL6 PE=1 SV=1	HUMAN	2
114	0	2.11	16.45	16.45	16.44999998	tr G8ILA2 G8ILA2_HUMAN	Myosin light polypeptide 6 OS=Homo sapiens GN=MYL6 PE=1 SV=1	HUMAN	2
114	0	2.11	21.74	21.74	21.73999999	tr G3V1Y7 G3V1Y7_HUMAN	Myosin light polypeptide 6 OS=Homo sapiens GN=MYL6 PE=1 SV=1	HUMAN	2
114	0	2.11	15.53	15.53	15.53000006	tr G3V1V0 G3V1V0_HUMAN	Myosin light polypeptide 6 OS=Homo sapiens GN=MYL6 PE=1 SV=1	HUMAN	2
114	0	2.11	17.24	17.24	17.23999998	tr F8W1R7 F8W1R7_HUMAN	Myosin light polypeptide 6 OS=Homo sapiens GN=MYL6 PE=1 SV=1	HUMAN	2
114	0	2.11	12.76	12.76	12.75999999	tr F8W180 F8W180_HUMAN	Myosin light polypeptide 6 OS=Homo sapiens GN=MYL6 PE=1 SV=1	HUMAN	2
114	0	2.11	24.27	24.27	24.26999996	tr F8VZU9 F8VZU9_HUMAN	Myosin light polypeptide 6 OS=Homo sapiens GN=MYL6 PE=1 SV=1	HUMAN	2
114	0	2.11	19.23	19.23	19.23000007	tr F8VPF3 F8VPF3_HUMAN	Myosin light polypeptide 6 (Fragment) OS=Homo sapiens GN=MYL6 PE=1 SV=1	HUMAN	2
114	0	2.11	10.5	10.5	10.49999997	tr B7Z6Z4 B7Z6Z4_HUMAN	Myosin light polypeptide 6 OS=Homo sapiens GN=MYL6 PE=1 SV=1	HUMAN	2
114	0	2.11	16.56	16.56	16.56000002	sp P60660 MYL6_HUMAN	Myosin light polypeptide 6 OS=Homo sapiens GN=MYL6 PE=1 SV=2	HUMAN	2
114	0	2.11	16.56	16.56	16.56000002	sp P60660-2 MYL6_HUMAN	Isoform 2 of Myosin light polypeptide 6 OS=Homo sapiens GN=MYL6	HUMAN	2
115	2.06	14.88	28.46	28.46	27.95000008	sp P48594 SPB4_HUMAN	Serpin B4 OS=Homo sapiens GN=SERPINB4 PE=1 SV=2	HUMAN	12
115	0	14.71	26.95	26.95	26.42000002	tr HOYSH9 HOYSH9_HUMAN	Serpin B4 (Fragment) OS=Homo sapiens GN=SERPINB4 PE=3 SV=1	HUMAN	11
115	0	10.55	22.49	22.49	21.88999995	tr F8W9L1 F8W9L1_HUMAN	Serpin B4 OS=Homo sapiens GN=SERPINB4 PE=3 SV=1	HUMAN	9
115	0	6.58	25.59	25.59	25.58999996	tr C9J265 C9J265_HUMAN	Serpin B4 (Fragment) OS=Homo sapiens GN=SERPINB4 PE=3 SV=1	HUMAN	6
116	2.06	2.06	41.51	35.85	35.85000004	sp P01834 IGKC_HUMAN	Ig kappa chain C region OS=Homo sapiens GN=IGKC PE=1 SV=1	HUMAN	2
117	2.04	8.73	15.17	5.83299994	sp Q9NSB2 KRT84_HUMAN	Keratin, type II cuticular Hb4 OS=Homo sapiens GN=KRT84 PE=2 SV=2	HUMAN	5	
118	2.03	2.03	4.228	0.4612	0.46120002	sp O75369 FLNB_HUMAN	Filamin-B OS=Homo sapiens GN=FLNB PE=1 SV=2	HUMAN	1
118	0	2.03	4.245	0.4631	0.46310001	sp O75369-9 FLNB_HUMAN	Isoform 9 of Filamin-B OS=Homo sapiens GN=FLNB	HUMAN	1

118	0	2.03	4.178	0.4558	0.45579998	sp O75369-8 FLNB_HUMAN	Isoform 8 of Filamin-B OS=Homo sapiens GN=FLNB	HUMAN	1
118	0	2.03	4.336	0.473	0.47300002	sp O75369-6 FLNB_HUMAN	Isoform 6 of Filamin-B OS=Homo sapiens GN=FLNB	HUMAN	1
118	0	2.03	4.295	0.4686	0.46859998	sp O75369-3 FLNB_HUMAN	Isoform 3 of Filamin-B OS=Homo sapiens GN=FLNB	HUMAN	1
118	0	2.03	4.467	0.4655	0.46549998	sp O75369-2 FLNB_HUMAN	Isoform 2 of Filamin-B OS=Homo sapiens GN=FLNB	HUMAN	1
118	0	2.03	3.57	0.4981	0.4981	tr E7EN95 E7EN95_HUMAN	Filamin-B OS=Homo sapiens GN=FLNB PE=1 SV=1	HUMAN	1
118	0	2.03	3.551	0.4955	0.49549998	sp O75369-7 FLNB_HUMAN	Isoform 7 of Filamin-B OS=Homo sapiens GN=FLNB	HUMAN	1
118	0	2.03	4.147	0.5592	0.55920002	sp O75369-5 FLNB_HUMAN	Isoform 5 of Filamin-B OS=Homo sapiens GN=FLNB	HUMAN	1
118	0	2.03	4.14	0.5581	0.55809999	sp O75369-4 FLNB_HUMAN	Isoform 4 of Filamin-B OS=Homo sapiens GN=FLNB	HUMAN	1
119	2.03	2.03	7.823	1.531	1.53099997	sp Q14134 TRI29_HUMAN	Tripartite motif-containing protein 29 OS=Homo sapiens GN=TRIM29 PE=1 SV=2	HUMAN	1
119	0	2.03	8.07	1.579	1.57900006	sp Q14134-2 TRI29_HUMAN	Isoform Beta of Tripartite motif-containing protein 29 OS=Homo sapiens GN=TRIM29	HUMAN	1
119	0	2.03	11.31	2.752	2.75199991	tr E9PRL4 E9PRL4_HUMAN	Tripartite motif-containing protein 29 OS=Homo sapiens GN=TRIM29 PE=1 SV=1	HUMAN	1
119	0	2.03	11.53	2.804	2.80399993	tr B7Z8U9 B7Z8U9_HUMAN	Tripartite motif-containing protein 29 OS=Homo sapiens GN=TRIM29 PE=1 SV=1	HUMAN	1
120	2.03	2.03	15.15	5.303	5.30299991	tr K7EK07 K7EK07_HUMAN	Histone H3 (Fragment) OS=Homo sapiens GN=H3F3B PE=1 SV=1	HUMAN	1
120	0	2.03	14.71	5.147	5.14700003	sp Q71D13 H32_HUMAN	Histone H3.2 OS=Homo sapiens GN=HIST3H3A PE=1 SV=3	HUMAN	1
120	0	2.03	14.71	5.147	5.14700003	sp Q16695 H31T_HUMAN	Histone H3.1t OS=Homo sapiens GN=HIST3H3 PE=1 SV=3	HUMAN	1
120	0	2.03	14.71	5.147	5.14700003	sp P84243 H33_HUMAN	Histone H3.3 OS=Homo sapiens GN=H3F3A PE=1 SV=2	HUMAN	1
120	0	2.03	14.71	5.147	5.14700003	sp P68431 H31_HUMAN	Histone H3.1 OS=Homo sapiens GN=HIST1H3A PE=1 SV=2	HUMAN	1
120	0	2.01	9.272	4.636	4.6360001	tr K7ES00 K7ES00_HUMAN	Histone H3.3 (Fragment) OS=Homo sapiens GN=H3F3B PE=1 SV=1	HUMAN	1
120	0	2.01	15.22	7.609	7.60900006	tr K7EMV3 K7EMV3_HUMAN	Histone H3 OS=Homo sapiens GN=H3F3B PE=1 SV=1	HUMAN	1
120	0	2.01	11.38	5.691	5.69100007	tr B4DEB1 B4DEB1_HUMAN	Histone H3 OS=Homo sapiens GN=H3F3A PE=1 SV=1	HUMAN	1
120	0	2.01	9.63	5.185	5.18499985	sp Q6NXT7 H3C_HUMAN	Histone H3.3C OS=Homo sapiens GN=H3F3C PE=1 SV=3	HUMAN	1
120	0	2	5.147	5.14700003	tr Q5TEC6 Q5TEC6_HUMAN	Histone H3 OS=Homo sapiens GN=HIST3H3 PE=1 SV=1	HUMAN	1	
120	0	2	6.195	6.195	6.19499981	tr K7EP01 K7EP01_HUMAN	Histone H3.3 OS=Homo sapiens GN=H3F3B PE=1 SV=1	HUMAN	1
121	2.02	2.02	12.34	3.048	3.04799993	sp O15231 ZNF185_HUMAN	Zinc finger protein 185 OS=Homo sapiens GN=ZNF185 PE=1 SV=3	HUMAN	2
121	0	2.02	12.32	3.043	3.04300003	sp O15231-3 ZNF185_HUMAN	Isoform 3 of Zinc finger protein 185 OS=Homo sapiens GN=ZNF185	HUMAN	2
121	0	2.02	11.23	2.913	2.91300006	sp O15231-6 ZNF185_HUMAN	Isoform 6 of Zinc finger protein 185 OS=Homo sapiens GN=ZNF185	HUMAN	2
122	2.02	2.02	11.75	4.046	4.04600017	tr F5H5D3 F5H5D3_HUMAN	Tubulin alpha-1C chain OS=Homo sapiens GN=TUBA1C PE=1 SV=1	HUMAN	2
122	0	2.02	13.59	4.677	4.67699999	sp Q9BQE3 TBA1C_HUMAN	Tubulin alpha-1C chain OS=Homo sapiens GN=TUBA1C PE=1 SV=1	HUMAN	2
122	0	2.02	13.53	4.656	4.65600006	sp Q71U36 TBA1A_HUMAN	Tubulin alpha-1A chain OS=Homo sapiens GN=TUBA1A PE=1 SV=1	HUMAN	2
122	0	2.02	14.66	5.048	5.04800007	sp Q71U36-2 TBA1A_HUMAN	Isoform 2 of Tubulin alpha-1A chain OS=Homo sapiens GN=TUBA1A	HUMAN	2
122	0	2.02	13.53	4.656	4.65600006	sp P68363 TBA1B_HUMAN	Tubulin alpha-1B chain OS=Homo sapiens GN=TUBA1B PE=1 SV=1	HUMAN	2
122	0	2.02	8.889	4.667	4.6670001	sp Q13748 TBA3C_HUMAN	Tubulin alpha-3C/D chain OS=Homo sapiens GN=TUBA3C PE=1 SV=3	HUMAN	2
122	0	2.02	9.569	5.024	5.02399988	sp Q13748-2 TBA3C_HUMAN	Isoform 2 of Tubulin alpha-3C/D chain OS=Homo sapiens GN=TUBA3C	HUMAN	2
122	0	2.01	13.43	6.269	6.26899973	sp P68363-2 TBA1B_HUMAN	Isoform 2 of Tubulin alpha-1B chain OS=Homo sapiens GN=TUBA1B	HUMAN	2
122	0	2.01	7.333	4.667	4.6670001	sp Q6PEV2 TBA3E_HUMAN	Tubulin alpha-3E chain OS=Homo sapiens GN=TUBA3E PE=1 SV=2	HUMAN	2
123	2.01	2.01	5.206	0.9332	0.93320003	tr G8JLL9 G8JLL9_HUMAN	Myosin-14 OS=Homo sapiens GN=MYH14 PE=1 SV=1	HUMAN	2
123	0	2.01	5.227	0.9369	0.93689999	tr F2Z2U8 F2Z2U8_HUMAN	Myosin-14 OS=Homo sapiens GN=MYH14 PE=1 SV=1	HUMAN	2
123	0	2.01	5.313	0.9524	0.95239999	sp Q72406 MYH14_HUMAN	Myosin-14 OS=Homo sapiens GN=MYH14 PE=1 SV=2	HUMAN	2
123	0	2.01	5.292	0.9486	0.94860001	sp Q72406-6 MYH14_HUMAN	Isoform 6 of Myosin-14 OS=Homo sapiens GN=MYH14	HUMAN	2
123	0	2.01	5.206	0.9332	0.93320003	sp Q72406-2 MYH14_HUMAN	Isoform 2 of Myosin-14 OS=Homo sapiens GN=MYH14	HUMAN	2
123	0	2	5.21	0.6766	0.67659998	sp Q72406-5 MYH14_HUMAN	Isoform 5 of Myosin-14 OS=Homo sapiens GN=MYH14	HUMAN	1
124	2	35.27	52.41	46.93	33.98999997	sp P19012 K1C15_HUMAN	Keratin, type I cytoskeletal 15 OS=Homo sapiens GN=KRT15 PE=1 SV=3	HUMAN	37
124	0	19.58	66.53	55.4600012	tr B3KRA2 B3KRA2_HUMAN	Keratin, type I cytoskeletal 15 OS=Homo sapiens GN=KRT15 PE=1 SV=1	HUMAN	16	
124	0	19.58	57.39	48.8	30.5799991	tr A8MT21 A8MT21_HUMAN	Keratin, type I cytoskeletal 15 OS=Homo sapiens GN=KRT15 PE=1 SV=1	HUMAN	16
124	0	11.16	59.09	52.73	28.6399999	tr C9JTG5 C9JTG5_HUMAN	Keratin, type I cytoskeletal 15 (Fragment) OS=Homo sapiens GN=KRT15 PE=1 SV=1	HUMAN	9
125	2	8.12	13.67	8.564	6.07700013	sp P08238 HS90B_HUMAN	Heat shock protein HSP 90-beta OS=Homo sapiens GN=HSP90AB1 PE=1 SV=4	HUMAN	4
125	0	6.1	15.75	11.02	7.87400007	sp Q58F78 H90B2_HUMAN	Putative heat shock protein HSP 90-beta 2 OS=Homo sapiens GN=HSP90AB2 PE=1 SV=2	HUMAN	3
125	0	6	10.05	5.863	5.86300008	sp Q58F77 H90B3_HUMAN	Putative heat shock protein HSP 90-beta 3 OS=Homo sapiens GN=HSP90AB3 PE=5 SV=1	HUMAN	3
125	0	4	7.327	4.158	4.15799999	sp Q58F76 H90B4_HUMAN	Putative heat shock protein HSP 90-beta 4 OS=Homo sapiens GN=HSP90AB4 PE=5 SV=1	HUMAN	2
125	0	4	24.4	12.5	12.5	tr Q5T9W8 Q5T9W8_HUMAN	Heat shock protein HSP 90-beta (Fragment) OS=Homo sapiens GN=HSP90AB1 PE=4 SV=1	HUMAN	2
125	0	2	3.861	1.494	1.49400001	sp P14625 ENPL_HUMAN	Endoplasmic OS=Homo sapiens GN=HSP90B1 PE=1 SV=1	HUMAN	1
125	0	2	25	25	25	tr F8W026 F8W026_HUMAN	Endoplasmic (Fragment) OS=Homo sapiens GN=HSP90B1 PE=1 SV=2	HUMAN	1
126	2	4.66	15.85	15.45	15.44999993	sp P31946 I433B_HUMAN	14-3-3 protein beta/alpha OS=Homo sapiens GN=YWHAB PE=1 SV=3	HUMAN	4
126	0	4.66	15.98	15.57	15.5699998	sp P31946-2 I433B_HUMAN	Isoform Short of 14-3-3 protein beta/alpha OS=Homo sapiens GN=YWHAB	HUMAN	4
127	2	4.43	13.39	5.477	3.85999982	sp P78385 KRT83_HUMAN	Keratin, type II cuticular Hb3 OS=Homo sapiens GN=KRT83 PE=1 SV=2	HUMAN	3
127	0	4.43	11.49	3.477	3.76200005	sp Q14533 KRT81_HUMAN	Keratin, type II cuticular Hb1 OS=Homo sapiens GN=KRT81 PE=1 SV=3	HUMAN	3
127	0	4.43	12.23	6.903	5.32499999	sp P78386 KRT85_HUMAN	Keratin, type II cuticular Hb5 OS=Homo sapiens GN=KRT85 PE=1 SV=1	HUMAN	4
127	0	4.43	11.93	5.556	3.90900001	sp O43790 KRT86_HUMAN	Keratin, type II cuticular Hb6 OS=Homo sapiens GN=KRT86 PE=1 SV=1	HUMAN	3
127	0	4.17	15.93	9.492	9.15300027	tr F5GY15 F5GY15_HUMAN	Keratin, type II cuticular Hb5 OS=Homo sapiens GN=KRT85 PE=3 SV=1	HUMAN	4
127	0	2	18.43	3.922	3.92200015	sp A6NCN2 KR87P_HUMAN	Putative keratin-87 protein OS=Homo sapiens GN=KRT87P PE=5 SV=4	HUMAN	1
128	2	2	9.524	1.587	1.58699993	sp P13797 PLST_HUMAN	Plastin-3 OS=Homo sapiens GN=PLS3 PE=1 SV=4	HUMAN	1
128	0	2	8.249	1.684	1.68399997	tr F8W8D8 F8W8D8_HUMAN	Plastin-3 OS=Homo sapiens GN=PLS3 PE=1 SV=1	HUMAN	1
128	0	2	8.376	1.709	1.70900002	tr B7Z6M1 B7Z6M1_HUMAN	Plastin-3 OS=Homo sapiens GN=PLS3 PE=1 SV=1	HUMAN	1
128	0	2	7.942	1.621	1.62099991	tr B4DGB4 B4DGB4_HUMAN	Plastin-3 OS=Homo sapiens GN=PLS3 PE=1 SV=1	HUMAN	1
129	2	2	7.403	1.129	1.12899998	sp Q9Y446 PKP3_HUMAN	Plakophilin-3 OS=Homo sapiens GN=PKP3 PE=1 SV=1	HUMAN	1
129	0	2	7.266	1.108	1.10799996	sp Q9Y446-2 PKP3_HUMAN	Isoform PKP3b of Plakophilin-3 OS=Homo sapiens GN=PKP3	HUMAN	1
129	0	2	13.68	4.245	4.24499996	tr E9PK71 E9PK71_HUMAN	Plakophilin-3 (Fragment) OS=Homo sapiens GN=PKP3 PE=1 SV=1	HUMAN	1
129	0	2	12.18	5.769	5.76899983	tr E9PRW6 E9PRW6_HUMAN	Plakophilin-3 (Fragment) OS=Homo sapiens GN=PKP3 PE=1 SV=1	HUMAN	1
129	0	2	9.645	4.569	4.56900001	tr E9PKC4 E9PKC4_HUMAN	Plakophilin-3 (Fragment) OS=Homo sapiens GN=PKP3 PE=1 SV=1	HUMAN	1
129	0	2	15.83	7.5	7.5000003	tr E9PJR7 E9PJR7_HUMAN	Plakophilin-3 (Fragment) OS=Homo sapiens GN=PKP3 PE=1 SV=1	HUMAN	1
129	0	2	11.84	11.84	11.84	tr E9PQ15 E9PQ15_HUMAN	Plakophilin-3 (Fragment) OS=Homo sapiens GN=PKP3 PE=1 SV=1	HUMAN	1
130	2	2	8.828	1.981	0.93240002	sp P13639 EF2_HUMAN	Elongation factor 2 OS=Homo sapiens GN=EEF2 PE=1 SV=4	HUMAN	1
131	2	2	10.82	4.329	4.32900004	tr G3V576 G3V576_HUMAN	Heterogeneous nuclear ribonucleoproteins C1/C2 OS=Homo sapiens GN=HNRNCP PE=1 SV=1	HUMAN	1
131	0	2	9.542	3.817	3.81699987	tr G3V4W0 G3V4W0_HUMAN	Heterogeneous nuclear ribonucleoproteins C1/C2 (Fragment) OS=Homo sapiens GN=HNRNF HUMAN	HUMAN	1
131	0	2	8.562	3.425	3.42499986	tr G3V4C1 G3V4C1_HUMAN	Heterogeneous nuclear ribonucleoproteins C1/C2 OS=Homo sapiens GN=HNRNCP PE=1 SV=1	HUMAN	1
131	0	2	8.197	3.279	3.27900015	tr G3V2Q1 G3V2Q1_HUMAN	Heterogeneous nuclear ribonucleoproteins C1/C2 OS=Homo sapiens GN=HNRNCP PE=1 SV=1	HUMAN	1
131	0	2	8.681	3.472	3.47199999	tr B4DY08 B4DY08_HUMAN	Heterogeneous nuclear ribonucleoproteins C1/C2 OS=Homo sapiens GN=HNRNCP PE=1 SV=1	HUMAN	1
131	0	2	8.17	3.268	3.26800011	sp P07910 HNRPC_HUMAN	Heterogeneous nuclear ribonucleoproteins C1/C2 OS=Homo sapiens GN=HNRNCP PE=1 SV=1	HUMAN	1
131	0	2	10	4	3.99999991	sp P07910-4 HNRPC_HUMAN	Isoform 4 of Heterogeneous nuclear ribonucleoproteins C1/C2 OS=Homo sapiens GN=HNRNCP HUMAN	HUMAN	1
131	0	2	11.06	4.425	4.42500003	sp P07910-3 HNRPC_HUMAN	Isoform 3 of Heterogeneous nuclear ribonucleoproteins C1/C2 OS=Homo sapiens GN=HNRNCP HUMAN	HUMAN	1
131	0	2	8.532	3.413	3.41299996	sp P07910-2 HNRPC_HUMAN	Isoform C1 of Heterogeneous nuclear ribonucleoproteins C1/C2 OS=Homo sapiens GN=HNRNCP HUMAN	HUMAN	1
131	0	2	8.889	5.556	5.55600002	tr G3V5V7 G3V5V7_HUMAN	Heterogeneous nuclear ribonucleoproteins C1/C2 (Fragment) OS=Homo sapiens GN=HNRNF HUMAN	HUMAN	1
131	0	2	7.477	4.673	4.67300005	tr G3V2D6 G3V2D6_HUMAN	Heterogeneous nuclear ribonucleoproteins C1/C2 (Fragment) OS=Homo sapiens GN=HNRNF HUMAN	HUMAN	1
131	0	2	5.461	3.413	3.41299996	sp O60812 HNRCL_HUMAN	Heterogeneous nuclear ribonucleoprotein C-like 1 OS=Homo sapiens GN=HNRNCP1 PE=1 SV=1	HUMAN	1
132	2	2	13.81	3.81	3.81000005	tr F5H423 F5H423_HUMAN	Uncharacterized protein OS=Homo sapiens PE=3 SV=1	HUMAN	1
132	0	2	20.14	5.556	5.55600002	tr B7ZB63 B7ZB63_HUMAN	ADP-ribosylation factor 3 OS=Homo sapiens GN=ARF3 PE=2 SV=1	HUMAN	1
132	0	2	16.02	4.42	4.41999994	sp P84077 ARF1_HUMAN	ADP-ribosylation factor 1 OS=Homo sapiens GN=ARF1 PE=1 SV=2	HUMAN	1
132	0	2	16.02	4.42	4.41999994	sp P61204 ARF3_HUMAN	ADP-ribosylation factor 3 OS=Homo sapiens GN=ARF3 PE=1 SV=2	HUMAN	1
133	2	2	9.06	2.685	2.685	sp P05141 ADT2_HUMAN	ADP/ATP translocase 2 OS=Homo sapiens GN=SLC25A5 PE=1 SV=7	HUMAN	1
133	0	2	8.173	3.846	3.84600013	tr V9GYG0 V9GYG0_HUMAN	ADP/ATP translocase 1 OS=Homo sapiens GN=SLC25A4 PE=1 SV=1	HUMAN	1
133	0	2	6.032	2.54	2.53999997	sp Q9HOC2 ADT4_HUMAN	ADP/ATP translocase 4 OS=Homo sapiens GN=SLC25A31 PE=2 SV=1	HUMAN	1
133	0	2	5.705	2.685	2.685	sp P12235 ADT1_HUMAN	ADP/ATP translocase 1 OS=Homo sapiens GN=SLC25A4 PE=1 SV=4	HUMAN	1
133	0	2	5.063	5.063	5.06299995	tr H7HJ0 H7HJ0_HUMAN	ADP/ATP translocase 3 (Fragment) OS=Homo sapiens GN=SLC25A6 PE=1 SV=1	HUMAN	1
133	0	2	2.685	2.685	2.685	sp P12236 ADT3_HUMAN	ADP/ATP translocase 3 OS=Homo sapiens GN=SLC25A6 PE=1 SV=4	HUMAN	1
134	2	2	2.105	0.6615	0.66149998	sp P01024 CO3_HUMAN	Complement C3 OS=Homo sapiens GN=C3 PE=1 SV=2	HUMAN	1
135	2	2	10.64	6.383	6.38300031	tr J3QX2 J3QX2_HUMAN	Rho GDP-dissociation inhibitor 1 OS=Homo sapiens GN=ARHGDI1 PE=1 SV=1	HUMAN	1
135	0	2	12.95	7.772	7.77200013	tr J3KTF8 J3KTF8_HUMAN	Rho GDP-dissociation inhibitor 1 (Fragment) OS=Homo sapiens GN=ARHGDI1 PE=1 SV=2	HUMAN	1
135	0	2	19.38	11.63	11.6300002	tr J3KRE2 J3KRE2_HUMAN	Rho GDP-dissociation inhibitor 1 OS=Homo sapiens GN=ARHGDI1 PE=1 SV=1	HUMAN	1

135	0	2	12.25	7.353	7.35300034	sp P52565 GDRI1_HUMAN	Rho GDP-dissociation inhibitor 1 OS=Homo sapiens GN=ARHGODIA PE=1 SV=3	HUMAN	1
136	2	2	3.09	2.528	2.52800006	tr F5H3P5 F5H3P5_HUMAN	Actin-related protein 3 OS=Homo sapiens GN=ACTR3 PE=1 SV=1	HUMAN	1
136	0	2	2.997	2.452	2.45200004	tr B4DXW1 B4DXW1_HUMAN	Actin-related protein 3 OS=Homo sapiens GN=ACTR3 PE=1 SV=1	HUMAN	1
136	0	2	2.632	2.153	2.15300005	sp P61158 ARP3_HUMAN	Actin-related protein 3 OS=Homo sapiens GN=ACTR3 PE=1 SV=3	HUMAN	1
136	0	2	2.153	2.153	2.15300005	sp Q9P1U1 ARP3B_HUMAN	Actin-related protein 3B OS=Homo sapiens GN=ACTR3B PE=2 SV=1	HUMAN	1
136	0	2	2.719	2.719	2.71899998	sp Q9P1U1-2 ARP3B_HUMAN	Isoform 2 of Actin-related protein 3B OS=Homo sapiens GN=ACTR3B	HUMAN	1
137	2	2	11.54	6.25	6.25	tr ABMUD9 ABMUD9_HUMAN	60S ribosomal protein L7 OS=Homo sapiens GN=RPL7 PE=1 SV=1	HUMAN	1
137	0	2	9.677	5.242	5.24200015	sp P18124 RL7_HUMAN	60S ribosomal protein L7 OS=Homo sapiens GN=RPL7 PE=1 SV=1	HUMAN	1
138	2	2	2.959	4.444	4.44400012	sp Q9H008 LHP_HUMAN	Phospholysine phosphohistidine inorganic pyrophosphate phosphatase OS=Homo sapiens	HUMAN	1
139	2	2	9.94	5.723	5.72299995	sp P29666 MARCS_HUMAN	Myristoylated alanine-rich C-kinase substrate OS=Homo sapiens GN=MARCS PE=1 SV=4	HUMAN	1
140	2	2	21.05	21.05	13.6800006	sp P25815 S100P_HUMAN	Protein S100-P OS=Homo sapiens GN=S100P PE=1 SV=2	HUMAN	1
141	2	2	7.429	7.429	7.42899999	tr K7ERT8 K7ERT8_HUMAN	60S ribosomal protein L23a (Fragment) OS=Homo sapiens GN=RPL23A PE=1 SV=1	HUMAN	1
141	0	2	18.57	18.57	18.56999999	tr K7EMA7 K7EMA7_HUMAN	60S ribosomal protein L23a OS=Homo sapiens GN=RPL23A PE=1 SV=1	HUMAN	1
141	0	2	7.647	7.647	7.64700025	tr K7EJ99 K7EJ99_HUMAN	60S ribosomal protein L23a (Fragment) OS=Homo sapiens GN=RPL23A PE=1 SV=1	HUMAN	1
141	0	2	8.228	8.228	8.22800025	tr H7BY10 H7BY10_HUMAN	60S ribosomal protein L23a (Fragment) OS=Homo sapiens GN=RPL23A PE=1 SV=1	HUMAN	1
141	0	2	6.701	6.701	6.70100003	tr ABMU53 ABMU53_HUMAN	60S ribosomal protein L23a OS=Homo sapiens GN=RPL23A PE=1 SV=1	HUMAN	1
141	0	2	8.333	8.333	8.33299998	sp P62750 RL23A_HUMAN	60S ribosomal protein L23a OS=Homo sapiens GN=RPL23A PE=1 SV=1	HUMAN	1
142	0	2	9.615	9.615	9.61500034	tr K7EJ44 K7EJ44_HUMAN	Profilin 1, isoform CRA_b OS=Homo sapiens GN=PFN1 PE=1 SV=1	HUMAN	1
142	0	2	7.143	7.143	7.14299977	sp P07737 PROF1_HUMAN	Profilin-1 OS=Homo sapiens GN=PFN1 PE=1 SV=2	HUMAN	1
143	2	2	4.663	4.663	4.66299988	tr J3QR09 J3QR09_HUMAN	Ribosomal protein L19 OS=Homo sapiens GN=RPL19 PE=1 SV=1	HUMAN	1
143	0	2	4.639	4.639	4.63900007	tr J3KTE4 J3KTE4_HUMAN	Ribosomal protein L19 OS=Homo sapiens GN=RPL19 PE=1 SV=1	HUMAN	1
143	0	2	4.592	4.592	4.59199995	sp P84098 RL19_HUMAN	60S ribosomal protein L19 OS=Homo sapiens GN=RPL19 PE=1 SV=1	HUMAN	1
144	2	2	10.59	10.59	10.58999997	tr F8VV13 F8VV13_HUMAN	Mucin-like protein 1 OS=Homo sapiens GN=MUCL1 PE=4 SV=1	HUMAN	1
144	0	2	10	10	10.0000001	sp Q96DR8 MUCL1_HUMAN	Mucin-like protein 1 OS=Homo sapiens GN=MUCL1 PE=1 SV=1	HUMAN	1
145	2	2	4.721	4.721	4.72100005	tr E7ETU3 E7ETU3_HUMAN	Cell division control protein 42 homolog OS=Homo sapiens GN=CDC42 PE=1 SV=1	HUMAN	1
145	0	2	5.759	5.759	5.75900003	sp P60953 CDC42_HUMAN	Cell division control protein 42 homolog OS=Homo sapiens GN=CDC42 PE=1 SV=2	HUMAN	1
145	0	2	5.759	5.759	5.75900003	sp P60953-1 CDC42_HUMAN	Isoform 1 of Cell division control protein 42 homolog OS=Homo sapiens GN=CDC42	HUMAN	1
146	2	2	2.128	2.128	2.128	sp Q9UL52 TM11E_HUMAN	Transmembrane peptidase serine 11E OS=Homo sapiens GN=TMPRSS11E PE=1 SV=2	HUMAN	1
147	2	2	4	4	3.99999991	sp Q6ZVX7 FBX50_HUMAN	F-box only protein 50 OS=Homo sapiens GN=NCCRPI1 PE=1 SV=1	HUMAN	1
148	2	2	7.031	7.031	7.03099996	sp Q14210 LY6D_HUMAN	Lymphocyte antigen 6D OS=Homo sapiens GN=LY6D PE=1 SV=1	HUMAN	1
149	2	2	2.833	2.833	2.83300001	sp P22626 ROA2_HUMAN	Heterogeneous nuclear ribonucleoproteins A2/B1 OS=Homo sapiens GN=HNRPA2B1 PE=1	HUMAN	1
149	0	2	2.933	2.933	2.93300003	sp P22626-2 ROA2_HUMAN	Isoform A2 of Heterogeneous nuclear ribonucleoproteins A2/B1 OS=Homo sapiens GN=HNR	HUMAN	1
150	2	2	18.95	18.95	18.95000004	sp P21145 MAL_HUMAN	Myelin and lymphocyte protein OS=Homo sapiens GN=MAL PE=1 SV=1	HUMAN	1
150	0	2	29.9	29.9	29.8999995	sp P21145-3 MAL_HUMAN	Isoform C of Myelin and lymphocyte protein OS=Homo sapiens GN=MAL	HUMAN	1
151	2	2	2.36	2.36	2.36000009	sp P07858 CATB_HUMAN	Cathepsin B OS=Homo sapiens GN=CTSB PE=1 SV=3	HUMAN	1
152	2	2	3.084	3.084	3.08400001	sp P00403 COX2_HUMAN	Cytochrome c oxidase subunit 2 OS=Homo sapiens GN=MT-CO2 PE=1 SV=1	HUMAN	1
153	2	2	3.14	3.14	3.13999988	sp O75874 IDHC_HUMAN	Isoictrate dehydrogenase [NADP] cytoplasmic OS=Homo sapiens GN=IDH1 PE=1 SV=2	HUMAN	1
154	1.83	1.83	9.543	4.97	3.57900001	tr F5H7G9 F5H7G9_HUMAN	Guanylate-binding protein 6 OS=Homo sapiens GN=GBP6 PE=4 SV=1	HUMAN	2
154	0	1.83	7.583	3.949	2.84400005	sp Q6ZN66 GBP6_HUMAN	Guanylate-binding protein 6 OS=Homo sapiens GN=GBP6 PE=2 SV=1	HUMAN	2
154	0	1.8	8.446	3.378	3.37800011	sp Q6ZN66-2 GBP6_HUMAN	Isoform 2 of Guanylate-binding protein 6 OS=Homo sapiens GN=GBP6	HUMAN	2
155	1.73	1.73	4.29	2.805	1.48499999	sp O75083 WDR1_HUMAN	WD repeat-containing protein 1 OS=Homo sapiens GN=WDR1 PE=1 SV=4	HUMAN	1
155	0	1.7	1.931	1.931	1.93099994	sp O75083-3 WDR1_HUMAN	Isoform 2 of WD repeat-containing protein 1 OS=Homo sapiens GN=WDR1	HUMAN	1
156	1.68	1.68	10.33	2.952	2.95199994	tr J3QL43 J3QL43_HUMAN	Eukaryotic initiation factor 4A-I (Fragment) OS=Homo sapiens GN=EIF4A1 PE=1 SV=1	HUMAN	1
156	0	1.68	8.211	2.346	2.34600008	tr J3KT12 J3KT12_HUMAN	Eukaryotic initiation factor 4A-I OS=Homo sapiens GN=EIF4A1 PE=1 SV=1	HUMAN	1
156	0	1.68	6.897	1.97	1.97000001	sp P60842 IF4A1_HUMAN	Eukaryotic initiation factor 4A-I OS=Homo sapiens GN=EIF4A1 PE=1 SV=1	HUMAN	1
156	0	1.68	8.069	2.305	2.30500009	sp P60842-2 IF4A1_HUMAN	Isoform 2 of Eukaryotic initiation factor 4A-I OS=Homo sapiens GN=EIF4A1	HUMAN	1
156	0	1.68	7.944	3.738	3.73799987	tr J3QR64 J3QR64_HUMAN	Eukaryotic initiation factor 4A-I (Fragment) OS=Homo sapiens GN=EIF4A1 PE=1 SV=1	HUMAN	1
156	0	1.68	10.43	4.908	4.90799993	tr J3QLN6 J3QLN6_HUMAN	Eukaryotic initiation factor 4A-I (Fragment) OS=Homo sapiens GN=EIF4A1 PE=1 SV=1	HUMAN	1
156	0	1.68	6.615	3.113	3.11299991	tr J3KTB5 J3KTB5_HUMAN	Eukaryotic initiation factor 4A-I (Fragment) OS=Homo sapiens GN=EIF4A1 PE=1 SV=1	HUMAN	1
156	0	1.68	5.249	2.21	2.20999997	tr E7EQG2 E7EQG2_HUMAN	Eukaryotic initiation factor 4A-I OS=Homo sapiens GN=EIF4A2 PE=1 SV=1	HUMAN	1
156	0	1.68	4.668	1.966	1.96599998	sp Q14240 IF4A2_HUMAN	Eukaryotic initiation factor 4A-II OS=Homo sapiens GN=EIF4A2 PE=1 SV=2	HUMAN	1
156	0	1.68	4.657	1.961	1.96100008	sp Q14240-2 IF4A2_HUMAN	Isoform 2 of Eukaryotic initiation factor 4A-II OS=Homo sapiens GN=EIF4A2	HUMAN	1
156	0	1.68	5.97	5.97	5.97000001	tr J3QKZ9 J3QKZ9_HUMAN	Eukaryotic initiation factor 4A-I (Fragment) OS=Homo sapiens GN=EIF4A1 PE=1 SV=2	HUMAN	1
156	0	1.68	7.339	7.339	7.33899996	tr J3KSN7 J3KSN7_HUMAN	Eukaryotic initiation factor 4A-II (Fragment) OS=Homo sapiens GN=EIF4A2 PE=1 SV=1	HUMAN	1
156	0	1.68	4.278	4.278	4.27800007	tr J3KS25 J3KS25_HUMAN	Eukaryotic initiation factor 4A-I (Fragment) OS=Homo sapiens GN=EIF4A1 PE=1 SV=2	HUMAN	1
157	1.64	1.64	2.145	2.145	2.14499999	sp P15104 GLNA_HUMAN	Glutamine synthetase OS=Homo sapiens GN=GLUL PE=1 SV=4	HUMAN	1
158	1.6	1.6	18.87	18.87	18.87000005	cont 000091	g 284262 pir S23202 kappa-casein - bovine [Bos taurus (contaminant)]	Bos taurus (c	1
159	1.55	1.55	14.95	7.477	7.47700036	tr B1AH87 B1AH87_HUMAN	Putative peripheral benzodiazepine receptor-related protein (Fragment) OS=Homo sapiens	(HUMAN	1
159	0	1.55	9.467	4.734	4.73399982	sp P03056 TSPOA_HUMAN	Translocator protein OS=Homo sapiens GN=TSPO PE=1 SV=3	HUMAN	1
160	1.49	1.49	6.883	2.024	2.02399995	sp P49189 ALSA1_HUMAN	4-trimethylaminobutyraldehyde dehydrogenase OS=Homo sapiens GN=ALDH9A1 PE=1 SV=3	HUMAN	1
160	0	1.49	4.717	2.358	2.35799998	tr B4DXY7 B4DXY7_HUMAN	4-trimethylaminobutyraldehyde dehydrogenase OS=Homo sapiens GN=ALDH9A1 PE=1 SV=1	HUMAN	1
161	1.47	1.47	3.955	3.955	3.95499989	sp P18510 IL1RA_HUMAN	Interleukin-1 receptor antagonist protein OS=Homo sapiens GN=IL1RN PE=1 SV=1	HUMAN	1
161	0	1.47	4.895	4.895	4.89500016	sp P18510-4 IL1RA_HUMAN	Isoform 4 of Interleukin-1 receptor antagonist protein OS=Homo sapiens GN=IL1RN	HUMAN	1
161	0	1.47	3.889	3.889	3.88900004	sp P18510-3 IL1RA_HUMAN	Isoform 3 of Interleukin-1 receptor antagonist protein OS=Homo sapiens GN=IL1RN	HUMAN	1
161	0	1.47	4.403	4.403	4.40299995	sp P18510-2 IL1RA_HUMAN	Isoform 2 of Interleukin-1 receptor antagonist protein OS=Homo sapiens GN=IL1RN	HUMAN	1
162	1.42	1.42	6.506	2.401	2.41	sp P05120 PAI2_HUMAN	Plasminogen activator inhibitor 2 OS=Homo sapiens GN=SERPINB2 PE=1 SV=2	HUMAN	1
163	1.35	1.35	5.882	1.505	1.50499996	sp Q9BSW2-2 EFC4B_HUMAN	Isoform 2 of EF-hand calcium-binding domain-containing protein 4B OS=Homo sapiens GN=	HUMAN	1
163	0.01	1.35	9	9	5.49999997	sp P61026 RAB10_HUMAN	Ras-related protein Rab-10 OS=Homo sapiens GN=RAB10 PE=1 SV=1	HUMAN	1
163	0	1.35	15.6	5.046	5.04599996	sp O00194 RB27B_HUMAN	Ras-related protein Rab-27B OS=Homo sapiens GN=RAB27B PE=1 SV=4	HUMAN	1
163	0	1.35	14.05	5.946	5.94599992	tr H3BN55 H3BN55_HUMAN	Ras-related protein Rab-27A (Fragment) OS=Homo sapiens GN=RAB27A PE=1 SV=1	HUMAN	1
163	0	1.35	11.35	1.486	1.48600005	sp Q8IZ41 RASEF_HUMAN	Ras and EF-hand domain-containing protein OS=Homo sapiens GN=RASEF PE=1 SV=1	HUMAN	1
163	0	1.35	1.716	4.977	4.97700013	sp P51159 RB27A_HUMAN	Ras-related protein Rab-27A OS=Homo sapiens GN=RAB27A PE=1 SV=3	HUMAN	1
163	0	1.35	12.21	5.164	5.16400002	sp P51159-2 RB27A_HUMAN	Isoform Short of Ras-related protein Rab-27A OS=Homo sapiens GN=RAB27A	HUMAN	1
163	0	1.35	20.83	6.548	6.54800013	tr E9PMJ1 E9PMJ1_HUMAN	Ras-related protein Rab-30 (Fragment) OS=Homo sapiens GN=RAB30 PE=1 SV=1	HUMAN	1
163	0	1.35	14.98	5.314	5.31399995	tr B4DEK7 B4DEK7_HUMAN	Ras-related protein Rab-8A OS=Homo sapiens GN=RAB8A PE=1 SV=1	HUMAN	1
163	0	1.35	10.38	8.491	5.18900007	sp Q86Y56 RAB43_HUMAN	Ras-related protein Rab-43 OS=Homo sapiens GN=RAB43 PE=1 SV=1	HUMAN	1
163	0	1.35	4.426	1.521	1.52099999	sp Q7Z6P3 RAB44_HUMAN	Ras-related protein Rab-44 OS=Homo sapiens GN=RAB44 PE=3 SV=3	HUMAN	1
163	0	1.35	17.24	5.419	5.41899987	sp Q15771 RAB30_HUMAN	Ras-related protein Rab-30 OS=Homo sapiens GN=RAB30 PE=1 SV=2	HUMAN	1
163	0	1.35	14.98	5.314	5.31399995	sp P61006 RAB8A_HUMAN	Ras-related protein Rab-8A OS=Homo sapiens GN=RAB8A PE=1 SV=1	HUMAN	1
163	0	1.35	11.05	6.077	6.07700013	tr X6RFL8 X6RFL8_HUMAN	Ras-related protein Rab-14 (Fragment) OS=Homo sapiens GN=RAB14 PE=3 SV=1	HUMAN	1
163	0	1.35	19.81	10.38	10.37999999	tr Q6MZ6 Q6MZ6_HUMAN	Putative uncharacterized protein DKFZp686I06205 OS=Homo sapiens GN=DKFZp686I06205	HUMAN	1
163	0	1.35	11.6	6.077	6.07700013	tr MOR1E0 MOR1E0_HUMAN	Ras-related protein Rab-4B (Fragment) OS=Homo sapiens GN=RAB4B PE=1 SV=1	HUMAN	1
163	0	1.35	10.94	5.729	5.72899999	tr MOROX1 MOROX1_HUMAN	Ras-related protein Rab-4B (Fragment) OS=Homo sapiens GN=RAB4B PE=1 SV=1	HUMAN	1
163	0	1.35	21.84	12.64	12.63999994	tr K7E541 K7E541_HUMAN	Ras-related protein Rab-27B (Fragment) OS=Homo sapiens GN=RAB27B PE=4 SV=1	HUMAN	1
163	0	1.35	15	7.857	7.85700008	tr J3QSF4 J3QSF4_HUMAN	Ras-related protein Rab-15 (Fragment) OS=Homo sapiens GN=RAB15 PE=1 SV=1	HUMAN	1
163	0	1.35	15.32	8.871	8.87100026	tr J3KR73 J3KR73_HUMAN	Ras-related protein Rab-6B (Fragment) OS=Homo sapiens GN=RAB6B PE=1 SV=1	HUMAN	1
163	0	1.35	13.01	7.534	7.53400028	tr H3BVB7 H3BVB7_HUMAN	Ras-related protein Rab-27A (Fragment) OS=Homo sapiens GN=RAB27A PE=1 SV=1	HUMAN	1
163	0	1.35	20	11.58	11.58000001	tr H3BUD9 H3BUD9_HUMAN	Ras-related protein Rab-27A (Fragment) OS=Homo sapiens GN=RAB27A PE=1 SV=1	HUMAN	1
163	0	1.35	13.97	8.088	8.08800012	tr H3BS49 H3BS49_HUMAN	Ras-related protein Rab-27A (Fragment) OS=Homo sapiens GN=RAB27A PE=1 SV=1	HUMAN	1
163	0	1.35	14.37	6.587	6.58700019	tr HOYDK7 HOYDK7_HUMAN	Ras-related protein Rab-30 (Fragment) OS=Homo sapiens GN=RAB30 PE=1 SV=1	HUMAN	1
163	0	1.35	12.97	5.946	5.94599992	tr F5H157 F5H157_HUMAN	Ras-related protein Rab-35 (Fragment) OS=Homo sapiens GN=RAB35 PE=1 SV=1	HUMAN	1
163	0	1.35	11.05	5.789	5.78900017	tr F5GY21 F5GY21_HUMAN	Ras-related protein Rab-8B OS=Homo sapiens GN=RAB8B PE=1 SV=1	HUMAN	1
163	0	1.35	15.83	7.914	7.914	tr E9PS06 E9PS06_HUMAN	Ras-related protein Rab-30 (Fragment) OS=Homo sapiens GN=RAB30 PE=1 SV=1	HUMAN	1
163	0	1.35	19.3	9.649	9.64900032	tr E9PRF7 E9PRF7_HUMAN	Ras-related protein Rab-30 (Fragment) OS=Homo sapiens GN=RAB30 PE=4 SV=1	HUMAN	1
163	0	1.35	18.03	9.016	9.01599973	tr E9PNB9 E9PNB9_HUMAN	Ras-related protein Rab-30 OS=Homo sapiens GN=RAB30 PE=4 SV=1	HUMAN	1
163	0	1.35	23.4	11.7	11.69999999	tr E9PLM3 E9PLM3_HUMAN	Ras-related protein Rab-30 OS=Homo sapiens GN=RAB30 PE=4 SV=1	HUMAN	1
163	0	1.35	22	11	10.99999999	tr E9PJQ5 E9PJQ5_HUMAN	Ras-related protein Rab-30 (Fragment) OS=Homo sapiens GN=RAB30 PE=4 SV=1	HUMAN	1
163	0	1.35	6.716	4.104	4.10399996	tr E7E560 E7E560_HUMAN	Uncharacterized protein OS=Homo sapiens GN=RAB34 PE=1 SV=2	HUMAN	1

163	0	1.35	9.424	5.759	5.75900003	tr A8MZ14 A8MZ14_HUMAN	Ras-related protein Rab-37 OS=Homo sapiens GN=RAB37 PE=3 SV=1	HUMAN	1
163	0	1.35	9.135	5.288	5.28800003	sp Q9NRW1 RAB6B_HUMAN	Ras-related protein Rab-6B OS=Homo sapiens GN=RAB6B PE=1 SV=1	HUMAN	1
163	0	1.35	9.744	5.641	5.64099997	sp Q9NRW1-2 RAB6B_HUMAN	Isoform 2 of Ras-related protein Rab-6B OS=Homo sapiens GN=RAB6B	HUMAN	1
163	0	1.35	7.895	4.265	4.82500009	sp Q96AX2-3 RAB37_HUMAN	Isoform 3 of Ras-related protein Rab-37 OS=Homo sapiens GN=RAB37	HUMAN	1
163	0	1.35	10.14	5.314	5.31399995	sp Q92930 RAB8B_HUMAN	Ras-related protein Rab-8B OS=Homo sapiens GN=RAB8B PE=1 SV=2	HUMAN	1
163	0	1.35	7.377	7.377	4.50799987	sp Q6IQ22 RAB12_HUMAN	Ras-related protein Rab-12 OS=Homo sapiens GN=RAB12 PE=1 SV=3	HUMAN	1
163	0	1.35	8.108	4.955	4.95500006	sp Q5JT25 RAB41_HUMAN	Ras-related protein Rab-41 OS=Homo sapiens GN=RAB41 PE=2 SV=2	HUMAN	1
163	0	1.35	8.145	4.977	4.97700013	sp Q5JT25-2 RAB41_HUMAN	Isoform 2 of Ras-related protein Rab-41 OS=Homo sapiens GN=RAB41	HUMAN	1
163	0	1.35	13.41	6.707	6.70699999	sp Q15717-2 RAB30_HUMAN	Isoform 2 of Ras-related protein Rab-30 OS=Homo sapiens GN=RAB30	HUMAN	1
163	0	1.35	9.302	5.116	5.11600003	sp P61106 RAB14_HUMAN	Ras-related protein Rab-14 OS=Homo sapiens GN=RAB14 PE=1 SV=4	HUMAN	1
163	0	1.35	9.859	5.164	5.16400002	sp P61018 RAB4B_HUMAN	Ras-related protein Rab-4B OS=Homo sapiens GN=RAB4B PE=1 SV=1	HUMAN	1
163	0	1.35	8.468	4.435	4.43499982	sp P61018-2 RAB4B_HUMAN	Isoform 2 of Ras-related protein Rab-4B OS=Homo sapiens GN=RAB4B	HUMAN	1
163	0	1.35	10.1	5.288	5.28800003	sp P59190-2 RAB15_HUMAN	Isoform 2 of Ras-related protein Rab-15 OS=Homo sapiens GN=RAB15	HUMAN	1
163	0	1.35	9.091	9.091	0.90100026	tr Q6PIK3 Q6PIK3_HUMAN	HCG1995540, isoform CRA_b OS=Homo sapiens GN=RAB4B PE=1 SV=1	HUMAN	1
163	0	1.35	3.481	3.481	3.48099992	tr J3KQW8 J3KQW8_HUMAN	Ras-related protein Rab-34, isoform NARR OS=Homo sapiens GN=RAB34 PE=1 SV=1	HUMAN	1
163	0	1.35	6.433	6.433	6.43299967	tr H7C0V7 H7C0V7_HUMAN	Ras-related protein Rab-34, isoform NARR OS=Homo sapiens GN=RAB34 PE=1 SV=2	HUMAN	1
163	0	1.35	6.322	6.322	6.32200018	tr H7BYW1 H7BYW1_HUMAN	Ras-related protein Rab-6A (Fragment) OS=Homo sapiens GN=RAB6A PE=1 SV=1	HUMAN	1
163	0	1.35	5.851	5.851	5.85100017	tr HOYNE9 HOYNE9_HUMAN	Ras-related protein Rab-8B (Fragment) OS=Homo sapiens GN=RAB8B PE=1 SV=1	HUMAN	1
163	0	1.35	11.96	11.96	11.95999998	tr HOYMN7 HOYMN7_HUMAN	Ras-related protein Rab-8B OS=Homo sapiens GN=RAB8B PE=4 SV=1	HUMAN	1
163	0	1.35	5.473	5.473	5.47300018	tr HOYGL6 HOYGL6_HUMAN	Ras-related protein Rab-6A (Fragment) OS=Homo sapiens GN=RAB6A PE=1 SV=1	HUMAN	1
163	0	1.35	6.627	6.627	6.62700012	tr G3V196 G3V196_HUMAN	Ras-related protein Rab-15 OS=Homo sapiens GN=RAB15 PE=1 SV=1	HUMAN	1
163	0	1.35	14.67	14.67	14.66999995	tr E9P181 E9P181_HUMAN	Ras-related protein Rab-30 (Fragment) OS=Homo sapiens GN=RAB30 PE=4 SV=1	HUMAN	1
163	0	1.35	4.264	4.264	4.26400006	tr C9JY26 C9JY26_HUMAN	Ras-related protein Rab-34, isoform NARR (Fragment) OS=Homo sapiens GN=RAB34 PE=1 SV=1	HUMAN	1
163	0	1.35	13.25	13.25	13.24999993	tr C9JU14 C9JU14_HUMAN	Ras-related protein Rab-6B (Fragment) OS=Homo sapiens GN=RAB6B PE=4 SV=3	HUMAN	1
163	0	1.35	12.79	12.79	12.79000047	tr C9JFM7 C9JFM7_HUMAN	Ras-related protein Rab-43 (Fragment) OS=Homo sapiens GN=RAB43 PE=4 SV=1	HUMAN	1
163	0	1.35	5.238	5.238	5.23799993	tr C9JBG0 C9JBG0_HUMAN	Ras-related protein Rab-34, isoform NARR (Fragment) OS=Homo sapiens GN=RAB34 PE=1 SV=1	HUMAN	1
163	0	1.35	22.45	22.45	22.45	tr C9JB90 C9JB90_HUMAN	Ras-related protein Rab-6B (Fragment) OS=Homo sapiens GN=RAB6B PE=4 SV=1	HUMAN	1
163	0	1.35	5.612	5.612	5.61200008	tr B7Z3L0 B7Z3L0_HUMAN	Ras-related protein Rab-37 OS=Homo sapiens GN=RAB37 PE=2 SV=1	HUMAN	1
163	0	1.35	4.231	4.231	4.23099995	tr A8MYQ9 A8MYQ9_HUMAN	Ras-related protein Rab-34, isoform NARR OS=Homo sapiens GN=RAB34 PE=1 SV=2	HUMAN	1
163	0	1.35	5.82	5.82	5.82000017	tr A8MTC6 A8MTC6_HUMAN	RAB37, member RAS oncogene family, isoform CRA_a OS=Homo sapiens GN=RAB37 PE=3 SV=1	HUMAN	1
163	0	1.35	6.044	6.044	6.04400001	tr A8MSP2 A8MSP2_HUMAN	RAB37, member RAS oncogene family, isoform CRA_e OS=Homo sapiens GN=RAB37 PE=2 SV=1	HUMAN	1
163	0	1.35	5.473	5.473	5.47300018	sp Q9NP90 RAB9B_HUMAN	Ras-related protein Rab-9B OS=Homo sapiens GN=RAB9B PE=1 SV=1	HUMAN	1
163	0	1.35	5.473	5.473	5.47300018	sp Q9H0U4 RAB1B_HUMAN	Ras-related protein Rab-1B OS=Homo sapiens GN=RAB1B PE=1 SV=1	HUMAN	1
163	0	1.35	4.803	4.803	4.80300002	sp Q9H082 R833B_HUMAN	Ras-related protein Rab-33B OS=Homo sapiens GN=RAB33B PE=1 SV=1	HUMAN	1
163	0	1.35	4.247	4.247	4.24700007	sp Q9BZG1 RAB34_HUMAN	Ras-related protein Rab-34 OS=Homo sapiens GN=RAB34 PE=1 SV=1	HUMAN	1
163	0	1.35	4.641	4.641	4.64100018	sp Q9BZG1-4 RAB34_HUMAN	Isoform 4 of Ras-related protein Rab-34 OS=Homo sapiens GN=RAB34	HUMAN	1
163	0	1.35	4.382	4.382	4.38200012	sp Q9BZG1-2 RAB34_HUMAN	Isoform 2 of Ras-related protein Rab-34 OS=Homo sapiens GN=RAB34	HUMAN	1
163	0	1.35	4.846	4.846	4.84599993	sp Q96E17 RAB3C_HUMAN	Ras-related protein Rab-3C OS=Homo sapiens GN=RAB3C PE=2 SV=1	HUMAN	1
163	0	1.35	5.164	5.164	5.16400002	sp Q96DA2 R839B_HUMAN	Ras-related protein Rab-39B OS=Homo sapiens GN=RAB39B PE=1 SV=1	HUMAN	1
163	0	1.35	4.933	4.933	4.93299998	sp Q96AX2 RAB37_HUMAN	Ras-related protein Rab-37 OS=Homo sapiens GN=RAB37 PE=1 SV=3	HUMAN	1
163	0	1.35	5.914	5.914	5.91400005	sp Q96AX2-4 RAB37_HUMAN	Isoform 4 of Ras-related protein Rab-37 OS=Homo sapiens GN=RAB37	HUMAN	1
163	0	1.35	5.093	5.093	5.09300008	sp Q96AX2-2 RAB37_HUMAN	Isoform 2 of Ras-related protein Rab-37 OS=Homo sapiens GN=RAB37	HUMAN	1
163	0	1.35	5.473	5.473	5.47300018	sp Q92928 RAB1C_HUMAN	Putative Ras-related protein Rab-1C OS=Homo sapiens GN=RAB1C PE=5 SV=2	HUMAN	1
163	0	1.35	7.097	7.097	7.09699988	sp Q86Y56-2 RAB43_HUMAN	Isoform 3 of Ras-related protein Rab-43 OS=Homo sapiens GN=RAB43	HUMAN	1
163	0	1.35	5.473	5.473	5.47300018	sp Q15286 RAB35_HUMAN	Ras-related protein Rab-35 OS=Homo sapiens GN=RAB35 PE=1 SV=1	HUMAN	1
163	0	1.35	7.237	7.237	7.23700002	sp Q15286-2 RAB35_HUMAN	Isoform 2 of Ras-related protein Rab-35 OS=Homo sapiens GN=RAB35	HUMAN	1
163	0	1.35	5.069	5.069	5.06899999	sp Q14964 R839A_HUMAN	Ras-related protein Rab-39A OS=Homo sapiens GN=RAB39A PE=2 SV=2	HUMAN	1
163	0	1.35	5.366	5.366	5.36600016	sp P62820 RAB1A_HUMAN	Ras-related protein Rab-1A OS=Homo sapiens GN=RAB1A PE=1 SV=3	HUMAN	1
163	0	1.35	5.189	5.189	5.18900007	sp P59190 RAB15_HUMAN	Ras-related protein Rab-15 OS=Homo sapiens GN=RAB15 PE=1 SV=1	HUMAN	1
163	0	1.35	5.288	5.288	5.28800003	sp P20340 RAB6A_HUMAN	Ras-related protein Rab-6A OS=Homo sapiens GN=RAB6A PE=1 SV=3	HUMAN	1
163	0	1.35	6.286	6.286	6.28599972	sp P20340-4 RAB6A_HUMAN	Isoform 4 of Ras-related protein Rab-6A OS=Homo sapiens GN=RAB6A	HUMAN	1
163	0	1.35	5.288	5.288	5.28800003	sp P20340-2 RAB6A_HUMAN	Isoform 2 of Ras-related protein Rab-6A OS=Homo sapiens GN=RAB6A	HUMAN	1
163	0	1.35	5.046	5.046	5.04599996	sp P20338 RAB4A_HUMAN	Ras-related protein Rab-4A OS=Homo sapiens GN=RAB4A PE=1 SV=3	HUMAN	1
163	0	1.35	5.023	5.023	5.02300002	sp P20337 RAB3B_HUMAN	Ras-related protein Rab-3B OS=Homo sapiens GN=RAB3B PE=1 SV=2	HUMAN	1
163	0	1.35	5	5	5.00000007	sp P20336 RAB3A_HUMAN	Ras-related protein Rab-3A OS=Homo sapiens GN=RAB3A PE=1 SV=1	HUMAN	1
163	0	1.35	5.023	5.023	5.02300002	sp O95716 RAB3D_HUMAN	Ras-related protein Rab-3D OS=Homo sapiens GN=RAB3D PE=1 SV=1	HUMAN	1
164	1.28	1.28	7.143	1.12	1.11999996	sp P07384 CAN1_HUMAN	Calpain-1 catalytic subunit OS=Homo sapiens GN=CAPN1 PE=1 SV=1	HUMAN	1
165	1.2	1.2	1.313	0.4179	0.41789999	sp Q00610 CLH1_HUMAN	Clathrin heavy chain 1 OS=Homo sapiens GN=CLTC PE=1 SV=5	HUMAN	1
165	0	1.2	1.342	0.4271	0.42710002	sp Q00610-2 CLH1_HUMAN	Isoform 2 of Clathrin heavy chain 1 OS=Homo sapiens GN=CLTC	HUMAN	1
165	0	1.2	3.153	3.153	3.15300003	tr K7EJIS K7EJIS_HUMAN	Clathrin heavy chain 1 (Fragment) OS=Homo sapiens GN=CLTC PE=1 SV=1	HUMAN	1
165	0	1.2	1.144	1.144	1.14399996	tr J3KS13 J3KS13_HUMAN	Clathrin heavy chain 1 OS=Homo sapiens GN=CLTC PE=1 SV=1	HUMAN	1
165	0	1.2	5.344	5.344	5.34400009	tr J3KRF5 J3KRF5_HUMAN	Clathrin heavy chain 1 (Fragment) OS=Homo sapiens GN=CLTC PE=1 SV=1	HUMAN	1
166	0.9	0.9	17.519	10.10	10.18999996	tr H3BPG0 H3BPG0_HUMAN	Cytochrome c oxidase subunit 4 isoform 1, mitochondrial (Fragment) OS=Homo sapiens GN=HUMAN	HUMAN	1
166	0	0.9	13.67	7.914	7.914	tr H3BNV9 H3BNV9_HUMAN	Cytochrome c oxidase subunit 4 isoform 1, mitochondrial OS=Homo sapiens GN=COX4I1 PE=1 SV=1	HUMAN	1
166	0	0.9	15.08	8.73	8.73000026	tr H3BN72 H3BN72_HUMAN	Cytochrome c oxidase subunit 4 isoform 1, mitochondrial OS=Homo sapiens GN=COX4I1 PE=1 SV=1	HUMAN	1
166	0	0.9	11.24	6.509	6.50900006	sp P13073 COX4I1_HUMAN	Cytochrome c oxidase subunit 4 isoform 1, mitochondrial OS=Homo sapiens GN=COX4I1 PE=1 SV=1	HUMAN	1
166	0	0.9	13.25	13.25	13.24999993	tr Q86WV2 Q86WV2_HUMAN	COX4I1 protein OS=Homo sapiens GN=COX4I1 PE=1 SV=1	HUMAN	1
167	0.82	0.82	5.625	5.625	5.62499985	tr U3KQR5 U3KQR5_HUMAN	60S ribosomal protein L6 (Fragment) OS=Homo sapiens GN=RPL6 PE=1 SV=1	HUMAN	1
167	0	0.82	5.66	5.66	5.66000007	tr F8VZ45 F8VZ45_HUMAN	60S ribosomal protein L6 (Fragment) OS=Homo sapiens GN=RPL6 PE=1 SV=1	HUMAN	1
167	0	0.82	14.29	14.29	14.29000005	tr F8VR69 F8VR69_HUMAN	60S ribosomal protein L6 (Fragment) OS=Homo sapiens GN=RPL6 PE=1 SV=2	HUMAN	1
167	0	0.82	3.125	3.125	3.125	sp Q02878 RL6_HUMAN	60S ribosomal protein L6 OS=Homo sapiens GN=RPL6 PE=1 SV=3	HUMAN	1
168	0.68	0.68	2.778	2.778	2.77800001	sp Q14201 BTG3_HUMAN	Protein BTG3 OS=Homo sapiens GN=BTG3 PE=1 SV=3	HUMAN	1
168	0	0.68	2.365	2.365	2.36499999	sp Q14201-2 BTG3_HUMAN	Isoform 2 of Protein BTG3 OS=Homo sapiens GN=BTG3	HUMAN	1
169	0.63	0.67	1.459	0.7817	0.78170002	sp Q8TDM6 DLG5_HUMAN	Disks large homolog 5 OS=Homo sapiens GN=DLG5 PE=1 SV=4	HUMAN	2
169	0	0.67	1.548	0.8292	0.82919998	sp Q8TDM6-4 DLG5_HUMAN	Isoform 4 of Disks large homolog 5 OS=Homo sapiens GN=DLG5	HUMAN	2
169	0	0.67	0.95	0.95	0.94999997	sp Q8TDM6-2 DLG5_HUMAN	Isoform 2 of Disks large homolog 5 OS=Homo sapiens GN=DLG5	HUMAN	2
169	0	0.63	1.187	1.187	1.18699996	sp Q8TDM6-5 DLG5_HUMAN	Isoform 5 of Disks large homolog 5 OS=Homo sapiens GN=DLG5	HUMAN	2
170	0.58	0.58	11.41	5.369	5.36900014	tr G3V1A4 G3V1A4_HUMAN	Cofilin 1 (Non-muscle), isoform CRA_a OS=Homo sapiens GN=CFL1 PE=1 SV=1	HUMAN	1
170	0	0.58	13.93	6.557	6.55699968	tr E9PQ87 E9PQ87_HUMAN	Cofilin-1 (Fragment) OS=Homo sapiens GN=CFL1 PE=1 SV=1	HUMAN	1
171	0.56	0.56	12.35	12.35	12.34999997	tr J3KJ73 J3KJ73_HUMAN	60S ribosomal protein L23 OS=Homo sapiens GN=RPL23 PE=1 SV=1	HUMAN	1
171	0	0.56	7.143	7.143	7.14299977	sp P62829 RL23_HUMAN	60S ribosomal protein L23 OS=Homo sapiens GN=RPL23 PE=1 SV=1	HUMAN	1
172	0.51	0.51	7.115	2.372	2.37199999	sp Q9Y696 CLIC4_HUMAN	Chloride intracellular channel protein 4 OS=Homo sapiens GN=CLIC4 PE=1 SV=4	HUMAN	1
172	0	0.51	4.11	4.11	4.10999991	sp P12273 PIP_HUMAN	Protein PIP OS=Homo sapiens GN=PIP PE=1 SV=1	HUMAN	1
173	0.5	0.5	1.563	0.6836	0.68359999	sp Q9NPP4 NLRCA_HUMAN	NLR family CARD domain-containing protein 4 OS=Homo sapiens GN=NLRCA PE=1 SV=2	HUMAN	1
173	0	0.5	4.457	1.95	1.95000004	sp Q9NPP4-2 NLRCA_HUMAN	Isoform 2 of NLR family CARD domain-containing protein 4 OS=Homo sapiens GN=NLRCA	HUMAN	1
174	0.42	0.42	5.364	5.364	5.36400005	sp P00414 COX3_HUMAN	Cytochrome c oxidase subunit 3 OS=Homo sapiens GN=MT-CO3 PE=1 SV=2	HUMAN	1
175	0	0.4	1.048	1.048	1.04799997	RRRRSP P04049-2 RAF1_HUMAN	REVERSED isoform 2 of RAF proto-oncogene serine/threonine-protein kinase OS=Homo sapiens	HUMAN	1
176	0	0.36	5.938	0.9335	0.93350001	sp Q9UL18 AGO1_HUMAN	Protein argonaute-1 OS=Homo sapiens GN=AGO1 PE=1 SV=3	HUMAN	1
176	0	0.36	5.11	0.9292	0.9292	sp Q9HCK5 AGO4_HUMAN	Protein argonaute-4 OS=Homo sapiens GN=AGO4 PE=1 SV=2	HUMAN	1
176	0	0.36	4.186	0.9302	0.93019996	sp Q9H9G7 AGO3_HUMAN	Protein argonaute-3 OS=Homo sapiens GN=AGO3 PE=1 SV=2	HUMAN	1
176	0	0.36	5.751	1.278	1.27800005	sp Q9H9G7-2 AGO3_HUMAN	Isoform 2 of Protein argonaute-3 OS=Homo sapiens GN=AGO3	HUMAN	1
176	0	0.36	0.9313	0.9313	0.93130004	sp Q9UKV8 AGO2_HUMAN	Protein argonaute-2 OS=Homo sapiens GN=AGO2 PE=1 SV=3	HUMAN	1
177	0	0.35	2.268	2.268	2.26799995	tr G5EA52 G5EA52_HUMAN	Protein disulfide-isomerase OS=Homo sapiens GN=PDIA3 PE=1 SV=1	HUMAN	1
177	0	0.35	2.178	2.178	2.17799991	sp P30101 PDIA3_HUMAN	Protein disulfide-isomerase A3 OS=Homo sapiens GN=PDIA3 PE=1 SV=4	HUMAN	1
178	0.32	0.32	7.424	3.93	3.92999984	sp P09497 CLCB_HUMAN	Clathrin light chain B OS=Homo sapiens GN=CLTB PE=1 SV=1	HUMAN	1
178	0	0.32	8.057	4.264	4.26499993	sp P09497-2 CLCB_HUMAN	Isoform Non-brain of Clathrin light chain B OS=Homo sapiens GN=CLTB	HUMAN	1
179	0	0.3	2.792	2.792	2.79200003	sp Q9U080 PA2G4_HUMAN	Proliferation-associated protein 2G4 OS=Homo sapiens GN=PA2G4 PE=1 SV=3	HUMAN	1

Appendix 2B



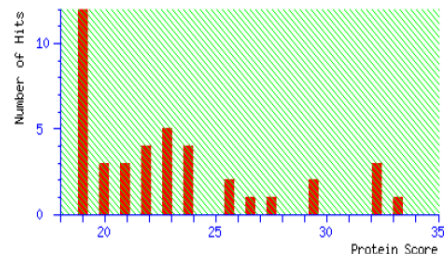
MALDI spectrum of koala blood recovered from under a fingernail 3hrs after deposition and after brief washing. The microswab was extracted in 50 % ACN and treated with 1:1 RapiGest solution followed by trypsin digestion at 37°C for 4hrs. The digested samples were spotted (1:1) with CHCA matrix (50 % ACN in 0.2 %TFA). Peak marked with an asterisk represents a peptide from β -hemoglobin proteins (HB-B). Note that blood proteins for koala are not on the database and the closest match is for a species of kangaroo, *Macropus giganteus*. Database search reports follow.

User : satish
 Email : satishmb@gmail.com
 Search title :
 Database : SwissProt 2016_10 (552884 sequences; 197760918 residues)
 Taxonomy : Other mammalia (13134 sequences)
 Timestamp : 16 Nov 2016 at 09:35:37 GMT
 Top Score : 33 for **K2C7_POTTR**, Keratin, type II cytoskeletal 7 OS=Potorous tridactylus GN=

[Re-Search All](#) [Search Unmatched](#)

Mascot Score Histogram

Protein score is $-10 \cdot \log(P)$, where P is the probability that the observed match is a random event. Protein scores greater than 54 are significant ($p < 0.05$).



Concise Protein Summary Report

[Format As](#) [Concise Protein Summary](#) [Help](#)
 Significance threshold $p < 0.05$ Max. number of hits

Protein View: HBB_MACGI

Hemoglobin subunit beta OS=Macropus giganteus GN=HBB PE=1 SV=1

Database: SwissProt
 Score: 33
 Expect: 7.2
 Nominal mass (M_r): 16005
 Calculated pI: 7.23
 Taxonomy: Macropus giganteus

Sequence similarity is available as [an NCBI BLAST search of HBB_MACGI against nr](#).

Search parameters

Enzyme: Trypsin: cuts C-term side of KR unless next residue is P. 11/16/2016
 Mass values searched: 31
 Mass values matched: 4

Protein sequence coverage: 29%

Matched peptides shown in **bold red**.

1 VHLTAEKNA ITSLWGKVAI EQTGGALGR **LLIVYPWTSR FFDHFGDLSN**
 51 **AKAVMANPKV LAHGAQVLVA** FGDAIKQLDN LKGTFAKLSE LHCDKLHVDP
 101 **ENFKLLGNII VICLAEHFGK** EFTIDTQVAW **QKLVAGVANA LAHKYH**

1. [K2C7_POTTR](#) Mass: 53254 Score: 33 Expect: 6.3 Matches: 7
 Keratin, type II cytoskeletal 7 OS=Potorous tridactylus GN=KRT7 PE=2 SV=1

2. [HBB_MACGI](#) Mass: 16005 Score: 33 Expect: 7.2 Matches: 4
 Hemoglobin subunit beta OS=Macropus giganteus GN=HBB PE=1 SV=1
[HBB_MACRU](#) Mass: 15991 Score: 33 Expect: 7.2 Matches: 4
 Hemoglobin subunit beta OS=Macropus rufus GN=HBB PE=1 SV=1
[HBB_MACEU](#) Mass: 16122 Score: 32 Expect: 7.4 Matches: 4
 Hemoglobin subunit beta OS=Macropus eugenii GN=HBB PE=2 SV=3
[TENAB_BOVIN](#) Mass: 21381 Score: 20 Expect: 1.4e+02 Matches: 3
 Interferon alpha-B OS=Bos taurus GN=IFNAB PE=3 SV=1

3. [HBB_POTTR](#) Mass: 15923 Score: 32 Expect: 8.3 Matches: 4
 Hemoglobin subunit beta OS=Potorous tridactylus GN=HBB PE=1 SV=1

4. [K2C7_BOVIN](#) Mass: 51546 Score: 32 Expect: 8.5 Matches: 7
 Keratin, type II cytoskeletal 7 OS=Bos taurus GN=KRT7 PE=2 SV=1

5. [EIF2D_BOVIN](#) Mass: 63606 Score: 30 Expect: 14 Matches: 6
 Eukaryotic translation initiation factor 2D OS=Bos taurus GN=EIF2D PE=2 SV=1

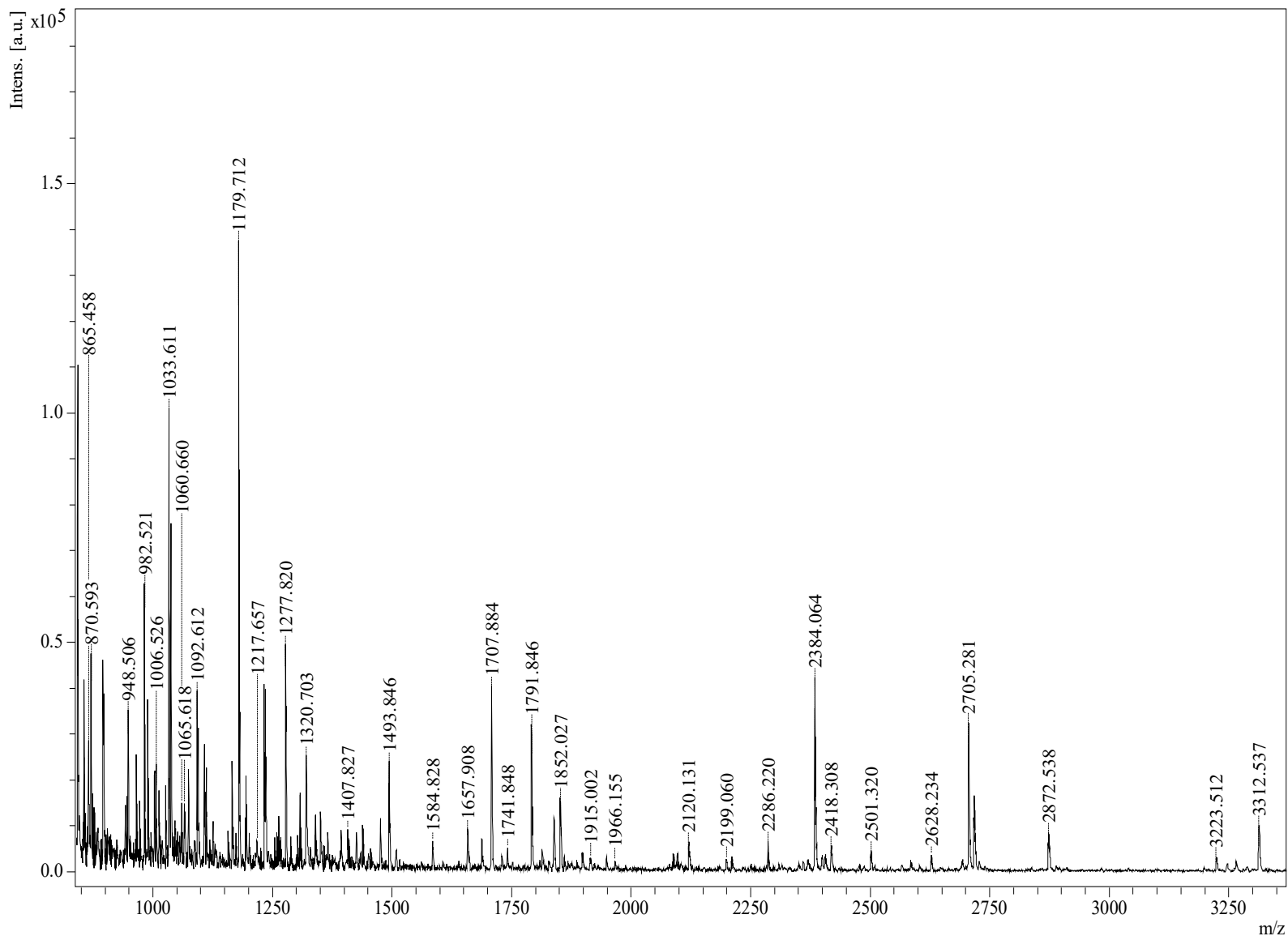
6. [IQCG_BOVIN](#) Mass: 51188 Score: 29 Expect: 16 Matches: 5
 IQ domain-containing protein G OS=Bos taurus GN=IQCG PE=2 SV=1

7. [CP2CG_RABIT](#) Mass: 55506 Score: 27 Expect: 24 Matches: 6
 Cytochrome P450 2C16 OS=Oryctolagus cuniculus GN=CYP2C16 PE=2 SV=1

8. [HNRPC_RABIT](#) Mass: 33664 Score: 26 Expect: 30 Matches: 5
 Heterogeneous nuclear ribonucleoprotein C OS=Oryctolagus cuniculus GN=HNRNPC PE=2 SV=1

Mascot Search Results: HBB_MACGI

31 - 40	1247.8640	1246.8567	1246.7074	0.1493	0	R.LLIVYPWTSR.F
41 - 52	1397.8260	1396.8187	1396.6412	0.1776	0	R.FFDHFGDLSNAK.A
96 - 104	1098.6640	1097.6567	1097.5506	0.1062	0	K.LHVDPENFK.L
133 - 144	1164.1210	1163.1137	1162.6822	0.4315	0	K.LVAGVANALAHK.Y

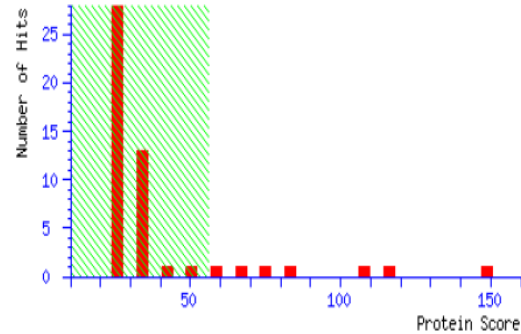


MALDI Spectrum of **control fingernail** scrapings (i.e., scrapings that had been collected from under a fingernail that had not been treated with vaginal fluid or koala blood. Database search results follow.

Database : SwissProt 2016_09 (552259 sequences; 197423140 residues)
 Taxonomy : Homo sapiens (human) (20161 sequences)
 Timestamp : 22 Oct 2016 at 10:21:14 GMT
 Top Score : 149 for Mixture 1, K2C1_HUMAN + K1C9_HUMAN + K2C6A_HUMAN

Mascot Score Histogram

Protein score is $-10 \cdot \log(P)$, where P is the probability that the observed match is a random match.
 Protein scores greater than 56 are significant ($p < 0.05$).



1. **Mixture 1** Total score: **149** Expect: 2.5e-11 Matches: 47
 Components (only one family member shown for each component):
[K2C1_HUMAN](#) Mass: 65999 Score: **106** Expect: 5.1e-07 Matches: 19
 Keratin, type II cytoskeletal 1 OS=Homo sapiens GN=KRT1 PE=1 SV=6
[K1C9_HUMAN](#) Mass: 62027 Score: **83** Expect: 9.6e-05 Matches: 15
 Keratin, type I cytoskeletal 9 OS=Homo sapiens GN=KRT9 PE=1 SV=3
[K2C6A_HUMAN](#) Mass: 60008 Score: **63** Expect: 0.0094 Matches: 16
 Keratin, type II cytoskeletal 6A OS=Homo sapiens GN=KRT6A PE=1 SV=3

2. **Mixture 2** Total score: **113** Expect: 1e-07 Matches: 41
 Components (only one family member shown for each component):
[K1C9_HUMAN](#) Mass: 62027 Score: **83** Expect: 9.6e-05 Matches: 15
 Keratin, type I cytoskeletal 9 OS=Homo sapiens GN=KRT9 PE=1 SV=3
[K22E_HUMAN](#) Mass: 65393 Score: **75** Expect: 0.00068 Matches: 15
 Keratin, type II cytoskeletal 2 epidermal OS=Homo sapiens GN=KRT2 PE=1 SV=2
[K1C10_HUMAN](#) Mass: 58792 Score: 54 Expect: 0.082 Matches: 12
 Keratin, type I cytoskeletal 10 OS=Homo sapiens GN=KRT10 PE=1 SV=6

3. [K2C1_HUMAN](#) Mass: 65999 Score: **106** Expect: 5.1e-07 Matches: 19
 Keratin, type II cytoskeletal 1 OS=Homo sapiens GN=KRT1 PE=1 SV=6

4. [K1C9_HUMAN](#) Mass: 62027 Score: **83** Expect: 9.6e-05 Matches: 15
 Keratin, type I cytoskeletal 9 OS=Homo sapiens GN=KRT9 PE=1 SV=3

5. [K22E_HUMAN](#) Mass: 65393 Score: **75** Expect: 0.00068 Matches: 15
 Keratin, type II cytoskeletal 2 epidermal OS=Homo sapiens GN=KRT2 PE=1 SV=2

6. [K2C6A_HUMAN](#) Mass: 60008 Score: **63** Expect: 0.0094 Matches: 16
 Keratin, type II cytoskeletal 6A OS=Homo sapiens GN=KRT6A PE=1 SV=3
[K2C6C_HUMAN](#) Mass: 59988 Score: 49 Expect: 0.24 Matches: 14
 Keratin, type II cytoskeletal 6C OS=Homo sapiens GN=KRT6C PE=1 SV=3

7. [K2C6B_HUMAN](#) Mass: 60030 Score: **57** Expect: 0.04 Matches: 15
 Keratin, type II cytoskeletal 6B OS=Homo sapiens GN=KRT6B PE=1 SV=5

8. [K1C10_HUMAN](#) Mass: 58792 Score: 54 Expect: 0.082 Matches: 12
 Keratin, type I cytoskeletal 10 OS=Homo sapiens GN=KRT10 PE=1 SV=6

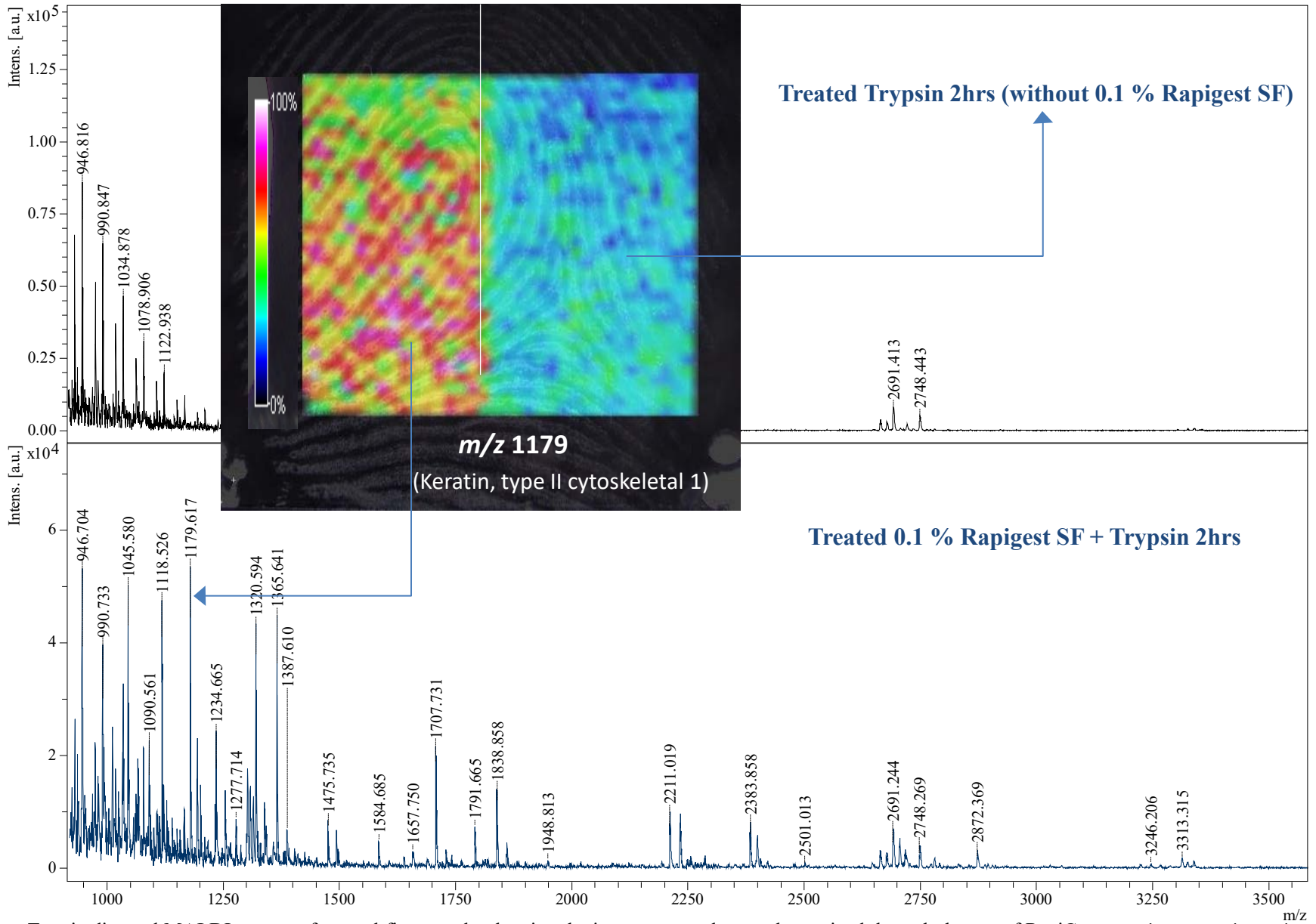
9. [NCF1_HUMAN](#) Mass: 44624 Score: 42 Expect: 1.2 Matches: 9
 Neutrophil cytosol factor 1 OS=Homo sapiens GN=NCF1 PE=1 SV=3

10. [CLC9A_HUMAN](#) Mass: 27306 Score: 38 Expect: 3.3 Matches: 6
 C-type lectin domain family 9 member A OS=Homo sapiens GN=CLEC9A PE=1 SV=1

Search Parameters

Type of search : Peptide Mass Fingerprint
 Enzyme : Trypsin
 Mass values : Monoisotopic
 Protein Mass : Unrestricted
 Peptide Mass Tolerance : ± 0.4 Da
 Peptide Charge State : 1+
 Max Missed Cleavages : 1
 Number of queries : 88

Appendix-2C

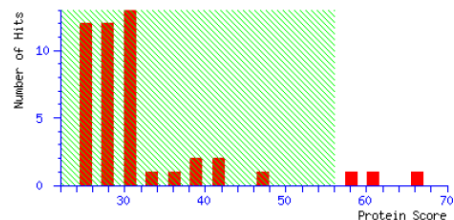


Trypsin digested MALDI spectra of control fingermarks showing the improvement that can be attained through the use of RapiGest. Database search results follow.

User : sati
 Email : satishkmb@gmail.com
 Search title :
 Database : SwissProt 2016_09 (552259 sequences; 197423140 residues)
 Taxonomy : Homo sapiens (human) (20161 sequences)
 Timestamp : 21 Oct 2016 at 04:15:17 GMT
 Top Score : 66 for **K2C1_HUMAN**, Keratin, type II cytoskeletal 1 OS=Homo sapiens GN=KRT1 PE=1 SV=6

Mascot Score Histogram

Protein score is $-10 \cdot \log(P)$, where P is the probability that the observed match is a random match.
 Protein scores greater than 56 are significant ($p < 0.05$).



10/21/2016

Concise Summary Report (./data/20161021/FTIcfxEST.dat)

1. [K2C1_HUMAN](#) Mass: 65999 Score: **66** Expect: 0.0047 Matches: 13
Keratin, type II cytoskeletal 1 OS=Homo sapiens GN=KRT1 PE=1 SV=6

2. [K1C10_HUMAN](#) Mass: 58792 Score: **62** Expect: 0.012 Matches: 12
Keratin, type I cytoskeletal 10 OS=Homo sapiens GN=KRT10 PE=1 SV=6

3. [K1C9_HUMAN](#) Mass: 62027 Score: **59** Expect: 0.026 Matches: 9
Keratin, type I cytoskeletal 9 OS=Homo sapiens GN=KRT9 PE=1 SV=3

4. [K22F_HUMAN](#) Mass: 65393 Score: 46 Expect: 0.52 Matches: 11
Keratin, type II cytoskeletal 2 epidermal OS=Homo sapiens GN=KRT2 PE=1 SV=2

5. [CLCC1_HUMAN](#) Mass: 61983 Score: 43 Expect: 1.1 Matches: 8
Chloride channel CLIC-like protein 1 OS=Homo sapiens GN=CLCC1 PE=1 SV=1

6. [CO4A1_HUMAN](#) Mass: 160514 Score: 41 Expect: 1.5 Matches: 10
Collagen alpha-1(IV) chain OS=Homo sapiens GN=COL4A1 PE=1 SV=3

7. [MED10_HUMAN](#) Mass: 15678 Score: 38 Expect: 3.4 Matches: 5
Mediator of RNA polymerase II transcription subunit 10 OS=Homo sapiens GN=MED10 PE=1 SV=1

8. [ADH4_HUMAN](#) Mass: 40196 Score: 38 Expect: 3.4 Matches: 7
Alcohol dehydrogenase 4 OS=Homo sapiens GN=ADH4 PE=1 SV=5

9. [CLC9A_HUMAN](#) Mass: 27306 Score: 36 Expect: 5.1 Matches: 5
C-type lectin domain family 9 member A OS=Homo sapiens GN=CLEC9A PE=1 SV=1

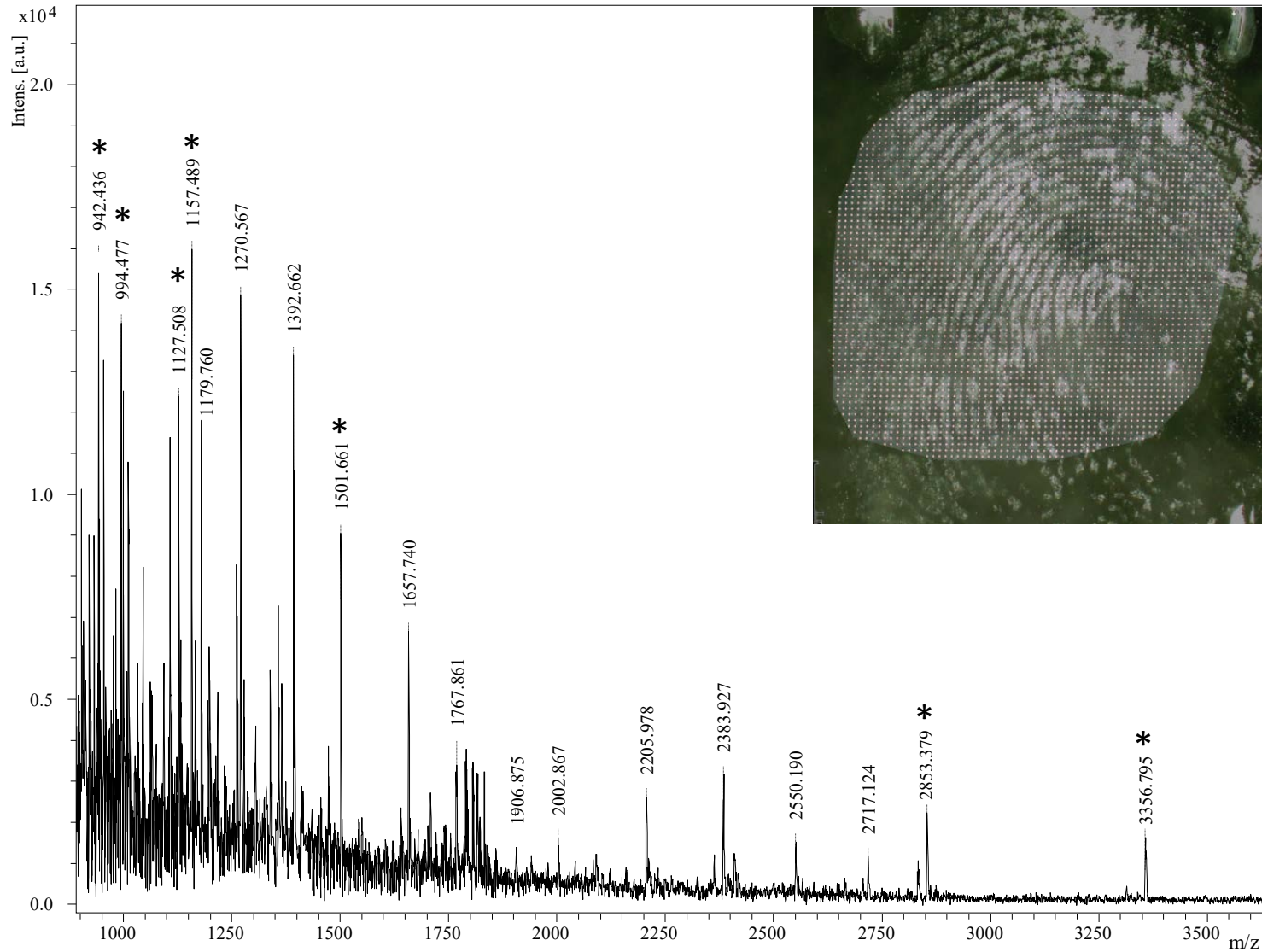
10. [PAP1L_HUMAN](#) Mass: 68348 Score: 32 Expect: 12 Matches: 8
Polyadenylate-binding protein 1-like OS=Homo sapiens GN=PABPC1L PE=2 SV=1

Keratin, type II cytoskeletal 1 OS=Homo sapiens GN=KRT1 PE=1 SV=6

Database: SwissProt
 Score: 66
 Expect: 0.0047
 Nominal mass (M_r): 65999
 Calculated pI: 8.15
 Taxonomy: [Homo sapiens](#)

Start - End	Observed	Mr (expt)	Mr (calc)	Delta M	Peptide	Expect: 13	Matches: 13
13 - 29	1657.6740	1656.6667	1656.7856	-0.1189 0	R.SGGGFSSGSAGIINYQR.R	SV=2	
212 - 223	1475.6630	1474.6557	1474.7416	-0.0859 0	K.WELLQQVDTSTR.T		
224 - 239	1993.8380	1992.8307	1992.9693	-0.1386 0	R.THNLEPYFESFINNLR.R		
224 - 240	2149.9190	2148.9117	2149.0705	-0.1587 1	R.THNLEPYFESFINNLR.R		
247 - 257	1277.6310	1276.6237	1276.6259	-0.0022 1	K.SDQSRDLSELK.N		
270 - 277	1066.4620	1065.4547	1065.5090	-0.0543 1	K.YEDEINKR.T		
377 - 386	1179.5330	1178.5257	1178.5931	-0.0674 0	K.YEELQITAGR.H		
393 - 403	1302.5960	1301.5887	1301.6939	-0.1052 1	R.NSKIEISELNR.V		
396 - 403	973.4820	972.4747	972.5240	-0.0492 0	K.IEISELNR.V		
418 - 432	1716.7320	1715.7247	1715.8438	-0.1191 0	K.QISNLQQSISDAEQR.G		
444 - 455	1357.6270	1356.6197	1356.6885	-0.0688 0	K.LNDLEDALQQAQ.E		
519 - 549	2383.7930	2382.7857	2382.9447	-0.1589 0	R.GGGGGYSGSGSSYSGSGGGYSGGGGGGR.G		
550 - 588	3312.3570	3311.3497	3311.3009	0.0488 0	R.GSYSGSGSSYSGSGGGYSGGGGGHGSYSGSSSGGYR.G		

Appendix-2D



MALDI spectrum of a mark made by a finger exposed to **vaginal fluid**, *indicates the matched tryptic peptides of cornulin (CRNN) protein. Inset: image showing region acquired for MALDI-IMS analysis. Database search results follow.

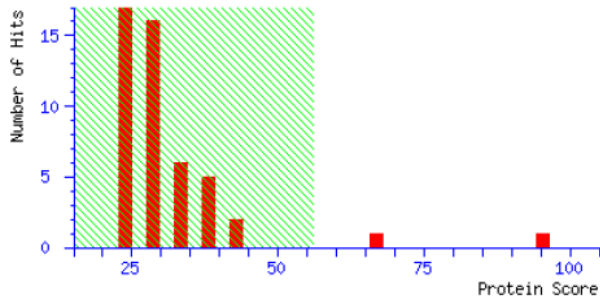
User : sati
 Email : satishmb@gmail.com
 Search title :
 Database : SwissProt 2016_06 (551385 sequences; 196948568 residues)
 Taxonomy : Homo sapiens (human) (20200 sequences)
 Timestamp : 7 Jul 2016 at 09:34:15 GMT
 Top Score : 95 for **CRNN_HUMAN**, Cornulin OS=Homo sapiens GN=CRNN PE=1 SV=1

Re-Search All Search Unmatched

- [CRNN_HUMAN](#) Mass: 53502 Score: **95** Expect: 5.8e-06 Matches: 14
Cornulin OS=Homo sapiens GN=CRNN PE=1 SV=1
- [K2C1_HUMAN](#) Mass: 65999 Score: **68** Expect: 0.0031 Matches: 12
Keratin, type II cytoskeletal 1 OS=Homo sapiens GN=KRT1 PE=1 SV=6
- [CHST5_HUMAN](#) Mass: 46131 Score: 41 Expect: 1.5 Matches: 8
Carbohydrate sulfotransferase 5 OS=Homo sapiens GN=CHST5 PE=2 SV=3
- [TDT_HUMAN](#) Mass: 58499 Score: 41 Expect: 1.5 Matches: 8
DNA nucleotidylxotransferase OS=Homo sapiens GN=DNTT PE=1 SV=3
- [SSX2_HUMAN](#) Mass: 21607 Score: 40 Expect: 1.9 Matches: 5
Protein SSX2 OS=Homo sapiens GN=SSX2 PE=1 SV=2
- [ATX10_HUMAN](#) Mass: 53455 Score: 39 Expect: 2.4 Matches: 7
Ataxin-10 OS=Homo sapiens GN=ATXN10 PE=1 SV=1

Mascot Score Histogram

Protein score is $-10 \cdot \log(P)$, where P is the probability that the observed match is a random event. Protein scores greater than 56 are significant ($p < 0.05$).



Matched CRNN peptides

Start - End	Observed	Mr(expt)	Mr(calc)	Delta M	Peptide
73 - 80	994.4770	993.4697	993.5899	-0.1202 0	K.EFLVLVFK.V
129 - 138	1157.4840	1156.4767	1156.5010	-0.0243 0	K.GQHYEGSSHR.Q
170 - 178	1062.4640	1061.4567	1061.4737	-0.0170 0	R.QAESQSQER.I
201 - 210	1261.5810	1260.5737	1260.5881	-0.0143 0	R.NQTTEMRPER.Q
220 - 252	3356.7960	3355.7887	3355.5262	0.2626 0	R.AHQTGETVTGSGTQTQAGATQVTEQDSSHQTR.T
256 - 266	1304.5490	1303.5417	1303.5753	-0.0335 0	K.QTQEATNDQNR.G
267 - 275	942.4340	941.4267	941.4315	-0.0048 0	R.GTETHGQGR.S
327 - 335	954.4580	953.4507	953.4679	-0.0172 0	R.GTEIHGQGR.S
336 - 362	2853.3950	2852.3877	2852.3285	0.0592 0	R.SQTSQAVTGGHTQIQAGSHTTETVEQDR.S
363 - 372	999.4780	998.4707	998.4894	-0.0186 0	R.SQTVSHGGAR.E
373 - 386	1501.6580	1500.6507	1500.6917	-0.0410 0	R.EQQQTQTQPGSGQR.W
387 - 414	2832.3440	2831.3367	2831.2781	0.0587 0	R.WMQVSNPEAGETVPGGQAQTGASTESGR.Q
415 - 423	1127.5060	1126.4987	1126.5156	-0.0168 0	R.QEWSSTHPR.R
434 - 448	1753.7820	1752.7747	1752.8067	-0.0320 0	R.QPTVVGEWVDDHSR.E

Cornulin OS=Homo sapiens GN=CRNN PE=1 SV=1

Database: SwissProt
 Score: 95
 Expect: 5.8e-06
 Nominal mass (Mr): 53502
 Calculated pI: 5.73
 Taxonomy: **Homo sapiens**

Sequence similarity is available as [an NCBI BLAST search of CRNN_HUMAN ag](#)

Search parameters

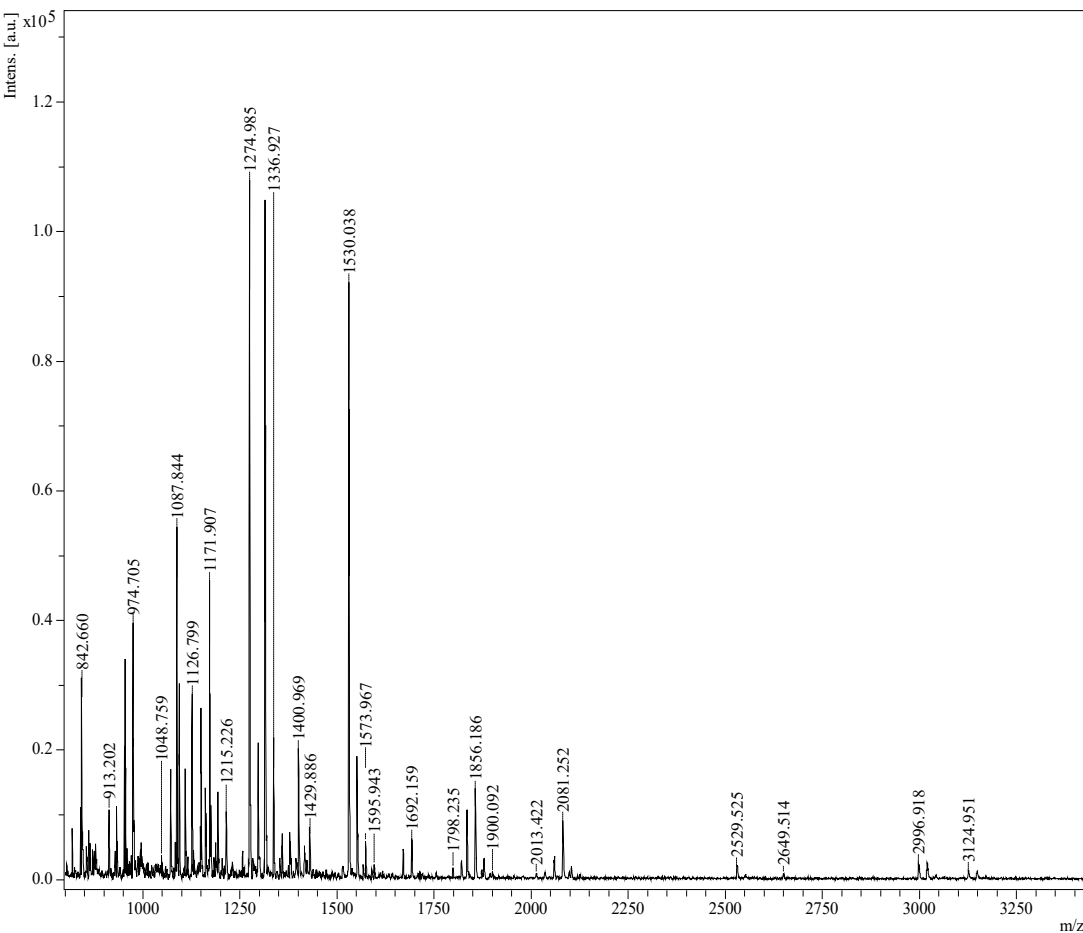
Enzyme: Trypsin: cuts C-term side of KR unless next residue is P
 Mass values searched: 61
 Mass values matched: 14

Protein sequence coverage: 40%

Matched peptides shown in **bold red**.

```

1  MPQLLNING IIEAFRRYAR TEGNCTALTR GELKRLLEQE FADVIVKPHD
51  PATVDEVLR L LDEDHTGTVE FK.EFLVLVFK VAQACFKTLS ESAEGACGSQ
101  ESGSLHSGAS QELGEGQSRG TEVGRAGKGG HYEGSSHRQS QQGSRGQNRP
151  GVQTQQGATG SAWVSSYDRQ AESQSQERIS PQIQLSGQTE QTQKAGEGKR
201  NQTTEMRPER QPQTREQDRA HQTGETVTGS GTQTAGATQ TVEQDSSHQ
251  GRTSKQTOEA TNDQNRGTET HGGQRSQTSQ AVTGGHAQIQ AGTHTQTPTQ
301  TVEQDSSHQ T GSTSTQTQES TNGQNRGTET HGGQRSQTSQ AVTGGHTQIQ
351  AGSHTTETVEQ DRSQTVSHGG AREGGQTQTQ PGSGQRWVQV SNPEAGETVP
401  GGQAQTGAST ESGRQEWSST HPRRCVTEGQ GDRQPTVVGE EWVDDHSRET
451  VILRLDQGNL HTSVSSAQGQ DAAQSEKRG ITARELYSYL RSTKP
    
```

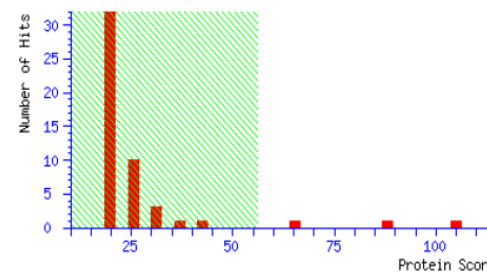


MALDI spectrum of fingerprint tryptic peptides (**human blood**) and database search results

Database : SwissProt 2016_09 (552259 sequences; 197423140 residues)
 Taxonomy : Homo sapiens (human) (20161 sequences)
 Timestamp : 19 Oct 2016 at 11:22:32 GMT
 Top Score : 105 for **Mixture 1**, HBB_HUMAN + HBA_HUMAN

Mascot Score Histogram

Protein score is $-10 \cdot \log(P)$, where P is the probability that the observed match is a random event. Protein scores greater than 56 are significant ($p < 0.05$).

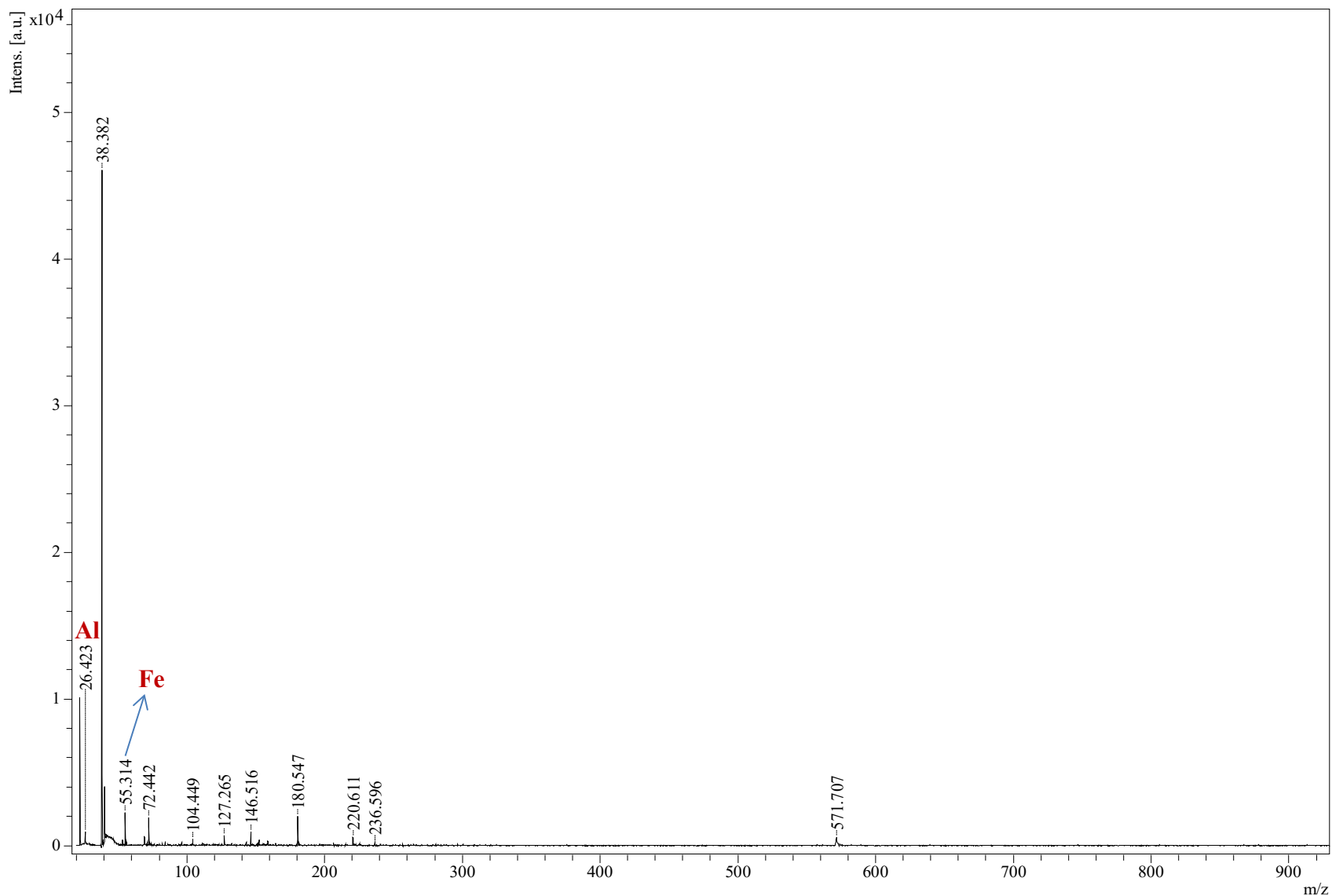


Concise Protein Summary Report

10192016 Concise Summary Report (.Jobs\20161010\FTrichTrE.dat)

1.	Mixture 1	Total score: 105	Expect: 6.4e-07	Matches: 19
Components (only one family member shown for each component):				
	HBB_HUMAN	Mass: 15988	Score: 88	Expect: 3.6e-05 Matches: 11
	Hemoglobin subunit beta OS=Homo sapiens GN=HBB PE=1 SV=2			
	HBA_HUMAN	Mass: 15248	Score: 64	Expect: 0.0086 Matches: 8
	Hemoglobin subunit alpha OS=Homo sapiens GN=HBA1 PE=1 SV=2			
2.	HBB_HUMAN	Mass: 15988	Score: 88	Expect: 3.6e-05 Matches: 11
	Hemoglobin subunit beta OS=Homo sapiens GN=HBB PE=1 SV=2			
3.	HBA_HUMAN	Mass: 15248	Score: 64	Expect: 0.0086 Matches: 8
	Hemoglobin subunit alpha OS=Homo sapiens GN=HBA1 PE=1 SV=2			
4.	HBD_HUMAN	Mass: 16045	Score: 41	Expect: 1.6 Matches: 7
	Hemoglobin subunit delta OS=Homo sapiens GN=HBD PE=1 SV=2			
5.	ODF2_HUMAN	Mass: 95342	Score: 35	Expect: 6.4 Matches: 14
	Outer dense fiber protein 2 OS=Homo sapiens GN=ODF2 PE=1 SV=1			
6.	KPRA_HUMAN	Mass: 39369	Score: 32	Expect: 12 Matches: 8
	Phosphorybosyl pyrophosphate synthase-associated protein 1 OS=Homo sapiens GN=PRPSAP1 PE=1 SV=2			

Appendix-2E



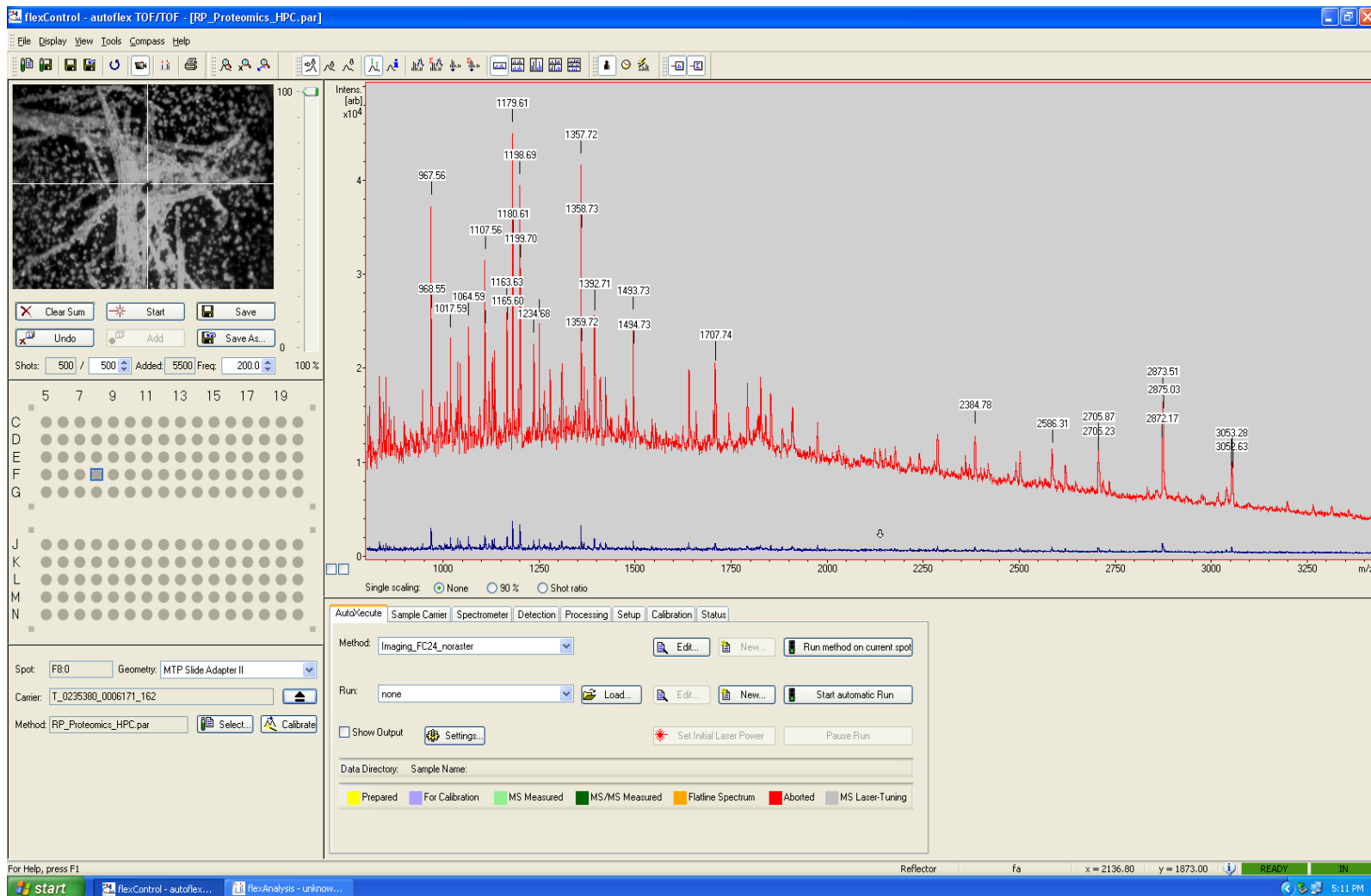
MALDI spectrum of silver-black magnetic dusting powder prior to exposure to fingerprints. The powder particles were dusted on a clean glass surface and collected using Kapton double-sided adhesive tape, then pasted onto ITO slide for MALDI analysis.

Appendix 3A

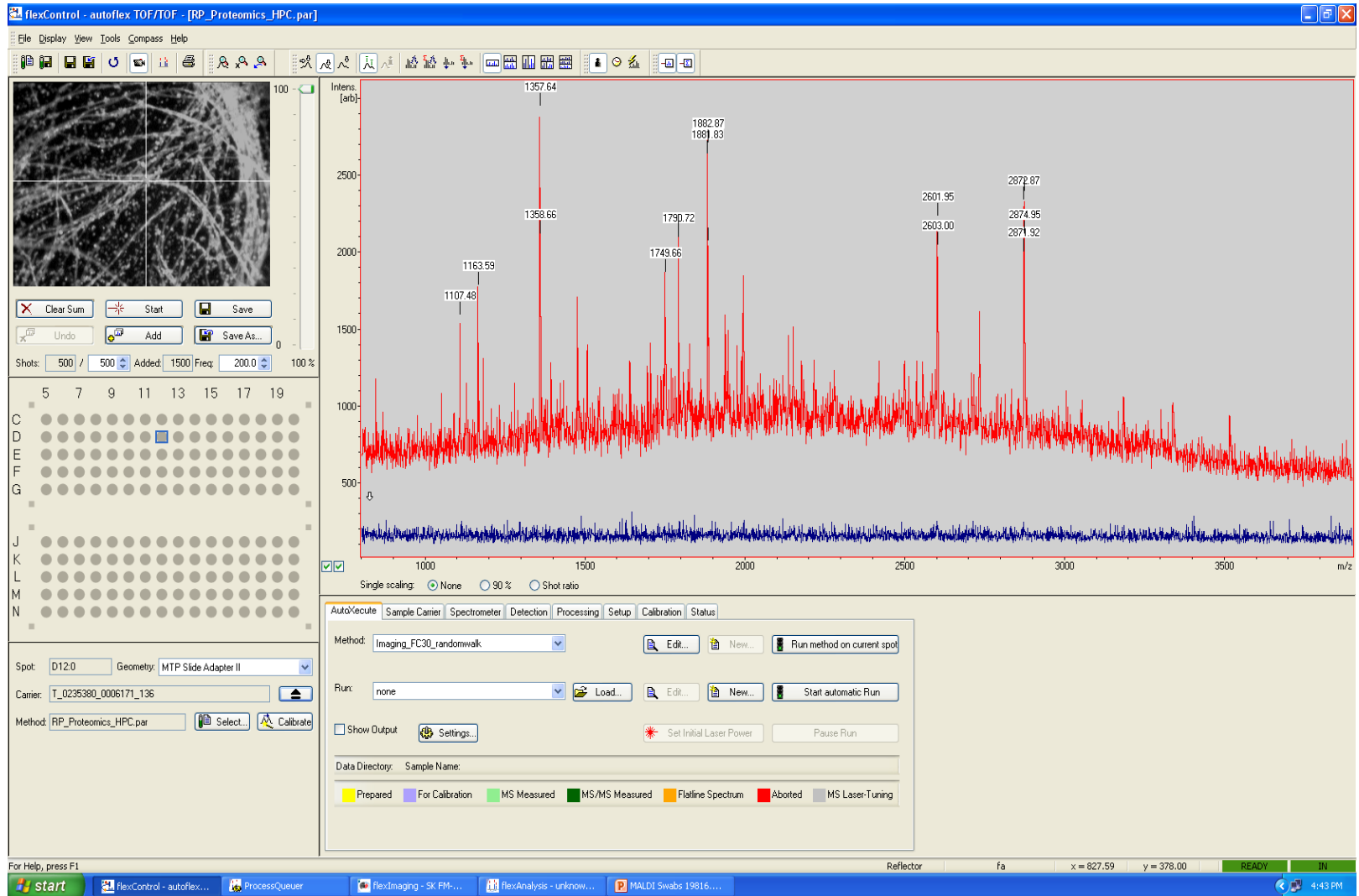
The data relating to Appendix 3A, 3C, 3D, 3E, 3F, 3G, are large, please refer to attached DVD files.

Appendix-3B

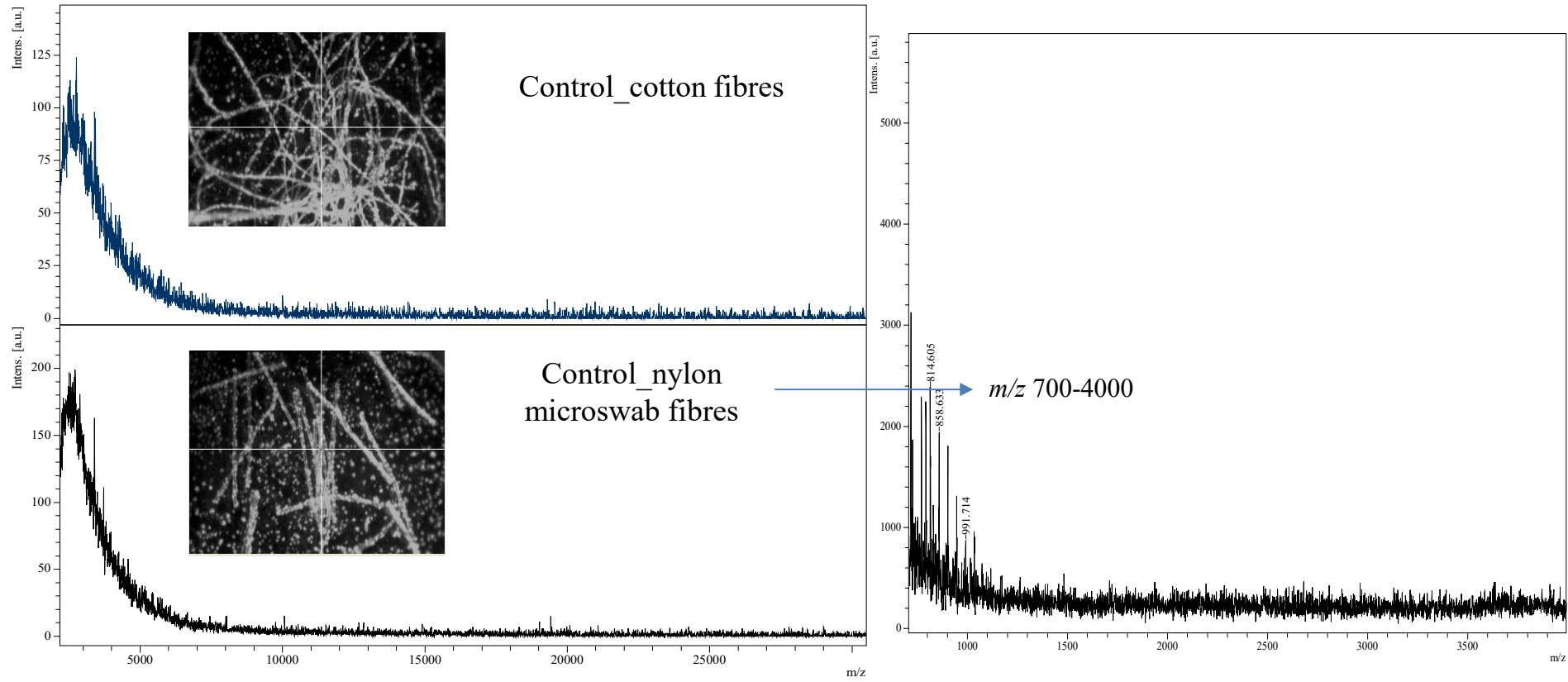
MALDI-ToF Flexcontrol image of data acquisition for 'on-nylon fibres' digested samples of fingernail deposited vaginal fluid (3 h). The fibres of nylon microswab were plucked directly onto ITO slide and digested with trypsin at the 37°C, for 3 h in a humid chamber. The peptide mass fingerprint (PMF) data were acquired on the fibres in RP (reflector positive) mode. 5 µL of CHCA (7 mg/mL in 60 %ACN and 0.2 %TFA) matrix were deposited onto the digested microfibrils.



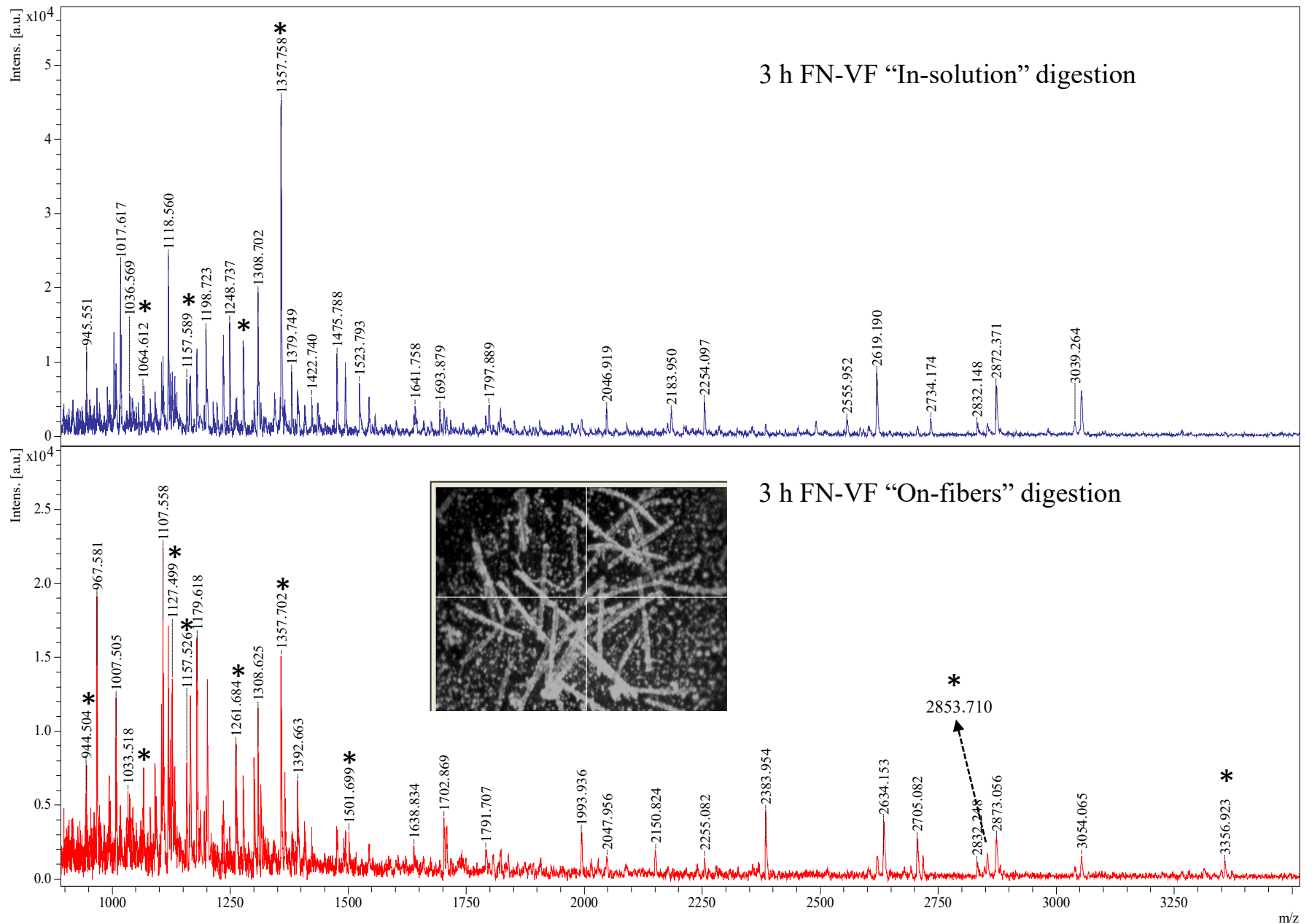
MALDI-ToF Flexcontrol image for 'on-cotton fibres' data acquisition. The cotton swab were used for direct swabbing of vaginal fluid. The several cotton fibres were plucked and the sample were processed as similar to nylon microswab.



Appendix-3B



MALDI-ToF MS spectra of **control** nylon microswab and cotton swabs, the spectra were collected from “on-fibres” data acquisition with detection range m/z 700-30000. CHCA (60 %ACN and 0.2 %TFA) were used as matrix.



MALDI-ToF MS spectra for 'in-solution' and 'on-fibres' digested microswab of fingernail-vaginal fluid (3 h) traces. Asterisk (*); detected tryptic peptides of vaginal cornulin (CRNN) protein. The same sample were carried out (approximate 50 % fibres of each experiment) for proteolysis.

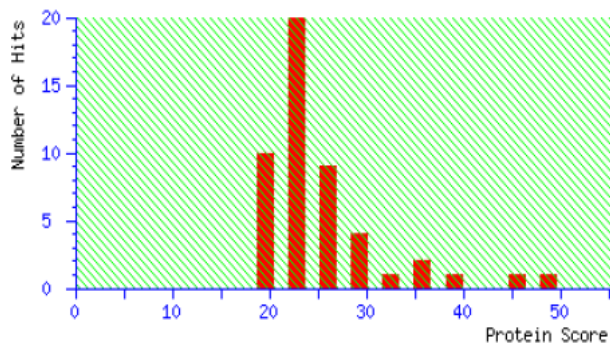
SwissProt database search results of the “in-solution” digested MALDI-PMF of fingernail scrapings (3 h) of vaginal fluid traces. The same sample (50-60 % fibres) were used for in-solution trypsin digestion followed by Mascot database identification, 9 peptides of the cornulin (CRNN) protein (vaginal marker) were detected in the extracted sample.

MATRIX SCIENCE Mascot Search Results

User : satish
 Email : satishkmb@gmail.com
 Search title :
 Database : SwissProt 2017_07 (555100 sequences; 198754198 residues)
 Taxonomy : Homo sapiens (human) (20215 sequences)
 Timestamp : 31 Aug 2017 at 06:37:20 GMT
 Top Score : 49 for **CRNN_HUMAN**, Cornulin OS=Homo sapiens GN=CRNN PE=1

Mascot Score Histogram

Protein score is $-10 \cdot \log(P)$, where P is the probability that the observed match is a Protein scores greater than 56 are significant ($p < 0.05$).



Concise Protein Summary Report

Format As [Help](#)

Significance threshold $p <$ Max. number of hits

Preferred taxonomy

1.	CRNN_HUMAN	Mass: 53502	Score: 49	Expect: 0.27	Matches: 9
Cornulin OS=Homo sapiens GN=CRNN PE=1 SV=1					
2.	K1C10_HUMAN	Mass: 58792	Score: 45	Expect: 0.62	Matches: 9
Keratin, type I cytoskeletal 10 OS=Homo sapiens GN=KRT10 PE=1 SV=6					
	YG041_HUMAN	Mass: 5615	Score: 24	Expect: 84	Matches: 2
Putative uncharacterized protein PNAS-138 OS=Homo sapiens GN=PNAS-138 PE=5 SV=1					
3.	C10T5_HUMAN	Mass: 25283	Score: 38	Expect: 3.3	Matches: 5
Complement C1q tumor necrosis factor-related protein 5 OS=Homo sapiens GN=C1QTNF5 PE=1 SV=1					
4.	AL2CL_HUMAN	Mass: 107680	Score: 35	Expect: 6.5	Matches: 10
ALS2 C-terminal-like protein OS=Homo sapiens GN=ALS2CL PE=1 SV=1					
5.	XAGE2_HUMAN	Mass: 12346	Score: 34	Expect: 7.3	Matches: 4
X antigen family member 2 OS=Homo sapiens GN=XAGE2 PE=1 SV=1					
6.	K1C13_HUMAN	Mass: 49557	Score: 32	Expect: 13	Matches: 8
Keratin, type I cytoskeletal 13 OS=Homo sapiens GN=KRT13 PE=1 SV=4					
7.	GULP1_HUMAN	Mass: 34468	Score: 31	Expect: 17	Matches: 8
PTB domain-containing engulfment adapter protein 1 OS=Homo sapiens GN=GULP1 PE=1 SV=1					
8.	DOK5_HUMAN	Mass: 35441	Score: 30	Expect: 18	Matches: 7
Docking protein 5 OS=Homo sapiens GN=DOK5 PE=1 SV=2					

SwissProt database search results of the MALDI-peptide mass fingerprint (PMF) for the fingernail scrapings (3 h) of vaginal fluid traces. The traces of microswab were subjected to “on-fibres” trypsin digestion and followed by Mascot database identification, 14 peptides of the cornulin (CRNN) protein (vaginal marker) were successfully detected by direct approach.

MASCOT SCIENCE Mascot Search Results

8/31/2017

Concise Summary Report (./data/20170831/FTieCrHwO.dat)

User : satish
 Email : satishkmb@gmail.com
 Search title :
 Database : SwissProt 2017_07 (555100 sequences; 198754198 resid
 Taxonomy : Homo sapiens (human) (20215 sequences)
 Timestamp : 31 Aug 2017 at 06:41:44 GMT
 Top Score : 92 for **CRNN_HUMAN**, Cornulin OS=Homo sapiens GN=CRNN

Re-Search All

Search Unmatched



1. [CRNN_HUMAN](#) Mass: 53502 Score: **92** Expect: 1.2e-05 Matches: 14
 Cornulin OS=Homo sapiens GN=CRNN PE=1 SV=1

2. [K2C1_HUMAN](#) Mass: 65999 Score: 41 Expect: 1.5 Matches: 11
 Keratin, type II cytoskeletal 1 OS=Homo sapiens GN=KRT1 PE=1 SV=6

3. [PRS37_HUMAN](#) Mass: 26428 Score: 39 Expect: 2.7 Matches: 6
 Probable inactive serine protease 37 OS=Homo sapiens GN=PRSS37 PE=2 SV=1

4. [K1C10_HUMAN](#) Mass: 58792 Score: 34 Expect: 7.2 Matches: 7
 Keratin, type I cytoskeletal 10 OS=Homo sapiens GN=KRT10 PE=1 SV=6
[YG041_HUMAN](#) Mass: 5615 Score: 24 Expect: 90 Matches: 2
 Putative uncharacterized protein PNAS-138 OS=Homo sapiens GN=PNAS-138 PE=5 SV=1

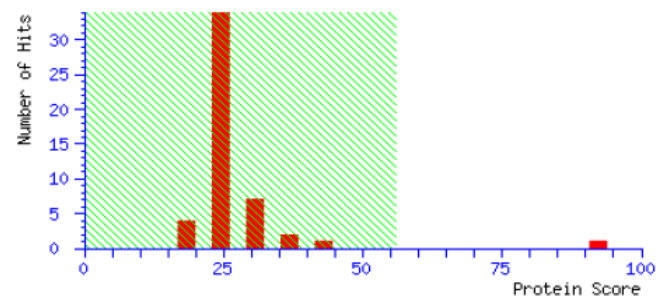
5. [MZB1_HUMAN](#) Mass: 20681 Score: 33 Expect: 9.5 Matches: 5
 Marginal zone B- and B1-cell-specific protein OS=Homo sapiens GN=MZB1 PE=1 SV=1

6. [ZN619_HUMAN](#) Mass: 63281 Score: 32 Expect: 12 Matches: 7
 Zinc finger protein 619 OS=Homo sapiens GN=ZNF619 PE=2 SV=1

7. [PEX19_HUMAN](#) Mass: 32786 Score: 29 Expect: 24 Matches: 4
 Peroxisomal biogenesis factor 19 OS=Homo sapiens GN=PEX19 PE=1 SV=1

Mascot Score Histogram

Protein score is $-10 \cdot \log(P)$, where P is the probability that the observed match is random. Protein scores greater than 56 are significant ($p < 0.05$).



Concise Protein Summary Report

Format As

Concise Protein Summary

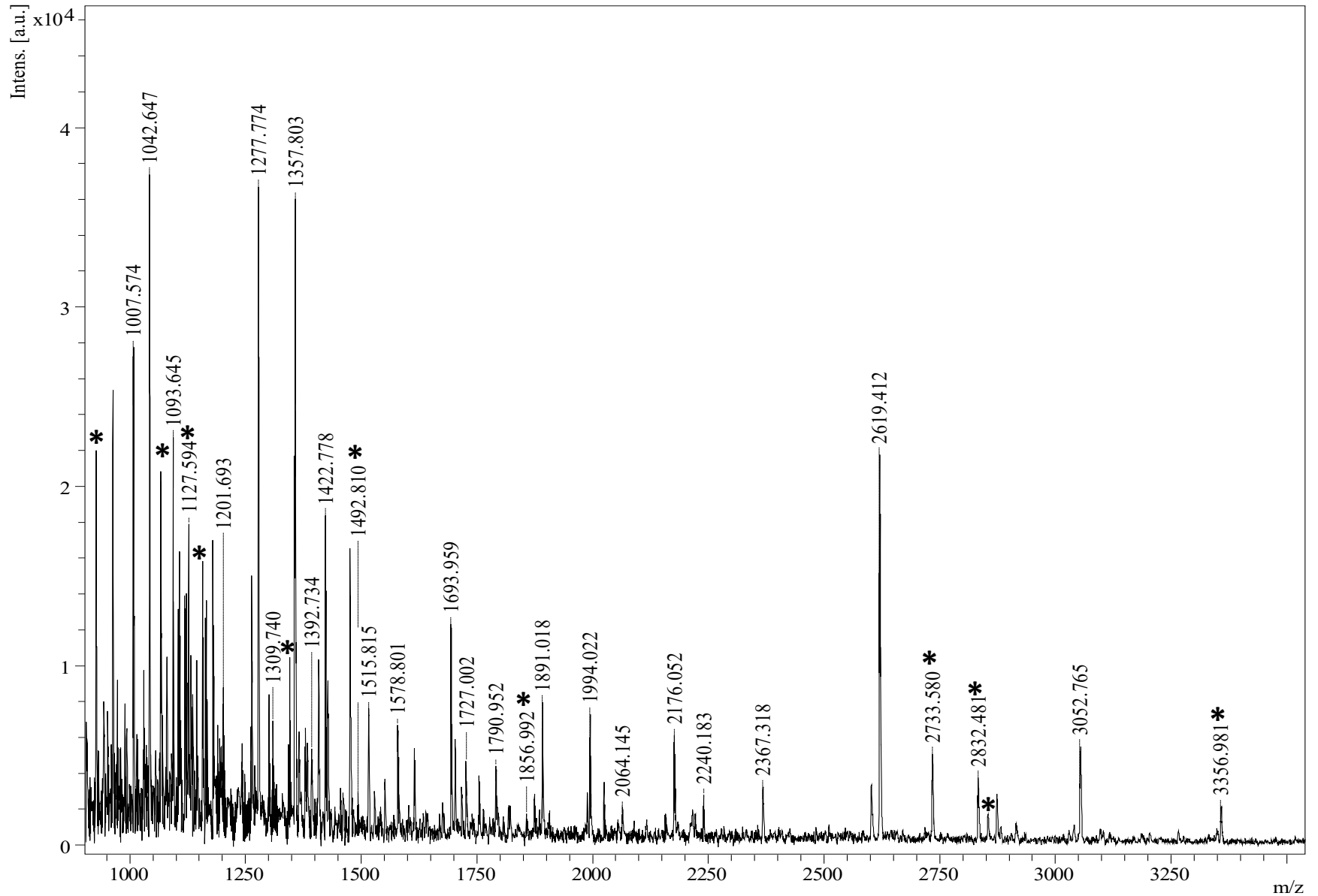
[Help](#)

Significance threshold p< 0.05

Max. number of hits

Preferred taxonomy All entries

Appendix-3 H



Supporting information for **Figure 5.5** MALDI-ToF spectrum of fingernail traces of vaginal fluid (collected after 1 h deposition), the same microswab were used for performing direct-PCR DNA profile and MALDI data acquisition. The several micro fibers were directly plucked onto ITO-slide and then “on-fiber” trypsin digestion was performed. *Indicates the matched cornulin peptides.

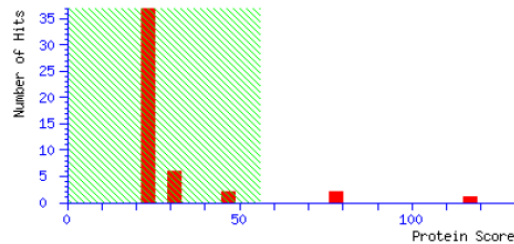
Appendix-3 H

MASCOT SCIENCE Mascot Search Results

User : Sati
Email : satishmb@gmail.com
Search title :
Database : SwissProt 2017_10 (556006 sequences; 199234755 residues)
Taxonomy : Homo sapiens (human) (20240 sequences)
Timestamp : 17 Nov 2017 at 11:36:26 GMT
Top Score : 117 for Mixture 1, CRNN_HUMAN + K1C13_HUMAN

Mascot Score Histogram

Protein score is $-10 \cdot \log(P)$, where P is the probability that the observed match is a
Protein scores greater than 56 are significant ($p < 0.05$).



11/17/2017

Concise Summary Report (./data/20171117/FTmtizEeO.da

- Mixture 1** Total score: **117** Expect: 4e-08 Matches: 28
Components (only one family member shown for each component):
[CRNN_HUMAN](#) Mass: 53502 Score: **81** Expect: 0.00015 Matches: 14
Cornulin OS=Homo sapiens GN=CRNN PE=1 SV=1
[K1C13_HUMAN](#) Mass: 49557 Score: **75** Expect: 0.00063 Matches: 14
Keratin, type I cytoskeletal 13 OS=Homo sapiens GN=KRT13 PE=1 SV=4

- [CRNN_HUMAN](#) Mass: 53502 Score: **81** Expect: 0.00015 Matches: 14
Cornulin OS=Homo sapiens GN=CRNN PE=1 SV=1

- [K1C13_HUMAN](#) Mass: 49557 Score: **75** Expect: 0.00063 Matches: 14
Keratin, type I cytoskeletal 13 OS=Homo sapiens GN=KRT13 PE=1 SV=4

- [K1C10_HUMAN](#) Mass: 58792 Score: 49 Expect: 0.24 Matches: 11
Keratin, type I cytoskeletal 10 OS=Homo sapiens GN=KRT10 PE=1 SV=6
[YG041_HUMAN](#) Mass: 5615 Score: 22 Expect: 1.2e+02 Matches: 2
Putative uncharacterized protein PNAS-138 OS=Homo sapiens GN=PNAS-138 PE=5 SV=1

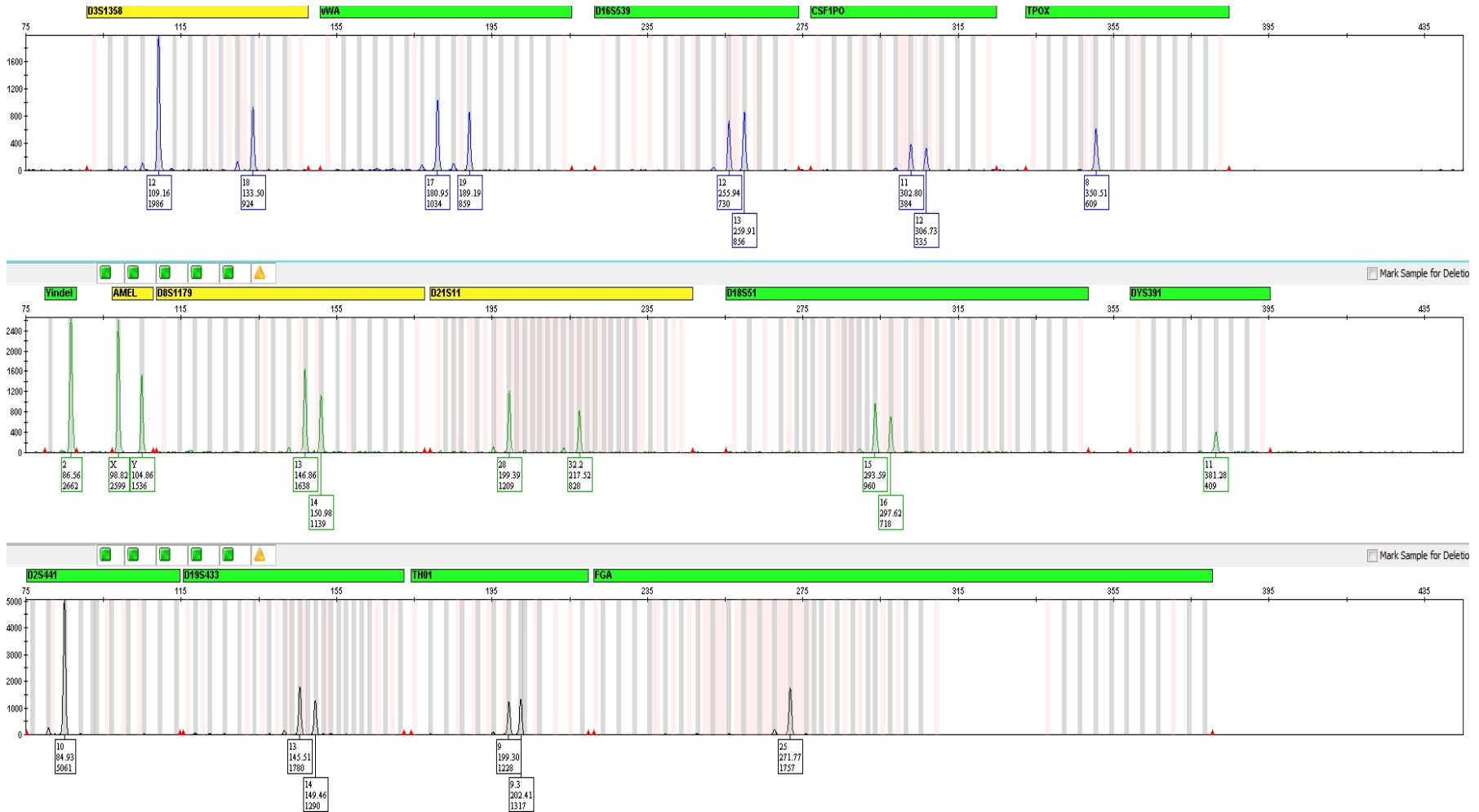
- [RS12_HUMAN](#) Mass: 14505 Score: 46 Expect: 0.56 Matches: 7
40S ribosomal protein S12 OS=Homo sapiens GN=RPS12 PE=1 SV=3

- [MYH2_HUMAN](#) Mass: 222906 Score: 33 Expect: 9.7 Matches: 19
Myosin-2 OS=Homo sapiens GN=MYH2 PE=1 SV=1

- [CDN2C_HUMAN](#) Mass: 18116 Score: 31 Expect: 16 Matches: 5
Cyclin-dependent kinase 4 inhibitor C OS=Homo sapiens GN=CDKN2C PE=1 SV=1

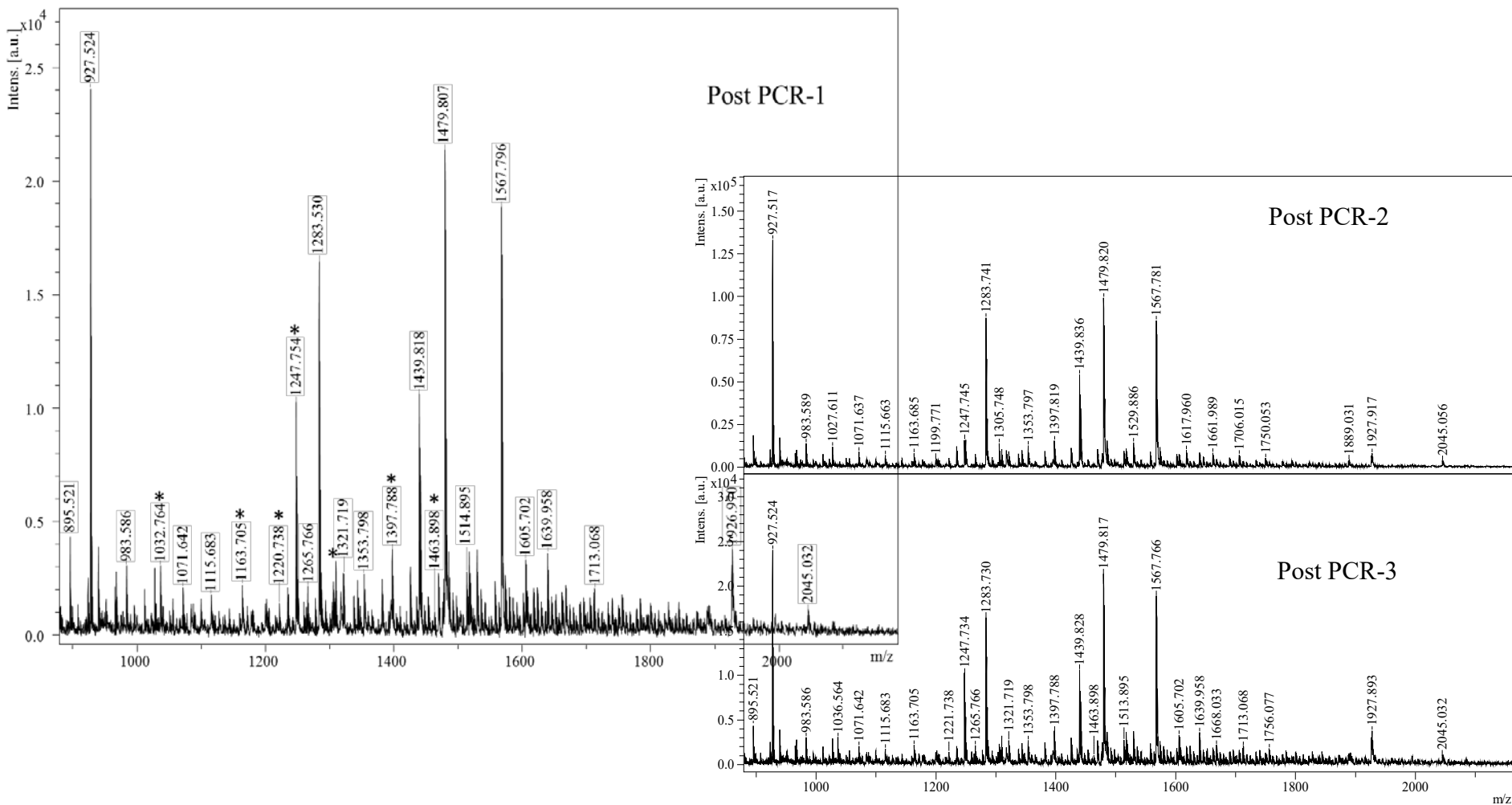
- [K2C4_HUMAN](#) Mass: 57250 Score: 31 Expect: 16 Matches: 10
Keratin, type II cytoskeletal 4 OS=Homo sapiens GN=KRT4 PE=1 SV=4

Appendix-3 I



Direct-PCR DNA profile data (selected loci) from traces of red kangaroo blood under fingernails collected 6 h after deposition. Globalfiler STR kit used. Note that the same male volunteer was involved in the collection of traces depicted below and those in the Figure above.

Appendix-3 I



MALDI-ToF PMF spectra for post PCR products of fingernail scraping (6 h) of *Macropus rufus* blood traces. The direct PCR were conducted in replicate samples with three different fingernail scrapings. The post PCR solutions (2 . L) were digested using trypsin at 37°C for overnight. CHCA (in 60% ACN and 0.2%TFA) was used as MALDI matrix. Asterisk (*) indicates the matched tryptic peptides of haemoglobin (*M. rufus*) protein.

MATRIX SCIENCE Mascot Search Results

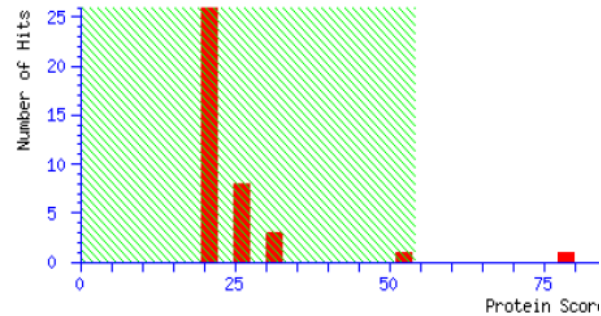
Appendix-3 I

User : Sathish
 Email : sathishmb@gmail.com
 Search title :
 Database : SwissProt 2017_08 (555426 sequences; 198919479 residues)
 Taxonomy : Other mammalia (13152 sequences)
 Timestamp : 19 Sep 2017 at 08:27:55 GMT
 Top Score : 78 for **HBB_MACGI**, Hemoglobin subunit beta OS=Macropus giganteus GN=HBB PE=1 SV=1

Concise Summary Report (./data/20170919/FTirrxTwL.dat)

Mascot Score Histogram

Protein score is $-10 \cdot \log(P)$, where P is the probability that Protein scores greater than 54 are significant ($p < 0.05$).

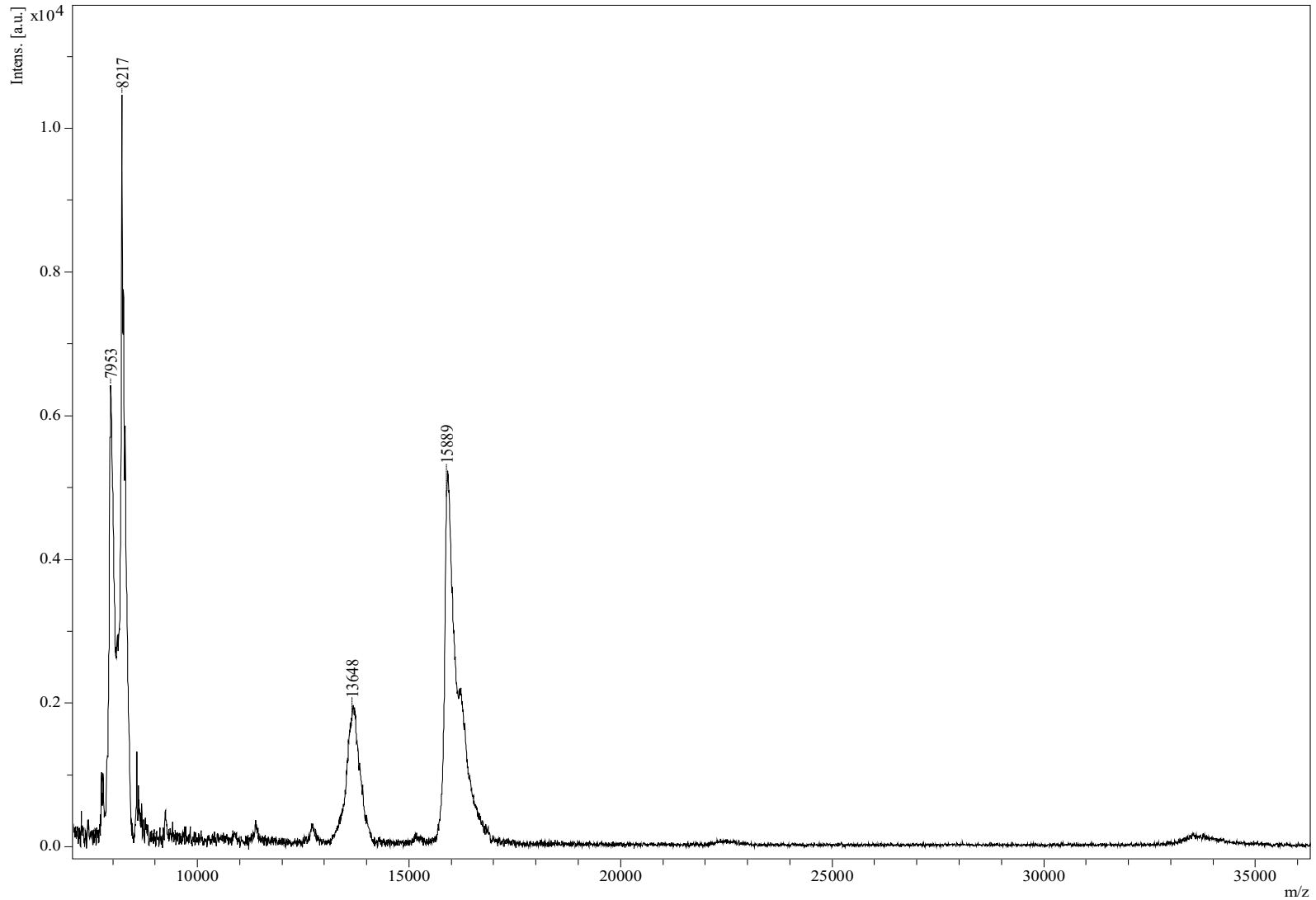


Concise Protein Summary Report

9/19/2017

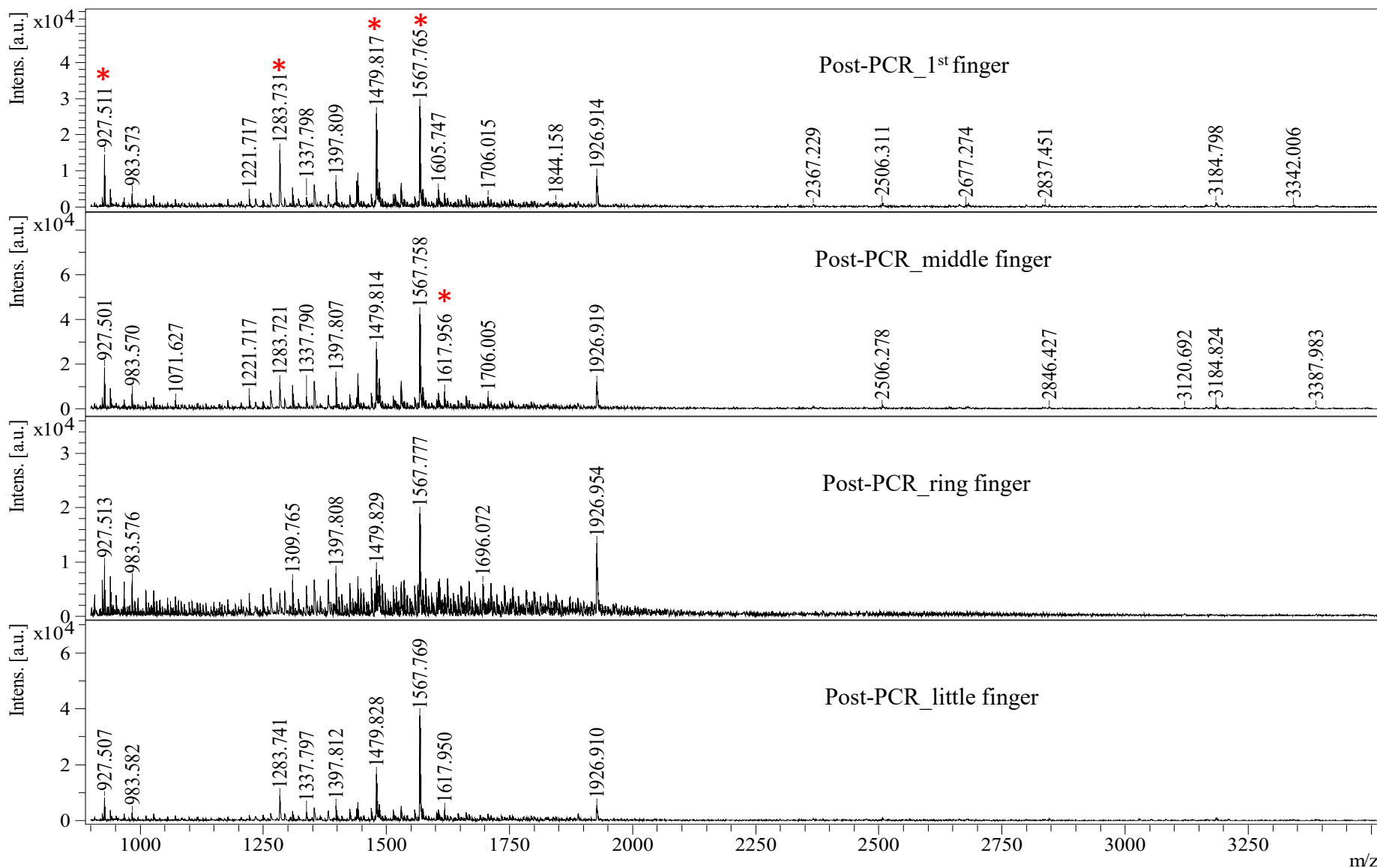
- [HBB_MACGI](#) Mass: 16005 Score: **78** Expect: 0.00019 Matches: 8
 Hemoglobin subunit beta OS=Macropus giganteus GN=HBB PE=1 SV=1
[HBB_MACRU](#) Mass: 15991 Score: **78** Expect: 0.00019 Matches: 8
 Hemoglobin subunit beta OS=Macropus rufus GN=HBB PE=1 SV=1
[HBB_MACEU](#) Mass: 16122 Score: **65** Expect: 0.0043 Matches: 7
 Hemoglobin subunit beta OS=Macropus eugenii GN=HBB PE=2 SV=3
[HBB_POTTR](#) Mass: 15923 Score: 30 Expect: 13 Matches: 4
 Hemoglobin subunit beta OS=Potorous tridactylus GN=HBB PE=1 SV=1
- [ALBU_BOVIN](#) Mass: 69248 Score: 52 Expect: 0.089 Matches: 11
 Serum albumin OS=Bos taurus GN=ALB PE=1 SV=4
- [ALDR_PIG](#) Mass: 35845 Score: 34 Expect: 5.4 Matches: 6
 Aldose reductase OS=Sus scrofa GN=AKR1B1 PE=1 SV=2
- [TCAL1_BOVIN](#) Mass: 18638 Score: 29 Expect: 15 Matches: 4
 Transcription elongation factor A protein-like 1 OS=Bos taurus GN=TCEAL1 PE=2 SV=1
- [PSB8_CANLE](#) Mass: 30479 Score: 29 Expect: 16 Matches: 5
 Proteasome subunit beta type-8 OS=Canis lupus familiaris GN=PSMB8 PE=1 SV=1
[DFBC7_BOVIN](#) Mass: 5646 Score: 19 Expect: 1.5e+02 Matches: 2
 Beta-defensin C7 (Fragment) OS=Bos taurus PE=2 SV=1
- [SNP25_RABIT](#) Mass: 6061 Score: 28 Expect: 20 Matches: 3
 Synaptosomal-associated protein 25 (Fragments) OS=Oryctolagus cuniculus GN=SNAP25 PE=1 SV=1
- [HBB_RANTA](#) Mass: 16156 Score: 26 Expect: 32 Matches: 4
 Hemoglobin subunit beta OS=Rangifer tarandus GN=HBB PE=1 SV=1
[HBBA_CAPHI](#) Mass: 16011 Score: 20 Expect: 1.3e+02 Matches: 3
 Hemoglobin subunit beta-A OS=Capra hircus PE=1 SV=1
[HBB_SHEEP](#) Mass: 16063 Score: 20 Expect: 1.3e+02 Matches: 3
 Hemoglobin subunit beta OS=Ovis aries GN=HBB PE=1 SV=2

Appendix-3 I



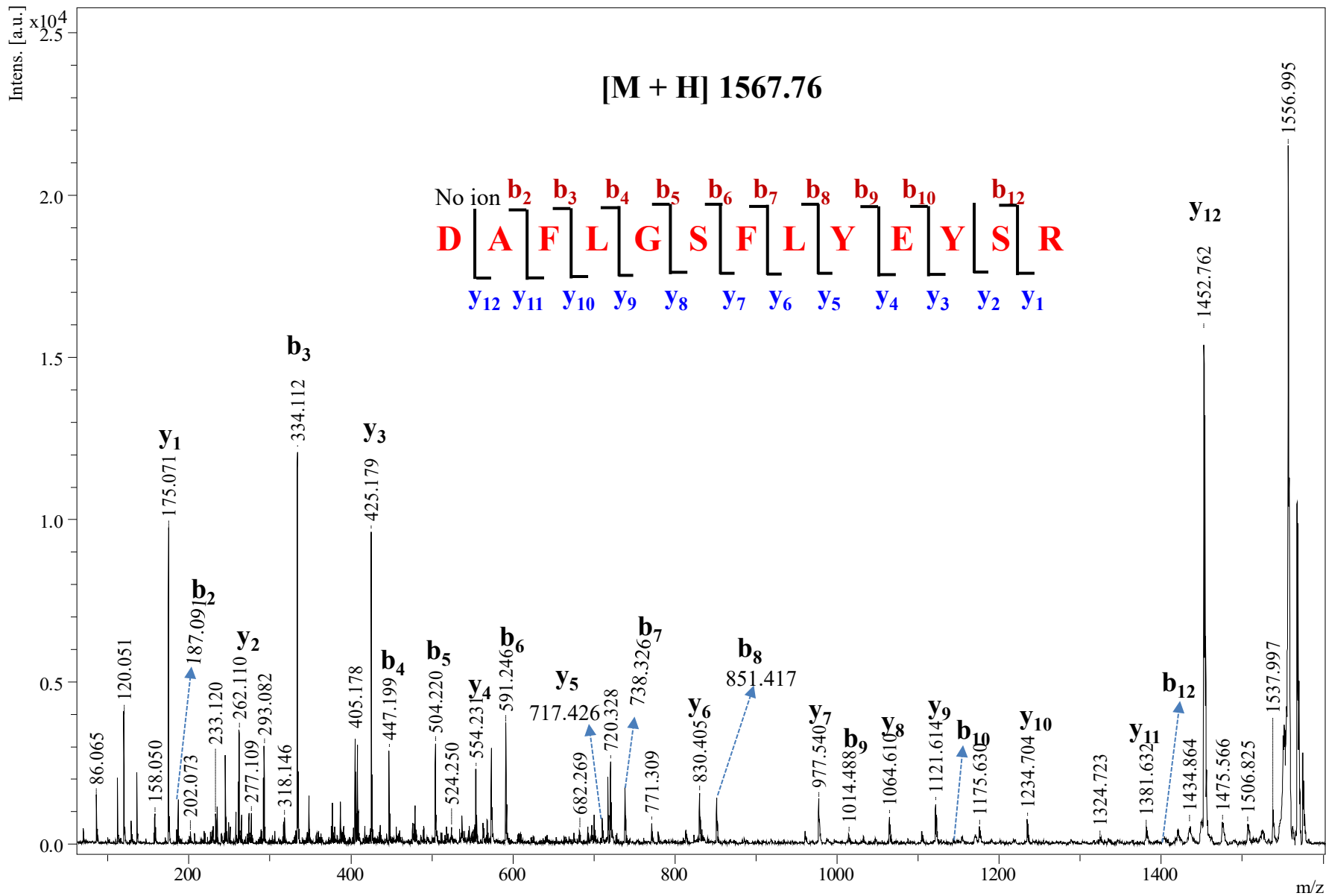
MALDI-ToF intact protein spectrum of post PCR (direct) solution of fingernail scraping (6 h) of *Macropus rufus* (Red kangaroo) blood.

Appendix -3 J



MALDI-peptide fingerprint mass (PMF) spectra of post-PCR products. The conventional PCR carried out solutions were used for trypsin digestion at the 37°C, for overnight. Asterisk* indicates the matched tryptic peptides of bovine serum albumin (BSA) protein which is present in PCR extraction solution (buffers). CHCA (10 mg/mL in 60 % ACN and 0.2 % TFA) was used as a matrix.

Appendix -3 J



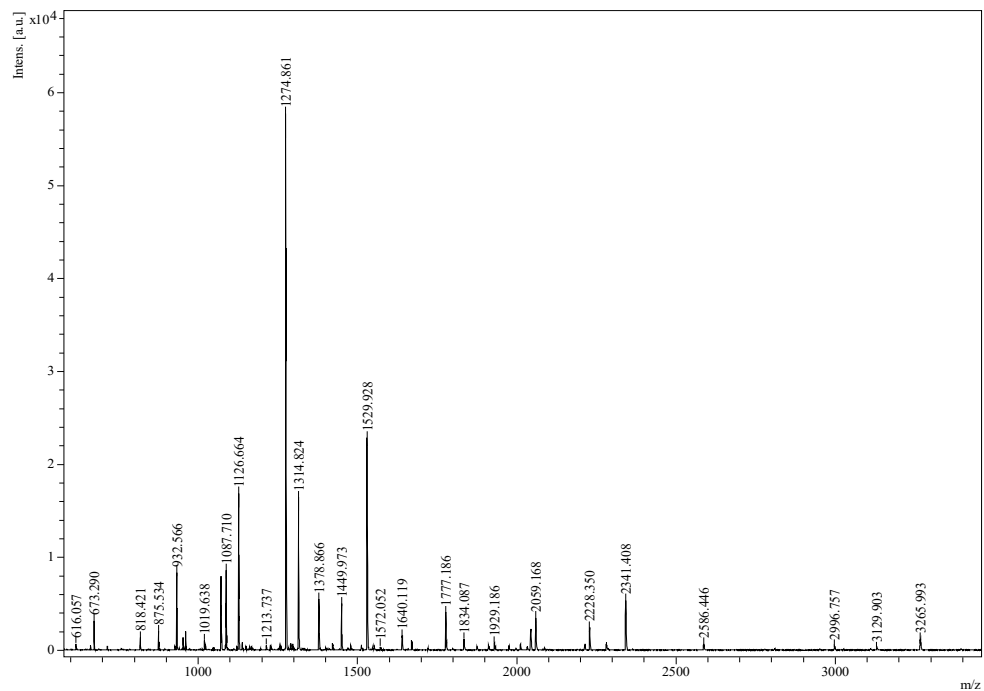
MALDI-ToF MS/MS spectrum of precursor ion at m/z 1567.76. A matched tryptic peptide arose from BSA protein. All the matched “b” and “y” product ions were indicated in the spectrum. The “LIFT” spectrum was acquired from post-PCR DNA (conventional extraction method) solution.

Appendix 4

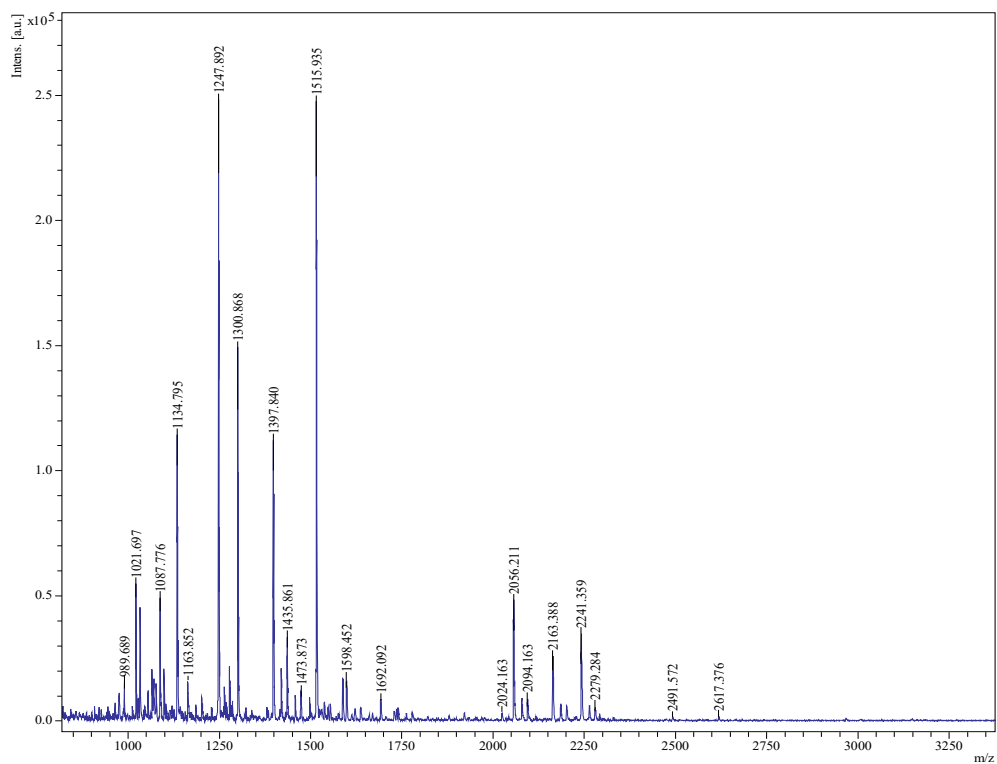
The data relating to Appendix 4B and 4H are large, please refer to attached DVD files.

Appendix-4A. MALDI-ToF MS tryptic peptide mass fingerprints (PMF) for human and non-human blood samples

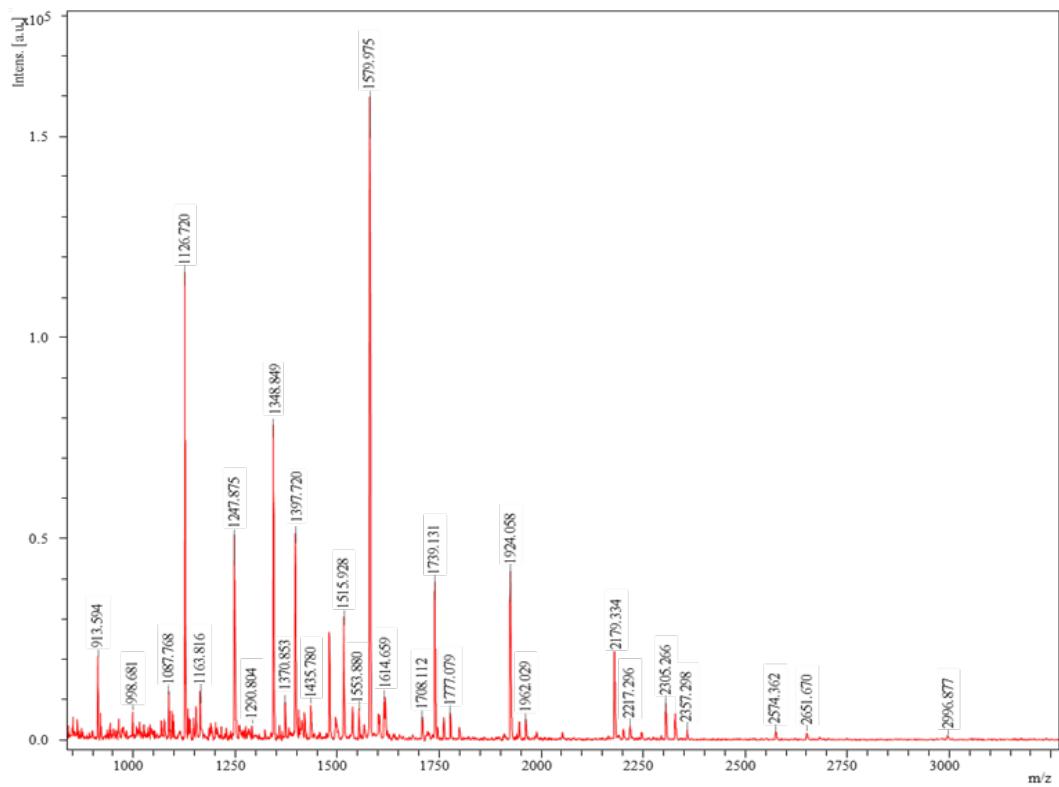
Human



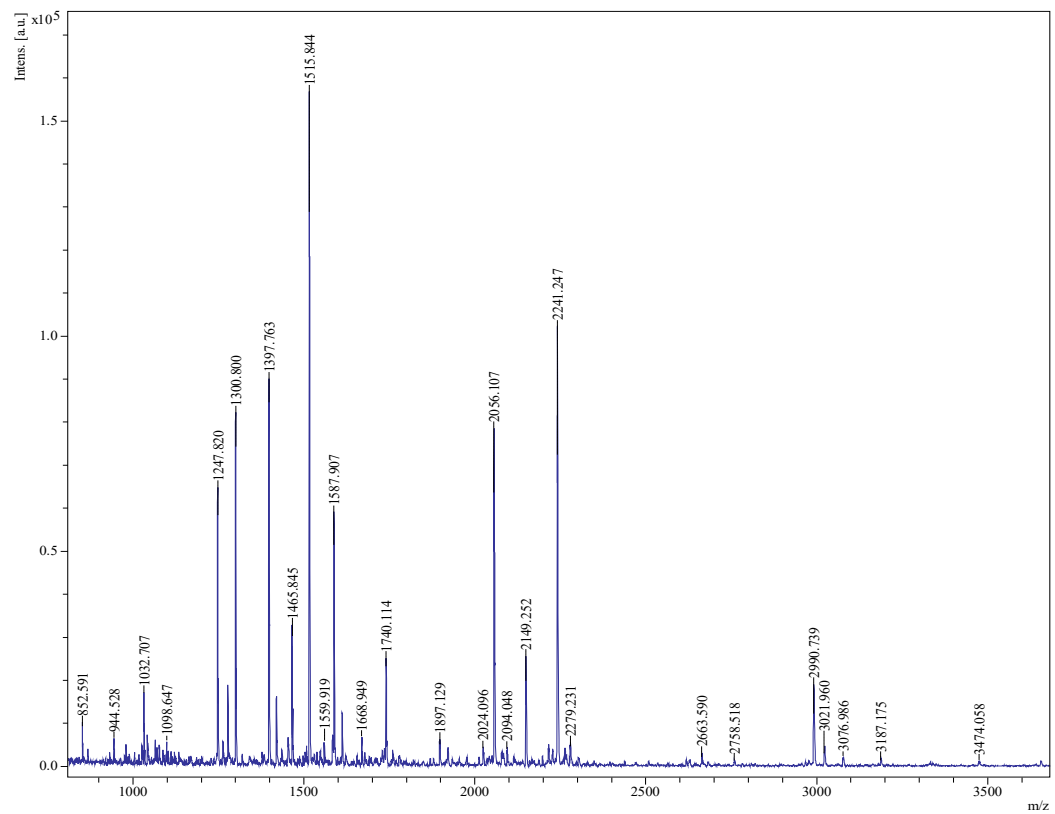
Dama Wallaby (*Macropus eugenii*)



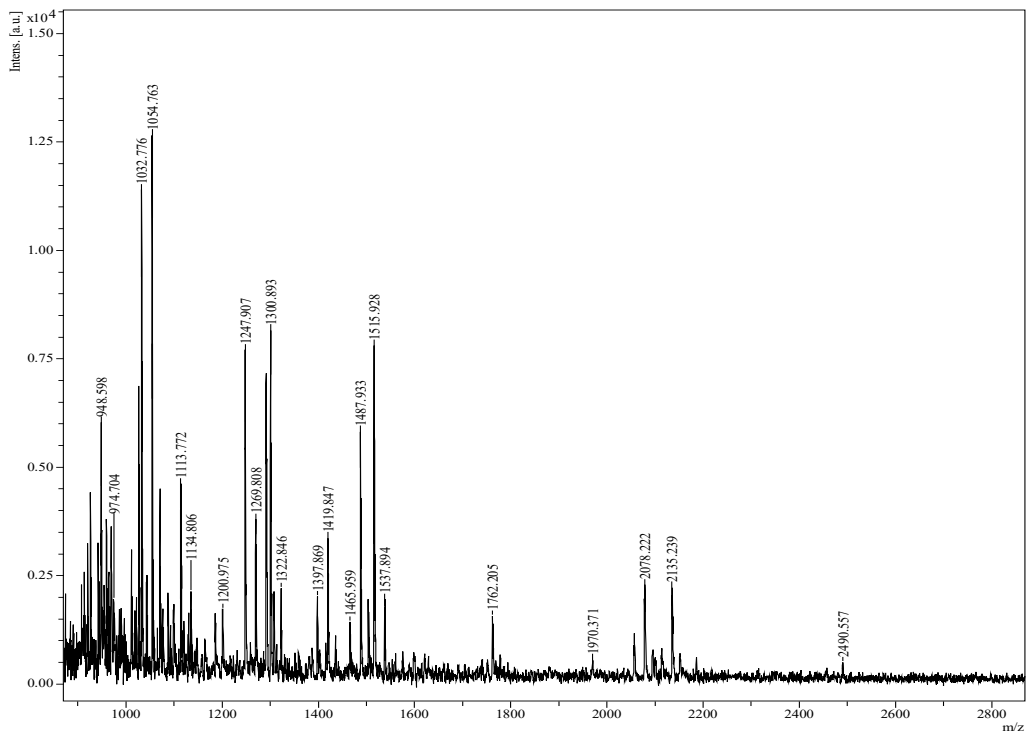
Koala (*Phascolarctos cinereus*)



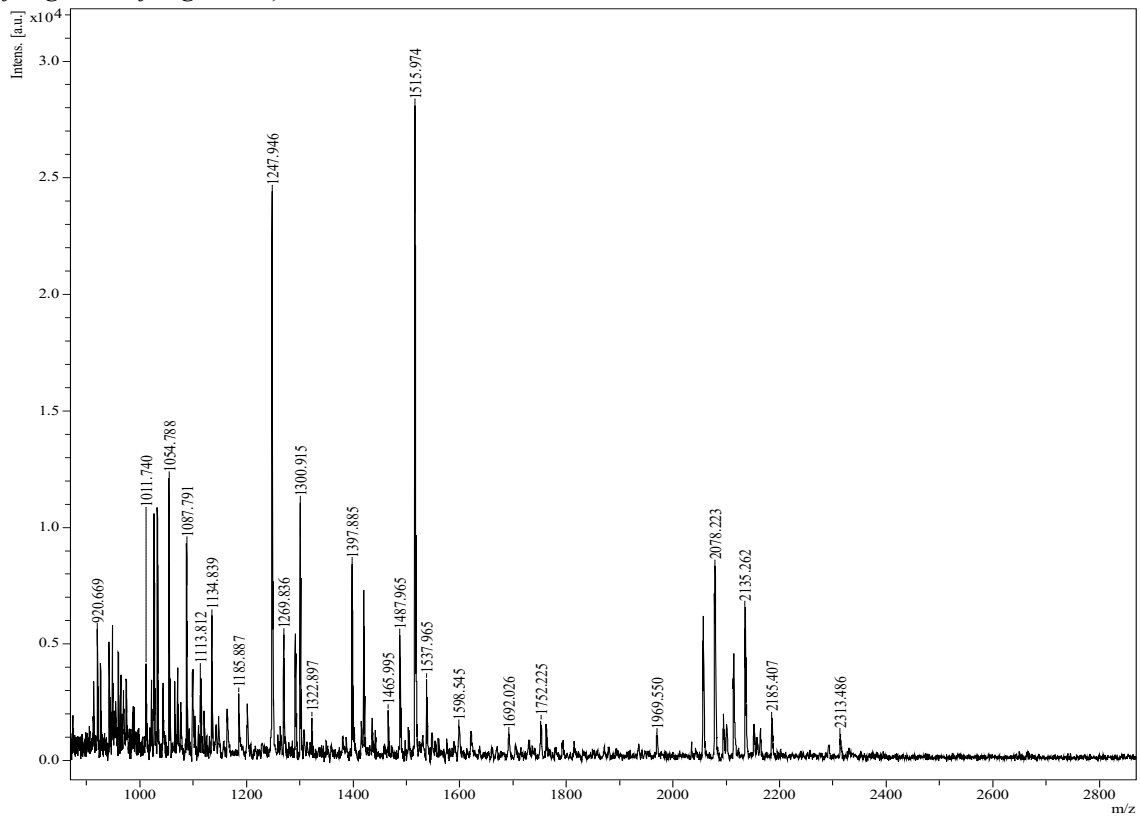
Swamp Wallaby (*Wallabia bicolor*)



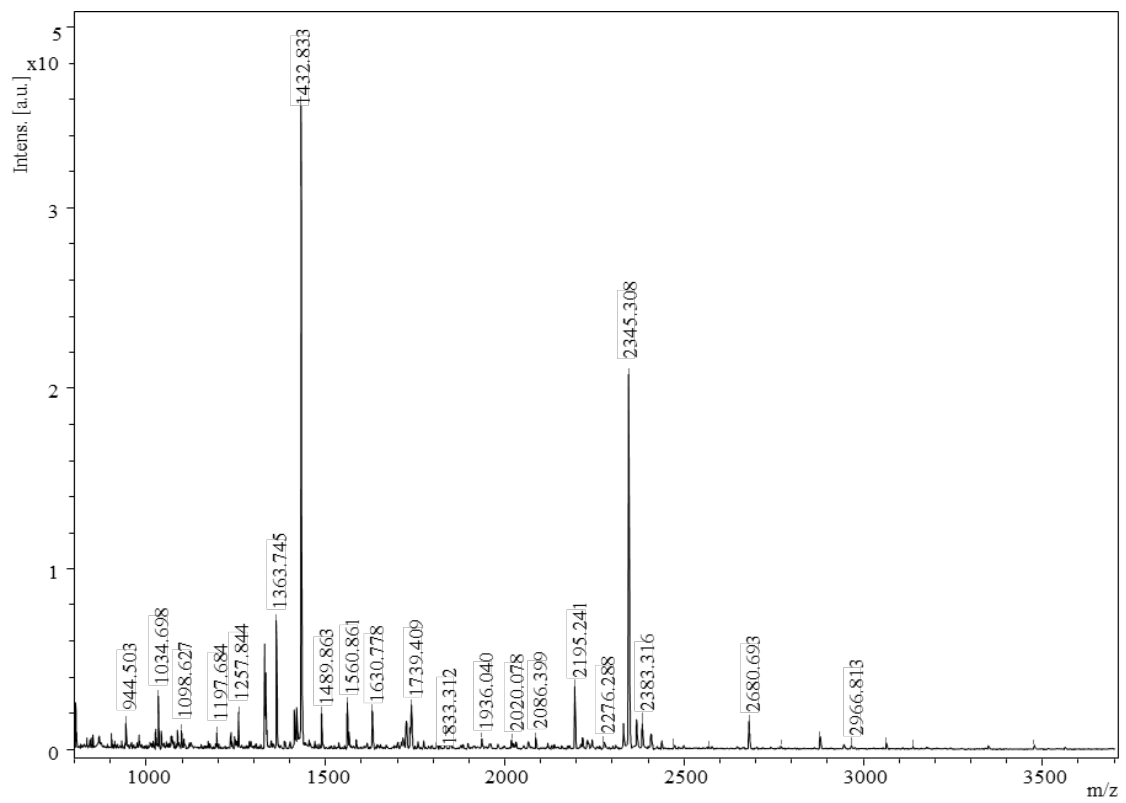
Eastern grey Kangaroo (*Macropus giganteus*)



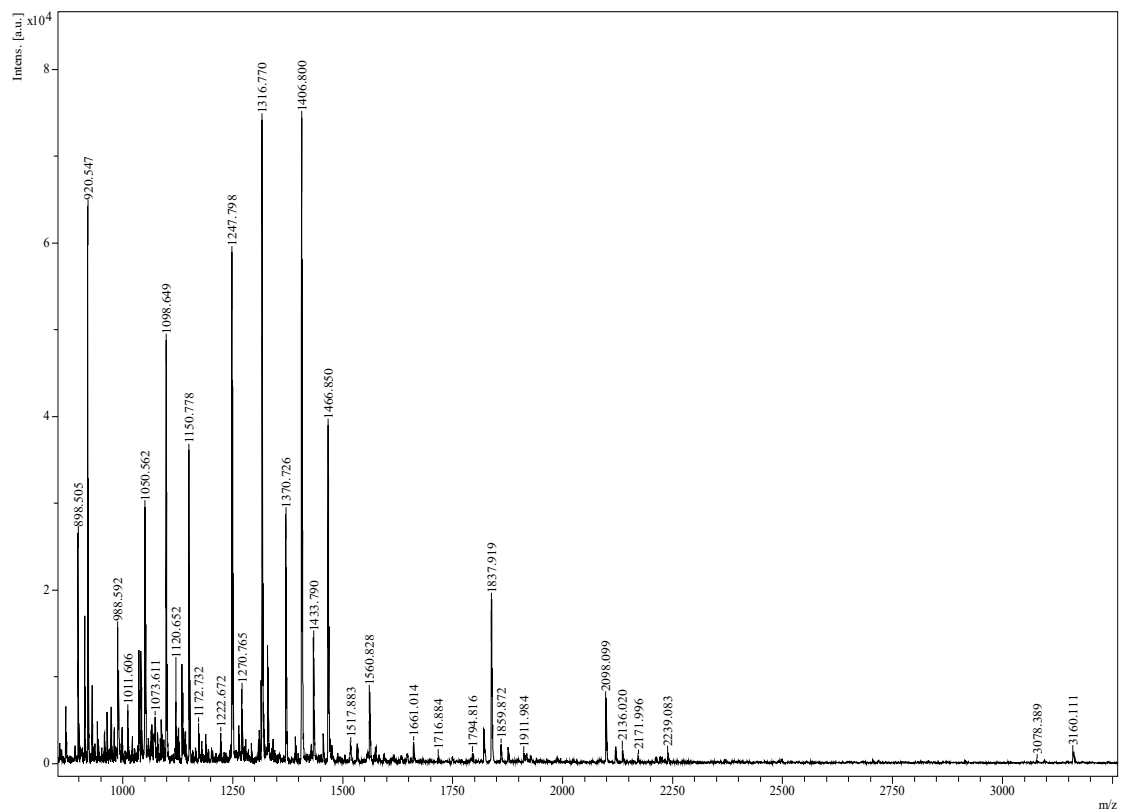
Western Grey Kangaroo and Kangaroo Island sub-species (*Macropus fuliginosus*, *Macropus fuliginosus fuliginosus*)



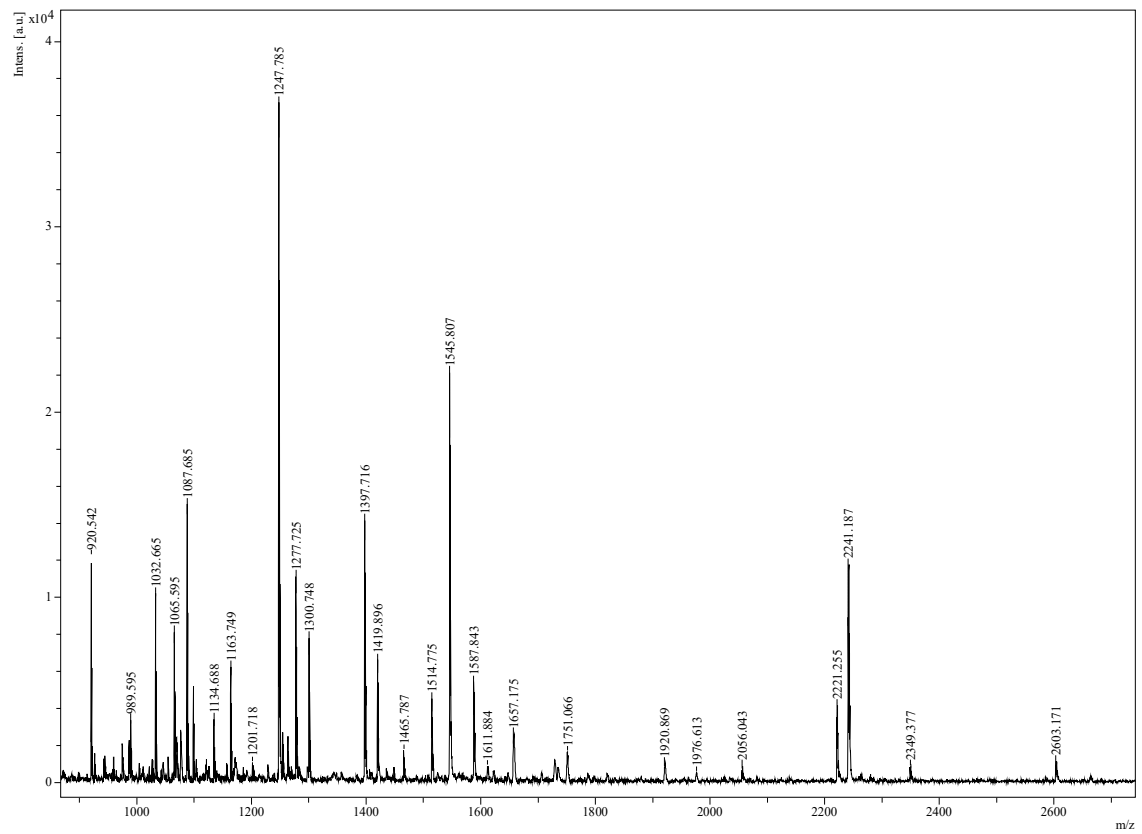
Brushtail POSSUM (*Trichosurus vulpecula*)



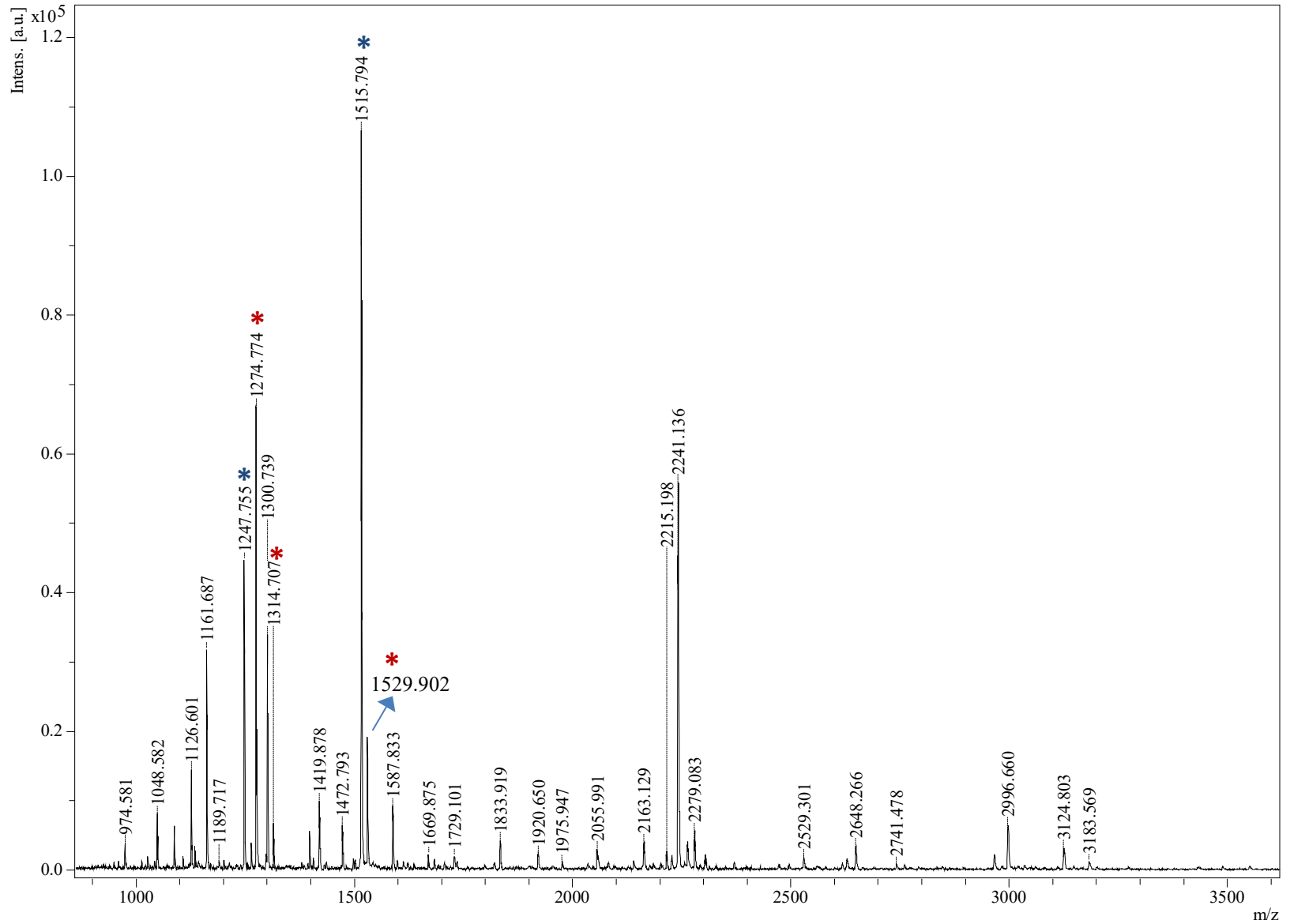
Tasmania devil (*Sarcophilus harrisii*)



Red Kangaroo (*Macropus rufus*)

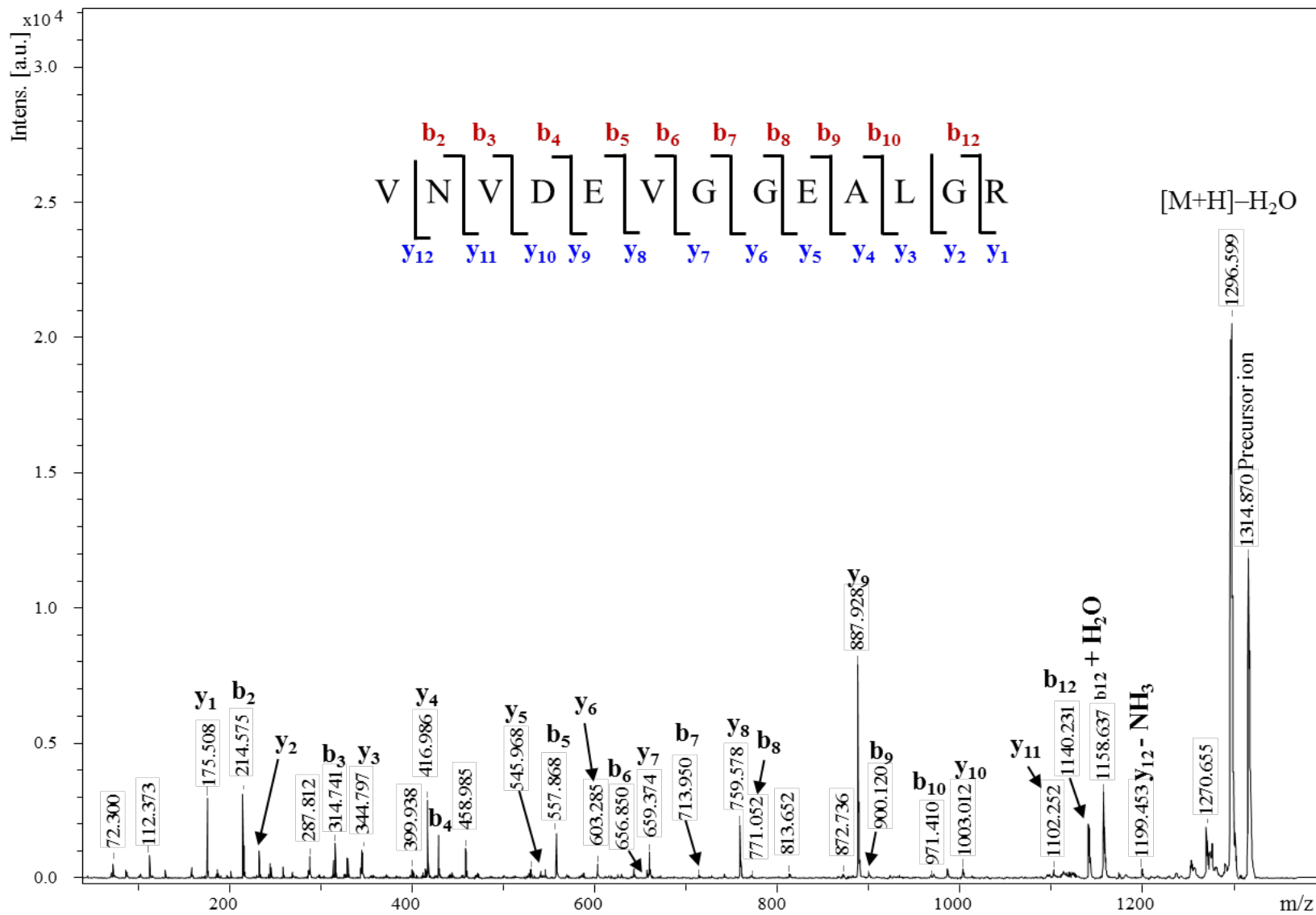


Appendix-4C



MALDI-ToF-MS tryptic peptide mass fingerprint (PMF) of Human (*) and Dama Wallaby (*) blood mixture (1:1). The spectrum was acquired on a bloodied fingerprint (the same mark used for MALDI-imaging). Homogenous CHCA (7mg/mL) matrix was deposited using the ImagePrep station.

Appendix-4D



MALDI-ToF MS/MS spectrum acquired from precursor ion m/z 1314.87 with its matched peptide sequence of human HB-B. Spectrum was acquired on bloodied fingermark.

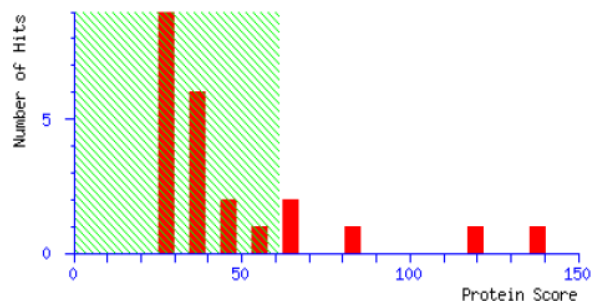
Appendix-4E. SwissProt database search results for a bloodied fingerprint made from mixed human and dama wallaby blood. The mark was enhanced using amido black protein stain solution and fixed with methanol and glacial acetic acid solutions. The intact protein and trypsin digest analyses were performed on dark blue coloured fingerprint ridges. MALDI-ToF-MS peptide mass fingerprint (PMF) data were searched against the SwissProt database using Mascot software database against “Mammalia” taxonomy. All the proteins detected were HB-A-subunits

MATRIX SCIENCE Mascot Search Results

User : sati
 Email : satishmb@gmail.com
 Search title :
 Database : SwissProt 2017_03 (553941 sequences; 198311666 residues)
 Taxonomy : Mammalia (mammals) (66595 sequences)
 Timestamp : 13 Apr 2017 at 10:15:25 GMT
 Top Score : 138 for **Mixture 1**, HBA_MACEU + HBA_HUMAN

Mascot Score Histogram

Protein score is $-10 \cdot \log(P)$, where P is the probability that the observed match is a random. Protein scores greater than 61 are significant ($p < 0.05$).



4/13/2017

Concise Summary Report (./data/20170413/FTipOeEnT.dat)

- Mixture 1** Total score: **138** Expect: 1.1e-09 Matches: 18
 Components (only one family member shown for each component):
[HBA_MACEU](#) Mass: 15327 Score: **119** Expect: 8.4e-08 Matches: 11
 Hemoglobin subunit alpha OS=Macropus eugenii GN=HBA PE=1 SV=3
[HBA_HUMAN](#) Mass: 15248 Score: **81** Expect: 0.00049 Matches: 8
 Hemoglobin subunit alpha OS=Homo sapiens GN=HBA1 PE=1 SV=2
- [HBA_MACEU](#) Mass: 15327 Score: **119** Expect: 8.4e-08 Matches: 11
 Hemoglobin subunit alpha OS=Macropus eugenii GN=HBA PE=1 SV=3
[HBA_MACGT](#) Mass: 15210 Score: **90** Expect: 6.7e-05 Matches: 9
 Hemoglobin subunit alpha OS=Macropus giganteus GN=HBA PE=1 SV=1
- [HBA_HUMAN](#) Mass: 15248 Score: **81** Expect: 0.00049 Matches: 8
 Hemoglobin subunit alpha OS=Homo sapiens GN=HBA1 PE=1 SV=2
[HBA_PANPA](#) Mass: 15248 Score: **81** Expect: 0.00049 Matches: 8
 Hemoglobin subunit alpha OS=Pan paniscus GN=HBA1 PE=1 SV=2
[HBA_PANTR](#) Mass: 15248 Score: **81** Expect: 0.00049 Matches: 8
 Hemoglobin subunit alpha OS=Pan troglodytes GN=HBA1 PE=1 SV=2
[HBA_SEMEN](#) Mass: 15112 Score: 35 Expect: 20 Matches: 5
 Hemoglobin subunit alpha OS=Sennopithecus entellus GN=HBA PE=1 SV=1
[HBA_CALAR](#) Mass: 15129 Score: 33 Expect: 31 Matches: 4
 Hemoglobin subunit alpha OS=Callithrix argentata GN=HBA PE=1 SV=1
[HBA_SAGOF](#) Mass: 15085 Score: 33 Expect: 31 Matches: 4
 Hemoglobin subunit alpha OS=Saguinus oedipus GN=HBA PE=1 SV=1
[HBA_ATEGE](#) Mass: 15216 Score: 33 Expect: 33 Matches: 4
 Hemoglobin subunit alpha OS=Ateles geoffroyi GN=HBA PE=1 SV=2
- [HBA_GORGO](#) Mass: 15103 Score: **65** Expect: 0.02 Matches: 7
 Hemoglobin subunit alpha OS=Gorilla gorilla gorilla GN=HBA PE=1 SV=1
[HBA1_HYLLA](#) Mass: 15258 Score: **65** Expect: 0.021 Matches: 7
 Hemoglobin subunit alpha-1 OS=Hylobates lar GN=HBA1 PE=2 SV=2
[HBA_PONPY](#) Mass: 15322 Score: 54 Expect: 0.24 Matches: 6
 Hemoglobin subunit alpha OS=Pongo pygmaeus GN=HBA1 PE=2 SV=2
[HBA_MACAS](#) Mass: 15111 Score: 47 Expect: 1.4 Matches: 6
 Hemoglobin subunit alpha-1/2/3 OS=Macaca assamensis PE=1 SV=1
[HBA_MACFA](#) Mass: 15102 Score: 47 Expect: 1.4 Matches: 6

Protein View: HBA_MACEU

Appendix-4E

Hemoglobin subunit alpha OS=Macropus eugenii GN=HBA PE=1 SV=3

Database: SwissProt
Score: 119
Expect: 8.4e-08
Monoisotopic mass (M_r): 15327
Calculated pI: 7.22
Taxonomy: Notamacropus eugenii

Sequence similarity is available as [an NCBI BLAST search of HBA_MACEU against nr](#).

Search parameters

Enzyme: Trypsin: cuts C-term side of KR unless next residue is P.
Mass values searched: 50 **Protein sequence coverage: 69%**
Mass values matched: 11

Protein sequence coverage: 69%

Matched peptides shown in **bold red**.

1 **MVLSAADKGH VKGIWGKVG HAGEYAAEGL ERTFHSFPTT KTYFPDFDLS**
51 **HGSAQIQAHG KKIADALGQA VEHIDDLPGT LSKLSDLHAH KLRVDPVNFK**
101 LLSHCLLVTF AAHLGDAFTP EVHASLDKFL AAVSTVLTSK YR

Unformatted sequence string: **142 residues** (for pasting into other applications).

Sort by residue number increasing mass decreasing mass
Show matched peptides only predicted peptides also

Start - End	Observed	Mr (expt)	Mr (calc)	Delta M	Peptide
2 - 12	1124.7550	1123.7477	1123.6349	0.1128 1	M.VLSAADKGHVK.G
9 - 17	981.6640	980.6567	980.5556	0.1011 1	K.GHVKGIWGK.V
13 - 32	2057.0880	2056.0807	2056.0126	0.0681 1	K.GIWGKVGGHAGEYAAEGLER.T
18 - 32	1515.8140	1514.8067	1514.7113	0.0954 0	K.VGGHAGEYAAEGLER.T
33 - 41	1065.6590	1064.6517	1064.5291	0.1226 0	R.TFHSFPTTK.T
42 - 61	2241.2210	2240.2137	2240.0763	0.1374 0	K.TYFPDFDLSHGSAQIQAHGK.K
42 - 62	2369.3160	2368.3087	2368.1713	0.1375 1	K.TYFPDFDLSHGSAQIQAHGKK.I
63 - 83	2163.2310	2162.2237	2162.1219	0.1018 0	K.IADALGQAVEHIDDLPGTLSK.L
84 - 91	920.6110	919.6037	919.4875	0.1162 0	K.LSDLHAHK.L
84 - 93	1189.8120	1188.8047	1188.6727	0.1320 1	K.LSDLHAHKLR.V
92 - 100	1087.6610	1086.6537	1086.6186	0.0351 1	K.LRVDPVNFK.L

Protein View: HBA_HUMAN

Appendix-4E

Hemoglobin subunit alpha OS=Homo sapiens GN=HBA1 PE=1 SV=2

Database: SwissProt
Score: 81
Expect: 0.00049
Monoisotopic mass (M_r): 15248
Calculated pI: 8.72
Taxonomy: Homo sapiens

Sequence similarity is available as [an NCBI BLAST search of HBA_HUMAN against nr.](#)

Search parameters

Enzyme: Trypsin: cuts C-term side of KR unless next residue is P.
Mass values searched: 50
Mass values matched: 8

Protein sequence coverage: 66%

Matched peptides shown in **bold red**.

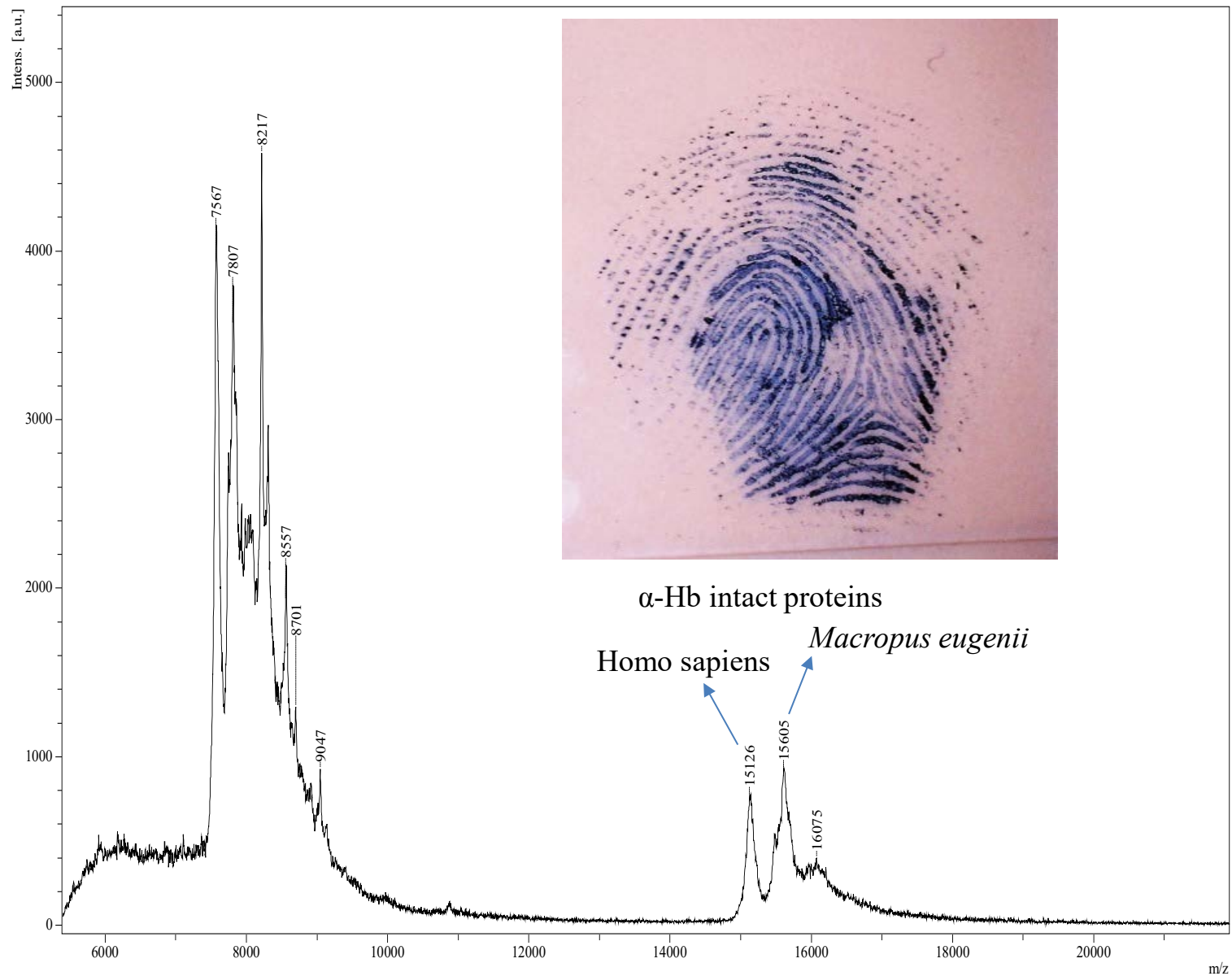
1 **MVLSPADKTN VKAAWGKVG A HAGEYGAEAL ERMFLSFPTT KTYFPHF DLS**
51 **HGSAQVKGHG KKVADALTNA VAHVDDMPNA LSALS DLHAH KLRVDPVNF K**
101 LLSHCLLVTL AAHLPAEFTP AVHASLDKFL ASVSTVLT SK YR

Unformatted sequence string: **142 residues** (for pasting into other applications).

Sort by residue number increasing mass decreasing mass
Show matched peptides only predicted peptides also

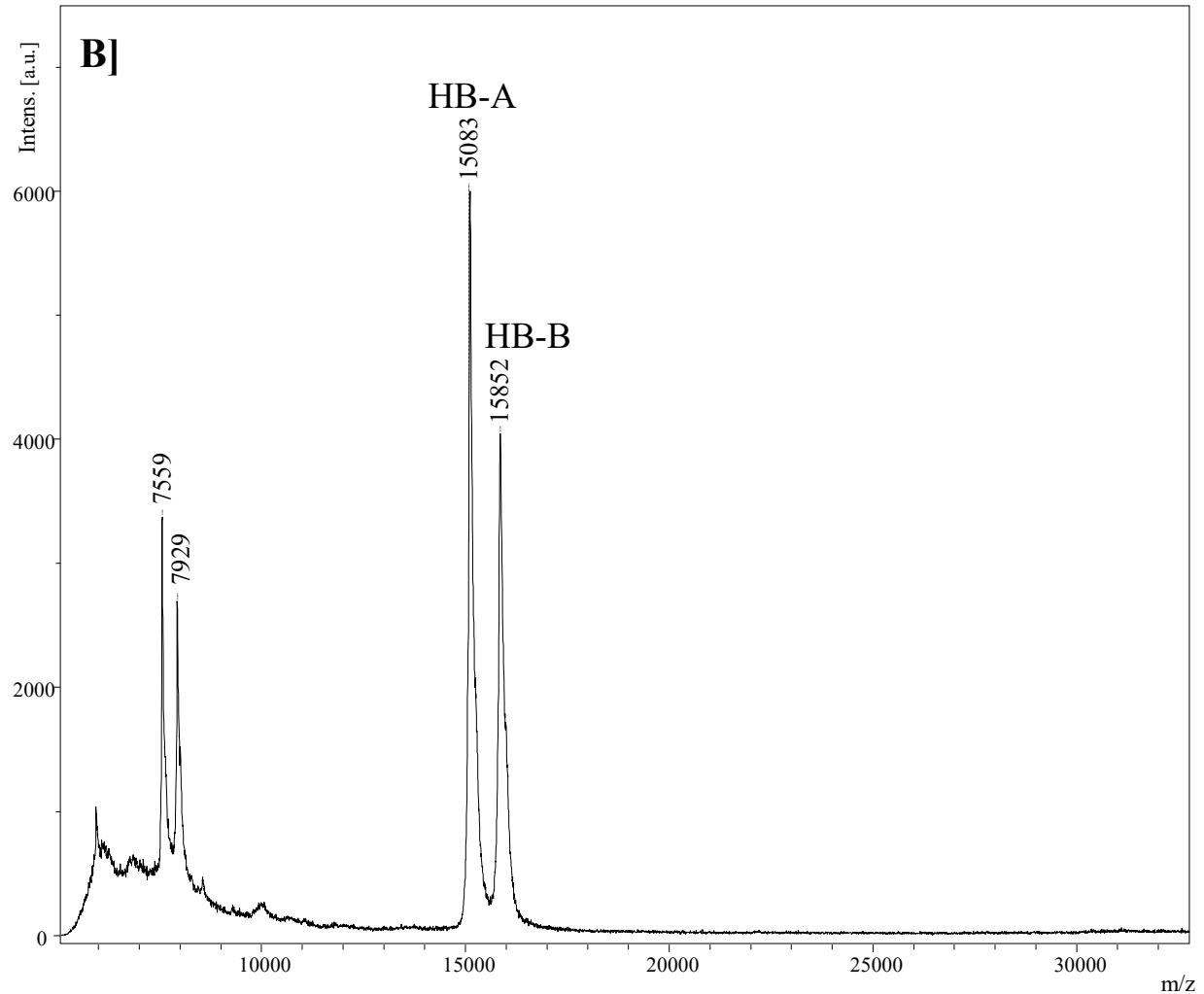
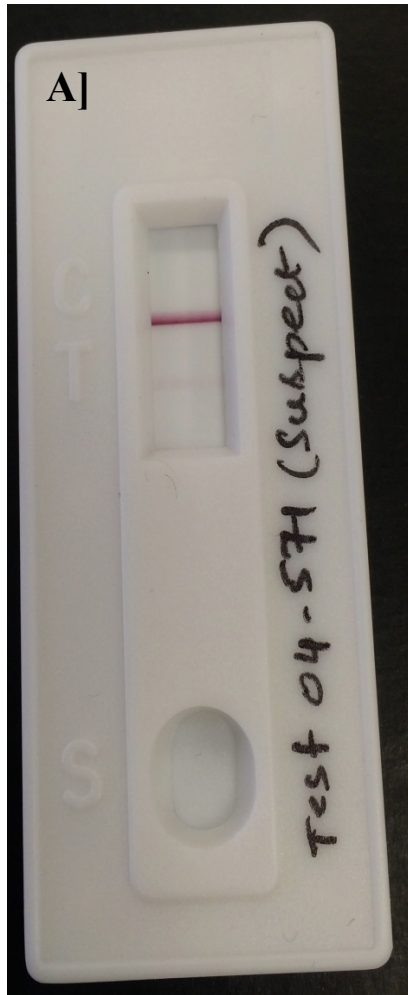
Start - End	Observed	Mr(expt)	Mr(calc)	Delta M	Peptide
2 - 12	1171.7890	1170.7817	1170.6608	0.1209 1	M.VLSPADKTNVK.A
9 - 17	974.6050	973.5977	973.5345	0.0632 1	K.TNVKAAWGK.V
18 - 32	1529.8650	1528.8577	1528.7270	0.1307 0	K.VGAHAGEYGAEALER.M
18 - 41	2582.2900	2581.2827	2581.2635	0.0192 1	K.VGAHAGEYGAEALERMFLSFPTTK.T
33 - 41	1071.6800	1070.6727	1070.5471	0.1257 0	R.MFLSFPTTK.T
42 - 57	1833.9960	1832.9887	1832.8846	0.1041 0	K.TYFPHF DLSHGSAQVK.G
63 - 93	3265.8840	3264.8767	3264.6673	0.2094 1	K.VADALTNAVAHVDDMPNALSALS DLHAHKLR.V
92 - 100	1087.6610	1086.6537	1086.6186	0.0351 1	K.LRVDPVNFK.L

Appendix-4E



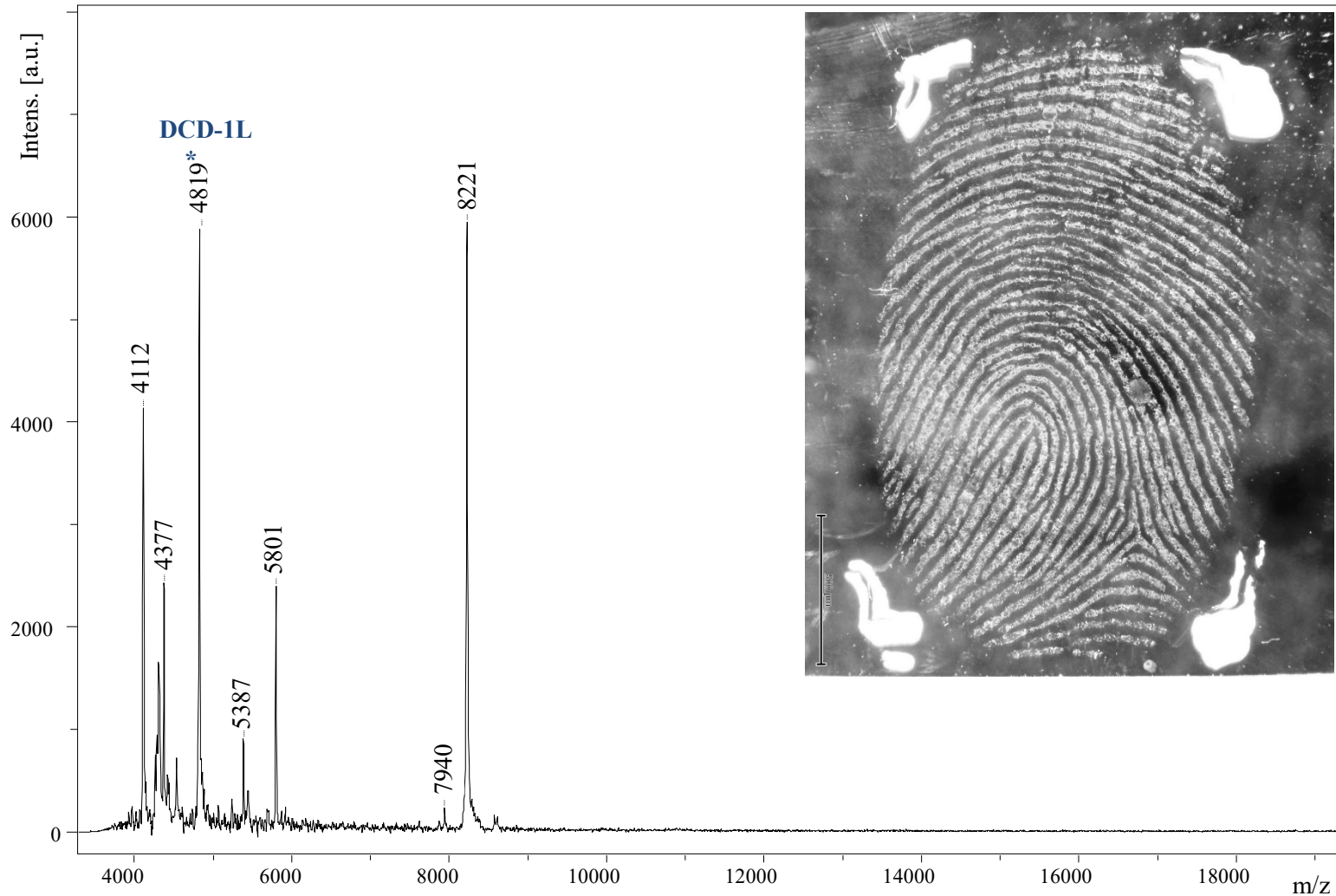
MALDI-TOF spectrum for intact proteins from the human and dama wallaby blood mixture. The spectra were acquired on an amido black stained bloodied fingerprint. Sinapinic acid (SA) matrix was used and data were recorded in linear positive mode.

Appendix-4F



A) ABAcard® Hematrace® test results of aged (January 2004) CTS proficiency test blood sample (04-571). Extraction solution of 200 μ L was added into ABA card at marked 'S' region. After 5 min a weak band was observed in the marked 'T' region. Control 'C' band appeared dark pink in colour. B) MALDI-ToF-MS intact protein spectrum using less than 1 μ L of the extraction solution. HB-A and HB-B hemoglobin proteins are evident.

Appendix-4G



MALDI-ToF-MS intact protein profiles of a control fingermark (i.e., not exposed to blood mixtures). The control mark was deposited onto an ITO coated slide and an intact protein spectrum was acquired over an m/z 3,500-20,000 detection range. Dermcidin (DCD 1L), an antimicrobial protein, was detected in the mark but blood traces were not. The spectrum was collected in linear mode (LP) and 10 mg/mL CHCA (in 60 %ACN and 0.2 % TFA) was used as MALDI matrix.

Appendix 5

ATR-IR data for Australian Marsupial blood samples are presented in the attached DVD.

Following are images of posters presented and awards received.

Mass Spectrometry-based Forensic “Omics” and MALDI-imaging analysis for the Identification/Visualization of Bodily Fluid traces in Fingermarks

Sathisha Kamanna¹, Adrian Linacre¹, Nico Voelcker², Julianne Henry³, Paul Kirkbride¹

Flinders University¹, University of South Australia², Forensic Science SA³, Australia





INTRODUCTION

Analysis of body fluids such as blood, saliva and vaginal secretions is very important to the investigation of crimes against the person such as murder and rape. Whereas DNA profiling is reliable in establishing from whom the body fluid originated, tests to positively identify the type of fluid involved (e.g., whether it is blood or saliva or a mixture of them) are much less refined and can be equivocal. Our recently published article [1] describes a streamlined and simplified direct approach for the identification of body fluids using matrix-assisted laser desorption/ionization time-of-flight mass spectrometry (MALDI-TOF-MS) that avoids pre-fractionation or isolation of proteins from mixtures. Here we show an extension of that work towards an integrated forensic Prote‘Omics’ and Gen‘Omics’ approach in regards to the analysis body fluids or fingermarks. In regards to fingermarks, the Prote‘Omics’ approach using MALDI-imaging mass spectrometry (MALDI-IMS) could indicate that a mark deposited by the male suspect contains a suspicious foreign fluid, such as vaginal fluid for example, while Gen‘Omics’ could identify the female contributor of the fluid. This would represent very powerful evidence.

MATERIALS AND METHODS

Body fluids/fingermark samples were sourced from volunteers pursuant to Southern Adelaide Clinical Human Research Ethics Committee Application 440.14-HREC/14/SAC/455. Proficiency test kits provided by Collaborative Testing Services (Stirling, Virginia, USA) were used as part of the validation program. All samples of direct and extracted fluids were analysed using MALDI-ToF MS and the identity of protein markers was confirmed by *de-novo* sequencing and nLC-MS/MS analysis. Genomics analysis of body fluids was performed using Applied Biosystems Globalfiler kits. Fingermarks contaminated with fluid (e.g., blood and saliva) were deposited on ITO-coated glass slides, treated with surfactant and trypsin for 2hrs, then homogenous CHCA matrix spray prior to MALDI imaging. Fingermarks results were visualized and evaluated using FlexImaging 4.0 (Bruker Daltonik, Bremen, Germany).

RESULTS

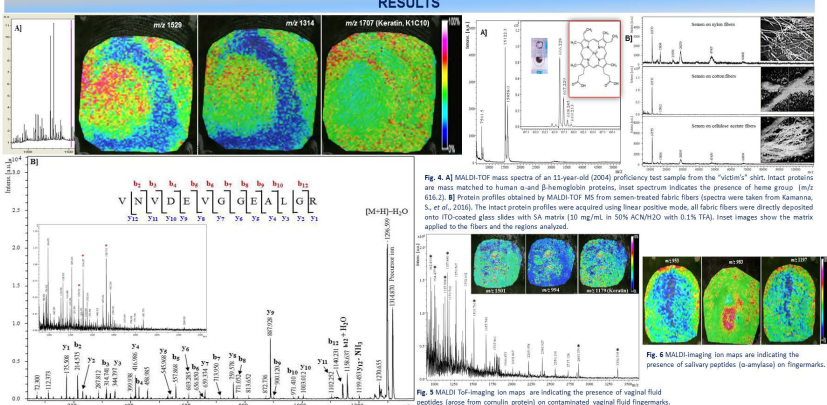
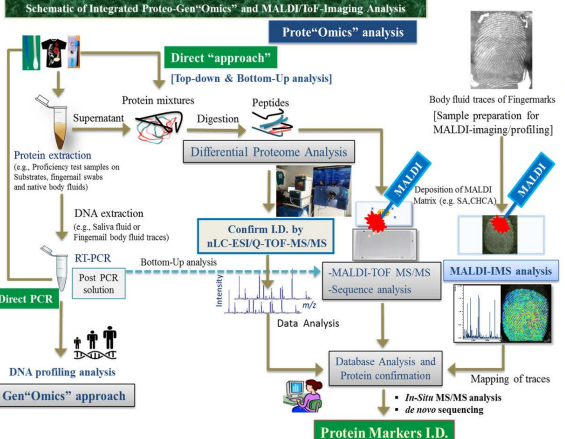


Fig. 4. A) MALDI-TOF mass spectra of an 15-year-old (2004) proficiency test sample from the “victim’s” shirt. Intact proteins are mass matched to human α - and β -hemoglobin proteins. Inset spectrum indicates the presence of heme group (m/z 653.2). **B)** Protein profiles obtained by MALDI-TOF MS from semen-treated fabric fibers (spectra were taken from Kamanna, S., et al., 2016). The intact protein profiles were acquired using linear positive mode, all fabric fibers were directly deposited onto ITO-coated glass slides with 54 matrix (10 mg/ml, in 50% ACN/20 with 0.1% TFA). Inset images show the matrix applied to the fibers and the regions analyzed.

Fig. 5. A) MALDI-TOF mass spectra of an 15-year-old (2004) proficiency test sample from the “victim’s” shirt. Intact proteins are mass matched to human α - and β -hemoglobin proteins. Inset spectrum indicates the presence of heme group (m/z 653.2). **B)** Protein profiles obtained by MALDI-TOF MS from semen-treated fabric fibers (spectra were taken from Kamanna, S., et al., 2016). The intact protein profiles were acquired using linear positive mode, all fabric fibers were directly deposited onto ITO-coated glass slides with 54 matrix (10 mg/ml, in 50% ACN/20 with 0.1% TFA). Inset images show the matrix applied to the fibers and the regions analyzed.

Fig. 6 MALDI-TOF mass spectra of intact protein profiles of fingermarks with presence of human desmoglein protein.



Schematic of Integrated Prote‘Omics’ and MALDI-ToF-Imaging Analysis

Prote‘Omics’ analysis

Direct “approach” [Top-down & Bottom-Up analysis]

Protein mixtures → Digestion → Peptides → MALDI-IMS analysis → Mapping of traces → Database Analysis and Protein confirmation → Protein Markers I.D.

Gen‘Omics’ approach

DNA extraction (e.g., Saliva fluid or Fingernail body fluid traces) → RT-PCR → Post PCR solution → DNA profiling analysis → Gen‘Omics’ approach → DNA STR profile

Bottom-Up analysis

Protein extraction (e.g., Proficiency test samples on Substrates, Fingernail swabs and native body fluids) → Digestion → Peptides → MALDI-IMS analysis → Mapping of traces → Database Analysis and Protein confirmation → Protein Markers I.D.

Confirm I.D. by nLC-ESI-Q-TOF-MS/MS

Differential Proteome Analysis

Deposition of MALDI Matrix (e.g. SA, CHCA)

MALDI-TOF MS/MS

Sequence analysis

In-Situ MS/MS analysis

de novo sequencing

CONCLUSION

Here, we have demonstrated on fingermarks a “bottom-up” enzymatic Prote‘Omics’ analysis with a homogenous trypsin digestion procedure for the simultaneous identification and mapping of traces such as blood and saliva using MALDI-imaging mass spectrometry. In addition, we show an *in situ* “top-down” and “bottom-up” direct MS identification of protein “markers” in body fluids and fluid stains on fabric fibres using an alternative enzymatic proteolytic cleavage procedure for tryptic peptide MALDI-imaging and classical proteome (e.g., nLC-MS/MS) analysis. In addition, an initial integrated Gen‘Omics’ and Prote‘Omics’ approach is described. Combined “Omics” approaches offer significant potential for application in forensic casework.

ACKNOWLEDGEMENTS

The authors wish to thank the SA Government Department of Justice for funding under the Ross Vining Research Fund. We also are indebted to Flinders fertility, which agreed to provide samples of semen to assist with this research. Finally, we gratefully acknowledge the contributions of the many volunteers from FSSA, Flinders University and the public who provided samples upon which experiments were carried out.

Fig. 1 A schematic of the overall experiment design developed to use for the identification of body fluid mixtures on different substrates or native solutions by Prote‘Omics’ approach. Traces of fingermarks analysis is performed using MALDI-imaging mass spectrometry.

Fig. 2. A) MALDI-imaging ion intensity maps of *in situ* proteolysis of a blooded fingermark. **B)** MALDI-LIFT MS/MS spectrum of precursor ion m/z 1314.87, tryptic peptide of β -subunit of hemoglobin B (HB- β). Inset indicates peptides of hemoglobin protein. Inset: sequence of HB- β peptide matched “y” and “y” ions are indicated in the LIFT MS/MS spectrum.

Fig. 3 Human DNA STR profile from body fluid on a microswab showing a mixed male (assault) and female (victim) typing.

REFERENCE

Kamanna, S., et al., *Direct identification of forensic body fluids using matrix-assisted laser desorption/ionization time-of-flight mass spectrometry* International Journal of Mass Spectrometry, 2016, **397-398**, p. 16-26.

ACKNOWLEDGEMENTS

The authors wish to thank the SA Government Department of Justice for funding under the Ross Vining Research Fund. We also are indebted to Flinders fertility, which agreed to provide samples of semen to assist with this research. Finally, we gratefully acknowledge the contributions of the many volunteers from FSSA, Flinders University and the public who provided samples upon which experiments were carried out.

CRICOS Provider No: 001144





INTRODUCTION

Body fluids such as blood and seminal fluid are very important evidence in the investigation of crimes against the person such as murder and rape. Whereas DNA profiling is extremely reliable in establishing from whom the body fluid originated, tests to positively identify the type of fluid involved (e.g., whether it is blood or semen or a mixture of them) are much less refined and can be equivocal. Several presumptive tests for body fluids are available but they can be ambiguous or provide false negative or false positive results, especially in the case of mixed deposits. Our recently published article [1] describes a streamlined and simplified direct approach for the identification of body fluids using matrix-assisted laser desorption/ionization time-of-flight mass spectrometry (MALDI-ToF-MS) that avoids pre-fractionation or isolation of proteins from mixtures.

Here we show an extension of forensic “omics” in regards to the examination of mixtures of proteins and small molecules present in fingermarks. This approach could provide investigators with both identity of the victim or suspect through the fingermark ridge pattern and what they might have touched in the moments before the crime.

MATERIALS AND METHODS

Body fluids/fingermark samples were sourced from volunteers pursuant to Southern Adelaide Clinical Human Research Ethics Committee Application 440.14–HREC/14/SAC/455.

Pieces of 100% nylon, cotton and cellulose acetate fabric (all white) were soaked with 10 μ L of body fluid mixtures. Proficiency test kits provided by Collaborative Testing Services (Stirling, Virginia, USA) were used as part of the validation program. The SEM images were collected using an FEI Inspect F50 instrument. All samples of direct and extracted fluids were analysed using MALDI-ToF MS and the identity of protein markers was confirmed by *de-novo* sequencing and nLC-MS/MS analysis.

Fingermarks contaminated with fluid (e.g., blood) were deposited on ITO-coated glass slides, treated with surfactant and trypsin for 2hrs, then homogenous CHCA matrix spray prior to MALDI imaging. Fingermarks results were visualized and evaluated using FlexImaging 4.0 (Bruker Daltonik, Bremen, Germany).

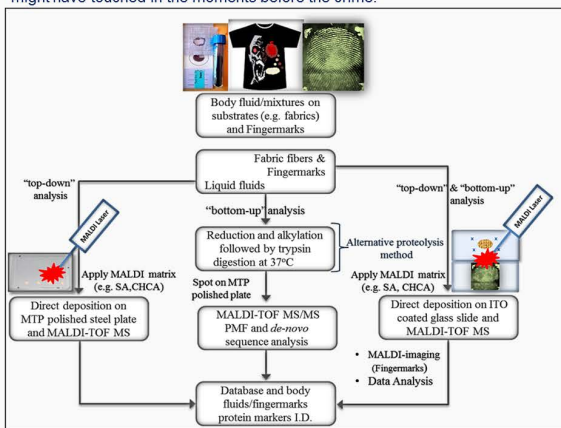


Fig. 1. A schematic of the overall experiment design developed to use for direct identification of body fluid mixtures by MALDI-ToF MS. The work flow is modified from Kamanna, S., *et al.*, 2016.

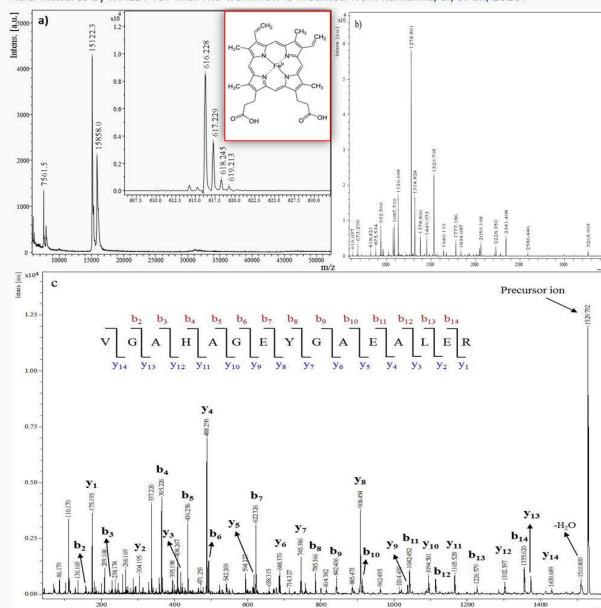


Fig. 3. MALDI-ToF mass spectra of an 11-year-old (2004) proficiency test sample from the “victim’s” shirt. (a) Intact protein mass matched to human α - and β -hemoglobin proteins, inset spectrum indicates the presence of heme group (m/z 616.2). (b) tryptic peptides. (c) MS/MS spectrum of precursor ion m/z 1529.79 of α -subunit of hemoglobin.

CONCLUSION

In situ “top-down” and “bottom-up” direct MS identification of protein “markers” in body fluids and stains on fabric fibres and an alternative enzymatic proteolytic cleavage procedure and tryptic peptide MALDI-imaging process for analysis of proteins and/or small molecules present in fingermarks offer significant potential for application in forensic casework.

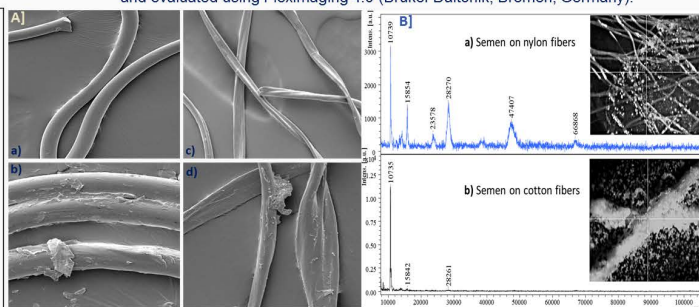


Fig. 2. (A) SEM images of fabric fibers, top row (a and c) are untreated nylon and cotton respectively, bottom row (b and d) depicts fibers from the same fabrics that have been treated with semen. (B) Protein profiles obtained by MALDI-TOF MS from semen-treated fabric fibers. The intact protein profiles were acquired using linear positive mode, all fabric fibers were directly deposited onto ITO-coated glass slides with SA matrix (10 mg/mL in 50% ACN/H₂O with 0.1% TFA). Inset images show the matrix applied to the fibers and the regions analyzed.

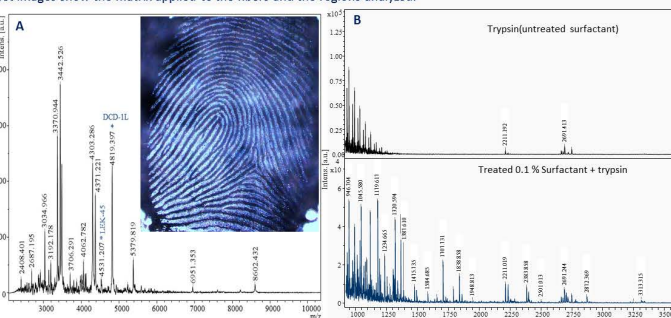


Fig. 4. A) MALDI-TOF mass spectra of intact protein profiles of Fingermarks. B) Treated and untreated Surfactant (e.g., Rapigest) based fingermarks trypsin digested (2 hrs) spectra.

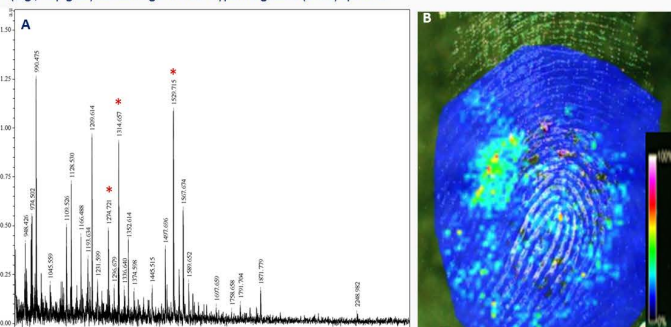


Fig. 5. a) MALDI-profiling and trypsin digested mass spectra of blood-contaminated fingermarks. b) MALDI-imaging ion map of m/z 1529 matched to α -subunit of hemoglobin.

REFERENCE

- Kamanna, S., *et al.*, Direct identification of forensic body fluids using matrix-assisted laser desorption/ionization time-of-flight mass spectrometry. International Journal of Mass Spectrometry, 2016. 397–398; p. 18-26.

ACKNOWLEDGEMENTS

The authors wish to thank the SA Government Department of Justice for funding under the Ross Vining Research Fund. We also are indebted to Flinders fertility, which agreed to provide samples of semen to assist with this research. Finally, we gratefully acknowledge the contributions of the many volunteers from FSSA, Flinders University and the public who provided samples upon which experiments were carried out.

Forensic Research & Technology

October 31-November 02, 2016 San Francisco, USA

Mass spectrometry-based forensic “Omics” in dir

otein markers

Sathisha Kamanna, Adrian Linacre, Nico Voelcker, Julianne Henry and Paul Kirkbride
Flinders University, Australia

Body fluids such as blood, seminal fluid, urine or saliva are very important in the investigation of crimes against the person such as murder and rape. Whereas DNA profiling is extremely reliable in establishing from whom the body fluid originated, tests to positively identify the type of fluid involved (e.g., whether it is semen or saliva or a mixture of them) are much less refined and can be ambiguous. Our recently submitted article describes a streamlined and simplified direct approach for the identification of body fluids using matrix-assisted laser desorption/ionization time-of-flight mass spectrometry (MALDI-ToF-MS) that avoids pre-fractionation or isolation of proteins. Microliter quantities (or less) of neat fluids or their extracts or deposits of them *in situ* on tufts of fibers plucked from evidence (such as garments) can be analysed directly and quickly. Here we describe extensions of our direct approach in regards to the examination of other fluids, both human and non-human, and explore its combination with analysis of miRNA.

Biography

Sathisha Kamanna is pursuing 3rd year PhD at Flinders University, South Australia. His PhD project is “Mass Spectrometry-based proteomics applications in forensic body fluids analysis”. He has 7 years work experience in biological mass spectrometry and is involved in the forensic analysis of body fluids and identification of protein/miRNA biomarkers using mass spectrometry based analytical techniques. He has 8 international publications (author/co-author) in reputed journals.

kama0073@flinders.edu.au
satishkmb@gmail.com

Notes:

conferenceseries.com

Conference Series LLC
Best Poster Award

Awarded to *Sathisha Kamanna*
Flinders University, Australia

for presenting the poster entitled:

*Mass Spectrometry-based Forensic "Omics" and
MALDI-imaging analysis for the identification/visualiz-
ation of bodily fluid traces in fingerprints*

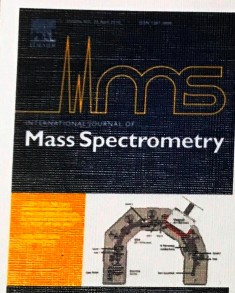
at the "5th International Conference on Forensic Research & Technology"

held during October 31-November 02, 2016 in San Francisco, USA

The award has been attributed in recognition of research paper quality, novelty and significance.

Yoshiaki Omura
Yoshiaki Omura
New York Medical College, USA

International Journal of Mass Spectrometry



Agilent Technologies



ELSEVIER

**IJMS Best Applied
Student Paper**

**Sathisha Kamanna
Flinders University, Adelaide, Australia**

**“Direct identification of forensic body fluids using matrix-assisted
laser desorption/ionization time-of-flight mass spectrometry”**

**Awarded at the 65th Conference on Mass Spectrometry and Allied Topics
June 4-8, 2017, Indianapolis, USA**

Perdita Barran
IJMS Editor-in-Chief

Zheng Ouyang
IJMS Editor-in-Chief

Micheal Bowers
IJMS Special Issue Consultant

Christian Schulz
Publisher, Elsevier

John C. Fjeldsted
Sen. Director, Agilent Technologies